frontiers | Research Topics

Aging, peripheral inflammation, and neurodegeneration

Edited by
Caroline Haikal and Robert Weissert

Published in
Frontiers in Aging Neuroscience
Frontiers in Immunology

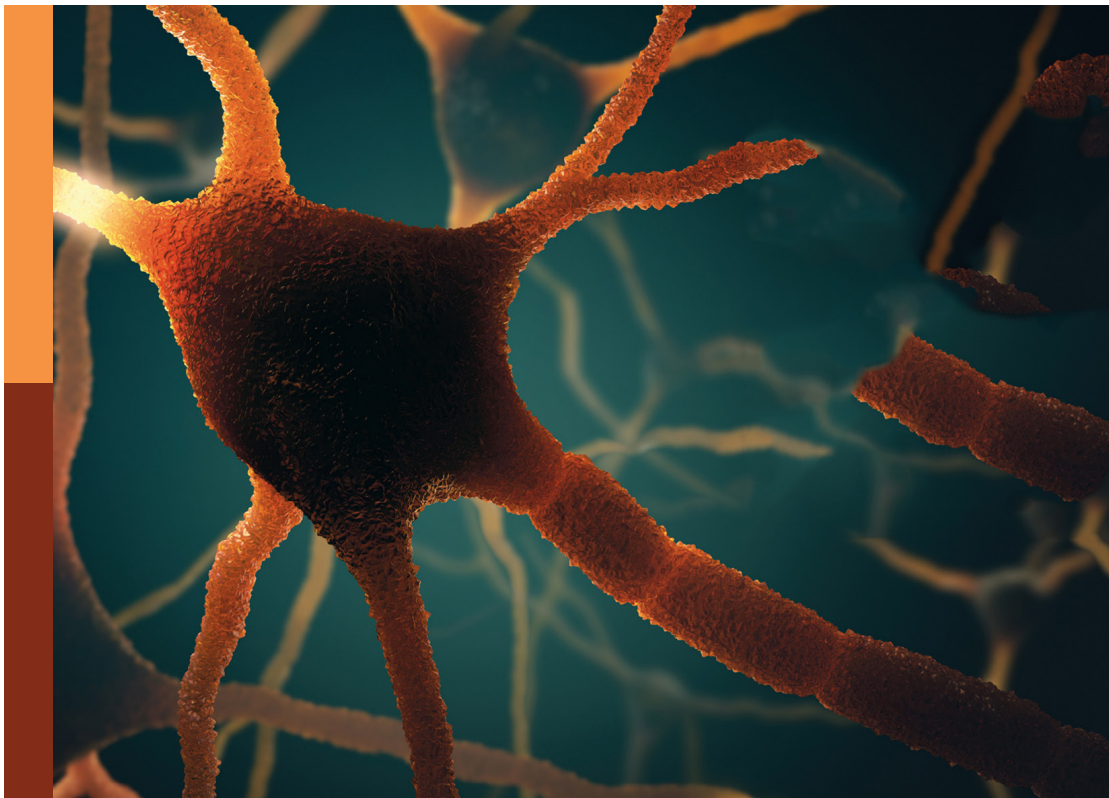

ISSN 1664-8714
ISBN 978-2-8325-5817-1
DOI 10.3389/978-2-8325-5817-1

About Frontiers

Frontiers is more than just an open access publisher of scholarly articles: it is a pioneering approach to the world of academia, radically improving the way scholarly research is managed. The grand vision of Frontiers is a world where all people have an equal opportunity to seek, share and generate knowledge. Frontiers provides immediate and permanent online open access to all its publications, but this alone is not enough to realize our grand goals.

Frontiers journal series

The Frontiers journal series is a multi-tier and interdisciplinary set of open-access, online journals, promising a paradigm shift from the current review, selection and dissemination processes in academic publishing. All Frontiers journals are driven by researchers for researchers; therefore, they constitute a service to the scholarly community. At the same time, the *Frontiers journal series* operates on a revolutionary invention, the tiered publishing system, initially addressing specific communities of scholars, and gradually climbing up to broader public understanding, thus serving the interests of the lay society, too.

Dedication to quality

Each Frontiers article is a landmark of the highest quality, thanks to genuinely collaborative interactions between authors and review editors, who include some of the world's best academicians. Research must be certified by peers before entering a stream of knowledge that may eventually reach the public - and shape society; therefore, Frontiers only applies the most rigorous and unbiased reviews. Frontiers revolutionizes research publishing by freely delivering the most outstanding research, evaluated with no bias from both the academic and social point of view. By applying the most advanced information technologies, Frontiers is catapulting scholarly publishing into a new generation.

What are Frontiers Research Topics?

Frontiers Research Topics are very popular trademarks of the *Frontiers journals series*: they are collections of at least ten articles, all centered on a particular subject. With their unique mix of varied contributions from Original Research to Review Articles, Frontiers Research Topics unify the most influential researchers, the latest key findings and historical advances in a hot research area.

Find out more on how to host your own Frontiers Research Topic or contribute to one as an author by contacting the Frontiers editorial office: frontiersin.org/about/contact

Aging, peripheral inflammation, and neurodegeneration

Topic editors

Caroline Haikal — Weill Cornell Medical Center, NewYork-Presbyterian, United States

Robert Weissert — University of Regensburg, Germany

Citation

Haikal, C., Weissert, R., eds. (2024). *Aging, peripheral inflammation, and neurodegeneration*. Lausanne: Frontiers Media SA. doi: 10.3389/978-2-8325-5817-1

Table of contents

frontiers | Frontiers in Aging Neuroscience

TYPE Editorial
PUBLISHED 10 December 2024
DOI 10.3389/fnagi.2024.1529026

OPEN ACCESS

EDITED AND REVIEWED BY
Yu-Min Kuo,
National Cheng Kung University, Taiwan

*CORRESPONDENCE
Caroline Haikal
✉ cah4014@med.cornell.edu
Robert Weissert
✉ robert.weissert@ukr.de

RECEIVED 15 November 2024
ACCEPTED 25 November 2024
PUBLISHED 10 December 2024

CITATION
Haikal C and Weissert R (2024) Editorial: Aging, peripheral inflammation, and neurodegeneration.
Front. Aging Neurosci. 16:1529026.
doi: 10.3389/fnagi.2024.1529026

Editorial: Aging, peripheral inflammation, and neurodegeneration

Caroline Haikal[1]* and Robert Weissert[2]*

[1]Neurological Surgery, Weill Cornell Medical Center, New York-Presbyterian, New York, NY, United States, [2]Department of Neurology, University of Regensburg Hospital, Regensburg, Germany

KEYWORDS

aging, amyotrophic lateral sclerosis, neurodegenerative diseases, neuroinflammation, inflammation, Parkinson's disease, Alzheimer's disease, oxidative stress

Editorial on the Research Topic
Aging, peripheral inflammation, and neurodegeneration

1 Editorial overview

Aging is the major risk factor for a multitude of diseases including neurodegenerative diseases such as Parkinson's disease (PD) and Alzheimer's disease (AD). Understanding aging-related biological changes is crucial to identifying why some individuals develop neurodegenerative diseases while others do not. Aging is a heterogeneous process, both in regard to individuals within a population, and within tissues and organs affected in an individual. As such, considerable effort has been put toward understanding the biological age of systems as opposed to relying on chronological age. Biological aging is characterized by 12 hallmarks (López-Otín et al., 2023), many of which are linked to neurodegenerative disease mechanisms. However, many of these hallmarks have bidirectional relationships with each other. Indeed, a recent review highlights the bidirectional relationship of chronic inflammation with each of the other 11 hallmarks (Baechle et al., 2023). An integrated view of aging and inflammation could aid in bettering the understanding of neurodegenerative diseases and identifying new avenues of research and effective therapeutic strategies. We have arranged this Research Topic into three broad subjects, as follows: (A) Oxidative stress and metabolic dysregulation in neurodegenerative diseases; (B) Immune system and inflammatory mechanisms in neurodegenerative and systemic diseases; and (C) Genetics, aging, and systemic conditions related to neurodegenerative risk.

2 Oxidative stress and metabolic dysregulation in neurodegenerative diseases

A recent study examined the directional relationships in which the biological age of one organ selectively affects the biological age of other organ systems and found that the advanced age of several body systems explained advanced brain age (Tian et al., 2023). In the review by Kong et al., the authors explore how oxidative stress links brain and lung health. Oxidative stress has damaging effects on lipids, proteins and DNA all of which are affected in pulmonary diseases, such as chronic obstructive pulmonary disease (COPD)

and fibrosis as well as brain diseases such as stroke, traumatic brain injury (TBI), and neurodegenerative diseases. They also examine the role of reactive oxygen species (ROS) in brain-lung crosstalk, identifying amongst other things, iron homeostasis disruption, breakdown of the blood brain barrier, and activation of the immune system. In their bibliometric analysis, Liu et al. map the research landscape of ferroptosis, an iron-dependent form of cell death, within neurodegenerative diseases. The study shows that ferroptosis research, particularly related to AD and PD, has grown significantly. This cell death pathway is associated with oxidative stress and lipid peroxidation, suggesting it may be a target for therapeutic intervention across neurodegenerative diseases. The role of iron dysregulation in neuroinflammation is further examined by Ashraf et al.. In this study, the authors examined the effects of lipopolysaccharide (LPS)-induced inflammation on cognitive performance and regional brain metabolism following mild iron priming. They reported that iron priming had different metabolic effects on the hippocampus and cortex but induced hyperramification of microglia in both regions following LPS administration. The nuanced, region-specific brain responses to iron priming-both alone and when combined with LPS-induced inflammation underscore the need for comprehensive analyses in such studies, and reinforce a link between iron dysregulation, inflammation, and neurodegenerative disease. Perturbation of iron (and copper) homeostasis is also discussed in Wimalasena et al.'s article. Here, the authors propose a new hypothesis to account for the selective vulnerability of neuromelanin-containing dopaminergic neurons in the substantia nigra pars compacta and noradrenergic neurons in the locus coeruleus. They argue that these neurons' high energy demands and complex metabolic roles render them more susceptible to oxidative stress and metal dysregulation (particularly iron and copper), which, in turn, promotes alpha-synuclein aggregation. This aggregation is a critical factor in Parkinson's disease pathology, providing a comprehensive framework for understanding selective neurodegeneration.

3 Immune system and inflammatory mechanisms in neurodegenerative and systemic diseases

Kitchener et al. studied a lysosomal enzyme, beta-galactosidase, the overexpression of which has previously been implicated in AD. Using immortalized BV-2 cells and primary mixed glial-neuronal cultures, as well as *in vivo* studies of young and aged mice, they show an upregulation of microglial beta-galactosidase cell-surface activity and extracellular release in response to inflammation which in turn promotes microglial activation-dependent neurotoxicity. This could be attenuated with the use of beta-galactosidase inhibitors, highlighting a potential target for neurodegenerative disease interventions, especially in conditions like AD and PD. Using differential gene expression analyses, An et al. identified shared crosstalk genes between AD and atherosclerosis, particularly related to complement activation and microglia signaling, emphasizing the role of immune pathways in both. They identified diagnostic genes which had over 80% predictive accuracy. They could also observe increased macrophage infiltration in both AD and atherosclerotic disease cohorts compared to healthy controls. In a single-center study, Alster et al. analyzed inflammatory markers in the cerebro-spinal fluid (CSF) and plasma of patients with supranuclear palsy, an atypical parkinsonism characterized by tauopathy, and healthy controls and correlated changes with brain volumes as examined by magnetic resonance imaging (MRI). IL-1 and IL-6 correlated variably with different brain regions, suggesting that the role of inflammatory factors in neurodegenerative disease may not be unequivocal and rather dependent on the type of inflammatory factor and selective vulnerability of certain tissues. This sentiment is echoed in Song, Li, Han, Xu, Ding et al.'s study where two-sample Mendelian randomization was employed to identify peripheral immune cells both positively and negatively associated with PD. The authors emphasize that different cell types may play different roles through the varying stages of PD and that potential therapeutic targets may be relevant at different times through the course of the pathogenesis. Similarly, Qin et al. utilized Mendelian randomization to evaluate the correlations between the plasma lipidome, circulating inflammatory proteins and risk of PD. The results show potential mediation by inflammatory proteins in the link between lipids and PD, adding to predictive markers and possible targets for PD treatment. When this method was employed by Xiao et al., to study the effects of inflammatory proteins on amyotrophic lateral sclerosis (ALS), they identified a bidirectional relationship between inflammatory markers and ALS, suggesting that ALS could also impact inflammatory protein levels, adding depth to ALS pathophysiology and potential therapeutic targets. Further examining the link between ALS and circulating inflammatory markers, Du et al. created a predictive model linking mitophagy and immune cell infiltration to ALS. They identified 40 genes with prognostic value and 4 genes with diagnostic value. They validated their differential expression in plasma from ALS patients and healthy controls. This work lays the groundwork for understanding progression of ALS and its immune and mitochondrial dynamics, potentially guiding early diagnostics and therapeutic developments.

4 Genetics, aging, and systemic conditions related to neurodegenerative risk

Aging is linked to altered microbiome composition, though its role in inflammation remains uncertain (Falony et al., 2016). Importantly, chronic inflammation and dysbiosis are both key features of neurodegenerative diseases and IBD. Several studies have examined the link between inflammatory bowel disease (IBD)-Crohn's disease, ulcerative colitis- and PD, yet controversy exists whether the correlation is real. Adding to this field, Wang et al. performed a large-scale cohort study and found no significant link between risk of IBD and risk of PD in general; however, specific subgroups, such as females with ulcerative colitis, did show a slight increased risk of PD. This finding provides evidence for a potential, but not universal, relationship between IBD and PD. Systemic lupus erythematosus (SLE) is an autoimmune

connective tissue disease in which neuropsychiatric, particularly cognitive dysfunction, can be prevalent. Histological examination has highlighted neuronal loss resulting in loss of volume of both white and gray matter areas and elevated levels of neurofilament light protein and glial fibrillary acidic protein (GFAP) in the CSF indicating the neurodegenerative nature of these changes. Kuchcinski et al. utilized a deep learning method called BrainAGE that estimates the age gap, i.e., the difference in chronological age vs. biological age of the brain, using magnetic resonance images of patients with SLE and age matched controls. They found a higher brain age gap in SLE patients, particularly those with higher disease activity, linking SLE's inflammatory effects with accelerated brain aging and cognitive decline. There is an epidemiological association between frailty-an increased state of vulnerability- and insomnia, both of which increase with age and are risk factors for neurodegenerative diseases. Song, Li, Han, Xu, Wang et al. utilized GWAS data to determine a positive genetic correlation between the two. They identified 2 SNPs at 3p21.31 mapping to genes related to sleep regulation and inflammation. Interestingly, they found tissue specific SNP heritability enrichment with the anterior cingulate cortex and cerebral amygdala.

This editorial collectively emphasizes the interconnected nature of aging, inflammation, immune responses, and systemic factors in neurodegeneration. By synthesizing findings across these three themes, the articles provide a comprehensive view of current research, offering promising avenues for targeted interventions in aging-related neurodegenerative diseases.

Author contributions

CH: Writing – original draft, Writing – review & editing. RW: Writing – review & editing.

Conflict of interest

The authors declare that the research was conducted in the absence of any commercial or financial relationships that could be construed as a potential conflict of interest.

The author(s) declared that they were an editorial board member of Frontiers, at the time of submission. This had no impact on the peer review process and the final decision.

Publisher's note

References

Baechle, J. J., Chen, N., Makhijani, P., Winer, S., Furman, D., and Winer, D. A. (2023). Chronic inflammation and the hallmarks of aging. *Molec. Metabol.* 74:101755. doi: 10.1016/j.molmet.2023.101755

Falony, G., Joossens, M., Vieira-Silva, S., Wang, J., Darzi, Y., Faust, K., et al. (2016). Population-level analysis of gut microbiome variation. *Science* 352, 560–564. doi: 10.1126/science.aad3503

López-Otín, C., Pietrocola, F., Roiz-Valle, D., Galluzzi, L., and Kroemer, G. (2023). Meta-hallmarks of aging and cancer. *Cell Metabol.* 35, 12–35. doi: 10.1016/j.cmet.2022.11.001

Tian, Y. E., Cropley, V., Maier, A. B., Lautenschlager, N. T., Breakspear, M., and Zalesky, A. (2023). Heterogeneous aging across multiple organ systems and prediction of chronic disease and mortality. *Nat. Med.* 29, 1221–1231. doi: 10.1038/s41591-023-02296-6

frontiers | Frontiers in Aging Neuroscience

TYPE Original Research
PUBLISHED 20 October 2023
DOI 10.3389/fnagi.2023.1274061

OPEN ACCESS

EDITED BY
Robert Weissert,
University of Regensburg, Germany

REVIEWED BY
Patricio Huerta,
Feinstein Institute for Medical Research, United States
Daniele Corbo,
University of Brescia, Italy

*CORRESPONDENCE
Grégory Kuchcinski
✉ gregory.kuchcinski@univ-lille.fr

RECEIVED 07 August 2023
ACCEPTED 09 October 2023
PUBLISHED 20 October 2023

CITATION
Kuchcinski G, Rumetshofer T, Zervides KA, Lopes R, Gautherot M, Pruvo J-P, Bengtsson AA, Hansson O, Jönsen A and Sundgren PCM (2023) MRI BrainAGE demonstrates increased brain aging in systemic lupus erythematosus patients. *Front. Aging Neurosci.* 15:1274061. doi: 10.3389/fnagi.2023.1274061

MRI BrainAGE demonstrates increased brain aging in systemic lupus erythematosus patients

Grégory Kuchcinski[1,2,3]*, Theodor Rumetshofer[1,4], Kristoffer A. Zervides[5], Renaud Lopes[3,6], Morgan Gautherot[6], Jean-Pierre Pruvo[3,6], Anders A. Bengtsson[5], Oskar Hansson[7,8], Andreas Jönsen[5] and Pia C. Maly Sundgren[1,2]

[1]Division of Diagnostic Radiology, Department of Clinical Sciences, Skåne University Hospital, Lund University, Lund, Sweden, [2]Lund University BioImaging Centre, Lund University, Lund, Sweden, [3]Inserm, CHU Lille, U1172 – LilNCog – Lille Neuroscience & Cognition, Univ. Lille, Lille, France, [4]Division of Logopedics, Phoniatrics and Audiology, Department of Clinical Sciences, Lund University, Lund, Sweden, [5]Division of Rheumatology, Department of Clinical Sciences, Skåne University Hospital, Lund University, Lund, Sweden, [6]Univ. Lille, CNRS, Inserm, CHU Lille, Institut Pasteur de Lille, Lille, France, [7]Clinical Memory Research Unit, Lund University, Lund, Sweden, [8]Memory Clinic, Skåne University Hospital, Malmö, Sweden

Introduction: Systemic lupus erythematosus (SLE) is an autoimmune connective tissue disease affecting multiple organs in the human body, including the central nervous system. Recently, an artificial intelligence method called BrainAGE (Brain Age Gap Estimation), defined as predicted age minus chronological age, has been developed to measure the deviation of brain aging from a healthy population using MRI. Our aim was to evaluate brain aging in SLE patients using a deep-learning BrainAGE model.

Methods: Seventy female patients with a clinical diagnosis of SLE and 24 healthy age-matched control females, were included in this post-hoc analysis of prospectively acquired data. All subjects had previously undergone a 3 T MRI acquisition, a neuropsychological evaluation and a measurement of neurofilament light protein in plasma (NfL). A BrainAGE model with a 3D convolutional neural network architecture, pre-trained on the 3D-T1 images of 1,295 healthy female subjects to predict their chronological age, was applied on the images of SLE patients and controls in order to compute the BrainAGE. SLE patients were divided into 2 groups according to the BrainAGE distribution (high vs. low BrainAGE).

Results: BrainAGE *z*-score was significantly higher in SLE patients than in controls (+0.6 [±1.1] vs. 0 [±1.0], $p = 0.02$). In SLE patients, high BrainAGE was associated with longer reaction times ($p = 0.02$), lower psychomotor speed ($p = 0.001$) and cognitive flexibility ($p = 0.04$), as well as with higher NfL after adjusting for age ($p = 0.001$).

Conclusion: Using a deep-learning BrainAGE model, we provide evidence of increased brain aging in SLE patients, which reflected neuronal damage and cognitive impairment.

KEYWORDS

systemic lupus erythematosus, brain, aging, deep learning, magnetic resonance imaging

1. Introduction

Systemic lupus erythematosus (SLE) is an autoimmune connective tissue disease that affects 0.1% of the general population, with a large female predominance. Neuropsychiatric symptoms are commonly observed in individuals with SLE, with reported frequencies ranging from 20 to 95%, depending on the classification criteria used (Brey et al., 2002). These symptoms have been associated with increased morbidity and mortality and decreased quality of life (Brey et al., 2002). The array of neuropsychiatric symptoms is diverse, encompassing conditions such as headaches, epilepsy, focal neurological deficits, mood disorders, and psychosis (Brey et al., 2002). Among these, cognitive dysfunction is particularly prevalent, affecting approximately 75% of patients (Leslie and Crowe, 2018). The pathophysiology of these symptoms remains widely debated.

Brain abnormalities observed in SLE patients are frequent and heterogeneous. Beyond the vascular and/or inflammatory lesions identified through MRI (Jennings et al., 2004) and histopathological studies (Hanly et al., 1992; Cohen et al., 2017), mounting evidence suggests an ongoing neurodegenerative process. Histological examinations have highlighted substantial and widespread neuronal loss among patients displaying neuropsychiatric symptoms (Ercan et al., 2016). Initial longitudinal imaging studies have confirmed progressive reductions in brain volume, affecting both white and gray matter, over relatively short time spans (19 months) (Appenzeller et al., 2007). The neurodegenerative nature of these changes has been further supported by elevated levels of CSF and plasma biomarkers associated with ongoing neuronal damage (neurofilament light protein [NfL] and glial fibrillary acidic protein) (Trysberg et al., 2003, 2004; Lauvsnes et al., 2022), even among patients without neuropsychiatric symptoms. Interestingly, this phenomenom has also been observed at the cellular level, with the accumulation of senescent neural cells in the hippocampus of murine models of SLE (MRL/Ipr mice) (Saito et al., 2021).

Nonetheless, these lesions lack specificity, exhibiting a continuum across patients with and without neuropsychiatric symptoms. In approximately 60% of cases, symptoms may be independent of brain damage, and instead attributed to chronic pain, altered sleep quality or corticosteroid therapy (Magro-Checa et al., 2016). The broad range of symptoms presented and the absence of a reliable biomarker therefore make diagnosis and management challenging in a large number of cases (Kalinowska-Lyszczarz et al., 2018).

Recently, an artificial intelligence method, called BrainAGE (Brain Age Gap Estimation), has been developed to measure the deviation in brain aging within a cohort of patients experiencing cognitive decline, in comparison to a healthy population without cognitive or psychiatric disorders (Franke and Gaser, 2019). The approach involves training a model to predict the age of healthy individuals based on MR images of their brain. Subsequently, this model can be applied to a group of patients with cognitive and/or psychiatric disorders, aiming to reveal the discrepancy between the predicted age generated by the algorithm and the actual age of the patient - termed BrainAGE score. A BrainAGE score near 0 indicates typical brain aging, while a BrainAGE score significantly higher than 0 suggests increased brain aging. This quantitative, cross-diagnostic marker effectively reflects the extent of disease-related structural changes. Notably, BrainAGE is sensitive to volume loss related to cerebral atrophy, but also to signal changes induced, for instance, by white matter lesions (Bretzner et al., 2023).

Our main objective was to evaluate brain aging in SLE by using a deep-learning BrainAGE model within an established cohort of extensively characterized SLE patients and matched healthy controls (Cannerfelt et al., 2018; Langensee et al., 2022; Zervides et al., 2022b). Our secondary objectives were to identify neuropsychological correlates and clinical factors contributing to increased brain aging.

2. Materials and methods

2.1. Population

The present study is a cross-sectional post-hoc MRI analysis of a well described single-center prospective SLE cohort (Cannerfelt et al., 2018; Langensee et al., 2022; Zervides et al., 2022b). The study cohort was approved by the regional ethics committee (reference #2012/254, #2012/677, #2014/778). The study was conducted in accordance with the Declaration of Helsinki. Written informed consent was obtained from the patients prior to data collection.

Between 2013 and 2016, consecutive prevalent patients with a diagnosis of SLE, attending the Department of Rheumatology, were prospectively enrolled. Inclusion criteria were as follows: diagnostic of SLE meeting at least 4 criteria of the American College of Rheumatology (ACR) classification (Tan et al., 1982), female gender, age between 18 and 55 years and right-handedness. Patients with any contra-indication to MRI were excluded (e.g., pace-maker, pregnancy).

During the same time period, female control subjects within the same age range, free of autoimmune, neurological or psychiatric disorders were recruited in a control group among health care workers and university employees at our institution. Seventy-one patients and 25 age-matched controls constituted the cohort population. Two participants (1 SLE patient and 1 healthy control) were secondarily excluded from the present analysis because of they had a focal brain lesion (meningioma, $n = 1$; cystic lesion, $n = 1$).

2.2. Clinical and neuropsychological evaluation

All patients were evaluated by a rheumatologist and a neurologist, as previously described (Zervides et al., 2022b). Neuropsychiatric manifestations were defined according to the Systemic Lupus International Collaborating Clinics (SLICC) attribution models (more stringent "SLICC A" and less stringent "SLICC B") (Hanly et al., 2007). Organ damage was recorded according to the SLICC/ACR damage index (SLICC/ACR-DI) (Gladman et al., 1996), and disease activity was assessed using the Systemic Lupus Erythematosus Disease Activity Index 2000 (SLEDAI-2 K) (Gladman et al., 2002).

All subjects underwent neuropsychological testing by a neuropsychologist using a standardized neurocognitive test battery (CNS Vital Signs; Gualtieri and Johnson, 2006), described elsewhere (Langensee et al., 2022). CNS Vital Signs has been previously tested and validated in SLE patients (Langensee et al., 2022), as well in traumatic brain injury, dementia and attention deficit hyperactivity disorder (Gualtieri and Johnson, 2006; Littleton et al., 2015). Briefly, seven established tests (verbal memory, visual memory, finger tapping,

symbol digit coding, Stroop, shifting attention and continuous performance) were used to compute age-adjusted scores in several cognitive domains. For the purpose of this study, we recorded composite memory, psychomotor speed, reaction time, complex attention and cognitive flexibility. These scores have a mean of 100 and a standard deviation of 15 in a normative sample provided by the CNS Vital Signs software. A psychologist, who remained present for the duration of the session, tested participants individually. A brief oral introduction by the psychologist, explaining the testing procedure was given to each participant. Following this, they completed the test battery independently according to the instructions that were given on the screen prior to each of the tests (Langensee et al., 2022). Additional clarifications were provided when requested. Each of the individual tests had to be performed for a predetermined amount of time and most tests were in turn timed internally, so that a response had to be given within the provided time window. Completing the entire test battery took approximately 30 min (variations occurred due to participants taking varying amounts of time to read the instructions).

Psychomotor speed was evaluated using two tests, the Finger Taping Test and the Symbol Digit Coding test (Gualtieri and Johnson, 2006). For the Finger Taping test, subjects are asked to press a space bar with left and right index finger as many times as they can in 10 s. For the Symbol Digit Coding test, the subject is given a training session to learn how to link numbers to digits. During the test session, the subject types in the number that corresponds to each symbol that is presented on the screen during 120 s. Psychomotor speed is a composite score calculated automatically by the software by adding the total of right and left taps from the Finger Taping Test and the total of correct responses during the Symbol Digit Test.

Reaction time was evaluated during a Stroop Test (Gualtieri and Johnson, 2006). During the first part of the test, the words RED, YELLOW, BLUE, and GREEN appear on the screen, printed in color. The subject is asked to press the space bar when the color of the word matches what the word says. This generates a complex reaction time score. During the second part of the test, the subject is asked to press the space bar when the color of the word does not match what the word says. This part also generates a complex reaction time score, called the "color-word reaction time." Averaging the two complex reaction time scores from the Stroop test generates a composite score for "reaction time."

2.3. Laboratory analyses

Serum and plasma samples were obtained from all patients within two weeks before or after MRI. Routine biochemical and immunological analyses were performed at the Departments of Laboratory Medicine and Immunology, including measurements of serum levels of complement factors, anti-double-stranded DNA antibodies, and antiphospholipid antibodies (including serum IgG anti-cardiolipin antibodies, serum IgG anti-beta-2-glycoprotein-1 antibodies and Lupus Anticoagulant). The concentrations of protein S100A8/A9 in serum were measured with the Bühlmann MRP8/14 ELISA kit, Switzerland, according to the manufacturers' instructions (Zervides et al., 2022b). Plasma NfL concentrations were measured using a single-molecule array (Quanterix; Billerica, MA) and the commercially available NfL assay was utilized (NF-light™ # 103186) (Zervides et al., 2022a).

2.4. Neuroimaging

2.4.1. MRI acquisitions

MRI acquisitions were performed on a 3T MRI (Siemens MAGNETOM Skyra, Erlangen, Germany), using a 20-channel head coil. The protocol included a 3D-T1 MPRAGE (magnetization-prepared rapid gradient-echo) (voxel size = 1 mm^3 isotropic, matrix = 256 × 256 × 176, TE = 2.54 ms, TR = 1900 ms, TI = 900 ms, flip angle = 9°) and a FLAIR sequence (voxel size = 0.7 × 0.7 × 3 mm, matrix = 280 × 320 × 33, TE = 81 ms, TR = 9000 ms, TI = 2500 ms, flip angle = 150°).

2.4.2. MRI visual analysis and white-matter hyperintensities segmentation

All scans were visually evaluated by a board certified neuroradiologist. A complete description of morphological abnormalities in this cohort has been reported elsewhere (Cannerfelt et al., 2018). For the purpose of this study, we reported only vascular lesions susceptible to influence BrainAGE prediction: previous ischemic or hemorrhagic lesions and white matter hyperintensities. White matter hyperintensities were automatically segmented by the lesion growth algorithm implemented in the Lesion Segmentation Toolbox (LST, version 2.0.14),[1] using 3D-T1 and FLAIR images (Schmidt et al., 2012).

2.4.3. BrainAGE preprocessing

Minimal preprocessing steps were applied on 3D-T1 brain images. First, images were corrected for magnetic field inhomogeneity effects and skull-stripped using VolBrain software version 1.0 (RRID:SCR_021020)[2] (Manjón and Coupé, 2016). Brain extractions were systematically checked, and manual corrections were performed by a neuroradiologist, when deemed necessary. Then, preprocessed 3D-T1 images were linearly registered and resampled into the MNI space using SPM software version 12 (RRID:SCR_007037). Finally, intensity normalization was performed using min–max normalization. Gray matter, white matter and CSF volumes were automatically calculated using VolBrain software.

2.4.4. Deep-learning BrainAGE model

For the prediction of chronological age based on brain images, our model was based on a 3D convolutional neural network architecture, as previously published (Gautherot et al., 2021). For the purpose of this study, the model was trained and validated on a dataset of brain MRI volumes from 1503 healthy female participants between 18 and 70 years (training $n = 1{,}295$, validation $n = 208$).

The training dataset was constituted of data compiled from several publicly available sources: IXI (Information eXtraction from Images),[3] HCP (Human Connectome Project),[4] OBRE (Center of Biomedical

1 https://www.applied-statistics.de/lst.html
2 https://fil.ion.ucl.ac.uk/spm/software/spm12/
3 https://brain-development.org/
4 https://www.humanconnectome.org/

Research Excellence),[5] MCIC (Mind Clinical Imaging Consortium),[6] NMorphCH (Neuromorphometry by Computer Algorithm Chicago),[7] NKI-RS (Enhanced Nathan Kline Institute-Rockland Sample),[8] PPMI (Parkinson's Progression Markers Initiative)[9] and ADNI (Alzheimer's Disease Neuroimaging Initiative).[10]

The model input was preprocessed 3D-T1 images with dimensions of 182 × 218 × 182 voxels. The model was based on a 3D convolutional neural network using an architecture previously described (Gautherot et al., 2021). The weights of the model were determined by minimizing the cost function, here the mean absolute error between chronological age and predicted brain age. To optimize the weights, we used a stochastic gradient descent optimization algorithm (Sutskever et al., 2013) with a learning rate of 0.001, a momentum of 0.1, and a learning rate decay of 5e-05. We used a batch size of 8 during 150 iterations. During the training phase, we performed a data augmentation strategy on-the-fly consisting of performing translation and rotation of the MR images. This technique generated additional artificial training images to prevent the model from overfitting and was empirically found to yield better performance (Shorten and Khoshgoftaar, 2019). We used a 5-fold cross-validation procedure on our training set for optimizing hyperparameters. The mean absolute error of the model on our validation dataset was 4.4 years.

As recommended in BrainAGE studies, we removed any common variance with chronological age before submitting the residualized version of BrainAGE, using linear regression (Liang et al., 2019):

$$Regressed\ predicted\ age = intercept + \alpha \times \text{chronological age} + \text{error} \quad (1)$$

α is the regression coefficient associated with the chronological age, and in our study α = 0.13.

Weights from the pre-trained model were used for the prediction of brain age for our SLE patients and matched controls. BrainAGE was calculated as the difference between predicted brain age and chronological age at the acquisition time, and converted in *z*-score taking the control group as reference (Gautherot et al., 2021).

To understand which brain regions were mainly used by the BrainAGE model, we computed attention maps using an occlusion sensitivity method adapted from Petsiuk et al. (2018). A sliding mask of 8 × 8 × 8 voxels was used to hide part of the input images and probe the model. The final attention map was generated as a linear combination of the binary masks where the combination weights come from the amplitude of the difference between predicted age with and without masking.

5 https://www.mrn.org/common/cobre-phase-3
6 https://www.nitrc.org/projects/mcic/
7 http://schizconnect.org/
8 http://fcon_1000.projects.nitrc.org/indi/enhanced/
9 www.ppmi-info.org/data
10 adni.loni.usc.edu

2.5. Statistical analysis

Statistical analyses were performed using SPSS version 26 (RRID:SCR_002865). Continuous variables are presented as mean (± standard deviation) and categorical variables are presented as numbers (percentage). The normality of the distribution of quantitative variables was assessed visually. Plasma NfL concentrations were log-transformed to satisfy the normality assumption. First, BrainAGE (*z*-score) and brain volumes were compared between controls and SLE patients using a student-*t* test. WMH volumes were compared using a Mann–Whitney *U* test. Then, in order to estimate the risk factors for increased BrainAGE, SLE patients were divided into 2 groups (high vs. low BrainAGE). To define the cut-off value between High and Low BrainAGE, we used the "reaction time" performance. Increased reaction time is one of the main neuropsychological landmarks of brain aging. We performed a ROC-analysis and calculated the Youden Index. The optimal threshold to identify patients with low "reaction time performance" (standardized score < 80) was BrainAGE z-score = 0.9. We therefore used this threshold to separate high and low BrainAGE groups. Group comparisons for biomarkers of neurodegeneration between high and low BrainAGE patients and healthy controls were done using a ANOVA (or Kruskal-Wallis ANOVA). As plasma concentrations of NfL increase with age, group comparisons were adjusted for age using an ANCOVA procedure. We also performed correlation analyses and calculated Pearson correlation coefficient (or Spearman correlation coefficient for non-normally distributed variables) in patients and healthy controls. Finally, to identify the clinical/biological predictors of high BrainAGE, group comparisons between high and low BrainAGE patients were done using a student t-test for continuous variables and a chi-square test for categorical variables. Parameters associated with BrainAGE with a value of $p < 0.2$ in univariate analysis were included in a multivariate logistic regression model with BrainAGE as a binary depend variable (high vs. low). To avoid multicollinearity, correlations between variables were checked and variables with r > 0.6 were excluded (disease duration and ongoing prednisolone treatment). A threshold of $p < 0.05$ was used for all statistical significance.

3. Results

3.1. BrainAGE is significantly increased in SLE patients

As described in material and methods, 70 right-handed female SLE patients and 24 age-matched controls were included in the present study. Table 1 displays the study population details. SLE disease activity (SLEDAI-2K) and organ damage (SLICC/ACR-DI) scores were low. Sixteen (22.9%) to 22 (31.4%) had a neuropsychiatric presentation according to "SLICC A" and "SLICC B" models, respectively. A detailed description of ongoing medications and neuropsychiatric manifestations is provided in Supplementary Tables S1, S2.

Mean chronological age of SLE patients and controls was 35.9 (±9.0) and 37.0 (±9.4) years, respectively ($p = 0.62$). BrainAGE z-score was significantly higher in SLE patients, revealing an increased brain aging (0.6 [±1.1] vs. 0 [±1]) (Figure 1 and Table 2). SLE patients had brains looking on average 3.6 years older than age-matched controls. Standard

10.3389/fnagi.2023.1274061

TABLE 1 Clinical, neuropsychological and biological characteristics of the SLE patients.

Characteristics	SLE ($n = 70$)
Clinical	
Age at MRI (y)	35.9 (±9.0)
Disease duration (y)	11.1 (±8.1)
SLICC/ACR-Damage Index	0.7 (±1.1)
SLEDAI-2 K	2.3 (±3.2)
Neuropsychiatric manifestations SLICC A model, *n* (%) SLICC B model, *n* (%)	16 (22.9%) 22 (31.4%)
Renal involvement, *n* (%)†	26 (37.1%)
Smoking (ever), *n* (%)	25 (35.8%)
Prednisolone (ongoing), *n* (%)	55 (78.6%)
Prednisolone daily dose (mg/day)	4.9 (±4.5)
Non-malarial DMARD (ongoing), *n* (%)	41 (58.6%)
Anti-hypertensive drug (ongoing), *n* (%)	21 (30.0%)
Neuropsychological evaluation	
Composite memory (standardized score)	95.9 (±6.1)
Psychomotor speed (standardized score)	96.3 (±10.9)
Reaction time (standardized score)	90.3 (±17.4)
Complex attention (standardized score)	96.6 (±22.6)
Cognitive flexibility (standardized score)	96.2 (±21.5)
Laboratory analyses	
Log-transformed Plasma NfL (pg/ml)	0.84 (±0.17)
Serum S100A8/A9 (ng/ml)	1.37 (±0.84)
Low complement (ever), *n* (%)	40 (57.1%)
Antiphospholipid antibodies (ever), *n* (%)	22 (31.4%)
Antibodies anti-double stranded DNA (ever), *n* (%)	41 (58.6%)

†According to SLICC SLE classification criteria. ACR, American College of Rheumatology; DMARD, disease-modifying antirheumatic drug; NfL, neurofilament light chain; SLE, systemic lupus erythematosus; SLEDAI-2K, Systemic Lupus Erythematosus Disease Activity Index 2000; SLICC, Systemic Lupus International Collaborating Clinics.

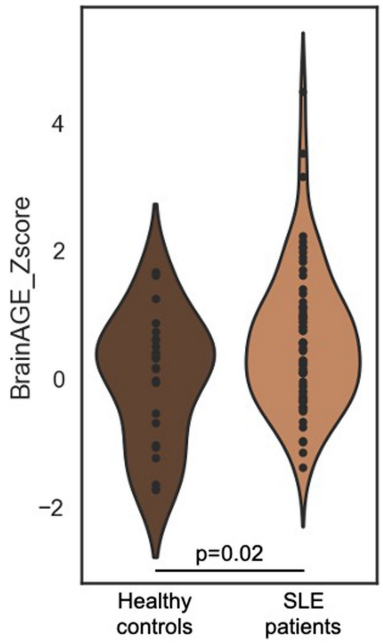

FIGURE 1
BrainAGE distribution in SLE patients and age-matched healthy controls. Violin plot of BrainAGE (*z*-score) distribution in SLE patients and age-matched controls. Mean BrainAGE is significantly higher in SLE (0.6 [±1.1] vs. 0 [±1], $p = 0.02$). BrainAGE, Brain Age Gap Estimation; SLE, systemic lupus erythematosus.

volumetry demonstrated a discrete brain atrophy with slightly increased cerebrospinal fluid volumes in SLE patients (11.96% [±2.50] vs. 10.80% [±2.13], $p = 0.045$) (Table 2). The volume of WMH was modest but significantly higher in SLE patients (0.179 [±0.339] vs. 0.061 [±0.156]). The visual assessment demonstrated no previous ischemic lesion.

Attention maps demonstrated that BrainAGE prediction was mainly based on the following brain areas: right lenticular nucleus, left and right medial prefrontal cortex, left dorso-lateral prefrontal cortex and inferior frontal cortex, posterior part of the body of the corpus callosum, pons, left and right cerebellum hemispheres (Figure 2).

3.2. In SLE patients, high BrainAGE is associated with biomarkers of neurodegeneration and poorer cognitive performance

To validate that BrainAGE was reflecting neurodegeneration in SLE patients, we analyzed the association between high BrainAGE (BrainAGE *z*-score > 0.9) and well-established biomarkers of neuronal damage (Table 3). Compared to low BrainAGE and healthy controls, high BrainAGE patients had brain atrophy with increased CSF volume ($p = 0.001$). White matter volume was also lower in high BrainAGE vs. low BrainAGE patients ($p = 0.02$). High BrainAGE patients had higher plasma NfL concentrations after adjusting for age, compared to low BrainAGE patients and healthy controls ($p < 0.001$) (Table 3). WMH volume was higher in high BrainAGE patients compared to healthy controls ($p = 0.03$), but there was no significant difference between high and low BrainAGE patients.

Then, we explored the neuropsychological correlates of increased BrainAGE.

Neuropsychiatric involvement according to the SLICC attribution models were not more prevalent in high BrainAGE patients ("SLICC A": 6/24 [25%] vs. 10/46 [21.7%], $p = 0.76$ and "SLICC B": 8/24 [33.3%] vs. 14/46 [30.4%], 0.80). Nevertheless, SLE patients with high BrainAGE had poorer performance compared to low BrainAGE (BrainAGE *z*-score ≤ 0.9) and/or healthy controls in several cognitive domains (Table 3 and Figure 3): psychomotor speed ($p = 0.001$), reaction time ($p = 0.02$) and cognitive flexibility ($p = 0.04$). Illustrative cases are presented in Figure 4.

Correlation analyses were consistent with the above-mentioned results (Supplementary Table S3). In SLE patients, higher BrainAGE was significantly correlated with lower grey and white matter volume, higher CSF volume, higher level of NfL in plasma, lower cognitive performance for psychomotor speed and reaction time. No significant correlations were found in healthy controls.

10.3389/fnagi.2023.1274061

TABLE 2 MRI characteristics of SLE patients and comparison with healthy controls.

MRI characteristics	SLE (n = 70)	Healthy controls (n = 24)	Cohen's d	Value of p
BrainAGE (z-score)	0.6 (±1.1)	0 (±1)	0.56	**0.02**
Gray matter volume (% of total intracranial volume)	51.19 (±2.43)	52.31 (±2.64)	−0.45	0.06
White matter volume (% of total intracranial volume)	36.85 (±1.99)	36.89 (±1.45)	−0.02	0.94
CSF volume (% of total intracranial volume)	11.96 (±2.50)	10.80 (±2.13)	0.48	**0.045**
WMH volume (mL)	0.179 (±0.339)	0.061 (±0.156)	0.39	**0.01**

BrainAGE, Brain Age Gap Estimation; SLE, systemic lupus erythematosus; WMH, white matter hyperintensities. Values of p inferior to 0.05 are presented in bold.

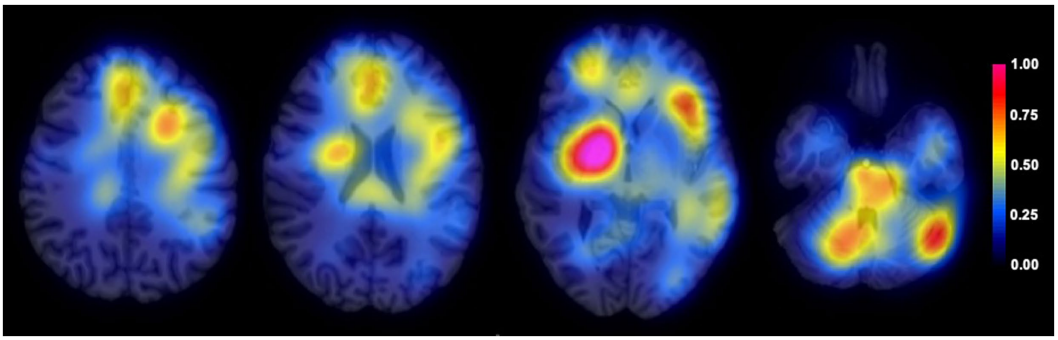

FIGURE 2
Average attention map for BrainAGE prediction. Average attention map (color-coded) for the entire population (n = 94) overlayed on an anatomical T1 image.

TABLE 3 Comparison of biomarkers of neurodegeneration in high BrainAGE, low BrainAGE SLE patients and healthy controls.

Variables	High BrainAGE (n = 24)	Low BrainAGE (n = 46)	Healthy controls (n = 24)	p-Value	Pairwise (adjusted $p < 0.05$)
BrainAGE (Z-score)	1.8 (±0.9)	0 (±0.6)	0 (±1)	**<0.001**	**High BA > Low BA and HC**
MRI volumes					
Gray matter volume (% of total intracranial volume)	50.87 (±3.32)	51.35 (±1.84)	52.31 (±2.64)	0.13	NA
White matter volume (% of total intracranial volume)	35.99 (±2.26)	37.31 (±1.70)	36.89 (±1.45)	**0.02**	**Low BA > High BA**
CSF volume (% of total intracranial volume)	13.14 (±2.92)	11.34 (±2.02)	10.80 (±2.13)	**0.001**	**High BA > Low BA and HC**
WMH volume (mL)	0.190 (±0.327)	0.173 (±0.348)	0.061 (±0.156)	**0.03**	**High BA > HC**
Laboratory markers					
Age-adjusted log-transformed plasma NfL	0.89 (±0.03)	0.81 (±0.02)	0.70 (±0.03)	**<0.001**	**High BA > Low BA > HC**
Cognitive performance					
Composite memory (standardized score)	95.3 (±15.1)	96.2 (±16.8)	100.6 (±12.0)	0.42	NA
Psychomotor speed (standardized score)	91.6 (±9.6)	98.8 (±10.8)	103.5 (±12.4)	**0.001**	**Low BA and HC > High BA**
Reaction time (standardized score)	82.2 (±19.9)	94.6 (±14.3)	93.1 (±21.2)	**0.02**	**HC > High BA**
Complex attention (standardized score)	93.8 (±28.0)	98.1 (±19.3)	105.2 (±8.1)	0.14	NA
Cognitive flexibility (standardized score)	89.0 (±23.9)	100.0 (±19.3)	102.2 (±13.0)	**0.04**	**HC > High BA**

High BrainAGE refers to BrainAGE z-score > 0.9. Low BrainAGE refers to BrainAGE z-score ≤ 0.9. BA, BrainAGE; BrainAGE, Brain Age Gap Estimation; HC, healthy controls; NfL, neurofilament light chain; SLE, systemic lupus erythematosus. Values of p inferior to 0.05 are presented in bold.

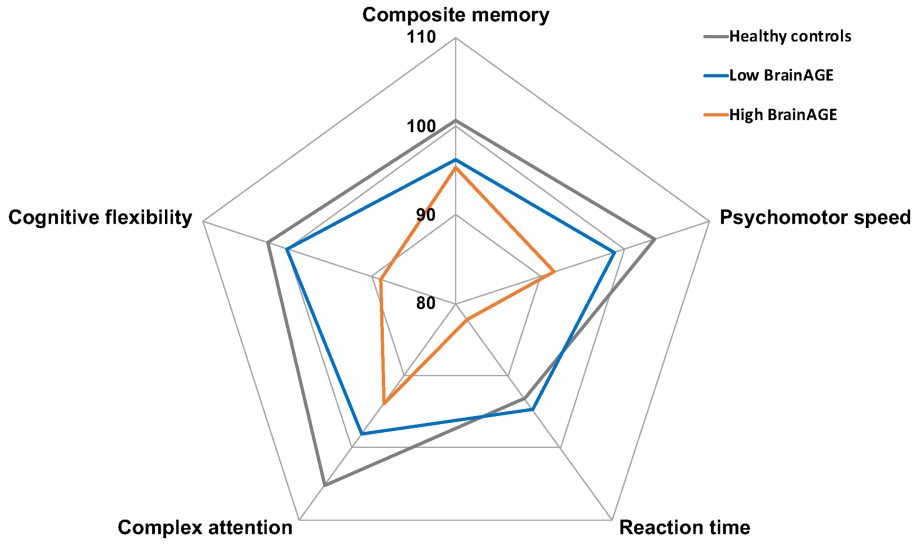

FIGURE 3
Neuropsychological profile of SLE patients according to BrainAGE. Graphical representation of mean standardized scores in five cognitive domains for healthy controls (gray), high BrainAGE (orange), and low BrainAGE patients (blue). BrainAGE, Brain Age Gap Estimation; SLE, systemic lupus erythematosus.

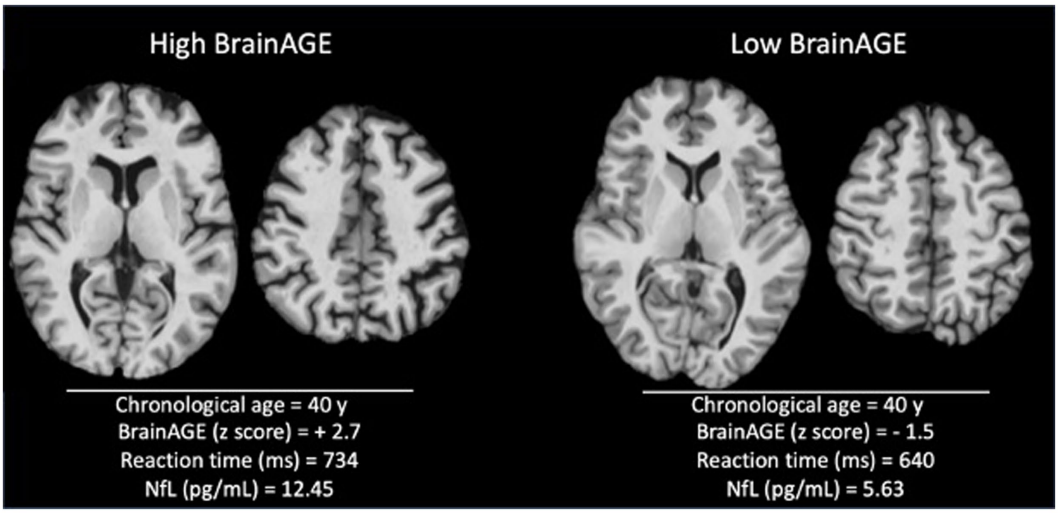

FIGURE 4
Illustrative cases with high versus low BrainAGE. Skull-striped 3D-T1 images from 40-year patients with high (left) and low BrainAGE (right). Visual inspection demonstrates a higher level of atrophy in the high BrainAGE patient, with enlarged ventricles and sulci. The patient with high BrainAGE has also longer reaction time and higher level of neurofilament light chain (NfL) in plasma.

3.3. Clinical and biological risk factors of high BrainAGE in SLE patients

Finally, we evaluated the association between BrainAGE and the clinical and biological characteristics of disease, to identify the main determinants of increased brain aging (Table 4). In univariate analysis, BrainAGE was associated with some indirect markers of active systemic inflammation. Patients with high BrainAGE were significantly younger at MRI (30.5 [±9.1] vs. 38.8 [±7.5] years, $p < 0.001$), had shorter disease duration (8.4 [±6.8] vs. 12.6 [±8.4] years, $p = 0.04$) and were more likely to have a non-malarial disease-modifying antirheumatic drug (DMARD) (19/24 [79.2%] vs. 22/46 [47.8%], $p < 0.001$). High BrainAGE tended to be associated with higher disease activity (SLEDAI-2K score = 3.1 [±4.2] vs. 1.9 [±2.5], $p = 0.15$), higher prednisolone daily dose (6.1 [±5.6] vs. 4.3 [±3.8], $p = 0.11$) and low complement levels (17/24 [70.8%] vs. 23/46 [50%], $p = 0.11$). We did not find any association between BrainAGE and the presence of anti-phospholipids antibody. In multivariate analysis (Table 5), age at MRI and non-malarial DMARD remained independently associated with BrainAGE ($p = 0.001$ and $p = 0.01$, respectively).

TABLE 4 Clinical/biological characteristics of SLE patients according to BrainAGE group: univariate analysis.

Variables	High BrainAGE ($n = 24$)	Low BrainAGE ($n = 46$)	*P*-value
Clinical			
Age at MRI (y)	30.5 (±9.1)	38.8 (±7.5)	**<0.001**
Disease duration (y)	8.4 (±6.8)	12.6 (±8.4)	**0.04**
SLICC/ACR-Damage Index	0.6 (±1.0)	0.7 (±1.1)	0.77
SLEDAI-2 K	3.1 (±4.2)	1.9 (±2.5)	0.13
Renal involvement, *n* (%)†	11 (45.8%)	15 (32.6%)	0.31
Smoking (ever), *n* (%)	9 (37.5%)	16 (34.8%)	0.64
Prednisolone (ongoing), *n* (%)	21 (87.5%)	34 (73.9%)	0.19
Prednisolone daily dose (ongoing) (mg/day)	6.1 (±5.6)	4.3 (±3.8)	0.11
Non-malarial DMARD (ongoing), *n* (%)	19 (79.2%)	22 (47.8%)	**0.01**
Anti-hypertensive drug (ongoing), *n* (%)	8 (33.3%)	12 (26.1%)	0.56
Laboratory tests			
Serum S100A8/A9 (ng/mL)	1.35 (±0.86)	1.38 (±0.84)	0.88
Low complement (ever), *n* (%)	17 (70.8%)	23 (50%)	0.11
Antibodies anti-double stranded DNA (ever), *n* (%)	15 (62.5%)	26 (56.5%)	0.63
Antiphospholipids antibodies (ever), *n* (%)	6 (25%)	16 (34.8%)	0.37

†According to SLICC SLE classification criteria. Values of $p < 0.05$ are presented in bold. High BrainAGE refers to BrainAGE *z*-score > 0.9. Low BrainAGE refers to BrainAGE *z*-score ≤ 0.9. ACR, American College of Rheumatology; BrainAGE, Brain Age Gap Estimation; DMARD, disease-modifying antirheumatic drug; SLE, systemic lupus erythematosus; SLEDAI-2K, Systemic Lupus Erythematosus Disease Activity Index 2000; SLICC, Systemic Lupus International Collaborating Clinics.

TABLE 5 Association between BrainAGE and clinical/biological characteristics of SLE patients: multivariate analysis.

Variables	*B* coefficient	OR	95%CI	*P*-value
Age at MRI	−0.14	0.87	0.80–0.94	**0.001**
SLEDAI-2 K	0	0.99	0.79–1.26	0.99
Prednisolone daily dose (ongoing)	0.07	1.07	0.91–1.27	0.41
Non-malarial DMARD (ongoing)	1.80	6.03	1.44–25.3	**0.01**
Low complement (ever)	0.43	1.54	0.37–6.34	0.55

Logistic regression model including all variables associated with BrainAGE in univariate analysis with a *p*-value < 0.2. Disease duration and prednisolone ongoing were not included due to multicollinearity. Values of $p < 0.05$ are presented in bold. BrainAGE, Brain Age Gap Estimation; DMARD, disease-modifying antirheumatic drug; SLE, systemic lupus erythematosus; SLEDAI-2K, Systemic Lupus Erythematosus Disease Activity Index 2000.

4. Discussion

In this retrospective cross-sectional analysis, we provided evidence of increased brain aging in SLE by applying a deep-learning model to brain MR images. We demonstrated that high BrainAGE was associated with established markers of neurodegeneration and with worse performance in several cognitive domains. Interestingly, higher BrainAGE scores were observed in younger patients and patients with ongoing non-malarial DMARD, suggesting a more active SLE phenotype.

One of the main strengths of our study lies in the use of a deep-learning model to compute a fully automated and time-efficient measurement of brain aging. This approach enables an individualized and non-invasive assessment, which could be implemented into clinical practice. Unlike conventional machine learning models based on brain parcellation and quantification of regional grey matter and white matter volumes, the use of a 3D CNN architecture allowed us to work directly on MR images registered in the MNI space, without introducing any prior assumptions. Processing steps were deliberately limited minimized, using a rigid co-registration method to preserve anatomical details. Notably, our model's performance to predict the age of healthy controls on the validation sample was in the range of other established models (Franke and Gaser, 2019). This approach has previously demonstrated efficacy in tracking the progression of neurodegeneration in Alzheimer's disease (Gautherot et al., 2021). Using attention maps, we demonstrated that BrainAGE prediction was based on widespread brain regions where age-related changes have been extensively documented, including the frontal lobe, lenticular nucleus, corpus callosum and cerebellum (Lemaitre et al., 2012; Tullo et al., 2019).

In this study, the utilization of a deep-learning model allowed us to capture brain changes indicative of neurodegeneration in SLE, even within the context of an average low disease activity and subtle differences in brain volumetry between patients and controls. We found that increased brain aging in SLE patients predominantly correlated with a reduction in white matter volume. This observation is consistent with standard MRI analyses showing white matter lesions in 60% of SLE patients with neuropsychiatric symptoms (Jennings et al., 2004). Beyond these clearly apparent lesions, advanced diffusion

MRI techniques (such as diffusion tensor imaging) have unveiled widespread alterations even in normal-appearing white matter regions (Kornaropoulos et al., 2022). NfL is another well-established biomarker of axonal damage (Khalil et al., 2018). Lauvsnes et al. (2022) reported a correlation between a loss of cerebral white matter (in the corpus callosum) and plasma NfL concentrations in SLE patients. Similarly, we found a correlation between brain aging and plasma NfL levels.

In our population, increased brain aging in SLE patients resulted in poorer cognitive performance. While SLE patients displaying low BrainAGE had cognitive test scores within the normal range, those with high BrainAGE performed significantly worse in several cognitive domains, reaction time and psychomotor speed being mostly affected. Processing speed is one of the main cognitive domains affected by normal ageing, which has been attributed to a decreased efficiency of interregional communication within the brain (Salthouse, 2016). Indeed, age-related cognitive slowing has been consistently associated with white matter volume reduction, white matter hyperintensities or altered white matter integrity assessed through DTI (Bendlin et al., 2010; Kochunov et al., 2010). Although complex attention was impaired in our SLE patients, in line with a recent meta-analysis (Leslie and Crowe, 2018), the association between complex attention and increased brain aging did not reach statistical significance in our study. Interestingly, neuropsychiatric involvement was not more prevalent in high BrainAGE patients. As already suggested, neuropsychiatric manifestations in SLE may hinge on functional alterations rather than structural modifications (Faust et al., 2010; Steup-Beekman et al., 2013).

Finally, we aimed at identifying the main risk factors of increased brain aging. We found that the clinical phenotype of SLE patients with high BrainAGE was a young subject, with short disease duration, high disease activity and low complement level, treated by non-malarial DMARD and high dose of prednisolone. Drawing from these exploratory results, we can speculate that increased brain age was mainly driven by persistent inflammatory activity under medication. Typically, disease activity in SLE tends to peak early in the disease course and subsequently decline over time (Zhang et al., 2010). Peschken et al. (2019) demonstrated that very high disease activity was associated with shorter disease duration, higher prednisolone dosage and use of DMARD. This initial active phase could be responsible for brain modifications, leading to a disproportionally high BrainAGE in younger patients. A link between chronic peripheral inflammation and modifications of brain structure has been established through murine models of SLE (Chesnokova et al., 2016; Schwartz et al., 2019). The suggested pathway is that ongoing systemic inflammation affects the communication between the peripheral immune system and the brain by activating resident microglial cells. Subsequent abnormal development of neuroprogenitor cells in the corpus callosum and increase neuronal death in the cortex and hippocampus have been observed (Leung et al., 2016; Shi et al., 2018). Direct immunologically mediated neuronal affliction is also involved in neuropsychiatric manifestations of SLE. Anti-NMDA receptor and anti-ribosomal P protein antibodies are considered to target especially the limbic system and are associated with diffuse neuropsychiatric presentations of SLE, while antiphospholipid antibodies are responsible for autoantibody mediated thrombosis and neurovascular manifestations (Schwartz et al., 2019). Of note, the brain changes could be partially reversible under treatment, as illustrated by Mak et al. (2016). Their longitudinal MRI study documented increased brain volume in SLE patients receiving immunosuppressive treatment to mitigate disease activity. We can therefore speculate that BrainAGE scores would decrease over time under a treatment that effectively controls disease activity.

Conversely, we did not find any association between increased brain age and antiphospholipid antibodies or WMH volume. A higher risk of ischemic and hemorrhagic stroke is attributed to SLE with a twofold increase compared to the general population (Wiseman et al., 2016b). Interestingly, ischemic brain changes in SLE patients have been associated with antiphospholipid antibodies (Kaichi et al., 2014; Magro-Checa et al., 2019), independently of SLE activity (Wiseman et al., 2016a). Although BrainAGE is sensitive to vascular lesions (Bretzner et al., 2023), these did not emerge as the main determinants of increased brain aging in our SLE population. The relatively low WMH burden in our population may account for this apparent discrepancy.

The main limitation of our study was its relatively small sample size, which currently curtails the applicability of BrainAGE on an individualized basis and precludes a comprehensive analysis of the intricate interplay between distinct neuropsychiatric manifestations and brain aging. We also acknowledge that the association with disease activity scores was close but did not reach statistical significance. This could be explained by the overall low disease activity observed in our cohort and it warrants validation across populations with a more severe phenotype. Future longitudinal studies will also provide additional insight into the association between age, disease duration and brain aging, as well as the role of glucocorticoids and immunosuppressive treatment.

In conclusion, using a deep-learning BrainAGE model, we provide evidence of increased brain aging in SLE patients, which reflected neuronal damage and cognitive impairment. BrainAGE could be evaluated as an adjunctive diagnostic tool for assessing brain involvement in SLE.

Data availability statement

The datasets presented in this article are not readily available because the data presented in this study are available from the corresponding author upon reasonable request and approval of the Institutional Review Board. Requests to access the datasets should be directed to pia.sundgren@med.lu.se.

Ethics statement

The studies involving humans were approved by regional ethics committee in Lund (reference #2012/254, #2012/677, #2014/778). The studies were conducted in accordance with the local legislation and institutional requirements. The participants provided their written informed consent to participate in this study.

Author contributions

GK: Conceptualization, Formal analysis, Funding acquisition, Methodology, Visualization, Writing – original draft. TR: Data curation, Investigation, Writing – review & editing. KZ: Data curation, Investigation, Writing – review & editing. RL: Formal analysis,

Methodology, Software, Writing – review & editing. MG: Methodology, Software, Writing – review & editing. J-PP: Resources, Supervision, Writing – review & editing. AB: Resources, Supervision, Writing – review & editing. OH: Funding acquisition, Resources, Writing – review & editing. AJ: Funding acquisition, Resources, Supervision, Writing – review & editing. PS: Conceptualization, Funding acquisition, Methodology, Project administration, Supervision, Writing – review & editing.

Funding

The author(s) declare financial support was received for the research, authorship, and/or publication of this article. This study has received funding by the French Society of Neuroradiology (SFNR), GK; the French Society of Radiology (SFR), GK; Collège des Enseignants en Radiologie de France (CERF), GK; Lille University, GK; Lille University Hospital, GK; Anna-Greta Crafoord Foundation, AJ; Greta and Johan Kock Foundation, AJ; Lund University, AJ; Stiftelsen Konung Gustaf V:80-årsfond, PS; Alfred Österlund Foundation, PS; Swedish Rheumatic Association, PS; Swedish Research Council (2016–00906), OH; the Knut and Alice Wallenberg foundation (2017–0383), OH; the Marianne and Marcus Wallenberg foundation (2015.0125), OH; the Strategic Research Area MultiPark (Multidisciplinary Research in Parkinson's disease) at Lund University, OH; the Swedish Alzheimer Foundation (AF-939932), OH; the Swedish Brain Foundation (FO2021-0293), OH; The Parkinson foundation of Sweden (1280/20), OH; the Cure Alzheimer's fund, OH; the Konung Gustaf V:s och Drottning Victorias Frimurarestiftelse, OH; the Skåne University Hospital Foundation (2020-O000028), OH; Regionalt Forskningsstöd (2020–0314), OH; and the Swedish federal government under the ALF agreement (2018-Projekt0279), OH. The funders had no role in the design of the study; in the collection, analyses, or interpretation of data; in the writing of the manuscript; or in the decision to publish the results.

Acknowledgments

The content of this manuscript has been presented in part at the European Society of Neuroradiology (ESNR), 45th annual meeting, Lisbon 2022 (Kuchcinski et al., 2022). The authors thank all participants of the study for their participation, and the "Lille Invivo Imaging and Functional Exploration - LIIFE" core facility (CI2C – http://www.ci2c.fr) for providing the conceptual framework for MRI analysis.

Conflict of interest

OH has acquired research support (for the institution) from ADx, AVID Radiopharmaceuticals, Biogen, Eli Lilly, Eisai, Fujirebio, GE Healthcare, Pfizer, and Roche. In the past 2 years, OH has received consultancy/speaker fees from AC Immune, Amylyx, Alzpath, BioArctic, Biogen, Cerveau, Fujirebio, Genentech, Novartis, Roche, and Siemens.

The remaining authors declare that the research was conducted in the absence of any commercial or financial relationships that could be construed as a potential conflict of interest.

Publisher's note

Supplementary material

The Supplementary material for this article can be found online at: https://www.frontiersin.org/articles/10.3389/fnagi.2023.1274061/full#supplementary-material

References

Appenzeller, S., Bonilha, L., Rio, P. A., Min Li, L., Costallat, L. T. L., and Cendes, F. (2007). Longitudinal analysis of gray and white matter loss in patients with systemic lupus erythematosus. *NeuroImage* 34, 694–701. doi: 10.1016/j.neuroimage.2006.09.029

Bendlin, B. B., Fitzgerald, M. E., Ries, M. L., Xu, G., Kastman, E. K., Thiel, B. W., et al. (2010). White matter in aging and cognition: a cross-sectional study of microstructure in adults aged eighteen to eighty-three. *Dev. Neuropsychol.* 35, 257–277. doi: 10.1080/87565641003696775

Bretzner, M., Bonkhoff, A. K., Schirmer, M. D., Hong, S., Dalca, A., Donahue, K., et al. (2023). Radiomics-derived brain age predicts functional outcome after acute ischemic stroke. *Neurology* 100, e822–e833. doi: 10.1212/WNL.0000000000201596

Brey, R. L., Holliday, S. L., Saklad, A. R., Navarrete, M. G., Hermosillo–Romo, D., Stallworth, C. L., et al. (2002). Neuropsychiatric syndromes in lupus: prevalence using standardized definitions. *Neurology* 58, 1214–1220. doi: 10.1212/wnl.58.8.1214

Cannerfelt, B., Nystedt, J., Jönsen, A., Lätt, J., van Westen, D., Lilja, A., et al. (2018). White matter lesions and brain atrophy in systemic lupus erythematosus patients: correlation to cognitive dysfunction in a cohort of systemic lupus erythematosus patients using different definition models for neuropsychiatric systemic lupus erythematosus. *Lupus* 27, 1140–1149. doi: 10.1177/0961203318763533

Chesnokova, V., Pechnick, R. N., and Wawrowsky, K. (2016). Chronic peripheral inflammation, hippocampal neurogenesis, and behavior. *Brain Behav. Immun.* 58, 1–8. doi: 10.1016/j.bbi.2016.01.017

Cohen, D., Rijnink, E. C., Nabuurs, R. J. A., Steup-Beekman, G. M., Versluis, M. J., Emmer, B. J., et al. (2017). Brain histopathology in patients with systemic lupus erythematosus: identification of lesions associated with clinical neuropsychiatric lupus syndromes and the role of complement. *Rheumatology (Oxford)* 56, 77–86. doi: 10.1093/rheumatology/kew341

Ercan, E., Magro-Checa, C., Valabregue, R., Branzoli, F., Wood, E. T., Steup-Beekman, G. M., et al. (2016). Glial and axonal changes in systemic lupus erythematosus measured with diffusion of intracellular metabolites. *Brain* 139, 1447–1457. doi: 10.1093/brain/aww031

Faust, T. W., Chang, E. H., Kowal, C., Berlin, R., Gazaryan, I. G., Bertini, E., et al. (2010). Neurotoxic lupus autoantibodies alter brain function through two distinct mechanisms. *Proc. Natl. Acad. Sci. U. S. A.* 107, 18569–18574. doi: 10.1073/pnas.1006980107

Franke, K., and Gaser, C. (2019). Ten years of BrainAGE as a neuroimaging biomarker of brain aging: what insights have we gained? *Front. Neurol.* 10:789. doi: 10.3389/fneur.2019.00789

Gautherot, M., Kuchcinski, G., Bordier, C., Sillaire, A. R., Delbeuck, X., Leroy, M., et al. (2021). Longitudinal analysis of brain-predicted age in amnestic and non-amnestic sporadic early-onset Alzheimer's disease. *Front. Aging Neurosci.* 13:729635. doi: 10.3389/fnagi.2021.729635

Gladman, D., Ginzler, E., Goldsmith, C., Fortin, P., Liang, M., Sanchez-Guerrero, J., et al. (1996). The development and initial validation of the systemic lupus international collaborating clinics/American College of Rheumatology damage index for systemic lupus erythematosus. *Arthritis Rheum.* 39, 363–369. doi: 10.1002/art.1780390303

Gladman, D. D., Ibañez, D., and Urowitz, M. B. (2002). Systemic lupus erythematosus disease activity index 2000. *J. Rheumatol.* 29, 288–291.

Gualtieri, C. T., and Johnson, L. G. (2006). Reliability and validity of a computerized neurocognitive test battery, CNS vital signs. *Arch. Clin. Neuropsychol.* 21, 623–643. doi: 10.1016/j.acn.2006.05.007

Hanly, J. G., Urowitz, M. B., Sanchez-Guerrero, J., Bae, S. C., Gordon, C., Wallace, D. J., et al. (2007). Neuropsychiatric events at the time of diagnosis of systemic lupus erythematosus: an international inception cohort study. *Arthritis Rheum.* 56, 265–273. doi: 10.1002/art.22305

Hanly, J. G., Walsh, N. M., and Sangalang, V. (1992). Brain pathology in systemic lupus erythematosus. *J. Rheumatol.* 19, 732–741.

Jennings, J. E., Sundgren, P. C., Attwood, J., McCune, J., and Maly, P. (2004). Value of MRI of the brain in patients with systemic lupus erythematosus and neurologic disturbance. *Neuroradiology* 46, 15–21. doi: 10.1007/s00234-003-1049-2

Kaichi, Y., Kakeda, S., Moriya, J., Ohnari, N., Saito, K., Tanaka, Y., et al. (2014). Brain MR findings in patients with systemic lupus erythematosus with and without antiphospholipid antibody syndrome. *AJNR Am. J. Neuroradiol.* 35, 100–105. doi: 10.3174/ajnr.A3645

Kalinowska-Lyszczarz, A., Pawlak, M. A., Pietrzak, A., Pawlak-Bus, K., Leszczynski, P., Puszczewicz, M., et al. (2018). Distinct regional brain atrophy pattern in multiple sclerosis and neuropsychiatric systemic lupus erythematosus patients. *Lupus* 27, 1624–1635. doi: 10.1177/0961203318781004

Khalil, M., Teunissen, C. E., Otto, M., Piehl, F., Sormani, M. P., Gattringer, T., et al. (2018). Neurofilaments as biomarkers in neurological disorders. *Nat. Rev. Neurol.* 14, 577–589. doi: 10.1038/s41582-018-0058-z

Kochunov, P., Coyle, T., Lancaster, J., Robin, D. A., Hardies, J., Kochunov, V., et al. (2010). Processing speed is correlated with cerebral health markers in the frontal lobes as quantified by neuroimaging. *NeuroImage* 49, 1190–1199. doi: 10.1016/j.neuroimage.2009.09.052

Kornaropoulos, E. N., Winzeck, S., Rumetshofer, T., Wikstrom, A., Knutsson, L., Correia, M. M., et al. (2022). Sensitivity of diffusion MRI to white matter pathology: influence of diffusion protocol, magnetic field strength, and processing pipeline in systemic lupus erythematosus. *Front. Neurol.* 13:837385. doi: 10.3389/fneur.2022.837385

Kuchcinski, G., Rumetshofer, T., Zervides, K. A., Lopes, R., Gautherot, M., Pruvo, J.-P., et al. (2022). Deep-learning BrainAGE demonstrates accelerated brain aging in Systemic Lupus Erythematosus patients. *Neuroradiology* 64, S1–S165. doi: 10.1007/s00234-022-03012-w

Langensee, L., Mårtensson, J., Jönsen, A., Zervides, K., Bengtsson, A., Nystedt, J., et al. (2022). Cognitive performance in systemic lupus erythematosus patients: a cross-sectional and longitudinal study. *BMC Rheumatol* 6:22. doi: 10.1186/s41927-022-00253-3

Lauvsnes, M. B., Zetterberg, H., Blennow, K., Kvaløy, J. T., Tjensvoll, A. B., Maroni, S., et al. (2022). Neurofilament light in plasma is a potential biomarker of central nervous system involvement in systemic lupus erythematosus. *J. Neurol.* 269, 3064–3074. doi: 10.1007/s00415-021-10893-z

Lemaitre, H., Goldman, A., Sambataro, F., Verchinski, B., Meyer-Lindenberg, A., Weinberger, D., et al. (2012). Normal age-related brain morphometric changes: nonuniformity across cortical thickness, surface area and grey matter volume? *Neurobiol. Aging* 33, 617.e1–617.e9. doi: 10.1016/j.neurobiolaging.2010.07.013

Leslie, B., and Crowe, S. F. (2018). Cognitive functioning in systemic lupus erythematosus: a meta-analysis. *Lupus* 27, 920–929. doi: 10.1177/0961203317751859

Leung, J. W.-H., Lau, B. W.-M., Chan, V. S.-F., Lau, C.-S., and So, K.-F. (2016). Abnormal increase of neuronal precursor cells and exacerbated neuroinflammation in the corpus callosum in murine model of systemic lupus erythematosus. *Restor. Neurol. Neurosci.* 34, 443–453. doi: 10.3233/RNN-160638

Liang, H., Zhang, F., and Niu, X. (2019). Investigating systematic bias in brain age estimation with application to post-traumatic stress disorders. *Hum. Brain Mapp.* 40, 3143–3152. doi: 10.1002/hbm.24588

Littleton, A. C., Register-Mihalik, J. K., and Guskiewicz, K. M. (2015). Test-retest reliability of a computerized concussion test: CNS vital signs. *Sports Health* 7, 443–447. doi: 10.1177/1941738115586997

Magro-Checa, C., Kumar, S., Ramiro, S., Beaart-van de Voorde, L. J., Eikenboom, J., Ronen, I., et al. (2019). Are serum autoantibodies associated with brain changes in systemic lupus erythematosus? MRI data from the Leiden NP-SLE cohort. *Lupus* 28, 94–103. doi: 10.1177/0961203318816819

Magro-Checa, C., Zirkzee, E. J., Huizinga, T. W., and Steup-Beekman, G. M. (2016). Management of Neuropsychiatric Systemic Lupus Erythematosus: current approaches and future perspectives. *Drugs* 76, 459–483. doi: 10.1007/s40265-015-0534-3

Mak, A., Ho, R. C.-M., Tng, H.-Y., Koh, H. L., Chong, J. S. X., and Zhou, J. (2016). Early cerebral volume reductions and their associations with reduced lupus disease activity in patients with newly-diagnosed systemic lupus erythematosus. *Sci. Rep.* 6:22231. doi: 10.1038/srep22231

Manjón, J. V., and Coupé, P. (2016). volBrain: an online MRI brain Volumetry system. *Front. Neuroinform.* 10:30. doi: 10.3389/fninf.2016.00030

Peschken, C. A., Wang, Y., Abrahamowicz, M., Pope, J., Silverman, E., Sayani, A., et al. (2019). Persistent disease activity remains a burden for patients with systemic lupus erythematosus. *J. Rheumatol.* 46, 166–175. doi: 10.3899/jrheum.171454

Petsiuk, V., Das, A., and Saenko, K. (2018). RISE: Randomized input sampling for explanation of black-box models. Available at: http://arxiv.org/abs/1806.07421 (Accessed October 2, 2023).

Saito, Y., Miyajima, M., Yamamoto, S., Sato, T., Miura, N., Fujimiya, M., et al. (2021). Accumulation of senescent neural cells in murine lupus with depression-like behavior. *Front. Immunol.* 12:692321. doi: 10.3389/fimmu.2021.692321

Salthouse, T. A. (2016). "Neural correlates of age-related slowing" in *Cognitive neuroscience of aging: Linking cognitive and cerebral aging*. eds. R. Cabeza, L. Nyberg and D. C. Park. *2nd* ed (New York: Oxford Academic)

Schmidt, P., Gaser, C., Arsic, M., Buck, D., Förschler, A., Berthele, A., et al. (2012). An automated tool for detection of FLAIR-hyperintense white-matter lesions in multiple sclerosis. *NeuroImage* 59, 3774–3783. doi: 10.1016/j.neuroimage.2011.11.032

Schwartz, N., Stock, A. D., and Putterman, C. (2019). Neuropsychiatric lupus: new mechanistic insights and future treatment directions. *Nat. Rev. Rheumatol.* 15, 137–152. doi: 10.1038/s41584-018-0156-8

Shi, D., Tian, T., Yao, S., Cao, K., Zhu, X., Zhang, M., et al. (2018). FTY720 attenuates behavioral deficits in a murine model of systemic lupus erythematosus. *Brain Behav. Immun.* 70, 293–304. doi: 10.1016/j.bbi.2018.03.009

Shorten, C., and Khoshgoftaar, T. M. (2019). A survey on image data augmentation for deep learning. *J. Big Data* 6:60. doi: 10.1186/s40537-019-0197-0

Steup-Beekman, G. M., Zirkzee, E. J. M., Cohen, D., Gahrmann, B. M. A., Emmer, B. J., Steens, S. C. A., et al. (2013). Neuropsychiatric manifestations in patients with systemic lupus erythematosus: epidemiology and radiology pointing to an immune-mediated cause. *Ann. Rheum. Dis.* 72, 76–79. doi: 10.1136/annrheumdis-2012-202369

Sutskever, I., Martens, J., Dahl, G., and Hinton, G. (2013). On the importance of initialization and momentum in deep learning. In Proceedings of the 30th international conference on machine learning (PMLR), 1139–1147

Tan, E. M., Cohen, A. S., Fries, J. F., Masi, A. T., Mcshane, D. J., Rothfield, N. F., et al. (1982). The 1982 revised criteria for the classification of systemic lupus erythematosus. *Arthritis Rheum.* 25, 1271–1277. doi: 10.1002/art.1780251101

Trysberg, E., Höglund, K., Svenungsson, E., Blennow, K., and Tarkowski, A. (2004). Decreased levels of soluble amyloid beta-protein precursor and beta-amyloid protein in cerebrospinal fluid of patients with systemic lupus erythematosus. *Arthritis Res. Ther.* 6, R129–R136. doi: 10.1186/ar1040

Trysberg, E., Nylen, K., Rosengren, L. E., and Tarkowski, A. (2003). Neuronal and astrocytic damage in systemic lupus erythematosus patients with central nervous system involvement. *Arthritis Rheum.* 48, 2881–2887. doi: 10.1002/art.11279

Tullo, S., Patel, R., Devenyi, G. A., Salaciak, A., Bedford, S. A., Farzin, S., et al. (2019). MR-based age-related effects on the striatum, globus pallidus, and thalamus in healthy individuals across the adult lifespan. *Hum. Brain Mapp.* 40, 5269–5288. doi: 10.1002/hbm.24771

Wiseman, S. J., Bastin, M. E., Jardine, C. L., Barclay, G., Hamilton, I. F., Sandeman, E., et al. (2016a). Cerebral small vessel disease burden is increased in systemic lupus erythematosus. *Stroke* 47, 2722–2728. doi: 10.1161/STROKEAHA.116.014330

Wiseman, S. J., Ralston, S. H., and Wardlaw, J. M. (2016b). Cerebrovascular disease in rheumatic diseases: a systematic review and Meta-analysis. *Stroke* 47, 943–950. doi: 10.1161/STROKEAHA.115.012052

Zervides, K. A., Janelidze, S., Nystedt, J., Gullstrand, B., Nilsson, P., Sundgren, P. C., et al. (2022a). Plasma and cerebrospinal fluid neurofilament light concentrations reflect neuronal damage in systemic lupus erythematosus. *BMC Neurol.* 22:467. doi: 10.1186/s12883-022-02998-3

Zervides, K. A., Jern, A., Nystedt, J., Gullstrand, B., Nilsson, P. C., Sundgren, P. C., et al. (2022b). Serum S100A8/A9 concentrations are associated with neuropsychiatric involvement in systemic lupus erythematosus: a cross-sectional study. *BMC Rheumatol* 6:38. doi: 10.1186/s41927-022-00268-w

Zhang, J., González, L. A., Roseman, J. M., Vilá, L. M., Reveille, J. D., and Alárcon, G. S. (2010). Predictors of the rate of change in disease activity over time in LUMINA, a multiethnic US cohort of patients with systemic lupus erythematosus: LUMINA LXX. *Lupus* 19, 727–733. doi: 10.1177/0961203309359289

frontiers | Frontiers in Aging Neuroscience

TYPE Original Research
PUBLISHED 12 January 2024
DOI 10.3389/fnagi.2023.1327756

OPEN ACCESS

EDITED BY
Caroline Haikal,
NewYork-Presbyterian, United States

REVIEWED BY
Deqiang Han,
Capital Medical University, China
Harald Neumann,
University of Bonn, Germany
Robert Adam Harris,
Karolinska Institutet (KI), Sweden

*CORRESPONDENCE
Guy C. Brown
✉ gcb3@cam.ac.uk

RECEIVED 25 October 2023
ACCEPTED 18 December 2023
PUBLISHED 12 January 2024

CITATION
Kitchener EJA, Dundee JM and Brown GC (2024) Activated microglia release β-galactosidase that promotes inflammatory neurodegeneration.
Front. Aging Neurosci. 15:1327756.
doi: 10.3389/fnagi.2023.1327756

Activated microglia release β-galactosidase that promotes inflammatory neurodegeneration

Emily J. A. Kitchener, Jacob M. Dundee and Guy C. Brown*

Department of Biochemistry, University of Cambridge, Cambridge, United Kingdom

Beta (β)-galactosidase is a lysosomal enzyme that removes terminal galactose residues from glycolipids and glycoproteins. It is upregulated in, and used as a marker for, senescent cells. Microglia are brain macrophages implicated in neurodegeneration, and can upregulate β-galactosidase when senescent. We find that inflammatory activation of microglia induced by lipopolysaccharide results in translocation of β-galactosidase to the cell surface and release into the medium. Similarly, microglia in aged mouse brains appear to have more β-galactosidase on their surface. Addition of β-galactosidase to neuronal-glial cultures causes microglial activation and neuronal loss mediated by microglia. Inhibition of β-galactosidase in neuronal-glial cultures reduces inflammation and neuronal loss induced by lipopolysaccharide. Thus, activated microglia release β-galactosidase that promotes microglial-mediated neurodegeneration which is prevented by inhibition of β-galactosidase.

KEYWORDS

microglia, β-galactosidase, neurodegeneration, senescence, neuroinflammation

Introduction

The mammalian enzyme β-galactosidase hydrolyses terminal galactose residues from glycolipids and glycoproteins. In humans, β-galactosidase deficiency causes neurodegeneration and death during development due to accumulation of the glycolipid/ganglioside GM1, which is normally metabolized by β-galactosidase to the ganglioside GM2 (Bonten et al., 2014). Almost all cellular β-galactosidase is located within the lysosomes, where it forms a complex with neuraminidase-1 (Neu1) and Protective Protein/Cathepsin A (PPCA), which protects β-galactosidase from degradation within the lysosomes (Bonten et al., 2014). Neu1 hydrolyses terminal sialic residues from glycolipids and glycoproteins, to reveal terminal galactose residues, which are then hydrolyzed by β-galactosidase (Puigdellívol et al., 2020).

Senescent cells are known to have an increased β-galactosidase activity; the β-galactosidase activity of cells measured at pH 6.0 (known as "senescence-associated beta-galactosidase activity") is commonly used as a marker of senescent cells, often detected by histochemical X-gal staining (Dimri et al., 1995). This was originally thought to be a β-galactosidase activity unique to senescent cells, but subsequently was shown to be due to the normal lysosomal β-galactosidase (i.e., the only β-galactosidase in mammals), which was found to be overexpressed in senescent cells, accounting for the increased X-gal staining of senescent cells (Lee et al., 2006).

The expression of lysosomes in cells (including expression of β-galactosidase) is regulated by transcription factor EB (TFEB), which also promotes the translocation of β-galactosidase to the plasma membrane/cell surface by lysosomal exocytosis (Magini et al., 2013). We recently reported that activation of microglia resulted in the translocation of Neu1 to the cell surface and extracellular space by lysosomal exocytosis (Allendorf and Brown, 2022). As Neu1 can be structurally and functionally coupled to β-galactosidase (Bonten et al., 2014), we were interested here in whether β-galactosidase was also released by activated microglia, and, if so, whether this had any functional consequences.

Microglia are resident brain macrophages and the main innate immune cell of the central nervous system. As such, microglia survey the brain for infection or damage, and if they detect these, become inflammatory activated in order to resolve the threat. However, chronic activation of microglia can be damaging to neurons and is implicated in many brain pathologies, including neurodegenerative diseases, such as Alzheimer's disease and Parkinson's disease (Thameem Dheen et al., 2007). Senescent microglia, overexpressing β-galactosidase, have been implicated in Alzheimer's disease (Greenwood and Brown, 2021). And β-galactosidase associated with the neuronal membrane is increased in Alzheimer's disease (Magini et al., 2015). β-galactosidase is increased in the CSF of Parkinson's disease patients, indicating an increase in extracellular β-galactosidase in the brain (van Dijk et al., 2013). Extracellular and cell surface β-galactosidase can potentially degrade cell surface GM1, which is neuroprotective (van Dijk et al., 2013). GM1 also potently inhibits microglial activation (Galleguillos et al., 2022), and decreases in Parkinson's disease (Chowdhury and Ledeen, 2022), potentially due to increased extracellular β-galactosidase in the PD brain (van Dijk et al., 2013).

In this study, we examined whether activated microglia release β-galactosidase, and, if so, whether β-galactosidase promoted inflammatory neurodegeneration.

Materials and methods

Cell culture and treatments

The immortalized cell line BV-2 (ECACC Cat# 0356, RRID:CVCL_0182) was maintained as previously described (Blasi et al., 1990; Shen et al., 2016). Neither cell line is listed as a commonly misidentified cell line by the International Cell Line Authentication Committee. Primary mixed neuron-glial cultures were prepared from the cerebellum of 3–5 day old Wistar rats (Charles River, RRID:RGD_2312511), following procedures described elsewhere (Carrillo-Jimenez et al., 2018; Allendorf et al., 2020). All animal experiments were approved by the Cambridge University Local Research Ethics Committee and undertaken in accordance with the UK Animals (Scientific Procedures) Act (1986).

Cells were treated as follows: adenosine triphosphate (ATP) was used at 1 mM and A23187 was used at 10 μM. LPS (100 ng/mL) and PMA (100 nM) were added over 18 or 72 h where indicated. Exogenous β-galactosidase from bovine liver (Sigma, St Louis, MO, USA) was used at 20 mU/mL for 72 h. For heat inactivation, β-galactosidase was first incubated at 70 °C for 5 min. For depletion experiments, mixed neuronal-glial co-cultures were treated 3 DIV with 5 μM PLX-3397 (PLX). β-galactosidase inhibitors, D-galactono-1,4-lactone (DGL, BioSynth, Staad, Switzerland) and 1-Deoxygalactonojirimycin (hydrochloride) (DGJ, Cambridge Bioscience) were used 1 mM or 10 mM for 72 h. Treatments were compared to a vehicle treated control group. The most appropriate vehicle was chosen for each experiment. Dimethyl sulfoxide (DMSO) for PLX treatments and phosphate buffered saline (PBS) for all other experiments.

β-galactosidase activity assays

BV-2 microglia were seeded at 1×10^5 cells/well in black, clear-bottom 96-well plates (Greiner) and treated as above. β-galactosidase activity on live cells was assessed in assay buffer adjusted to pH 7.0 or pH 4.0 for supernatant activity assays. The supernatant activity was assayed at final pH 4.7 as a result of diluting DMEM (which uses a sodium bicarbonate buffer system) with pH 4.0 assay buffer at a 1: 1 ratio. For the assay, media was removed from live cells and immediately replaced with 50 μL PBS. For supernatants, debris was removed by centrifugation 150 RCM, 5 min and 50 μL used for the assay. The assay was initiated by the addition of 50 μL of 2X assay buffer. Assay buffer (1X) contained 100 mM sodium phosphate (pH 7.0) or 100 mM citric acid/200 mM sodium phosphate buffer (pH 4.0), 1 mM MgCl2, 50 μM β-mercaptoethanol and 0.5 mg/mL 4-Methylumbelliferyl-β-D-galactopyranoside (MUG, GlycoSynth) in distilled water. 0.2 mU/mL β-galactosidase from bovine liver (Sigma, St Louis, MO, USA) was used as a positive control. Kinetic experiments were performed using a plate reader (FlexStation 3, Molecular Devices), pre-heated to 37°C, with fluorescence determinations beginning immediately upon the addition of assay buffer and taken every minute for 2 h, using 360/40 nm excitation and 460/40 nm emission filters. A standard curve was produced using 4-methylumbelliferone (MUB) which was used to convert arbitrary fluorescent units and calculate concentration of MUB produced in μM.

For assessing inhibitors of β-galactosidase, D-galactono-1,4-lactone and DGJ were diluted to 2X the indicated concentrations (1 mM or 10 mM) in PBS containing 2X the final concentration (0.2 mU/mL) of β-galactosidase from bovine liver, then the assay was initiated as above.

Cell viability and density quantification

After treatment some culture media was removed and saved for analysis where necessary, then cell viability, defined as % necrotic (PI-positive) cells, was measured at indicated endpoints by differential dye uptake of propidium iodide (identifying necrotic cells) and Hoechst 33342 (identifying all cells) using a fluorescent microscope (EVOS M5000). Cell densities were quantified as described previously (Birkle and Brown, 2023). Briefly, Alexa Fluor-488 NeuO (Stemcell Technologies, Cambridge, UK) was used to identify neurons and Alexa Fluor-594 IB4 (Invitrogen, Paisley, UK) was used to identify microglia. Cultures were imaged using 10× objective, with four images taken in consistent positions

around each well. Image sets were analyzed for the number of each cell type using a custom CellProfiler (Stirling et al., 2021b)/CellProfiler Analyst (Stirling et al., 2021a) pipeline.

BV-2 cell viability and density quantification

BV-2 microglia were seeded at 5×10^3 in 96-well plates and treated with vehicle or 20 mU/mL β-galactosidase from bovine liver (Sigma, St Louis, MO, USA) for 48 h. Density and cell viability, defined as % necrotic (PI-positive) cells, was measured at 0, 24, and 48 h by differential dye uptake of propidium iodide (identifying necrotic cells) and Hoechst 33342 (identifying all cells) using a fluorescent microscope (EVOS M5000). Cultures were imaged using a 10× objective, with four images taken in consistent positions around each well. Images were analyzed using FIJI.

Measurement of β-galactosidase and inflammatory cytokines

Following treatments, β-galactosidase concentration from BV-2 supernatants and β-galactosidase concentration from mixed neuronal-glial cultures was determined using Mouse Beta-Galactosidase (GLB1) ELISA Kit (Abbexa, Cambridge, UK) and Rat Beta-Galactosidase (GLB1) ELISA Kit (Abbexa, Cambridge, UK), respectively, according to the manufacturer's instructions. TNFα and IL-6 detection was achieved by ELISA as per the manufacturer's instructions (BioLegend, San Diego, CA, USA).

Immunohistochemistry and imaging of free-floating brain slices

Transcardial perfusion, tissue sectioning, tissue staining, image acquisition and analysis were done as previously described (Dundee et al., 2023). Briefly, 25 μm serial coronal sections were prepared using a sliding microtome and stored in PBS containing 0.025% sodium azide as free-floating sections. For each of five wild-type (WT) mice, aged 4 and 17 months old, three sections were used, taken 300 μm apart per mouse. Sections were incubated with mouse anti-Iba1 (1:200, Sigma, St Louis, MO, USA), rabbit anti-β-galactosidase (1:200, Thermo Fisher, Waltham, MA, USA) and rat anti-CD68 (1:200, Thermo Fisher, Waltham, MA, USA) antibodies in blocking solution for 2 h at 37°C (Xiao et al., 2017), then washed with PBS and incubated for 2 h at 37°C with secondary antibodies, Alexa Fluor-488 goat anti-mouse (1:200, Thermo Fisher, Waltham, MA, USA), Alexa Fluor-568 goat anti-rabbit (1:200, Thermo Fisher, Waltham, MA, USA) and Alexa Fluor-647 goat anti-rat (1:200, Thermo Fisher, Waltham, MA, USA). Sections were washed with PBS and mounted on poly-L-lysine treated glass slides in DAPI-containing Vectashield mounting medium (Vector Laboratories, Newark, CA, USA) and imaged on a confocal microscope (Nikon C2si, 63×, 1.35 NA oil immersion objective using 405, 488, and 561 nm lasers). For imaging, Z-stacks (0.5 μm step intervals) were taken of the somatosensory cortex. Fifteen microglia were analyzed across the three sections from each mouse. Image analysis was done in FIJI and Imaris (version 9.1.2). Briefly, background subtraction and intensity normalization were done, then microglial surface rendering (using Iba1 staining) and β-galactosidase staining intensity within Iba1+ structures was analyzed in Imaris. The results for the surface-rendered objects were represented as volume (μm^3) and β-galactosidase intensity as MFI.

Statistical analysis

Statistical analysis was performed using GraphPad Prism (version 9.0) and data was collected from a minimum of 3 independent experiments. Shapiro–Wilk test of normality was performed. Statistical significance was assessed by *t*-test, or repeated measures one-way or two-way ANOVA, followed by Šídák's or Dunnett's *post-hoc* test (see figure legends). Error bars represent the standard error of the mean of experiments (SEM). *p*-values refer to the probability of the null hypothesis that the means do not differ. $p < 0.05$ was considered significant, and $p \geq 0.05$ not significant.

Results

Activation of microglia induces β-galactosidase release

It is unknown whether intact microglia can release β-galactosidase, so we measured this with BV-2 microglia and primary microglia in various conditions. To measure cell surface β-galactosidase activity, we added the β-galactosidase substrate, 4-methylumbelliferyl-β-D-galactopyranoside (MUG), to a monolayer of live BV-2 cells in the well of their cell culture plate, and followed the rate at which MUG was converted to the fluorogenic product 4-methylumbelliferone (MUB) in a plate reader. MUG is cell impermeant, so when added to intact cells, the assay only measures the cell surface or extracellular activity (Aureli et al., 2009). The culture medium was changed to PBS just prior to the assay, so that only cell surface or acute release of β-galactosidase was measured by the assay. In the absence of cells, there was no measurable β-galactosidase activity, but in the presence of live BV-2 cells, there was a significant β-galactosidase activity, which very slowly increased with assay time (**Figure 1A**). This indicates that there is a β-galactosidase activity present on the surface of BV-2 microglia. Addition of β-galactosidase isolated from bovine liver to the assay in the absence of cells resulted in steady activity (**Figures 1A, B**). The cell surface β-galactosidase activity was measured at pH 7.0, and therefore is likely to be active extracellularly.

One potential cause of β-galactosidase release from lysosomes is lysosomal exocytosis (Magini et al., 2013), which can be induced by a rise in intracellular calcium (Reddy et al., 2001). To induce a rise in intracellular calcium, we added A23187 (a calcium ionophore) or ATP (a P2X7 agonist) to BV-2 microglia. Addition of A23187 induced an immediate, artifactual increase in fluorescence due to the fluorescence of the compound itself, then an increase in rate

10.3389/fnagi.2023.1327756

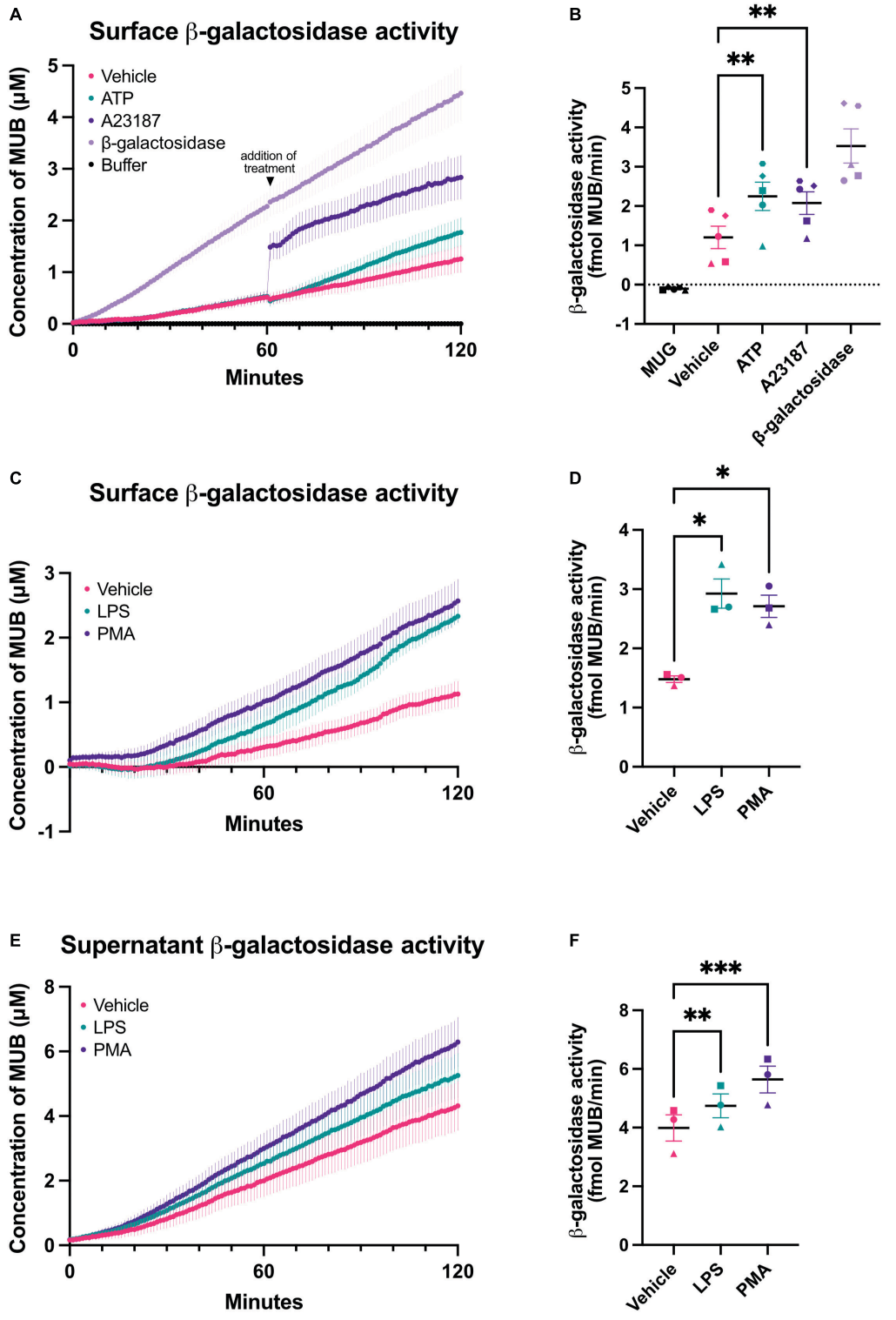

FIGURE 1
Chronic and acute activation of BV-2 microglia induces β-galactosidase release. β-galactosidase activity on the surface of BV-2 cells and released into the supernatant was determined using the rate of MUG to MUB conversion when added to a monolayer of cells or to the cleared supernatant from these cells. β-galactosidase activity on live cells was assessed in assay buffer adjusted to pH 7.0 or pH 4.0 for supernatant activity assays. Buffer refers to the 1X assay buffer containing 0.5 mg/mL MUG in the absence of cells (negative control). β-galactosidase (0.2 mU/mL) from bovine liver was used as a positive control for the assay. **(A)** Cells were acutely treated with ATP (1 mM) or A23187 (10 μM) 1 h after the initiation of the MUG assay and the rate of MUG-MUB conversion after treatment addition was calculated in **(B)**. **(C)** BV-2 cells were treated with LPS (100 ng/mL) or PMA (100 nM) for 18 h, then supernatant was removed and β-galactosidase activity was assayed on the cell surface. **(D)** The rate at which MUG was converted to MUB was determined from **(C)**. **(E)** The supernatants of LPS and PMA treated cells from **(C)** were cleared and assayed for β-galactosidase activity and rate determined in **(F)**. Data represents mean values ± SEM of at least 3 independent experiments. Statistical comparisons were made by repeated measures one-way ANOVA with Dunnett's *post hoc* comparisons test. Asterisk (*) indicate significance compared to untreated control (*$p < 0.05$, **$p < 0.01$, ***$p < 0.001$).

for 5–10 min, and finally a return to baseline rate. ATP induced an increase in rate for about 60 min (Figure 1B). This is consistent with an intracellular calcium rise causing β-galactosidase release by lysosomal exocytosis.

To test whether β-galactosidase is released from inflammatory activated microglia, we treated BV-2 microglia for 18 h with lipopolysaccharide (LPS). LPS induced a significant increase in β-galactosidase activity on the surface of the cells, compared to cells not treated with LPS (Figures 1C, D). We also measured the β-galactosidase activity released from the cells into the cell culture medium during the course of the 18 h incubation ± LPS, and we found that LPS induced a significant increase in extracellular β-galactosidase activity (Figures 1E, F), consistent with LPS-induced release from microglia.

Phorbol 12-myristate 13-acetate (PMA) is a protein kinase C activator that has been reported to induce β-galactosidase and senescence of microglia (Cao et al., 2020). So, we tested whether PMA treatment of microglia could induce β-galactosidase release, and found that BV-2 microglia cultured with PMA had significantly more β-galactosidase activity on the cell surface (Figures 1C, D) and released significantly more β-galactosidase activity into the culture medium (Figures 1E, F).

The above assay measured β-galactosidase activity, but not protein. To measure whether β-galactosidase protein was released from activated microglia, we assayed β-galactosidase protein by ELISA in the cell culture media of BV-2 microglia pretreated with LPS or PMA. We found that PMA increased extracellular β-galactosidase protein 3 fold, and LPS increased extracellular β-galactosidase protein 7 fold, as measured by ELISA (Figure 2A). As cell death might, in principle, release β-galactosidase from lysosomes into the medium, we also checked whether LPS or PMA induced cell death, but there was no such increase in cell death (Figure 2B). Thus, activated microglia can release β-galactosidase to their surface and into their extracellular environment.

As BV-2 microglia release β-galactosidase into their extracellular medium, we tested the effect of adding isolated β-galactosidase to the extracellular medium of BV-2 microglia. We added 20 mU/mL β-galactosidase (isolated from bovine liver) to proliferating cultures of BV-2 cells, and measured cell density and cell death over 48 h. β-galactosidase had no significant effect on cell density or the increase in cell density caused by proliferation, and induced no cell death, as measured by propidium iodide staining of the cells (Supplementary Figure 1).

Having found that microglial activation can induce β-galactosidase on the microglial cell surface in culture, we wanted to test this *in vivo*. Microglia are known to become activated and senesce with age in mice (Matsudaira et al., 2023). So, we examined sections from the brains of mice at 4- and 17-months-old. For this, coronal brain slices were immunostained using antibodies to β-galactosidase and Iba1 (microglial marker) (Figures 3A, B). There was no significant difference with age in microglial Iba1 volume, indicating no effect of age on microglial size (Figure 3C). We then analyzed the staining intensity of β-galactosidase in Iba1-positive cells in the somatosensory cortex using confocal microscopy. We found that the intensity of β-galactosidase on Iba1-positive structures was significantly increased in 17-month-old compared with 4-month-old mice (Figure 3D), indicating a significant increase in β-galactosidase levels with age. Much of the

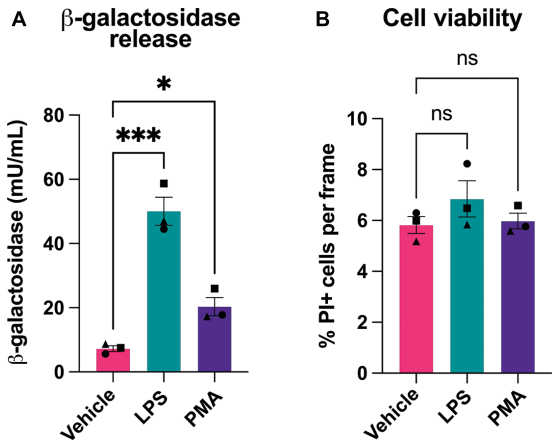

FIGURE 2
Microglial activation induces release of β-galactosidase protein without affecting cell death. **(A)** BV-2 cells were treated with LPS (100 ng/mL) or PMA (100 nM) for 18 h, then supernatant was collected and β-galactosidase concentration was determined by ELISA. **(B)** Cell viability of BV-2 microglia, post-treatment ± LPS or PMA, was assessed by propidium iodide uptake and presented as % of total cells (determined by Hoechst staining). Data represents mean values ± SEM of 3 independent experiments. Statistical comparisons were made by repeated measures one-way ANOVA with Dunnett's *post hoc* comparisons test. Asterisk (*) indicate significance compared to untreated control (ns: $p \geq 0.05$, *$p < 0.05$, ***$p < 0.001$).

β-galactosidase staining appeared to be on the microglial surface in aged brains, rather than in intracellular lysosomes (Figure 3A), consistent with translocation to the cell surface. This was further supported by staining of slices with Iba1 and the lysosomal marker, CD68 (Supplementary Figure 2). This confirmed that although lysosomes appear larger in aged brains, the lysosomes are still largely confined to the perinuclear cell body (Supplementary Figure 2), and their distribution is distinct from that of β-galactosidase in aged brains (Figure 3).

Primary cultures release β-galactosidase, and added β-galactosidase promotes neuronal loss and microglial activation

As activated microglia released β-galactosidase, we were interested in whether this released β-galactosidase could contribute to neurodegeneration in primary neuronal-glial cultures. These cultures were isolated from the cerebellum of P3-P5 rats and cultured for 7 days (Carrillo-Jimenez et al., 2018), and contain 83 ± 3% neurons, 11 ± 2% astrocytes and 4 ± 1% microglia (Kinsner et al., 2005). We first measured whether LPS or PMA would induce β-galactosidase release in these cultures. We found that addition of 100 ng/mL LPS or 100 nM PMA induced a significant increase in β-galactosidase protein in the culture medium (Figure 4A).

As LPS and PMA induced an increase in extracellular β-galactosidase, we next tested whether addition of isolated β-galactosidase affected neuronal viability and microglial activation in mixed neuronal-glial cultures. We added 20 mU/mL β-galactosidase (or 100 ng/mL LPS for comparison) to these cultures

10.3389/fnagi.2023.1327756

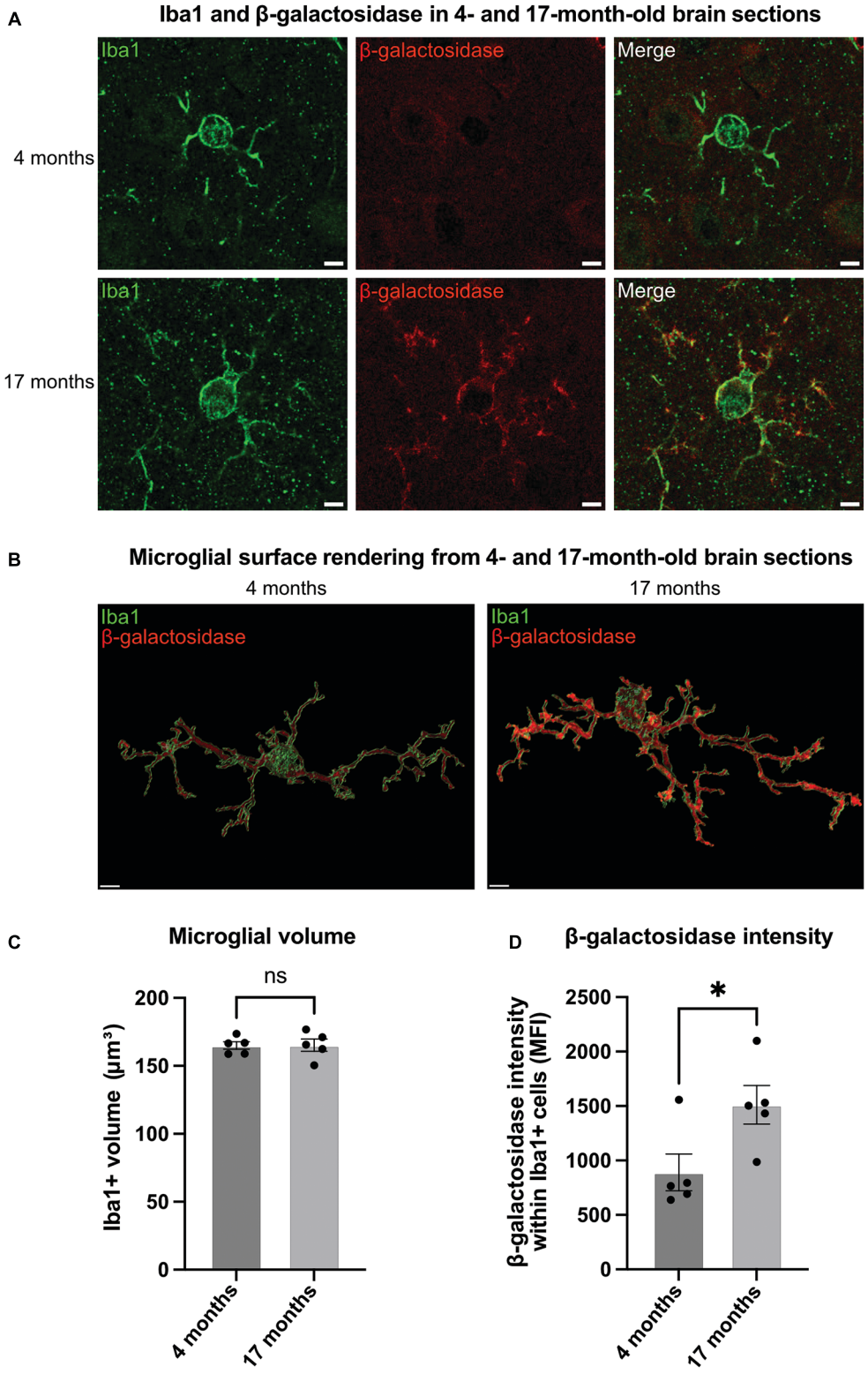

FIGURE 3
Microglia in aged brains have increased levels of β-galactosidase. **(A)** Representative confocal microscopy images of microglia from 4- to 17-month-old mice stained for Iba1 (green, microglial marker) and β-galactosidase (red) in the somatosensory cortex. Scale bar = 2 µm. **(B)** Representative renders of microglia from confocal images generated in Imaris. Scale bar = 2 µm. **(C)** Microglial volume as measured by area (μm^3) of Iba1 staining. **(D)** Mean fluorescence intensity (MFI) of β-galactosidase within Iba1-positive microglia. Each point represents one animal comprised of 15 microglia analyzed across three equidistant sections. Error bars represent SEM and statistical comparisons were made via unpaired *t*-test. Asterisk (*) indicate significance (ns: $p \geq 0.05$, *$p < 0.05$).

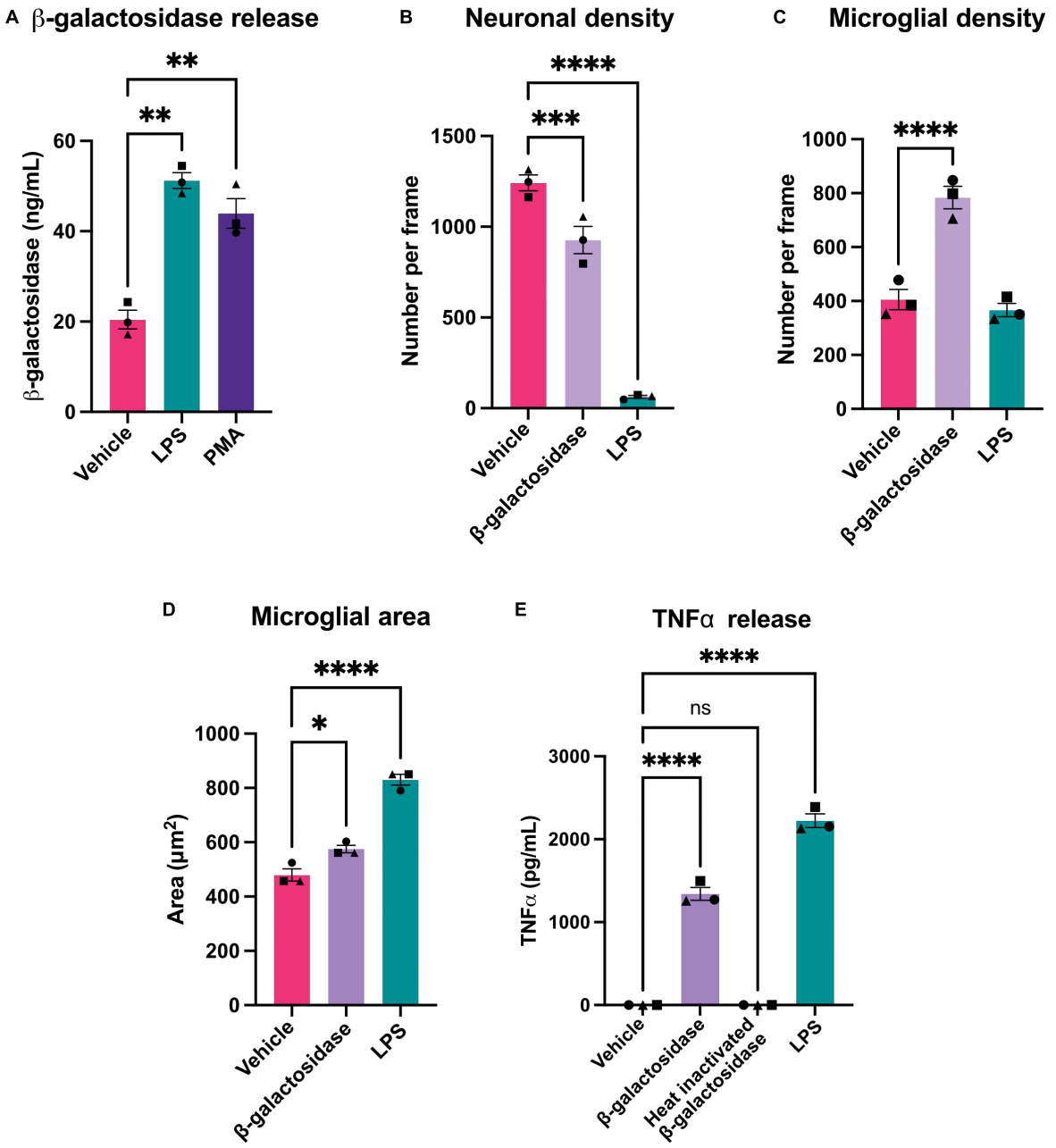

FIGURE 4
β-galactosidase promotes neuronal loss and microglial activation. **(A)** Mixed neuronal-glial cultures were treated with LPS (100 ng/mL) or PMA (100 nM) for 72 h and supernatants were assessed for β-galactosidase levels by ELISA. **(B)** Mixed neuronal-glial cultures were treated with β-galactosidase (20 mU/mL) and LPS (100 ng/mL) for 72 h then cultures were stained with Hoechst 33342 (to identify nuclei and apoptotic cells), isolectin B4 (to identify microglia), NeuO (to identify live neurons) and live neuronal cell numbers quantified using CellProfiler. **(C)** Microglial cell numbers quantified by fluorescent microscopy using CellProfiler. **(D)** Microglial cell area was quantified in CellProfiler. **(E)** Mixed neuronal-glial cultures were treated with β-galactosidase (20 mU/mL), heat inactivated β-galactosidase (20 mU/mL) and LPS (100 ng/mL) for 72 h then supernatants were assessed for TNFα levels by ELISA. Data represents mean values ± SEM of 3 independent experiments. Statistical comparisons were made by repeated measures one-way ANOVA with Dunnett's *post hoc* comparisons test. Asterisk (*) indicate significance compared to untreated control (ns: $p \geq 0.05$, *$p < 0.05$, **$p < 0.01$, ***$p < 0.001$, ****$p < 0.0001$).

for 72 h. Addition of β-galactosidase induced a loss of about 25% of the neurons over 72 h (Figure 4B and Supplementary Table 1), and doubled the number of microglia in the cultures, compared to the untreated control (Figure 4C and Supplementary Table 1). β-galactosidase also changed microglial area and morphology in a similar way (but lower extent) to LPS (Figure 4D and Supplementary Figure 3).

Having found that microglia proliferate and undergo morphological changes with β-galactosidase addition, both indicators of activation, we tested whether β-galactosidase can induce release of pro-inflammatory cytokines by measuring the amount of extracellular TNFα (tumor necrosis factor alpha) by ELISA. Untreated cultures had no detectable TNFα; LPS-treated cultures had a high level of TNFα; while cultures treated

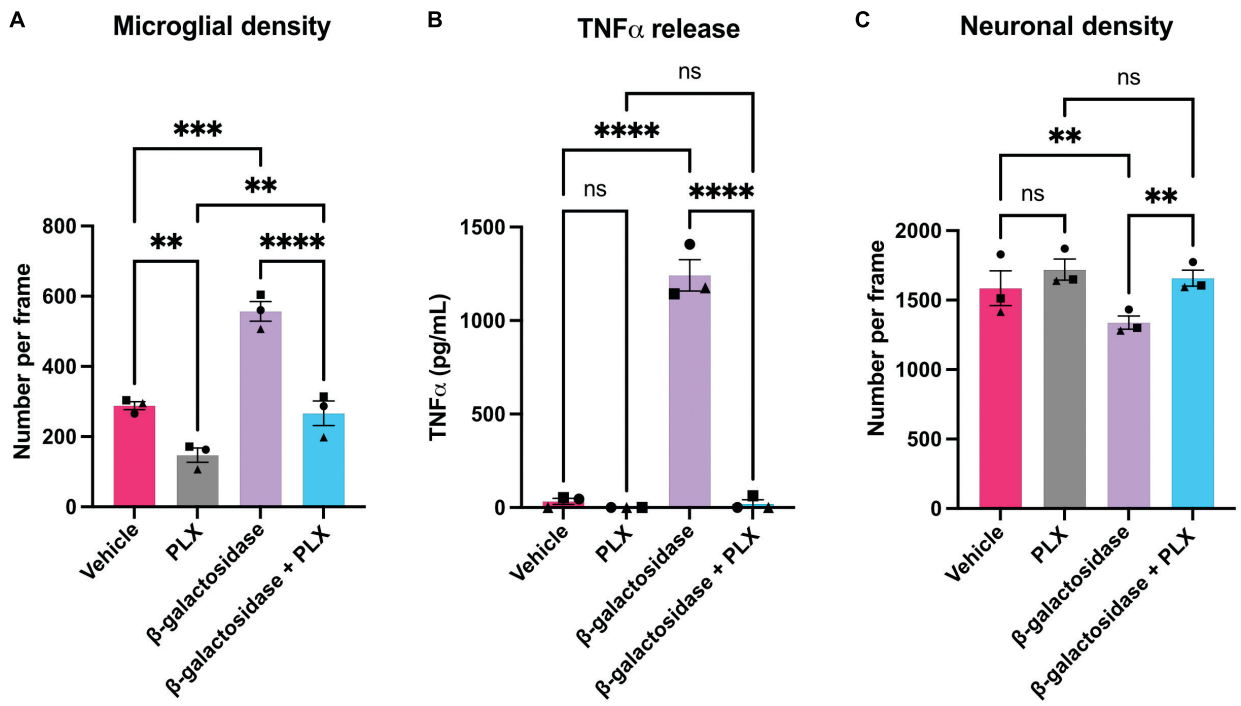

FIGURE 5
Microglial depletion prevents β-galactosidase-induced TNFα release and neuronal loss. Mixed neuronal-glial cultures were treated with PLX-3397 (5 μM) 3 DIV, then ± β-galactosidase (20 mU/mL) 7 DIV for 72 h. Cultures were then stained with Hoechst 33342 (to identify nuclei and apoptotic cells), isolectin B4 (to identify microglia), NeuO (to identify live neurons). **(A)** Microglial cell numbers were quantified by fluorescent microscopy using CellProfiler. **(B)** Supernatants were assessed for TNFα levels by ELISA. **(C)** Live neuronal cell numbers were quantified by fluorescent microscopy using CellProfiler. Data represents mean values ± SEM of 3 independent experiments. Statistical comparisons were made by repeated measures two-way ANOVA with Šídák's *post hoc* comparisons test. Asterisk (*) indicate significance compared to untreated control (ns: $p \geq 0.05$, **$p < 0.01$, ***$p < 0.001$, ****$p < 0.0001$).

with 20 mU/mL β-galactosidase had an intermediate level of TNFα (1342 pg/mL) (Figure 4E). To test whether the effects of added β-galactosidase were due to the β-galactosidase activity, rather than the protein or potential contaminants, we added heat-inactivated β-galactosidase, and found this had no effect on TNFα release (Figure 4E), neuronal or microglial count, or microglial morphology (Supplementary Figure 4). Hence, exogenous β-galactosidase activity promotes neuronal loss and activates microglia to a pro-inflammatory state.

To investigate whether the effects of β-galactosidase on neurotoxicity and inflammation require microglia, we depleted microglia in the mixed neuronal-glial cultures using PLX-3394, a colony stimulating factor 1 receptor (CSF1R) inhibitor, prior to β-galactosidase treatment. PLX treatment depleted the microglia in these cultures by at least 50% both in the absence and presence of exogenous β-galactosidase treatment, as measured using fluorescent isolectin-B4 to specifically label and quantify microglia (Figure 5A and Supplementary Table 2). And PLX treatment completely prevented the dramatic increase in TNFα levels induced by addition of β-galactosidase (Figure 5B). Furthermore, depletion of microglia prevented the loss of neurons induced by addition of β-galactosidase (Figure 5C and Supplementary Table 2). Together, these results suggest β-galactosidase is not directly neurotoxic, but that β-galactosidase induced neuronal loss is mediated by the activation of microglia and subsequent inflammation.

Inhibiting β-galactosidase protects against LPS-induced neuronal loss and microglial activation

As LPS induced β-galactosidase release in primary cultures, and added β-galactosidase induced microglial activation and neuronal loss, we wanted to test whether inhibiting β-galactosidase activity would affect LPS-induced microglial activation and neuronal loss. To do this, we tested the ability of several commercially available β-galactosidase inhibitors to inhibit the activity of isolated bovine β-galactosidase, and found two structurally dissimilar inhibitors, D-galactono-1,4-lactone (DGL) and 1-deoxygalactonojirimycin (hydrochloride) (DGJ), which significantly reduced activity of exogenous β-galactosidase (Supplementary Figure 5). We then tested whether these inhibitors affected the neuronal loss induced by LPS. Addition of LPS to mixed neuronal-glial cultures for 72 h resulted in neuronal loss as expected, but co-treatment with 10 mM D-galactono-1,4-lactone significantly protected against this loss (Figures 6A, B). D-galactono-1,4-lactone also reduced the effects of LPS on: TNFα levels (Figure 6C) and IL-6 levels (Figure 6D). Thus, inhibition of β-galactosidase by D-galactono-1,4-lactone reduced LPS-induced neuronal loss and microglial activation.

Similarly, we assessed the effects of the β-galactosidase inhibitor DGJ on mixed neuronal-glial cultures. Again, addition of LPS for 72 h resulted in neuronal loss, and co-treatment with 10 mM DGJ

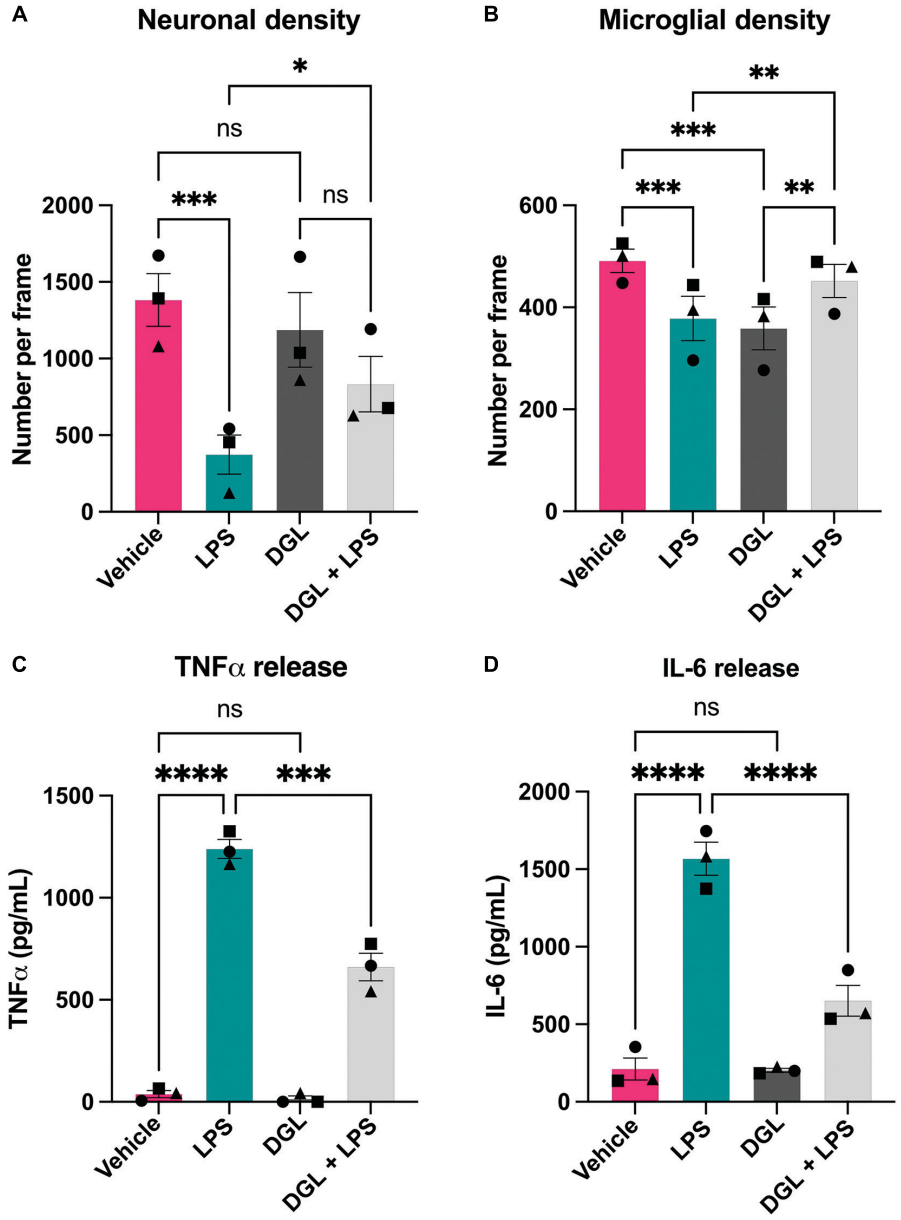

FIGURE 6
D-galactono-1,4-lactone protects against neuronal loss and microglial activation. Mixed neuronal-glial cultures were treated with LPS (100 ng/mL) ± 10 mM D-galactono-1,4-lactone (DGL) for 72 h then cultures were stained with Hoechst 33342 (to identify nuclei and apoptotic cells), isolectin B4 (to identify microglia), NeuO (to identify live neurons). **(A)** Live neuronal cell numbers and, **(B)** microglial cell numbers were quantified by fluorescent microscopy using CellProfiler. Supernatants were assessed for TNFα **(C)** and IL-6 **(D)** levels by ELISA. Data represents mean values ± SEM of 3 independent experiments. Statistical comparisons were made by repeated measures two-way ANOVA with Šídák's *post hoc* comparisons test. Asterisk (*) indicate significance compared to untreated control (ns: $p \geq 0.05$, *$p < 0.05$, **$p < 0.01$, ***$p < 0.001$, ****$p < 0.0001$).

substantially protected against this loss (Figure 7A). DGJ caused no significant change in microglial numbers (Figure 7B), but reduced LPS-induced release of TNFα (Figure 7C) and LPS-induced release of IL-6 (Figure 7D).

Discussion

It has previously been shown that LPS induces β-galactosidase protein and activity in BV-2 microglia (Yu et al., 2012; Borgonetti and Galeotti, 2022). We found that inflammatory activation of BV-2 microglia with LPS induced release of β-galactosidase onto the cell surface of microglia and into the medium, as measured by β-galactosidase protein or β-galactosidase activity. LPS also induced β-galactosidase release in primary neuronal-glial cultures, and addition of isolated β-galactosidase to these cultures induced microglial activation and neuronal loss, which was prevented by depleting microglia from these cultures. LPS-induced microglial activation and neuronal loss in these primary cultures was substantially reduced by two different β-galactosidase inhibitors. Overall, this suggests that LPS-activated

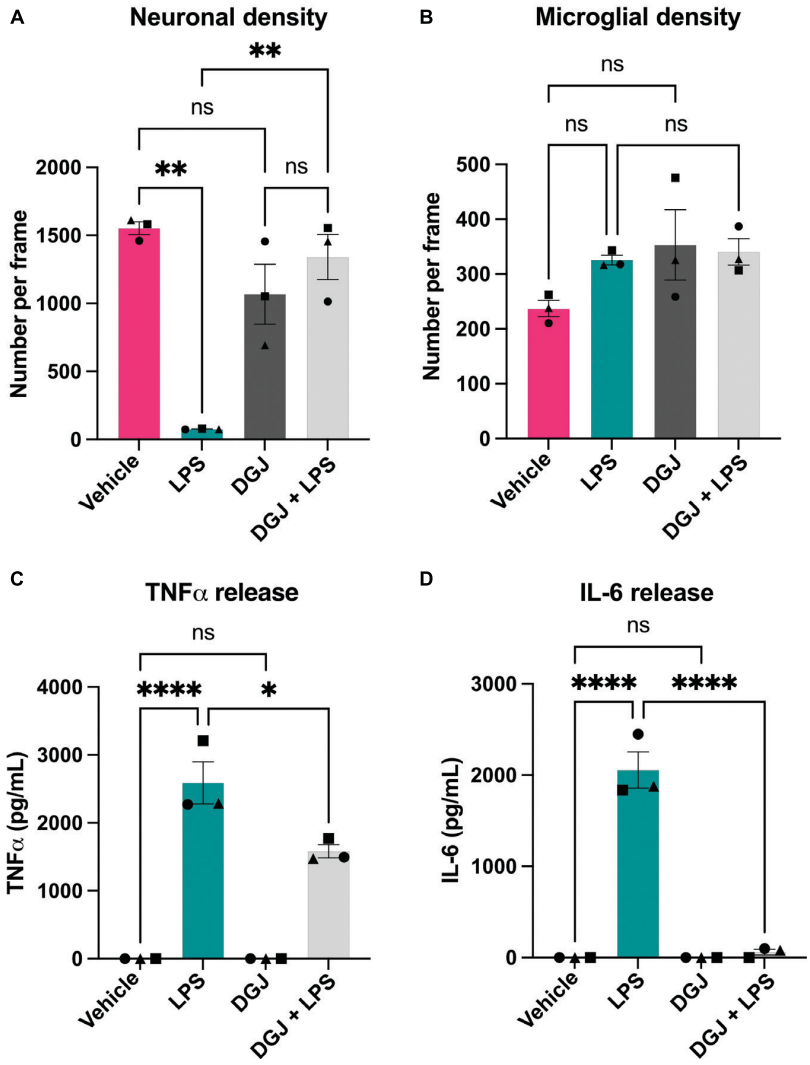

FIGURE 7
1-Deoxygalactonojirimycin protects against neuronal loss and microglial activation. Mixed neuronal-glial cultures were treated with LPS (100 ng/mL) ± 10 mM 1-Deoxygalactonojirimycin (DGJ) for 72 h then cultures were stained with Hoechst 33342 (to identify nuclei and apoptotic cells), isolectin B4 (to identify microglia), NeuO (to identify live neurons). **(A)** Live neuronal cell numbers and, **(B)** microglial cell numbers were quantified by fluorescent microscopy using CellProfiler. Supernatants were assessed for TNFα **(C)** and IL-6 **(D)** levels by ELISA. Data represents mean values ± SEM of 3 independent experiments. Statistical comparisons were made by repeated measures two-way ANOVA with Šídák's *post hoc* comparisons test. Asterisk (*) indicate significance compared to untreated control (ns: $p \geq 0.05$, *$p < 0.05$, **$p < 0.01$, ****$p < 0.0001$).

microglia release β-galactosidase, which promotes microglial toxicity to neurons.

We did not investigate the mechanism by which LPS induces β-galactosidase release, but it has previously been shown that β-galactosidase can be released by lysosomal exocytosis (Magini et al., 2013), and that LPS can induce lysosomal exocytosis by microglia (Liu et al., 2008; Allendorf and Brown, 2022). Consistent with this, A23187 and ATP, which can induce a calcium rise and lysosomal exocytosis (Jaiswal et al., 2002), caused an acute increase in cell surface β-galactosidase activity. However, confirming that release was by lysosomal exocytosis would require further study.

Addition of β-galactosidase to primary cultures caused: increased microglia, altered microglial morphology, release of TNFα, and loss of neurons. We do not know why β-galactosidase increased microglial numbers, but microglial proliferation is commonly associated with microglial activation, and the TNFα release induced by addition of β-galactosidase is a potent mitogen for microglia (Mander et al., 2006). Hence, β-galactosidase might indirectly promote microglial proliferation by inducing microglial activation. However, a proliferative effect of β-galactosidase would need to be confirmed using a proliferation marker, such as Ki67. β-galactosidase altered microglial morphology as indicated by a flattening down of the microglia onto the culture well, but it might be useful to further characterize this morphological transition, for example by Scholl analysis.

Depletion of microglia from the primary cultures using PLX, prevented β-galactosidase-induced release of TNFα and loss of neurons. PLX is known to specifically deplete microglia without affecting astrocytes (Van Zeller et al., 2022), and we confirmed a depletion of microglia with no significant effect on neurons (**Figure 5C**) or astrocytes (**Supplementary Figure 6**). Therefore, β-galactosidase-induced neuroinflammation and neuronal loss

requires microglia. This suggests that β-galactosidase activated microglia in a way that promoted neuronal loss. We did not further investigate the mechanism of this microglial activation or neuronal loss. However, mammalian β-galactosidase functions to remove terminal galactose residues from glycolipids and glycoproteins, including particularly the ganglioside GM1 (Li and Li, 1999). GM1 is anti-inflammatory in microglia and neuroprotective, both in culture and *in vivo* (van Dijk et al., 2013; Galleguillos et al., 2022). Thus, it is possible that cell surface β-galactosidase degrades GM1, resulting in microglial activation and neuronal loss. However, testing this would require further investigation, for example by staining for GM1 on microglia, and extracellular β-galactosidase may remove terminal galactose residues from receptors and other cell surface glycoproteins to change microglial and neuronal function. The mechanism of neuronal loss induced by β-galactosidase in these cultures was not further investigated, but possibilities include: (i) release of TNFα and IL-6, which are both sufficient to induce neuronal loss (Conroy et al., 2004; De Lella Ezcurra et al., 2010; Smith et al., 2012; Neniskyte et al., 2014), (ii) microglial phagocytosis of the neurons, induced by microglial activation (Neher et al., 2011), and (iii) exposure of N-acetylglucosamine residues on the cell surface, which may induce phagocytosis or complement activation (Cockram et al., 2021).

Lipopolysaccharide (LPS) induced β-galactosidase release in primary mixed neuronal-glial cultures, and two different β-galactosidase inhibitors reduced LPS-induced neuronal loss in these cultures. This suggests that β-galactosidase, in particular extracellular β-galactosidase, may be a good target to prevent inflammatory neurodegeneration. Unfortunately, these two inhibitors, D-galactono-1,4-lactone and DGJ, had to be used at millimolar levels, as this was the concentration at which they inhibited isolated β-galactosidase activity. We found no other commercially-available inhibitors of mammalian β-galactosidase that were more potent. Thus, further testing and translating the role of β-galactosidase may require the development of more potent inhibitors or other methods. Targeting all β-galactosidase may be toxic long-term, because lysosomal β-galactosidase is beneficial by degrading glycolipids and glycoproteins (Bonten et al., 2014), and lysosomes may be upregulated in microglia in a variety of conditions, for example to degrade cellular debris or amyloid beta. However, it might in principle be possible to specifically target extracellular β-galactosidase, using drugs that do not enter cells, or to target inhibitors to specific cell types, using for example myeloid-specific nanosystems (Zhu et al., 2022). For example, cell-impermeant β-galactosidase inhibitors could be injected into the brain with LPS to test whether inhibition of extracellular β-galactosidase prevents LPS-induced neuronal loss in rodents (Neher et al., 2014).

Senescent cells are characterized by the overexpression of β-galactosidase and lysosomes generally (Dimri et al., 1995; Kurz et al., 2000). This can be driven by the transcription factor TFEB, which can also promote lysosomal exocytosis (Magini et al., 2013). Thus, it is possible that part of the β-galactosidase in senescent cells could end up on the cell surface. This is at least consistent with our findings that: (i) PMA and LPS induce β-galactosidase release [as both PMA and LPS are reported to induce microglial senescence (Yu et al., 2012; Cao et al., 2020)], and (ii) microglia in the brains of aged mice appear to have β-galactosidase on their cell surface. Note, however, that we do not know whether PMA or LPS induced microglial senescence in our cultures, and much more work would be required to confirm that senescent microglia expose β-galactosidase. If so, this might provide an explanation of why senescent microglia appear to promote neurodegeneration (Bussian et al., 2018; Martínez-Cué and Rueda, 2020).

Aberrant and chronic microglial activation and neuroinflammation are implicated in many neurodegenerative disorders including AD and PD (Perry et al., 2010). In PD patients, GM1 deficiency has been reported, and GM1 replacement may provide some clinical benefit in PD patients (Wu et al., 2012; Schneider et al., 2013). Moreover, β-galactosidase activity is increased in the CSF of PD patients (van Dijk et al., 2013). Thus, it is possible that cell surface or extracellular β-galactosidase degrades protective GM1, resulting in microglial activation and neuronal loss. Furthermore, removal of the terminal galactose residue of GM1, generates GM2 ganglioside, which can be pro-inflammatory (Mizutani et al., 1999). In AD, accumulation of GM2 has been reported (Kracun et al., 1992). Thus, it could be that activated microglia release β-galactosidase that degrades neuroprotective and anti-inflammatory GM1, to produce pro-inflammatory GM2, resulting in chronic inflammation and microglia-mediated neurodegeneration. However, this is a hypothesis that requires testing *in vivo*.

Overall, we have shown that activated microglia can release β-galactosidase, and extracellular β-galactosidase can induce neuronal loss via microglia, such that inhibiting β-galactosidase can prevent inflammatory neuronal loss in culture. Thus, extracellular β-galactosidase is a potential target to prevent neurodegeneration induced by inflammation or aging.

Data availability statement

The original contributions presented in this study are included in this article/**Supplementary material**, further inquiries can be directed to the corresponding author.

Ethics statement

The animal study was approved by the University of Cambridge Animal Welfare and Ethical Review Board. The study was conducted in accordance with the local legislation and institutional requirements.

Author contributions

EK: Formal analysis, Investigation, Methodology, Visualization, Writing – original draft, Writing – review & editing. JD: Investigation, Writing – review & editing. GB: Conceptualization, Supervision, Writing – original draft, Writing – review & editing.

Funding

The authors declare financial support was received for the research, authorship, and/or publication of this article. This work received funding from the Biotechnology and Biological Sciences Research Council UK (BBSRC BB/M011194/1 and BB/T508160/1).

Acknowledgments

We gratefully acknowledge the Cambridge Advanced Imaging Centre for their support and assistance in this work. We thank Leanne Dundee for the creation of the graphical abstract.

Conflict of interest

The authors declare that the research was conducted in the absence of any commercial or financial relationships that could be construed as a potential conflict of interest.

Publisher's note

All claims expressed in this article are solely those of the authors and do not necessarily represent those of their affiliated organizations, or those of the publisher, the editors and the reviewers. Any product that may be evaluated in this article, or claim that may be made by its manufacturer, is not guaranteed or endorsed by the publisher.

Supplementary material

The Supplementary Material for this article can be found online at: https://www.frontiersin.org/articles/10.3389/fnagi.2023.1327756/full#supplementary-material

References

Allendorf, D. H., and Brown, G. C. (2022). Neu1 is released from activated microglia, stimulating microglial phagocytosis and sensitizing neurons to glutamate. *Front. Cell. Neurosci.* 16:267. doi: 10.3389/fncel.2022.917884

Allendorf, D. H., Puigdellívol, M., and Brown, G. C. (2020). Activated microglia desialylate their surface, stimulating complement receptor 3-mediated phagocytosis of neurons. *Glia* 68, 989–998. doi: 10.1002/glia.23757

Aureli, M., Masilamani, A. P., Illuzzi, G., Loberto, N., Scandroglio, F., Prinetti, A., et al. (2009). Activity of plasma membrane β-galactosidase and β-glucosidase. *FEBS Lett.* 583, 2469–2473. doi: 10.1016/j.febslet.2009.06.048

Birkle, T. J. Y., and Brown, G. C. (2023). Syk inhibitors protect against microglia-mediated neuronal loss in culture. *Front. Aging Neurosci.* 15:1120952. doi: 10.3389/fnagi.2023.1120952

Blasi, E., Barluzzi, R., Bocchini, V., Mazzolla, R., and Bistoni, F. (1990). Immortalization of murine microglial cells by a v-raf / v-myc carrying retrovirus. *J. Neuroimmunol.* 27, 229–237. doi: 10.1016/0165-5728(90)90073-V

Bonten, E. J., Annunziata, I., and D'Azzo, A. (2014). Lysosomal multienzyme complex: pros and cons of working together. *Cell. Mol. Life Sci.* 71, 2017–2032. doi: 10.1007/s00018-013-1538-3

Borgonetti, V., and Galeotti, N. (2022). Rosmarinic acid reduces microglia senescence: a novel therapeutic approach for the management of neuropathic pain symptoms. *Biomedicines* 10:1468. doi: 10.3390/biomedicines10071468

Bussian, T. J., Aziz, A., Meyer, C. F., Swenson, B. L., van Deursen, J. M., and Baker, D. J. (2018). Clearance of senescent glial cells prevents tau-dependent pathology and cognitive decline. *Nature* 562, 578–582. doi: 10.1038/s41586-018-0543-y

Cao, D., Li, X. H., Luo, X. G., Yu, H. M., Wan, L. S., Wei, L., et al. (2020). Phorbol myristate acetate induces cellular senescence in rat microglia in vitro. *Int. J. Mol. Med.* 46, 415–426. doi: 10.3892/ijmm.2020.4587

Carrillo-Jimenez, A., Puigdellívol, M., Vilalta, A., Venero, J. L., Brown, G. C., StGeorge-Hyslop, P., et al. (2018). Effective knockdown of gene expression in primary microglia with siRNA and magnetic nanoparticles without cell death or inflammation. *Front. Cell. Neurosci.* 12:313. doi: 10.3389/fncel.2018.00313

Chowdhury, S., and Ledeen, R. (2022). The key role of GM1 ganglioside in Parkinson's disease. *Biomolecules* 12:173. doi: 10.3390/biom12020173

Cockram, T. O. J., Dundee, J. M., Popescu, A. S., and Brown, G. C. (2021). The phagocytic code regulating phagocytosis of mammalian cells. *Front. Immunol.* 12:629979. doi: 10.3389/fimmu.2021.629979

Conroy, S. M., Nguyen, V., Quina, L. A., Blakely-Gonzales, P., Ur, C., Netzeband, J. G., et al. (2004). Interleukin-6 produces neuronal loss in developing cerebellar granule neuron cultures. *J. Neuroimmunol.* 155, 43–54. doi: 10.1016/j.jneuroim.2004.06.014

De Lella Ezcurra, A. L., Chertoff, M., Ferrari, C., Graciarena, M., and Pitossi, F. (2010). Chronic expression of low levels of tumor necrosis factor-α in the substantia nigra elicits progressive neurodegeneration, delayed motor symptoms and microglia/macrophage activation. *Neurobiol. Dis.* 37, 630–640. doi: 10.1016/j.nbd.2009.11.018

Dimri, G. P., Lee, X., Basile, G., Acosta, M., Scott, G., Roskelley, C., et al. (1995). A biomarker that identifies senescent human cells in culture and in aging skin in vivo. *Proc. Natl. Acad. Sci. U.S.A.* 92, 9363–9367. doi: 10.1073/pnas.92.20.9363

Dundee, J. M., Puigdellívol, M., Butler, R., Cockram, T. O. J., and Brown, G. C. (2023). P2Y6 receptor-dependent microglial phagocytosis of synapses mediates synaptic and memory loss in aging. *Aging Cell* 22, 1–14. doi: 10.1111/acel.13761

Galleguillos, D., Wang, Q., Steinberg, N., Zaidi, A., Shrivastava, G., Dhami, K., et al. (2022). Anti-inflammatory role of GM1 and other gangliosides on microglia. *J. Neuroinflamm.* 19, 1–18. doi: 10.1186/s12974-021-02374-x

Greenwood, E. K., and Brown, D. R. (2021). Senescent microglia: the key to the ageing brain? *Int. J. Mol. Sci* 22, 4402. doi: 10.3390/ijms22094402

Jaiswal, J. K., Andrews, N. W., and Simon, S. M. (2002). Membrane proximal lysosomes are the major vesicles responsible for calcium-dependent exocytosis in nonsecretory cells. *J. Cell Biol.* 159, 625–635. doi: 10.1083/jcb.200208154

Kinsner, A., Pilotto, V., Deininger, S., Brown, G. C., Coecke, S., Hartung, T., et al. (2005). Inflammatory neurodegeneration induced by lipoteichoic acid from *Staphylococcus aureus* is mediated by glia activation, nitrosative and oxidative stress, and caspase activation. *J. Neurochem.* 95, 1132–1143. doi: 10.1111/j.1471-4159.2005.03422.x

Kracun, I., Kalanj, S., Talan-Hranilovic, J., and Cosovic, C. (1992). Cortical distribution of gangliosides in Alzheimer's disease. *Neurochem. Int.* 20, 433–438. doi: 10.1016/0197-0186(92)90058-Y

Kurz, D. J., Decary, S., Hong, Y., and Erusalimsky, J. D. (2000). Senescence-associated β-galactosidase reflects an increase in lysosomal mass during replicative ageing of human endothelial cells. *J. Cell Sci.* 113, 3613–3622. doi: 10.1242/jcs.113.20.3613

Lee, B. Y., Han, J. A., Im, J. S., Morrone, A., Johung, K., Goodwin, E. C., et al. (2006). Senescence-associated β-galactosidase is lysosomal β-galactosidase. *Aging Cell* 5, 187–195. doi: 10.1111/j.1474-9726.2006.00199.x

Li, Y. T., and Li, S. C. (1999). Enzymatic hydrolysis of glycosphingolipids. *Anal. Biochem.* 273, 1–11. doi: 10.1006/abio.1999.4191

Liu, J., Hong, Z., Ding, J., Liu, J., Zhang, J., and Chen, S. (2008). Predominant release of lysosomal enzymes by newborn rat microglia after LPS treatment revealed by proteomic studies. *J. Proteome Res.* 7, 2033–2049. doi: 10.1021/pr7007779

Magini, A., Polchi, A., Tozzi, A., Tancini, B., Tantucci, M., Urbanelli, L., et al. (2015). Abnormal cortical lysosomal β-hexosaminidase and β-galactosidase activity at post-synaptic sites during Alzheimer's disease progression. *Int. J. Biochem. Cell Biol.* 58, 62–70. doi: 10.1016/j.biocel.2014.11.001

Magini, A., Polchi, A., Urbanelli, L., Cesselli, D., Beltrami, A., Tancini, B., et al. (2013). TFEB activation promotes the recruitment of lysosomal glycohydrolases β-hexosaminidase and β-galactosidase to the plasma membrane. *Biochem. Biophys. Res. Commun.* 440, 251–257. doi: 10.1016/j.bbrc.2013.09.060

Mander, P. K., Jekabsone, A., and Brown, G. C. (2006). Microglia proliferation is regulated by hydrogen peroxide from NADPH oxidase1. *J. Immunol.* 176, 1046–1052. doi: 10.4049/jimmunol.176.2.1046

Martínez-Cué, C., and Rueda, N. (2020). Cellular senescence in neurodegenerative diseases. *Front. Cell. Neurosci.* 14:16. doi: 10.3389/fncel.2020.00016

Matsudaira, T., Nakano, S., Konishi, Y., Kawamoto, S., Uemura, K., Kondo, T., et al. (2023). Cellular senescence in white matter microglia is induced during ageing in mice and exacerbates the neuroinflammatory phenotype. *Commun. Biol.* 6:665. doi: 10.1038/s42003-023-05027-2

Mizutani, K., Oka, N., Akiguchi, I., Satoi, H., Kawasaki, T., Kaji, R., et al. (1999). Enhancement of TNF-α production by ganglioside GM2 in human mononuclear cell culture. *Neuroreport* 10, 703–706. doi: 10.1097/00001756-199903170-00008

Neher, J. J., Neniskyte, U., Hornik, T., and Brown, G. C. (2014). Inhibition of UDP/P2Y6 purinergic signaling prevents phagocytosis of viable neurons by activated microglia in vitro and in vivo. *Glia* 62, 1463–1475. doi: 10.1002/glia.22693

Neher, J. J., Neniskyte, U., Zhao, J.-W., Bal-Price, A., Tolkovsky, A. M., and Brown, G. C. (2011). Inhibition of microglial phagocytosis is sufficient to prevent inflammatory neuronal death. *J. Immunol.* 186, 4973–4983. doi: 10.4049/jimmunol.1003600

Neniskyte, U., Vilalta, A., and Brown, G. C. (2014). Tumour necrosis factor alpha-induced neuronal loss is mediated by microglial phagocytosis. *FEBS Lett.* 588, 2952–2956. doi: 10.1016/j.febslet.2014.05.046

Perry, V. H., Nicoll, J. A. R., and Holmes, C. (2010). Microglia in neurodegenerative disease. *Nat. Rev. Neurol.* 6, 193–201. doi: 10.1038/nrneurol.2010.17

Puigdellívol, M., Allendorf, D. H., and Brown, G. C. (2020). Sialylation and galectin-3 in microglia-mediated neuroinflammation and neurodegeneration. *Front. Cell. Neurosci.* 14:162. doi: 10.3389/fncel.2020.00162

Reddy, A., Caler, E. V., and Andrews, N. W. (2001). Plasma membrane repair is mediated by Ca2+-regulated exocytosis of lysosomes. *Cell* 106, 157–169. doi: 10.1016/S0092-8674(01)00421-4

Schneider, J. S., Gollomp, S. M., Sendek, S., Colcher, A., Cambi, F., and Du, W. (2013). A randomized, controlled, delayed start trial of GM1 ganglioside in treated Parkinson's disease patients. *J. Neurol. Sci.* 324, 140–148. doi: 10.1016/j.jns.2012.10.024

Shen, X., Burguillos, M. A., Osman, A. M., Frijhoff, J., Carrillo-Jiménez, A., Kanatani, S., et al. (2016). Glioma-induced inhibition of caspase-3 in microglia promotes a tumor-supportive phenotype. *Nat. Immunol.* 17, 1282–1290. doi: 10.1038/ni.3545

Smith, J. A., Das, A., Ray, S. K., and Banik, N. L. (2012). Role of pro-inflammatory cytokines released from microglia in neurodegenerative diseases. *Brain Res. Bull.* 87, 10–20. doi: 10.1016/j.brainresbull.2011.10.004

Stirling, D. R., Carpenter, A. E., and Cimini, B. A. (2021a). CellProfiler Analyst 3.0: accessible data exploration and machine learning for image analysis. *Bioinformatics* 37, 3992–3994. doi: 10.1093/bioinformatics/btab634

Stirling, D. R., Swain-Bowden, M. J., Lucas, A. M., Carpenter, A. E., Cimini, B. A., and Goodman, A. (2021b). CellProfiler 4: improvements in speed, utility and usability. *BMC Bioinform.* 22:433. doi: 10.1186/s12859-021-04344-9

Thameem Dheen, S., Kaur, C., and Ling, E.-A. (2007). Microglial activation and its implications in the brain diseases. *Curr. Med. Chem* 14, 1189–1197. doi: 10.2174/092986707780597961

van Dijk, K. D., Persichetti, E., Chiasserini, D., Eusebi, P., Beccari, T., Calabresi, P., et al. (2013). Changes in endolysosomal enzyme activities in cerebrospinal fluid of patients with Parkinson's disease. *Mov. Disord.* 28, 747–754. doi: 10.1002/mds.25495

Van Zeller, M., Sebastião, A. M., and Valente, C. A. (2022). Microglia depletion from primary glial cultures enables to accurately address the immune response of astrocytes. *Biomolecules* 12:666. doi: 10.3390/biom12050666

Wu, G., Lu, Z. H., Kulkarni, N., and Ledeen, R. W. (2012). Deficiency of ganglioside GM1 correlates with Parkinson's disease in mice and humans. *J. Neurosci. Res.* 90, 1997–2008. doi: 10.1002/jnr.23090

Xiao, X., Feng, Y. P., Du, B., Sun, H. R., Ding, Y. Q., and Qi, J. G. (2017). Antibody incubation at 37°c improves fluorescent immunolabeling in free-floating thick tissue sections. *Biotechniques* 62, 115–122. doi: 10.2144/000114524

Yu, H. M., Zhao, Y. M., Luo, X. G., Feng, Y., Ren, Y., Shang, H., et al. (2012). Repeated lipopolysaccharide stimulation induces cellular senescence in BV2 cells. *Neuroimmunomodulation* 19, 131–136. doi: 10.1159/000330254

Zhu, K., Wang, Y., Sarlus, H., Geng, K., Nutma, E., Sun, J., et al. (2022). Myeloid cell-specific topoisomerase 1 inhibition using DNA origami mitigates neuroinflammation. *EMBO Rep.* 23:e54499. doi: 10.15252/embr.202154499

frontiers | Frontiers in Aging Neuroscience

TYPE Original Research
PUBLISHED 15 January 2024
DOI 10.3389/fnagi.2023.1294879

OPEN ACCESS

EDITED BY
Bogdan O. Popescu,
Carol Davila University of Medicine and Pharmacy, Romania

REVIEWED BY
Yutaka Oji,
Juntendo University, Japan
Caroline Haikal,
NewYork-Presbyterian, United States

*CORRESPONDENCE
Chang-he Shi
✉ shichanghe@gmail.com

†These authors have contributed equally to this work

RECEIVED 15 September 2023
ACCEPTED 31 December 2023
PUBLISHED 15 January 2024

CITATION
Wang H-l, Wang Z-y, Tian J, Ma D-r and Shi C-h (2024) Association between inflammatory bowel disease and Parkinson's disease: a prospective cohort study of 468,556 UK biobank participants. *Front. Aging Neurosci.* 15:1294879. doi: 10.3389/fnagi.2023.1294879

Association between inflammatory bowel disease and Parkinson's disease: a prospective cohort study of 468,556 UK biobank participants

Hai-li Wang[1†], Zhi-yun Wang[2†], Jie Tian[3†], Dong-rui Ma[2] and Chang-he Shi[2*]

[1]Department of Surgery ICU, The First Affiliated Hospital of Zhengzhou University, Zhengzhou University, Zhengzhou, Henan, China, [2]Department of Neurology, The First Affiliated Hospital of Zhengzhou University, Zhengzhou University, Zhengzhou, Henan, China, [3]Zhengzhou Railway Vocational and Technical College, Zhengzhou, Henan, China

Introduction: Inflammatory Bowel Disease (IBD) and Parkinson's disease (PD) are both chronic, progressive disorders. As such, given the inconclusive results of extensive research on the association between IBD and PD, our study intends to examine this relationship further using the UK Biobank database.

Methods: We conducted a prospective cohort study using the Cox proportional hazards model, analyzing data from the UK Biobank to investigate the relationship between IBD and PD, following subjects until PD diagnosis, loss to follow up, death or study termination on 30 June, 2023.

Results: The results show that IBD had no effect on the risk of PD (HR: 1.356, 95% CI: 0.941–1.955, $p = 0.103$), and the effect remained consistent in specific Crohn's disease, ulcerative colitis or unclassified IBD populations. In addition, after sensitivity analysis using propensity matching scores and excluding patients diagnosed with PD 5 or 10 years after baseline, IBD had no effect on the risk of PD. However, in the subgroup analysis, we found that in females (HR: 1.989, 95% CI: 1.032–3.835, $p = 0.040$), the polygenic risk score was highest (HR: 2.476, 95% CI: 1.401–4.374, $p = 0.002$), and having ulcerative colitis without hypertension (HR: 2.042, 95% CI: 1.128–3.697, $p = 0.018$) was associated with an increased risk of PD.

Conclusion: In conclusion, over an average follow-up period of 13.93 years, we found no significant association between IBD and PD.

KEYWORDS

Parkinson's disease, inflammatory bowel disease, prospective cohort study, propensity score matching, polygenic risk score

1 Introduction

Parkinson's disease (PD) ranks as the second-most prevalent neurodegenerative disorder globally (Tolosa et al., 2021). With the anticipated influx of elder populations, both the prevalence and associated global healthcare burden of PD are expected to rise substantially (Collaborators, 2019). Classified as a multifactorial condition, PD emerged from the

interaction of genetic predispositions, environmental factors, and immune mechanisms. In addition to being characterized by motor symptoms, including resting tremor, bradykinesia, muscular rigidity, and postural instability (Hawkes et al., 2007), a range of non-motor manifestations, including gastrointestinal dysfunction, anxiety, and insomnia, have been observed to precede the onset of the aforementioned motor symptoms in PD by several years (Gallagher et al., 2010). The hallmark features of PD include the progressive loss of dopaminergic neurons within the substantia nigra and the emergence of Lewy bodies, which are aggregates primarily composed of abnormally folded α-synuclein (α-syn) (Kalia and Lang, 2015). Intriguingly, Lewy bodies have been observed to manifest at early stages within the gastrointestinal tract of individuals diagnosed with PD, thereby lending credence to existing theories regarding gastrointestinal origins of the disease (Guarino et al., 2008; Lebouvier et al., 2010; Shannon et al., 2012). According to Braak's pioneering hypothesis, the gastrointestinal tract is proposed as the initial site of PD pathogenesis, where an unidentified pathogen penetrates the gastric mucosal barrier, initiating the aggregation of α-syn. Subsequently, this aggregation is believed to propagate to the central nervous system via the vagus nerve in a manner akin to prions, traveling retrograde along neuronal axons, ascending from the lower brain stem through the medulla oblongata and midbrain, and eventually reaching the cerebral cortex (Braak et al., 2003). Significant changes in the gut microbiome (Rogers et al., 2016; Cryan et al., 2019; Morais et al., 2021), which is crucial to the gut-brain axis and observed in both PD and Inflammatory Bowel Disease (IBD) (Burokas et al., 2015; Weingarden and Vaughn, 2017; Lee et al., 2021; Wang et al., 2021), suggest a potential impact on the progression of these conditions, lending further support to this hypothesis.

IBD is characterized by chronic, recurrent inflammation of the intestines (Zhang, 2014), encompassing ulcerative colitis (UC) and Crohn's disease (CD) (Harris and Chang, 2018; Younis et al., 2020). The etiology of IBD is considered multifactorial, likely stemming from the complex interplay among genetic predisposition, environmental influences, and altered gut microbiota (Torres et al., 2017), all of which contribute to dysregulation in both innate and adaptive immune responses, contributing to the current upward trajectory of IBD (Larsen et al., 2023). Individuals diagnosed with PD demonstrate an increase in pro-inflammatory factors within the gastrointestinal tract. Both IBD and PD exhibit similar alterations in gut microbiota, including changes in key bacterial communities and reduced butyrate levels, which in turn contribute to the impairment of intestinal mucosal integrity (Romano et al., 2021). Mutations in leucine-rich repeat kinase 2 (LRRK2), which are associated with PD (Myasnikov et al., 2021), have also recently been reported to connected with IBD (Lee et al., 2021). In addition to gastrointestinal symptoms, IBD can also cause neurological effects in both the central and peripheral nervous systems, potentially coinciding with such conditions as PD, Multiple Sclerosis, and stroke (Ferro and Oliveira, 2021). Furthermore, the observed correlation between IBD and PD, particularly in terms of genetic overlap, inflammatory processes, and intestinal permeability, may suggest a link between the two conditions (Devos et al., 2013; Li et al., 2021).

Utilizing participant data from the UK Biobank, we conducted a large-scale prospective cohort study employing Cox proportional hazard model to investigate the association between IBD and PD. In addition, propensity score matching (PSM) was implemented to adjust for confounding variables and to mitigate their interference in the analysis (Figure 1). Consequently, after excluding participants who developed PD within 5 or 10 years following the baseline, the data were subsequently reanalyzed.

2 Materials and methods

2.1 Study population

The UK Biobank is a large prospective cohort study that collected genetic, physical and health data from more than 500,000 participants aged 40 to 69 from 22 assessment centers across the UK between 2006 and 2010, with a response rate of 5.47 percent. The richness and comprehensiveness of the data enable investigators to conduct an extensive array of epidemiological research, and we can browse the data of UK Biobank through its website.[1] In addition, the UK Biobank study was approved by the Northwest Multi-Center Research Ethics Committee, and all participants signed written informed consent.

Among all 502,364 participants in the UK Biobank study, we first excluded participants ($n = 49,535$) with other gastrointestinal diseases (Supplementary Table 1). Further, after calculating the time interval between PD or IBD diagnosis and inclusion in the study, we further excluded participants who had PD at the baseline ($n = 804$) and who were diagnosed with IBD during the follow-up period ($n = 1,846$), so all IBD patients were diagnosed before baseline and participants were diagnosed with PD during follow-up, establishing that all recorded instances of PD transpired subsequent to an IBD diagnosis. Finally, we excluded participants with incomplete baseline data ($n = 25,067$), leaving 425,112 participants in total to be included in the final study.

2.2 Definition of IBD and PD

IBD, encompassing CD (K50) and UC (K51), along with PD (G20), was identified based on the International Classification of Diseases, Tenth Revision (ICD-10) codes. The diagnostic records were sourced from primary care databases, self-reported medical histories and hospital admission records, and we divided the participants into a healthy control group and an IBD group. Thereafter, the IBD group was further categorized into three distinct subgroups based on specific diagnostic criteria: "CD", "UC", and "IBD-U", where the latter refers to participants diagnosed with both CD and UC concurrently.

2.3 Covariates

In the baseline characteristics section, information on participants' age (a continuous variable), gender (male/female), and Townsend Deprivation Index score (a continuous variable) is available. The Townsend Deprivation Index is calculated based on the most recent national census output areas, employing the postal codes available at the time of participant enrolment in the UK Biobank study. This provides a corresponding deprivation score for

1 https://biobank.ndph.ox.ac.uk/

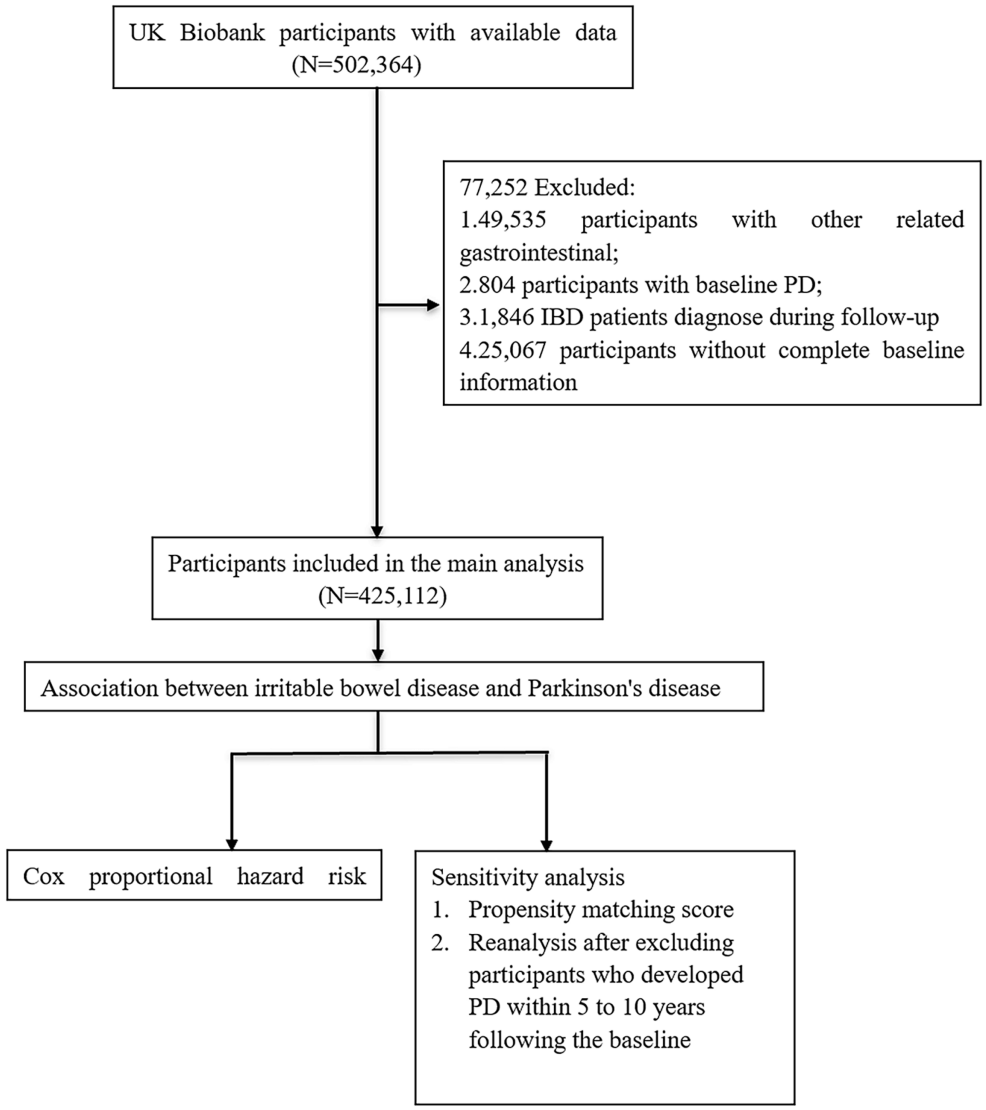

FIGURE 1
Analytical workflow for the research. PD, Parkinson's disease; IBD, inflammatory bowel disease.

each respective geographic location, offering a measure for assessing the level of socioeconomic deprivation in a population, where higher index values indicate greater socioeconomic deprivation. The data collected via the Assessment Centre's touchscreen interface also include such variables such as ethnicity (White/Non-White), education level (University/Non-University), smoking status (Never/Previous/Current), and frequency of alcohol intake (0/1/2/3/4), where scoring for the latter is determined as follows: '0' denotes abstinence or drinking only on special occasions; "1" indicates 1–3 instances per month; "2" suggests 1–2 instances per week; "3" implies 3–4 instances per week; and "4" represents daily or near-daily consumption. Regarding education level, we define a "university" education as possessing a "college or university degree", whereas all other categories are defined as "non-university". In addition, covariates also include Body Mass Index (BMI, a continuous variable) as well as the presence of diabetes (coded as E10-E14) and hypertension (coded as I10-I15) based on the ICD-10 classifications.

In addition, the UK Biobank contains polygenic risk scores (PRSs) for 25 quantitative traits and 25 diseases, demonstrating a good and stable performance in predicting individual disease risk (Lewis and Vassos, 2020). The PRS serves as an effective tool for clinical risk prediction, functioning by evaluating individual variations in multiple genetic loci to predict the risk of specific diseases (Lu et al., 2022), where the higher the score, the greater the risk of developing related diseases. We used the Standard PRS for PD to assess an individua's risk of developing PD at the genetic level, and risk categories were stratified among all 502,364 participants, the top 25% of whom were defined as low risk, 25–75% as moderate risk, and the bottom 25% as high risk. Ultimately, we included 11 covariates in total.

2.4 Statistical analysis

Continuous variables of the baseline characteristics are presented as means and standard deviations, and categorical variables are

presented as percentages. For continuous variables, the analysis of variance was used, while for categorical variables, the chi-square test was used to compare the baseline characteristics of the two groups, and a baseline table was drawn.

Cox proportional hazards models were used to test the association between IBD and PD, with end point events including the first PD diagnosis, loss to follow-up, death or end of the study (June 2023), after which, the time interval from baseline to end point events was calculated. In our analysis, the hazard ratio (HR) value of the first level of the categorical variables was normalized to 1, serving as a reference for comparison with other levels. Then, we performed a survival analysis of the healthy control and IBD groups, drew survival curves using the Kaplan–Meier method and used the Log-rank test to examine the difference. Univariate Cox regression analysis was conducted to include variables that were statistically significant, which were then incorporated into a multivariate Cox regression model, and forest plots were drawn. Three multivariate Cox regression models were further constructed: Model 1 adjusted for age, gender, and ethnicity; Model 2 incorporated additional variables, including education level, frequency of alcohol consumption, smoking status and BMI; Model 3 included all 11 covariates for a comprehensive analysis. In the multivariate Cox regression analysis, we compared the incidence of PD among CD, UC and IBD-U and healthy controls, respectively. In addition, an interaction term between IBD status and PRS was created to examine whether the risk of PD is modified when genetic predisposition are considered. Further stratified analyses were performed by age and categorical variable to explore how the relationship between IBD status and PD risk might vary across subgroups. Finally, a sensitivity analysis was performed using PSM (nearest neighbor ratio of 1:1 without replacement and a caliper width of 0.02) to ensure robustness of the findings after adjusting for confounding factors. In addition, prodromal symptoms of PD, such as REM sleep behavior disorder, olfaction dysfunction, and autonomic nerve impairment, often appear years before a formal clinical diagnosis, so it is possible that some PD patients were prodromal at baseline and were assigned to be healthy controls (Berg et al., 2021). Then after excluding participants who developed PD within 5 to 10 years following the baseline, we re-conducted our analysis using multivariable Cox regression models. The Schoenfeld residual test was used to validate the proportional hazards assumption, and all statistical analyses were executed in R version 4.3.0, with $p < 0.05$ considered significant.

3 Results

3.1 Baseline characteristics

In the present study, 425,112 participants in total were included, comprising 421,825 individuals in the healthy control group and 3,287 patients in the IBD group (Supplementary Table 2). The latter group included 956 individuals with CD, 1,980 with UC, and 351 with IBD-U, whereas 29 participants from the IBD cohort were diagnosed with PD during the follow-up period. Over an average follow-up period of 13.92 years, there were 2,821 newly diagnosed cases of PD; however, no statistically significant differences were observed between the two groups in terms of gender, Townsend Deprivation Index or PRS. The proportion of White individuals (96.8% vs. 94.8%) and those with a non-university education level (70.3% vs. 66.5%) was higher in the IBD group compared to the healthy control group, which exhibited a larger proportion of individuals who never smoked (55.4% vs. 47.8%) and had a higher frequency of alcohol consumption (20.7% vs. 18.4%) compared to the IBD group. Moreover, within the healthy control group, a greater percentage of participants were without diabetes (91.8% vs. 88.9%) and hypertension (70.3% vs. 65.6%).

3.2 Association between IBD and PD

Based on the Kaplan–Meier method, during an average follow-up period of 13.93 years, there was no significant difference in the risk of developing PD between the healthy control group and the IBD group (Log-rank: $p = 0.1$) (Figure 2). Further, the Schoenfeld residual test indicated that the proportional hazards assumption was met in both groups. According to the results of the univariate Cox regression analysis (Figure 3), the IBD group exhibited an elevated but statistically non-significant risk of developing PD compared to the healthy control group (HR: 1.356, 95% CI: 0.941–1.955, $p = 0.103$), whereas in the three IBD subgroups (CD, UC, and IBD-U), we independently investigated their respective associations with PD employing multivariable Cox regression models for each subgroup, and consistent conclusions were obtained across all three categories.

The subgroup analysis (Figure 4) revealed that within the overall IBD population, the risk of developing PD was elevated among females, those categorized at a high risk of PRS and participants without a history of hypertension and diabetes. The presence of IBD amplified the risk of PD in these specific subgroups. Consequently, we further examined the risk of developing PD within the UC (Supplementary Figure 1) and CD (Supplementary Figure 2) populations. Our findings suggest that the occurrence of PD was not influenced by the presence of CD. However, among UC patients, we still observed an increased risk of PD among females, those categorized as "High Risk" in the PRS, and individuals without hypertension. Nonetheless, the interaction term created to examine the effects of having CD (Figure 5) or UC (Figure 6) along with the genetic risk did not yield significant results for interactive effects.

The sensitivity analysis was conducted utilizing PSM to attenuate the impact of confounding variables. The 1:1 matching was successfully executed for all 3,287 participants (Supplementary Table 3). Aside from drinking frequency and BMI, no statistically significant difference was observed in the baseline characteristics between the matched healthy control and IBD groups. In addition, a subsequent survival analysis revealed that even among the matched cohorts, there remained no statistically significant divergence in the risk of developing PD between the two groups (Supplementary Figure 3). In addition, upon excluding patients who were diagnosed with PD within 5 ($n = 411$) or 10 years ($n = 1,576$) of the baseline, our analysis also did revealed no connection between IBD and PD (Supplementary Tables 4, 5), which might suggest that even when considering a longer period prior to diagnosis, there is no association between IBD and PD.

4 Discussion

Throughout disease progression, the motor symptoms (tremor, myotonia, motor retardation and postural balance disorders, etc.) and

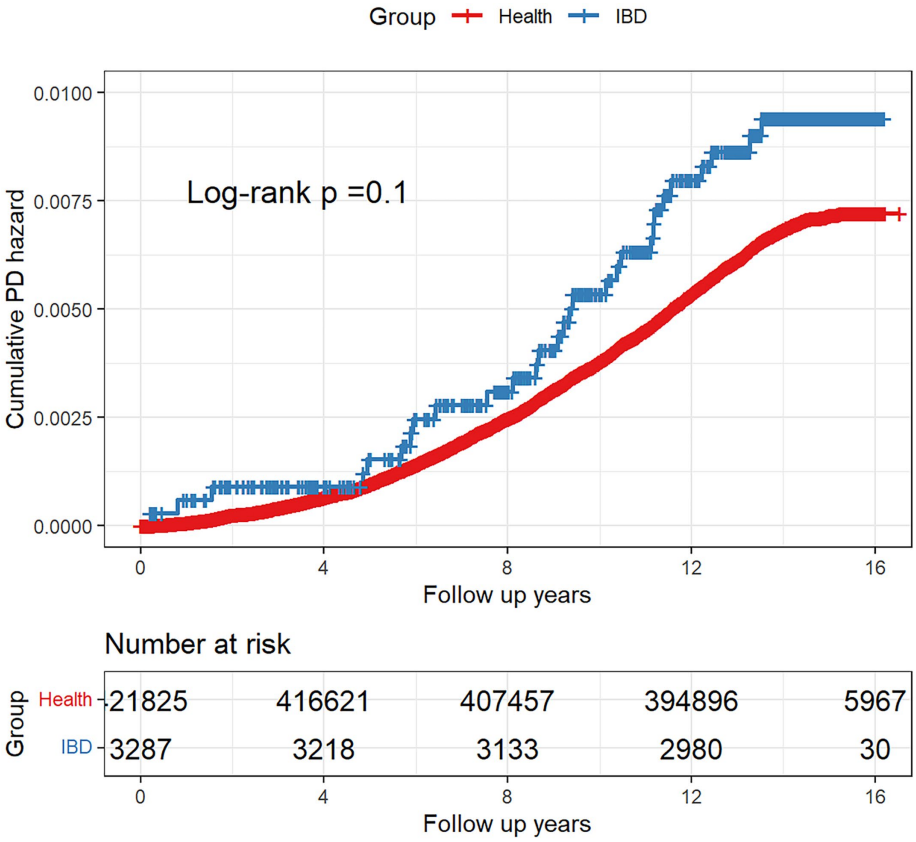

FIGURE 2
Kaplan–Meier plot for the cumulative probability of PD risk.

non-motor symptoms (sleep disorders, autonomic nervous dysfunction, mental and behavioral abnormalities, etc.) of PD will gradually increase, seriously affecting the quality of life of PD patients (Santos Garcia et al., 2021). Meanwhile, IBD encompasses two primary subtypes: CD and UC (Miyoshi and Chang, 2017), where the latter restricted to the colon, characterized by superficial mucosal inflammation that extends continuously proximally, potentially resulting in ulcers, significant bleeding, and toxic megacolon. In contrast, CD can affect any part of the digestive tract and is typically marked by discontinuous lesions. Its hallmark is transmural inflammation, which can lead to complications such as fibrosis, stenosis, fistulae and abscesses (Khor et al., 2011; Wright et al., 2018). Pathophysiological changes in the gastrointestinal system have also been implicated in the onset of PD (Böttner et al., 2012; Fasano et al., 2015), where, increasingly, empirical evidence supports the hypothesis that PD may have its etiological origins in the gastrointestinal tract (Sampson et al., 2016; Knudsen et al., 2018). Beyond the potential common risk gene LRRK2, a genome-wide association study (GWAS) identified an overlap of seven genes presenting a risk for PD with CD (MROH3P, HLA, CCNY, LRRK2, APT, SYMPK and RSPH6A) and four with UC (GUCY1A3, HLA, BTNL2 and TRIM10, Witoelar et al., 2017). Biological pathways involving gut microbiota, autoimmunity, mitochondrial functionality, autophagy and lysosomal activity may forge a close connection between IBD and PD (Lee et al., 2021), but despite the inconclusive role of IBD in predisposing individuals to PD in the present study cohort, the association between these two disorders remains an open question warranting further investigation.

During the 13.93-year follow-up period in this study, 2,821 new cases of PD in total were diagnosed. In response, a univariate Cox regression analysis indicated no significant association between IBD and PD (HR:1.356, 95% CI: 0.941–1.955, $p = 0.103$). When further dissecting the IBD group into CD, UC, and IBD-U, no significant relationships with PD were observed, findings that are consistent even after adjusting for confounding variables across three distinct multivariate models. IBD and PD also show marked differences in clinical presentations among different genders (Cerri et al., 2019). Nonetheless, in subgroup analyses, distinct populations with IBD showed an elevated risk of PD, especially females (HR: 1.855, 95% CI: 1.094–3.143, $p = 0.022$). Based on previous research, UC is more prevalent in male patients (Goodman et al., 2020), while in the case of PD the incidence rate in males is more than double that in females. The reasons for the observed increase in PD risk among females remain unclear, but similarly, in two analogous studies that performed subgroup analyses, an elevated incidence of PD was noted among female with IBD (Park et al., 2019; Villumsen et al., 2019). Existing studies present an inconclusive correlation between hypertension and PD risk (Paganini-Hill, 2001; Ng et al., 2021), the use of antihypertensive agents, specifically calcium channel blockers (Becker et al., 2008), has been implicated in reducing the incidence of PD. Meanwhile, diabetes might elevate the risk of PD (Hu et al., 2007; Pagano et al., 2018), but this association appears to be potentially

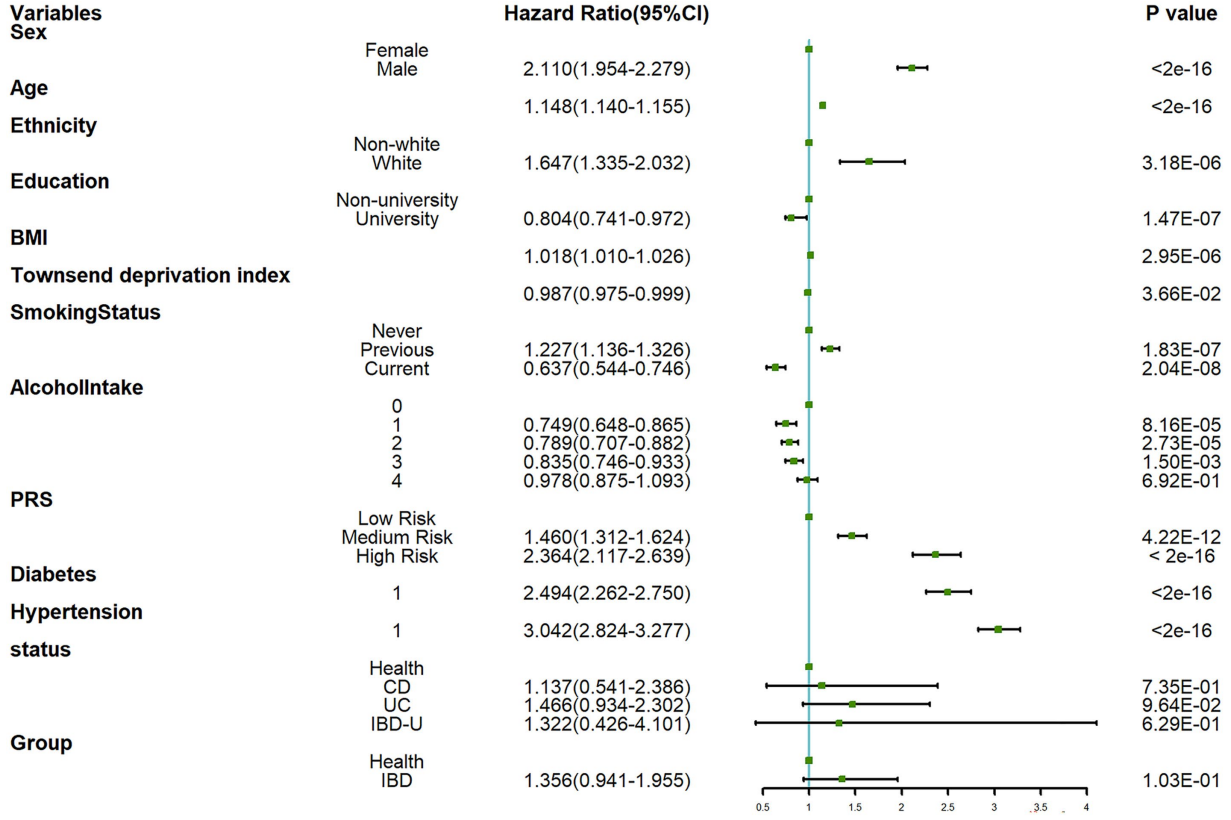

FIGURE 3
Forest plot for univariate Cox regression analysis.

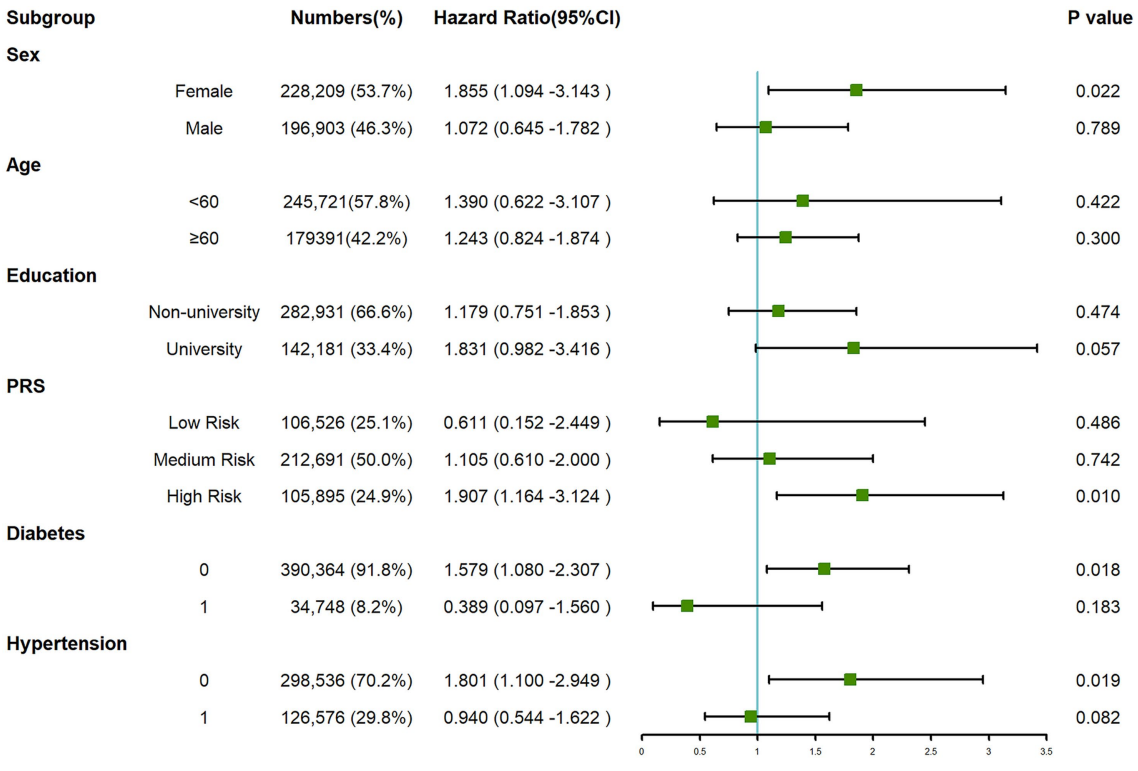

FIGURE 4
Forest plot for subgroup analysis between IBD and PD.

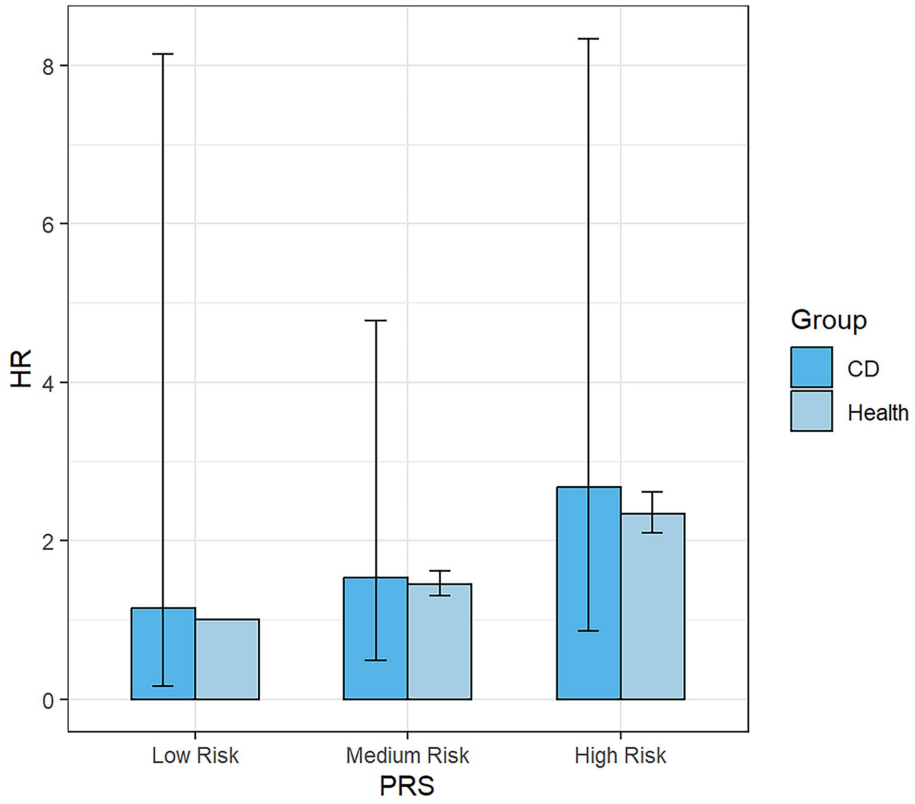

FIGURE 5
Bar Chart for the impact of the interaction term created by UC status and PRS on the risk of PD. UC, ulcerative colitis; PRS, polygenic risk score.

linked to BMI (Foltynie and Athauda, 2020). In our research, those without hypertension (HR: 1.801, 95% CI: 1.100–2.949, $p = 0.019$) or diabetes (HR: 1.579, 95% CI: 1.080–2.307, $p = 0.018$) also face an increased risk, possibly indicating that unique inflammatory or immune pathways in IBD contribute to neurodegenerative changes. The specific mechanisms remain unclear, warranting further investigation, but nterestingly, this elevated risk was not observed in the CD subgroup, despite remaining significant in the UC subgroup.

Our findings are consistent with several previous studies. For instance, existing Mendelian randomization studies do not support a causal relationship between UC, CD, and PD (Freuer and Meisinger, 2022; Li and Wen, 2022; Zeng et al., 2023). Further, one cross-sectional study found no difference in the co-occurrence of PD between IBD patients and non-IBD controls (Bahler et al., 2017), whereas a nationwide epidemiological survey from Sweden examined the risk of developing PD subsequent to autoimmune diseases and found that neither CD nor UC increased the incidence of subsequent PD diagnosis (Li et al., 2012). Another nationwide cohort study in Sweden from 2002 to 2004, which included 39,652 IBD participants, suggested that UC increases the risk of PD (HR: 1.3, 95% CI: 1.0–1.7, $p = 0.04$), but this association disappeared upon adjusting for the number of medical visits as a covariate (Weimers et al., 2019). Further, one retrospective cohort study using the Truven Health Markets can database included 154,051 IBD patients and an equal number of controls. After adjusting for age, gender, residence type, US region, comorbidities, and behavior, they found no statistically significant association between the two diseases (Coates et al., 2022). However, several studies have reached conflicting conclusions. In another retrospective cohort study, 144,018 patients with IBD were matched with a healthy control group at a 1: 5 ratio, based on age, gender, and the index year of IBD diagnosis and the findings suggest that IBD patients had a higher incidence rate of PD compared to matched controls (RR: 1.28, 95% CI: 1.14–1.44, $p < 0.001$) (Peter et al., 2018). In addition, in a study conducted on the Korean population, which included 24,830 patients with IBD and 99,320 non-IBD controls (Kim et al., 2022), the analysis revealed an increased risk of PD among IBD patients. Meanwhile, in two independent national cohort studies from Danish and Taiwan (Lin et al., 2016; Villumsen et al., 2019), after adjusting for key confounding factors such as age, gender and comorbid conditions, the results from both studies converged to indicate an increased risk of PD among patients with IBD. In another study that included 38,861 individuals with IBD and a control group —matched at a 1:3 ratio for the age and gender—consistent results were obtained. Further, a case–control study and another Spanish cross-sectional study, which utilized 5-aminosalicylic acid (5-ASA) as a proxy for possible IBD groups, proposed that IBD might exert a protective effect against PD (Camacho-Soto et al., 2018; Pinel Rios et al., 2019). Finally, we summarized the previous studies into a table (Supplementary Table 6). Given the inconsistencies in previous studies, our research contributes to the existing body of knowledge. Thus, future endeavors are essential to delve deeper into the specific mechanisms involved.

Compared to previous studies, our research utilized participant data from the UK Biobank and employed Cox

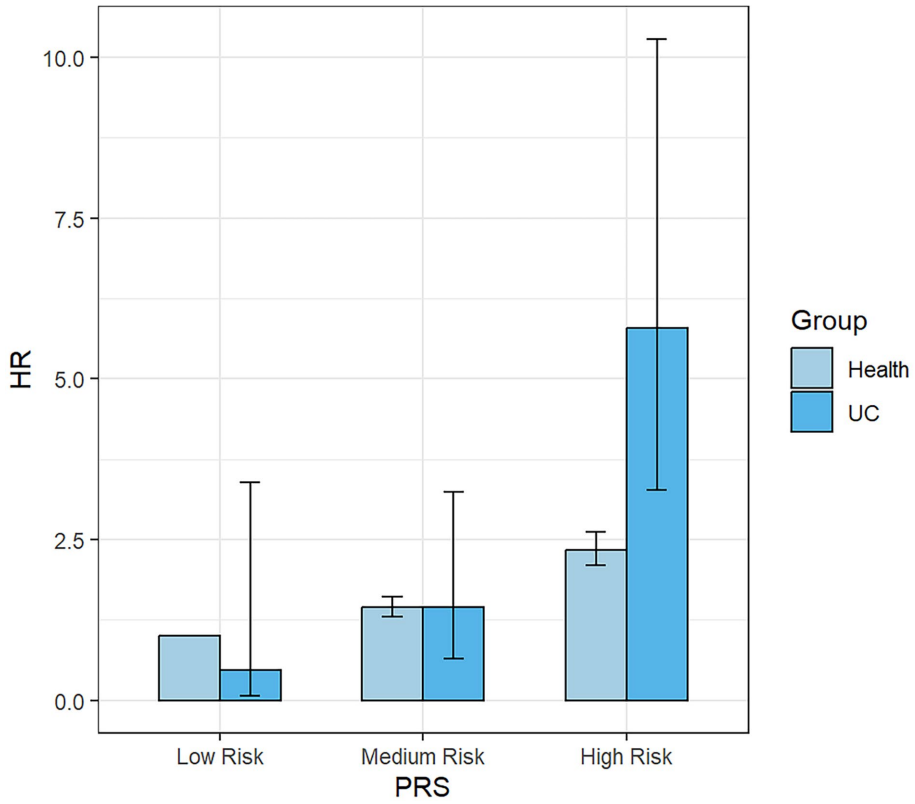

FIGURE 6
Bar Chart for the impact of the interaction term created by CD status and PRS on the risk of PD. CD, Crohn's disease.

Proportional Hazards Model to explore the association between IBD and PD. In addition, we carried out case–control matching and adopted an extended follow-up time. At the time of inclusion, we excluded patients with related gastrointestinal diseases to minimize confounding factors, such as irritable bowel syndrome, colorectal tumors and steatorrhea, whereas in the Cox regression analysis, we adjusted for multiple confounding factors such as age, gender, BMI, and the Townsend Deprivation Index. Furthermore, we separately investigated the relationships of UC and CD with PD. Subgroup analyses were employed to examine disparities in disease risk among different populations, and PSM was used to control for confounding factors. However, while our study adds to the body of literature examining the relationship between IBD and PD, certain limitations should be considered when interpreting our findings and designing future research. First, the sample size of IBD patients was relatively small, consisting of only 3,287 participants. Second, some baseline characteristics of the participants may have changed during the follow-up period, such as BMI, smoking status, and alcohol consumption, which could introduce bias. In addition, both IBD and PD were identified based on ICD-10 coding, which may introduce potential coding biases.

In summary, we confirm no significant association between IBD and PD, except in females (HR:1.989, 95% CI: 1.032–3.835, $p = 0.040$), PRS is at high risk (HR:2.476, 95% CI: 1.401–4.374, $p = 0.002$), participants without hypertension (HR:2.042, 95% CI: 1.128–3.697, $p = 0.018$), C was associated with an increased risk of PD.

Data availability statement

The data analyzed in this study is subject to the following licenses/restrictions: Researchers may obtain access to the UK Biobank dataset upon application. Requests to access these datasets should be directed to https://biobank.ndph.ox.ac.uk/.

Author contributions

H-lW: Writing – original draft, Writing – review & editing, Formal analysis. Z-yW: Writing – original draft, Methodology. JT: Writing – original draft, Visualization. D-rM: Writing – original draft, Data curation. C-hS: Writing – original draft, Funding acquisition, Supervision.

Funding

The author(s) declare financial support was received for the research, authorship, and/or publication of this article. This work was supported by the National Natural Science Foundation of China to C-hS [grant numbers 82171247 and 82371433], the Scientific Research and Innovation Team of the First Affiliated Hospital of Zhengzhou University to C-hS [grant number ZYCXTD2023011], the Scientific and Technological Research Projects in Henan Province to JT [grant number 222102310033], and the Key Research Project in Higher Education Institutions of Henan Province to JT [grant number 22B320022].

Acknowledgments

The authors appreciate greatly to the UK Biobank participants and the highly-competent staff overseeing data acquisition and database upkeep, whose collective efforts have been crucial in providing the foundational data that enabled this study to be realized.

Conflict of interest

The authors declare that the research was conducted in the absence of any commercial or financial relationships that could be construed as a potential conflict of interest.

Publisher's note

All claims expressed in this article are solely those of the authors and do not necessarily represent those of their affiliated organizations, or those of the publisher, the editors and the reviewers. Any product that may be evaluated in this article, or claim that may be made by its manufacturer, is not guaranteed or endorsed by the publisher.

Supplementary material

The Supplementary material for this article can be found online at: https://www.frontiersin.org/articles/10.3389/fnagi.2023.1294879/full#supplementary-material

References

Bahler, C., Schoepfer, A. M., Vavricka, S. R., Brungger, B., and Reich, O. (2017). Chronic comorbidities associated with inflammatory bowel disease: prevalence and impact on healthcare costs in Switzerland. *Eur. J. Gastroenterol. Hepatol.* 29, 916–925. doi: 10.1097/MEG.0000000000000891

Becker, C., Jick, S., and Meier, C. (2008). Use of antihypertensives and the risk of Parkinson disease. *Neurology* 70, 1438–1444. doi: 10.1212/01.wnl.0000303818.38960.44

Berg, D., Borghammer, P., Fereshtehnejad, S. M., Heinzel, S., Horsager, J., Schaeffer, E., et al. (2021). Prodromal Parkinson disease subtypes - key to understanding heterogeneity. *Nat. Rev. Neurol.* 17, 349–361. doi: 10.1038/s41582-021-00486-9

Böttner, M., Zorenkov, D., Hellwig, I., Barrenschee, M., Harde, J., Fricke, T., et al. (2012). Expression pattern and localization of alpha-synuclein in the human enteric nervous system. *Neurobiol. Dis.* 48, 474–480. doi: 10.1016/j.nbd.2012.07.018

Braak, H., Rub, U., Gai, W. P., and Del Tredici, K. (2003). Idiopathic Parkinson's disease: possible routes by which vulnerable neuronal types may be subject to neuroinvasion by an unknown pathogen. *J. Neural Transm. (Vienna)* 110, 517–536. doi: 10.1007/s00702-002-0808-2

Burokas, A., Moloney, R. D., Dinan, T. G., and Cryan, J. F. (2015). Microbiota regulation of the mammalian gut-brain axis. *Adv. Appl. Microbiol.* 91, 1–62. doi: 10.1016/bs.aambs.2015.02.001

Camacho-Soto, A., Gross, A., Searles Nielsen, S., Dey, N., and Racette, B. A. (2018). Inflammatory bowel disease and risk of Parkinson's disease in Medicare beneficiaries. *Parkinsonism Relat. Disord.* 50, 23–28. doi: 10.1016/j.parkreldis.2018.02.008

Cerri, S., Mus, L., and Blandini, F. (2019). Parkinson's disease in women and men: What's the difference? *J. Parkinsons Dis.* 9, 501–515. doi: 10.3233/JPD-191683

Coates, M. D., Ba, D. M., Liu, G., Dalessio, S., Leslie, D. L., and Huang, X. (2022). Revisiting the association between inflammatory bowel disease and Parkinson's disease. *Inflamm. Bowel Dis.* 28, 850–854. doi: 10.1093/ibd/izab175

Collaborators, G. B. D. N. (2019). Global, regional, and national burden of neurological disorders, 1990-2016: a systematic analysis for the global burden of disease study 2016. *Lancet Neurol.* 18, 459–480. doi: 10.1016/S1474-4422(18)30499-X

Cryan, J. F., O'Riordan, K. J., Cowan, C. S. M., Sandhu, K. V., Bastiaanssen, T. F. S., Boehme, M., et al. (2019). The microbiota-gut-brain Axis. *Physiol. Rev.* 99, 1877–2013. doi: 10.1152/physrev.00018.2018

Devos, D., Lebouvier, T., Lardeux, B., Biraud, M., Rouaud, T., Pouclet, H., et al. (2013). Colonic inflammation in Parkinson's disease. *Neurobiol. Dis.* 50, 42–48. doi: 10.1016/j.nbd.2012.09.007

Fasano, A., Visanji, N. P., Liu, L. W., Lang, A. E., and Pfeiffer, R. F. (2015). Gastrointestinal dysfunction in Parkinson's disease. *Lancet Neurol.* 14, 625–639. doi: 10.1016/S1474-4422(15)00007-1

Ferro, J. M., and Oliveira, S. M. (2021). Neurology of inflammatory bowel disease. *J. Neurol. Sci.* 424:117426. doi: 10.1016/j.jns.2021.117426

Foltynie, T., and Athauda, D. (2020). Diabetes, BMI, and Parkinson's. *Mov. Disord.* 35, 201–203. doi: 10.1002/mds.27941

Freuer, D., and Meisinger, C. (2022). Association between inflammatory bowel disease and Parkinson's disease: a Mendelian randomization study. *NPJ Park. Dis.* 8:55. doi: 10.1038/s41531-022-00318-7

Gallagher, D. A., Lees, A. J., and Schrag, A. (2010). What are the most important nonmotor symptoms in patients with Parkinson's disease and are we missing them? *Mov. Disord.* 25, 2493–2500. doi: 10.1002/mds.23394

Goodman, W. A., Erkkila, I. P., and Pizarro, T. T. (2020). Sex matters: impact on pathogenesis, presentation and treatment of inflammatory bowel disease. *Nat. Rev. Gastroenterol. Hepatol.* 17, 740–754. doi: 10.1038/s41575-020-0354-0

Guarino, M. P., Carotti, S., Morini, S., Perrone, G., Behar, J., Altomare, A., et al. (2008). Decreased number of activated macrophages in gallbladder muscle layer of cholesterol gallstone patients following ursodeoxycholic acid. *Gut* 57, 1740–1741. doi: 10.1136/gut.2008.160333

Harris, K. G., and Chang, E. B. (2018). The intestinal microbiota in the pathogenesis of inflammatory bowel diseases: new insights into complex disease. *Clin. Sci. (Lond.)* 132, 2013–2028. doi: 10.1042/CS20171110

Hawkes, C. H., Del Tredici, K., and Braak, H. (2007). Parkinson's disease: a dual-hit hypothesis. *Neuropathol. Appl. Neurobiol.* 33, 599–614. doi: 10.1111/j.1365-2990.2007.00874.x

Hu, G., Jousilahti, P., Bidel, S., Antikainen, R., and Tuomilehto, J. (2007). Type 2 diabetes and the risk of Parkinson's disease. *Diabetes Care* 30, 842–847. doi: 10.2337/dc06-2011

Kalia, L. V., and Lang, A. E. (2015). Parkinson's disease. *Lancet* 386, 896–912. doi: 10.1016/S0140-6736(14)61393-3

Khor, B., Gardet, A., and Xavier, R. J. (2011). Genetics and pathogenesis of inflammatory bowel disease. *Nature* 474, 307–317. doi: 10.1038/nature10209

Kim, G. H., Lee, Y. C., Kim, T. J., Kim, E. R., Hong, S. N., Chang, D. K., et al. (2022). Risk of neurodegenerative diseases in patients with inflammatory bowel disease: a Nationwide population-based cohort study. *J. Crohns Colitis* 16, 436–443. doi: 10.1093/ecco-jcc/jjab162

Knudsen, K., Fedorova, T. D., Hansen, A. K., Sommerauer, M., Otto, M., Svendsen, K. B., et al. (2018). In-vivo staging of pathology in REM sleep behaviour disorder: a multimodality imaging case-control study. *Lancet Neurol.* 17, 618–628. doi: 10.1016/S1474-4422(18)30162-5

Larsen, L., Karachalia Sandri, A., Fallingborg, J., Jacobsen, B. A., Jacobsen, H. A., Bøgsted, M., et al. (2023). Has the incidence of inflammatory bowel disease peaked? Evidence from the population-based NorDIBD cohort 1978–2020. *Am. J. Gastroenterol.* 118, 501–510. doi: 10.14309/ajg.0000000000002187

Lebouvier, T., Neunlist, M., Bruley des Varannes, S., Coron, E., Drouard, A., N'Guyen, J. M., et al. (2010). Colonic biopsies to assess the neuropathology of Parkinson's disease and its relationship with symptoms. *PLoS One* 5:e12728. doi: 10.1371/journal.pone.0012728

Lee, H. S., Lobbestael, E., Vermeire, S., Sabino, J., and Cleynen, I. (2021). Inflammatory bowel disease and Parkinson's disease: common pathophysiological links. *Gut* 70, 408–417. doi: 10.1136/gutjnl-2020-322429

Lewis, C. M., and Vassos, E. (2020). Polygenic risk scores: from research tools to clinical instruments. *Genome Med.* 12:44. doi: 10.1186/s13073-020-00742-5

Li, Y., Chen, Y., Jiang, L., Zhang, J., Tong, X., Chen, D., et al. (2021). Intestinal inflammation and Parkinson's disease. *Aging Dis.* 12, 2052–2068. doi: 10.14336/AD.2021.0418

Li, X., Sundquist, J., and Sundquist, K. (2012). Subsequent risks of Parkinson disease in patients with autoimmune and related disorders: a nationwide epidemiological study from Sweden. *Neurodegener Dis* 10, 277–284. doi: 10.1159/000333222

Li, H., and Wen, Z. (2022). Effects of ulcerative colitis and Crohn's disease on neurodegenerative diseases: a Mendelian randomization study. *Front. Genet.* 13:846005. doi: 10.3389/fgene.2022.846005

Lin, J. C., Lin, C. S., Hsu, C. W., Lin, C. L., and Kao, C. H. (2016). Association between Parkinson's disease and inflammatory bowel disease: a Nationwide Taiwanese retrospective cohort study. *Inflamm. Bowel Dis.* 22, 1049–1055. doi: 10.1097/MIB.0000000000000735

Lu, X., Liu, Z., Cui, Q., Liu, F., Li, J., Niu, X., et al. (2022). A polygenic risk score improves risk stratification of coronary artery disease: a large-scale prospective Chinese cohort study. *Eur. Heart J.* 43, 1702–1711. doi: 10.1093/eurheartj/ehac093

Miyoshi, J., and Chang, E. B. (2017). The gut microbiota and inflammatory bowel diseases. *Transl. Res.* 179, 38–48. doi: 10.1016/j.trsl.2016.06.002

Morais, L. H., Schreiber, H. L. IV, and Mazmanian, S. K. (2021). The gut microbiota-brain axis in behaviour and brain disorders. *Nat. Rev. Microbiol.* 19, 241–255. doi: 10.1038/s41579-020-00460-0

Myasnikov, A., Zhu, H., Hixson, P., Xie, B., Yu, K., Pitre, A., et al. (2021). Structural analysis of the full-length human LRRK2. *Cells* 184, 3519–3527.e10. doi: 10.1016/j.cell.2021.05.004

Ng, Y. F., Ng, E., Lim, E. W., Prakash, K. M., Tan, L. C. S., and Tan, E. K. (2021). Case-control study of hypertension and Parkinson's disease. *NPJ Park. Dis.* 7:63. doi: 10.1038/s41531-021-00202-w

Paganini-Hill, A. (2001). Risk factors for parkinson's disease: the leisure world cohort study. *Neuroepidemiology* 20, 118–124. doi: 10.1159/000054770

Pagano, G., Polychronis, S., Wilson, H., Giordano, B., Ferrara, N., Niccolini, F., et al. (2018). Diabetes mellitus and Parkinson disease. *Neurology* 90, e1654–e1662. doi: 10.1212/WNL.0000000000005475

Park, S., Kim, J., Chun, J., Han, K., Soh, H., Kang, E. A., et al. (2019). Patients with inflammatory bowel disease are at an increased risk of Parkinson's disease: a South Korean Nationwide population-based study. *J. Clin. Med.* 8:1191. doi: 10.3390/jcm8081191

Peter, I., Dubinsky, M., Bressman, S., Park, A., Lu, C., Chen, N., et al. (2018). Anti-tumor necrosis factor therapy and incidence of Parkinson disease among patients with inflammatory bowel disease. *JAMA Neurol.* 75, 939–946. doi: 10.1001/jamaneurol.2018.0605

Pinel Rios, J., Madrid Navarro, C. J., Perez Navarro, M. J., Cabello Tapia, M. J., Pina Vera, M. J., Campos Arillo, V., et al. (2019). Association of Parkinson's disease and treatment with aminosalicylates in inflammatory bowel disease: a cross-sectional study in a Spain drug dispensation records. *BMJ Open* 9:e025574. doi: 10.1136/bmjopen-2018-025574

Rogers, G. B., Keating, D. J., Young, R. L., Wong, M. L., Licinio, J., and Wesselingh, S. (2016). From gut dysbiosis to altered brain function and mental illness: mechanisms and pathways. *Mol. Psychiatry* 21, 738–748. doi: 10.1038/mp.2016.50

Romano, S., Savva, G. M., Bedarf, J. R., Charles, I. G., Hildebrand, F., and Narbad, A. (2021). Meta-analysis of the Parkinson's disease gut microbiome suggests alterations linked to intestinal inflammation. *NPJ Park. Dis.* 7:27. doi: 10.1038/s41531-021-00156-z

Sampson, T. R., Debelius, J. W., Thron, T., Janssen, S., Shastri, G. G., Ilhan, Z. E., et al. (2016). Gut microbiota regulate motor deficits and Neuroinflammation in a model of Parkinson's disease. *Cells* 167, 1469–1480.e12. doi: 10.1016/j.cell.2016.11.018

Santos Garcia, D., de Deus, F. T., Cores, C., Munoz, G., Paz Gonzalez, J. M., Martinez Miro, C., et al. (2021). Predictors of clinically significant quality of life impairment in Parkinson's disease. *NPJ Park. Dis.* 7:118. doi: 10.1038/s41531-021-00256-w

Shannon, K. M., Keshavarzian, A., Mutlu, E., Dodiya, H. B., Daian, D., Jaglin, J. A., et al. (2012). Alpha-synuclein in colonic submucosa in early untreated Parkinson's disease. *Mov. Disord.* 27, 709–715. doi: 10.1002/mds.23838

Tolosa, E., Garrido, A., Scholz, S. W., and Poewe, W. (2021). Challenges in the diagnosis of Parkinson's disease. *Lancet Neurol.* 20, 385–397. doi: 10.1016/S1474-4422(21)00030-2

Torres, J., Mehandru, S., Colombel, J. F., and Peyrin-Biroulet, L. (2017). Crohn's disease. *Lancet* 389, 1741–1755. doi: 10.1016/S0140-6736(16)31711-1

Villumsen, M., Aznar, S., Pakkenberg, B., Jess, T., and Brudek, T. (2019). Inflammatory bowel disease increases the risk of Parkinson's disease: a Danish nationwide cohort study 1977-2014. *Gut* 68, 18–24. doi: 10.1136/gutjnl-2017-315666

Wang, Q., Luo, Y., Ray Chaudhuri, K., Reynolds, R., Tan, E. K., and Pettersson, S. (2021). The role of gut dysbiosis in Parkinson's disease: mechanistic insights and therapeutic options. *Brain* 144, 2571–2593. doi: 10.1093/brain/awab156

Weimers, P., Halfvarson, J., Sachs, M. C., Saunders-Pullman, R., Ludvigsson, J. F., Peter, I., et al. (2019). Inflammatory bowel disease and Parkinson's disease: a Nationwide Swedish cohort study. *Inflamm. Bowel Dis.* 25, 111–123. doi: 10.1093/ibd/izy190

Weingarden, A. R., and Vaughn, B. P. (2017). Intestinal microbiota, fecal microbiota transplantation, and inflammatory bowel disease. *Gut Microbes* 8, 238–252. doi: 10.1080/19490976.2017.1290757

Witoelar, A., Jansen, I. E., Wang, Y., Desikan, R. S., Gibbs, J. R., Blauwendraat, C., et al. (2017). Genome-wide pleiotropy between Parkinson disease and autoimmune diseases. *JAMA Neurol.* 74, 780–792. doi: 10.1001/jamaneurol.2017.0469

Wright, E. K., Ding, N. S., and Niewiadomski, O. (2018). Management of inflammatory bowel disease. *Med. J. Aust.* 209, 318–323. doi: 10.5694/mja17.01001

Younis, N., Zarif, R., and Mahfouz, R. (2020). Inflammatory bowel disease: between genetics and microbiota. *Mol. Biol. Rep.* 47, 3053–3063. doi: 10.1007/s11033-020-05318-5

Zeng, R., Wang, J., Zheng, C., Jiang, R., Tong, S., Wu, H., et al. (2023). Lack of causal associations of inflammatory bowel disease with Parkinson's disease and other neurodegenerative disorders. *Mov. Disord.* 38, 1082–1088. doi: 10.1002/mds.29386

Zhang, Y.-Z. (2014). Inflammatory bowel disease: pathogenesis. *World J. Gastroenterol.* 20:91. doi: 10.3748/wjg.v20.i1.91

frontiers | Frontiers in Aging Neuroscience

TYPE Original Research
PUBLISHED 15 February 2024
DOI 10.3389/fnagi.2024.1358996

OPEN ACCESS

EDITED BY
Robert Weissert,
University of Regensburg, Germany

REVIEWED BY
Wenhua Xu,
University of Kentucky, United States
Xikang Tang,
Sun Yat-Sen Memorial Hospital, China
Haoxin Zhang,
University of California, Irvine, United States

*CORRESPONDENCE
Yinzhou Wang
✉ yinzhouw@163.com

RECEIVED 21 December 2023
ACCEPTED 29 January 2024
PUBLISHED 15 February 2024

CITATION
Song Z, Li W, Han Y, Xu Y and Wang Y (2024) Investigating the shared genetic architecture between frailty and insomnia.
Front. Aging Neurosci. 16:1358996.
doi: 10.3389/fnagi.2024.1358996

Investigating the shared genetic architecture between frailty and insomnia

Zhiwei Song[1], Wangyu Li[2], Yupeng Han[3], Yiya Xu[1] and Yinzhou Wang[1,4]*

[1]Department of Neurology, Fujian Provincial Hospital, Shengli Clinical Medical College of Fujian Medical University, Fuzhou, Fujian, China, [2]Department of Pain Management, Fujian Provincial Hospital, Shengli Clinical Medical College of Fujian Medical University, Fuzhou, Fujian, China, [3]Department of Anesthesiology, Fujian Provincial Hospital, Shengli Clinical Medical College of Fujian Medical University, Fuzhou, Fujian, China, [4]Fujian Key Laboratory of Medical Analysis, Fujian Academy of Medical Sciences, Fuzhou, Fujian, China

Background: The epidemiological association between frailty and insomnia is well established, yet the presence of a common genetic etiology is still uncertain. Further exploration is needed to ascertain the causal relationship between frailty and insomnia.

Methods: Utilizing data obtained from genome-wide association studies (GWAS) summaries, we utilized the linkage disequilibrium score regression (LDSC) to determine the genetic correlation existing between frailty and insomnia. The determination of causality was achieved through the application of two-sample Mendelian randomization. We investigated the enrichment of single nucleotide polymorphism (SNP) at various tissue types utilizing stratified LD score regression (S-LDSC) and multimarker analysis of genome annotation (MAGMA). Common risk SNPs were identified using Multi-Trait Analysis of GWAS (MTAG) and Cross-Phenotype Association (CPASSOC). We further investigated the expression profiles of risk genes in tissues using Summary-data-based Mendelian randomization(SMR) based on pooled data, to explore potential functional genes.

Results: Our findings indicated a significant genetic correlation between frailty and insomnia, highlighting SNPs sharing risk (rs34290943, rs10865954), with a pronounced correlation in the localized genomic region 3p21.31. Partitioned genetic analysis revealed 24 functional elements significantly associated with both frailty and insomnia. Furthermore, mendelian randomization revealed a causal connection between frailty and insomnia. The genetic correlation between frailty and insomnia showed enrichment in 11 brain regions (S-LDSC) and 9 brain regions (MAGMA), where four functional genes (RMB6, MST1R, RF123, and FAM212A) were identified.

Conclusion: This study suggests the existence of a genetic correlation and common risk genes between frailty and insomnia, contributing to a deeper comprehension of their pathogenesis and assists in identifying potential therapeutic targets.

KEYWORDS

frailty, insomnia, shared genetic architecture, Mendelian randomization, causal relationship

1 Background

Frailty, a common geriatric syndrome, is defined as an age-related state characterized by impaired biological reserves, a reduced ability to maintain physiologic homeostasis, and an increased vulnerability to adverse outcomes (Dent et al., 2019). With the increasing rate of population aging, concerns about frailty and its impact on the global health burden are intensifying. Frailty is commonly assessed using the frailty index (FI) (Atkins et al., 2021), defined as the proportion of accumulated health deficits (signs, symptoms, dysfunctions, and laboratory abnormalities) over a lifetime. FI is better at identifying frailty in its low to mid-range spectrum compared to the frailty phenotype (FP), rendering it more sensitive in younger individuals. Additionally, FI is considered predictive of the risk of falls, fractures, disability, and death (Shi et al., 2021). Insomnia, a prevalent sleep disorder, affects approximately 10% of adults chronically and an additional 20% experience occasional insomnia symptoms (Perlis et al., 2022). Insomnia prevalence is higher among women, the elderly, and individuals facing economic hardship. Growing evidence suggests that individuals with insomnia may experience multiple somatic and psychological disorders, impaired quality of life, and higher all-cause mortality rates (Ge et al., 2019). Evidence indicates that insomnia can result in sleep dysfunction, fatigue, unsteady gait, and decreased physical activity, all factors that elevate the risk of frailty (Fan et al., 2022). Furthermore, the variety of psychological and somatic disorders induced by insomnia may heighten vulnerability to frailty. Recently, there has been an increasing body of evidence suggesting the coexistence of frailty and insomnia. A recent meta-analysis encompassing 12 observational studies (Pourmotabbed et al., 2020) suggests an association between sleep disturbances and frailty. However, prior studies exploring the potential association between frailty and insomnia have produced inconsistent results (Nemoto et al., 2021; Tang et al., 2021; Wen et al., 2023), making it challenging to establish causality.

Frailty and insomnia both possess a substantial genetic basis. Studies have shown that frailty has a genetic foundation, with estimates of heritability varying from 30 to 45% (Livshits et al., 2018). A recent extensive GWAS study identified 202 common genetic loci associated with insomnia (Jansen et al., 2019). Few studies to date have explored the link between frailty and insomnia at a genetic level, and it remains unclear as to whether and how their genetic structures overlap. Based on the established link between frailty and insomnia in epidemiological studies, we hypothesize that frailty and insomnia could share a common genetic structure and that their relationship might entail a causal connection. Based on this hypothesis, it is anticipated that this study will yield new insights into the pathophysiological mechanisms underlying the co-morbidity of frailty and insomnia, and identify new therapeutic targets for the two diseases, whether occurring individually or in combination, thereby contributing to healthier, more independent aging.

Cross-trait analysis (Zhu et al., 2021) employs various meta-analytic methods to integrate summary statistics of distinct yet potentially related traits. This approach aims to identify specific loci with shared associations within a meta-analytic framework. It contributes significantly to the comprehension of the genetic architecture of complex traits, facilitating the exploration of genetic sharing, trait interactions, and potential biological mechanisms. Multi-trait analysis of GWAS (MTAG) (Turley et al., 2018) represents a methodology for concurrent multi-phenotypic analyses, utilizing GWAS generalized new data. This approach enables the leveraging of information from associated phenotypes to augment the statistical power of tests for target phenotypes, offering an advantage over single-phenotype GWAS. Cross-Phenotype Association (CPASSOC) (Zhu et al., 2021) employs aggregated single SNP-trait associations from GWAS to ascertain which variants are associated with at least one trait. It exhibits several benefits in identifying cross-phenotypic associations, including the ability to accommodate opposite risk effects and various types of phenotypic traits. Cross-trait analyses are currently being applied in the field of neurology. For example, Tian et al. (2023) have demonstrated a shared genetic framework between amyotrophic lateral sclerosis and Parkinson's disease, encompassing 9 single-nucleotide polymorphisms, 3 risk loci, and 7 genes. These genes are linked to neuronal projection development pathways. In another study, Zeng et al. (2023) discovered a notable positive genetic link between body mass index and multiple sclerosis, indicated by 39 common risk SNPs. Such results provide new perspectives on the mechanisms driving their co-morbidities and guide upcoming treatment strategies.

Mendelian randomization has been utilized in studies of frailty and insomnia, leveraging its ability to mitigate the effects of confounders and diminish reverse causal inference (Emdin et al., 2017). For instance, Deng et al. (2023) demonstrated a bidirectional causal relationship between frailty and depression from a genetic standpoint via Mendelian randomization. This suggests that routine frailty screening for depressed patients is necessary, and treating depression may also moderately reduce the risk of frailty. Utilizing Mendelian randomization, researchers have determined that various sleep characteristics (short sleep, long sleep, continuous sleep duration) not only are associated with but also causally influence the prognosis of ischaemic stroke, potentially serving as a therapeutic target to enhance stroke prognosis (Zhang et al., 2023).

In our research, we explored the genetic links and the possibility of a causal connection between frailty and insomnia, using extensive GWAS data. Initially, to comprehend the shared genetic bases of frailty and insomnia, we established the genetic correlations and local genetic correlations. Subsequently, we utilized cross-trait GWAS meta-analyses for identifying common SNPs. Moreover, we implemented two-sample Mendelian randomization analyses to examine the causative link between frailty and insomnia. Furthermore, our study involved analyzing the tissue-specific enrichment of genetic associations linking frailty and insomnia. Summary data-based Mendelian randomization (SMR) (Zhu et al., 2016) utilizing pooled data, is a methodology that merges summary data from GWAS with data from expression quantitative trait loci (eQTL) studies in order to identify genes whose expression levels are linked to complex traits owing to pleiotropy. Utilizing SMR, we pinpointed genes with shared functionality between frailty and insomnia. The STROBE-MR guidelines (Skrivankova et al., 2021a,b) were followed throughout the course of the study. Figure 1 presents a flowchart depicting our analytical strategy.

2 Materials and methods

2.1 Study samples

The genesis of the GWAS data on frailty can be traced to a study led by Atkins et al. (2021). This research involved a GWAS on frailty

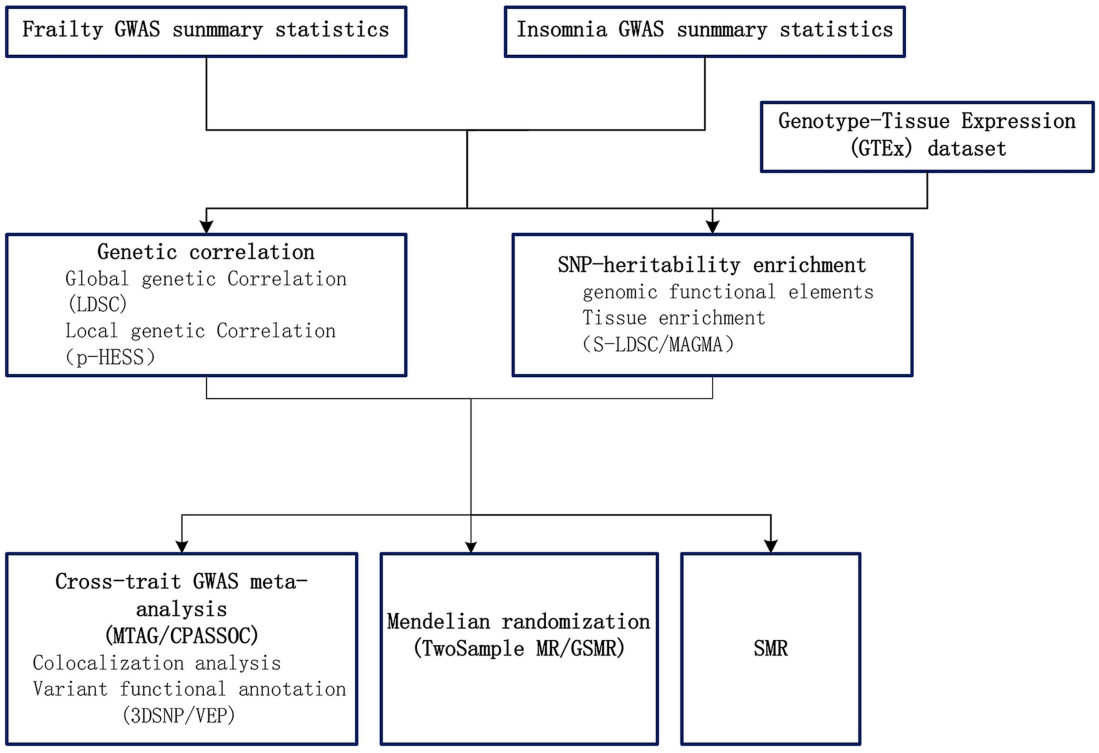

FIGURE 1
Overview of analytical strategy performed in the study.

indices among participants from the British Biobank of European descent ($n = 164,610$, aged between 60 and 70) and those from the Swedish TwinGene project ($n = 10,616$, aged 41–87). Calculations for the FI were based on 49 or 44 self-reported elements, including symptoms, disabilities, and diagnosed illnesses. The complete GWAS summary statistics are available for download from the GWAS catalog (project number: GCST90020053). Meanwhile, the summary statistics for insomnia were derived from a GWAS using UK Biobank data (project number: ukb-b-3957), which included 462,341 participants.

2.2 Heritability and genetic correlation

Utilizing GWAS summary statistics and LD scores from European lineage reference data in the 1,000 Genomes Project, we applied the linkage disequilibrium score regression (LDSC) (Bulik-Sullivan et al., 2015) to ascertain the heritability of frailty and insomnia, as well as to determine the genetic correlation between these traits. Heritabilities of SNPs for frailty and insomnia were measured using S-LDSC (Finucane et al., 2015) in combination with the baseline LD model (Gazal et al., 2017). This baseline LD model approach distinctly determines SNP heritabilities based on continuous, rather than binary, annotation sets. The use of S-LDSC (Finucane et al., 2015) facilitates the analysis of the genetic structure of complex traits by dividing heritability among various genomic annotations. Following this, bivariate LDSC with unconstrained intercepts was utilized to gauge genetic correlations between frailty and insomnia (rg). Considering the population overlap in the GWAS data for frailty and insomnia, an LDSC with constrained intercepts was also conducted as part of a sensitivity analysis.

2.3 Local genetic correlation analysis

Heritability Estimation from Summary Statistics (ρ-HESS) (Shi et al., 2017) is employed for estimating local SNP heritability and genetic correlation from summary statistics. Local genetic correlations were estimated using ρ-HESS to determine whether frailty and insomnia are genetically correlated in locally independent regions of the genome. Subsequently, the local SNP heritabilities and genetic correlations between the two traits were calculated, employing the 1,000 Genomes Project data provided on the ρ-HESS webpage as a reference. Subsequently, the Bonferroni correction method was utilized to adjust for multiple testing, considering the factor of 0.05 divided by the number of regions.

2.4 Partitioned heritability

Our study provided further insight into the genetic correlation between frailty and insomnia through the analysis of various genomic functional elements via S-LDSC (Okamura et al., 2016), which operates by categorizing SNPs into functional groups and subsequently calculating LD scores for each categorized SNP. The calculated LD scores were subsequently utilized to estimate the genetic correlation within each functional category. Consequently, this approach enabled the estimation of genetic correlations across over 30 functional

components, thereby elucidating the contribution of diverse components to the overarching genetic correlation between frailty and insomnia.

2.5 Tissue specific enrichment of SNP heritability

2.5.1 S-LDSC

We conducted a GTEx tissue enrichment analysis using S-LDSC to determine the tissues most strongly associated with shared genes (Finucane et al., 2015). GTEx (version 8) offers insights into 53 distinct tissue types, encompassing data on SNP mutations linked to quantitative traits of gene expression across various tissues.

2.5.2 MAGMA

For a sensitivity analysis of S-LDSC, tissue-specific enrichment and gene set enrichment analyses were performed using MAGMA (de Leeuw et al., 2015). The process began with a gene-level association analysis to assess the relationship between genes and phenotypes, utilizing the *p*-values of SNPs in proximity to the genes in question. Subsequently, gene set enrichment analyses were performed using the designated gene set of FUMA (MSigDB_20231Hs_MAGMA). Finally, for the assessment of the tissue specificity of the phenotype, MAGMA gene characterization was employed. This analysis investigated the relationship between tissue-specific gene expression profiles and disease gene associations, utilizing data from GTEx v8 (gtex_v8_ts_avg_log2TPM), which encompasses information from 54 distinct tissues.

2.6 Cross-trait GWAS meta-analysis

In order to pinpoint shared risk SNPs associated with frailty and insomnia, cross-trait meta-analyses were conducted employing MTAG (Turley et al., 2018) and CPASSOC (Zhu et al., 2021). In MTAG analyses, the estimation of SNP effects for each trait can be enhanced by including related, distinct traits (Yoshida and Yáñez, 2021). Additionally, a paired cross-trait meta-analysis was executed using CPASSOC to consider the variance in heritability of the two phenotypes. CPASSOC operates on the assumption that cross-trait heterogeneity effects exist, and it calculates cross-trait statistical heterogeneity (SHet) and *p*-values via a meta-analysis weighted by sample size. SHom is typified as a fixed-effects meta-analysis approach with diminished efficacy when faced with between-study heterogeneity. In cases of heterogeneous effects, SHet serves as an expansion of SHom, providing enhanced statistical stability and power. We utilized SHet to combine summary statistics for frailty and insomnia.

SNPs of significance were identified based on their notable associations with both phenotypes, characterized by a *p*-value less than 5 × 10^-8 in both MTAG and CPASSOC analyses. The summary statistics for frailty and insomnia were merged using SHet, followed by clustering them using parameters in PLINK (1.9). Independent SNPs, significantly associated with the phenotype, were identified by applying specific parameters through PLINK's "clustering" function: -clump-p1 5e-8 -clump-p2 1e-5 -clump-r2 0.2 - clump-kb 500.

2.7 Mendelian randomization

To investigate the potential causal relationship between frailty and insomnia, the "TwoSampleMR" and "GSMR" R packages were employed to analyze associations suggestive of causality ($p < 0.05$). Mendelian stochastic analyses were conducted using six principal MR methods, namely MR-Egger (Burgess and Thompson, 2017), inverse variance weighting (IVW) (Burgess et al., 2017), weighted median, weighted mode, simple mode, and GSMR, with varying assumptions regarding the level of multinomiality. Evaluations of horizontal pleiotropy and heterogeneity were performed using the MR-Egger intercept test and Cochran's Q statistic. MR-PRESSO (Verbanck et al., 2018) were utilized to identify pleiotropy and outliers. Variant selection was predicated on three fundamental assumptions: that the variants are (1) exposure-related, (2) not influenced by confounders, and (3) devoid of a direct impact on the outcomes.

2.8 Summary-data-based Mendelian randomization

SMR (Krishnamoorthy et al., 2023) uses genetic variation as an instrumental variable for estimating the impact of a gene's expression level on the phenotype. To identify shared functional genes in tissue enrichment, both the Benjamini-Hochberg FDR test and the HEIDI-outlier test (Yang et al., 2021) were utilized.

3 Results

3.1 Genetic correlations

The liability-scale SNP heritability (without constrained intercept) was determined to be 11.69% (95% CI = 11.68–11.70%) for frailty and 6.65% (95% CI = 6.65–6.65%) for insomnia, with a significantly positive genetic correlation between frailty and insomnia (rg = 1.14, $p = 0.00$). Additionally, LDSC with constrained intercepts was conducted (rg = 0.61, $p = 4.63E\text{-}189$), and the findings continued to be significant (Supplementary Table S1).

3.2 Local genetic correlations

After applying multiple corrections, the ρ-HESS method was employed to determine a significant local genetic correlation between frailty and insomnia. A significant local correlation was identified in a singular region between frailty and insomnia at 3p21.31 (chr3:47727212 … 0.49316972) ($p = 9.45e\text{-}06$) (Supplementary Figure S1; Supplementary Table S2).

3.3 Partitioned genetic correlations

SNPs partially genetically related to frailty demonstrated enrichment in 31 of 98 functional categories, with the leading category being GERP.RSsup4L2_0 (enrichment = 12.8, $p = 0.00$). SNPs associated with insomnia showed enrichment in 36 of 97 functional categories, notably led by GERP.RSsup4L2_0 (enrichment = 16.6, $p = 0.00$). Twenty-four functional categories

exhibited significant associations with both frailty and insomnia (Figure 2; Supplementary Table S3).

3.4 Cross-trait GWAS meta-analysis

Cross-trait analyses were conducted using both MTAG and CPASSO, resulting in 124 shared independent SNPs achieving genome-wide significance (Supplementary Table S4). In the screening of SNPs at 3p21.31, after excluding SNPs that were only significant in GWAS for frailty or insomnia, or those in linkage disequilibrium (LD $r^2 \geq 0.02$) with previously significant SNPs, two SNPs were identified as being associated with both frailty and insomnia (Table 1). The rs34290943 SNP was mapped to the DALRD3 gene, and locus rs10865954 to the MIR191 gene.

3.5 Mendelian randomization

Two-sample Mendelian randomization was conducted using loci significantly associated with either the frailty or insomnia phenotype as instrumental variables ($F > 10$). Given the genetic commonalities identified in the preceding section, causality may arise from instrumental variables exhibiting pleiotropic effects. Upon exclusion of potentially biased polytropic instrumental variables, MR was reanalyzed, revealing a strong causal relationship (OR 1.14, $p < 0.001$) (Figure 3; Supplementary Table S5). The Egger intercept did not deviate from 0, indicating that the remaining instrumental variables (IVs) were not affected by polytropy. Conversely, the causal relationship between insomnia and frailty was found to be unstable. Insomnia potentially played a role in elevating the risk of frailty (OR 1.98, $p = 0.00$), yet the

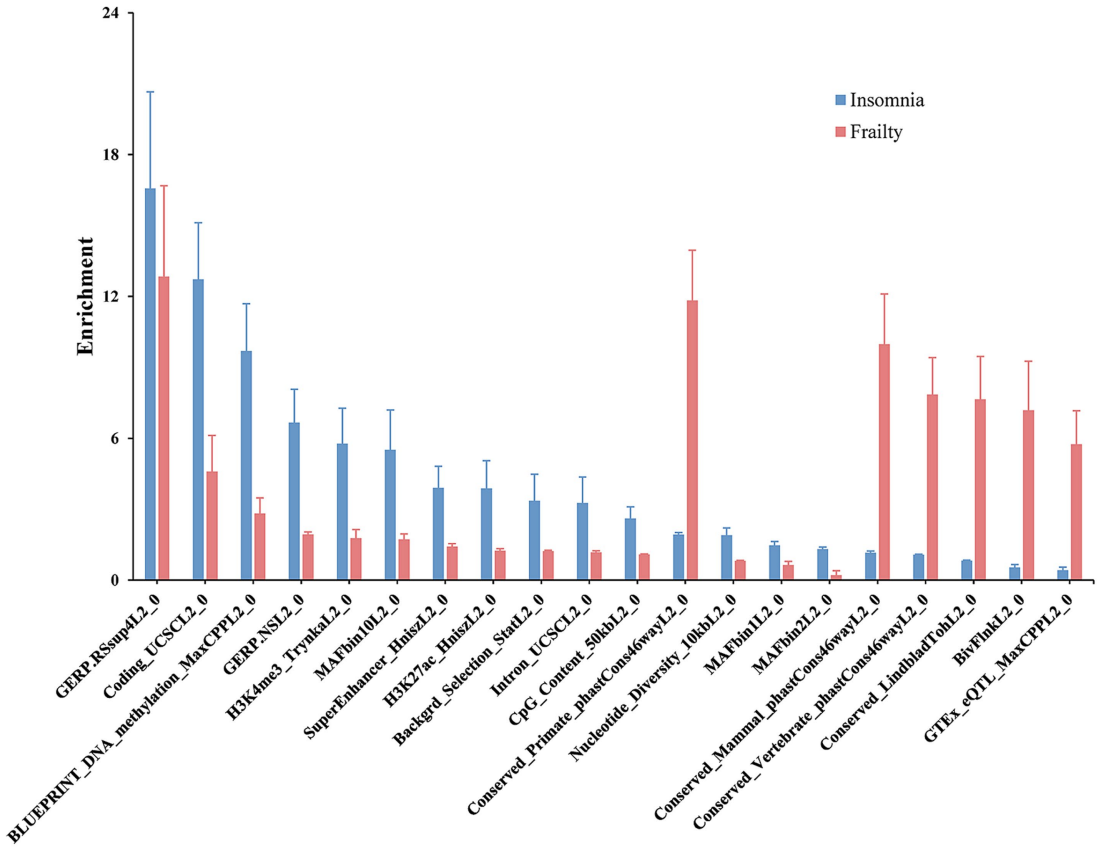

FIGURE 2
Partitioned genetic correlation between frailty and insomnia. The display highlighted genomic functional elements common to both frailty and insomnia. The vertical axis depicted estimates of enrichment, and error bars indicated the standard error of enrichment.

TABLE 1 Shared risk regions in different analyses.

SNP	CHR	BP	Effect allele	Non-effect allele	Mtag_pval_frailty	Mtag_pval_insomnia	CPASSOC *p*-value	ρ-HESS *p*-value
rs34290943	3	49,161,660	C	T	5.81E-10	5.63E-10	7.55E-09	9.45E-06
rs10865954	3	49,211,989	C	T	4.73E-12	3.53E-12	5.38E-13	9.45E-06

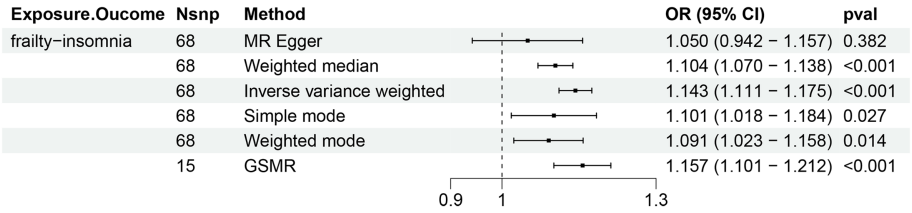

FIGURE 3
Bi-directional Mendelian randomization (MR) analyses between frailty and insomnia. (Causal effect of frailty on insomnia). Estimates and 95% confidence intervals (CI) are shown using square plots and error bars.

presence of horizontal pleiotropy could not be discounted (Egger intercept = 0.004, $p = 0.007$) (Supplementary Table S6).

3.6 Tissue-level SNP heritability enrichment

The enrichment of SNP heritability for frailty and insomnia at the tissue level was evaluated using S-LDSC analysis, which involved GTEx data across different tissues. Tissues exhibiting significant SNP heritability enrichment for frailty and insomnia, predominantly located in the brain, were identified. Specifically, SNPs associated with frailty showed notable enrichment in 11 different brain regions, primarily in the anterior cingulate cortex (BA24) and cerebellar hemispheres.

In the case of insomnia, distinct enrichment of SNPs was noted in 19 different brain regions, predominantly concentrated in the anterior cingulate cortex (BA24) and the cerebral amygdala. SNPs co-associated with frailty and insomnia exhibited enrichment in 11 brain regions, mainly in the anterior cingulate cortex (BA24) and cerebral amygdala (Figure 4; Supplementary Table S7). Furthermore, MAGMA tissue-specific analyses revealed that SNPs linked to frailty showed specific enrichment in 11 distinct brain regions, whereas for insomnia, such enrichment was observed in 14 different brain areas. SNPs co-associated with frailty and insomnia were enriched in 9 brain regions, primarily in the cerebellum and cerebellar hemispheres (Figure 5; Supplementary Table S8).

3.7 Identification of shared functional genes

SMR was utilized to pinpoint shared functional genes related to frailty and insomnia by jointly analyzing GWAS summary data for these conditions and eQTL summary data from GTEx. The S-LDSC and MAGMA analyses indicated associations with enriched SNP heritability in both diseases. Among these genes, four were shared between weakness and insomnia following HEIDI outlier testing. RMB6 was detected in various brain regions including the caudate basal ganglia (pSMR = 1.34E-06, pHEIDI = 0.99; pSMR = 2.99E-07, pHEIDI = 0.05), the frontal cortex (BA9) (pSMR = 1.28E-06, pHEIDI = 0.74; pSMR = 3.03E-07, pHEIDI = 0.07), and the cerebral hypothalamus (pSMR = 4.31E-06, pHEIDI = 0.74; pSMR = 1.26E-06, pHEIDI = 0.09). MST1R was identified in the cerebellar hemisphere (pSMR = 9.11E-06, pHEIDI = 0.58; pSMR = 4.50E-06, pHEIDI = 0.15), cerebellum (pSMR = 2.49E-06, pHEIDI = 0.75; pSMR = 6.30E-07, pHEIDI = 0.12), and the basal ganglia of the nucleus ambiguus (pSMR = 3.35E-05, pHEIDI = 0.95; pSMR = 2.14E-05, pHEIDI = 0.40). RF123 and FAM212A were detected in the cerebellar hemisphere, cerebellum, and cerebral hemisphere (Figure 6; Supplementary Table S9).

4 Discussion

To our knowledge, this study is the first genome-wide cross-trait analysis to systematically assess the shared genetic foundations of frailty and insomnia. Our research, leveraging a detailed GWAS dataset along with tissue-specific expression data, reveals potential genetic connections between frailty and insomnia. This is supported by several critical observations: Initially, we found that specific genomic regions and functional elements are linked to both frailty and insomnia. Second, bidirectional MR analyses indicate that frailty exerts a causal effect on insomnia, albeit not reciprocally. Finally, our investigation into genetic commonalities between frailty and insomnia, particularly in brain tissue, led to the identification of numerous potential functional genes impacting both phenotypes.

A path-analysis study revealed that poor sleep quality contributes to increased frailty susceptibility in older adults, potentially linked to poor physical functioning (Tang et al., 2021), and indicated that over half of pre-frail and frail older adults exhibit insomnia symptoms (Nemoto et al., 2021). The association between insomnia and aging is believed to initiate a chronic low-grade inflammatory state in older adults, leading to alterations in the immune system, a phenomenon termed inflammatory aging (Besedovsky et al., 2019; Irwin, 2019). Transitioning from a state of homeostasis to low-grade inflammation induces an inflammatory response, the severity of which is predictive of mortality in older adults (Ingiosi et al., 2013). Prolonged activation of a low-grade inflammatory state may impede the return to homeostasis during sleep repair, potentially leading to disease in older adults (Pak et al., 2020). Furthermore, extended sleep latency is known to elevate insulin resistance via the activation of inflammatory markers (Kim et al., 2016), thereby exacerbating protein synthesis impairment and muscle loss, potentially worsening limb movement.

To date, there has been no comprehensive analysis of the genetic link between frailty and insomnia in any study. Following a local genetic correlation analysis, the independent region 3p21.31 (chr3:47727212 … 0.49316972) was identified. One study reported a correlation between 3p21.31 and the incidence of gliomas and glioblastomas in women (Ostrom et al., 2018). Additionally, the TMIE gene located at 3p21.31 is believed to

10.3389/fnagi.2024.1358996

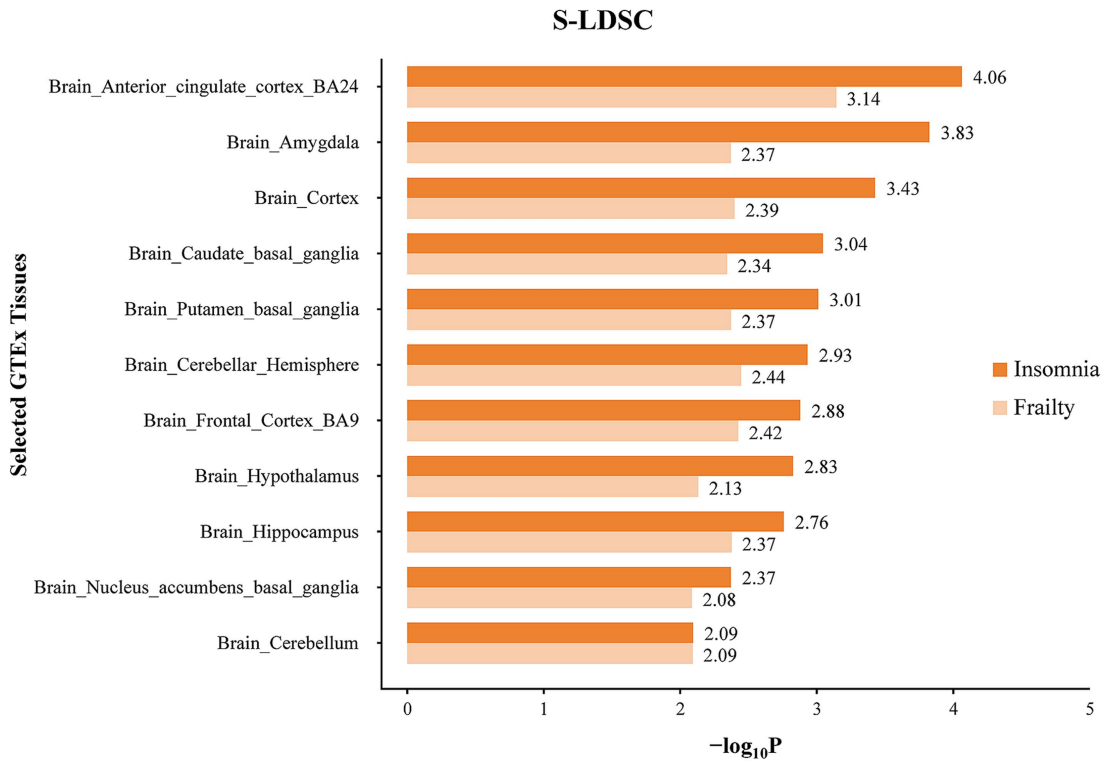

FIGURE 4
Tissue specific enrichment of SNP heritability for frailty and insomnia through S-LDSC. The x-axis represents negative log10 *p*-values of enrichment for each individual test.

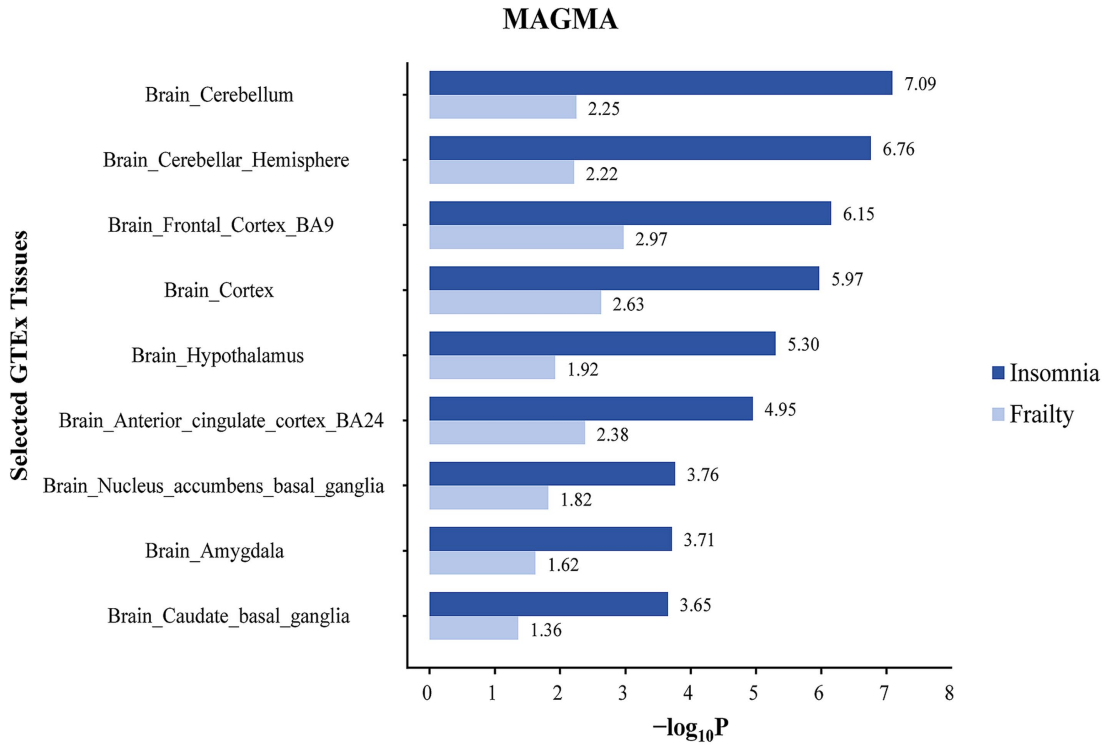

FIGURE 5
Tissue specific enrichment of SNP heritability for frailty and insomnia through MAGMA. The x-axis represents negative log10 *p*-values of enrichment for each individual test.

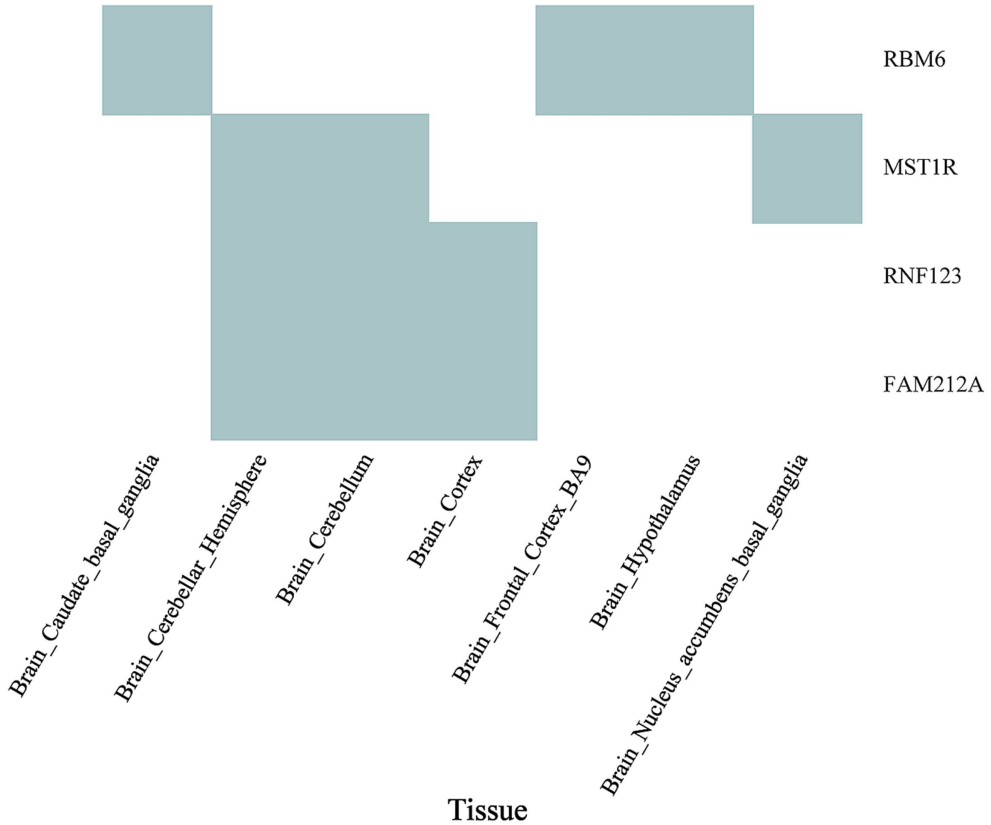

FIGURE 6
Overlap of significant genes associated with both frailty and insomnia in SMR in enriched tissues. Cyan plots indicate significant genes that met the FDR threshold of <5% in SMR analyses with GWAS for both frailty and insomnia, and also cleared the HEIDI-outlier test ($p > 0.05$).

be significantly associated with sleep duration (Meng et al., 2022). Considering the notable gene-level correlations, a cross-trait GWAS analysis was conducted to identify 124 SNPs co-associated with frailty and insomnia, including two SNPs at 3p21.31: rs34290943 and rs10865954. The SNP rs34290943 was mapped to the DALRD3 gene, while rs10865954 was located in the MIR191 gene locus. The protein encoded by the DALRD3 gene possesses a DALR anticodon binding domain, akin to that found in the leucyl aminoacyl tRNA synthetase class. It has been shown that the expression level of DALRD3 in the brain tissue of patients with insomnia is significantly lower compared to controls, and significant dynamic changes in the expression level of this gene were observed in the mouse cerebral cortex during sleep and sleep deprivation states (Sun et al., 2020). Previous studies have suggested that significantly reduced plasma levels of MIR191 in elderly patients are associated with age-related frailty syndrome, with its notable age-related downregulation in plasma aligning with prior observations in monocytes (Serna et al., 2012). Furthermore, miR-191 is a component of a distinctive circulating 7-miRNA signature that differentiates Alzheimer's disease patients from normal controls (Nagpal and Kulshreshtha, 2014).

Subsequent analyses of functional components uncovered 24 annotated regions linked to frailty and insomnia. It is suggested that the Coding_UCSCL2_0 region may have associations with neuropsychiatric disorders including Alzheimer's disease, major depression, bipolar disorder, and sporadic Creutzfeldt-Jakob disease (de Souza et al., 2010). In the study by Hnisz et al. mutations in MAFbin1L2_0 were found to be associated with Alzheimer's disease (Hnisz et al., 2013). Animal experiments demonstrated that increased H3K27ac enrichment in early gene promoters of neurons enhances memory capacity in mice, thereby influencing aging (Li et al., 2021). Intron_UCSCL2_0 is crucial for forebrain inhibitory neuronal differentiation and exhibits a strong association with restless legs syndrome (RLS) and insomnia (Lam et al., 2022). These functional components linked to frailty and insomnia require additional experimental validation.

We investigated the causal relationship between frailty and insomnia using a GSMR approach, an extension of the SMR approach that utilizes all SNPs of the highest genome-wide significance levels associated with the exposure as IVs for causal testing. The GSMR method excelled in efficacy for discovering causal effects, surpassing methods such as IVW and MR-Egger. It also demonstrated considerable robustness in the face of pleiotropy in the instrumental variables and linkage disequilibrium among instrumental variables (Zhu et al., 2018). Two-sample Mendelian randomization analyses disclosed a causal effect of frailty on insomnia and indicated horizontal pleiotropy in the causal effect of insomnia on frailty. This implies that older frail patients are more prone to insomnia symptoms, that the onset of insomnia leading to frailty could be impacted by other confounders, and that a shared genetic risk exists between frailty

and insomnia. One meta-analysis suggested that insomnia independently correlates with frailty among older adults in the community or nursing homes; however, the inclusion of six studies using the FP to identify frailty partly accounts for the inconsistency in findings (Wen et al., 2023). Compared to randomized controlled trials (RCTs), Mendelian randomization offers the benefits of lower cost, diminished confounding, and lessened reverse causal inference, thus serving as a 'natural' RCT that mitigates traditional observational study biases and is superior in deducing causality (Emdin et al., 2017).

Tissue enrichment analysis for key genes associated with frailty and insomnia was conducted, revealing significant enrichment in brain tissues for both conditions. S-LDSC analysis demonstrated that SNPs co-associated with frailty and insomnia were enriched in 11 brain regions, mainly in the anterior cingulate cortex (BA24) and the amygdala. Similarly, MAGMA tissue-specificity analyses indicated enrichment in 9 brain regions, especially in the cerebellum and cerebellar hemispheres. This enrichment, particularly in the cerebellum and cerebellar hemispheres, suggests a potential mechanism for the co-morbidity of frailty and insomnia in brain structures. Aligned with our findings, a genome-wide analysis of insomnia (involving 593,724 cases and 1,771,286 controls) demonstrated that genes linked to insomnia were primarily enriched in brain tissues [including cerebellar hemispheres, cerebellum, frontal cortex (BA9), cerebral cortex, anterior cingulate cortex (BA24)] (Watanabe et al., 2022). A GWAS study with 386,565 participants of European ancestry from the UK Biobank revealed that genes related to frailty were predominantly enriched in specific brain areas (cerebellar hemispheres, frontal cortex BA9, cerebellum, anterior cingulate cortex BA24, nucleus ambiguus in the basal ganglia) (Ye et al., 2023). Neuroimaging meta-analyses on insomnia have suggested a critical role for the anterior cingulate cortex and amygdala in insomnia disorders (Reimann et al., 2023). Voxel-based studies have revealed that frailty is associated with multiple brain regions, potentially leading to reduced grey matter volume in areas such as the hippocampus, amygdala, fusiform gyrus, and several cortical regions (Nishita et al., 2019). Additionally, reduced grey matter in the cerebellum is recognized as a neurological feature of frailty (Chen et al., 2015). Through SMR exploration of functional genes linked to frailty and insomnia in specific enriched tissues, four genes were identified: RMB6, MST1R, RF123, and FAM212A. In line with our study, MST1R and RF123 are considered to be associated with brain function or psychiatric disorders, exhibiting upregulated expression in various brain regions (Qiu et al., 2022). The role of these identified genes in frailty and insomnia necessitates further experimental verification.

Our study presents several limitations. Firstly, the genetic data on frailty and insomnia in this study originated exclusively from European populations, potentially diminishing the heterogeneity of the results to some extent. However, this aspect also restricts the generalization of our results to other ethnic populations, and therefore, future analyses should incorporate data from diverse ethnicities. Secondly, the genetic data encompassed a large cohort of patients with insomnia symptoms, thereby enlarging the sample size of the data, but also introduced a certain level of heterogeneity in the findings. Incorporating additional GWAS data that integrate genetic information with comprehensive clinical characteristics (e.g., varying severities of insomnia, duration of symptoms, frequency of occurrence) in subsequent studies may yield a more nuanced comprehension of the role genetic factors play in the varied clinical manifestations of frailty and insomnia. Thirdly, our analyses were confined to the genetic characteristics of the traits, acknowledging that epigenetic influences on these traits are equally crucial.

5 Conclusion

In conclusion, our research revealed a notable genetic link between frailty and insomnia, highlighted by the identification of shared risk SNPs. This correlation was found to be more distinct in certain genomic areas. Partitioned genetic analyses revealed 24 functional elements significantly linked to both frailty and insomnia. Mendelian randomization was additionally employed to demonstrate a causal relationship between frailty and insomnia. The genetic correlation was found to be enriched in 11/9 brain regions, within which 4 functional genes were detected. These findings may offer insights into the shared genetic architecture of frailty and insomnia, contributing to an enhanced understanding of their pathogenesis and the development of therapeutic targets aimed at alleviating insomnia symptoms and potentially preventing or reversing aging.

Data availability statement

Publicly available datasets were analyzed in this study. Data about the frailty index can be found at: https://www.ebi.ac.uk/gwas/downloads/summary-statistics GCST90020053. Data about insomnia can be found at https://gwas.mrcieu.ac.uk/datasets/ukb-b-3957.

Ethics statement

Written informed consent was not required for any of the potentially identifiable images or data included in this study, as all statistical analyses were based on existing publicly available summary data and thus no additional ethical approval was required.

Author contributions

ZS: Visualization, Writing – review & editing. WL: Formal analysis, Writing – original draft. YH: Formal analysis, Writing – original draft. YX: Data curation, Writing – original draft. YW: Supervision, Writing – review & editing.

Funding

The author(s) declare financial support was received for the research, authorship, and/or publication of this article. This work was

financially supported in part by research grants from Natural Science Foundation of Fujian Province, China (2023J02024) and Medical Innovation Project of Fujian Province (2022CXA047).

Acknowledgments

The authors would like to thank all the colleagues who contributed to this work.

Conflict of interest

The authors declare that the research was conducted in the absence of any commercial or financial relationships that could be construed as a potential conflict of interest.

Publisher's note

All claims expressed in this article are solely those of the authors and do not necessarily represent those of their affiliated organizations, or those of the publisher, the editors and the reviewers. Any product that may be evaluated in this article, or claim that may be made by its manufacturer, is not guaranteed or endorsed by the publisher.

Supplementary material

The Supplementary material for this article can be found online at: https://www.frontiersin.org/articles/10.3389/fnagi.2024.1358996/full#supplementary-material

References

Atkins, J. L., Jylhävä, J., Pedersen, N. L., Magnusson, P. K., Lu, Y., Wang, Y., et al. (2021). A genome-wide association study of the frailty index highlights brain pathways in ageing. *Aging Cell* 20:e13459. doi: 10.1111/acel.13459

Besedovsky, L., Lange, T., and Haack, M. (2019). The sleep-immune crosstalk in health and disease. *Physiol. Rev.* 99, 1325–1380. doi: 10.1152/physrev.00010.2018

Bulik-Sullivan, B., Finucane, H. K., Anttila, V., Gusev, A., Day, F. R., Loh, P. R., et al. (2015). An atlas of genetic correlations across human diseases and traits. *Nat. Genet.* 47, 1236–1241. doi: 10.1038/ng.3406

Burgess, S., Small, D. S., and Thompson, S. G. (2017). A review of instrumental variable estimators for Mendelian randomization. *Stat. Methods Med. Res.* 26, 2333–2355. doi: 10.1177/0962280215597579

Burgess, S., and Thompson, S. G. (2017). Interpreting findings from Mendelian randomization using the MR-egger method. *Eur. J. Epidemiol.* 32, 377–389. doi: 10.1007/s10654-017-0255-x

Chen, W. T., Chou, K. H., Liu, L. K., Lee, P. L., Lee, W. J., Chen, L. K., et al. (2015). Reduced cerebellar gray matter is a neural signature of physical frailty. *Hum. Brain Mapp.* 36, 3666–3676. doi: 10.1002/hbm.22870

de Leeuw, C. A., Mooij, J. M., Heskes, T., and Posthuma, D. (2015). MAGMA: generalized gene-set analysis of GWAS data. *PLoS Comput. Biol.* 11:e1004219. doi: 10.1371/journal.pcbi.1004219

de Souza, M. B., de Lemos, R. R., da Cunha, J. E., de Lima Filho, J. L., and de Oliveira, J. R. (2010). Searching for new genetic risk factors for neuropsychiatric disorders in expression databases. *J. Mol. Neurosci.* 41, 193–197. doi: 10.1007/s12031-009-9321-5

Deng, M. G., Liu, F., Liang, Y., Wang, K., Nie, J. Q., and Liu, J. (2023). Association between frailty and depression: a bidirectional Mendelian randomization study. *Sci. Adv.* 9:eadi3902. doi: 10.1126/sciadv.adi3902

Dent, E., Martin, F. C., Bergman, H., Woo, J., Romero-Ortuno, R., and Walston, J. D. (2019). Management of frailty: opportunities, challenges, and future directions. *Lancet* 394, 1376–1386. doi: 10.1016/S0140-6736(19)31785-4

Emdin, C. A., Khera, A. V., and Kathiresan, S. (2017). Mendelian randomization. *JAMA* 318, 1925–1926. doi: 10.1001/jama.2017.17219

Fan, J., Liu, Y., Wang, Q., Zhao, H., Kong, L., and Li, J. (2022). Association of insomnia and multidimensional frailty in community-dwelling older adults: a cross-sectional survey. *J. Clin. Nurs.* 31, 167–173. doi: 10.1111/jocn.15893

Finucane, H. K., Bulik-Sullivan, B., Gusev, A., Trynka, G., Reshef, Y., Loh, P. R., et al. (2015). Partitioning heritability by functional annotation using genome-wide association summary statistics. *Nat. Genet.* 47, 1228–1235. doi: 10.1038/ng.3404

Gazal, S., Finucane, H. K., Furlotte, N. A., Loh, P. R., Palamara, P. F., Liu, X., et al. (2017). Linkage disequilibrium-dependent architecture of human complex traits shows action of negative selection. *Nat. Genet.* 49, 1421–1427. doi: 10.1038/ng.3954

Ge, L., Guyatt, G., Tian, J., Pan, B., Chang, Y., Chen, Y., et al. (2019). Insomnia and risk of mortality from all-cause, cardiovascular disease, and cancer: systematic review and meta-analysis of prospective cohort studies. *Sleep Med. Rev.* 48:101215. doi: 10.1016/j.smrv.2019.101215

Hnisz, D., Abraham, B. J., Lee, T. I., Lau, A., Saint-André, V., Sigova, A. A., et al. (2013). Super-enhancers in the control of cell identity and disease. *Cell* 155, 934–947. doi: 10.1016/j.cell.2013.09.053

Ingiosi, A. M., Opp, M. R., and Krueger, J. M. (2013). Sleep and immune function: glial contributions and consequences of aging. *Curr. Opin. Neurobiol.* 23, 806–811. doi: 10.1016/j.conb.2013.02.003

Irwin, M. R. (2019). Sleep and inflammation: partners in sickness and in health. *Nat. Rev. Immunol.* 19, 702–715. doi: 10.1038/s41577-019-0190-z

Jansen, P. R., Watanabe, K., Stringer, S., Skene, N., Bryois, J., Hammerschlag, A. R., et al. (2019). Genome-wide analysis of insomnia in 1,331,010 individuals identifies new risk loci and functional pathways. *Nat. Genet.* 51, 394–403. doi: 10.1038/s41588-018-0333-3

Kim, T. H., Carroll, J. E., An, S. K., Seeman, T. E., Namkoong, K., and Lee, E. (2016). Associations between actigraphy-assessed sleep, inflammatory markers, and insulin resistance in the midlife development in the United States (MIDUS) study. *Sleep Med.* 27-28, 72–79. doi: 10.1016/j.sleep.2016.07.023

Krishnamoorthy, S., Li, G. H., and Cheung, C. L. (2023). Transcriptome-wide summary data-based Mendelian randomization analysis reveals 38 novel genes associated with severe COVID-19. *J. Med. Virol.* 95:e28162. doi: 10.1002/jmv.28162

Lam, D. D., Antic Nikolic, A., Zhao, C., Mirza-Schreiber, N., Krężel, W., Oexle, K., et al. (2022). Intronic elements associated with insomnia and restless legs syndrome exhibit cell-type-specific epigenetic features contributing to MEIS1 regulation. *Hum. Mol. Genet.* 31, 1733–1746. doi: 10.1093/hmg/ddab355

Li, X., Zhang, J., Li, D., He, C., He, K., Xue, T., et al. (2021). Astrocytic ApoE reprograms neuronal cholesterol metabolism and histone-acetylation-mediated memory. *Neuron* 109, 957–970.e8. doi: 10.1016/j.neuron.2021.01.005

Livshits, G., Ni Lochlainn, M., Malkin, I., Bowyer, R., Verdi, S., Steves, C. J., et al. (2018). Shared genetic influence on frailty and chronic widespread pain: a study from TwinsUK. *Age Ageing* 47, 119–125. doi: 10.1093/ageing/afx122

Meng, P., Pan, C., Cheng, S., Li, C., Yao, Y., Liu, L., et al. (2022). Evaluating the role of rare genetic variation in sleep duration. *Sleep Health* 8, 536–541. doi: 10.1016/j.sleh.2022.05.007

Nagpal, N., and Kulshreshtha, R. (2014). miR-191: an emerging player in disease biology. *Front. Genet.* 5:99. doi: 10.3389/fgene.2014.00099

Nemoto, Y., Sato, S., Kitabatake, Y., Nakamura, M., Takeda, N., Maruo, K., et al. (2021). Bidirectional relationship between insomnia and frailty in older adults: a 2-year longitudinal study. *Arch. Gerontol. Geriatr.* 97:104519. doi: 10.1016/j.archger.2021.104519

Nishita, Y., Nakamura, A., Kato, T., Otsuka, R., Iwata, K., Tange, C., et al. (2019). Links between physical frailty and regional gray matter volumes in older adults: a voxel-based morphometry study. *J. Am. Med. Dir. Assoc.* 20, 1587–1592.e7. doi: 10.1016/j.jamda.2019.09.001

Okamura, K., Kawai, T., Hata, K., and Nakabayashi, K. (2016). Lists of HumanMethylation450 BeadChip probes with nucleotide-variant information obtained from the phase 3 data of the 1000 genomes project. *Genom Data.* 7, 67–69. doi: 10.1016/j.gdata.2015.11.023

Ostrom, Q. T., Kinnersley, B., Wrensch, M. R., Eckel-Passow, J. E., Armstrong, G., Rice, T., et al. (2018). Sex-specific glioma genome-wide association study identifies new risk locus at 3p21.31 in females, and finds sex-differences in risk at 8q24.21. *Sci. Rep.* 8:7352. doi: 10.1038/s41598-018-24580-z

Pak, V. M., Onen, S. H., Bliwise, D. L., Kutner, N. G., Russell, K. L., and Onen, F. (2020). Sleep disturbances in MCI and AD: Neuroinflammation as a possible mediating pathway. *Front. Aging Neurosci.* 12:69. doi: 10.3389/fnagi.2020.00069

Perlis, M. L., Posner, D., Riemann, D., Bastien, C. H., Teel, J., and Thase, M. (2022). Insomnia. *Lancet* 400, 1047–1060. doi: 10.1016/S0140-6736(22)00879-0

Pourmotabbed, A., Boozari, B., Babaei, A., Asbaghi, O., Campbell, M. S., Mohammadi, H., et al. (2020). Sleep and frailty risk: a systematic review and meta-analysis. *Sleep Breath.* 24, 1187–1197. doi: 10.1007/s11325-020-02061-w

Qiu, S., Hu, Y., Zou, Q., and Liu, G. (2022). Genetic variant rs9848497 up-regulates MST1R expression, thereby influencing leadership phenotypes. *Proc. Natl. Acad. Sci. USA* 119:e2207847119. doi: 10.1073/pnas.2207847119

Reimann, G. M., Küppers, V., Camilleri, J. A., Hoffstaedter, F., Langner, R., Laird, A. R., et al. (2023). Convergent abnormality in the subgenual anterior cingulate cortex in insomnia disorder: a revisited neuroimaging meta-analysis of 39 studies. *Sleep Med. Rev.* 71:101821. doi: 10.1016/j.smrv.2023.101821

Serna, E., Gambini, J., Borras, C., Abdelaziz, K. M., Belenguer, A., Sanchis, P., et al. (2012). Centenarians, but not octogenarians, up-regulate the expression of microRNAs. *Sci. Rep.* 2:961. doi: 10.1038/srep00961

Shi, H., Mancuso, N., Spendlove, S., and Pasaniuc, B. (2017). Local genetic correlation gives insights into the shared genetic architecture of complex traits. *Am. J. Hum. Genet.* 101, 737–751. doi: 10.1016/j.ajhg.2017.09.022

Shi, S. M., Olivieri-Mui, B., McCarthy, E. P., and Kim, D. H. (2021). Changes in a frailty index and association with mortality. *J. Am. Geriatr. Soc.* 69, 1057–1062. doi: 10.1111/jgs.17002

Skrivankova, V. W., Richmond, R. C., Woolf, B., Davies, N. M., Swanson, S. A., VanderWeele, T. J., et al. (2021a). Strengthening the reporting of observational studies in epidemiology using mendelian randomisation (STROBE-MR): explanation and elaboration. *BMJ* 375:n2233. doi: 10.1136/bmj.n2233

Skrivankova, V. W., Richmond, R. C., Woolf, B., Yarmolinsky, J., Davies, N. M., Swanson, S. A., et al. (2021b). Strengthening the reporting of observational studies in epidemiology using Mendelian randomization: the STROBE-MR statement. *JAMA* 326, 1614–1621. doi: 10.1001/jama.2021.18236

Sun, H., Zhang, J., Ma, Y., and Liu, J. (2020). Integrative genomics analysis identifies five promising genes implicated in insomnia risk based on multiple omics datasets. *Biosci. Rep.* 40:BSR20201084. doi: 10.1042/BSR20201084

Tang, J. Y., Luo, H., Tse, M., Lum, T. Y., Wong, G. H., and Li, S. X. (2021). The relationship between insomnia symptoms and frailty in community-dwelling older persons: a path analysis. *Sleep Med.* 84, 237–243. doi: 10.1016/j.sleep.2021.05.039

Tian, Y., Ma, G., Li, H., Zeng, Y., Zhou, S., Wang, X., et al. (2023). Shared genetics and comorbid genes of amyotrophic lateral sclerosis and Parkinson's disease. *Mov. Disord.* 38, 1813–1821. doi: 10.1002/mds.29572

Turley, P., Walters, R. K., Maghzian, O., Okbay, A., Lee, J. J., Fontana, M. A., et al. (2018). Multi-trait analysis of genome-wide association summary statistics using MTAG. *Nat. Genet.* 50, 229–237. doi: 10.1038/s41588-017-0009-4

Verbanck, M., Chen, C. Y., Neale, B., and Do, R. (2018). Detection of widespread horizontal pleiotropy in causal relationships inferred from Mendelian randomization between complex traits and diseases. *Nat. Genet.* 50, 693–698. doi: 10.1038/s41588-018-0099-7

Watanabe, K., Jansen, P. R., Savage, J. E., Nandakumar, P., Wang, X., 23andMe Research Teamet al. (2022). Genome-wide meta-analysis of insomnia prioritizes genes associated with metabolic and psychiatric pathways. *Nat. Genet.* 54, 1125–1132. doi: 10.1038/s41588-022-01124-w

Wen, Q., Yan, X., Ren, Z., Wang, B., Liu, Y., and Jin, X. (2023). Association between insomnia and frailty in older population: a meta-analytic evaluation of the observational studies. *Brain Behav.* 13:e2793. doi: 10.1002/brb3.2793

Yang, Y., Musco, H., Simpson-Yap, S., Zhu, Z., Wang, Y., Lin, X., et al. (2021). Investigating the shared genetic architecture between multiple sclerosis and inflammatory bowel diseases. *Nat. Commun.* 12:5641. doi: 10.1038/s41467-021-25768-0

Ye, Y., Noche, R. B., Szejko, N., Both, C. P., Acosta, J. N., Leasure, A. C., et al. (2023). A genome-wide association study of frailty identifies significant genetic correlation with neuropsychiatric, cardiovascular, and inflammation pathways. *Geroscience.* 45, 2511–2523. doi: 10.1007/s11357-023-00771-z

Yoshida, G. M., and Yáñez, J. M. (2021). Multi-trait GWAS using imputed high-density genotypes from whole-genome sequencing identifies genes associated with body traits in Nile tilapia. *BMC Genomics* 22:57. doi: 10.1186/s12864-020-07341-z

Zeng, R., Jiang, R., Huang, W., Wang, J., Zhang, L., Ma, Y., et al. (2023). Dissecting shared genetic architecture between obesity and multiple sclerosis. *EBioMedicine* 93:104647. doi: 10.1016/j.ebiom.2023.104647

Zhang, Z., Wang, M., Gill, D., Zhu, W., and Liu, X. (2023). Genetically predicted sleep traits and functional outcome after ischemic stroke: a Mendelian randomization study. *Neurology* 100, e1159–e1165. doi: 10.1212/WNL.0000000000206745

Zhu, Z., Hasegawa, K., Camargo, C. A. Jr., and Liang, L. (2021). Investigating asthma heterogeneity through shared and distinct genetics: insights from genome-wide cross-trait analysis. *J. Allergy Clin. Immunol.* 147, 796–807. doi: 10.1016/j.jaci.2020.07.004

Zhu, Z., Zhang, F., Hu, H., Bakshi, A., Robinson, M. R., Powell, J. E., et al. (2016). Integration of summary data from GWAS and eQTL studies predicts complex trait gene targets. *Nat. Genet.* 48, 481–487. doi: 10.1038/ng.3538

Zhu, Z., Zheng, Z., Zhang, F., Wu, Y., Trzaskowski, M., Maier, R., et al. (2018). Causal associations between risk factors and common diseases inferred from GWAS summary data. *Nat. Commun.* 9:224. doi: 10.1038/s41467-017-02317-2

frontiers | Frontiers in Aging Neuroscience

TYPE Hypothesis and Theory
PUBLISHED 21 February 2024
DOI 10.3389/fnagi.2024.1339295

OPEN ACCESS

EDITED BY
Caroline Haikal,
New York-Presbyterian, United States

REVIEWED BY
Carla Masala,
University of Cagliari, Italy
Juan Segura-Aguilar,
University of Chile, Chile

*CORRESPONDENCE
Kandategе Wimalasena
kandategе.wimalasena@wichita.edu

†These authors have contributed equally to this work

RECEIVED 15 November 2023
ACCEPTED 09 February 2024
PUBLISHED 21 February 2024

CITATION
Wimalasena K, Adetuyi O and Eldani M (2024) Metabolic energy decline coupled dysregulation of catecholamine metabolism in physiologically highly active neurons: implications for selective neuronal death in Parkinson's disease.
Front. Aging Neurosci. 16:1339295.
doi: 10.3389/fnagi.2024.1339295

Metabolic energy decline coupled dysregulation of catecholamine metabolism in physiologically highly active neurons: implications for selective neuronal death in Parkinson's disease

Kandategе Wimalasena *, Oluwatosin Adetuyi† and Maya Eldani†

Department of Chemistry and Biochemistry, Wichita State University, Wichita, KS, United States

Parkinson's disease (PD) is an age-related irreversible neurodegenerative disease which is characterized as a progressively worsening involuntary movement disorder caused by the loss of dopaminergic (DA) neurons in substantia nigra pars compacta (SNpc). Two main pathophysiological features of PD are the accumulation of inclusion bodies in the affected neurons and the predominant loss of neuromelanin-containing DA neurons in substantia nigra pars compacta (SNpc) and noradrenergic (NE) neurons in locus coeruleus (LC). The inclusion bodies contain misfolded and aggregated α-synuclein (α-Syn) fibrils known as Lewy bodies. The etiology and pathogenic mechanisms of PD are complex, multi-dimensional and associated with a combination of environmental, genetic, and other age-related factors. Although individual factors associated with the pathogenic mechanisms of PD have been widely investigated, an integration of the findings to a unified causative mechanism has not been envisioned. Here we propose an integrated mechanism for the degeneration of DA neurons in SNpc and NE neurons in LC in PD, based on their unique high metabolic activity coupled elevated energy demand, using currently available experimental data. The proposed hypothetical mechanism is primarily based on the unique high metabolic activity coupled elevated energy demand of these neurons. We reason that the high vulnerability of a selective group of DA neurons in SNpc and NE neurons in LC in PD could be due to the cellular energy modulations. Such cellular energy modulations could induce dysregulation of DA and NE metabolism and perturbation of the redox active metal homeostasis (especially copper and iron) in these neurons.

KEYWORDS

Parkinson's disease, Catecholamine metabolism, neuromelanin, alphasynuclein, catecholamine biosynthesis and regulation, neurodegeneration, oxidative stress

1 Introduction

Parkinson's disease (PD) is an age-related irreversible neurodegenerative disease which is the second most common among all neurodegenerative diseases. PD is largely characterized as a progressively worsening involuntary movement disorder caused by the loss of dopaminergic (DA) neurons in substantia nigra pars compacta (SNpc). Two main pathological hallmarks of PD are the accumulation of inclusion bodies in the cytosol of affected neurons known as Lewy bodies and the predominant loss of neuromelanin-containing DA neurons in substantia nigra pars compacta (SNpc) and noradrenergic (NE) neurons in locus coeruleus (LC) (Zecca et al., 2004, 2006; Zucca et al., 2006; Rommelfanger and Weinshenker, 2007; Vila, 2019). The Lewy bodies contain misfolded and aggregated α-synuclein (α-Syn) fibrils [however, precise role of α-SYN in PD or its regular physiological function is not fully understood, at present; for recent reviews see (Sulzer and Edwards, 2019; Bernal-Conde et al., 2020; Sharma and Burré, 2023)]. Although environmental, genetic, and other age-related causes of PD have been studied for several decades, an integration of the findings to a unified causative mechanism has not been achieved. Most experimental observations to date suggest that the causes of PD are multidimensional and thus, any integrated mechanism must satisfy the key findings in all relevant areas. Here we envision an integrated mechanism for the degeneration of DA neurons in SNpc and NE neurons in LC in PD using available experimental data.

1.1 The hypothesis

The proposed hypothetical mechanism is primarily based on the unique high metabolic activity coupled elevated energy demand of these neurons. We reason that the high vulnerability of a selective group of DA neurons in SNpc and NE neurons in LC in PD could be due to the cellular energy modulations induced dysregulation of DA and NE metabolism and perturbation of the redox active metal homeostasis (especially copper and iron) in these neurons as argued below.

2 Critical evaluation and discussion of the evidence for the hypothesis

2.1 Catecholamine biosynthesis, storage, and recycling

Numerous studies suggest that oxidatively labile cytosolic catecholamines, their metabolic intermediates, and biosynthetic precursors such as L-3,4-dihydroxyphenylalanine (L-DOPA) could collectively contribute to the degeneration of SNpc DA and LC NE neurons in PD. The intrinsic oxidative lability of the 3,4-dihydoxy phenyl functionality of DA, NE, their biosynthetic precursors and metabolites make them selectively and significantly more vulnerable to autoxidation under cytosolic conditions (Umek et al., 2018), particularly in the presence of redox active transition metals such as iron or copper, with an elevated tendency to produce increased oxidative stress (Miller et al., 1990). Thus, the perturbations of DA and NE metabolisms leading to increase cytosolic concentrations could cause increased oxidative stress and degeneration of affected neurons. Therefore, it is logical to focus on the biochemical, bioenergetic and biophysiological aspects of biosynthesis, storage, and cellular distributions of DA and NE in their respective neurons, initially [for a general rev. see ref. (Eisenhofer et al., 2004)]. Briefly, the first step in the catecholamine biosynthetic pathway is the conversion of aromatic amino acid, tyrosine, to L-DOPA by iron containing monooxygenase, tyrosine hydroxylase (TH), in the cytosol of catecholaminergic neurons (**Scheme 1**). TH reaction is the first and rate-limiting step in the catecholamine biosynthetic pathway and is under tight short-term regulation by cytosolic catecholamine mediated feedback inhibition (especially DA) in conjunction with the phosphorylation/dephosphorylation of the regulatory domain Ser residues (40, 31, and 19) by a number of protein kinases/phosphatases (Dickson and Briggs, 2013). In the second step, cytosolic L-DOPA is effectively decarboxylated by a pyridoxal phosphate dependent enzymes, DOPA decarboxylase or non-specific aromatic amino acid decarboxylases (AADC) (Bertoldi, 2014) to DA in the cytosol and, cytosolic DA is actively sequestered into the synaptic vesicles for transient storage through a H^+ coupled transmembrane antiporter, vesicular monoamine transporter-2 (VMAT2) (**Scheme 2**; Wimalasena, 2011). The intragranular H^+ ion gradient required for functioning of VMAT2 mediated active vesicular uptake of DA against a steep concentration gradient is generated by an inward H^+ translocating V-ATPase in the synaptic vesicle membrane (Wimalasena, 2011). In NE and E neurons, DA is converted to NE by the copper enzyme, dopamine β-monooxygenase (DβM), located inside the synaptic vesicles, employing ascorbic acid as the physiological reductant (**Schemes 3**, **4**; Gonzalez-Lopez and Vrana, 2020). In adrenergic neurons, NE is transported back to the cytosol from the synaptic vesicles and N-methylated by phenyl ethanolamine N-methyltransferase (PNMT) using S-adenosylmethionine (SAM) as a CH_3 donor (Ziegler et al., 2002) to produce epinephrine (E) in the cytosol and sequestered back into adrenergic synaptic vesicles by a process analogous to DA, employing VMAT2. Furthermore, a fraction of DA and NE released by exocytosis is taken up back into the corresponding presynaptic neurons through Na^+ and Cl^- co-transport coupled plasma membrane DA transporter (DAT) in DA neurons (**Scheme 5**) or NE transporter (NET) (Torres et al., 2003) in NE neurons (**Scheme 6**) for recycling. Cytosolic DA or NE derived from re-uptake pathway is combined with newly synthesized cytosolic DA or NE and effectively sequestered into the corresponding synaptic vesicles through VMAT2 as above (**Schemes 5**, **6**).

Abbreviations: ASC, ascorbate; α-SYN, α-synuclein; LC, locus coeruleus; DA, dopamine or dopaminergic; DβM, dopamine beta-monooxygenase; DAT, plasma membrane dopamine transporter; L-DOPA, L-3,4-dihydroxy-phenylalanine; E, epinephrine; NE, norepinephrine or noradrenergic; GSH, reduced glutathione; NET, plasma membrane norepinephrine transporter; NM, neuromelanin; PD, Parkinson's disease; SNpc, substantia nigra pars compacta; VMAT, vesicular monoamine transporter; TH, tyrosine hydroxylase; V-ATPase, Vacuolar ATPase; VMAT2, vesicular monoamine transporter type 2.

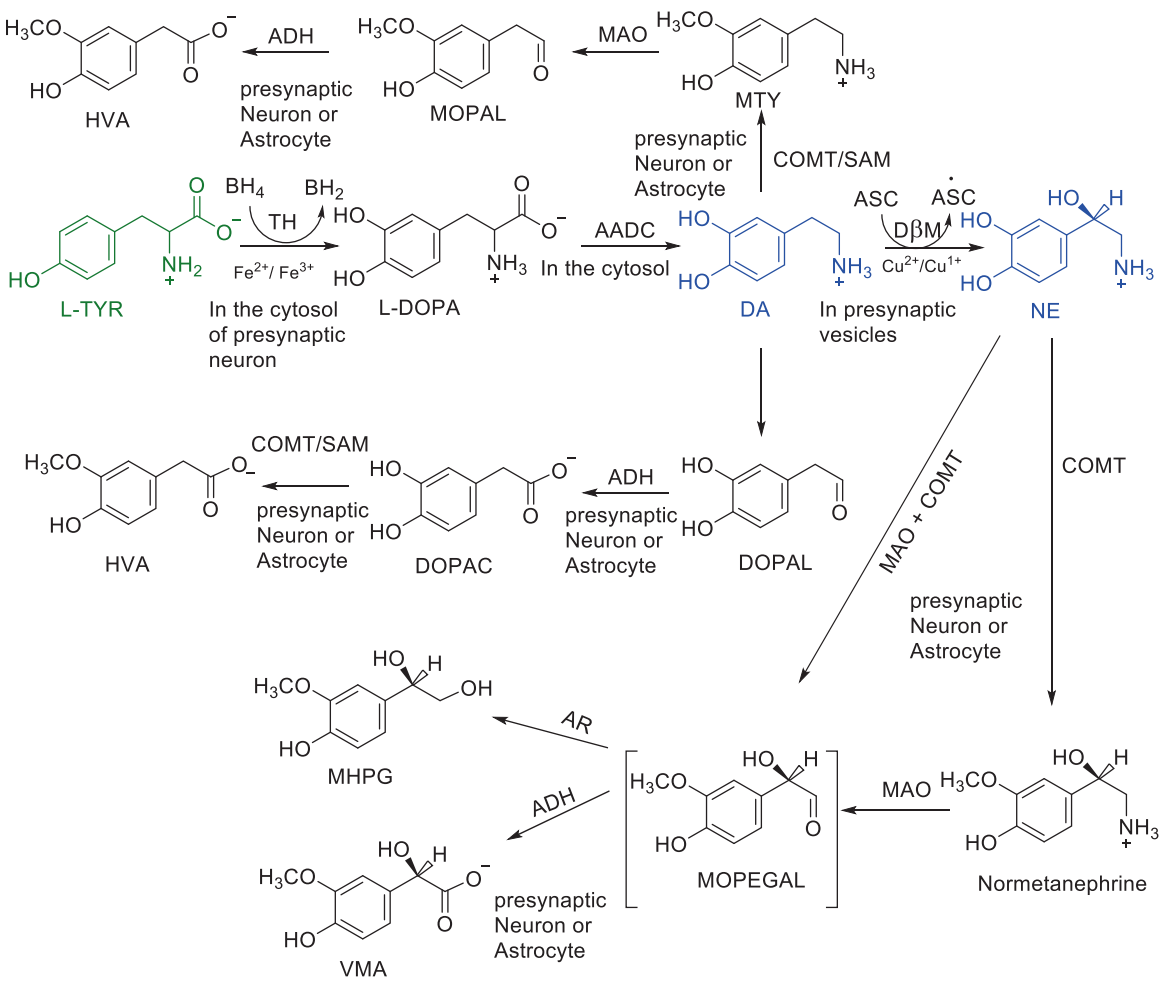

SCHEME 1
Major pathways of DA and NE metabolism. Enzymes: AADC, aromatic amino acid decarboxylase; ADH, aldehyde dehydrogenase; COMT, catechol O-methyl transferase; DβM, dopamine β-hydroxylase; MAO, monoamine oxidase; TH, tyrosine Hydroxylase Cofactors: ASC, Ascorbic acid; BH4; Tetrahydrobiopterin; SAM S-adenosylmethionine Substrates and products; DA, dopamine; DOPA, L-3,4-dihydroxyphenylalanine; DOPAC, 3,4-dihydroxyphenyacetic acid; DOPAL, 3,4-dihydroxyphenylacetaldehyde; HVA, Homo-vanillic acid; MHPG, 3-methoxy-4-hydroxyphenylglycol; MOPAL, 3-methoxy-4-hydroxyphenyl acetaldehyde; MOPEGAL, 3-methoxy-4-hydroxyphenylglycolaldehyde; MTY, 3-methoxy tyramine; L-NE, L-norepinephrine; L-Tyr, L-tyrosine; VMA, 3-methoxy-4-hydroxymandelic acid.

2.2 SNpc DA and LC NE neurons require a large investment of metabolic energy because of their specialized physiological functions in comparison to other DA and NE neurons

The biosynthesis outlined above suggest that catecholaminergic neurons generally require a relatively high investment of metabolic energy for their regulated transmitter biosynthesis, storage, and recycling, in comparison to other types of neurons. For example, energy stored in synaptic vesicle transmembrane pH gradients (**Schemes 2**, **4**) and neuronal plasma membrane Na^+ and Cl^- ion gradients (**Schemes 5**, **6**) are vital for effective synaptic vesicle sequestration and recycling of DA and NE in their respective neurons (Eisenhofer et al., 2004). More importantly, most these processes are interdependent and must be integrated and collectively regulated for optimal functioning of these neurons. Thus, perturbations of one or more of these processes could lead to dysregulation of DA and NE metabolisms leading to harmful downstream effects. For example, our previous studies have shown that the inhibition of V-ATPase or reduction of cytosolic ATP levels dissipate intragranular pH gradients and DA (or NE) gradients within a brief period in resealed chromaffin granule ghosts *in vitro* (Wimalasena et al., 2007). In addition to these general bioenergetic requirements of most DA and NE neurons, unique and specific characteristic of SNpc DA neurons and LC NE neurons require additional metabolic energy for their optimal physiological functions. For example, autonomous pacemaking and L-type Ca^{2+} channel activities (Guzman et al., 2009; Putzier et al., 2009; de Oliveira et al., 2019) specifically associated with these neurons require additional metabolic energy (Ni and Ernst, 2022) for their survival. This is because a continuous influx of extracellular Ca^{2+} into neurons during specialized processes requires efflux back into the extracellular medium through plasma membrane Ca^{2+} ATPase. Alternatively, it can be compartmentalized into endoplasmic reticulum (ER) or mitochondrial Ca^{2+} stores through membrane Ca^{2+} ATPases. These processes occur against

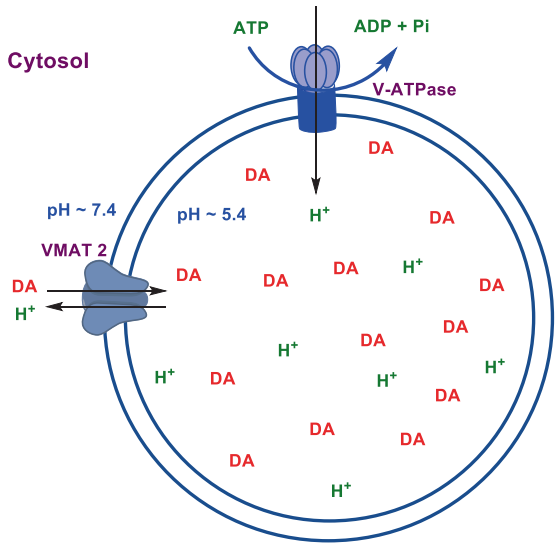

SCHEME 2
Transient storage of cytosolic DA in dopaminergic synaptic vesicles.

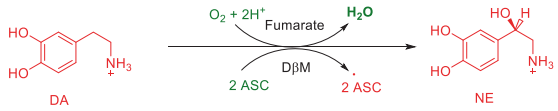

SCHEME 3
Conversion of DA to NE by dopamine β-monooxygenase (DβM).

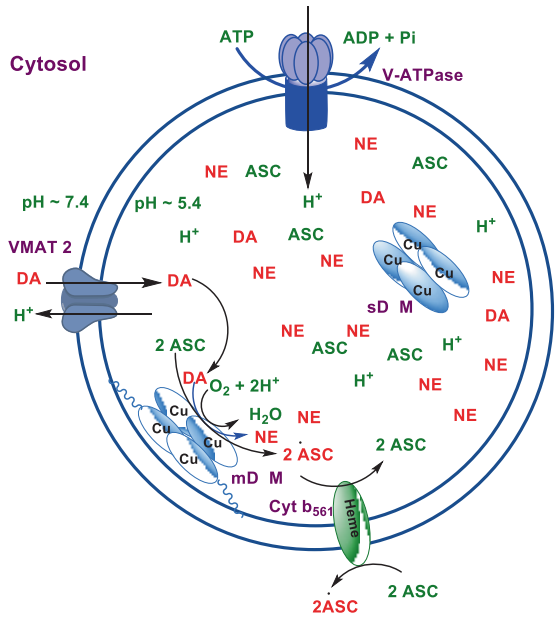

SCHEME 4
Conversion of DA to NE in synaptic vesicles of adrenergic/noradrenergic neurons.

steep concentration gradients, ensuring the maintenance of physiological cytosolic Ca^{2+} levels essential for optimal neuronal functioning (Gleichmann and Mattson, 2011; Duda et al., 2016).

In addition, extensive axonal arborization with multiple synaptic neurotransmitter release of DA neurons in SNpc and NE neurons in LC require even more metabolic energy to maintain their normal physiological activities (Oertel et al., 2019). Therefore, SNpc DA and LC NE neuronal demand for metabolic energy are even higher than that of regular DA or NE neurons. Thus, an efficient and continuous mitochondrial metabolic energy production is essential for functioning of SNpc DA and LC NE neurons, since energy requirements of these neurons are generally met by the mitochondrial electron transport coupled oxidative phosphorylation (Exner et al., 2012; Hall et al., 2012). *Consequently, reduction of mitochondrial energy production efficiency due to the inhibition of electron transport chain components by environmental toxins, loss of function mutations in various mitochondrial proteins and factors, or age-related general reduction of the mitochondrial metabolic energy production efficiency could be detrimental to the physiological functions of these neurons. Reduced cellular energy supply* (Exner et al., 2012) *could result in the dysregulation of SNpc DA and LC NE metabolisms leading to increased oxidative stress associated downstream adverse effects. Thus, the selective degeneration of SNpc DA and LC NE neurons in PD could be due to a combination of environmental* (Ball et al., 2019), *genetic* (Klein and Westenberger, 2012), *and age-related factors associated with inefficient mitochondrial metabolic energy production* (Bose and Beal, 2016) *leading to dysregulation of DA and NE metabolism in these neurons.*

2.3 NM was spontaneously produced from oxidized DA or NE in metabolically highly active SNpc DA and LC NE neurons as a defensive mechanism against the metabolic energy coupled frequent dysregulation of DA and NE metabolism

As mentioned above, neuromelanin (NM)-containing DA neurons in SNpc and NE neurons in LC are the most vulnerable in PD (Vila et al., 2019). However, the role of NM in PD or the molecular details of NM biosynthesis is not fully understood at present. On the other hand, limited structural information available to date suggest that the initial step of NM biosynthesis is the oxidation of cytosolic DA or NE (but, not synaptic vesicle DA or NE) to the corresponding quinones (**Scheme 7**; Wakamatsu et al., 2003, 2012, 2019). Although, relatively well understood peripheral melanin biosynthesis is initiated with tyrosinase (or TH) catalyzed oxidation of tyrosine to DOPA and then to dopaquinone (Bisaglia et al., 2007; Nagatsu et al., 2022), since significant levels of tyrosinase expression in SNpc, LC or other areas of the brain has not been detected (Tribl et al., 2007), transition metal (most likely copper or iron) assisted catalytic autoxidation of cytosolic DA or NE to corresponding quinones has been proposed as the initial step in NM production (Sulzer et al., 2000; Zhang et al., 2019). Thus, NM is most likely produced non-enzymatically, from oxidized cytosolic DA or NE and other protein and non-protein components (Sulzer et al., 2000). [Although some derivatives of dopaquinones are neurotoxic

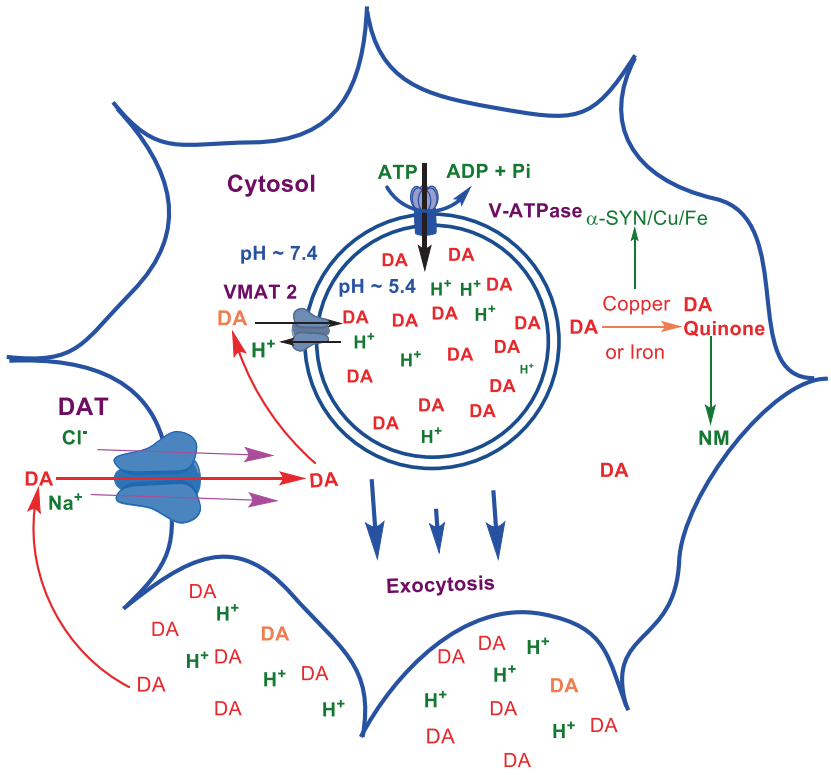

SCHEME 5
Exocytotic release and recycling of DA in dopaminergic neurons.

(i.e., aminochrome), their toxicity could be mitigated through the reduction by DT-diaphorase which is in turn converted to NM in dopaminergic neurons. In addition, these derivatives stimulate expression of glutathione S-transferase μ 2 (GSTM2) which is then released by astrocytes into inter-synaptic space where it gets internalized by dopaminergic neurons. GSTM2 converts dopaquinone and its derivatives into stable products and eventually to NM and therefore DT-diaphorase and GSTM2 could moderate the neurotoxicity of dopaquinone and its derivatives (**Scheme 7** and for a recent review see Segura-Aguilar et al., 2022)]. Interestingly, insoluble NM particles are also known to bind redox active metals including iron and copper (Zecca et al., 2001) and cationic mitochondrial toxins such as MPP^+ and Paraquat (Capucciati et al., 2021).

According to the above envisioned high metabolic activity coupled elevated energy demand hypothesis, NM production from the oxidized cytosolic DA or NE could be defined as a defensive mechanism against the low metabolic energy coupled frequent dysregulation of DA and NE metabolism in SNpc DA and LC NE neurons. Metabolically highly active SNpc DA and LC NE neurons with a high demand for metabolic energy (Ni and Ernst, 2022)*, could be significantly more susceptible to frequent low metabolic energy coupled dysregulation of DA and NE metabolism resulting in high levels of NM production. On the other hand, frequent DA and NE metabolism dysregulations could also lead to cytosolic DA and NE accumulations, making these neurons more susceptible to increased oxidative stress and eventual degeneration. This occurs when the net rate of cytosolic DA and NE accumulations (biosynthesis plus recycling) exceed the rates of NM production plus VMAT2 mediated synaptic sequestration. Even if these rates were similar, and no net accumulation of cytosolic DA or NE occurs, progressive and prolong cytosolic accumulation of insoluble NM complexes above a certain threshold could interfere with the regular physiological functions of these neurons (e.g., exocytotic release of transmitters and free movement of intracellular organelles such as mitochondria and synaptic vesicles), leading to their malfunctions and degeneration. This proposal is also consistent with the recent demonstration* (Carballo-Carbajal et al., 2019) *that over-expression of human tyrosinase in rat SNpc DA neurons result in age dependent progressive accumulation of NM and their degeneration above specific threshold of accumulation similar to that of PD. Thus,* while the production of neuromelanin (NM) from cytosolic dopamine (DA) or norepinephrine (NE) may initially offer neuroprotection, persistent dysregulation of DA or NE metabolism due to frequent low metabolic energy could result in the accumulation of cytosolic DA or NE. This accumulation, especially beyond a critical threshold, may lead to progressive and selective death of neuromelanin-containing DA and NE neurons in PD. *Thus, metabolically highly active, NM containing SNpc DA and LC NE neurons could be selectively more vulnerable to degeneration in PD. Furthermore, the ability of NM to sequester redox active metal and mitochondrial toxins from the soluble cytosolic milieu will help to maintain the cellular copper and iron homeostasis and to protect electron transport complexes in these neurons form environmental toxins. However, under degenerative conditions, NM containing neurons could release intracellular NM complexes containing redox metals to the extra neuronal space stimulating the progression of neural death to the*

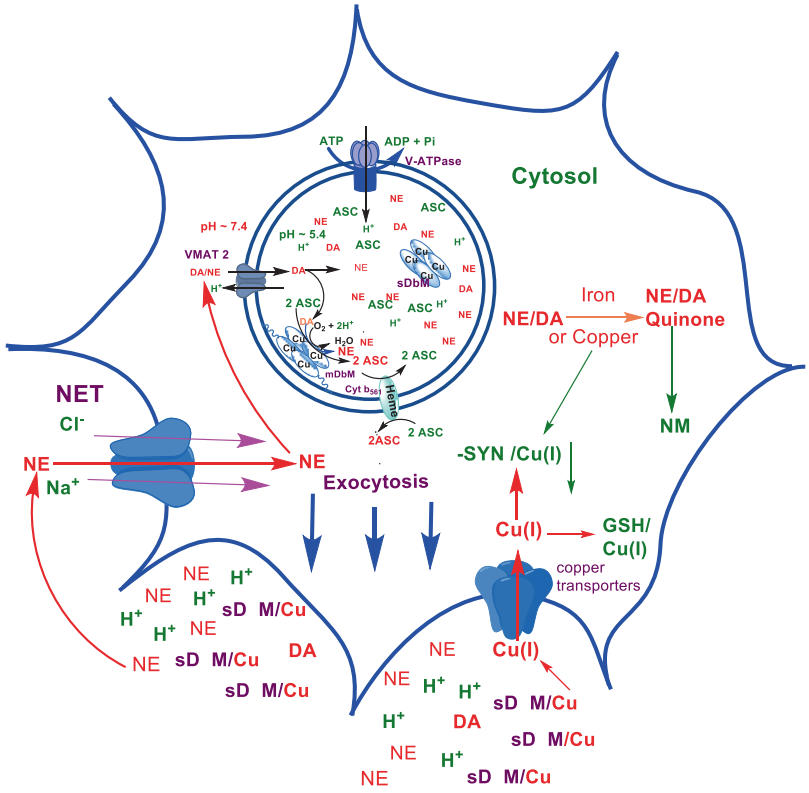

SCHEME 6
Exocytotic release and recycling of NE in noradrenergic neurons.

adjacent neurons and activation of microglia induced inflammation (Liddelow et al., 2017; Tansey et al., 2022), *further stimulating the neural death pathways.*

2.4 The physiological role of α-SYN could be to assist the maintenance of cellular toxic metal homeostasis

The early observation that misfolded and aggregated α-SYN containing inclusion bodies (Lewy bodies) are present in SNpc DA neurons of most PD patients has led to the proposal that the accumulation of α-SYN containing Lewy bodies contribute to the dopaminergic degeneration in PD (Lücking and Brice, 2000; Mehra et al., 2019; Srinivasan et al., 2021). *However, whether α-SYN containing Lewy body accumulation is the cause, or it is a downstream symptom of PD pathology has not been convincingly established yet and many questions remain unanswered at present.* For example, total α-SYN levels were consistently reduced in PD patient brains compared to non-PD controls (Stefanis, 2012). Similarly, PD therapies and diagnostic tools developed based on targeting spread, production, aggregation, and degradation of α-SYN have provided a limited or variable success in curing, halting, or diagnosing the progression of PD (Brundin and Olsson, 2011). On the other hand, the ability of α-SYN to bind numerous redox active metals, especially in the context of PD, has been widely studied (Binolfi et al., 2006; Mezzaroba et al., 2019). Among many metals known to bind α-SYN, copper (Wang et al., 2010; Valensin et al., 2016) and iron (Peng et al., 2010) has taken center stage due to the high affinities of these metals toward α-SYN and the general consensus is that these metals are closely associated with the pathophysiology of PD (Montes et al., 2014). The high affinity binding site of α-SYN binds both Cu(I) and Cu(II) with dissociation constants in the nanomolar range [$K_d \sim 1.10 \times 10^{-10}$ M for Cu(II) (Dudzik et al., 2013) and 3.9×10^{-9} M for Cu(I)] (Gentile et al., 2018). Although Fe(II) binds weakly ($K_d = 1.7 \times 10^{-4}$ M), Fe (III) binds strongly ($K_d = 8.3 \times 10^{-14}$ M) to α-SYN (Peng et al., 2010). More importantly, both copper and iron binding to α-SYN increases its tendency to aggregation and formation of insoluble amyloid fibrils *in vitro* (Wang et al., 2010). Additionally, in contrast to the previous proposals that α-SYN bound copper is more effective in redox oxygen activation in the presence of biological reductant such as ascorbate or catecholamines (Valensin et al., 2016), recent studies suggest that binding to α-SYN, reduces oxygen activation efficacy of free copper (Dell'Acqua et al., 2015; Bacchella et al., 2023) further validating the significance of copper binding characteristics of α-SYN. *Thus, it is conceivable that α-SYN could be a physiologically relevant auxiliary in vivo copper/iron buffering system that could contribute to the maintenance of cellular copper/iron homeostasis in SNpc DA and LC NE neurons, especially under stressed conditions.* For example, copper/iron α-SYN interaction could effectively complement other neuronal copper buffering systems such as glutathione [$K_d = 9 \times 10^{-12}$ M (Banci et al., 2010)] and metallothionein, and ferrous binding systems such as ferritin [$K_d = 4.7 \times 10^{-9}$ M (Hulet et al., 1999)]. *Based on these arguments, we propose that*α-synuclein (α-SYN) in dopamine (DA) and norepinephrine

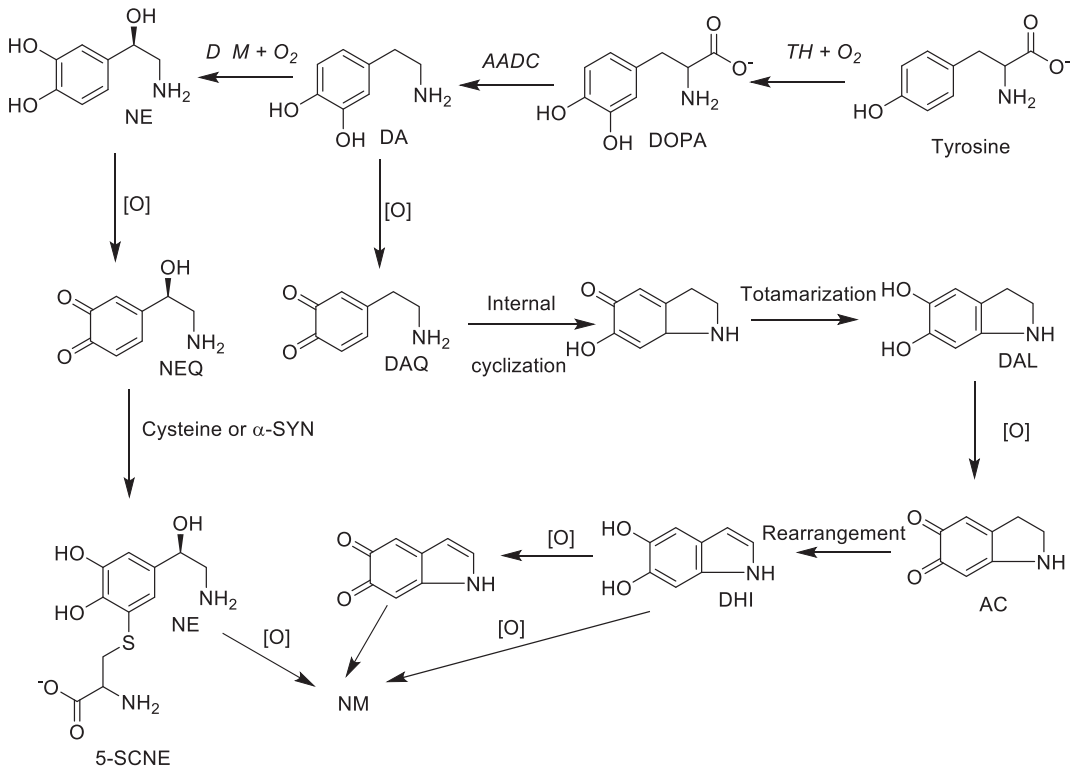

SCHEME 7
Possible major oxidative pathways for the formation of neuromelanin from dopamine and norepinephrine: AC, aminochrome DA, dopamine; DAL, leuco-dopamine chrome; DAQ, dopamine quinone; DHI, 5,6- hydroxy indole; DOPA L-3,4-dihydroxyphenylalanine; NE, norepinephrine; NEQ norepinephrine quinone; 5SCNE, 5-S-cysteinylnorepinephrine Enzymes: TH, tyrosine hydroxylase; AADC, aromatic amino acid decarboxylase; DβM, dopamine beta-monooxygenase; [O], autoxidation in the presence of transition metal ions; NM, neuromelanin.

(NE) neurons may play a physiological role by serving as an auxiliary cytosolic copper/iron detoxifying/buffering system. These functions protect DA and NE neurons from heightened oxidative stress induced by free copper and iron, particularly in situations where copper/iron homeostasis and/or catecholamine metabolism are dysregulated. *However, as discussed below copper-α-SYN interaction could be physiologically more relevant to the protection of LC NE neurons (in comparison to SNpc DA neurons) from copper/NE induced oxidative stress and downstream adverse effects.*

2.5 Copper binding properties of α-SYN could be especially critical to maintain copper homeostasis in LC NE neurons

As mentioned above, the copper enzyme, DβM, catalyzes the conversion of DA to NE in NE and E synaptic vesicles [for reviews see refs (Stewart and Klinman, 1988; Gonzalez-Lopez and Vrana, 2020; **Schemes 4**, **5**)]. Early estimates have demonstrated that equal amounts of sequentially and structurally related (Stewart and Klinman, 1988; Gonzalez-Lopez and Vrana, 2020) membrane bound (mDβM) and soluble (sDβM) forms of DβM are present in NE and E synaptic vesicles (Lewis and Asnani, 1992). After exocytotic release, while sDβM is discarded (**Scheme 6**), mDβM is recycled through synaptic membrane recycling pathway (Wimalasena and Wimalasena, 2004). The observation that free copper concentration in the synaptic cleft area of NE neurons is relatively higher in comparison to other aminergic neurons under normal physiological conditions (Rihel, 2018) suggest that disposed sDβM may contribute to the increase of free copper in synaptic cleft areas of these neurons. Thus, exocytotic release of the synaptic content of NE neurons must be accompanied by a decrease in intracellular copper levels. Thus, the synaptic release must be coupled with a suitable copper re-uptake system to maintain the overall copper homeostasis in NE neurons. A major portion of extracellular copper enters into neurons through a highly abundant copper transporter 1 (CTR1) (Davies et al., 2013; An et al., 2022) as Cu(I) (An et al., 2022; **Scheme 6**). Since cytosolic free copper is toxic, especially in the presence of catecholamines, it must be immediately and transiently recruited by medium-affinity intracellular copper buffering systems such as glutathione (K_d = 9 × 10^{-12} M) or metallothionines (**Scheme 6**). Subsequently, it is selectively transferred to high affinity copper chaperones (i.e., Atox1, Cox 1, and CCS) in the cytosol (Hatori and Lutsenko, 2016) and eventually recruited for the synthesis of various copper containing proteins. Since metabolically highly active LC NE neurons (see above) must be highly susceptible to frequent dysregulation of cellular copper homeostasis, the copper binding tendency of α-SYN could provide an additional avenue to maintain the neuronal copper homeostasis reducing their vulnerability to produce cytosolic copper/catecholamine induced high oxidative stress. In fact, copper binding and buffering characteristics of

α-SYN could be even more critical in PD, since PD pathology is intimately associated with high oxidative stress and significant depletion of cellular reduced glutathione levels (Sian et al., 1994; Martin and Teismann, 2009).

3 Conclusion

Salient features of the above envisioned integrated causes of PD are: (1) The high metabolic activity associated elevated energy demand of DA neurons in SNpc and NE neurons in LC makes them selectively more vulnerable to inadequate energy supply associated dysregulation of catecholamine metabolism, increased oxidative stress, and degeneration. (2) Frequent inadequate metabolic energy supply for these neurons could be a consequence of low mitochondrial metabolic energy output, most likely due to the continuous exposure to environmental mitochondrial toxins, age related decline of overall mitochondrial energy production efficiency, or specific mutations in vital mitochondrial proteins and other factors affecting the normal physiological functions of the mitochondria. (3) The selective NM production in PD sensitive DA and NE neurons could be an initial defense mechanism against the inadequate metabolic energy supply coupled dysregulation of catecholamine metabolism. This is because spontaneous insoluble NM production transiently removes toxic cytosolic DA/NE and redox active iron/copper from the soluble cytosolic medium leading to their detoxification. However, frequent dysregulation of DA/NE metabolism leading to their cytosolic accumulations or increased synthesis of insoluble NM complexes above a certain threshold obstructing the normal functions of these neurons could lead to their malfunctions and degenerations. (4) Major physiological function of α-SYN in metabolically highly active SNpc DA and LC NE neurons could be to transiently buffer the redox active cytosolic transition metals (especially, copper and iron). Metal binding stimulated aggregation of insoluble α-SYN/copper/iron complexes facilitate maintenance of the copper and iron homeostasis and lessen the tendency for cytosolic copper/iron/catecholamine induced increase oxidative stress in these neurons. However, progressive, and excessive accumulation of insoluble α-SYN/iron/copper complexes above a specific threshold may interfere with the normal physiological functions of these neurons leading to their malfunctions and degeneration. Taken together, integrated causes envisioned here suggest that long-term preventive strategies of PD must include an adequate continuous supply of cellular metabolic energy to these neurons to minimize the frequent dysregulation of DA and NE metabolisms.

Data availability statement

The original contributions presented in this study are included in this article/supplementary materials, further inquiries can be directed to the corresponding author.

Author contributions

KW: Conceptualization, Writing–original draft, Writing—review and editing. OA: Writing–review and editing, Writing–original draft. ME: Writing–review and editing.

Funding

The author(s) declare that no financial support was received for the research, authorship, and/or publication of this article. This research did not receive any specific grant from funding agencies in the public, commercial, or not-for profit sectors.

Acknowledgments

We would like to thank Wichita State University Chemistry and Biochemistry Department for partial financial support.

Conflict of interest

The authors declare that the research was conducted in the absence of any commercial or financial relationships that could be construed as a potential conflict of interest.

Publisher's note

All claims expressed in this article are solely those of the authors and do not necessarily represent those of their affiliated organizations, or those of the publisher, the editors and the reviewers. Any product that may be evaluated in this article, or claim that may be made by its manufacturer, is not guaranteed or endorsed by the publisher.

References

An, Y., Li, S., Huang, X., Chen, X., Shan, H., and Zhang, M. (2022). The role of copper homeostasis in brain disease. *Int. J. Mol. Sci.* 23, 13850. doi: 10.3390/ijms232213850

Bacchella, C., Camponeschi, F., Kolkowska, P., Kola, A., Tessari, I., Baratto, M., et al. (2023). Copper binding and redox activity of α-synuclein in membrane-like environment. *Biomolecules* 13, 287. doi: 10.3390/biom13020287

Ball, N., Teo, W., Chandra, S., and Chapman, J. (2019). Parkinson's disease and the environment. *Front. Neurol.* 10:218. doi: 10.3389/fneur.2019.00218

Banci, L., Bertini, I., Ciofi-Baffoni, S., Kozyreva, T., Zovo, K., and Palumaa, P. (2010). Affinity gradients drive copper to cellular destinations. *Nature* 465, 645–648. doi: 10.1038/nature09018

Bernal-Conde, L., Ramos-Acevedo, R., Reyes-Hernández, M., Balbuena-Olvera, A., Morales-Moreno, I., Argüero-Sánchez, R., et al. (2020). Alpha-synuclein physiology

and pathology: A perspective on cellular structures and organelles. *Front. Neurosci.* 13:1399. doi: 10.3389/fnins.2019.01399

Bertoldi, M. (2014). Mammalian Dopa decarboxylase: structure, catalytic activity and inhibition. *Arch. Biochem. Biophys.* 546, 1–7. doi: 10.1016/j.abb.2013.12.020

Binolfi, A., Rasia, R., Bertoncini, C., Ceolin, M., Zweckstetter, M., Griesinger, C., et al. (2006). Interaction of alpha-synuclein with divalent metal ions reveals key differences: a link between structure, binding specificity and fibrillation enhancement. *J. Am. Chem. Soc.* 128, 9893–9891. doi: 10.1021/ja0618649

Bisaglia, M., Mammi, S., and Bubacco, L. (2007). Kinetic and structural analysis of the early oxidation products of dopamine: analysis of the interactions with alpha-synuclein. *J. Biol. Chem.* 282, 15597–15605. doi: 10.1074/jbc.M610893200

Bose, A., and Beal, M. (2016). Mitochondrial dysfunction in Parkinson's disease. *J. Neurochem.* 139 Suppl 1, 216–231. doi: 10.1111/jnc.13731

Brundin, P., and Olsson, R. (2011). Can α-synuclein be targeted in novel therapies for Parkinson's disease? *Expert. Rev. Neurother.* 11, 917–919. doi: 10.1586/ern.11.73

Capucciati, A., Zucca, F., Monzani, E., Zecca, L., Casella, L., and Hofer, T. (2021). Interaction of neuromelanin with xenobiotics and consequences for neurodegeneration; promising experimental models. *Antioxidants*10, 824. doi: 10.3390/antiox10060824

Carballo-Carbajal, I., Laguna, A., Romero-Giménez, J., Cuadros, T., Bové, J., Martinez-Vicente, M., et al. (2019). Brain tyrosinase overexpression implicates age-dependent neuromelanin production in Parkinson's disease pathogenesis. *Nat. Commun.* 10, 973. doi: 10.1038/s41467-019-08858-y

Davies, K., Hare, D., Cottam, V., Chen, N., Hilgers, L., Halliday, G., et al. (2013). Localization of copper and copper transporters in the human brain. *Metallomics* 5, 43–51. doi: 10.1039/c2mt20151h

de Oliveira, R., Petiz, L., Lim, R., Lipski, J., Gravina, F., Brichta, A., et al. (2019). Crosstalk between mitochondria, calcium channels and actin cytoskeleton modulates noradrenergic activity of locus coeruleus neurons. *J. Neurochem.* 149, 471–487. doi: 10.1111/jnc.14692

Dell'Acqua, S., Pirota, V., Anzani, C., Rocco, M., Nicolis, S., Valensin, D., et al. (2015). Reactivity of copper-α-synuclein peptide complexes relevant to Parkinson's disease. *Metallomics* 7, 1091–1092. doi: 10.1039/c4mt00345d

Dickson, P., and Briggs, G. (2013). Tyrosine hydroxylase: regulation by feedback inhibition and phosphorylation. *Adv. Pharmacol.* 68, 13–21. doi: 10.1016/B978-0-12-411512-5.00002-6

Duda, J., Pötschke, C., and Liss, B. (2016). Converging roles of ion channels, calcium, metabolic stress, and activity pattern of Substantia nigra dopaminergic neurons in health and Parkinson's disease. *J. Neurochem* 139 Suppl 1, 156–178. doi: 10.1111/jnc.13572

Dudzik, C., Walter, E. D., Abrams, B., Jurica, M., and Millhauser, G. (2013). Coordination of copper to the membrane-bound form of α-synuclein. *Biochemistry* 52, 53–60. doi: 10.1021/bi301475q

Eisenhofer, G., Kopin, I., and Goldstein, D. (2004). Catecholamine metabolism: a contemporary view with implications for physiology and medicine. *Pharmacol. Rev.* 56, 331–349. doi: 10.1124/pr.56.3.1

Exner, N., Lutz, A., Haass, C., and Winklhofer, K. (2012). Mitochondrial dysfunction in Parkinson's disease: molecular mechanisms and pathophysiological consequences. *EMBO J.* 31, 3038–3062. doi: 10.1038/emboj.2012.170

Gentile, I., Garro, H., Delgado Ocaña, S., Gonzalez, N., Strohäker, T., Schibich, D., et al. (2018). Interaction of Cu(i) with the Met-X3-Met motif of alpha-synuclein: binding ligands, affinity and structural features. *Metallomics* 10, 1383–1389. doi: 10.1039/c8mt00232k

Gleichmann, M., and Mattson, M. (2011). Neuronal calcium homeostasis and dysregulation. *Antioxid. Redox Signal.* 14, 1261–1273. doi: 10.1089/ars.2010.3386

Gonzalez-Lopez, E., and Vrana, K. (2020). Dopamine beta-hydroxylase and its genetic variants in human health and disease. *J. Neurochem.* 152, 157–181. doi: 10.1111/jnc.14893

Guzman, J., Sánchez-Padilla, J., Chan, C., and Surmeier, D. (2009). Robust pacemaking in substantia nigra dopaminergic neurons. *J. Neurosci.* 29, 11011–11019. doi: 10.1523/JNEUROSCI.2519-09.2009

Hall, C., Klein-Flügge, M., Howarth, C., and Attwell, D. (2012). Oxidative phosphorylation, not glycolysis, powers presynaptic and postsynaptic mechanisms underlying brain information processing. *J. Neurosci.* 32, 8940–8951. doi: 10.1523/JNEUROSCI.0026-12.2012

Hatori, Y., and Lutsenko, S. (2016). The role of copper chaperone Atox1 in coupling redox homeostasis to intracellular copper distribution. *Antioxidants* 5, 25. doi: 10.3390/antiox5030025

Hulet, S., Hess, E., Debinski, W., Arosio, P., Bruce, K., Powers, S., et al. (1999). Characterization and distribution of ferritin binding sites in the adult mouse brain. *J. Neurochem.* 72, 868–874. doi: 10.1046/j.1471-4159.1999.720868.x

Klein, C., and Westenberger, A. (2012). Genetics of Parkinson's disease. *Cold Spring Harb. Perspect. Med.* 2, a008888. doi: 10.1101/cshperspect.a008888

Lewis, E., and Asnani, L. (1992). Soluble and membrane-bound forms of dopamine beta-hydroxylase are encoded by the same mRNA. *J. Biol. Chem.* 267, 494–500.

Liddelow, S., Guttenplan, K., Clarke, L., Bennett, F., Bohlen, C., Schirmer, L., et al. (2017). Neurotoxic reactive astrocytes are induced by activated microglia. *Nature* 541, 481–487. doi: 10.1038/nature21029

Lücking, C., and Brice, A. (2000). Alpha-synuclein and Parkinson's disease. *Cell Mol. Life Sci.* 57, 1894–1908. doi: 10.1007/PL00000671

Martin, H., and Teismann, P. (2009). Glutathione–a review on its role and significance in Parkinson's disease. *FASEB J.* 23, 3263–3272. doi: 10.1096/fj.08-125443

Mehra, S., Sahay, S., and Maji, S. (2019). α-Synuclein misfolding and aggregation: Implications in Parkinson's disease pathogenesis. *Biochim. Biophys. Acta Proteins Proteom.* 1867, 890–908. doi: 10.1016/j.bbapap.2019.03.001

Mezzaroba, L., Alfieri, D., Colado Simão, A., and Vissoci Reiche, E. (2019). The role of zinc, copper, manganese and iron in neurodegenerative diseases. *Neurotoxicology* 74, 230–241. doi: 10.1016/j.neuro.2019.07.007

Miller, D., Buettner, G., and Aust, S. (1990). Transition metals as catalysts of "autoxidation" reactions. *Free Radic. Biol. Med.* 8, 95–108. doi: 10.1016/0891-5849(90)90148-c

Montes, S., Rivera-Mancia, S., Diaz-Ruiz, A., Tristan-Lopez, L., and Rios, C. (2014). Copper and copper proteins in Parkinson's disease. *Oxid. Med. Cell Longev.* 2014, 147251. doi: 10.1155/2014/147251

Nagatsu, T., Nakashima, A., Watanabe, H., Ito, S., and Wakamatsu, K. (2022). Neuromelanin in Parkinson's Disease: Tyrosine Hydroxylase and Tyrosinase. *Int. J. Mol. Sci.* 23, 4176. doi: 10.3390/ijms23084176

Ni, A., and Ernst, C. (2022). Evidence that substantia nigra pars compacta dopaminergic neurons are selectively vulnerable to oxidative stress because they are highly metabolically active. *Front. Cell Neurosci.* 16:826193. doi: 10.3389/fncel.2022.826193

Oertel, W., Henrich, M., Janzen, A., and Geibl, F. (2019). The locus coeruleus: Another vulnerability target in Parkinson's disease. *Mov. Disord.* 34, 1423–1429. doi: 10.1002/mds.27785

Peng, Y., Wang, C., Xu, H., Liu, Y., and Zhou, F. (2010). Binding of alpha-synuclein with Fe(III) and with Fe(II) and biological implications of the resultant complexes. *J. Inorg. Biochem.* 104, 365–370. doi: 10.1016/j.jinorgbio.2009.11.005

Putzier, I., Kullmann, P., Horn, J., and Levitan, E. (2009). Cav1.3 channel voltage dependence, not Ca2+ selectivity, drives pacemaker activity and amplifies bursts in nigral dopamine neurons. *J. Neurosci.* 29, 15414–15419. doi: 10.1523/JNEUROSCI.4742-09.2009

Rihel, J. (2018). Copper on the brain. *Nat. Chem. Biol.* 14, 638–639. doi: 10.1038/s41589-018-0089-1

Rommelfanger, K., and Weinshenker, D. (2007). Norepinephrine: The redheaded stepchild of Parkinson's disease. *Biochem. Pharmacol.* 74, 177–190. doi: 10.1016/j.bcp.2007.01.036

Segura-Aguilar, J., Muñoz, P., Inzunza, J., Varshney, M., Nalvarte, I., and Mannervik, B. (2022). Neuroprotection against Aminochrome Neurotoxicity: Glutathione Transferase M2-2 and DT-Diaphorase. *Antioxidants* 11, 296. doi: 10.3390/antiox11020296

Sharma, M., and Burré, J. (2023). α-Synuclein in synaptic function and dysfunction. *Trends Neurosci.* 46, 153–166. doi: 10.1016/j.tins.2022.11.007

Sian, J., Dexter, D., Lees, A., Daniel, S., Agid, Y., Javoy-Agid, F., et al. (1994). Alterations in glutathione levels in Parkinson's disease and other neurodegenerative disorders affecting basal ganglia. *Ann. Neurol.* 36, 348–355. doi: 10.1002/ana.410360305

Srinivasan, E., Chandrasekhar, G., Chandrasekar, P., Anbarasu, K., Vickram, A., Karunakaran, R., et al. (2021). Alpha-Synuclein Aggregation in Parkinson's Disease. *Front. Med.* 8:736978. doi: 10.3389/fmed.2021.736978

Stefanis, L. (2012). α-Synuclein in Parkinson's disease. *Cold Spring Harb. Perspect. Med.* 2, a009399. doi: 10.1101/cshperspect.a009399

Stewart, L., and Klinman, J. (1988). Dopamine beta-hydroxylase of adrenal chromaffin granules: structure and function. *Annu. Rev. Biochem.* 57, 551–592. doi: 10.1146/annurev.bi.57.070188.003003

Sulzer, D., Bogulavsky, J., Larsen, K., Behr, G., Karatekin, E., Kleinman, M., et al. (2000). Neuromelanin biosynthesis is driven by excess cytosolic catecholamines not accumulated by synaptic vesicles. *Proc. Natl. Acad. Sci. U. S. A.* 97, 11869–11874. doi: 10.1073/pnas.97.22.11869

Sulzer, D., and Edwards, R. (2019). The physiological role of α-synuclein and its relationship to Parkinson's Disease. *J. Neurochem.* 150, 475–486. doi: 10.1111/jnc.14810

Tansey, M., Wallings, R., Houser, M., Herrick, M., Keating, C., and Joers, V. (2022). Inflammation and immune dysfunction in Parkinson disease. *Nat. Rev. Immunol.* 22, 657–673. doi: 10.1038/s41577-022-00684-6

Torres, G., Gainetdinov, R., and Caron, M. (2003). Plasma membrane monoamine transporters: structure, regulation and function. *Nat. Rev. Neurosci.* 4, 13–25. doi: 10.1038/nrn1008

Tribl, F., Arzberger, T., Riederer, P., and Gerlach, M. (2007). Tyrosinase is not detected in human catecholaminergic neurons by immunohistochemistry and

Western blot analysis. *J. Neural Transm. Suppl.* 72, 51–55. doi: 10.1007/978-3-211-73574-9_8

Umek, N., Geršak, B., Vintar, N., Šoštarič, M., and Mavri, J. (2018). Dopamine autoxidation is controlled by acidic pH. *Front. Mol. Neurosci.* 11:467. doi: 10.3389/fnmol.2018.00467

Valensin, D., Dell'Acqua, S., Kozlowski, H., and Casella, L. (2016). Coordination and redox properties of copper interaction with α-synuclein. *J. Inorg. Biochem.* 163, 292–300. doi: 10.1016/j.jinorgbio.2016.04.012

Vila, M. (2019). Neuromelanin, aging, and neuronal vulnerability in Parkinson's disease. *Mov. Disord.* 34, 1440–1451. doi: 10.1002/mds.27776

Vila, M., Laguna, A., and Carballo-Carbajal, I. (2019). Intracellular crowding by age-dependent neuromelanin accumulation disrupts neuronal proteostasis and triggers Parkinson disease pathology. *Autophagy* 15, 2028–2030. doi: 10.1080/15548627.2019.1659621

Wakamatsu, K., Fujikawa, K., Zucca, F., Zecca, L., and Ito, S. (2003). The structure of neuromelanin as studied by chemical degradative methods. *J. Neurochem.* 86, 1015–1023. doi: 10.1046/j.1471-4159.2003.01917.x

Wakamatsu, K., Murase, T., Zucca, F., Zecca, L., and Ito, S. (2012). Biosynthetic pathway to neuromelanin and its aging process. *Pigment. Cell Melanoma Res.* 25, 792–803. doi: 10.1111/pcmr.12014

Wakamatsu, K., Nakao, K., Tanaka, H., Kitahori, Y., Tanaka, Y., Ojika, M., et al. (2019). The oxidative pathway to dopamine-protein conjugates and their pro-oxidant activities: implications for the neurodegeneration of Parkinson's disease. *Int. J. Mol. Sci.* 20, 2575. doi: 10.3390/ijms20102575

Wang, X., Moualla, D., Wright, J., and Brown, D. (2010). Copper binding regulates intracellular alpha-synuclein localisation, aggregation and toxicity. *J. Neurochem.* 113, 704–714. doi: 10.1111/j.1471-4159.2010.06638.x

Wimalasena, D., Wiese, T., and Wimalasena, K. (2007). Copper ions disrupt dopamine metabolism via inhibition of V-H+-ATPase: a possible contributing factor to neurotoxicity. *J. Neurochem.* 101, 313–326. doi: 10.1111/j.1471-4159.2006.04362.x

Wimalasena, D., and Wimalasena, K. (2004). Kinetic evidence for channeling of dopamine between monoamine transporter and membranous dopamine-beta-monooxygenase in chromaffin granule ghosts. *J. Biol. Chem.* 279, 15298–15304. doi: 10.1074/jbc.M313325200

Wimalasena, K. (2011). Vesicular monoamine transporters: structure-function, pharmacology, and medicinal chemistry. *Med. Res. Rev.* 31, 483–519. doi: 10.1002/med.20187

Zecca, L., Stroppolo, A., Gatti, A., Tampellini, D., Toscani, M., Gallorini, M., et al. (2004). The role of iron and copper molecules in the neuronal vulnerability of locus coeruleus and substantia nigra during aging. *Proc. Natl. Acad. Sci. U. S. A.* 101, 9843–9848. doi: 10.1073/pnas.0403495101

Zecca, L., Tampellini, D., Gerlach, M., Riederer, P., Fariello, R., and Sulzer, D. (2001). Substantia nigra neuromelanin: structure, synthesis, and molecular behaviour. *Mol. Pathol.* 54, 414–418.

Zecca, L., Zucca, F., Albertini, A., Rizzio, E., and Fariello, R. G. (2006). A proposed dual role of neuromelanin in the pathogenesis of Parkinson's disease. *Neurology* 67, S8–S11. doi: 10.1212/wnl.67.7_suppl_2.s8

Zhang, S., Wang, R., and Wang, G. (2019). Impact of dopamine oxidation on dopaminergic neurodegeneration. *ACS Chem. Neurosci.* 10, 945–953. doi: 10.1021/acschemneuro.8b00454

Ziegler, M., Bao, X., Kennedy, B., Joyner, A., and Enns, R. (2002). Location, development, control, and function of extraadrenal phenylethanolamine N-methyltransferase. *Ann. N. Y. Acad. Sci.* 971, 76–82. doi: 10.1111/j.1749-6632.2002.tb04437.x

Zucca, F., Bellei, C., Giannelli, S., Terreni, M., Gallorini, M., Rizzio, E., et al. (2006). Neuromelanin and iron in human locus coeruleus and substantia nigra during aging: consequences for neuronal vulnerability. *J. Neural Transm.* 113, 757–767. doi: 10.1007/s00702-006-0453-2

frontiers | Frontiers in Aging Neuroscience

TYPE Original Research
PUBLISHED 22 February 2024
DOI 10.3389/fnagi.2024.1340110

OPEN ACCESS

EDITED BY
Robert Weissert,
University of Regensburg, Germany

REVIEWED BY
Cristoforo Comi,
University of Eastern Piedmont, Italy
Cristhian Mendoza,
San Sebastian University, Chile

*CORRESPONDENCE
Yinzhou Wang
✉ yinzhouw@163.com

RECEIVED 20 November 2023
ACCEPTED 12 February 2024
PUBLISHED 22 February 2024

CITATION
Song Z, Li W, Han Y, Xu Y, Ding H and Wang Y (2024) Association of immune cell traits with Parkinson's disease: a Mendelian randomization study.
Front. Aging Neurosci. 16:1340110.
doi: 10.3389/fnagi.2024.1340110

Association of immune cell traits with Parkinson's disease: a Mendelian randomization study

Zhiwei Song[1], Wangyu Li[2], Yupeng Han[3], Yiya Xu[1], Haiqi Ding[4] and Yinzhou Wang[1,5]*

[1]Department of Neurology, Fujian Provincial Hospital, Shengli Clinical Medical College of Fujian Medical University, Fuzhou, Fujian, China, [2]Department of Pain Management, Fujian Provincial Hospital, Shengli Clinical Medical College of Fujian Medical University, Fuzhou, Fujian, China, [3]Department of Anesthesiology, Fujian Provincial Hospital, Shengli Clinical Medical College of Fujian Medical University, Fuzhou, Fujian, China, [4]Department of Orthopedic Surgery, The First Affiliated Hospital, Fujian Medical University, Fuzhou, Fujian, China, [5]Fujian Key Laboratory of Medical Analysis, Fujian Academy of Medical Sciences, Fuzhou, Fujian, China

Background: Immunity and neuroinflammation play crucial roles in the pathogenesis of Parkinson's disease (PD). Nonetheless, prior investigations into the correlation between immune inflammation and PD have produced varying results. Identifying specific immune cell phenotypes that are truly associated with PD is challenging, and the causal relationship between immune cells and PD remains elusive.

Methods: This study conducted a comprehensive two-sample Mendelian randomization (MR) analysis, employing five distinct analytical approaches, to clarify the causal connection between immune cell characteristics and the risk of PD. Utilizing GWAS data, we investigated the causal relationship between 731 immune cell traits and PD. These immune cell phenotypes encompass absolute cell (AC) counts, median fluorescence intensity (MFI), and relative cell (RC) counts for B cells, cDCs, mature stage T cells, monocytes, myeloid cells, TBNK (T cells, B cells, and natural killer cells), and Tregs, as well as the logistic parameter (MP) for cDCs and TBNK.

Results: The inverse variance weighted (IVW) analysis indicated that Myeloid DCs ($p = 0.004$), HVEM expression on CD45RA– CD4+ T cells ($p = 0.007$), CD62L– CD86+ Myeloid DCs ($p = 0.015$), and HLA DR expression on monocytes ($p = 0.019$) were associated with a reduced risk of PD. CD14+ CD16+ monocytes ($p = 0.005$), HLA DR+ NK cells within CD3– lymphocytes ($p = 0.023$), and CD28 expression on activated & secreting Tregs ($p = 0.032$) were associated with an increased risk of PD.

Conclusion: This study establishes a causal link between immune cell phenotype and the pathogenesis of PD, identifying several specific immune cell characteristics associated with PD. This could inspire researchers to delve into the pathogenesis of PD at the cellular subtype level, and aid in the identification of potential pharmacological protein targets for PD.

KEYWORDS

Mendelian randomization, immune cells, Parkinson's disease, causal relationship, single nucleotide polymorphisms

1 Background

Parkinson's disease (PD) is a progressive neurodegenerative disorder primarily characterized by the progressive loss of dopaminergic neurons in the substantia nigra and abnormal α-synuclein aggregation in Lewy vesicles (Bloem et al., 2021). In 2016, it was estimated that over 6 million individuals worldwide were affected by PD, a number that is projected to increase as the population ages (GBD 2016 Neurology Collaborators, 2019). The precise cause of PD remains elusive; however, research has indicated that neuroinflammation significantly contributes to PD's development, with central nervous system (CNS)-resident immune cells (microglia, astrocytes) engaging in interactions with peripheral immune cells (macrophages, lymphocytes, etc.), leading to neuroinflammation, which markedly influences PD's progression (Tansey et al., 2022).

Prior research has established the role of immune dysfunction, characterized by alterations in cytokine levels and irregularities in immune cell functionality, in the development of PD. Furthermore, PD shares numerous genetic risk factors with other autoimmune diseases, and several of the over 90 risk variants for PD identified by genome-wide association studies (GWAS) are related to immune function genes (Nalls et al., 2019). Furthermore, the identification of shared genetic variants in PD patients and those with other autoimmune diseases (Witoelar et al., 2017) further underscores the role of immunity in the pathogenesis of PD. Immune system dysregulation may occur in patients with autoimmune diseases, who are more likely to develop PD compared to the general population. A national epidemiological study involving 310,522 patients with autoimmune diseases revealed that 932 of these patients developed PD during the follow-up period (De Virgilio et al., 2016). Inflammatory cells (e.g., microglia, CD4+ and CD8+ T cells; Marogianni et al., 2020) and inflammatory factors (e.g., IL-1α, IL-2, IL-1β, TNF-α, IL-6, TGF-β, IFN-γ, and IL-9; Karpenko et al., 2018) serve as key mediators between the brain and the immune system and play a pivotal role in the pathogenesis of PD. In the brain tissue of PD patients, the levels of activated microglia and CD3+ T cells were found to be higher compared to those in control patients (Lin et al., 2019; Li et al., 2022). Studies have also demonstrated that PD patients exhibit elevated serum levels of pro-inflammatory cytokines, such as TNF, IFNγ, IL-1β, IL-6, IL-2, CXC-chemokine ligand 8 (CXCL 8), and CCL 2, which correlate with disease severity and disability (Wang et al., 2015). In recent research, it has been discovered that immune cells (NK cells, monocytes/macrophages, neutrophils, and T cells) from the peripheral system can penetrate the blood–brain barrier in individuals with PD (Huang et al., 2022). However, the role of immune cells in PD remains controversial; they may play a protective role in the acute phase of neuroinflammation in PD through the production of trophic factors and inhibition of inflammation (Hoogland et al., 2015), and in the chronic phase of neuroinflammation through inflammatory factors and autoantibodies that may exert toxic effects on neurons (Channer et al., 2023), which explains to some extent that one type of immune cell may lead to different conclusions in different studies about the pathogenesis of PD. While previous research has identified numerous associations between immune cells and PD, the exploration of the causal relationship between various immune cell phenotypes and the pathogenesis of PD is still pending. Furthermore, the specific phenotypic characteristics through which immune cells influence the course of PD have yet to be elucidated.

Mendelian Randomization (MR) employs variations in genetics as a pivotal instrument for evaluating the causal relationships between exposures and subsequent outcomes (Bowden and Holmes, 2019), and is primarily employed for etiological inference in epidemiology, aiding researchers in reducing bias in experimental results and in drawing conclusions about causality (Emdin et al., 2017). Although randomized controlled trials (RCTs) are effective tools for causal inference, their implementation can be resource-intensive and is often limited by sample size and ethical issues. However, MR offers advantages such as lower cost, reduced confounding, and diminished reverse causal inference compared to observational study (Sekula et al., 2016), and is thus regarded as a "natural" RCT that aids in mitigating the traditional bias inherent in observational studies (Emdin et al., 2017). The primary objectives of this study involve assessing the causal relationship between various immune phenotypes and PD, while the secondary objectives include identifying potential key immune cell phenotypes, deepening the understanding of PD pathogenesis, and providing new directions and strategies for PD treatment and drug development.

2 Materials and methods

2.1 Study design

Throughout its duration, the study was conducted in strict adherence to the STROBE-MR guidelines (Skrivankova et al., 2021). In this study utilizing two-sample Mendelian Randomization, loci of single nucleotide polymorphism (SNP) from the database of genome-wide association analysis (GWAS) were employed as instrumental variables for examining the influence of risk between immune phenotypes and PD. A total of 731 immune cell characteristics were defined as exposure factors in relation to the occurrence of PD, constituting the study outcome. The analysis utilizing MR adheres to three foundational principles: firstly, the exposure (immune phenotype) maintains a robust association with the chosen SNPs; secondly, these SNPs are not influenced by external confounding factors; and thirdly, while these polymorphisms do not have a direct relationship with the outcome (PD), their causal connection is exclusively through the immune phenotype (Burgess and Labrecque, 2018). The design and hypotheses and flow chat of the MR study are outlined in Figure 1.

2.2 Source of exposure data

Publicly available immune trait data were obtained from Valeria Orrù's study (Orrù et al., 2020), encompassing a total of 731 immunophenotypes. This dataset includes a total of 118 cell counts, 389 median fluorescence intensities (MFIs) associated with surface antigens, in addition to 32 cell morphology parameters, and 192 relative counts, which refer to the ratio among different cells. This data were sourced from a cohort of 3,757 Sardinians, encompassing 20,143,392 SNPs (Orrù et al., 2020).

2.3 Collection of outcome data

Extensive GWAS genetic data were obtained from the International Parkinson's Disease Genomics Consortium (IPDGC), encompassing 7.8 million SNPs from 37,700 cases, 18,600 proxy cases (individuals without PD yet having a familial history of the condition),

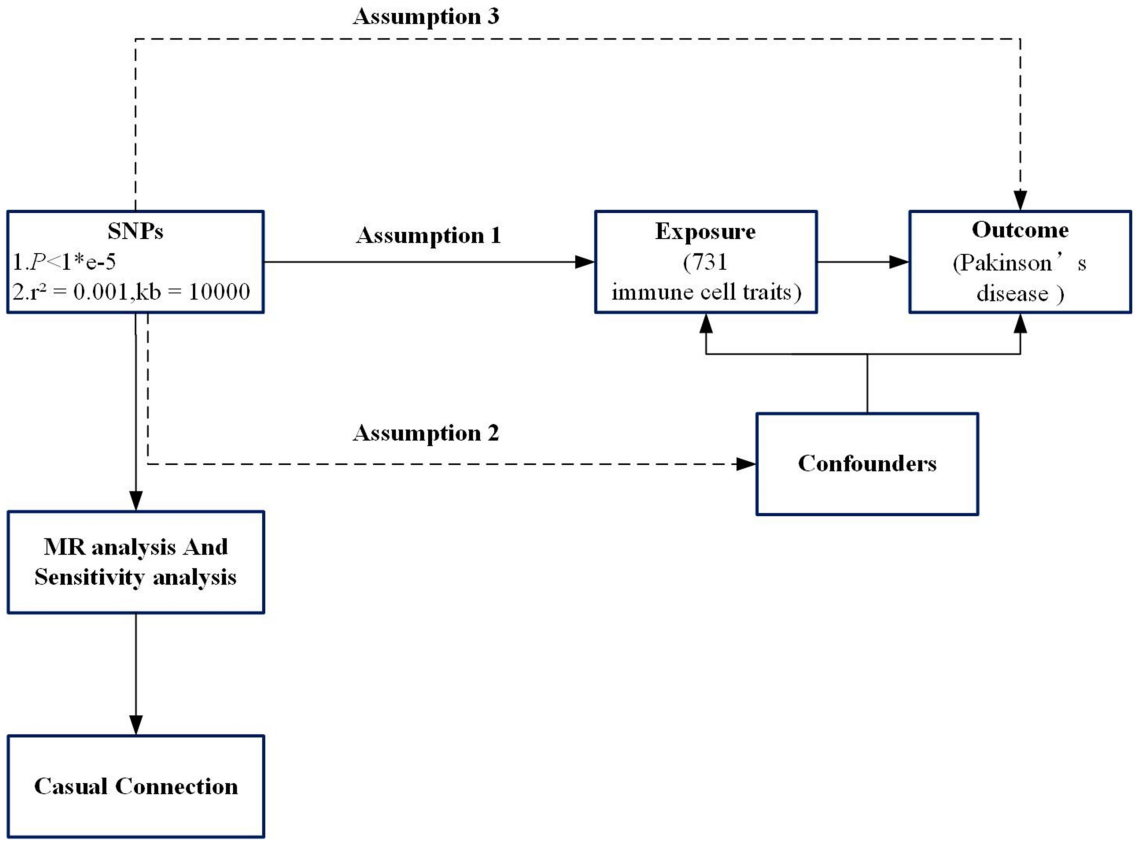

FIGURE 1
Flowchart of the study. Assumption 1, the exposure (immune phenotype) maintains a robust association with the chosen single-nucleotide polymorphisms (SNPs); Assumption 2, SNPs are not influenced by external confounding factors; Assumption 3, SNPs do not have a direct relationship with the outcome (PD), their causal connection is exclusively through the immune phenotype. SNP, Single-nucleotide poly-morphism; MR, Mendelian randomization.

and 1.4 million controls (Nalls et al., 2019). This constitutes one of the largest GWAS studies to date on PD patients of European ancestry, with data from the United Kingdom Biobank being openly accessible.

2.4 Identification of SNPs

The causal relationship between immunophenotype and PD was assessed. The specific screening steps included using the TwoSampleMR package to extract relevant SNPs (Woolf et al., 2022). SNPs that exhibited significant differences across the genome ($p < 1^*e{-}5$) (VanderWeele et al., 2014) were selected and tested for linkage disequilibrium ($r^2 = 0.001$, kb = 10,000), followed by the elimination of linkage disequilibrium SNPs and the removal of echo sequences. To reduce bias due to weak instruments, SNPs displaying *F*-statistics (a measure of the SNP's robustness; Burgess et al., 2016; indicative of the SNP's strength) lower than 10 were omitted.

2.5 Statistics and sensitivity analyses

In this study, R 4.3.2 software (Yavorska and Burgess, 2017) was primarily utilized to conduct Inverse Variance Weighted (IVW), MR Egger, Weighted Median, Simple Mode, and Weighted Mode analyses. The IVW method served as the principal analytical approach to ascertain the causal relationship between immunophenotypes and PD. Additionally, reverse Mendelian randomization was employed to investigate the influence of PD onset on immunophenotype (Davey Smith and Hemani, 2014). The heterogeneity among the estimated effects of SNPs was assessed by calculating both the *Q*-value and *p* value, following Cochran's method. In the presence of heterogeneity, causal inference was conducted using the IVW random effects model (Burgess et al., 2017). The MR-Egger intercept examination and the MR-PRESSO approach were applied to investigate horizontal pleiotropy. Subsequently, a Leave-one-out sensitivity analysis (Burgess and Thompson, 2017) was performed to evaluate the impact of individual SNPs on the overall causal effect. Moreover, funnel plots and scatter plots were produced to visually illustrate the possible presence of horizontal pleiotropy.

3 Results

3.1 SNP screening and MR analysis results

Following the aforementioned steps, which involved matching data on immunophenotypes and PD and excluding SNPs with low F-statistics (< 10), a total of 147 SNPs were ultimately included in the study.

3.2 Exploration of the role of immunophenotype on the pathogenicity of PD

At a significance threshold of $p < 0.05$ using the IVW method, it was observed that Myeloid DC within the DC (cDC group), CD14+ CD16+ monocytes (monocyte group), HVEM on CD45RA− CD4+ T cells (Maturation stages of T cell group), CD62L− CD86+ myeloid DC within the DC (cDC group), HLA DR on monocytes (monocyte group), HLA DR+ NK cells in CD3− lymphocytes (TBNK group), and CD28 on activated & secreting Treg cells (Treg group) demonstrated significant associations with PD (Figure 2). Results derived from five distinct MR methods are presented in Figure 2. MR analyses employing a random-effects model with the IVW method yielded the following results: myeloid DC of DC (OR = 0.924, 95%CI: 0.876–0.975, $p = 0.004$), HVEM on CD45RA− CD4+ T cell (OR = 0.945, 95%CI: 0.907–0.985, $p = 0.007$), CD62L− CD86+ myeloid DC of DC (OR = 0.945, 95%CI: 0.903–0.989, $p = 0.015$), and HLA DR on monocyte (OR = 0.951, 95%CI: 0.911–0.992, $p = 0.019$) indicated a protective effect against reduced PD risk. The CD14+ CD16+ monocyte (OR = 1.091, 95%CI: 1.027–1.158, $p = 0.005$), HLA DR+ NK cell in CD3− lymphocytes (OR = 1.062, 95%CI: 1.008–1.119, $p = 0.023$), and CD28 on activated & secreting Treg (OR = 1.043, 95%CI: 1.004–1.083, $p = 0.032$) were identified as being associated with an increased risk of PD. Four additional analytical methods—MR Egger, Weighted Median, Simple Mode, and Weighted Mode—were employed to ascertain the stability of the results, yet the Simple Mode method did not substantiate a causal relationship for Myeloid DC within DCs (OR = 0.975, 95% CI: 0.848–1.120, $p = 0.725$), CD14+ CD16+ Monocytes (OR = 0.982, 95% CI: 0.831–1.161, $p = 0.837$),

ID	Nsnp	Method	Pval	OR (95% CI)
Myeloid DC %DC	25	Inverse variance weighted	0.004	0.924 (0.876 - 0.975)
	25	MR Egger	0.010	0.883 (0.810 - 0.964)
	25	Weighted median	0.002	0.892 (0.829 - 0.961)
	25	Simple mode	0.725	0.975 (0.848 - 1.120)
	25	Weighted mode	0.007	0.894 (0.830 - 0.963)
CD14+ CD16+ monocyte %monocyte	23	Inverse variance weighted	0.005	1.091 (1.027 - 1.158)
	23	MR Egger	0.003	1.182 (1.073 - 1.301)
	23	Weighted median	0.011	1.101 (1.022 - 1.186)
	23	Simple mode	0.837	0.982 (0.831 - 1.161)
	23	Weighted mode	0.022	1.105 (1.020 - 1.197)
HVEM on CD45RA- CD4+	18	Inverse variance weighted	0.007	0.945 (0.907 - 0.985)
	18	MR Egger	0.042	0.913 (0.842 - 0.990)
	18	Weighted median	<0.001	0.906 (0.854 - 0.960)
	18	Simple mode	0.063	0.905 (0.819 - 0.999)
	18	Weighted mode	0.025	0.900 (0.827 - 0.979)
CD62L- CD86+ myeloid DC %DC	18	Inverse variance weighted	0.015	0.945 (0.903 - 0.989)
	18	MR Egger	0.185	0.956 (0.897 - 1.019)
	18	Weighted median	0.014	0.931 (0.880 - 0.986)
	18	Simple mode	0.024	0.854 (0.754 - 0.967)
	18	Weighted mode	0.023	0.936 (0.889 - 0.986)
HLA DR on monocyte	16	Inverse variance weighted	0.019	0.951 (0.911 - 0.992)
	16	MR Egger	0.446	0.972 (0.905 - 1.044)
	16	Weighted median	0.431	0.973 (0.910 - 1.041)
	16	Simple mode	0.760	0.983 (0.880 - 1.097)
	16	Weighted mode	0.979	1.001 (0.931 - 1.077)
HLA DR+ NK %CD3- lymphocyte	22	Inverse variance weighted	0.023	1.062 (1.008 - 1.119)
	22	MR Egger	0.013	1.129 (1.035 - 1.232)
	22	Weighted median	0.043	1.081 (1.003 - 1.166)
	22	Simple mode	0.576	1.049 (0.889 - 1.237)
	22	Weighted mode	0.026	1.100 (1.018 - 1.189)
CD28 on activated & secreting Treg	25	Inverse variance weighted	0.032	1.043 (1.004 - 1.083)
	25	MR Egger	0.155	1.037 (0.988 - 1.087)
	25	Weighted median	0.167	1.039 (0.984 - 1.097)
	25	Simple mode	0.618	1.019 (0.947 - 1.097)
	25	Weighted mode	0.219	1.031 (0.983 - 1.082)

FIGURE 2
Forest plots showed the causal associations between immune cell traits and PD by using different methods. SNP, Single-nucleotide poly-morphism; OR, Odd radio; and CI, Confidence interval.

HVEM on CD45RA− CD4+ T cells (OR = 0.905, 95% CI: 0.819–0.999, $p = 0.063$), or HLA DR+ NK cells within CD3− lymphocytes (OR = 1.049, 95% CI: 0.889–1.237, $p = 0.576$) in relation to PD. Furthermore, the MR Egger method also failed to demonstrate a causal relationship between CD62L− CD86+ Myeloid DCs within DCs (OR = 0.956, 95% CI: 0.897–1.019, $p = 0.185$) and PD, additionally, numerous analyses did not corroborate a causal relationship between HLA DR+ NK cells within CD3− lymphocytes and CD28 on activated and secreting Tregs in relation to PD, but the IVW results were significant, with no detected pleiotropy or heterogeneity, and the outcomes of all five analytical methods aligned in the same direction, suggesting a positive result overall (Birney, 2022; Figure 2).

Concurrently, a reverse Mendelian randomization analysis was carried out to evaluate the influence of PD manifestation on immunophenotypes. Although the results varied significantly across different analysis methods, they failed to satisfy both the MR-Egger intercept test and the MR-PRESSO method, indicating the presence of horizontal pleiotropy and leading to an unreliable result.

3.3 Sensitivity analyses

During the analysis of these seven causal links, all p values derived from Cochran's Q test for heterogeneity surpassed the significance level set at 0.05. This suggests the absence of substantial heterogeneity among the SNPs associated with PD, as detailed in Table 1. Additionally, our MR-Egger-intercept analysis revealed the absence of significant directional pleiotropy for each immunophenotype ($p > 0.05$). This implies included SNPs were not associated with the outcome via confounding factors. Causal effects, as estimated by the MR-PRESSO method, remained significant both prior to and following outlier correction. Furthermore, global analyses did not uncover any evidence of horizontal pleiotropy (global test $p > 0.05$). The leave-one-out analysis illustrates that none of the individual SNP exert a significant effect on the overall causal estimate, thereby bolstering the reliability of the MR results (Figure 3). Additionally, the funnel plot exhibited a predominantly symmetrical distribution of causal effects, indicating minimal bias (Figure 4). Scatter plots showed that the regression lines illustrating the connection between immunophenotypes and PD risk, as obtained from different analytical approaches, were broadly consistent (Figure 5).

4 Discussion

Peripheral immunity may contribute to PD pathogenesis through mechanisms including inflammatory responses, cellular infiltration, dysregulation of lymphocyte subsets, and autoimmune responses. The findings from the two-sample Mendelian randomization indicated that CD14+ CD16+ monocytes, HLA DR+ NK cells in CD3− lymphocytes, and CD28 on activated & secreting Tregs were positively correlated with an increased risk of PD. Furthermore, it was observed that Myeloid DCs, HVEM on CD45RA− CD4+ T cells, CD62L− CD86+ Myeloid DCs, and HLA DR on monocytes exerted a protective causal effect against the development of PD. Sensitivity analyses and quality control affirmed the robustness of these findings. Exposure factors in this study, derived from peripheral blood immune cell phenotypes as detected by flow cytometry, partially substantiate the causal relationship between peripheral immunity and PD's development.

In the evolving process of immune-brain crosstalk, it appears that the systemic immune response constitutes an integral component of the pathogenesis of PD, wherein myeloid-derived dendritic cells (Myeloid DCs) assume a pivotal role (Tansey et al., 2022). In PD, a subset of myeloid-derived dendritic cells, which have metastasized from the peripheral blood, may infiltrate the brain, harvesting cerebrospinal fluid (CSF) brain antigens in the choroid plexus or meninges. This process induces immune cells to adopt dysregulated phenotypes, thereby contributing to an inflammatory environment that plays a pathological role in neurodegeneration (Bossù et al., 2015). A Ciaramella et al. observed that PD patients showed significantly lower levels of peripheral blood Myeloid DCs compared to control subjects, with the number of peripheral blood Myeloid DCs being negatively correlated with the severity of motor symptoms (Goldeck et al., 2016). This is consistent with our findings, suggesting that Myeloid DC might play a protective role in the pathogenesis of PD. We hypothesized that a reduction in the level of peripheral blood Myeloid DC is associated with increased recruitment of this cell from the circulatory system to the brain, potentially explaining the more active cellular infiltration and inflammatory response in the brain of PD patients. Consequently, peripheral blood myeloid cells reflect, to some degree, the extent of neuroinflammation and may serve as a potential biomarker for evaluating PD's progression.

TABLE 1 Sensitivity analysis for immune cell traits vs. PD by MR analysis.

Exposure	Horizontal pleiotropy		Heterogeneity	MR-PRESSO global test
	MR egger-interpreter	MR egger-interpreter	Cochran's Q	p value
		p value	p value	
Myeloid DC %DC	0.014	0.209	0.760	0.720
CD14+ CD16+ monocyte %monocyte	0.029	0.057	0.375	0.271
HVEM on CD45RA− CD4+	0.013	0.344	0.546	0.569
CD62L− CD86+ myeloid DC %DC	0.007	0.614	0.315	0.377
HLA DR on monocyte	0.011	0.463	0.6037	0.516
HLA DR+ NK % CD3− lymphocyte	0.021	0.104	0.769	0.580
CD28 on activated & secreting Treg	0.004	0.697	0.469	0.575

OR: Odd radio; CI: Confidence interval.

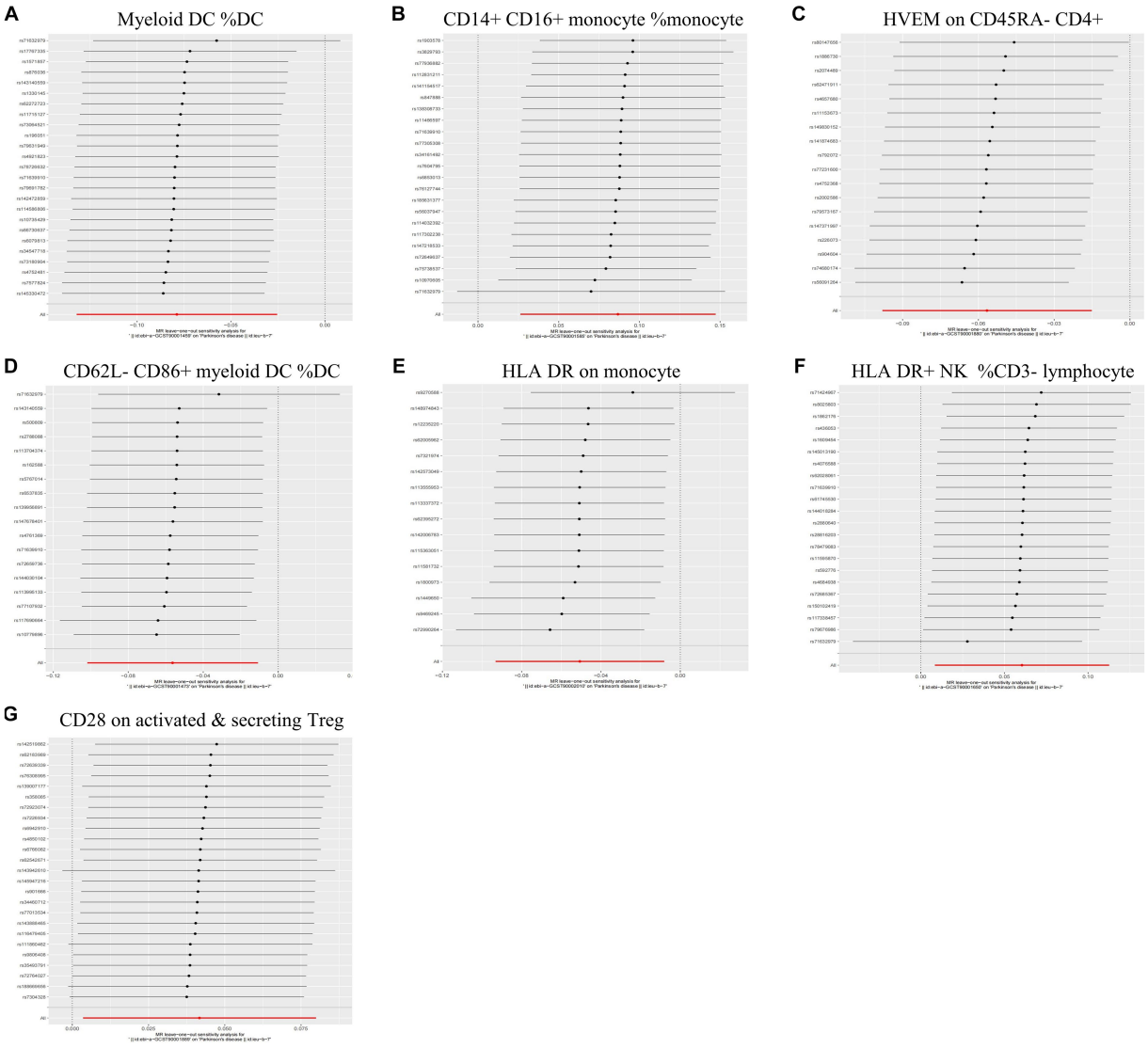

FIGURE 3
Leave-one-out analysis of each immunophenotype on the risk of PD. The error line represents a 95% confidence interval. **(A)** Myeloid DC of DC; **(B)** CD14+ CD16+ monocyte of monocyte; **(C)** HVEM on CD45RA– CD4+ T cell; **(D)** CD62L– CD86+ myeloid DC of DC; **(E)** HLA DR on monocyte; **(F)** HLA DR+ NK of CD3– lymphocyte; and **(G)** CD28 on activated & secreting Treg.

Our results suggest that an elevation in the levels of CD14+CD16+ monocyte subsets is associated with an increased risk of PD. The peripheral immune system, particularly its monocytes, has been implicated in the neuroinflammation associated with PD. α-Synuclein, identified as a damage-associated molecular pattern (DAMP) released by neurons, contributes to the *in vivo* activation of monocytes. This activation prompts the monocytes to produce pro-inflammatory mediators (Grozdanov et al., 2019). Monocytes, a heterogeneous group of cells, are primarily characterized by variations in the expression of CD14 and CD16 molecules. In PD patients, alterations in the phenotype and function of these monocytes are evident, as indicated by a rise in the number of CD14+CD16+ monocyte subpopulations in the blood. This particular subpopulation may exhibit high expression of TLR10 (da Rocha Sobrinho et al., 2021). Emerging data suggest a correlation between the frequency of CD14+CD16+TLR10+ monocytes and the severity of PD (da Rocha Sobrinho et al., 2021), these observations align with the results of our findings. The role of CD14+CD16+ monocytes in PD continues to be a topic of debate in the scientific community. Conversely, Schlachetzki et al. (2018) observed no change in the frequency of CD14+CD16+ monocyte subpopulations in PD patients compared to healthy controls. However, Grozdanov et al. (2014) reported a decrease in the number of CD14+CD16+ monocytes in PD patients. Variations in the age of onset, duration, and severity of PD among patient populations, as well as the overall sample sizes of the studies, may contribute to the divergent findings. The use of MR in our study helped to partially negate the effects of confounding factors and reverse causality.

CD4+ T cells potentially play a critical role in neurodegeneration associated with PD. Prior research has demonstrated that CD4-deficient mice exhibit attenuated dopaminergic neuronal death due to α-synuclein overexpression. IFN-γ-producing CD4+ T cells are crucial for CNS myeloid MHCII responses and TH nerve neuronal

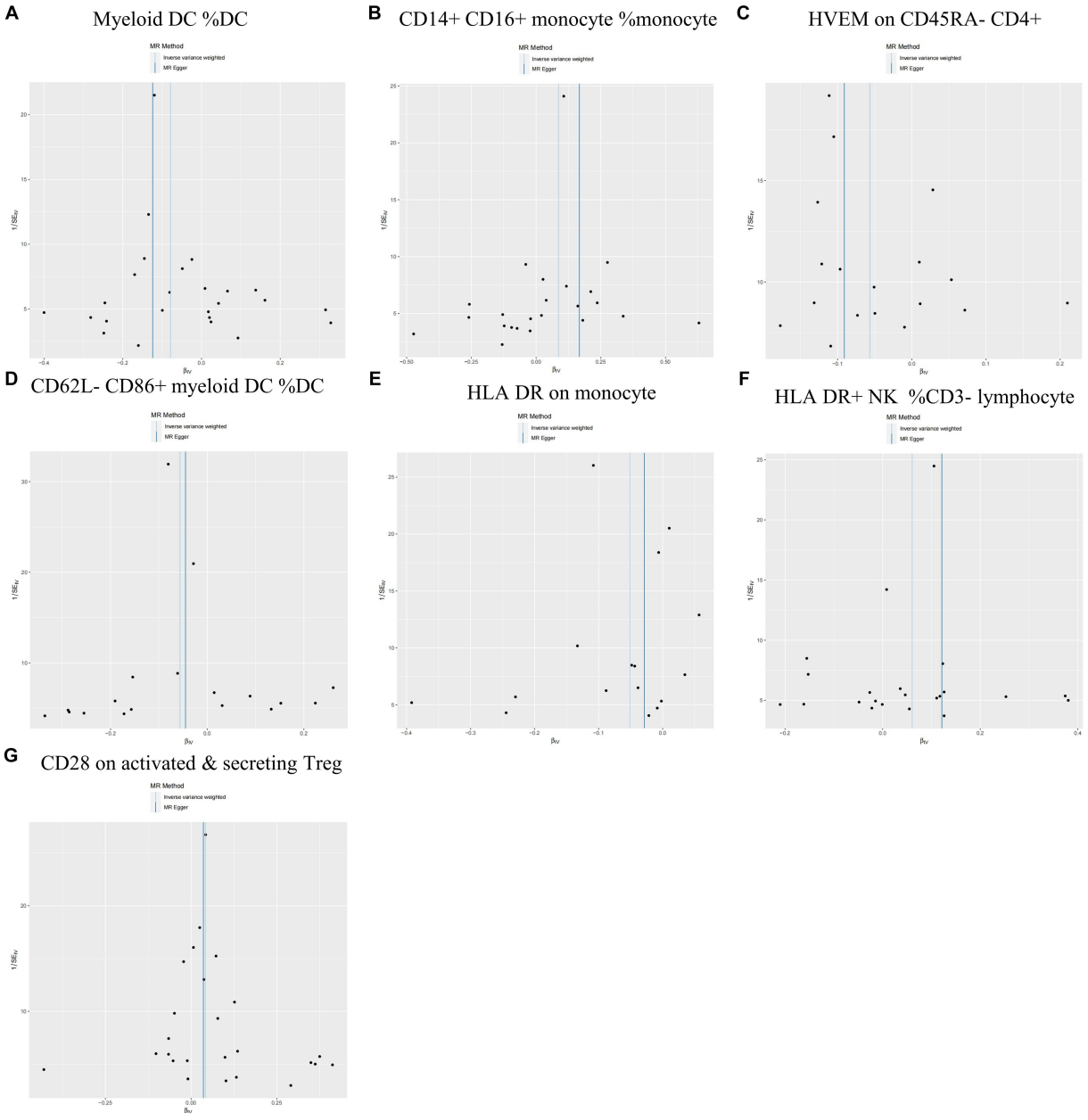

FIGURE 4
Funnel plots are utilized in sensitivity analysis to examine the causal relationship between immunophenotype and the risk of PD. **(A)** Myeloid DC of DC; **(B)** CD14+ CD16+ monocyte of monocyte; **(C)** HVEM on CD45RA− CD4+ T cell; **(D)** CD62L− CD86+ myeloid DC of DC; **(E)** HLA DR on monocyte; **(F)** HLA DR+ NK of CD3− lymphocyte; and **(G)** CD28 on activated & secreting Treg.

loss attributed to α-synuclein overexpression (Deng et al., 2021). Additionally, it has been observed by some researchers that CD4+ and CD8+ T cells infiltrate the brain parenchyma in brain tissue samples from PD patients, as well as in mouse models of PD (Sanchez-Guajardo et al., 2010). A meta-analysis of 21 case–control trials (Jiang et al., 2017), encompassing 943 PD cases, indicated that the number of peripheral blood CD4+ T cell subsets is reduced in PD patients, aligning with our findings. Furthermore, HVEM, a member of the tumor necrosis factor receptor (TNFR) superfamily (Aubert et al., 2021), inhibits T-cell proliferation when bound to the B and T lymphocyte attenuator (BTLA). This inhibition occurs through the phosphoacyl esterase SHP-1 and SHP-2 downstream signaling pathways, ultimately suppressing T cell activation and immune responses (Deng et al., 2021). Zhong et al. provided evidence that elevated HVEM expression in CD4+ T cells could act as a protective factor in myasthenia gravis. Our study echoes these findings, proposing that HVEM expression in CD45RA− CD4+ T cells might play a protective role in the development of PD by attenuating the immune response.

Prior research has demonstrated that PD patients exhibit reduced levels of peripheral blood myeloid DC (Ciaramella et al., 2013). Conversely, our current study reveals that CD62L− CD86+ myeloid DC within the dendritic cell (DC) genus play a protective role in preventing PD. DCs are critical in initiating T cell responses and

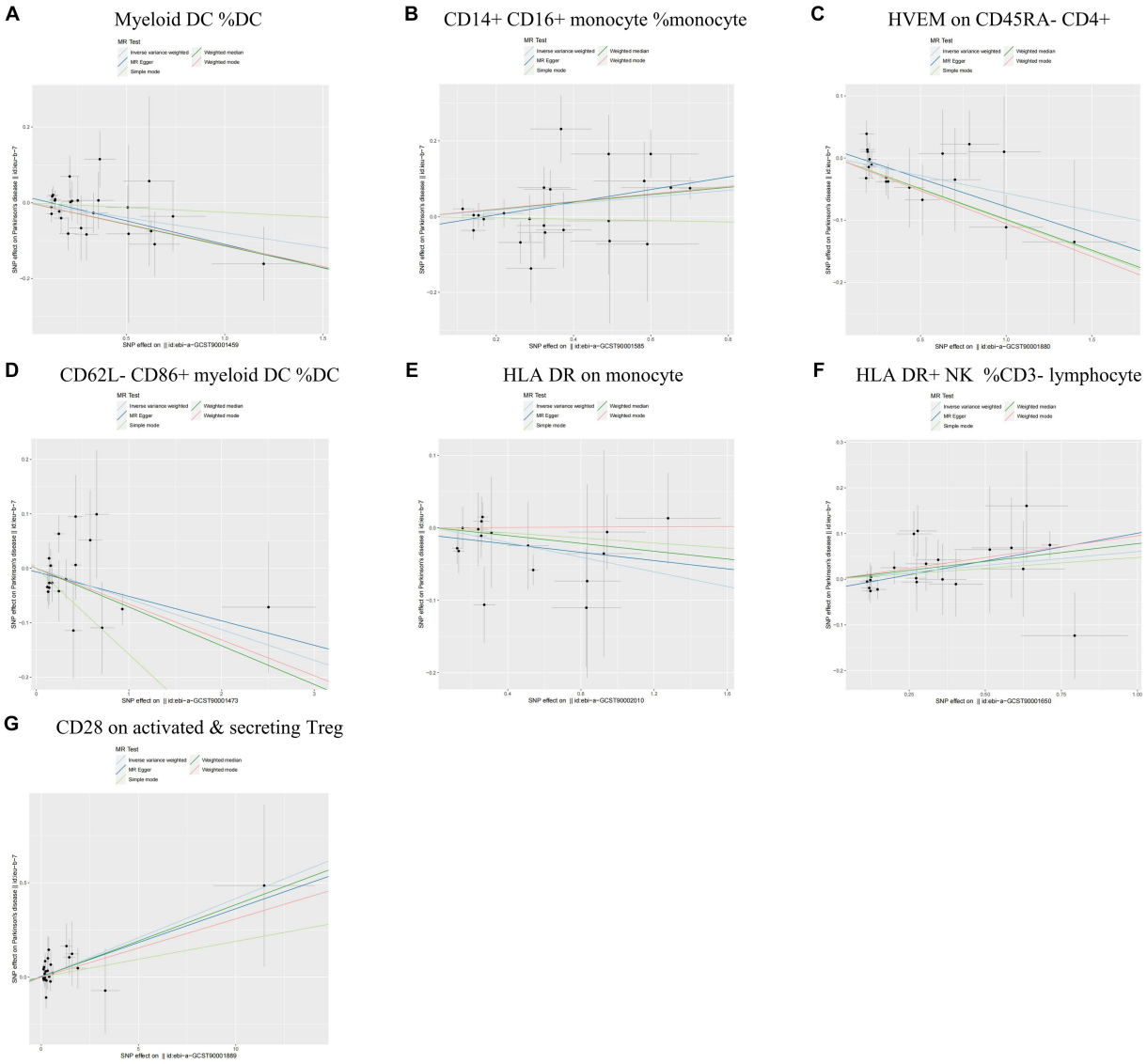

FIGURE 5
Scatter plots of sensitivity analysis for the causal relationship between immunophenotype and the risk of PD. **(A)** Myeloid DC of DC; **(B)** CD14+ CD16+ monocyte of monocyte; **(C)** HVEM on CD45RA– CD4+ T cell; **(D)** CD62L– CD86+ myeloid DC of DC; **(E)** HLA DR on monocyte; **(F)** HLA DR+ NK of CD3– lymphocyte; and **(G)** CD28 on activated & secreting Treg.

coordinating immune responses, while CD86, a co-stimulatory molecule, is believed to promote the Th2 response. *In vitro* studies have shown that IFN-β upregulates CD86 expression on DCs and inhibits the Th1 response via these cells (Tekguc et al., 2021). DCs are crucial in initiating T cell responses and coordinating immune reactions. Peng et al. (2022) reported that extracellular vesicles derived from mesenchymal stromal cells may suppress the Th2 response in allergic rhinitis patients by inhibiting CD86 expression on DCs. Furthermore, numerous investigators have noted diminished levels of CD86 expression in the blood DCs of individuals with multiple sclerosis (MS), suggesting that CD86+ myeloid DCs may have a protective effect in MS (Huang et al., 2001). Limited research exists on the association between CD62L– CD86+ myeloid DC of DC and PD; it is hypothesized that these cells may mitigate PD risk by modulating the Th2 response.

Parkinson's disease have identified changes linked to innate immune abnormalities in CSF (Wijeyekoon et al., 2020a,b) and peripheral blood, notably in monocyte subtypes and their marker expression (Su et al., 2022). Our results indicate that HLA-DR expression on monocytes within the Monocyte genus plays a protective role in the pathogenesis of PD. In a study by Wijeyekoon et al. (2020a,b), it revealed no significant variance in the overall count of serum monocytes between PD patients and controls, however, the phenotype of these monocytes had changed. The surface expression levels of monocyte HLA-DR were found to be associated with better cognitive function, semantic fluency, and motor function. Therefore, reduced levels of HLA-DR may result in ineffective clearance of pathological proteins, potentially triggering neuronal dysfunction and ultimately leading to cognitive and motor deficits (Wijeyekoon et al., 2020a,b). However, this finding contrasts with some animal models of PD, where increased HLA-DR has shown negative effects (Harms et al., 2013). The expression of the MHCII complex plays a crucial role in α-synuclein-induced microglia activation within the pathological

framework of PD (Harms et al., 2013), with HLA-DR being a component of the MHCII complex. Inconsistent findings concerning HLA-DR might stem from microglial activation triggered by HLA-DR during acute toxin/protein injections or pathology in PD animal models, where the deleterious effects of pro-inflammatory cytokine release surpass the benefits of enhanced pathological protein clearance. Conversely, in chronic clinical disease scenarios, the benefits of increased antigen presentation and α-synuclein clearance by HLA-DR may exceed its potential deleterious impacts.

Natural killer (NK) cells, a crucial component of innate immunity, modulate neuroinflammation when infiltrated into the CNS (Earls and Lee, 2020). Research conducted by Sun et al. (2019) demonstrated that the proportion of NK cells was significantly higher in PD patients compared to controls. Additionally, individuals with peripheral blood NK cell levels exceeding the reference range had a significantly increased risk of developing PD. This aligns with our observation that HLA-DR+ NK cells in CD3− lymphocytes could potentially increase the risk of developing PD. In a mouse model of amyotrophic lateral sclerosis (ALS), NK cells within the spinal cord prompt microglia to transition to the M1 type, releasing inflammatory mediators via interferon γ (IFN-γ) (Garofalo et al., 2020). Additionally, HLA-DR+ NK cells have been linked to substantial IFN-γ production (Erokhina et al., 2018). IFN-γ could potentially exacerbate neuroinflammation in the mid and late stages of PD, resulting in further deterioration of neuronal damage (Panagiotakopoulou et al., 2020). Therefore, we hypothesize that the heightened risk of PD development due to HLA-DR+ NK cells in CD3− lymphocytes might be linked to neuroinflammation, potentially mediated by elevated levels of inflammatory cytokines like IFN-γ.

Prior research has shown that CD4 + CD25 + Foxp3+ regulatory T cells (Treg) uphold immune homeostasis via their immunosuppressive action on effector T cells (Teff) (Ohkura and Sakaguchi, 2020). Additionally, observations that PD patients commonly exhibit a decreased ability of Treg to suppress Teff (DeMaio et al., 2022), indicate that the development of PD may lead to a significant reduction in Treg's ability to suppress inflammation. However, there remains a debate in the literature regarding how the ratio of peripheral blood Treg changes in PD patients. Findings by Kustrimovic et al. (2018) indicated that the number of circulating Treg cells was significantly lower in PD patients, with CD4+ T cells showing a preferential differentiation toward the Th1 lineage. On the other hand, a study conducted by Cen et al. (2017) showed that there was no significant disparity in Treg ratios between the PD group and the control group; however, the Treg/Th17 ratio was significantly higher in female PD patients compared to female controls. These discrepancies could be attributed to biases arising from differences in the race of the PD patients included in the study, the severity of the disease, and the overall sample size. Additionally, CD28 receptor, expressed on Treg cells, acts as a co-stimulatory molecule, providing a secondary signal crucial for full T cell activation. In the hαSyn mouse model of PD, Treg activation and expansion occur through binding to the CD28 receptor via a hyper-excitable anti-CD28 monoclonal antibody (CD28SA). This process attenuates neuroinflammatory responses and mitigates dopaminergic neuronal degeneration (Badr et al., 2022), evidencing neuroprotective effects. Notably, our results indicate that CD28 on activated and secreting Treg may increase the risk of developing PD. We contend that Mendelian randomization analysis, which employs genetic variants as instrumental variables, is not influenced by extraneous factors such as the environment, since these variables are established at the time of conception. Therefore, the results of MR are indicative of the effects of lifetime perturbations of risk factors (Larsson et al., 2023), potentially leading to a distinct acute effect compared to that observed in animal models with CD28. In other words, the impact of enhanced Treg immunosuppression, resulting from increased CD28 signaling in PD, may vary during different stages of PD onset and progression. Enhanced Treg function in the initial stages of the disease might aid in controlling the brain's inflammatory response, potentially slowing PD progression. Conversely, prolonged Treg activation could lead to excessive immune suppression, impacting neural tissue clearance and repair, and indirectly advancing disease progression. Future research should focus on conducting more prospective studies to further explore the molecular role of CD28 on activated and secreting Treg in PD and other neuroinflammatory diseases.

The current study found insufficient statistical evidence to support an inverse relationship between immune cell phenotype and PD. While the IVW method indicated a correlation and differential significance between PD development and various immune phenotypes, the pronounced multiplicity of these associations contravenes the exclusionary assumptions of MR. This indicates that certain SNPs might influence changes in the immune phenotype via confounding factors other than PD (Skrivankova et al., 2021).

This study investigates immune cell phenotypic characteristics that could assist researchers in identifying potential drug targets. For instance, elevated CD27 expression on memory B cell subsets is associated with an increased risk of Crohn's disease; therapeutic targeting of CD27 on B cells may aid in reducing this risk (Zheng et al., 2017). Secondly, this study facilitates the development of personalized prevention and treatment strategies for PD: immune cell phenotypes, reflecting individual variations, enable the identification of individuals at elevated risk of the disease. Initiating interventions or targeted treatments at an early stage can significantly enhance an individual's quality of life. For instance, individuals exhibiting low HLA-DR expression on monocytes, who are at a heightened risk for PD, could benefit from early lifestyle modifications, including changes in diet, increased exercise, and minimizing exposure to environmental hazards, to mitigate PD risk. This study's primary advantage is its position as the most extensive genetic analysis conducted thus far in exploring the causal connection between immune cell phenotypes and PD. Unlike previous research focusing on a single cell type (Jensen et al., 2021) or limited immune cell phenotypes (Tian et al., 2022), our study encompasses a broad range of immune cell types.

This study has certain limitations. Firstly, our data selection was limited to studies measuring immune cell phenotypes in blood samples, despite evidence suggesting elevated levels in CSF samples of PD patients (Guan et al., 2022). However, this approach offers significant insight into the role of peripheral immunity in PD. Secondly, while two-sample Mendelian randomization offers a robust approach for causal inference, further validation via randomized controlled trials and animal studies is essential. Finally, the selection of immune cell data from Sardinians, due to the higher prevalence of certain immune-related genetic variants in Sardinia (Steri et al., 2017), necessitates validation of our study's conclusions in broader population-based data.

5 Conclusion

Variants correlated with clinical outcomes frequently influence a multitude of immune phenotypes, rendering the identification of the

specific immune phenotype genuinely associated with the disease process challenging. This study delves into the immune-related mechanisms of PD from the perspective of cellular subtypes, utilizing GWAS data analysis to identify immune phenotypes genuinely associated with PD. This facilitates the identification of potential druggable protein targets and lays a theoretical foundation for the development of future therapeutic strategies with immunomodulatory effects.

Data availability statement

The raw data supporting the conclusions of this article will be made available by the authors, without undue reservation.

Ethics statement

Ethical approval was not required for the study involving humans in accordance with the local legislation and institutional requirements. Written informed consent to participate in this study was not required from the participants or the participants' legal guardians/next of kin in accordance with the national legislation and the institutional requirements.

Author contributions

ZS: Writing – original draft. WL: Writing – original draft. YH: Writing – original draft. YX: Writing – original draft. HD: Formal analysis, Writing – original draft. YW: Writing – review & editing.

Funding

The author(s) declare that financial support was received for the research, authorship, and/or publication of this article. This work was financially supported in part by research grants from Natural Science Foundation of Fujian Province, China (2023J02024) and Medical innovation project of Fujian Province (2022CXA047).

Acknowledgments

The authors would like to thank all the colleagues who contributed to this work.

Conflict of interest

The authors declare that the research was conducted in the absence of any commercial or financial relationships that could be construed as a potential conflict of interest.

Publisher's note

References

Aubert, N., Brunel, S., and Olive, D., And Marodon, G. (2021). Blockade of Hvem for prostate Cancer immunotherapy in humanized mice. *Cancers (Basel)* 13::3009. doi: 10.3390/Cancers13123009

Badr, M., Mcfleder, R. L., Wu, J., Knorr, S., Koprich, J. B., Hünig, T., et al. (2022). Expansion of regulatory T cells by Cd28 Superagonistic antibodies attenuates neurodegeneration in A53t-A-Synuclein Parkinson's disease mice. *J. Neuroinflammation* 19:319. doi: 10.1186/S12974-022-02685-7

Birney, E. (2022). Mendelian randomization. *Cold Spring Harb. Perspect. Med.* 12:A041302. doi: 10.1101/Cshperspect.A041302

Bloem, B. R., and Okun, M. S., And Klein, C. (2021). Parkinson's disease. *Lancet* 397, 2284–2303. doi: 10.1016/S0140-6736(21)00218-X

Bossù, P., Spalletta, G., and Caltagirone, C., And Ciaramella, A. (2015). Myeloid dendritic cells are potential players in human neurodegenerative diseases. *Front. Immunol.* 6::632. doi: 10.3389/Fimmu.2015.00632

Bowden, J., And Holmes, M. V. (2019). Meta-analysis and Mendelian randomization: a review. *Res. Synth. Methods* 10, 486–496. doi: 10.1002/Jrsm.1346

Burgess, S., and Davies, N. M., And Thompson, S. G. (2016). Bias due to participant overlap in two-sample Mendelian randomization. *Genet. Epidemiol.* 40, 597–608. doi: 10.1002/Gepi.21998

Burgess, S., And Labrecque, J. A. (2018). Mendelian randomization with a binary exposure variable: interpretation and presentation of causal estimates. *Eur. J. Epidemiol.* 33, 947–952. doi: 10.1007/S10654-018-0424-6

Burgess, S., and Small, D. S., And Thompson, S. G. (2017). A review of instrumental variable estimators for Mendelian randomization. *Stat. Methods Med. Res.* 26, 2333–2355. doi: 10.1177/0962280215597579

Burgess, S., And Thompson, S. G. (2017). Interpreting findings from Mendelian randomization using the Mr-egger method. *Eur. J. Epidemiol.* 32, 377–389. doi: 10.1007/S10654-017-0255-X

Cen, L., Yang, C., Huang, S., Zhou, M., Tang, X., Li, K., et al. (2017). Peripheral lymphocyte subsets as a marker of Parkinson's disease in a Chinese population. *Neurosci. Bull.* 33, 493–500. doi: 10.1007/S12264-017-0163-9

Channer, B., Matt, S. M., Nickoloff-Bybel, E. A., Pappa, V., Agarwal, Y., Wickman, J., et al. (2023). Dopamine, immunity, and disease. *Pharmacol. Rev.* 75, 62–158. doi: 10.1124/pharmrev.122.000618

Ciaramella, A., Salani, F., Bizzoni, F., Pontieri, F. E., Stefani, A., Pierantozzi, M., et al. (2013). Blood dendritic cell frequency declines in idiopathic Parkinson's disease and is associated with motor symptom severity. *PLoS One* 8:e65352. doi: 10.1371/journal.pone.0065352

da Rocha Sobrinho, H. M., Saar Gomes, R., Da Silva, D. J., Quixabeira, V., Joosten, L., De Barros, R., et al. (2021). Toll-like receptor 10 controls Tlr2-induced cytokine production in monocytes from patients with Parkinson's disease. *J. Neurosci. Res.* 99, 2511–2524. doi: 10.1002/Jnr.24916

Davey Smith, G., And Hemani, G. (2014). Mendelian randomization: genetic anchors for causal inference in epidemiological studies. *Hum. Mol. Genet.* 23, R89–R98. doi: 10.1093/Hmg/Ddu328

De Virgilio, A., Greco, A., Fabbrini, G., Inghilleri, M., Rizzo, M. I., Gallo, A., et al. (2016). Parkinson's disease: autoimmunity and neuroinflammation. *Autoimmun. Rev.* 15, 1005–1011. doi: 10.1016/J.Autrev.2016.07.022

DeMaio, A., Mehrotra, S., and Sambamurti, K., And Husain, S. (2022). The role of the adaptive immune system and T cell dysfunction in neurodegenerative diseases. *J. Neuroinflammation* 19::251. doi: 10.1186/S12974-022-02605-9

Deng, Z., Zheng, Y., and Cai, P., And Zheng, Z. (2021). The role of B and T lymphocyte attenuator in respiratory system diseases. *Front. Immunol.* 12::635623. doi: 10.3389/fimmu.2021.635623

Earls, R. H., And Lee, J. K. (2020). The role of natural killer cells in Parkinson's disease. *Exp. Mol. Med.* 52, 1517–1525. doi: 10.1038/S12276-020-00505-7

Emdin, C. A., and Khera, A. V., And Kathiresan, S. (2017). Mendelian randomization. *JAMA* 318, 1925–1926. doi: 10.1001/Jama.2017.17219

Erokhina, S. A., Streltsova, M. A., Kanevskiy, L. M., Telford, W. G., and Sapozhnikov, A. M., And Kovalenko, E. I. (2018). Hla-Dr(+) Nk cells are mostly characterized by less mature phenotype and high functional activity. *Immunol. Cell Biol.* 96, 212–228. doi: 10.1111/imcb.1032

Garofalo, S., Cocozza, G., Porzia, A., Inghilleri, M., Raspa, M., Scavizzi, F., et al. (2020). Natural killer cells modulate motor neuron-immune cell cross talk in models

of amyotrophic lateral sclerosis. *Nat. Commun.* 11:1773. doi: 10.1038/S41467-020-15644-8

GBD 2016 Neurology Collaborators (2019). Global, regional, and national burden of neurological disorders, 1990-2016: a systematic analysis for the global burden of disease study 2016. *Lancet Neurol.* 18, 459–480. doi: 10.1016/S1474-4422(18)30499-X

Goldeck, D., Maetzler, W., Berg, D., and Oettinger, L., And Pawelec, G. (2016). Altered dendritic cell subset distribution in patients with Parkinson's disease: impact of cmv Serostatus. *J. Neuroimmunol.* 290, 60–65. doi: 10.1016/J.Jneuroim.2015.11.008

Grozdanov, V., Bliederhaeuser, C., Ruf, W. P., Roth, V., Fundel-Clemens, K., Zondler, L., et al. (2014). Inflammatory dysregulation of blood monocytes in Parkinson's disease patients. *Acta Neuropathol.* 128, 651–663. doi: 10.1007/S00401-014-1345-4

Grozdanov, V., Bousset, L., Hoffmeister, M., Bliederhaeuser, C., Meier, C., Madiona, K., et al. (2019). Increased immune activation by pathologic A-Synuclein in Parkinson's disease. *Ann. Neurol.* 86, 593–606. doi: 10.1002/ana.25557

Guan, Q., Liu, W., Mu, K., Hu, Q., Xie, J., Cheng, L., et al. (2022). Single-cell Rna sequencing of Csf reveals neuroprotective Rac1(+) Nk cells in Parkinson's disease. *Front. Immunol.* 13:992505. doi: 10.3389/Fimmu.2022.992505

Harms, A. S., Cao, S., Rowse, A. L., Thome, A. D., Li, X., Mangieri, L. R., et al. (2013). MHCII is required for A-Synuclein-induced activation of microglia, Cd4 T cell proliferation, and dopaminergic neurodegeneration. *J. Neurosci.* 33, 9592–9600. doi: 10.1523/jneurosci.5610-12.2013

Hoogland, I. C., Houbolt, C., Van Westerloo, D. J., Van Gool, W. A., and Van De Beek, D. (2015). Systemic inflammation and microglial activation: systematic review of animal experiments. *J. Neuroinflammation* 12:114. doi: 10.1186/S12974-015-0332-6

Huang, Y. M., Kouwenhoven, M., Jin, Y. P., Press, R., and Huang, W. X., And Link, H. (2001). Dendritic cells derived from patients with multiple sclerosis show high Cd1a and low Cd86 expression. *Multiple Sclerosis (Houndmills, Basingstoke, England)* 7, 95–99. doi: 10.1177/135245850100700204

Huang, B., Zhenxin, Y., Chen, S., Tan, Z., Zong, Z., Zhang, H., et al. (2022). The innate and adaptive immune cells in Alzheimer's and Parkinson's diseases. *Oxidative Med. Cell. Longev.* 2022:1315248. doi: 10.1155/2022/1315248

Jensen, M. P., Jacobs, B. M., Dobson, R., Bandres-Ciga, S., Blauwendraat, C., Schrag, A., et al. (2021). Lower lymphocyte count is associated with increased risk of Parkinson's disease. *Ann. Neurol.* 89, 803–812. doi: 10.1002/Ana.26034

Jiang, S., Gao, H., Luo, Q., and Wang, P., And Yang, X. (2017). The correlation of lymphocyte subsets, natural killer cell, and Parkinson's disease: a meta-analysis. *Neurol. Sci.* 38, 1373–1380. doi: 10.1007/S10072-017-2988-4

Karpenko, M. N., Vasilishina, A. A., Gromova, E. A., Muruzheva, Z. M., and Miliukhina, I. V., And Bernadotte, A. (2018). Interleukin-1β, Interleukin-1 receptor antagonist, Interleukin-6, Interleukin-10, and tumor necrosis factor-A levels in Csf and serum in relation to the clinical diversity of Parkinson's disease. *Cell. Immunol.* 327, 77–82. doi: 10.1016/J.Cellimm.2018.02.011

Kustrimovic, N., Comi, C., Magistrelli, L., Rasini, E., Legnaro, M., Bombelli, R., et al. (2018). Parkinson's disease patients have a complex phenotypic and functional Th1 Bias: cross-sectional studies of Cd4+ Th1/Th2/T17 and Treg in drug-Naïve and drug-treated patients. *J. Neuroinflammation* 15:205. doi: 10.1186/S12974-018-1248-8

Larsson, S. C., and Butterworth, A. S., And Burgess, S. (2023). Mendelian randomization for cardiovascular diseases: principles and applications. *Eur. Heart J.* 44, 4913–4924. doi: 10.1093/eurheartj/ehad736

Li, R., Tropea, T. F., Baratta, L. R., Zuroff, L., Diaz-Ortiz, M. E., Zhang, B., et al. (2022). Abnormal B-cell and Tfh-cell profiles in patients with Parkinson disease: a cross-sectional study. *Neurology(R) Neuroimmunology & Neuroinflammation* 9:E1125. doi: 10.1212/nxi.0000000000001125

Lin, C. H., Chen, C. C., Chiang, H. L., Liou, J. M., Chang, C. M., Lu, T. P., et al. (2019). Altered gut microbiota and inflammatory cytokine responses in patients with Parkinson's disease. *J. Neuroinflammation* 16:129. doi: 10.1186/S12974-019-1528-Y

Marogianni, C., Sokratous, M., Dardiotis, E., Hadjigeorgiou, G. M., and Bogdanos, D., And Xiromerisiou, G. (2020). Neurodegeneration and inflammation-an interesting interplay in Parkinson's disease. *Int. J. Mol. Sci.* 21::8421. doi: 10.3390/ijms21228421

Nalls, M. A., Blauwendraat, C., Vallerga, C. L., Heilbron, K., Bandres-Ciga, S., Chang, D., et al. (2019). Identification of novel risk loci, causal insights, and heritable risk for Parkinson's disease: a Meta-analysis of genome-wide association studies. *Lancet Neurol.* 18, 1091–1102. doi: 10.1016/S1474-4422(19)30320-5

Ohkura, N., and Sakaguchi, S. (2020). Transcriptional and epigenetic basis of Treg cell development and function: its genetic anomalies or variations in autoimmune diseases. *Cell Res.* 30, 465–474. doi: 10.1038/S41422-020-0324-7

Orrù, V., Steri, M., Sidore, C., Marongiu, M., Serra, V., Olla, S., et al. (2020). Complex genetic signatures in immune cells underlie autoimmunity and inform therapy. *Nat. Genet.* 52, 1036–1045. doi: 10.1038/S41588-020-0684-4

Panagiotakopoulou, V., Ivanyuk, D., De Cicco, S., Haq, W., Arsić, A., Yu, C., et al. (2020). Interferon-Γ signaling synergizes with Lrrk2 in neurons and microglia derived from human induced pluripotent stem cells. *Nat. Commun.* 11:5163. doi: 10.1038/S41467-020-18755-4

Peng, Y. Q., Wu, Z. C., Xu, Z. B., Fang, S. B., Chen, D. H., Zhang, H. Y., et al. (2022). Mesenchymal stromal cells-derived Small extracellular vesicles modulate dc function to suppress Th2 responses via Il-10 in patients with allergic rhinitis. *Eur. J. Immunol.* 52, 1129–1140. doi: 10.1002/Eji.202149497

Sanchez-Guajardo, V., Febbraro, F., and Kirik, D., And Romero-Ramos, M. (2010). Microglia acquire distinct activation profiles depending on the degree of alpha-Synuclein neuropathology in a Raav based model of Parkinson's disease. *PLoS One* 5::E8784. doi: 10.1371/journal.pone.0008784

Schlachetzki, J., Prots, I., Tao, J., Chun, H. B., Saijo, K., Gosselin, D., et al. (2018). A monocyte gene expression signature in the early clinical course of Parkinson's disease. *Sci. Rep.* 8:10757. doi: 10.1038/S41598-018-28986-7

Sekula, P., del Greco M, F., Pattaro, C., and Köttgen, A. (2016). Mendelian randomization as an approach to assess causality using observational data. *J. Am. Soc. Nephrol.* 27, 3253–3265. doi: 10.1681/asn.2016010098

Skrivankova, V. W., Richmond, R. C., Woolf, B., Yarmolinsky, J., Davies, N. M., Swanson, S. A., et al. (2021). Strengthening the reporting of observational studies in epidemiology using Mendelian randomization: the Strobe-Mr statement. *JAMA* 326, 1614–1621. doi: 10.1001/jama.2021.18236

Steri, M., Orrù, V., Idda, M. L., Pitzalis, M., Pala, M., Zara, I., et al. (2017). Overexpression of the cytokine Baff and autoimmunity risk. *N. Engl. J. Med.* 376, 1615–1626. doi: 10.1056/Nejmoa1610528

Su, Y., Shi, C., Wang, T., Liu, C., Yang, J., Zhang, S., et al. (2022). Dysregulation of peripheral monocytes and pro-inflammation of alpha-Synuclein in Parkinson's disease. *J. Neurol.* 269, 6386–6394. doi: 10.1007/S00415-022-11258-W

Sun, C., Zhao, Z., Yu, W., Mo, M., Song, C., Si, Y., et al. (2019). Abnormal subpopulations of peripheral blood lymphocytes are involved in Parkinson's disease. *Ann Transl Med* 7:637. doi: 10.21037/Atm.2019.10.105

Tansey, M. G., Wallings, R. L., Houser, M. C., Herrick, M. K., and Keating, C. E., And Joers, V. (2022). Inflammation and immune dysfunction in Parkinson disease. *Nat. Rev. Immunol.* 22, 657–673. doi: 10.1038/S41577-022-00684-6

Tekguc, M., Wing, J. B., Osaki, M., and Long, J., And Sakaguchi, S. (2021). Treg-expressed Ctla-4 depletes Cd80/Cd86 by Trogocytosis, releasing free Pd-L1 on antigen-presenting cells. *Proc. Natl. Acad. Sci. USA* 118::E2023739118. doi: 10.1073/pnas.2023739118

Tian, J., Dai, S. B., Jiang, S. S., Yang, W. Y., Yan, Y. Q., Lin, Z. H., et al. (2022). Specific immune status in Parkinson's disease at different ages of onset. *Npj Parkinson's Disease* 8:5. doi: 10.1038/S41531-021-00271-X

Vanderweele, T. J., Tchetgen Tchetgen, E. J., and Cornelis, M., And Kraft, P. (2014). Methodological challenges in Mendelian randomization. *Epidemiology* 25, 427–435. doi: 10.1097/ede.0000000000000081

Wang, Q., and Liu, Y., And Zhou, J. (2015). Neuroinflammation in Parkinson's disease and its potential as therapeutic target. *Transl Neurodegener* 4::19. doi: 10.1186/S40035-015-0042-0

Wijeyekoon, R. S., Kronenberg-Versteeg, D., Scott, K. M., Hayat, S., Kuan, W. L., Evans, J. R., et al. (2020a). Peripheral innate immune and bacterial signals relate to clinical heterogeneity in Parkinson's disease. *Brain Behav. Immun.* 87, 473–488. doi: 10.1016/J.Bbi.2020.01.018

Wijeyekoon, R. S., Moore, S. F., Farrell, K., Breen, D. P., Barker, R. A., and Williams-Gray, C. H. (2020b). Cerebrospinal fluid cytokines and neurodegeneration-associated proteins in Parkinson's disease. *Mov. Disord.* 35, 1062–1066. doi: 10.1002/mds.28015

Witoelar, A., Jansen, I. E., Wang, Y., Desikan, R. S., Gibbs, J. R., Blauwendraat, C., et al. (2017). Genome-wide pleiotropy between Parkinson disease and autoimmune diseases. *JAMA Neurol.* 74, 780–792. doi: 10.1001/jamaneurol.2017.0469

Woolf, B., Di Cara, N., Moreno-Stokoe, C., Skrivankova, V., Drax, K., Higgins, J., et al. (2022). Investigating the transparency of reporting in two-sample summary data Mendelian randomization studies using the Mr-Base platform. *Int. J. Epidemiol.* 51, 1943–1956. doi: 10.1093/ije/dyac074

Yavorska, O. O., and Burgess, S. (2017). Mendelianrandomization: an R package for performing Mendelian randomization analyses using summarized data. *Int. J. Epidemiol.* 46, 1734–1739. doi: 10.1093/ije/dyx034

Zheng, Y., Ge, W., Ma, Y., Xie, G., Wang, W., Han, L., et al. (2017). Mir-155 regulates Il-10-producing Cd24(hi)Cd27(+) B cells and impairs their function in patients with Crohn's disease. *Front. Immunol.* 8:914. doi: 10.3389/fimmu.2017.00914

frontiers | Frontiers in Aging Neuroscience

TYPE Original Research
PUBLISHED 27 March 2024
DOI 10.3389/fnagi.2024.1367106

OPEN ACCESS

EDITED BY
Robert Weissert,
University of Regensburg, Germany

REVIEWED BY
Deepti Lall,
Cedars Sinai Medical Center, United States
Fuyi Xu,
University of Tennessee Health Science Center (UTHSC), United States

*CORRESPONDENCE
Jing Shen
✉ 165344440@qq.com

†These authors have contributed equally to this work and share first authorship

RECEIVED 09 January 2024
ACCEPTED 18 March 2024
PUBLISHED 27 March 2024

CITATION
Xiao C, Gu X, Feng Y and Shen J (2024) Two-sample Mendelian randomization analysis of 91 circulating inflammatory protein levels and amyotrophic lateral sclerosis. *Front. Aging Neurosci.* 16:1367106. doi: 10.3389/fnagi.2024.1367106

Two-sample Mendelian randomization analysis of 91 circulating inflammatory protein levels and amyotrophic lateral sclerosis

Chenxu Xiao[1†], Xiaochu Gu[2†], Yu Feng[3,4†] and Jing Shen[1*†]

[1]The Affiliated Jiangsu Shengze Hospital of Nanjing Medical University, Suzhou, China, [2]Medical Laboratory, Suzhou Psychiatric Hospital, The Affiliated Guangji Hospital of Soochow University, Suzhou, China, [3]The University of New South Wales, Kensington, NSW, Australia, [4]The University of Melbourne, Parkville, VIC, Australia

Introduction: Amyotrophic Lateral Sclerosis (ALS) is a neurodegenerative disease with poorly understood pathophysiology. Recent studies have highlighted systemic inflammation, especially the role of circulating inflammatory proteins, in ALS.

Methods: This study investigates the potential causal link between these proteins and ALS. We employed a two-sample Mendelian Randomization(MR) approach, analyzing data from large-scale genome-wide association studies to explore the relationship between 91 circulating inflammatory proteins and ALS. This included various MR methods like MR Egger, weighted median, and inverse-variance weighted, complemented by sensitivity analyses for robust results.

Results: Significant associations were observed between levels of inflammatory proteins, including Adenosine Deaminase, Interleukin-17C, Oncostatin-M, Leukemia Inhibitory Factor Receptor, and Osteoprotegerin, and ALS risk. Consistencies were noted across different *P*-value thresholds. Bidirectional MR suggested that ALS risk might influence levels of certain inflammatory proteins.

Discussion: Our findings, via MR analysis, indicate a potential causal relationship between circulating inflammatory proteins and ALS. This sheds new light on ALS pathophysiology and suggests possible therapeutic targets. Further research is required to confirm these results and understand the specific roles of these proteins in ALS.

KEYWORDS

amyotrophic lateral sclerosis, circulating inflammatory protein, two-sample mendelian randomization, osteoprotegerin, tumor necrosis factor

1 Introduction

Amyotrophic Lateral Sclerosis (ALS), also known as Lou Gehrig's disease, is a neurodegenerative condition that primarily affects motor neurons. This disease is characterized by the progressive degeneration of motor neurons, leading to fatal paralysis. ALS manifests in two forms: familial and sporadic, differentiated by family history. Despite significant research efforts, the underlying pathogenesis of ALS remains elusive, and effective treatments are scarce (Ralli et al., 2019; Masrori and Van Damme, 2020; Yang et al., 2021).

In the last decade, substantial progress has been made in understanding the genetic architecture, pathophysiological mechanisms, and potential biomarkers of ALS (Yang et al., 2021; Witzel et al., 2022; Mead et al., 2023). These advancements have opened new avenues for therapeutic intervention, particularly in the domain of neuroinflammation, which is increasingly associated with ALS. Recent focus in ALS research has centered on systemic inflammation, especially the role of circulating inflammatory proteins (Henkel et al., 2004; Murdock et al., 2015; Zondler et al., 2016). Studies have linked proteins like PIKFYVE kinase and TDP-43 to neuronal damage in ALS, associating their inhibition or misfolding with neuronal injury (Gleixner et al., 2022; Shao et al., 2022; Tejwani et al., 2023). This growing body of evidence underscores the importance of these proteins as both biomarkers and potential therapeutic targets (Akiyama et al., 2022; Jiang et al., 2022; Hosaka et al., 2023).

Concurrently, the application of bioinformatics, molecular biology, and genetics in ALS research has significantly enhanced our understanding of the disease's complexity (Sankaran et al., 2021; Carroll, 2022; Sari et al., 2022). Innovations in these fields have led to the identification of new genetic and molecular pathways in ALS, laying the groundwork for targeted therapies (Lehrach et al., 2011; Akinduro et al., 2021; Wu and Lin, 2022). One key methodology employed in this context is Mendelian Randomization (MR). MR leverages genetic variations as instrumental variables to establish causal relationships between exposures (inflammatory proteins) and outcomes (ALS), thus enhancing the credibility of causal inferences drawn from observational studies by reducing common confounders and reverse causation (Song et al., 2022; Lee et al., 2023; Liu et al., 2023; Rajasundaram and Gill, 2023).

Our study employs a two-sample MR approach, utilizing multiple *p*-value thresholds to increase the accuracy of our findings while acknowledging the trade-offs involved. Lower *p*-values, such as <5.0E−08, are typically used to ensure robustness of associations, reduce heterogeneity, and improve study precision. However, such stringent criteria may also exclude potentially meaningful associations. Therefore, by adopting different *p*-value thresholds, our analysis aims to strike a balance between minimizing false positives and not overlooking significant associations that could be crucial for understanding the pathophysiology of ALS (Liu et al., 2023; Soremekun et al., 2023).

2 Methods

The research process is illustrated in the flowchart figure (Figure 1).

2.1 Data sources

Data on 91 circulating inflammatory proteins were sourced from GWAS data measured using the Olink Target Inflammation panel across 11 cohorts, involving a total of 14,824 European ancestry participants (Zhao et al., 2023). Data on Amyotrophic Lateral Sclerosis were derived from a meta-analysis of GWAS by van Rheenen et al., "GCST90027164",[1] including 27,205 ALS cases and 110,881 European ancestry controls (van Rheenen et al., 2021) (Supplementary Table S1). The ALS validation group comprises two GWAS datasets curated by van Rheenen and Nicolas. The initial dataset consists of sporadic ALS cases, while the validation sets include one sporadic ALS dataset and another dataset that does not differentiate between familial or sporadic ALS (Supplementary Table S1). Specific details regarding data curation are thoroughly explained in the original articles.

2.2 Mendelian randomization

We utilized a two-sample MR (TSMR) analysis to explore the causal relationship between circulating inflammatory proteins and ALS. In our MR analysis, inflammatory proteins were the exposure of interest, ALS was the outcome, and SNPs were used as instrumental variables. The TSMR approach was based on the following assumptions: (I) instrumental variables are closely associated with the risk of inflammatory proteins; (II) instrumental variables affect ALS risk only through their impact on inflammatory proteins; (III) instrumental variables are independent of confounding factors (Davey Smith and Hemani, 2014).

We selected SNPs associated with inflammatory proteins across the whole genome ($p<5\times10^{-8}$), ($p<5\times10^{-7}$), and ($p<5\times10^{-6}$) for forward TSMR analysis. For reverse TSMR analysis of ALS GWAS instrumental variables, we used SNPs ($p<5\times10^{-8}$). Additionally, PLINK clumping was employed to calculate linkage disequilibrium between each exposure's SNPs on the basis of the 1,000 Genomes European panel, using an $r^2<0.01$ (clumping distance = 5,000 kb) as the threshold for SNPs in linkage equilibrium. The *F*-statistic was calculated using $F=\text{beta}^2/\text{se}^2$, with all *F*-statistics >10, indicating robustness of the instrumental variables.

Several MR methods were used, including MR Egger, weighted median, IVW, Wald ratio, simple mode, and weighted mode. IVW was selected as the primary analysis method, using Wald ratio when snp < 2, with a *p*-value <0.05 considered significant (Burgess et al., 2013; Verbanck et al., 2018). Cochran's *Q* statistic was used to assess heterogeneity between individual SNPs. If no significant heterogeneity was observed ($p<0.05$), a fixed-effect model was adopted (Hemani et al., 2018); otherwise, the causal significance relationship needed cautious interpretation. Sensitivity analyses were also conducted to verify the robustness of our results. Furthermore, MR-Egger and MR-PRESSO methods were employed to determine the presence of pleiotropy. The intercept obtained from MR-Egger regression was used to measure directional pleiotropy, and MR-PRESSO was used for enhanced detection of pleiotropy (Bowden et al., 2016). Steiger testing was performed to determine the direction of causality. Leave-one-out sensitivity analysis was conducted to determine whether individual SNPs had a significant impact on MR results.

2.3 Statistical software

All statistical analyses were performed using R software version 4.3.0.[2] MR analysis and Steiger filtering were performed using the "TwoSampleMR" R package (Smith and Ebrahim, 2003; Emdin et al., 2017; The Telomeres Mendelian Randomization Collaboration et al.,

1 https://www.ebi.ac.uk/gwas/studies/GCST90027164

2 https://www.r-project.org/

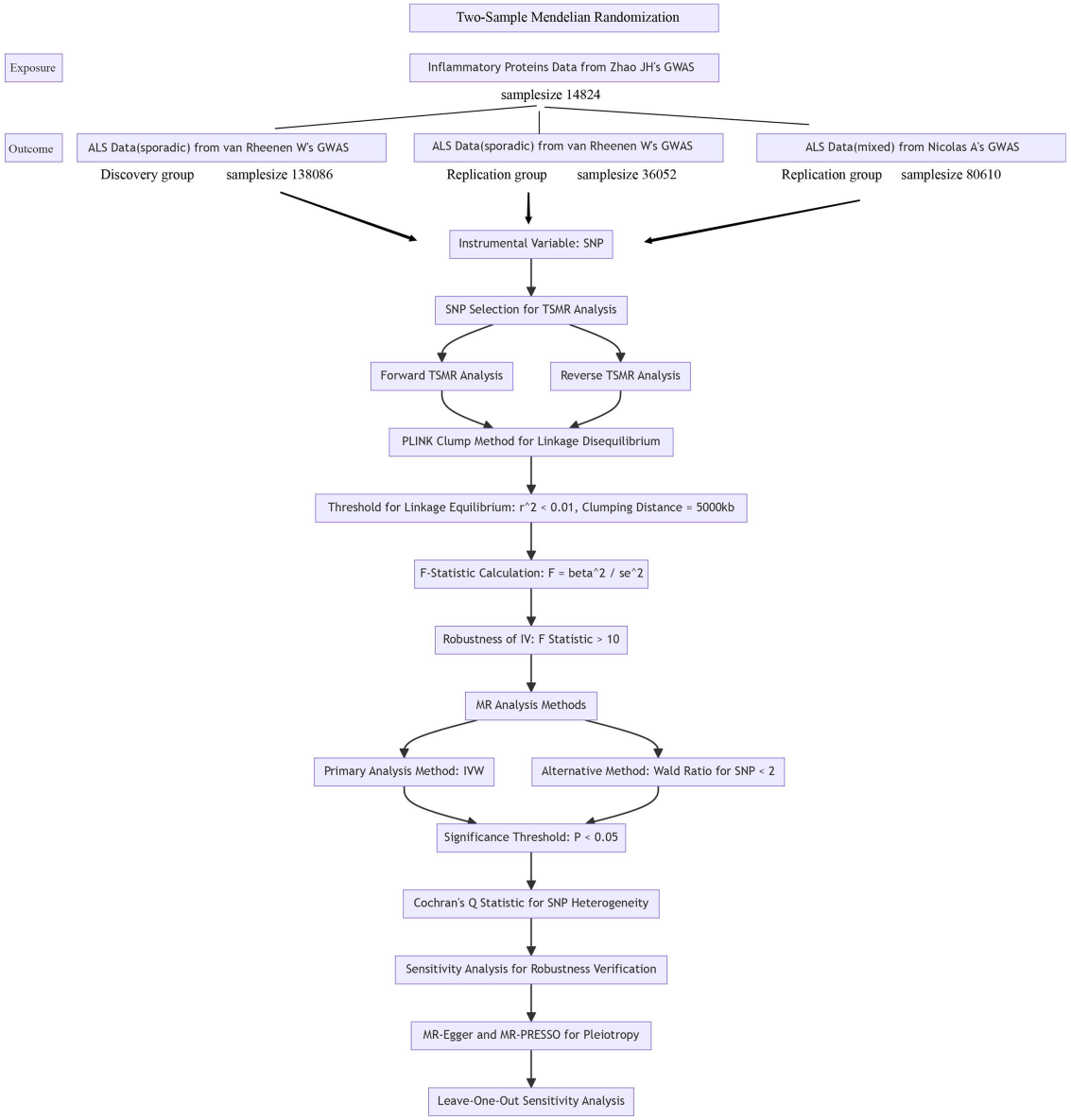

FIGURE 1
Flowchart figure.

2017). MR-PRESSO was carried out using the "MRPRESSO" R package.

2.4 Selection of external datasets for validation

During the initial exploration phase of the study, we refrained from using *p*-value correction to capture more potential associations. To ensure the reliability of our preliminary results, we chose to validate them using two external datasets. One dataset focuses on sporadic ALS, while the other does not distinguish between familial or sporadic ALS. By including both sporadic ALS and non-differentiated familial or sporadic ALS datasets, we can comprehensively assess the generalizability of our findings. In the preliminary screening process, we incorporated potentially key proteins previously identified, including 12 inflammation-related proteins. By utilizing these datasets, we are able to validate the associations observed in our study (van Rheenen et al., 2016; Nicolas et al., 2018).

3 Results

3.1 Forward Mendelian randomization results

Using the threshold of SNPs ($p < 5 \times 10^{-8}$), instrumental variables were extracted for 73 inflammatory proteins for TSMR analysis. The results indicated that increased levels of Adenosine Deaminase are associated with a higher risk of ALS (OR = 1.068, PIVW = 0.048). This

analysis showed no significant heterogeneity (MR Egger $Q = 5.658$, Q p-value = 0.059) and no horizontal pleiotropy (P Egger Intercept = 0.806, P MR Presso = 0.361). An increase in Interleukin-17C levels was also found to increase ALS risk (OR = 1.199, PIVW = 0.047) (SNPs <3). Higher Oncostatin-M levels were associated with a decreased risk of ALS (OR = 0.84, PIVW = 0.016), with the analysis showing no significant heterogeneity (MR Egger $Q = 0.359$, Q p-value = 0.836) and no horizontal pleiotropy (P Egger Intercept = 0.596, P MR Presso = 0.864). Increased levels of Leukemia inhibitory factor receptor were associated with a decreased risk of ALS (OR = 0.903, PIVW = 0.017), with no significant heterogeneity (MR Egger $Q = 2.064$, Q p-value = 0.151) or horizontal pleiotropy (P Egger Intercept = 0.913) observed (Figure 2) (Supplementary Tables S2, S3, S8).

Due to the initial selection criteria, some proteins did not yield SNPs, leading us to relax the conditions. We selected SNPs with a threshold of $p < 5 \times 10^{-7}$ as instrumental variables, and conducted TSMR analysis on 86 inflammatory proteins. The results revealed the following:

Adenosine Deaminase Levels: an increase in Adenosine Deaminase levels was associated with an increased risk of ALS (OR = 1.07, PIVW = 0.025). The analysis showed no significant heterogeneity (MR Egger $Q = 6.654$, Q p-value = 0.084) and no evidence of horizontal pleiotropy (P Egger Intercept = 0.820, P MR Presso = 0.339).

Interleukin-5 Levels: higher levels of Interleukin-5 were also linked to an increased risk of ALS (OR = 1.5, PIVW = 0.015), with fewer than three SNPs involved.

SIR2-like Protein 2 Levels: an elevation in SIR2-like protein 2 levels was correlated with an increased risk of ALS (OR = 1.24, PIVW = 0.024), again with fewer than three SNPs.

Neurturin Levels: increased levels of Neurturin were found to raise the risk of ALS (OR = 1.237, PIVW = 0.040), with fewer than three SNPs.

Leukemia Inhibitory Factor Receptor Levels: conversely, an increase in Leukemia inhibitory factor receptor levels was associated with a decreased risk of ALS (OR = 0.912, PIVW = 0.029). This analysis also showed no significant heterogeneity (MR Egger $Q = 2.966$, Q p-value = 0.227) and no horizontal pleiotropy (P Egger Intercept = 0.713, P MR Presso = 0.566).

Osteoprotegerin Levels: higher levels of Osteoprotegerin were linked to a reduced risk of ALS (OR = 0.89, PIVW = 0.020). The analysis indicated no significant heterogeneity (MR Egger $Q = 16.163$, Q p-value = 0.064) and no horizontal pleiotropy (P Egger Intercept = 0.979, P MR Presso = 0.118) (Figure 3) (Supplementary Tables S2, S4, S9).

In an effort to include more inflammatory proteins, the criteria were adjusted by setting the SNP threshold to $p < 5 \times 10^{-6}$. This enabled the extraction of instrumental variables for all 91 inflammatory proteins, which were then analyzed using TSMR. The findings were as follows:

ADA (Adenosine Deaminase) Levels: an increase in ADA levels was associated with an increased risk of ALS (OR = 1.072, PIVW = 0.037). This analysis indicated the presence of heterogeneity (MR Egger $Q = 29.224$, Q p-value = 0.004) and no evidence of horizontal pleiotropy (P Egger Intercept = 0.735, P MR Presso = 0.389).

TNF-beta Levels: elevated TNF-beta levels were associated with a reduced risk of ALS (OR = 0.951, PIVW = 0.012). The analysis showed heterogeneity (MR Egger $Q = 34.518$, Q p-value = 0.184) and no horizontal pleiotropy ($p = 0.454$, P MR Presso = 0.723).

Osteoprotegerin Levels: an increase in Osteoprotegerin levels was linked to a decreased risk of ALS (OR = 0.916, PIVW = 0.031). The analysis did not show significant heterogeneity (MR Egger $Q = 27.915$, Q p-value = 0.085) and no horizontal pleiotropy was found (P Egger Intercept = 0.440, P MR Presso = 0.125).

Interleukin-10 Levels: higher levels of Interleukin-10 were associated with a decreased risk of ALS (OR = 0.901, PIVW = 0.011). This analysis indicated no significant heterogeneity (MR Egger $Q = 11.062$, Q p-value = 0.853) and no horizontal pleiotropy (P Egger Intercept = 0.751, P MR Presso = 0.056) (Figure 4) (Supplementary Tables S2, S5, S10).

From the three sets of analyses conducted, we can draw several conclusions:

ADA Levels: an increase in ADA levels was found to heighten the risk of ALS. This finding was significant across all three sets of analyses (P IVW < 0.05). Although there was heterogeneity in the results with the threshold at $p < 5 \times 10^{-6}$, the IVW results were relatively stable.

exposure	method	nsnp	pval	OR(95%CI)	Q_pval.MR.Egger.	MR.egger.intercept.P	MR.PRESSO.Global.Test.P
Adenosine Deaminase levels	MR Egger	4	0.322091965	1.08(0.96 to 1.21)			
	Weighted median	4	0.006638358	1.08(1.02 to 1.14)			
	Inverse variance weighted	4	0.047865044	1.07(1.00 to 1.14)	0.059069422	0.806223267	0.361
	Simple mode	4	0.790138424	0.98(0.86 to 1.12)			
	Weighted mode	4	0.043046057	1.11(1.04 to 1.17)			
Oncostatin-M levels	MR Egger	4	0.979734923	0.99(0.58 to 1.70)			
	Weighted median	4	0.071872041	0.86(0.73 to 1.01)			
	Inverse variance weighted	4	0.016016951	0.84(0.73 to 0.97)	0.835659445	0.595813979	0.864
	Simple mode	4	0.246173065	0.85(0.69 to 1.06)			
	Weighted mode	4	0.205177641	0.86(0.72 to 1.03)			
Leukemia inhibitory factor receptor levels	MR Egger	3	0.511171984	0.89(0.70 to 1.13)			
	Weighted median	3	0.036044510	0.91(0.84 to 0.99)			
	Inverse variance weighted	3	0.016672743	0.90(0.83 to 0.98)	0.150826793	0.912885596	
	Simple mode	3	0.482012378	0.94(0.82 to 1.08)			
	Weighted mode	3	0.242926096	0.93(0.84 to 1.02)			
Interleukin-17C levels	Inverse variance weighted	2	0.047331455	1.20(1.00 to 1.43)			

P<0.05 was considered statistically significant

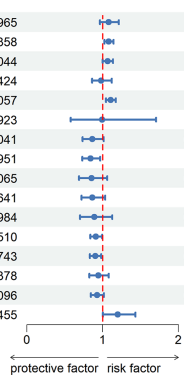

FIGURE 2
Adopt a significance threshold for selecting SNPs of $p < 5 \times 10^{-8}$. In this Mendelian randomization analysis, inflammatory proteins are analyzed as the exposure factor, with ALS as the resultant outcome. Significant findings are denoted by a P_IVW value less than 0.05.

10.3389/fnagi.2024.1367106

exposure	method	nsnp	pval	OR(95%CI)	Q_pval.MR.Egger.	MR.egger.intercept.P	MR.PRESSO.Global.Test.P
Interleukin-5 levels	Wald ratio	1	0.015440661	1.50(1.08 to 2.08)			
SIR2-like protein 2 levels	Inverse variance weighted	2	0.023797281	1.24(1.03 to 1.49)			
Neurturin levels	Inverse variance weighted	2	0.039940201	1.24(1.01 to 1.52)			
Leukemia inhibitory factor receptor levels	MR Egger	4	0.330188545	0.88(0.72 to 1.07)			
	Weighted median	4	0.066449423	0.92(0.84 to 1.01)			
	Inverse variance weighted	4	0.029061127	0.91(0.84 to 0.99)	0.226932871	0.712724048	0.566
	Simple mode	4	0.620674990	0.96(0.82 to 1.12)			
	Weighted mode	4	0.201360642	0.92(0.84 to 1.02)			
Osteoprotegerin levels	MR Egger	11	0.376230343	0.89(0.70 to 1.13)			
	Weighted median	11	0.011225750	0.86(0.77 to 0.97)			
	Inverse variance weighted	11	0.020225965	0.89(0.81 to 0.98)	0.063559731	0.979019685	0.118
	Simple mode	11	0.082399961	0.81(0.65 to 1.00)			
	Weighted mode	11	0.117033676	0.89(0.79 to 1.02)			
Adenosine Deaminase levels	MR Egger	5	0.280790595	1.06(0.97 to 1.16)			
	Weighted median	5	0.003749396	1.08(1.03 to 1.14)			
	Inverse variance weighted	5	0.024805448	1.07(1.01 to 1.14)	0.083791053	0.820178088	0.339
	Simple mode	5	0.813721901	1.02(0.90 to 1.15)			
	Weighted mode	5	0.042119092	1.09(1.03 to 1.15)			

P<0.05 was considered statistically significant

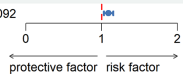

FIGURE 3
Adopt a significance threshold for selecting SNPs of $p < 5 \times 10^{-7}$. In this Mendelian randomization analysis, inflammatory proteins are analyzed as the exposure factor, with ALS as the resultant outcome. Significant findings are denoted by a P_IVW value less than 0.05.

exposure	method	nsnp	pval	OR(95%CI)	Q_pval.MR.Egger.	MR.egger.intercept.P	MR.PRESSO.Global.Test.P
TNF-beta levels	MR Egger	30	0.318031934	0.97(0.91 to 1.03)			
	Weighted median	30	0.175117441	0.97(0.92 to 1.02)			
	Inverse variance weighted	30	0.011761730	0.95(0.91 to 0.99)	0.184333283	0.454012996	0.723
	Simple mode	30	0.660874963	0.98(0.89 to 1.08)			
	Weighted mode	30	0.138414805	0.96(0.92 to 1.01)			
Adenosine Deaminase levels	MR Egger	14	0.177995682	1.06(0.98 to 1.15)			
	Weighted median	14	0.007297604	1.08(1.02 to 1.14)			
	Inverse variance weighted	14	0.036546363	1.07(1.00 to 1.14)	0.003648523	0.734957416	0.389
	Simple mode	14	0.689116904	0.97(0.86 to 1.10)			
	Weighted mode	14	0.007490589	1.09(1.03 to 1.15)			
Osteoprotegerin levels	MR Egger	21	0.106643578	0.86(0.73 to 1.02)			
	Weighted median	21	0.206034244	0.94(0.85 to 1.04)			
	Inverse variance weighted	21	0.030994346	0.92(0.85 to 0.99)	0.085073049	0.439992627	0.125
	Simple mode	21	0.073390936	0.84(0.69 to 1.01)			
	Weighted mode	21	0.389023265	0.94(0.83 to 1.07)			
Interleukin-10 levels	MR Egger	19	0.175393047	0.88(0.73 to 1.05)			
	Weighted median	19	0.473386110	0.96(0.86 to 1.07)			
	Inverse variance weighted	19	0.010947869	0.90(0.83 to 0.98)	0.85334866	0.751464761	0.056
	Simple mode	19	0.040167391	0.78(0.63 to 0.97)			
	Weighted mode	19	0.958315524	1.00(0.85 to 1.17)			

P<0.05 was considered statistically significant

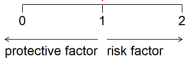

FIGURE 4
Adopt a significance threshold for selecting SNPs of $p < 5 \times 10^{-6}$. In this Mendelian randomization analysis, inflammatory proteins are analyzed as the exposure factor, with ALS as the resultant outcome. Significant findings are denoted by a P_IVW value less than 0.05.

Leukemia Inhibitory Factor Receptor Levels: higher levels of the Leukemia inhibitory factor receptor were associated with a decreased risk of ALS. This was significantly observed in the first two sets of analyses (P IVW < 0.05).

Osteoprotegerin Levels: an increase in Osteoprotegerin levels also appeared to reduce the risk of ALS. This outcome was significant in the latter two sets of analyses (P IVW < 0.05).

Next, we conducted a leave-one-out analysis on the three key results mentioned above. This involved sequentially excluding each SNP and estimating the effect sizes for the remaining SNPs. For both Leukemia inhibitory factor receptor levels and Osteoprotegerin levels, the analysis showed no significant difference in effect size before and after exclusion, indicating that no single SNP had a significant impact on the MR estimates. However, in the three sets of analyses for ADA levels, the exclusion of the SNP "rs112665079" led to a deviation in results, suggesting that rs112665079 has a significant influence on the MR estimation results (Figure 5) (Supplementary Table S7).

After excluding rs112665079 and reanalyzing TSMR with ADA levels as the exposure and ALS as the outcome, the results were contrary to the previous findings, showing no significant correlation. This indeed demonstrates the significant impact of rs112665079 on the MR estimation results (Figure 6).

3.2 Reverse Mendelian randomization results

In the reverse Mendelian randomization analysis involving ALS and 91 inflammatory proteins, the following results were obtained:

C-C Motif Chemokine 20 Levels: an increase in the risk of ALS was associated with elevated levels of C-C motif chemokine 20

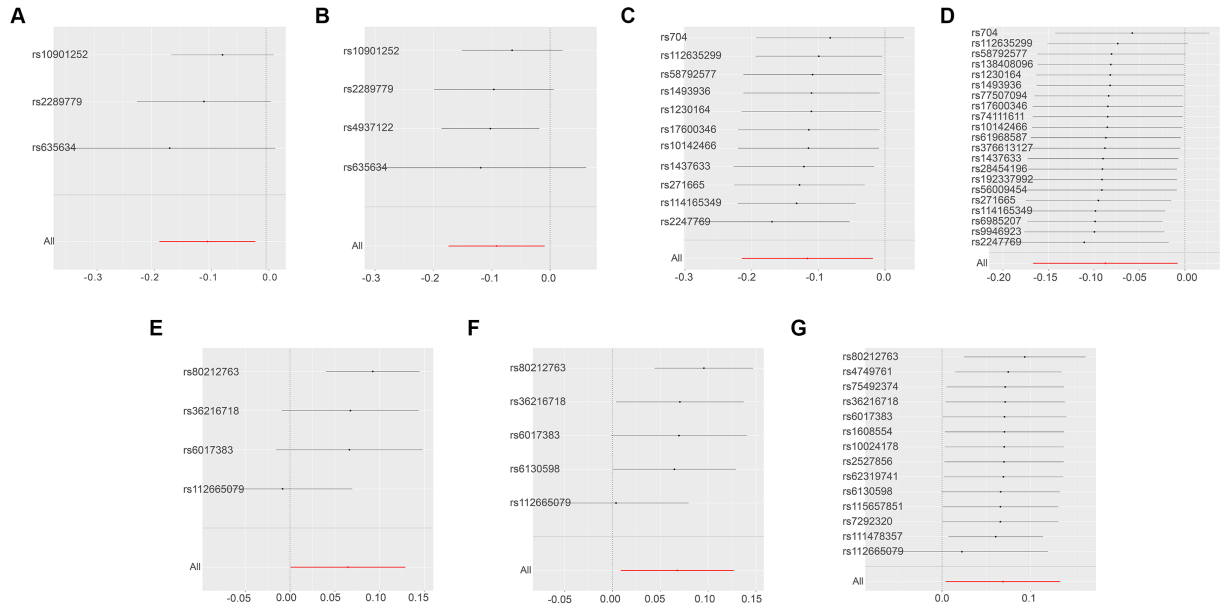

FIGURE 5
Displays the leave-one-out analysis results using the IVW method, assessing the impact of individual SNPs on the overall MR findings by sequentially excluding each SNP. The *Y*-axis corresponds to each excluded rsID and the aggregate IVW method result without any SNP exclusions. The *X*-axis represents the specific IVW values, where black and red dots denote beta effect values, and the lines indicate the confidence intervals of the beta values. Specifically, **(A,B)** illustrate the leukemia inhibitory factor receptor levels as the exposure, with SNP thresholds set at $p < 5 \times 10^{-8}$ and $p < 5 \times 10^{-7}$, respectively. **(C,D)** focus on osteoprotegerin levels as the exposure, applying SNP thresholds of $p < 5 \times 10^{-7}$ and $p < 5 \times 10^{-6}$. Finally, the levels of adenosine deaminase as the exposure factor are examined in **(E–G)**, with SNP thresholds set at $p < 5 \times 10^{-8}$, $p < 5 \times 10^{-7}$, and $p < 5 \times 10^{-6}$, respectively.

exposure	method	nsnp	pval	OR(95%CI)	snps.threshold
Adenosine Deaminase levels	MR Egger	3	0.6241362	0.96(0.85 to 1.08)	
	Weighted median	3	0.5035207	0.97(0.90 to 1.05)	
	Inverse variance weighted	3	0.8342857	0.99(0.92 to 1.07)	P < 5×10 -8
	Simple mode	3	0.6979696	0.97(0.86 to 1.10)	
	Weighted mode	3	0.6324832	0.97(0.88 to 1.07)	
Adenosine Deaminase levels	MR Egger	4	0.4351065	0.95(0.85 to 1.06)	
	Weighted median	4	0.5030855	0.97(0.90 to 1.05)	
	Inverse variance weighted	4	0.9233064	1.00(0.93 to 1.08)	P < 5×10 -7
	Simple mode	4	0.7862434	0.98(0.86 to 1.12)	
	Weighted mode	4	0.6462847	0.98(0.89 to 1.07)	
Adenosine Deaminase levels	MR Egger	13	0.6688425	0.97(0.85 to 1.11)	
	Weighted median	13	0.5404853	0.97(0.89 to 1.06)	
	Inverse variance weighted	13	0.6510011	1.02(0.93 to 1.13)	P < 5×10 -6
	Simple mode	13	0.6950588	0.97(0.84 to 1.12)	
	Weighted mode	13	0.6741573	0.98(0.90 to 1.07)	

P<0.05 was considered statistically significant

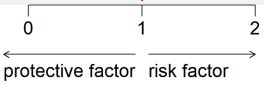

FIGURE 6
MR Results with Adenosine Deaminase Correction. SNP selection thresholds are applied with *p*-values $<5 \times 10^{-8}$, $p < 5 \times 10^{-7}$, and $p < 5 \times 10^{-6}$, respectively. Adenosine Deaminase protein is considered as the exposure factor, and ALS as the outcome in the Mendelian randomization analysis.

(OR = 1.089, PIVW = 0.020). The analysis showed no significant heterogeneity (MR Egger $Q = 9.884$, Q *p*-value = 0.626) and no horizontal pleiotropy (*P* Egger Intercept = 0.742, *P* MR Presso = 0.725).

Tumor Necrosis Factor Ligand Superfamily Member 12 Levels: similarly, an increased risk of ALS was associated with higher levels of Tumor necrosis factor ligand superfamily member 12 (OR = 1.097, PIVW = 0.010). No significant heterogeneity was observed in this analysis (MR Egger $Q = 7.787$, Q *p*-value = 0.802), and there was no evidence of horizontal pleiotropy (*P* Egger Intercept = 0.127, *P* MR Presso = 0.586).

Interleukin-5 Levels: in contrast, an increased risk of ALS was associated with decreased levels of Interleukin-5 (OR = 0.915, PIVW = 0.031). This analysis also showed no significant

10.3389/fnagi.2024.1367106

outcome	method	nsnp	pval	OR(95%CI)	Q_pval.MR.Egger.	MR.egger.intercept.P	MR.PRESSO.Global.Test.P
C-C motif chemokine 20 levels	MR Egger	14	0.427605824	1.06(0.92 to 1.24)			
	Weighted median	14	0.133109302	1.08(0.98 to 1.19)			
	Inverse variance weighted	14	0.019917956	1.09(1.01 to 1.17)	0.626145768	0.741854431	0.725
	Simple mode	14	0.658866776	1.03(0.90 to 1.19)			
	Weighted mode	14	0.328330013	1.07(0.94 to 1.21)			
Interleukin-5 levels	MR Egger	14	0.373249835	0.92(0.78 to 1.09)			
	Weighted median	14	0.392296423	0.95(0.86 to 1.06)			
	Inverse variance weighted	14	0.030586136	0.92(0.84 to 0.99)	0.592141552	0.898468324	0.686
	Simple mode	14	0.688692026	0.96(0.80 to 1.16)			
	Weighted mode	14	0.714762055	0.97(0.83 to 1.13)			
Tumor necrosis factor ligand	MR Egger	14	0.840052224	0.98(0.85 to 1.14)			
superfamily member 12 levels	Weighted median	14	0.124003620	1.09(0.98 to 1.21)			
	Inverse variance weighted	14	0.009698159	1.10(1.02 to 1.18)	0.801547445	0.127064464	0.586
	Simple mode	14	0.181645142	1.15(0.95 to 1.41)			
	Weighted mode	14	0.862038085	0.98(0.83 to 1.17)			

P<0.05 was considered statistically significant

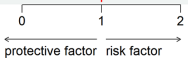

FIGURE 7
Reverse MR Results. Mendelian randomization analysis with ALS as the exposure factor and inflammatory proteins as the outcome, considering significance with p_ivw < 0.05.

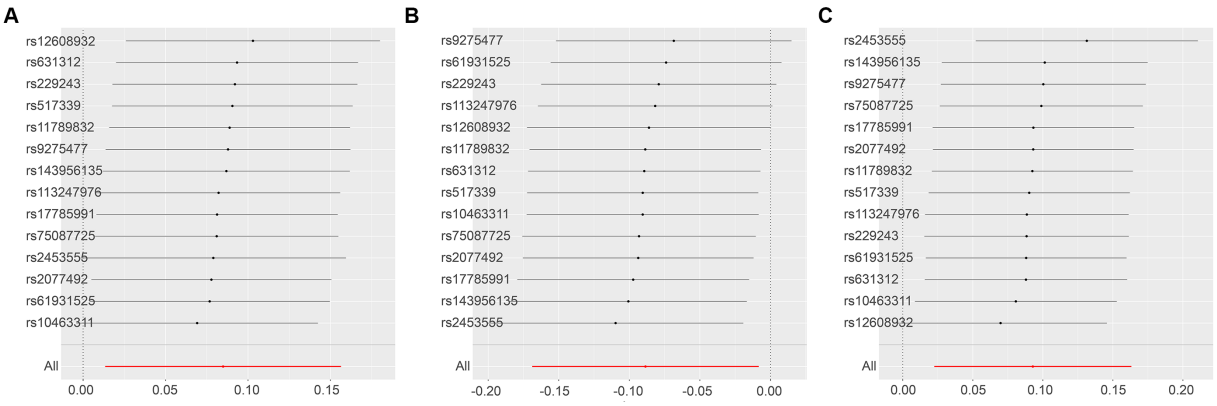

FIGURE 8
Leave-One-Out Analysis Results for Various Outcomes with ALS Exposure. This series illustrates the influence of ALS as an exposure factor on different inflammatory markers, using the leave-one-out methodology to assess the impact of individual SNPs on the overall results. **(A)**: C-C motif chemokine 20 levels as the outcome, with ALS as the exposure; **(B)**: Interleukin-5 levels as the outcome, with ALS as the exposure; **(C)**: Tumor necrosis factor ligand superfamily member 12 levels as the outcome, with ALS as the exposure.

heterogeneity (MR Egger $Q = 10.272$, Q p-value = 0.592) and no horizontal pleiotropy (P Egger Intercept = 0.898, P MR Presso = 0.686) (Figure 7).

A sensitivity analysis using the leave-one-out approach demonstrated robust results (Figure 8) (Supplementary Tables S2, S6, S11).

3.3 Validation group results

We selected three SNP thresholding tool variables ($p < 5 \times 10^{-8}$, $p < 5 \times 10^{-7}$, $p < 5 \times 10^{-6}$) and 12 inflammatory proteins as exposures, with ALS as the outcome, for two-sample Mendelian randomization analysis. The clumping conditions are the same as those for the test set. We were surprised to find that, whether in the initial exploration phase or in the validation set, the levels of osteoprotegerin showed significance for sporadic ALS (OR < 1, PIVW < 0.05) (Figure 9) (Supplementary Tables S2–S4). This result suggests that there may be an association between Osteoprotegerin levels and sporadic ALS, where Osteoprotegerin levels may play a protective role.

Another remarkable discovery is the correlation of Tumor Necrosis Factor Ligand Superfamily Member 12 levels with the sporadic ALS validation set across three different SNP threshold groups, with a potential association observed with the mixed ALS set at SNP ($p < 5 \times 10^{-6}$) (OR > 1, P IVW < 0.05) (Figure 9) (Supplementary Tables S2–S4). This suggests that an increase in Tumor necrosis factor ligand superfamily member 12 levels may be a risk factor for ALS. However, we observed the opposite causal relationship in the initial GWAS set.

These results suggest complex interactions between ALS and Tumor Necrosis Factor Ligand Superfamily Member 12 levels, possibly involving bidirectional causal relationships.

4 Discussion

This study utilized the TSMR approach to explore the potential causal relationship between circulating inflammatory proteins and ALS. Our analysis revealed several significant associations between

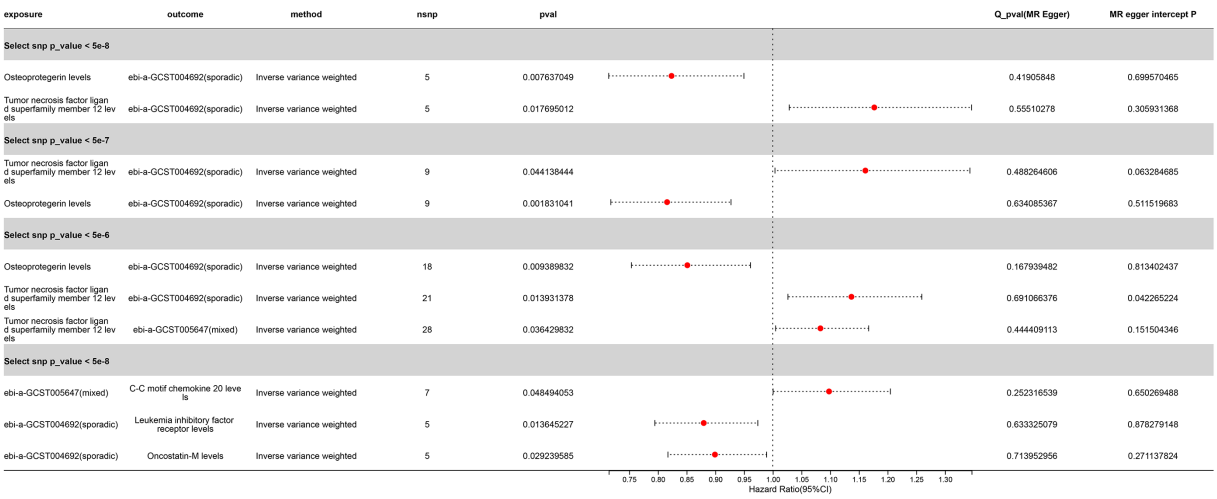

FIGURE 9
Significant Mendelian Randomization Results of Inflammatory Proteins with ALS Validation Sets (p_ivw < 0.05 denotes significance). "Sporadic" denotes a cohort of sporadic ALS, while "Mixed" refers to a combined cohort of familial and sporadic ALS.

inflammatory proteins and the risk of ALS, offering new insights into the pathophysiology of ALS and potentially unveiling new therapeutic targets.

In our study, different *p*-value thresholds significantly impacted the results. Lower *p*-value thresholds (e.g., < 5.0E−08) are commonly employed to ensure robustness of associations, reduce heterogeneity, and enhance the accuracy of the research. However, such stringent criteria might also exclude potentially meaningful associations (Bottigliengo et al., 2022; Chen et al., 2023; Liu et al., 2023; Ren et al., 2023). Our analysis indicated that some associations, previously insignificant, became significant when the *p*-value threshold was relaxed, underscoring the importance and complexity of *p*-value selection in research on the relationship between inflammatory proteins and ALS.

Our study employed both forward and reverse MR analyses, a method that allows for a more comprehensive exploration of the potential causal relationship between inflammatory proteins and ALS (Perry et al., 2021; Huimei Huang et al., 2022; Wang et al., 2022; Yin et al., 2023). The forward MR analysis revealed associations between increased levels of specific inflammatory proteins and an increased risk of ALS, whereas the reverse MR analysis provided evidence that an increased risk of ALS could lead to changes in certain inflammatory protein levels. These findings suggest a possible bidirectional causal relationship between inflammatory proteins and ALS, further complicating their interaction.

In our research, multiple inflammatory proteins identified across various *p*-value thresholds showed significant positive results related to ALS risk. For instance, increased levels of ADA were significantly associated with an increased risk of ALS. Previous studies have suggested that ADA may play an important role in neurodegenerative diseases, linked to neuronal damage and inflammatory responses. Allen et al. identified a defect in adenosine to inosine deamination in astrocytes of ALS patients caused by reduced ADA expression. This defect led to increased sensitivity to adenosine-mediated toxicity (Allen et al., 2019). Supplementing inosine could reverse motor neuron toxicity observed in co-cultured patient astrocytes (Allen et al., 2018). Song et al. explored gene therapy for ALS by upregulating ADAR2 in mouse motor neurons using adeno-associated viral vectors. This treatment prevented progressive motor dysfunction and rescued motor neurons from death by normalizing TDP-43 expression, suggesting a potential gene therapy approach for ALS (Song and Pan, 2014).

In summary, this section of the study discusses the significant associations found between changes in Leukemia inhibitory factor receptor and Osteoprotegerin levels and the risk of ALS. It highlights the diverse roles of cytokines, including LIFR, in skeletal muscle physiology and their impact on muscle cell growth, differentiation, metabolism, nerve innervation, and inflammatory cell recruitment to muscle injury sites (Hunt and White, 2016). The research also touches on the limited but emerging findings linking AIFR and Osteoprotegerin to ALS, as well as their roles in neuropsychiatric disorders, emphasizing the importance of inflammation and immune mechanisms in these conditions (Ham et al., 2018; Hashioka et al., 2019; Novellino et al., 2020; Xu et al., 2023).

Furthermore, the study finds significant correlations between ALS risk and changes in levels of various inflammatory proteins, such as Interleukin-17C, Oncostatin-M, Interleukin-5 levels, SIR2-like protein 2 levels, Neurturin levels, TNF-beta levels and Interleukin-10, under different *p*-value thresholds. Reverse MR analysis suggests that increased ALS risk could lead to changes in certain inflammatory protein levels, such as motif chemokine 20 levels, Tumor necrosis factor ligand superfamily member 12 levels and Interleukin-5 levels. These findings offer new perspectives for research into the roles of these proteins in neuroprotection, neuroregeneration, and inflammation, potentially contributing to understanding and treating ALS and related neuropsychiatric disorders.

In summary, our study, based on GWAS data from European populations, suggests that Osteoprotegerin levels confer a protective effect against sporadic ALS, validated in two datasets. Additionally, we observed a complex bidirectional relationship between Tumor Necrosis Factor Ligand Superfamily Member 12 levels and sporadic ALS. Furthermore, some correlations were found in the GWAS dataset combining Tumor Necrosis Factor Ligand Superfamily

Member 12 with familial and sporadic ALS, highlighting the potential complex bidirectional association between Tumor Necrosis Factor Ligand Superfamily Member 12 levels and ALS. Future research can delve into the specific roles of Osteoprotegerin and Tumor Necrosis Factor Ligand Superfamily Member 12 in the pathogenesis of ALS, assess their potential as biomarkers, and explore therapeutic strategies targeting them.

The findings of this study rely on data from the European population, implying that the applicability of its conclusions may have certain limitations. Although these inflammatory proteins show significant associations for some ALS patients within the European population, we must acknowledge that ALS patients in other populations worldwide may exhibit different levels of correlation and significance. Therefore, to comprehensively understand the role of these inflammatory proteins and their differences across diverse populations, future research should focus on collecting and analyzing data from more varied population groups. Such research endeavors will help uncover the population-specific aspects of ALS pathogenesis, thereby laying the groundwork for the discovery of universally applicable therapeutic strategies.

5 Conclusion

In summary, our study offers new insights into the role of circulating inflammatory proteins in ALS and paves the way for future research and the development of therapeutic strategies. Future research should focus on validating these findings and exploring the relationships between other potential inflammatory proteins and ALS. Furthermore, a deeper investigation into the specific roles of these inflammatory proteins in ALS pathophysiology will be crucial.

Data availability statement

The original contributions presented in the study are included in the article/Supplementary material, further inquiries can be directed to the corresponding author.

Author contributions

CX: Conceptualization, Data curation, Formal analysis, Funding acquisition, Investigation, Methodology, Project administration, Resources, Software, Supervision, Validation, Visualization, Writing – original draft, Writing – review & editing. XG: Writing – original draft, Writing – review & editing. YF: Writing – original draft, Writing – review & editing. JS: Conceptualization, Data curation, Formal analysis, Funding acquisition, Investigation, Methodology, Project administration, Resources, Software, Supervision, Validation, Visualization, Writing – original draft, Writing – review & editing.

Funding

The author(s) declare that financial support was received for the research, authorship, and/or publication of this article. This work was supported by basic research in medical application and applied research in medical innovation project (SKY2023101) and Suzhou Science and Technology Bureau - Key Technology (SS202089 and SZFCXK202107).

Acknowledgments

In the vastness of space and immensity of time, it is my joy to spend a planet and an epoch with her.

Conflict of interest

The authors declare that the research was conducted in the absence of any commercial or financial relationships that could be construed as a potential conflict of interest.

Publisher's note

Supplementary material

The Supplementary material for this article can be found online at: https://www.frontiersin.org/articles/10.3389/fnagi.2024.1367106/full#supplementary-material

References

Akinduro, O. O., Suarez-Meade, P., Garcia, D., Brown, D. A., Sarabia-Estrada, R., Attia, S., et al. (2021). Targeted therapy for Chordoma: key molecular Signaling pathways and the role of multimodal therapy. *Target. Oncol.* 16, 325–337. doi: 10.1007/s11523-021-00814-5

Akiyama, T., Koike, Y., Petrucelli, L., and Gitler, A. (2022). Cracking the cryptic code in amyotrophic lateral sclerosis and frontotemporal dementia: towards therapeutic targets and biomarkers. *Clin. Transl. Med.* 12:e818. doi: 10.1002/ctm2.818

Allen, S. P., Hall, B., Castelli, L., Francis, L., Woof, R., Higginbottom, A., et al. (2018). Inosine reverses motor neuron toxicity observed in amyotrophic lateral sclerosis patient astrocytes with an adenosine deaminase deficiency. *Biochimica et Biophysica Acta* 1859:e23. doi: 10.1016/J.BBABIO.2018.09.071

Allen, S. P., Hall, B., Castelli, L., Francis, L., Woof, R., Siskos, A., et al. (2019). Astrocyte adenosine deaminase loss increases motor neuron toxicity in amyotrophic lateral sclerosis. *Brain* 142:586. doi: 10.1093/brain/awy353

Bottigliengo, D., Foco, L., Seibler, P., Klein, C., König, I., and Del Greco, M. (2022). A Mendelian randomization study investigating the causal role of inflammation on Parkinson's disease. *Brain* 145, 3444–3453. doi: 10.1093/brain/awac193

Bowden, J., Davey Smith, G., Haycock, P. C., and Burgess, S. (2016). Consistent estimation in Mendelian randomization with some invalid instruments using a weighted median estimator. *Genet. Epidemiol.* 40, 304–314. doi: 10.1002/gepi.21965

Burgess, S., Butterworth, A., and Thompson, S. G. (2013). Mendelian randomization analysis with multiple genetic variants using summarized data. *Genet. Epidemiol.* 37, 658–665. doi: 10.1002/gepi.21758

Carroll, D. (2022). Integrating experience with databases, bioinformatics, and wet lab exercises for students in an introductory genetics course. *Biochem. Mol. Biol. Educ.* 50, 457–459. doi: 10.1002/bmb.21649

Chen, J., Song, B., Feng, Q., Feng, Y., Yu, Q., He, P., et al. (2023). AB0154 MENDELIAN randomization study implies causal linkage between POLYMYOSITIS and physical ACTIVITY. *Ann. Rheum. Dis.* 82, 1256.2–1256.1256. doi: 10.1136/annrheumdis-2023-eular.4215

Davey Smith, G., and Hemani, G. (2014). Mendelian randomization: genetic anchors for causal inference in epidemiological studies. *Hum. Mol. Genet.* 23, R89–R98. doi: 10.1093/hmg/ddu328

Emdin, C. A., Khera, A. V., and Kathiresan, S. (2017). Mendelian Randomization. *JAMA* 318, 1925–1926. doi: 10.1001/jama.2017.17219

Gleixner, A., Morris Verdone, B., Otte, C. G., Anderson, E. N., Ramesh, N., Shapiro, O. R., et al. (2022). NUP62 localizes to ALS/FTLD pathological assemblies and contributes to TDP-43 insolubility. *Nat. Commun.* 13, 3380–3317. doi: 10.1038/s41467-022-31098-6

Ham, S., Kim, T., Hong, H., Kim, Y. S., Tang, Y., and Im, H. I. (2018). Big data analysis of genes associated with neuropsychiatric disorders in an Alzheimer's disease animal model. *Front. Neurosci.* 12:407. doi: 10.3389/fnins.2018.00407

Hashioka, S., Inoue, K., Miyaoka, T., Hayashida, M., Wake, R., Oh-Nishi, A., et al. (2019). The possible causal link of periodontitis to neuropsychiatric disorders: more than psychosocial mechanisms. *Int. J. Mol. Sci.* 20:3723. doi: 10.3390/ijms20153723

Hemani, G., Bowden, J., and Davey Smith, G. (2018). Evaluating the potential role of pleiotropy in Mendelian randomization studies. *Hum. Mol. Genet.* 27, R195–r208. doi: 10.1093/hmg/ddy163

Henkel, J. S., Engelhardt, J. I., Siklós, L., Simpson, E. P., Kim, S. H., Pan, T., et al. (2004). Presence of dendritic cells, MCP-1, and activated microglia/macrophages in amyotrophic lateral sclerosis spinal cord tissue. *Ann. Neurol.* 55, 221–235. doi: 10.1002/ana.10805

Hosaka, T., Tsuji, H., and Kwak, S. (2023). Roles of aging, circular RNAs, and RNA editing in the pathogenesis of amyotrophic lateral sclerosis: potential biomarkers and therapeutic targets. *Cells* 12:1443. doi: 10.3390/cells12101443

Huimei Huang, S., Cheng, C.̀e. L., Cheng, B., Liu, L., Xuena Yang, P., Meng, Y. Y., et al. (2022). Dissecting the association between psychiatric disorders and neurological proteins: a genetic correlation and two-sample bidirectional Mendelian randomization study. *Neuropsychopharmacology* 34, 311–317. doi: 10.1017/neu.2022.10

Hunt, L., and White, J. (2016). The role of Leukemia inhibitory factor receptor Signaling in skeletal muscle growth, injury and disease. *Advances in experimental medicine and biology*, *900*, 45–59. Springer, Cham

Jiang, Z. Z., Wang, Z., Wei, X. J., and Yu, X. F. (2022). Inflammatory checkpoints in amyotrophic lateral sclerosis: from biomarkers to therapeutic targets. *Front. Immunol.* 13:59994. doi: 10.3389/fimmu.2022.1059994

Lee, G., Yao, C., Hwang, S.-J., Ma, J., Joehanes, R., Lee, D. H., et al. (2023). Integrative Mendelian randomization reveals the soluble receptor for advanced glycation end products as protective in relation to rheumatoid arthritis. *Sci. Rep.* 13:8002. doi: 10.1038/s41598-023-35098-4

Lehrach, H., Schäfer, R., and Schlag, P. M. (2011). "Deep sequencing"und prädiktive Modellierung als Konzept therapeutischer Entscheidungsfindungen in der Onkologie [deep sequencing and predictive modeling as a concept for therapeutic decision-making in oncology]. *Onkologe* 17, 477–486. doi: 10.1007/s00761-011-2025-9

Liu, R., Shi, X., Feng, J., Piao, J., Yang, Z., Zhao, Y., et al. (2023). Ischemic stroke and cerebral microbleeds: a two-sample bidirectional Mendelian randomization study. *Neurol Ther* 12, 1299–1308. doi: 10.1007/s40120-023-00500-w

Liu, W.-S., Zhang, Y.-R., Ge, Y.-J., Wang, H., Cheng, W., and Yu, J. (2023). *Inflammation and brain structure in Alzheimer's disease and other neurodegenerative disorders: A Mendelian randomization study*

Masrori, P., and Van Damme, P. (2020). Amyotrophic lateral sclerosis: a clinical review. *Eur. J. Neurol.* 27, 1918–1929. doi: 10.1111/ene.14393

Mead, R. J., Shan, N., Reiser, J., Marshall, F., and Shaw, P. J. (2023). Amyotrophic lateral sclerosis: a neurodegenerative disorder poised for successful therapeutic translation. *Nat. Rev. Drug Discov.* 22, 185–212. doi: 10.1038/s41573-022-00612-2

Murdock, B. J., Bender, D. E., Segal, B. M., and Feldman, E. L. (2015). The dual roles of immunity in ALS: injury overrides protection. *Neurobiol. Dis.* 77, 1–12. doi: 10.1016/j.nbd.2014.12.015

Nicolas, A., Kenna, K. P., Renton, A. E., Ticozzi, N., Faghri, F., Chia, R., et al. (2018). Genome-wide analyses identify KIF5A as a novel ALS gene. *Neuron* 97, 1268–1283.e6. doi: 10.1016/j.neuron.2018.02.027

Novellino, F., Sacca, V., Donato, A., Zaffino, P., Spadea, M., Vismara, M., et al. (2020). Innate immunity: a common denominator between neurodegenerative and neuropsychiatric diseases. *Int. J. Mol. Sci.* 21:1115. doi: 10.3390/ijms21031115

Perry, B., Burgess, S., Jones, H., Zammit, S., Upthegrove, R., Mason, A., et al. (2021). The potential shared role of inflammation in insulin resistance and schizophrenia: a bidirectional two-sample mendelian randomization study. *PLoS Med.* 18:e1003455. doi: 10.1371/journal.pmed.1003455

Rajasundaram, S., and Gill, D. (2023). *Tumour necrosis factor receptor 1 inhibition and cardiovascular disease: A cis-Mendelian randomization study*

Ralli, M., Lambiase, A., Artico, M., de Vincentiis, M., and Greco, A. (2019). Amyotrophic lateral sclerosis: autoimmune pathogenic mechanisms, clinical features, and therapeutic perspectives. *Israel Med. Assoc. J.* 21, 438–443.

Ren, F., Jin, Q.-Y., Qian, Y., Ren, X., Liu, T., and Zhan, Y. (2023). Genetic evidence supporting the causal role of gut microbiota in chronic kidney disease and chronic systemic inflammation in CKD: a bilateral two-sample Mendelian randomization study. *Front. Immunol.* 14:87698. doi: 10.3389/fimmu.2023.1287698

Sankaran, S. M., Smith, J. D., and Roy, K. R. (2021). CRISPR-Cas9 gene editing in yeast: a molecular biology and bioinformatics laboratory module for undergraduate and high school students. *J. Microbiol. Biol. Educ.* 22:e21. doi: 10.1128/jmbe.00106-21

Sari, I. J., Pongsophon, P., Vongsangnak, W., Pimthong, P., and Pitiporntapin, S. (2022). The development of molecular genetics concept test for senior high school students using Rasch analysis. *Int. J. Eval. Res. Educ.* 11, 1687–1458. doi: 10.11591/ijere.v11i4.21846

Shao, W., Todd, T. W., Wu, Y., Jones, C. Y., Tong, J., Jansen-West, K. R., et al. (2022). Two FTD-ALS genes converge on the endosomal pathway to induce TDP-43 pathology and degeneration. *Science* 378:94. doi: 10.1126/science.abq7860

Smith, G. D., and Ebrahim, S. (2003). Mendelian randomization: can genetic epidemiology contribute to understanding environmental determinants of disease? *Int. J. Epidemiol.* 32, 1–22. doi: 10.1093/ije/dyg070

Song, C. J., Bian, M. Y., Lei, L., and Chen, L. L. (2022). *Mendelian randomization and its application in periodontitis*

Song, Y., and Pan, W. (2014). Exploration of the pathogenesis of amyotrophic lateral sclerosis from the perspective of motor neuron TDP-43 protein expression and ADAR2 Activity. *Neurodegener. Dis.* 1, 119–125. doi: 10.1159/000368927

Soremekun, O. S., Musanabaganwa, C., Uwineza, A., Ardissino, M., Rajasundaram, S., Wani, A., et al. (2023). *Transl Psychiatry* 13:2542. doi: 10.1038/s41398-023-02542-y

Tejwani, L., Jung, Y., Kokubu, H., Sowmithra, S., Ni, L., Lee, C., et al. (2023). Reduction of nemo-like kinase increases lysosome biogenesis and ameliorates TDP-43–related neurodegeneration. *J. Clin. Invest.* 133:e138207. doi: 10.1172/JCI138207

The Telomeres Mendelian Randomization CollaborationHaycock, P. C., Burgess, S., Nounu, A., Zheng, J., Okoli, G. N., et al. (2017). Association between telomere length and risk of cancer and non-neoplastic diseases: a Mendelian randomization study. *JAMA Oncol.* 3, 636–651. doi: 10.1001/jamaoncol.2016.5945

van Rheenen, W., Shatunov, A., Dekker, A. M., McLaughlin, R. L., Diekstra, F. P., Pulit, S. L., et al. (2016). Genome-wide association analyses identify new risk variants and the genetic architecture of amyotrophic lateral sclerosis. *Nat. Genet.* 48, 1043–1048. doi: 10.1038/ng.3622

van Rheenen, W., van der Spek, R. A. A., Bakker, M. K., van Vugt, J. J. F. A., Hop, P. J., Zwamborn, R. A. J., et al. (2021). Common and rare variant association analyses in amyotrophic lateral sclerosis identify 15 risk loci with distinct genetic architectures and neuron-specific biology. *Nat. Genet.* 53, 1636–1648. doi: 10.1038/s41588-021-00973-1

Verbanck, M., Chen, C. Y., Neale, B., and do, R. (2018). Detection of widespread horizontal pleiotropy in causal relationships inferred from Mendelian randomization between complex traits and diseases. *Nat. Genet.* 50, 693–698. doi: 10.1038/s41588-018-0099-7

Wang, Q., Shi, Q., Jiawen, L., Wang, Z., and Hou, J. (2022). Causal relationships between inflammatory factors and multiple myeloma: a bidirectional Mendelian randomization study. *Int. J. Cancer* 151, 1750–1759. doi: 10.1002/ijc.34214

Witzel, S., Mayer, K., and Oeckl, P. (2022). Biomarkers for amyotrophic lateral sclerosis. *Curr. Opin. Neurol.* 35, 699–704. doi: 10.1097/WCO.0000000000001094

Wu, J., and Lin, Z. (2022). Non-small cell lung cancer targeted therapy: drugs and mechanisms of drug resistance. *Int. J. Mol. Sci.* 23:15056. doi: 10.3390/ijms232315056

Xu, H., Zheng, L., Wang, L., Gao, H., Wei, Y., and Chen, J. (2023). Albumin and associated biomarkers in severe neuropsychiatric disorders: acute-phase schizophrenia and bipolar disorder. *Neuropsychiatr. Dis. Treat.* 19, 2027–2037. doi: 10.2147/NDT.S423399

Yang, X., Ji, Y., Wang, W., Zhang, L., Chen, Z., Yu, M., et al. (2021). Amyotrophic lateral sclerosis: molecular mechanisms, biomarkers, and therapeutic strategies. *Antioxidants (Basel)* 10:1012. doi: 10.3390/antiox10071012

Yin, Z., Chen, J., Xia, M., Zhang, X.-y., Li, Y., Chen, Z.-h., et al. (2023). Assessing causal relationship between circulating cytokines and age-related neurodegenerative diseases: a bidirectional two-sample Mendelian randomization analysis. *Sci. Rep.* 13:12325. doi: 10.1038/s41598-023-39520-9

Zhao, J. H., Stacey, D., Eriksson, N., Macdonald-Dunlop, E., Hedman, Å. K., Kalnapenkis, A., et al. (2023). Genetics of circulating inflammatory proteins identifies drivers of immune-mediated disease risk and therapeutic targets. *Nat. Immunol.* 24, 1540–1551. doi: 10.1038/s41590-023-01588-w

Zondler, L., Müller, K., Khalaji, S., Bliederhäuser, C., Ruf, W. P., Grozdanov, V., et al. (2016). Peripheral monocytes are functionally altered and invade the CNS in ALS patients. *Acta Neuropathol.* 132, 391–411. doi: 10.1007/s00401-016-1596-9

frontiers | Frontiers in Immunology

TYPE Original Research
PUBLISHED 27 March 2024
DOI 10.3389/fimmu.2024.1360527

OPEN ACCESS

EDITED BY
Robert Weissert,
University of Regensburg, Germany

REVIEWED BY
Rohat Geran,
Charité University Medicine Berlin, Germany
Kelsi West,
Catalytic Data Science, United States
Guohao Wang,
National Institutes of Health (NIH), United States

*CORRESPONDENCE
Xusheng Huang
lewish301@163.com

RECEIVED 23 December 2023
ACCEPTED 18 March 2024
PUBLISHED 27 March 2024

CITATION
Du R, Chen P, Li M, Zhu Y, He Z and Huang X (2024) Developing a novel immune infiltration-associated mitophagy prediction model for amyotrophic lateral sclerosis using bioinformatics strategies.
Front. Immunol. 15:1360527.
doi: 10.3389/fimmu.2024.1360527

Developing a novel immune infiltration-associated mitophagy prediction model for amyotrophic lateral sclerosis using bioinformatics strategies

Rongrong Du[1,2], Peng Chen[3,4], Mao Li[2], Yahui Zhu[2,3], Zhengqing He[5] and Xusheng Huang[1,2,3]*

[1]School of Medicine, Nankai University, Tianjin, China, [2]Department of Neurology, The First Medical Center, Chinese People's Liberation Army (PLA) General Hospital, Beijing, China, [3]Medical School of Chinese People's Liberation Army (PLA), Beijing, China, [4]Department of General Surgery & Institute of General Surgery, The First Medical Center of Chinese People's Liberation Army (PLA) General Hospital, Beijing, China, [5]Department of Neurology, Beijing Friendship Hospital, Capital Medical University, Beijing, China

Background: Amyotrophic lateral sclerosis (ALS) is a fatal neurodegenerative disease, which leads to muscle weakness and eventual paralysis. Numerous studies have indicated that mitophagy and immune inflammation have a significant impact on the onset and advancement of ALS. Nevertheless, the possible diagnostic and prognostic significance of mitophagy-related genes associated with immune infiltration in ALS is uncertain. The purpose of this study is to create a predictive model for ALS using genes linked with mitophagy-associated immune infiltration.

Methods: ALS gene expression profiles were downloaded from the Gene Expression Omnibus (GEO) database. Univariate Cox analysis and machine learning methods were applied to analyze mitophagy-associated genes and develop a prognostic risk score model. Subsequently, functional and immune infiltration analyses were conducted to study the biological attributes and immune cell enrichment in individuals with ALS. Additionally, validation of identified feature genes in the prediction model was performed using ALS mouse models and ALS patients.

Results: In this study, a comprehensive analysis revealed the identification of 22 mitophagy-related differential expression genes and 40 prognostic genes. Additionally, an 18-gene prognostic signature was identified with machine learning, which was utilized to construct a prognostic risk score model. Functional enrichment analysis demonstrated the enrichment of various pathways, including oxidative phosphorylation, unfolded proteins, KRAS, and mTOR signaling pathways, as well as other immune-related pathways. The analysis of immune infiltration revealed notable distinctions in certain congenital immune cells and adaptive immune cells between the low-risk and high-risk groups, particularly concerning the T lymphocyte subgroup. ALS mouse models and ALS clinical samples demonstrated consistent expression levels of four mitophagy-related immune infiltration genes (*BCKDHA*, *JTB*, *KYNU*, and *GTF2H5*) with the results of bioinformatics analysis.

Conclusion: This study has successfully devised and verified a pioneering prognostic predictive risk score for ALS, utilizing eighteen mitophagy-related genes. Furthermore, the findings indicate that four of these genes exhibit promising roles in the context of ALS prognostic.

KEYWORDS

amyotrophic lateral sclerosis, mitophagy, immune infiltration, gene, prediction model, prognosis

1 Introduction

Amyotrophic lateral sclerosis (ALS) is a neurodegenerative disease affecting upper and lower motor neurons, characterized by progressive muscle weakness, atrophy leading to paralysis, and eventual fatality. ALS has insidious onset, rapid progression, heterogeneous clinical manifestations, and currently lacks effective treatment options. The majority of patients succumb to respiratory failure within 3-5 years of onset (1, 2), imparting a heavy burden on patients, their families, and society. Presently, ALS diagnosis primarily relies on neurophysiological and neuroimaging examinations, yet early diagnosis and treatment remain challenging. Thus, the identification of practical early diagnostic markers and the construction of a more accurate ALS diagnostic and prognostic model may offer new hope for ALS patient treatment.

Mitophagy is a crucial process for mitochondrial quality control, its malfunction leads to the accumulation of defective mitochondria, posing a risk of damage to high-energy-demanding neuronal cells. Studies have indicated that mitophagy dysfunction is a key factor in the occurrence and progression of various neurodegenerative diseases such as ALS, Parkinson's disease, and Alzheimer's disease (3). Furthermore, research has pointed out that energy metabolism disturbances resulting from mitochondrial dysfunction are central to the pathophysiology of ALS (4, 5). To date, nearly 40 ALS-related genes have been identified. Some of these genes (*OPTN, SQSTM1/p62TBK1, SOD1, C9ORF72, VCP*) are directly or indirectly associated with the mitophagy pathway, influencing different stages of the mitophagy process (6, 7). The findings of these studies indicate that mitophagy is a significant factor in the pathogenesis of ALS. Nevertheless, the specific involvement of mitophagy-related genes (MRGs) in the progression of ALS remains largely unexplored. Consequently, a comprehensive investigation into mitophagy-related markers in ALS using bioinformatics tools may facilitate the discovery of novel biomarkers with therapeutic potential for ALS. Furthermore, it has been observed that mitophagy also contributes to the regulation of the immune response. Mitophagy has the potential to exert an anti-inflammatory effect by suppressing the excessive production of interleukin (IL)-1β and IL-18 (8). Dysregulation of mitophagy, on the other hand, triggers inflammation by activating the pyrin domain-containing protein 3 (NLRP3) inflammasomes, resulting in an overexpression of IL-1β and IL-18 (9, 10). Additionally, the release of mitochondrial DNA has been shown to promote the transcription of various inflammatory cytokines, including tumor necrosis factor (TNF-α) and IL-6 (11). The unique anatomy of spinal motor neurons makes ALS particularly susceptible to peripheral immune responses (12). Blood monocytes and macrophages react to degenerating motor nerves, producing cytokines that can act locally or travel through the blood-brain barrier to the central nervous system. These cytokines are being studied as potential early biomarkers for ALS (13). A meta-analysis on ALS revealed a consistent trend towards elevated blood levels of pro-inflammatory cytokines, including IL-1B, IL-6, and TNF, which are known to be produced by reactive monocytes/macrophages (13–15).

The objective of this study is to conduct multifaceted analyses of different datasets related to ALS in the GEO database. Limma and Spearman correlation analyses were used to identify mitophagy-related DEGs in ALS and filter for mitophagy genes. Subsequently, machine learning methods (forest plot, univariate analysis, and least absolute shrinkage and selection operator (LASSO) regression) were used to filter and identify prognostic markers and construct a risk model. Finally, we used Gene Set Enrichment Analysis (GSEA) and Receiver Operating Characteristic (ROC) curve analysis to create and evaluate the prediction model molecule drugs. We also collected ALS mouse models and ALS patients to confirm the expression levels of the model's feature genes. The study aimed to elucidate the relationship between mitophagy, ALS, and immune infiltration by constructing a mitophagy-associated prediction model and examining its association with immune infiltration. Our study sheds new light on the role of mitophagy and immune inflammation in predicting the prognosis and diagnosis of ALS.

2 Materials and methods

2.1 Acquisition and preprocessing of expression profiling data

The ALS patient dataset was sourced from the Gene Expression Omnibus (https://www.ncbi.nlm.nih.gov/geo/), with the candidate dataset being selected based on specific inclusion criteria, including

ALS diagnosis, human gene expression profile, availability of follow-up information (survival information), and related clinical data. The gene expression data from GSE112676 and GSE112680, obtained from Illumina HumanHT-12 V3.0 and HumanHT-12 V4.0 expression bead chip arrays, were incorporated into the study. The dataset GSE112676 consisted of 233 ALS samples and 508 control (CON) samples, while the dataset GSE112680 cohort, comprised 164 ALS samples and 137 control samples. Survival information was available for all 397 ALS patients. Demographic details of the cohorts have been previously documented (16). In summary, the ALS and CON groups exhibited a higher proportion of male participants (≥58.54%) with mean ages of 63.92 and 63.58, respectively. The majority of patients (>60%) presented with spinal-onset ALS rather than bulbar-onset ALS. The GSE112680 cohort had a higher percentage of individuals with C9orf72 repeat expansions (12.8% vs. 5.2%). Survival was operationally defined as the duration from disease onset to death, tracheostomy, or noninvasive ventilation (16). According to this operationalization, the median survival time was 2.42 years, with 50% of patients surviving. As shown in Table 1.

The methodology employed by Swindell et al. (16) was consulted for a comprehensive account of the data processing procedures and outcomes, with particular attention to mitigating platform-specific biases and batch confounders. The relevant GSE dataset was obtained by directly downloading the preprocessed and standardized probe expression matrix. Gene probes were converted to gene symbols utilizing the respective annotation profiles within each dataset. Normalization of gene expression values and the generation of normally distributed expression values were achieved using the 'limma' package in R software. In cases where multiple probes corresponded to the same gene, the final gene expression value was determined by calculating the average expression value.

2.2 Differential expression pattern analysis

The differential expression analysis between the ALS and CON groups was conducted utilizing the GSE112676 dataset. This analysis was performed employing the R package limma (version V-3.84.3, https://www.bioconductor.org/packages/release/bioc/html/limma.html) within R version 4.3.0. Gene-specific information, including P-values and logFC values, was obtained and analyzed using the Benjamini & Hochberg method to account for multiple tests. This method yielded adjusted p-values (adj.P.Value). Differentially expressed genes (DEGs) were identified using significant differences in fold change and statistical significance, with a threshold set at adj.P.Val < 0.05.

2.3 Mitophagy-related gene screening

To investigate the correlation between mitophagy genes and DEGs, a collection of thirty-four mitophagy genes associated with ALS was identified based on the Relevance score > 1.5 in the Genecards database (http://www.genecards.org/), searched using the keyword "Mitophagy". Further analysis was performed to investigate the relationship between these mitophagy genes and the identified DEGs. the corrplot package (v-0.90, https://cran.r-project.org/web/packages/corrplot/vignettes/corrplot-intro.html) was utilized. Genes that exhibited a significant correlation (P<0.05) and a correlation coefficient (r) exceeding 0.3 were deemed relevant and selected as relevant genes. These relevant genes, in conjunction with the mitophagy genes, were designated as mitophagy-related genes for subsequent analysis.

TABLE 1 Baseline characteristics.

Variable	Overall, N = 397[1]	Cohort		p-value[2]
		Training cohort N = 233 (59%)[1]	Validation cohort N = 164 (41%)[1]	
Age of onset	63.78 [55.60,70.72]	63.92 [56.37,70.75]	63.58 [54.81,70.66]	0.696
Survival time (years)	2.42 [1.59, 3.52]	2.50 [1.64, 3.79]	2.34 [1.56, 3.35]	0.263
Sex				0.642
Female	158 (39.80%)	90 (38.63%)	68 (41.46%)	
Male	239 (60.20%)	143 (61.37%)	96 (58.54%)	
Site of onset				0.420
Bulbar	146 (36.78%)	90 (38.63%)	56 (34.15%)	
Spinal	251 (63.22%)	143 (61.37%)	108 (65.85%)	
Status				0.022
Dead	342 (86.15%)	209 (89.70%)	133 (81.10%)	
Survival	55 (13.85%)	24 (10.30%)	31 (18.90%)	

[1]Median [IQR]; n (%).
[2]Wilcoxon rank sum test; Pearson's Chi-squared test.

2.4 Identification of prognostic significance genes

Utilizing the aforementioned mitophagy-related genes, conducted univariate Cox regression analysis using the survival-V3.2.13 package (https://github.com/therneau/survival) to identify potential genes associated with ALS. The corresponding P-value for each gene was assessed, and a threshold of $P<0.05$ was established for evaluation purposes.

2.5 Development and validation of risk scoring

The glmnet package (V-4.1-2, https://cran.r-project.org/web/packages/glmnet/index.html) was utilized to perform LASSO Cox analysis on the candidate prognostic genes obtained from the training set GSE112676. This analysis aimed to select feature genes with nonzero regression coefficients to construct a risk-scoring model. To assess the accuracy of the risk scoring model, the prognostic model construction method was followed, wherein the Risk score for each diseased sample was calculated by adding the expression level of each gene multiplied by its corresponding coefficient (e.g., Risk score = (expression level of gene A * coefficient of gene A) + (expression level of gene B * coefficient of gene B) +…), the Risk score values were calculated for each diseased sample in the training dataset GSE112676. Subsequently, employing the optimal threshold value derived from the median Risk score, the diseased samples within the training dataset GSE112676 were partitioned into two groups: High_Risk (comprising samples with a Risk score greater than or equal to the median Risk score) and Low_Risk (comprising samples with a Risk score lower than the median Risk score). The survival package in R4.1.0 was utilized to generate survival prognostic curves, enabling the evaluation of the relationship between the aforementioned grouping of High_Risk and Low_Risk samples and the actual survival prognosis information. The log-rank test was used to determine the statistical significance of the survival prognosis disparity among the two groups. Furthermore, the prognostic significance of the feature genes in the training dataset GSE112676 was assessed by calculating the Area Under Curve (AUC) values of the ROC curve at 5, 7, and 10 years. It should be noted that the AUC for validation sets at 1, 2, and 3 years is 0, as the classification data for survival time in these sets consists solely of either all 1 or all 0. Similarly, the accuracy of the risk scoring model was confirmed in the external validation dataset GSE112680 from GEO using the appropriate signature construction method.

2.6 The relationship between high- and low-risk groups and immune infiltration

Mitophagy and immunity are closely related, and peripheral immune cells play a significant role in disease progression in ALS patients (17). Therefore, it is meaningful to link with immune infiltration in the study. CIBERSORT analysis (accessible at https://cibersortx.stanford.edu/) was used to estimate the proportions of 22 human immune cell subsets based on gene expression data. Finally, the disparities in the distribution of TMB scores and proportions of immune cell infiltration between the high-risk and low-risk groups were evaluated using the Wilcoxon test.

2.7 Prognostic model genes and immune correlation analysis

Conducting correlation analysis on the feature genes and immune infiltration proportions was performed using the corrplot package (v-0.90, https://cran.r-project.org/web/packages/corrplot/vignettes/corrplot-intro.html).

2.8 Differences in checkpoint genes and HLA family genes between high-risk and low-risk groups

The expression data of common immune checkpoint genes and the Human Leukocyte Antigen (HLA) gene family, which comprises 17 HLA genes, were extracted from the training set GSE112676. The differential expression of immune checkpoint genes and the HLA gene family between the high-risk and low-risk groups was compared using the Wilcoxon test.

2.9 Analysis of molecular mechanisms between high- and low-risk groups

To conduct a more comprehensive examination of the molecular mechanisms underlying the distinction between high- and low-risk groups in ALS, 50 hallmark gene sets from the MSigDB database (http://www.gsea-msigdb.org/gsea/index.jsp) were obtained. The hallmark enrichment scores were computed using the GSEA function from the clusterProfiler package (V-4.6.2, https://www.bioconductor.org/packages/release/bioc/html/clusterProfiler.html).

2.10 Differential gene selection between high- and low-risk groups

Differential expression analysis was conducted on the high- and low-risk groups using the GSE112676 dataset. The limma package (V-3.84.3, available at https://www.bioconductor.org/packages/release/bioc/html/limma.html) in R version 4.3.0 was employed to obtain gene-specific information, including P-values and logFC values. Furthermore, multiple testing correction was performed using the Benjamini & Hochberg method to derive adjusted p-values (adj.P.Value). DEGs were identified using the following criteria: adj.P.Value < 0.05 and $|logFC| > 1.5$.

2.11 Enrichment analysis of differential genes between high- and low-risk groups

The DEGs obtained from the high- and low-risk groups were subjected to Gene Ontology (GO) analysis using the clusterProfiler package (V-4.6.2, https://www.bioconductor.org/packages/release/bioc/html/clusterProfiler.html). This analysis encompassed the categories of cellular component (CC), molecular function (MF), and biological process (BP). Additionally, the Kyoto Encyclopedia of Genes and Genomes (KEGG) pathway enrichment analysis was conducted. A significance threshold of P-value < 0.05 was applied to ascertain significant enrichment.

2.12 Diagnostic analysis of model genes

The differential expression of the feature genes between the ALS and CON groups was assessed through the utilization of the Wilcox test on both the training dataset GSE112676 and the validation dataset GSE112680. The pROC package (V-1.18.2, https://www.rdocumentation.org/packages/pROC/versions/1.18.2) was employed to generate ROC curves for the feature genes.

2.13 Real-time polymerase chain reaction

A group of 10 patients diagnosed with ALS and 10 healthy individuals of the same age and gender were selected for the study. Blood samples were collected from both groups to investigate the gene expression patterns of specific genes in a diagnostic model using real-time quantitative polymerase chain reaction (RT-qPCR). The ALS mouse model (B6SJL-Tg(SOD1^{G93A})) was acquired from The Jackson Laboratory in the United States, and RT-qPCR was conducted on the lumbar spinal cord of SOD1^{G93A} mice to evaluate the gene expression trends of characteristic genes in the disease model. The procedure for collecting the samples was approved by the Ethics Committee of the First Medical Center of Chinese PLA General Hospital. Total RNA was isolated from peripheral blood and spinal cord tissues using the RNAprep Pure High-Efficiency Total RNA Extraction Kit and the RNAeasy Fast Animal Tissue/Cell Total RNA Extraction Kit, respectively. RT-PCR was conducted using the FastKing One-Step RT-PCR Kit. Gene primers were designed using Primer 5 and synthesized by Biomed. GAPDH expression was utilized as an internal control, and relative expression was determined using the $2^{-\Delta\Delta Ct}$ method.

2.14 Statistical analysis

All statistical analyses were conducted using R software (version 4.1.0 and 4.3.0) and R studio (Version 3.84.3). The Wilcoxon test was utilized to compare the proportions of immune cell infiltration between the high- and low-risk groups and to analyze the differential expression of the feature genes in the ALS and CON groups. LASSO-Cox regression was used for feature gene selection. The log-rank test was then conducted to compare the survival rates of low- and high-risk groups. Univariate Cox regression analyses were also performed to identify genes that may be associated with ALS. A two-tailed P value<0.05 was considered statistically significant, with some exceptions where a specific P value was set.

3 Results

3.1 Acquisition and preprocessing of expression profile data

The study's schematic diagram is presented in Figure 1. The training set, GSE112676, was acquired and comprised 508 control samples and 233 ALS samples, all of which had survival information available. The validation set, GSE112680, consisted of 137 control samples and 164 ALS samples, all of which had survival information available. To explore the association between mitophagy genes and differentially expressed genes (DEGs), a set of thirty-four mitophagy genes (Supplementary Materials 1) linked to ALS was identified using a Relevance score > 1.5 in the Genecards database (http://www.genecards.org/), utilizing the keyword "Mitophagy". Subsequent analysis was conducted to examine the connection between these mitophagy genes and the identified DEGs, employing the corrplot package (v-0.90, https://cran.r-project.org/web/packages/corrplot/vignettes/corrplot-intro.html). Genes demonstrating a significant correlation (P<0.05) and a correlation coefficient (r) greater than 0.3 were considered pertinent and chosen as relevant genes. These relevant genes, in conjunction with the mitophagy genes, were designated as mitophagy-related genes for subsequent analysis.

3.2 Identification of prognostic significance genes in mitophagy-related genes

Firstly, the limma package was used to analyze the DEGs between CON and ALS on all expression matrices of the training set GSE112676, with adjust P-value <0.05 as a significance

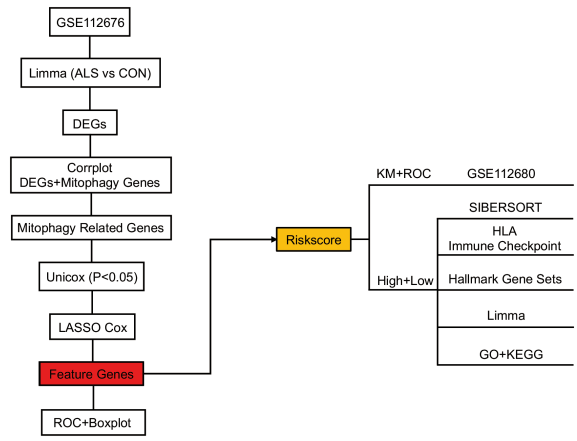

FIGURE 1
Overview of the schematic diagram of this study.

threshold. A total of, 5256 DEGs were identified from this analysis, including, 2822 upregulated genes and, 2434 downregulated genes (Figure 2A). Similarly, we analyzed differentially expressed genes in the validation set. A total of 1079 genes were down-regulated and 1300 genes were up-regulated (Supplementary Figure 1). Additionally, a heatmap was employed to visually represent the DEGs (Figure 2B). According to the mitophagy database, a total of 34 genes involved in the process of mitophagy were obtained (Supplementary Material 1). After comparing training set GSE112676 genes with all mitophagy-related genes, 25 overlapping genes were identified (Supplementary Material 2). A Spearman correlation analysis was performed on a set of 25 genes associated with mitophagy. The correlation among these 25 mitophagy-related genes is depicted in Figure 2C, while an examination of the expression levels of these 25 mitophagy genes in the CON group compared to the ALS group is presented in Figure 2D. Among them, the expression level of eight genes (*ATG12, ATG5, MAP1LC3B, MFN1, OPTN, SRC, TOMM20, TOMM7*) was upregulated, while the expression level of four genes (*CDC37, MFN2, SQSTM1, TOMM40*) were downregulated. Using the corrplot package, Spearman correlation analysis was conducted between the, 5256 DEGs and the 25 mitophagy genes. In light of the extensive number of genes, a correlation heatmap analysis specifically targeted the top 20 DEGs with the highest logFC values, as well as the genes associated with mitophagy (Figure 2E). Subsequently, employing a significance threshold of $P < 0.05$ and $|r| > 0.3$, 4405 genes were identified, comprising, 4383 DEGs and 22 mitophagy genes (*MFN2, OPTN, MAP1LC3B, ATG12, PINK1, MFN1, TOMM20, TOMM7, TOMM40, ULK1, ATF5, CDC37, CSNK2A1, UBC, VDAC1, UBA52, SQSTM1, TOMM22, CSNK2B, VPS13C, UBB, CSNK2A2*) (Supplementary Material 3). To further investigate their prognostic potential, univariate Cox analysis on the aforementioned, 4405 genes, led to the discovery of 40 genes with significant prognostic value, as indicated by a P-value < 0.05 (Figure 2F).

3.3 Construction and validation of risk score

Through the utilization of LASSO-Cox regression analysis on the aforementioned candidate genes, a subset of 18 genes (*VPS3TA, TR1M46, TIGD6, TAF1B, SEH1L, PARVB, NCK1PSD, MRS2, MMP21, KYNU, JTB, IFNW1, GTF2H5, FUBP1, DNAJB14, CDK5RAP1, BCKDHA, ATG2B*) was identified for the development of a prognostic risk score based on the minimal criteria of λ (Figures 3A, B). The risk score for each sample was calculated using the formula: Risk score = [(2.298 x *VPS3TA* expression value) + (-1.112 x *TR1M46* expression value) + (1.835 x *TIGD6* expression value) + (1.409 x *TAF1B* expression value) + (0.846 x *SEH1L* expression value) + (1.177 x *PARVB* expression value) + (0.027 x *NCK1PSD* expression value) + (2.525 x *MRS2* expression value) + (0.087 x *MMP21* expression value) + (0.228 x *KYNU* expression value) + (-1.391 x *JTB* expression value) +(1.456 x *IFNW1* expression value) + (0.247 x *GTF2H5* expression value) + (3.198 x *FUBP1* expression value) + (0.043 x *DNAJB14* expression value) + (-0.7 x *CDK5RAPI* expression value) + (0.623 x *BCKDHA* expression value) + (0.828 x *ATG2B* expression value)] (Figure 3C). Subsequently, the 164 patients were stratified into two risk groups based on the median risk score, with 113 patients categorized as low-risk and 51 patients as high-risk (Figure 3D). Patients in the high-risk group exhibited higher mortality rates (Figure 3E), as evidenced by the Kaplan-Meier curve demonstrating superior survival rates among patients in the low-risk group ($P < 0.0001$, Figure 3F). Time-dependent ROC analysis of the risk score revealed that the area under the curve (AUC) was 0.933, 0.966, and 1 for 5-, 7-, and 10-year survival, respectively (Figure 3G).

To Validate the prognostic risk score, patients in the validation set, GSE112680, were divided into two groups based on the median risk score (Figure 4A). Patients in the high-risk groups experienced a higher incidence of mortality (Figure 4B), as evidenced by the Kaplan-Meier curve demonstrating significantly greater survival rates among patients in the low-risk group compared to those in the high-risk group (validation set: $P = 0.0058$ Figure 4C). These findings demonstrate the reliability of the ROC analysis and indicate that the risk scoring model is highly feasible, with AUC values of 0.643, 0.709, and 0.63 for 5-year, 7-year, and 10-year predictions, respectively (Figure 4D).

3.4 Relationship between high- and low-risk groups and immune response

An investigation was conducted to determine the connection between immune-related genes and ALS High- and Low-Risk groups through the analysis of immune cell infiltration. The CIBERSORT algorithm was used to estimate the relative infiltration abundance of immune cell types in each sample (Figure 5A). Additionally, the differences in immune cells between the two risk groups were compared and their significance was assessed using the Wilcoxon test. A total of 22 immune cells infiltrating between the ALS high- and low-risk groups were screened with values of $p<0.05$, as shown in (Figure 5A). Patients with higher scores exhibited significantly elevated levels of CD4 memory resting Tcells, gamma delta Tcells, and M1 Macrophages while showing relatively lower proportions of CD8 Tcells, M0 macrophages, and NK cells, Mast cell activated and regulatory Tregs T cells. Additional examination of the 18 mitophagy-related genes that were chosen, along with their association with immune cells (Figure 5B), unveiled a noteworthy inverse association between MRS2 and M0 macrophages ($r=-0.47$, $P<0.001$, Figure 5C). Conversely, there was a noteworthy positive correlation between DNAJB14 and resting memory CD4 T cells($r=0.47$, $P<0.001$, Figure 5D). Further analysis of eight immune checkpoint genes showed that the expressions of *HAVCR2, CD274, PDCD1*, and CD86 were elevated and the expressions of CD80 were relatively lower in the high-risk group of ALS

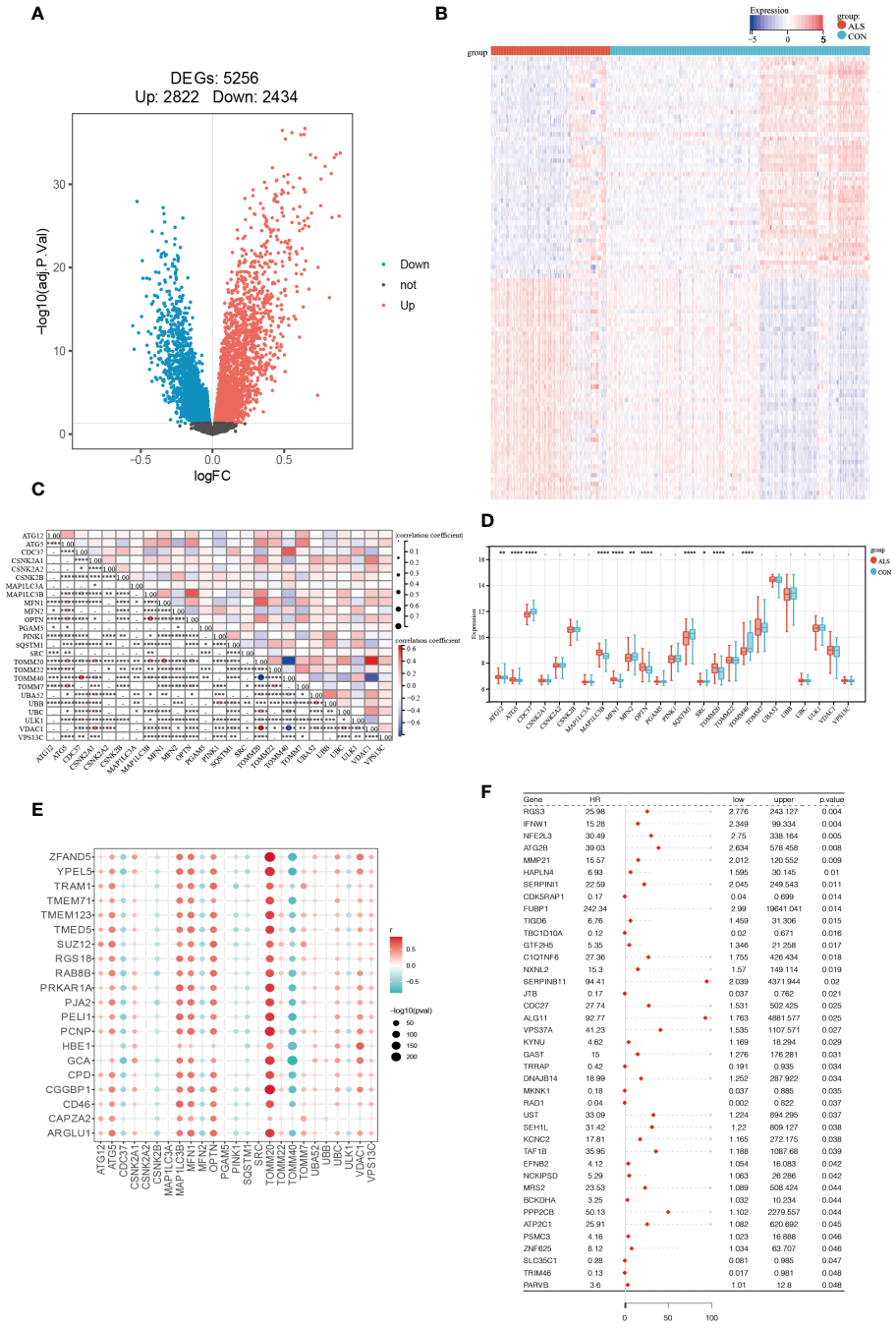

FIGURE 2
Identification of Prognostic Significance Mitophagy-Related Genes in ALS. **(A)** Differential analysis volcano plot (red represents significantly upregulated genes, blue represents significantly downregulated genes, and black represents non-significant genes). **(B)** Heatmap of differentially expressed mitophagy-related genes between ALS and control samples. **(C)** The correlation of 25 mitophagy-related genes. **(D)** The expression levels of 25 mitophagy genes in the CON group vs. the ALS group. **(E)** Scatter plot showing the correlation between the top 20 DEG genes with the largest logFC and mitophagy genes. The redder the point, the stronger the positive correlation; the bluer the point, the stronger the negative correlation. The larger the shape of the point, the smaller the p-value; the smaller the shape, the larger the p-value. **(F)** Forest plot displaying the results of the univariate Cox analysis. ****P<0.0001, ***P<0.001, **P<0.01, *P<0.05, ns P>0.05.

(Figure 5E). Since HLA family genes play a crucial role in immune response, we also analyzed the association between HLA family genes and high- and low-risk groups. we found that patients with higher scores exhibited significantly elevated levels of *HLA-DPB1*, *HLA-DRA*, and *HLA-DMB* while showing relatively lower proportions of *HLA-G* (Figure 5F).

3.5 Molecular mechanism analysis between high- and low-risk groups

The enrichment scores for multiple hallmark pathways were calculated using GSEA. Among these pathways, a total of 10 showed significant enrichment, with normalized enrichment scores (NES)

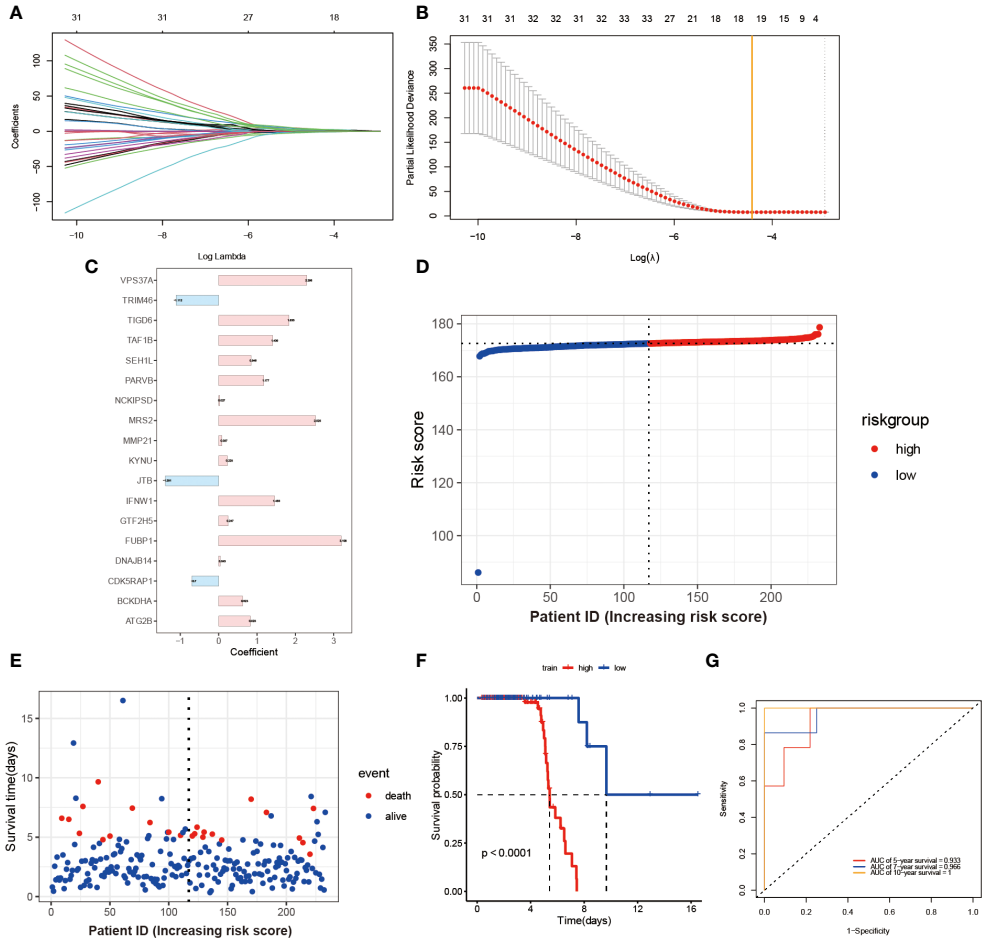

FIGURE 3
Construction and Validation of Risk Score Model. **(A)** Each curve in the figure represents the trajectory of each independent variable coefficient. The y-axis represents the coefficient values, while the lower x-axis represents log(λ) and the upper x-axis represents the number of non-zero coefficients in the model at that time. **(B)** The lowest point on the curve indicates the optimal lambda, which is the intersection between the yellow line and the red dot. **(C)** The histogram shows the distribution of coefficient values for the selected features. The distribution of risk scores **(D)** and survival times for each patient sample **(E)** in the training set GSE112676 is shown. The Kaplan-Meier survival curves **(F)** and time-dependent ROC curves **(G)** are presented for both high and low-risk groups.

greater than 0 indicating activation in the high-risk group and NES less than 0 indicating inhibition in the high-risk group (Figure 6A). To further analyze the high- and low-risk groups in the training set (GSE112676), differential analysis was performed using the limma package with the criteria of adj.P.Val < 0.05 and |logFC| > 1.5. This analysis identified 100 DEGs, including 23 upregulated and 77 downregulated genes (Figure 6B). GO and KEGG pathway enrichment analyses were performed on these 100 DEGs using R software to explore their potential biological functions and pathways. The results of GO functional analysis revealed that the most significant items of GO enrichment included leukocyte mediated immunity, leukocyte cell-cell adhesion, regulation of immune effector process in biological process (BP), secretory granule lumen, cytoplasmic vesicle lumen, mitochondrial outer membrane in cellular component (CC) and transcription coactivator activity in molecular function (MF) (Figures 6C–E). The results of KEGG pathway enrichment analysis showed that they were mainly enriched in Thermogenesis, NOD-like receptor signaling pathway, and Amino sugar and nucleotide sugar metabolism (Figure 6F).

3.6 Diagnostic analysis of model genes and validation of the four key DEGs in SOD1^{G93A} mice lumbar spinal cord tissue and clinical samples

To verify whether the model genes we screened have significant differences in diagnosis, ROC curves were drawn based on the expression levels of 18 feature genes both in the GSE112676 and GSE112680 datasets. According to it, four of eighteen genes (*BCKDHA, JTB, KYNU, GTF2H5*) have good diagnostic value in the diagnosis of ALS with AUC>0.6 in both the GSE112676 and GSE112680 dataset (Figures 7A, B), suggesting that these four genes not only have the prognostic effect but also have the potential diagnostic value.

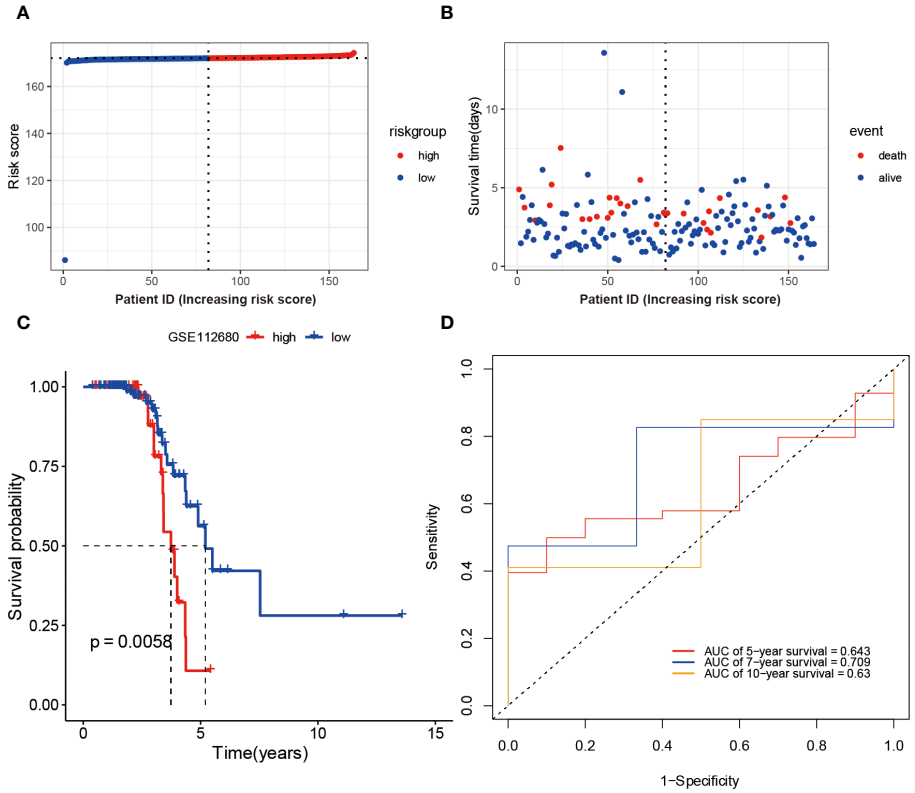

FIGURE 4
Validation of Risk Score Model in GSE112680 geneset. Risk scores **(A)** and survival time distribution **(B)** for each patient sample in the validation set GSE112680 were plotted. Kaplan-Meier survival curves **(C)** for the high and low-risk groups, as well as time-dependent ROC curves **(D)**, were generated.

Branched Chain Keto Acid Dehydrogenase E1 Subunit Alpha (*BCKDHA*), Jumping Translocation Breakpoint (*JTB*), *KYNU*, and General Transcription Factor IIH Subunit 5 (*GTF2H5*) (Figures 7C, D) exhibited notable variations in both peripheral blood of ALS patients and the lumbar spinal cord of $SOD1^{G93A}$ mice. Analysis of mRNA expression in $SOD1^{G93A}$ lumbar spinal cord tissue samples revealed an increase in *JTB* and *KYNU* expression, while *BCKDHA* and *GTF2H5* expression were found to be downregulated (Figure 7E). Furthermore, to enhance the credibility of these four genes that exhibit differential expression, peripheral blood samples were procured from a cohort of 10 individuals diagnosed with ALS and 10 healthy volunteers to conduct RT-qPCR. The outcomes revealed a significant reduction in mRNA expression levels of *BCKDHA* and *GTF2H5* in the ALS group as compared to the control group ($P<0.05$), whereas *JTB* and *KYNU* exhibited upregulation ($P<0.05$) (Figure 7F). These findings strongly imply that these four genes possess the potential to function as diagnostic and prognostic biomarkers for ALS.

4 Discussion

ALS is a complex pathological process, that involves oxidative stress, mitochondrial dysfunction, excitotoxicity, and neuroinflammatory responses (18). The exact pathogenesis of ALS remains unclear, leading to a lack of practical early diagnostic markers and treatment options, posing challenges for clinical management. Although ALS primarily affects motor neurons in the brain and spinal cord, peripheral blood analysis may provide noninvasive biomarkers. Hence, it is still important to explore new biomarkers and provide new insight.

In our analysis of the GEO dataset, we found two large patient cohorts (GSE112676 and GSE112680) with prognostic information: a microarray dataset from peripheral blood of ALS patients and controls, with a total of, 1117 participants (19). This dataset is the best resource for identifying ALS blood biomarkers. Swindell et al. conducted a meta-analysis and found 752 ALS-increased DEGs with consistent differential expression in both cohorts (GSE112676 and GSE112680) (16). Genes most strongly elevated in ALS blood included ribosomal protein L9 (*RPL9*), ribosomal L24 domain containing 1 (*RSL24D1*), vanin 2 (*VNN2*), mitochondrial amidoxime reducing component 1 (*MARC1*) and kynureninase (*KYNU*).

In this study, genes from the GSE112676 dataset with those involved in the mitophagy process to screen, 4383 DEGs and 22 mitophagy-related DEGs using selection criteria. Subsequently, through single-factor Cox regression analysis of these, 4405 mitophagy-related genes, identified 40 prognosis-related genes. After conducting further LASSO Cox regression analysis, we identified 18 signature genes and used them to establish a risk-

10.3389/fimmu.2024.1360527

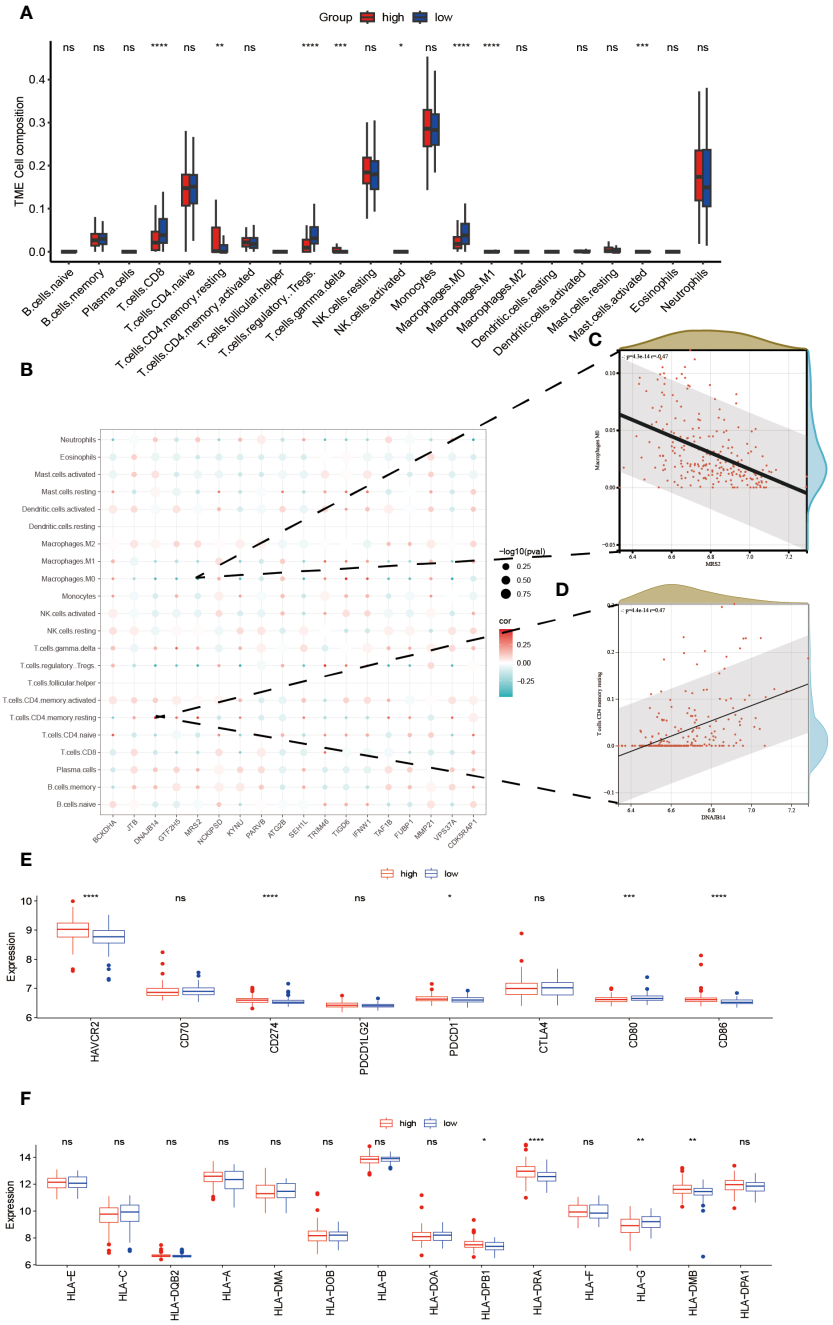

FIGURE 5
Relationship Between High- and Low-Risk Groups and Immune Response. The infiltration abundance distribution using the CIBERSORT algorithm **(A)**. **(B)** Scatter plot illustrating the correlation between the expression levels of model genes and the levels of immune cell infiltration. The color of the points indicates the strength of positive correlation (red) or negative correlation (blue). The size of the points reflects the p-value, with larger points indicating smaller p-values. **(C)** MRS2 showed a marked negative correlation with M0 macrophages. **(D)** DNAJB14 exhibited a significant positive correlation with T cells CD4 memory. Box plots displaying the expression levels of immune checkpoint genes **(E)** and HLA genes **(F)** between high- and low-risk groups. ****P<0.0001, ***P<0.001, **P<0.01, *P<0.05, ns P>0.05.

scoring model. By stratifying patients into high- and low-risk groups, the relationship between the prognostic model genes and immune infiltration was elucidated. Finally, GSEA and GO/KEGG analyses clarified the pathways enriched by DEGs. ROC curve analysis on the validation set demonstrated the good predictive capability of the model. Finally, we found that four out of the eighteen genes also have prognostic and diagnostic value for ALS. To further determine the expression of these four genes in the disease, we used animal models and clinical samples for the four overlapping genes in the test and training sets. Consistently, *JTB* and *KYNU* were upregulated, while *BCKDHA* and GTF2H5 were downregulated in the ALS group compared to the control group.

Increasing evidence suggests that mitochondrial dysfunction resulting in disrupted energy metabolism is a key pathological feature of ALS (4, 5). The accumulation of impaired mitochondria is regarded as a catalyst for ALS, and concomitantly, deficiencies in

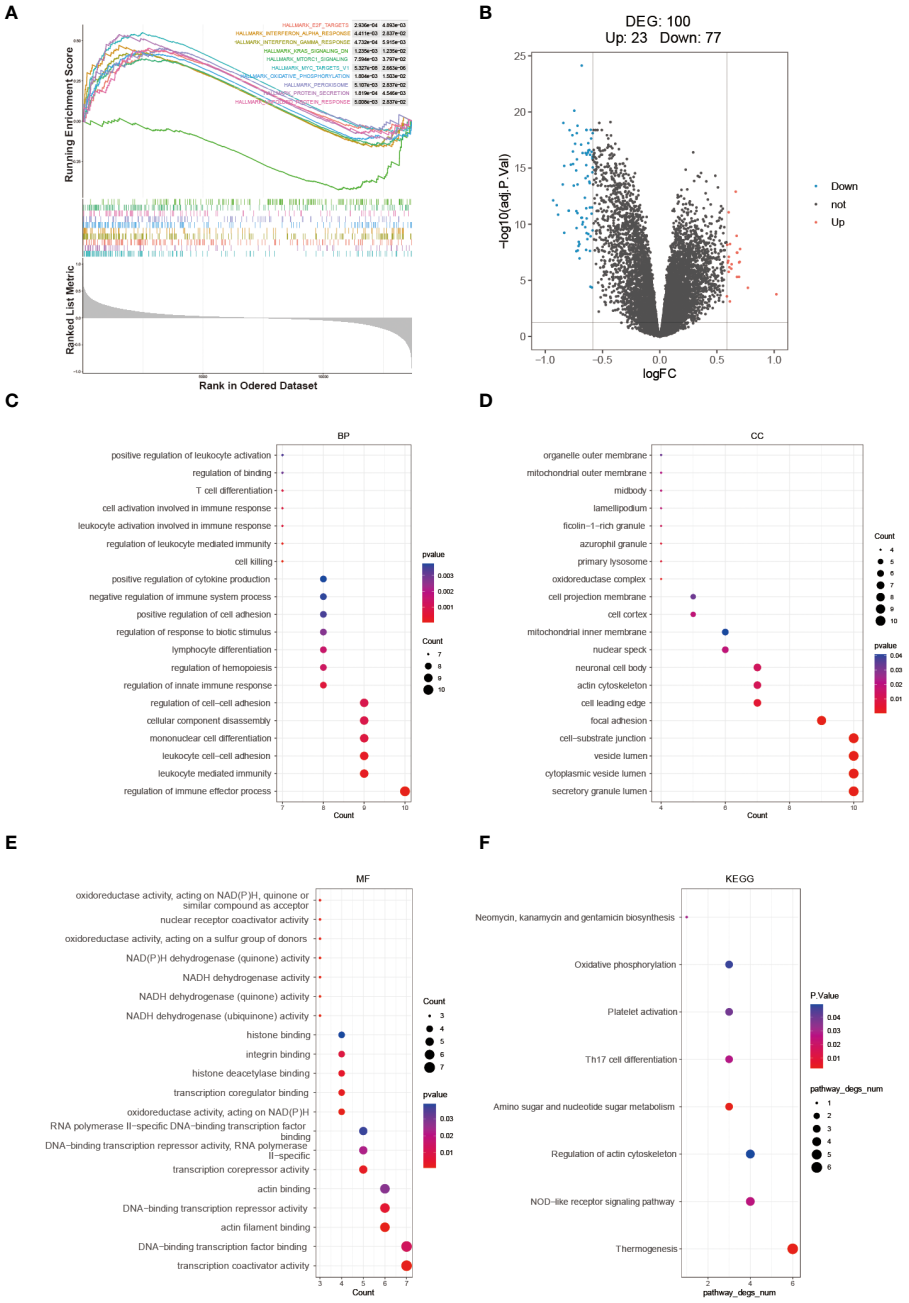

FIGURE 6
Molecular mechanism analysis between high- and low-risk groups. **(A)** GSEA Enrichment Analysis Plot. **(B)** Volcano plot depicting the differential expression between high- and low-risk groups. GO **(C–E)** and KEGG **(F)** enrichment analysis results are displayed, with stronger significance indicated by redder color and lower significance indicated by bluer color.

mitophagy are also evident in ALS models (20).To date, various genes associated with ALS have been identified to participate in the degradation of damaged mitochondria through the process of mitophagy, such as *p62*, *OPTN*, and *TBK1* as discussed previously (21, 22). A study showed that mutant SOD1 affects mitophagy by preventing autophagy receptors from binding to damaged mitochondria (23). Wang et al. found that *C9ORF72* helps regulate energy balance by stabilizing mitochondrial complex I (24). Mutations in *TARDBP* lead to TDP-43 buildup in mitochondria. A recent study by Yu et al. suggests a link between TDP-43, mtDNA, and inflammation in ALS development (25). The VCP protein is crucial for maintaining mitochondrial quality control and mutant VCP disrupts the labeling of mitochondria for mitophagy (26, 27). These discoveries suggest that impaired mitochondrial transport may play a role in the development of ALS. However, investigations into mitophagy in ALS have been limited to morphological examinations of autophagosomes and mitochondrial changes. The connection between mitophagy and ALS is not fully understood, and mitophagy-related genes in ALS have not been thoroughly studied using bioinformatics analysis. This study aims to create a prediction

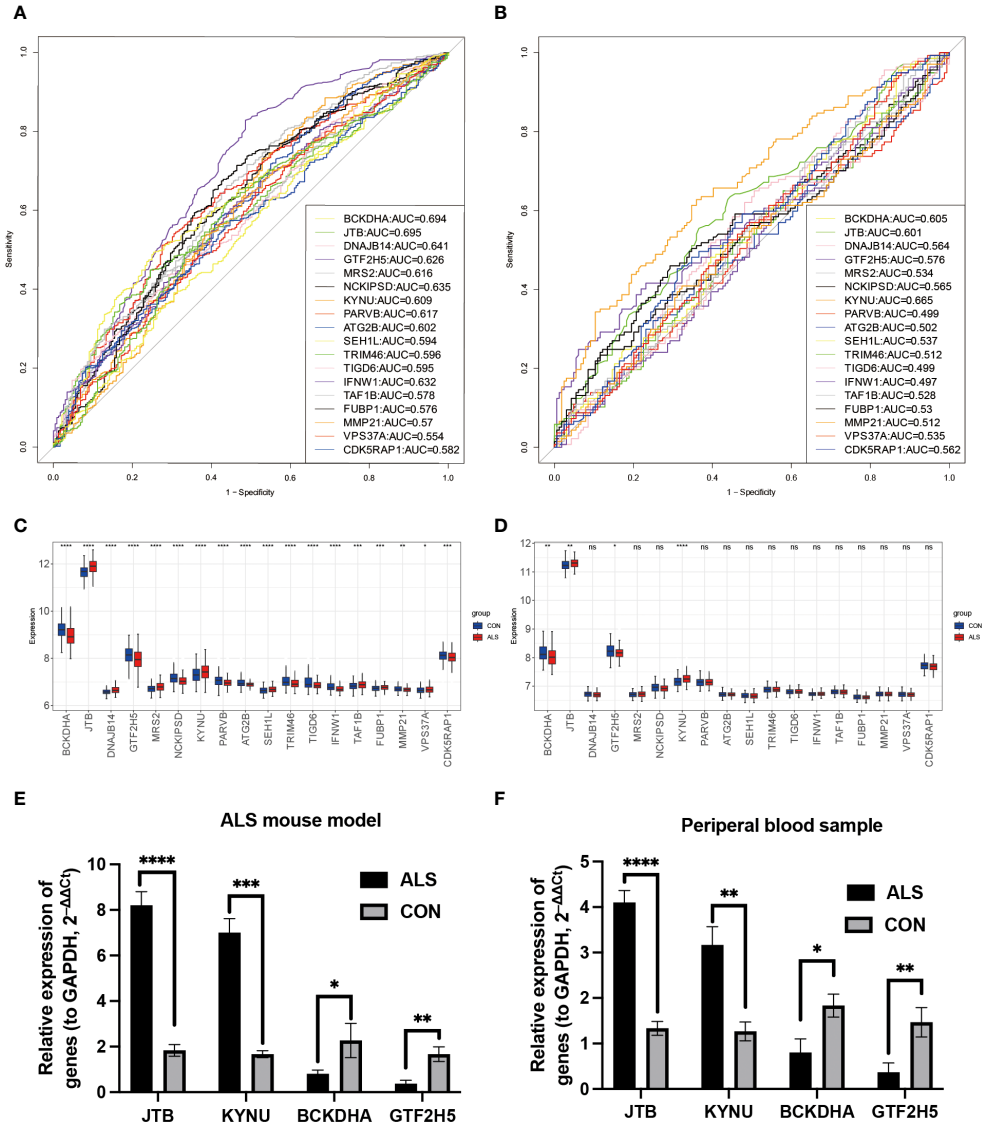

FIGURE 7
Diagnostic analysis of model genes and Validation of the four key DEGs in the lumbar spinal cord tissue of SOD1^{G93A} mice and clinical samples. In the training set GSE112676, the ROC plot to assess disease prediction performance **(A)**, as well as box plots were used to depict the differential distribution of model genes **(C)**. **(B, D)** The same analysis was performed in the validation set GSE112680. Additionally, the expression levels of four key genes were validated by RT-qPCR in ALS mice lumbar spinal cord **(E)** and peripheral blood samples from ALS patients **(F)**. ****P<0.0001, ***P<0.001, **P<0.01, *P<0.05, ns P>0.05.

model related to mitophagy and explore the relationship between mitophagy-related genes and immune infiltration in ALS to uncover potential immune mechanisms and identify new biomarkers.

JTB regulates cell proliferation during mitosis and can inhibit TGFB1-induced apoptosis (28). Moreover, *JTB* affects cell proliferation and growth by increasing AURKB activity (29), and its overexpression induces mitochondrial swelling and reduces mitochondrial membrane potential. The results revealed increased mRNA levels of *JTB* in the serum of ALS patients and the lumbar spinal cord of SOD1^{G93A} mouse models, consistent with the bioinformatics analysis. Other studies have also reported mitochondrial defects and impairment of the autophagy pathway in ALS patients (23, 30). Furthermore, research has shown that overexpression of JTB in cells leads to perinuclear aggregation and swelling of mitochondria, accompanied by a significant decrease in membrane potential, as detected by JC-1 staining (28). Thus, the overexpression of *JTB* in ALS may induce mitochondrial damage, suggesting a novel key factor in mitochondrial dysfunction associated with ALS.

BCKDHA, together with *BCKDHB*, forms the E1 subunit of the mitochondrial branched-chain alpha-keto acid dehydrogenase (BCKD) complex (31). This study showed decreased mRNA levels of *BCKDHA* in the serum of ALS patients and the lumbar spinal cord tissue of SOD1^{G93A} mouse models, consistent with the bioinformatics analysis. *BCKDHA* and *VDAC1* are both mitochondrial proteins that jointly participate in lipid metabolism processes. Research has indicated that *BCKDHA* and *VDAC1* can undergo immunoprecipitation with APOE in mouse liver extracts

(32). This interaction plays a crucial role in the energy production processes of mitochondria and helps the liver to adapt to its energy demands. Furthermore, additional studies suggest that *BCKDHA* (33) induces β-cell mitochondrial dysfunction, stress signal transduction, and cell apoptosis related to type 2 diabetes mellitus (T2DM). Since there are a limited number of studies on *BCKDHA* and ALS, our study may provide some insights for future research.

KYNU is an enzyme involved in the kynurenine pathway (KP), which generates metabolites with immunomodulatory properties. The activation of the KP and the subsequent overproduction of the KP metabolite quinolinic acid due to neuroinflammation are prevalent characteristics in various neurodegenerative disorders, such as ALS. Mutations in the *WARS* and *KYNU* genes negatively impact protein synthesis and cell viability, and cause neurite degeneration in neuronal cells and rat motor neurons (34). The experimental results indicate elevated mRNA levels of *KYNU* in serum from ALS patients and lumbar spinal cord tissue of $SOD1^{G93A}$ mouse models compared to healthy individuals. This result ties well with previous studies wherein the presence of a functional KP in NSC-34 cells, with KYNU and *TDO2* being among the components of the KP in these cells (35). Jennifer et al. identified five genes within the KP (*AFMID, CCBL1, GOT2, KYNU, HAAO*) that exhibit either unique protein-altering variants or an accumulation of rare protein-altering variants in sporadic ALS cases compared to controls (34). Swindell found *KYNU* genes most strongly elevated in ALS blood (16). Our results were consistent with these findings and we also showed that a higher expression of *KYNU* is associated with a better prognosis. Further studies are still needed to clarify why the expression patterns of those genes are different even though they trigger the same canonical pathway of pyroptosis.

GTF2H5 encodes a subunit of the transcription/repair factor TFIIH, which plays a role in gene transcription (36). *GTF2H5* and *PINK1* are involved in gene expression, transcription pathways, and RNA polymerase II transcription. The results indicate decreased mRNA levels of *GTF2H5* in serum from ALS patients and lumbar spinal cord tissue of $SOD1^{G93A}$ mouse models compared to healthy individuals. PHB2 depletion disrupts the stability of PINK1 in mitochondria, thereby blocking the recruitment of PRKN/Parkin, ubiquitin, and OPTN to mitochondria, resulting in inhibited mitophagy (37). Furthermore, *GTF2H5* deficiency leads to resistance to free celastrol, a compound derived from Tripterygium (TP) (38). Therefore, decreased expression levels of *GTF2H5* in ALS patients may lead to impaired mitophagy.

Neuroinflammation serves as one of the pathological hallmarks of ALS. After central nervous system (CNS) injury, various types of innate and adaptive immune cells from the peripheral circulation, including granulocytes, monocyte-derived macrophages, lymphocytes, and natural killer (NK) cells, can be recruited across the blood-brain barrier (BBB) (39, 40). Post-mortem analysis of ALS patient tissue revealed infiltration of peripheral cells, such as CD4+ and CD8+ T cells, macrophages, and NK cells, into multiple CNS regions, indicating the involvement of immune-mediated events in ALS pathogenesis (41, 42). An annotation-based enrichment analysis revealed that DEGs associated with neutrophils were increased in patients with ALS (16).Our study identified peripheral blood immune cells potentially associated with ALS prognosis, including B naive cells, CD4 naive T cells, CD8 T cells, M0 and M2 macrophages, and neutrophils. Shi et al. also used the GSE112676 and GSE112680 datasets to construct a risk model involving four genes (*TRPM2, ROCK1, HSP90AA1, and HSPA4*) (43). Moreover, external validation from dataset GSE112681 confirmed the predictive power of the model. *TRPM2* down-regulation and *ROCK1* up-regulation were also found at the initial stage of our study, but they were not aggregated into further studies due to different directions of subsequent research. Currently, the establishment of prediction models for ALS solely considers DEGs as a single factor, disregarding the variability of the disease. By constructing a gene model, this study not only improves the accuracy of feature gene selection but also enhances the specificity of gene screening.

Currently, there is limited research on mitophagy and immune infiltration in ALS. The expression levels of four key genes in peripheral blood and lumbar spinal cord tissues of ALS mic and found statistically significant expression differences, indicating that *JTB, KYNU, BCKDHA*, and *GTF2H5* in peripheral blood can serve as practical clinical biomarkers for diagnosing ALS patients. However, this study also has some limitations (1): Even though the prognostic risk score performed well, large prospective cohort studies are still needed to validate it; (2) As mitophagy-related genes continue to be discovered, the model needs constant improvement; (3) The expression levels of four prognostic model genes were verified using qRT-PCR *in vitro* through the collection of clinical samples and mouse models, without delving into the underlying mechanism. Hence, additional research is warranted to elucidate the molecular mechanisms involved.

In conclusion, we have created and verified a new prognostic predictive risk score for ALS based on four mitophagy-related genes. This risk score demonstrated its independence as a prognostic factor for ALS outcomes. Furthermore, the analysis of the correlation between these four genes and immune infiltration in ALS indicated a potential involvement of the interaction between mitophagy-related genes and immune cell infiltration in the regulation of ALS pathogenesis. These results offer a fresh perspective on the roles of mitophagy and immune infiltration in ALS and lay the groundwork for further investigations.

Data availability statement

The original contributions presented in the study are included in the article/Supplementary Material. Further inquiries can be directed to the corresponding author.

Ethics statement

The studies involving humans were approved by The Ethics Committee of the Chinese People's Liberation Army (PLA) General Hospital. The studies were conducted in accordance with the local legislation and institutional requirements. The participants provided their written informed consent to participate in this

study. The animal study was approved by The Institutional Animal Care and Use Committee of the Chinese PLA General Hospital. The study was conducted in accordance with the local legislation and institutional requirements.

Author contributions

RD: Conceptualization, Data curation, Investigation, Writing – original draft, Writing – review & editing. PC: Formal analysis, Methodology, Software, Visualization, Writing – review & editing. ML: Data curation, Formal analysis, Software, Writing – review & editing. YZ: Data curation, Software, Writing – review & editing. ZH: Data curation, Investigation, Methodology, Writing – review & editing. XH: Conceptualization, Funding acquisition, Supervision, Validation, Writing – review & editing.

Funding

The author(s) declare that no financial support was received for the research, authorship, and/or publication of this article.

Acknowledgments

We are grateful to the contributors to the public databases used in this study. We would like to thank the patients and their families and nurses. We thank the Chinese PLA General Hospital which has provided materials essential for this study and all the neurologists of the Neurology Department for the support in this study.

Conflict of interest

The authors declare that the research was conducted in the absence of any commercial or financial relationships that could be construed as a potential conflict of interest.

Publisher's note

Supplementary material

The Supplementary Material for this article can be found online at: https://www.frontiersin.org/articles/10.3389/fimmu.2024.1360527/full#supplementary-material

References

1. Nijssen J, Aguila J, Hoogstraaten R, Kee N, Hedlund E. Axon-seq decodes the motor axon transcriptome and its modulation in response to als. *Stem Cell Rep.* (2018) 11:1565–78. doi: 10.1016/j.stemcr.2018.11.005

2. Osking Z, Ayers JI, Hildebrandt R, Skruber K, Brown H, Ryu D, et al. Als-linked sod1 mutants enhance neurite outgrowth and branching in adult motor neurons. *iScience.* (2019) 19:448–9. doi: 10.1016/j.isci.2019.08.004

3. Li X, Huang L, Lan J, Feng X, Li P, Wu L, et al. Molecular mechanisms of mitophagy and its roles in neurodegenerative diseases. *Pharmacol Res.* (2021) 163:105240. doi: 10.1016/j.phrs.2020.105240

4. Sassani M, Alix JJ, McDermott CJ, Baster K, Hoggard N, Wild JM, et al. Magnetic resonance spectroscopy reveals mitochondrial dysfunction in amyotrophic lateral sclerosis. *Brain.* (2020) 143:3603–18. doi: 10.1093/brain/awaa340

5. Vandoorne T, De Bock K, Van Den Bosch L. Energy metabolism in als: An underappreciated opportunity? *Acta Neuropathol.* (2018) 135:489–509. doi: 10.1007/s00401-018-1835-x

6. Park J, Matralis AN, Berghuis AM, Tsantrizos YS. Human isoprenoid synthase enzymes as therapeutic targets. *Front Chem.* (2014) 2:50. doi: 10.3389/fchem.2014.00050

7. Chua JP, De Calbiac H, Kabashi E, Barmada SJ. Autophagy and als: Mechanistic insights and therapeutic implications. *Autophagy.* (2022) 18:254–82. doi: 10.1080/15548627.2021.1926656

8. Xu Y, Shen J, Ran Z. Emerging views of mitophagy in immunity and autoimmune diseases. *Autophagy.* (2020) 16:3–17. doi: 10.1080/15548627.2019.1603547

9. Saitoh T, Fujita N, Jang MH, Uematsu S, Yang BG, Satoh T, et al. Loss of the autophagy protein atg16l1 enhances endotoxin-induced il-1beta production. *Nature.* (2008) 456:264–8. doi: 10.1038/nature07383

10. Zhou R, Yazdi AS, Menu P, Tschopp J. A role for mitochondria in nlrp3 inflammasome activation. *Nature.* (2011) 469:221–5. doi: 10.1038/nature09663

11. Oka T, Hikoso S, Yamaguchi O, Taneike M, Takeda T, Tamai T, et al. Mitochondrial DNA that escapes from autophagy causes inflammation and heart failure. *Nature.* (2012) 485:251–5. doi: 10.1038/nature10992

12. Chiot A, Zaidi S, Iltis C, Ribon M, Berriat F, Schiaffino L, et al. Modifying macrophages at the periphery has the capacity to change microglial reactivity and to extend als survival. *Nat Neurosci.* (2020) 23:1339–51. doi: 10.1038/s41593-020-00718-z

13. Staats KA, Borchelt DR, Tansey MG, Wymer J. Blood-based biomarkers of inflammation in amyotrophic lateral sclerosis. *Mol Neurodegener.* (2022) 17:11. doi: 10.1186/s13024-022-00515-1

14. Moreno-Martinez L, Calvo AC, Munoz MJ, Osta R. Are circulating cytokines reliable biomarkers for amyotrophic lateral sclerosis? *Int J Mol Sci.* (2019) 20(11):2759. doi: 10.3390/ijms20112759

15. Hu Y, Cao C, Qin XY, Yu Y, Yuan J, Zhao Y, et al. Increased peripheral blood inflammatory cytokine levels in amyotrophic lateral sclerosis: A meta-analysis study. *Sci Rep.* (2017) 7:9094. doi: 10.1038/s41598-017-09097-1

16. Swindell WR, Kruse CPS, List EO, Berryman DE, Kopchick JJ. Als blood expression profiling identifies new biomarkers, patient subgroups, and evidence for neutrophilia and hypoxia. *J Transl Med.* (2019) 17:170. doi: 10.1186/s12967-019-1909-0

17. Berriat F, Lobsiger CS, Boillee S. The contribution of the peripheral immune system to neurodegeneration. *Nat Neurosci.* (2023) 26:942–54. doi: 10.1038/s41593-023-01323-6

18. Renton AE, Chio A, Traynor BJ. State of play in amyotrophic lateral sclerosis genetics. *Nat Neurosci.* (2014) 17:17–23. doi: 10.1038/nn.3584

19. van Rheenen W, Diekstra FP, Harschnitz O, Westeneng HJ, van Eijk KR, Saris CGJ, et al. Whole blood transcriptome analysis in amyotrophic lateral sclerosis: A biomarker study. *PLoS One.* (2018) 13:e0198874. doi: 10.1371/journal.pone.0198874

20. Evans CS, Holzbaur ELF. Autophagy and mitophagy in als. *Neurobiol Dis.* (2019) 122:35–40. doi: 10.1016/j.nbd.2018.07.005

21. Moore AS, Holzbaur EL. Dynamic recruitment and activation of als-associated tbk1 with its target optineurin are required for efficient mitophagy. *Proc Natl Acad Sci U.S.A.* (2016) 113:E3349–58. doi: 10.1073/pnas.1523810113

22. Yilmaz R, Muller K, Brenner D, Volk AE, Borck G, Hermann A, et al. Sqstm1/P62 variants in 486 patients with familial als from Germany and Sweden. *Neurobiol Aging.* (2020) 87:139 e9–e15. doi: 10.1016/j.neurobiolaging.2019.10.018

23. Tak YJ, Park JH, Rhim H, Kang S. Als-related mutant sod1 aggregates interfere with mitophagy by sequestering the autophagy receptor optineurin. *Int J Mol Sci.* (2020) 21(20):7525. doi: 10.3390/ijms21207525

24. Wang T, Liu H, Itoh K, Oh S, Zhao L, Murata D, et al. C9orf72 regulates energy homeostasis by stabilizing mitochondrial complex I assembly. *Cell Metab*. (2021) 33:531–46.e9. doi: 10.1016/j.cmet.2021.01.005

25. Yu CH, Davidson S, Harapas CR, Hilton JB, Mlodzianoski MJ, Laohamonthonkul P, et al. Tdp-43 triggers mitochondrial DNA release via mptp to activate cgas/sting in als. *Cell*. (2020) 183:636–49.e18. doi: 10.1016/j.cell.2020.09.020

26. Kim NC, Tresse E, Kolaitis RM, Molliex A, Thomas RE, Alami NH, et al. Vcp is essential for mitochondrial quality control by pink1/parkin and this function is impaired by vcp mutations. *Neuron*. (2013) 78:65–80. doi: 10.1016/j.neuron.2013.02.029

27. Johnson JO, Mandrioli J, Benatar M, Abramzon Y, Van Deerlin VM, Trojanowski JQ, et al. Exome sequencing reveals vcp mutations as a cause of familial als. *Neuron*. (2010) 68:857–64. doi: 10.1016/j.neuron.2010.11.036

28. Kanome T, Itoh N, Ishikawa F, Mori K, Kim-Kaneyama JR, Nose K, et al. Characterization of jumping translocation breakpoint (Jtb) gene product isolated as a tgf-beta1-inducible clone involved in regulation of mitochondrial function, cell growth and cell death. *Oncogene*. (2007) 26:5991–6001. doi: 10.1038/sj.onc.1210423

29. Platica M, Ionescu A, Ivan E, Holland JF, Mandeli J, Platica O. Par, a protein involved in the cell cycle, is functionally related to chromosomal passenger proteins. *Int J Oncol*. (2011) 38:777–85. doi: 10.3892/ijo.2011.900

30. Genin EC, Madji Hounoum B, Bannwarth S, Fragaki K, Lacas-Gervais S, Mauri-Crouzet A, et al. Mitochondrial defect in muscle precedes neuromuscular junction degeneration and motor neuron death in chchd10(S59l/+) mouse. *Acta Neuropathol*. (2019) 138:123–45. doi: 10.1007/s00401-019-01988-z

31. Margutti AVB, Silva WA Jr., Garcia DF, de Molfetta GA, Marques AA, Amorim T, et al. Maple syrup urine disease in Brazilian patients: Variants and clinical phenotype heterogeneity. *Orphanet J Rare Dis*. (2020) 15:309. doi: 10.1186/s13023-020-01590-7

32. Rueter J, Rimbach G, Treitz C, Schloesser A, Luersen K, Tholey A, et al. The mitochondrial bckd complex interacts with hepatic apolipoprotein E in cultured cells in vitro and mouse livers in vivo. *Cell Mol Life Sci*. (2023) 80:59. doi: 10.1007/s00018-023-04706-x

33. Lynch CJ, Adams SH. Branched-chain amino acids in metabolic signalling and insulin resistance. *Nat Rev Endocrinol*. (2014) 10:723–36. doi: 10.1038/nrendo.2014.171

34. Fifita JA, Chan Moi Fat S, McCann EP, Williams KL, Twine NA, Bauer DC, et al. Genetic analysis of tryptophan metabolism genes in sporadic amyotrophic lateral sclerosis. *Front Immunol*. (2021) 12:701550. doi: 10.3389/fimmu.2021.701550

35. Chen Y, Brew BJ, Guillemin GJ. Characterization of the kynurenine pathway in nsc-34 cell line: Implications for amyotrophic lateral sclerosis. *J Neurochem*. (2011) 118:816–25. doi: 10.1111/j.1471-4159.2010.07159.x

36. Singh A, Compe E, Le May N, Egly JM. Tfiih subunit alterations causing xeroderma pigmentosum and trichothiodystrophy specifically disturb several steps during transcription. *Am J Hum Genet*. (2015) 96:194–207. doi: 10.1016/j.ajhg.2014.12.012

37. Yan C, Gong L, Chen L, Xu M, Abou-Hamdan H, Tang M, et al. Phb2 (Prohibitin 2) promotes pink1-prkn/parkin-dependent mitophagy by the parl-pgam5-pink1 axis. *Autophagy*. (2020) 16:419–34. doi: 10.1080/15548627.2019.1628520

38. Yuan F, Sun M, Liu H, Qian F. Albumin-conjugated drug is irresistible by single gene mutation of endocytic system: Verification by genome-wide crispr-cas9 loss-of-function screens. *J Control Release*. (2020) 323:311–20. doi: 10.1016/j.jconrel.2020.04.035

39. Greenhalgh AD, David S, Bennett FC. Immune cell regulation of glia during cns injury and disease. *Nat Rev Neurosci*. (2020) 21:139–52. doi: 10.1038/s41583-020-0263-9

40. Engelhardt B, Vajkoczy P, Weller RO. The movers and shapers in immune privilege of the cns. *Nat Immunol*. (2017) 18:123–31. doi: 10.1038/ni.3666

41. Henkel JS, Engelhardt JI, Siklos L, Simpson EP, Kim SH, Pan T, et al. Presence of dendritic cells, mcp-1, and activated microglia/macrophages in amyotrophic lateral sclerosis spinal cord tissue. *Ann Neurol*. (2004) 55:221–35. doi: 10.1002/ana.10805

42. Garofalo S, Cocozza G, Porzia A, Inghilleri M, Raspa M, Scavizzi F, et al. Natural killer cells modulate motor neuron-immune cell cross talk in models of amyotrophic lateral sclerosis. *Nat Commun*. (2020) 11:1773. doi: 10.1038/s41467-020-15644-8

43. Shi Y, Zhu R. Analysis of damage-associated molecular patterns in amyotrophic lateral sclerosis based on scrna-seq and bulk rna-seq data. *Front Neurosci*. (2023) 17:1259742. doi: 10.3389/fnins.2023.1259742

frontiers | Frontiers in Aging Neuroscience

TYPE Review
PUBLISHED 03 April 2024
DOI 10.3389/fnagi.2024.1389454

OPEN ACCESS

EDITED BY
Robert Weissert,
University of Regensburg, Germany

REVIEWED BY
Sabina Galiniak,
University of Rzeszów, Poland
Xi-Xi Yin,
Hubei University of Science and Technology, China
Ana Cristina Breithaupt-Faloppa,
University of São Paulo, Brazil

*CORRESPONDENCE
Qinglu Wang
✉ wql_zcq@126.com

RECEIVED 21 February 2024
ACCEPTED 19 March 2024
PUBLISHED 03 April 2024

CITATION
Kong J, Fan R, Zhang Y, Jia Z, Zhang J, Pan H and Wang Q (2024) Oxidative stress in the brain–lung crosstalk: cellular and molecular perspectives. *Front. Aging Neurosci.* 16:1389454. doi: 10.3389/fnagi.2024.1389454

Oxidative stress in the brain–lung crosstalk: cellular and molecular perspectives

Jianda Kong[1], Rao Fan[1], Yuanqi Zhang[1], Zixuan Jia[2], Jing Zhang[2], Huixin Pan[2] and Qinglu Wang[2]*

[1]College of Sports Science, Qufu Normal University, Jining, China, [2]College of Sport and Health, Shandong Sport University, Jinan, China

Oxidative stress is caused by an imbalance between the production of reactive oxygen species (ROS) and the body's ability to counteract their harmful effects, playing a key role in the pathogenesis of brain and lung-related diseases. This review comprehensively examines the intricate mechanisms by which oxidative stress influences cellular and molecular pathways, contributing to neurodegenerative, cardiovascular, and respiratory disorders. Emphasizing the detrimental effects on both brain and lung health, we discuss innovative diagnostic biomarkers, such as 8-hydroxy-2′-deoxyguanosine (8-OHdG), and the potential of antioxidant therapies. For these topics, we provide insights into future research directions in the field of oxidative stress treatment, including the development of personalized treatment approaches, the discovery and validation of novel biomarkers, and the development of new drug delivery systems. This review not only provides a new perspective on understanding the role of oxidative stress in brain and lung-related diseases but also offers new insights for future clinical treatments.

KEYWORDS

oxidative stress, reactive oxygen species, brain, lung, brain–lung crosstalk, reactive nitrogen species, 8-hydroxy-2′-deoxyguanosine

1 Introduction

Oxidative stress, characterized by the imbalance between the production of reactive oxygen and nitrogen species (ROS/RNS) and the detoxification capacity of the body toward these reactive intermediates, plays a crucial role in various diseases including the brain and lungs. In the cellular environment, oxidative stress disrupts cell signaling, gene expression, and protein function through the accumulation of ROS and RNS, leading to cell damage and death (Forman and Zhang, 2021; Jelinek et al., 2021). Under physiological conditions, ROS and RNS indeed play pivotal roles in cellular signaling, immune function, and the homeostasis of the cellular environment. They act both as signaling molecules that promote physiological responses and, when in excess, can lead to oxidative stress pathologies characterized by cellular and biochemical complexities (Zarkovic, 2020). However, an excess of ROS and RNS can indeed have deleterious effects, including the oxidative damage to DNA, proteins, and lipids, thereby compromising cellular function and integrity (Schieber and Chandel, 2014).

In the brain, oxidative stress is closely associated with a range of neurodegenerative diseases, stroke, and traumatic brain injury (TBI). Accumulation of ROS can result in

neuronal damage and loss, making significant contributions to the pathophysiology of these diseases. Furthermore, oxidative stress is also linked to neuroinflammation and blood–brain barrier dysfunction, which are key features in the progression of neurological disorders (Jelinek et al., 2021). Accumulation of ROS in the brain can cause oxidative damage to DNA, proteins, and lipids, leading to neuronal injury and loss (Radak et al., 2011). In addition, oxidative stress is closely associated with neuroinflammation, which serves as a defensive but potentially harmful response of the brain's immune system to various damages (Teleanu et al., 2022). Oxidative stress also disrupts the integrity of the blood–brain barrier, resulting in increased permeability and functional impairment. This disruption allows inflammatory cells and potentially harmful substances to infiltrate the brain, further contributing to neuronal damage and the progression of neurodegenerative diseases (Katsi et al., 2020).

Similarly, in the lungs, oxidative stress is a critical factor in the pathogenesis of diseases such as chronic obstructive pulmonary disease (COPD), pulmonary fibrosis, and acute respiratory distress syndrome (ARDS). Oxidative damage in lung tissue can lead to disruption of cellular barrier function, enhanced inflammatory response, and aggravated fibrosis process (Hecker, 2018; Bezerra et al., 2023). This pathological condition arises when there is an imbalance between the production of ROS and the lung's ability to detoxify these harmful compounds or to repair the resulting damage (Snezhkina et al., 2019). Reactive oxygen species, such as free radicals and peroxides, are generated as byproducts of normal cellular metabolism; however, their levels can become excessively elevated due to environmental factors such as pollution, cigarette smoke, or infections (Sies and Jones, 2020).

Despite the anatomical and functional differences between the brain and lungs, they engage in complex bidirectional communication under conditions of oxidative stress. For instance, brain injury can activate the neuroimmune lung axis, potentially leading to pulmonary pathology (Ziaka and Exadaktylos, 2021). Conversely, lung diseases can impact neural function through oxidative stress and inflammatory pathways (Bezerra et al., 2023). These interactions emphasize the importance of considering the health of two organs in the context of a disease that may initially affect one organ, implying that when one organ experiences stress or damage, it can trigger a cascade of reactions in another organ.

Based on the information presented above, this review aims to delve into the molecular mechanisms of oxidative stress in the interplay between the brain and lungs, with a specific focus on dynamic changes under healthy and disease conditions. By synthesizing existing research, we aim to elucidate how oxidative stress affects the interaction between these two critical organ systems and its potential implications for future therapeutic strategies.

2 Basic concepts of oxidative stress

2.1 The generation and regulation of free radicals and ROS

Free radicals and ROS are molecules with at least one unpaired electron, making them highly reactive. These substances include oxygen free radicals (such as superoxide anion, hydroxyl radical, perhydroxyl radical, and singlet oxygen) as well as nitrogen free radicals. Under physiological conditions, ROS are produced in liver cells and macrophages through cellular processes such as aerobic respiration or inflammatory processes. ROS primarily function as signaling molecules and also participate in cell differentiation and apoptosis, thereby promoting the natural aging process (Jakubczyk et al., 2020). Excessive production of ROS may be caused by prolonged exposure to UV radiation, chronic stress, intense physical activity, improper diet, and the use of irritants (Lushchak, 2015).

2.2 The effects of oxidative stress on cell function

Reactive oxygen species are chemically reactive molecules containing oxygen that play a dual role within biological systems, acting both as vital signaling molecules and as detrimental agents when present in excess. They interact with several molecules within cells, significantly affecting cell function. Specifically, ROS can react with three major classes of macromolecules: lipids, proteins, and DNA.

Lipids are susceptible to ROS through a process known as lipid peroxidation, where ROS attack the polyunsaturated fatty acids in cell membranes (Kim et al., 2023). This attack leads to the formation of lipid peroxides, disrupting the membrane's integrity and fluidity, and can result in cell lysis or apoptosis. Additionally, proteins can also be modified by ROS through oxidation of amino acid residues, particularly cysteine and methionine, leading to changes in protein structure and function (Kim et al., 2014). This modification can affect enzyme activity, receptor function, and signal transduction pathways, altering the cell's normal operations and responses. DNA is another critical target of ROS. Oxidative damage to DNA includes base modifications, strand breaks, and cross-linking, which can result in mutations and chromosomal aberrations. These genetic alterations can disrupt normal cell cycle progression, affect gene expression, and lead to carcinogenesis (Lovell and Markesbery, 2007; Tung et al., 2012). Moreover, ROS influence cellular processes such as proliferation, differentiation, and apoptosis by modulating various signal transduction pathways and gene expression mechanisms. For instance, ROS can activate or inhibit transcription factors like NF-κB and AP-1, which are involved in the regulation of genes responsible for cell survival, growth, and death (Fujioka et al., 2004; Morgan and Liu, 2011). However, the accumulation of excessive ROS within cells can trigger cellular stress responses, such as the activation of antioxidant defense mechanisms or the induction of programmed cell death pathways. When the balance tips toward an overproduction of ROS, it can lead to oxidative stress, resulting in significant cell damage or death. This oxidative stress is a key pathogenic factor in the development of various diseases, including neurodegenerative disorders, cardiovascular diseases, and cancer (Schieber and Chandel, 2014).

In summary, ROS interact with and can damage key cellular molecules like lipids, proteins, and DNA, thereby disrupting normal cellular functions and contributing to disease pathogenesis. The body's ability to counteract or repair such damage is crucial

TABLE 1 Reactive oxygen species interactions with cellular macromolecules and their biological effects.

Molecule class	Interaction with ROS	Effects	References
Lipids	ROS attack polyunsaturated fatty acids in cell membranes through lipid peroxidation.	Leads to the formation of lipid peroxides, disrupting membrane integrity and fluidity, potentially causing cell lysis or apoptosis.	Kim et al., 2023
Proteins	ROS modify proteins through oxidation of amino acid residues, particularly cysteine and methionine.	Changes in protein structure and function affecting enzyme activity, receptor function, and signal transduction pathways.	Kim et al., 2014
DNA	ROS cause oxidative damage to DNA, including base modifications, strand breaks, and cross-linking.	Lead to mutations and chromosomal aberrations, disrupting cell cycle, affecting gene expression, and potentially leading to carcinogenesis.	Tung et al., 2012
Signal transduction pathways	ROS modulate various signal transduction pathways and gene expression mechanisms, influencing cellular processes like proliferation, differentiation, and apoptosis.	Activation or inhibition of transcription factors such as NF-κB and AP-1, regulating genes responsible for cell survival, growth, and death.	Fujioka et al., 2004; Morgan and Liu, 2011

for maintaining cellular health and preventing disease progression. **Table 1** demonstrates an overview of ROS interactions with cellular macromolecules and their biological roles.

2.3 The association between oxidative stress and disease

A myriad of intricate connections between oxidative stress and diseases has been substantiated. Oxidative stress is a state that can lead to damage to cellular structure and function, characterized by the involvement of oxygen-containing free radicals capable of undergoing oxidation reactions. These radicals are produced during normal cellular metabolism and play crucial roles in vital physiological processes such as cell signaling and immune function (Chaudhary et al., 2023). However, when the accumulation of free radicals surpasses the scavenging capacity of antioxidants within the body, oxidative stress ensues, potentially leading to damage to proteins, lipids, and DNA, thereby precipitating the development of various diseases (Chaudhary et al., 2023). Consequently, a close association exists between oxidative stress and diseases related to the brain and lungs. For instance, an acute increase in ROS production following ischemic stroke overwhelms antioxidant defenses, leading to further tissue damage. Reperfusion therapy, despite facilitating blood reflow, results in the generation of highly detrimental ROS, culminating in oxidative stress that contributes to the majority of ischemic reperfusion injuries and, consequently, brain tissue damage (Allen and Bayraktutan, 2009). Furthermore, oxidative stress and inflammation play significant roles in both acute and chronic lung injury, where new therapeutic targets include mitochondrial ROS, NLRP3 inflammasomes, DNA sensors, cell death pathways, and IL-1 inhibitors (Wiegman et al., 2020).

In the progression of cancer, oxidative stress also plays a pivotal role. Oxidative stress can promote the onset and progression of tumors, including brain and lung cancers. Regarding brain cancer, oxidative stress can accelerate tumor cell proliferation and invasion through mechanisms such as DNA damage, promotion of inflammatory responses, and alteration of cell signaling pathways. For instance, glioblastoma multiforme (GBM), a highly aggressive form of brain cancer, is associated with oxidative stress-related DNA damage (Rezatabar et al., 2019). Moreover, by altering the tumor microenvironment, such as affecting angiogenesis around the tumor, oxidative stress further promotes the growth and metastasis of brain cancer (Aboelella et al., 2021). Similarly, oxidative stress plays a key role in lung cancer. Smoking, a major risk factor for lung cancer, produces a significant amount of free radicals, leading to oxidative stress. This not only directly damages the DNA of lung cells, increasing the risk of mutations and thus promoting carcinogenesis, but also activates inflammatory responses, facilitating the establishment of a tumor microenvironment conducive to the development of lung cancer (Caliri et al., 2021). Additionally, oxidative stress, including that mediated by the nicotinamide adenine dinucleotide phosphate (NADPH) oxidase family, can further promote cancer progression through mechanisms affecting apoptosis, cell cycle regulation, and intercellular signaling, potentially following the same mechanisms in lung cancer (Vermot et al., 2021).

3 Role of oxidative stress in the lung

3.1 The biological basis of oxidative stress in the lungs

In the pathophysiology of asthma, recruitment and activation of inflammatory cells such as neutrophils, macrophages, and eosinophils lead to increased levels of ROS and RNS, triggering oxidative/nitrosative stress and reducing antioxidant enzyme activity. This process activates transcription factors such as nuclear factor erythroid 2-related factor 2 (NRF2) and nuclear factor-kappa B (NF-κB). The pathophysiology of COPD is influenced by oxidative substances, resulting in chronic inflammation and the development of diseases such as emphysema and bronchitis. Gao et al. (2015) emphasized the decreased expression of Klotho in airway epithelial cells of COPD patients and its impact on inflammation and oxidative damage in their study. Sokolowska et al. (2019) investigated the effects of ozone exposure on the respiratory barrier in a mouse model, revealing how oxidative stress triggers inflammation and airway remodeling. Additionally, Wiegman et al. (2015) explored how oxidative stress-induced mitochondrial dysfunction drives inflammation and airway smooth

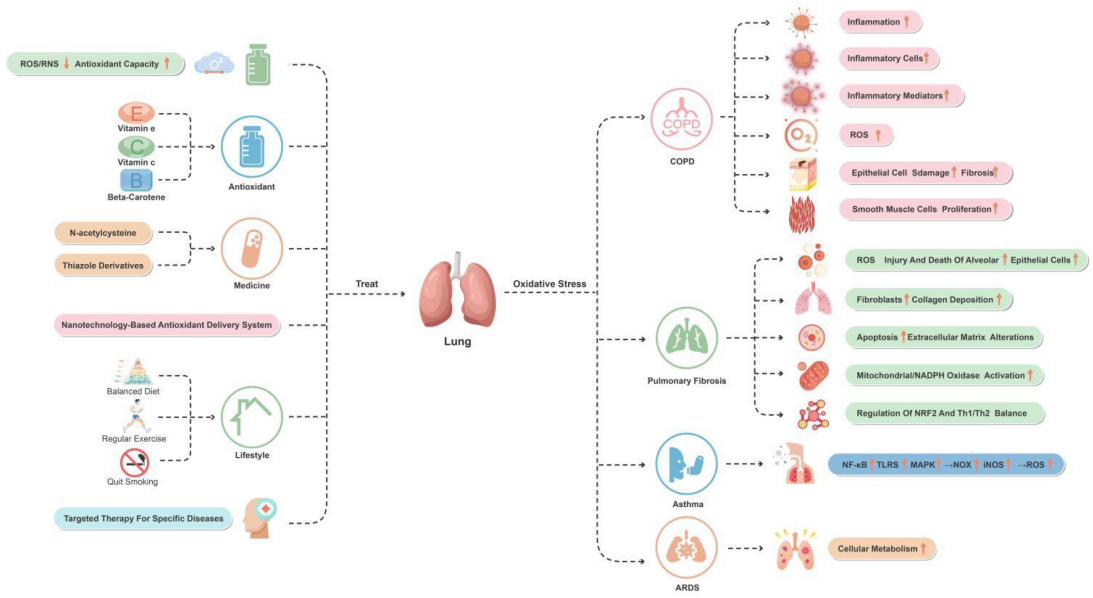

FIGURE 1
The role of oxidative stress in lung disease with associated and therapeutic strategies. This figure provides an overview of the oxidative stress mechanisms and improvement strategies for lung-related diseases and conditions. The major diseases and conditions include COPD, pulmonary fibrosis, asthma, and ARDS. By reducing ROS/RNS levels and increasing antioxidant capacity, using antioxidants and medications, and making lifestyle changes, oxidative stress in these diseases and conditions can effectively be reduced.

muscle remodeling in COPD patients. Antioxidant mechanisms play a crucial role in the lung's response to inflammation caused by tobacco smoke and other substances (Wiegman et al., 2015). In idiopathic pulmonary fibrosis (IPF), factors such as age and environmental exposure promote its development. Oxidative stress and inflammation play important roles in tissue repair and remodeling. Over-oxygenation of healthy lungs leads to injury and inflammation, exacerbating lung inflammation under existing conditions and activating pathways such as mitogen-activated protein kinase (MAPK), c-Jun N-terminal kinase (JNK), and NF-κB (Alharbi et al., 2022).

3.2 The role of oxidative stress in lung diseases

3.2.1 COPD

Oxidative stress plays a crucial role in the pathogenesis of COPD. COPD is characterized by chronic airway inflammation, and oxidative stress exacerbates this process by promoting the activation of inflammatory cells and the release of inflammatory mediators. Accumulation of ROS is considered a key factor in airway remodeling in COPD, leading to epithelial cell damage, fibrosis, and airway smooth muscle proliferation (Rahman, 2005). In addition, oxidative stress is associated with systemic inflammation and lung function impairment in COPD patients (Nucera et al., 2022).

Long-term smoking is a major cause of COPD, providing an important source of chronic inhaled oxidants. Additionally, several inflammatory and structural cells in the lower airways of COPD patients act as endogenous sources of oxidants, even in ex-smokers (Mumby and Adcock, 2022). A systematic review have indicated that oxidative stress in the lower airways increases during stable and exacerbation periods in COPD patients compared to age-matched smokers (Zinellu et al., 2021). Therefore, antioxidant therapy strategies such as N-acetylcysteine and antioxidant supplementation have been shown to be beneficial in COPD patients, suggesting that reducing oxidative stress can improve disease symptoms and quality of life (Nucera et al., 2022). **Figure 1** depicts these mechanisms.

3.2.2 Pulmonary fibrosis

Pulmonary fibrosis is a disease characterized by abnormal repair and fibrosis of lung tissue, in which oxidative stress plays a crucial role in its development. During the process of pulmonary fibrosis, there is an increased production of ROS, resulting in damage and death of alveolar epithelial cells, subsequently triggering activation of fibroblasts and excessive deposition of collagen. This process involves various molecular mechanisms, including cell apoptosis and alteration of extracellular matrix. Studies have indicated that environmental toxins, activation of mitochondria/NADPH oxidase, and depletion of antioxidant defense are the main sources of oxidative stress in pulmonary fibrosis (Mastruzzo et al., 2002).

Furthermore, oxidative stress also promotes inflammation, exacerbating lung tissue damage and the fibrotic process. For instance, NRF2 plays a role in regulating oxidative stress levels in the lungs and T helper type 1/T helper type 2 (Th1/Th2) balance, which may have important implications in the development of pulmonary fibrosis (Walters et al., 2008).

Antioxidant therapy has shown potential in managing pulmonary fibrosis. For example, the use of antioxidants such as N-acetylcysteine may help slow down the progression of the

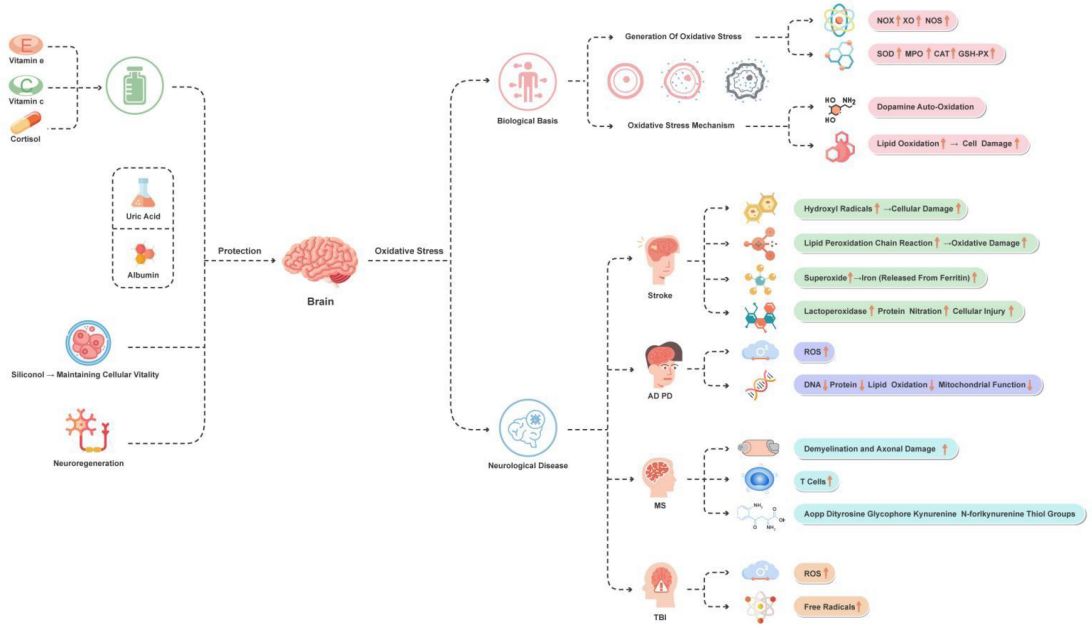

FIGURE 2
Main manifestations of oxidative stress in the brain and protection strategies. This figure illustrates the oxidative stress mechanisms and improvement strategies of brain-related diseases. The main diseases and conditions include stroke, AD, PD, MS, and TBI. The main improvement strategies involve the use of antioxidants, uric acid, albumin, silicic acid (for maintaining cell vitality), and promoting neural regeneration.

disease and improve lung function in patients. The effectiveness of this treatment approach may be attributed to its role in neutralizing ROS and enhancing antioxidant defense mechanisms (Walters et al., 2008). **Figure 2** depicts these mechanisms.

3.2.3 Other pulmonary diseases

In addition to COPD and pulmonary fibrosis, oxidative stress also plays a crucial role in other pulmonary diseases. The role of oxidative stress varies greatly among different pulmonary diseases. In the case of asthma, oxidative stress promotes its development by affecting redox-sensitive signaling pathways. Low levels of oxidative stress activate the Keap1-NRF2-ARE signaling pathway, inducing the expression of antioxidant and detoxification enzyme genes to eliminate excessive ROS (Liu K. et al., 2022). On the other hand, higher levels of oxidative stimulation activate the NF-κB, Toll-like receptors (TLRs), and MAPK signaling pathways, leading to the upregulation of inflammatory mediators, including pro-inflammatory cytokines and pro-oxidant enzymes, such as NADPH oxidase (NOX) and inducible nitric oxide synthase (iNOS), resulting in excessive ROS production. Additionally, TLRs also promote increased ROS production by mitochondria (Liu K. et al., 2022).

In the pathogenesis of asthma, the imbalance between excessive ROS production and reduced antioxidant defense mechanisms leads to the generation of oxidative stress. Oxidative stress plays an important role in the development and progression of asthma, which is characterized by the accumulation of inflammation and immune events. In asthma, the generation of oxidative stress occurs due to the imbalance between excessive ROS production and reduced antioxidant defense mechanisms (Liu K. et al., 2022; Michaeloudes et al., 2022).

In addition to the well-established mechanisms of oxidative stress in asthma, recent studies have expanded our understanding of nitrosative stress and its biomarkers in other pulmonary conditions. For instance, Galiniak et al. (2023) explored biomarkers of nitrosative stress in cystic fibrosis, revealing significant findings in the serum of patients, which underscores the complex interplay between oxidative and nitrosative stress in pulmonary diseases. Another study highlights the critical roles of oxidative stress in pulmonary disease progression, further emphasizing the need for detailed investigations into these mechanisms across a range of conditions (Pinzaru et al., 2023).

In ARDS, oxidative stress has been studied from a multidisciplinary perspective regarding its role in cellular metabolism in lung health and disease. For instance, a study investigated the effects of *Taxus cuspidata* ethanol extract (TO) and TO-mediated photodynamic therapy (TO-PDT) on A549 lung cancer cells. Morphological changes in the cell nucleus and cell membrane were observed in cells treated with TO and TO-PDT. These findings suggest that TO can serve as a photosensitizer during PDT to enhance its direct cytotoxic effects on cancer cells (Arunachalam et al., 2022; Liu K. et al., 2022).

3.3 Therapeutic strategies for oxidative stress

In the treatment of oxidative stress-related diseases, such as brain and lung diseases, therapeutic strategies indeed involve reducing the generation of ROS/RNS and enhancing the body's antioxidant defense capacity. These diseases include neurodegenerative diseases, cardiovascular diseases, and cancer,

among others. In this regard, traditional antioxidants, such as vitamin E, vitamin C, and beta-carotene, have been used to neutralize free radicals in the body and reduce oxidative stress. These antioxidants lower the levels of ROS/RNS by directly reacting with free radicals, thereby protecting cells from oxidative damage (Firuzi et al., 2011). Certain drugs, such as n-acetylcysteine (NAC) (Zhang et al., 2011)and thiazolidine derivatives (TZDs) (Sá et al., 2017), can increase the intracellular levels of glutathione, an important intracellular antioxidant that helps neutralize ROS (Firuzi et al., 2011).

Recent research has shown that antioxidant delivery systems based on nanotechnology are being studied to more effectively deliver antioxidants to cells and tissues affected by oxidative stress. These systems enhance treatment efficacy by improving the bioavailability and targeting of the drugs. For instance, antioxidant-based nanotherapy has demonstrated advantages in alleviating oxidative stress in neurodegenerative diseases, effectively neutralizing oxidative stress by improving the half-life and bioavailability of antioxidants and enhancing their ability to cross the blood–brain barrier (Ashok et al., 2022).

In addition, lifestyle improvements such as a balanced diet, regular exercise, and avoiding smoking are also considered effective means of reducing oxidative stress. These changes help enhance the natural antioxidant defense system and reduce the risk of chronic diseases caused by oxidative stress (Sorriento et al., 2018). Targeted treatments for specific diseases, such as alleviating the condition of COPD or neurodegenerative diseases using certain medications, may also involve reducing oxidative stress. These therapies may include specific antioxidants or anti-inflammatory drugs (Firuzi et al., 2011; Gonçalves and Romeiro, 2019). These are briefly depicted in **Figure 1**.

4 Oxidative stress in the brain

4.1 Biological basis of brain oxidative stress

In the brain, oxidative stress is a condition caused by an excessive production of free radicals and ROS, which are effectively neutralized under normal physiological conditions through antioxidant mechanisms. When this balance is disrupted, oxidative stress occurs in the brain. Enzymes such as NOX, xanthine oxidase (XO), nitric oxide synthase (NOS), superoxide dismutase (SOD), myeloperoxidase (MPO), catalase (CAT), and glutathione peroxidase (GSH-Px) are major contributors to oxidative stress (Jelinek et al., 2021).

Oxidative stress in the brain involves multiple mechanisms, including neurotransmitter auto-oxidation, lipid peroxidation, and redox signaling. For example, dopamine auto-oxidation produces semiquinone radicals, which further generate superoxide anions and hydrogen peroxide. Lipid peroxidation involves a multistep process, including generation of free radicals, oxidation, and propagation of chain reactions, all of which can lead to cell damage in the brain (Cobley et al., 2018).

Furthermore, oxidative stress in the brain is closely associated with neurofunction, pathological changes, and aging. Redox biology plays a crucial role in neurofunction, dysfunction, and aging. Studies have shown that redox signaling plays an important role in neurotransmitter release, cognitive function, and aging processes (Franco and Vargas, 2018).

4.2 Oxidative stress in neurological disorders

4.2.1 Stroke

Ischemic stroke is a severe neurological disorder, and its pathogenesis is mainly related to oxidative stress. Oxidative stress plays a crucial role in the occurrence of stroke, directly affecting the severity of the condition and the recovery process of function.

Hydroxyl radicals are potent oxidants that rapidly oxidize neighboring molecules, leading to cell damage. Lipid peroxidation chain reactions are important oxidative stress reactions, which are initiated by hydroxyl radicals (Lushchak, 2014). Superoxide not only directly causes oxidative stress reactions but also acts as a precursor for hydrogen peroxide and peroxynitrite, further exacerbating the extent of oxidative damage (Quijano et al., 2007). Lipid peroxidation reactions result in damage to the brain cell membrane and play a vital role in the stroke process, intensifying cell injury (Manzanero et al., 2013). Additionally, superoxide promotes the release of iron from iron-sulfur proteins, catalyzing the production of more oxidative stress reactions (Kurtz, 2004). Peroxynitrite is a non-radical strong oxidant that can cause protein nitration, altering its function and leading to cell damage (Pisoschi and Pop, 2015).

All these mechanisms collectively contribute to the aggravation of oxidative stress reactions in stroke, resulting in neuronal damage and death. Studies have shown that the levels of malondialdehyde (MDA), a biomarker of lipid peroxidation, are related to the severity of stroke and functional recovery. Mendioroz et al. (2011) found that 59.9% of stroke patients showed a moderate to severe NIHSS score (16–20) at admission, while Mansour et al. (2015) reported a median NIHSS score of 22 (16–30) within 24 h and 20 (11–30) after 72 h (Elsayed et al., 2020). Moreover, the generation of superoxide and the formation of peroxynitrite are the main sources of oxidative stress in stroke. Studies have indicated that peroxynitrite, the non-radical form of peroxynitrite, is a very strong oxidant with reactivity of its decomposition intermediate, capable of rapidly causing protein nitration and altering protein function (Forman and Zhang, 2021).

Overall, these mechanisms collectively contribute to the exacerbation of oxidative stress during the stroke process, thereby affecting the pathophysiology of stroke and the recovery of patients. These aspects are all reflected in **Figure 2**.

4.2.2 Neurodegenerative diseases

Neurodegenerative diseases such as Alzheimer's disease (AD), Parkinson's disease (PD), Huntington's disease (HD), and multiple sclerosis (MS) exhibit significant effects of oxidative stress throughout their progression.

Reactive oxygen species production is a crucial process in neurodegenerative diseases. These ROS, including superoxide anions, hydroxyl radicals, hydroxide ions, and hydrogen peroxide, are the main mediators of oxidative stress (Kim et al., 2015). Oxidative stress leads to the oxidation of nucleic acids, proteins,

and lipids, resulting in the formation of advanced glycation end products, impairment of mitochondrial function, activation of glial cells, deposition of amyloid-β plaques, cell apoptosis, cytokine production and inflammatory response, as well as dysfunction of proteasomes (Yaribeygi et al., 2018). Oxidative stress is considered a major factor contributing to neurodegeneration and cell death in AD, PD, and other neurodegenerative diseases. These diseases typically manifest as progressive loss of neurons and impaired motor or cognitive function (Niedzielska et al., 2016). Mitochondrial dysfunction is closely associated with oxidative stress, especially in the context of neurodegenerative diseases. Mitochondrial damage leads to cellular metabolic imbalance and reduced energy production, further exacerbating oxidative stress (Liu et al., 2017). Intriguingly, research into MS has revealed the pivotal role of oxidative stress in its pathogenesis. One article has demonstrated that ROS play a significant role in the etiology of MS, leading to demyelination and axonal damage, as well as the activation and proliferation of T cells (Ohl et al., 2016). Furthermore, an increase in oxidative and glycoxidative damage to serum proteins in MS patients has been identified, offering potential biomarkers for monitoring therapeutic efficacy and understanding the role of oxidative stress in the pathophysiology of MS. These biomarkers include protein carbonyls, advanced oxidation protein products (AOPP), dityrosine, glycophore, kynurenine, N′-formylkynurenine, and thiol groups, among others (Sadowska-Bartosz et al., 2013).

Due to the key role of oxidative stress in neurodegenerative diseases, antioxidant therapeutic strategies are considered potential approaches for these diseases. However, the effectiveness of these strategies is still controversial, and further research is needed to clarify their role in the treatment of neurodegenerative diseases. The above content is briefly outlined in **Figure 2**.

4.2.3 TBI

In recent years, oxidative stress has increasingly been acknowledged as a key factor in the pathophysiology of TBI. Research has revealed the potential value of antioxidant therapy in mitigating the impact of TBI, particularly in combating the excessive generation of ROS and free radicals induced by brain injury (Hall et al., 2010). Additionally, mitochondrial dysfunction plays a significant role in the degradation of neuronal cytoskeleton following TBI, suggesting that targeting the mitochondrial pathway may be an effective intervention (Hill et al., 2017).

On the other hand, the administration of high-dose intravenous vitamin C as a novel approach for treating TBI has garnered considerable attention due to its demonstrated effectiveness in reducing oxidative stress and improving clinical outcomes (Leichtle et al., 2020). Furthermore, the development of novel antioxidant neuroprotective drugs has emerged as a crucial area of investigation, targeting specifically the oxidative stress pathway with the aim of protecting neurons from damage (Hall et al., 2019).

To comprehensively understand the impact of antioxidant therapy on TBI cases, a series of systematic reviews have been conducted. These evaluations extensively analyze how oxidative stress affects TBI patients and explore the potential benefits of antioxidant therapy (Shen et al., 2016). Moreover, research has identified an increased expression of mitochondrial deubiquitinase ubiquitin-specific protease 30 (USP30) following TBI, leading to impaired mitochondrial quality control. This finding suggests that targeting USP30 may be a novel strategy for alleviating secondary brain injury after TBI (Wu et al., 2023).

Overall, these studies collectively underscore the importance of addressing oxidative stress in the treatment of TBI and highlight the necessity of further exploring targeted therapeutic approaches to mitigate oxidative stress-induced damage to the brain. Therefore, oxidative stress holds crucial significance in the advancement of TBI research. **Figure 2** reflects the above content.

4.3 Neuroprotection strategies

When oxidative stress damages the nervous system, various intervention strategies have shown potential effects. The application of antioxidants is considered a key approach. Studies have found a strong association between intake of vitamins C and E and delayed onset of AD in elderly individuals (Kontush and Schekatolina, 2004; Costanzi et al., 2008). Free radicals trigger neurodegenerative diseases through mechanisms such as lipid peroxidation, protein oxidation, and DNA damage (Franzoni et al., 2021). Kim et al.'s (2015) research further demonstrated that ROS cause cellular damage by disrupting the structure and function of biomolecules. Additionally, natural compounds such as quercetin possess neuroprotective properties. Arredondo et al.'s (2010) study revealed that quercetin can protect against oxidative stress-induced neuronal damage by promoting NRF2 nuclear translocation and increasing glutathione levels.

In the treatment of ischemic stroke, antioxidants such as uric acid and albumin have been proven to reduce stroke risk, with mechanisms involving the clearance of harmful ROS (Lee et al., 2020). Furthermore, maintaining cellular vitality during hypoxia is critical for neuroprotection strategies. Chtourou et al.'s (2012) research found that silibinin has a protective effect against manganese-induced neurotoxicity, achieved through improvements in cerebellar redox state and cholinergic functioning. Finally, significant progress has been made in research on neural regeneration in the field of neurodegenerative diseases. Despite the limited self-healing and regenerative capabilities in the central nervous system, current studies are exploring regenerative therapeutic approaches for neurodegenerative diseases (Simon and Standaert, 1999).

These research directions and findings provide a series of potential neuroprotection strategies, highlighting the potential value of antioxidants and natural compounds, as well as revealing new treatment targets and methods. These achievements lay a solid foundation for future research and clinical practice. **Figure 2** depicts these treatment strategies.

5 Oxidative stress in brain–lung crosstalk

5.1 How oxidative stress impacts brain–lung communication

The significant role of oxidative stress in lung diseases has been established through research, particularly in the context of

aging and chronic diseases such as COPD. Studies have highlighted the impact of cellular aging on respiratory tract infections and emphasized the importance of understanding plasma membrane repair mechanisms in pulmonary diseases (Cong et al., 2017; Yanagi et al., 2017). In addition, Cho and Stout-Delgado (2020) stressed the influence of aging on lung diseases, with oxidative stress potentially exacerbating this impact. Extensive literature supports the involvement of oxidative stress in neurodegenerative diseases. It contributes to the pathophysiology of conditions like AD, PD, and amyotrophic lateral sclerosis, promoting an imbalance in dopamine, iron, and alpha-synuclein in the brain, thereby generating oxidative stress (Bedard and Krause, 2007; Feitosa et al., 2018).

Research on oxidative stress genes associated with acute lung injury (ALI) has unveiled crucial biomarkers, highlighting the close relationship between oxidative stress and ALI and indicating the intertwining of immune response and oxidative stress in pulmonary diseases (Liu et al., 2023). The NOX, which generate ROS, play a significant role under both physiological and pathological conditions. Understanding the dynamics of these enzymes is essential for managing oxidative stress-related diseases affecting both the brain and lungs (Begum et al., 2022).

Oxidative stress-mediated disruption of the blood–brain barrier is a critical factor in neurological disorders. Iron metabolism, closely linked to oxidative stress, plays a crucial role in various neurological conditions. This aspect of oxidative stress has been demonstrated to impact diseases such as HD, PD, and AD (Song et al., 2020).

Thus, the relationship between oxidative stress and brain–lung crosstalk is intricate and multifaceted, involving a range of cellular and molecular processes. These studies provide a foundation for further exploration of oxidative stress-targeted therapeutic strategies in neurodegenerative and pulmonary diseases.

5.2 The role of ROS in brain–lung crosstalk: bridging neural, immune, and endocrine pathways

This section delves into the pivotal role of ROS in mediating brain–lung crosstalk through neural, immune, and endocrine pathways (**Table 2**). It illustrates how severe TBI can trigger pulmonary dysfunction via neuro-immune interactions facilitated by ROS, which disrupt the blood–brain barrier and enhance systemic inflammation, leading to conditions like ARDS. Furthermore, the immune pathways highlight ROS's critical function in activating brain's immune cells and macrophages, contributing to inflammation and influencing lung health. This is further compounded by endocrine pathways, where the hypothalamic-pituitary-adrenal (HPA) axis's regulation by oxidative stress affects immune responses and susceptibility to lung infections and inflammation. Additionally, at a molecular level, ROS influence key signaling pathways such as NF-κB and MAPK, crucial for regulating inflammation and cellular stress responses, thus underscoring ROS's comprehensive role in bridging neural, immune, and endocrine mechanisms affecting both brain and lung health.

5.2.1 Neural pathways

Neurological injuries, particularly severe TBI, have been shown to induce pulmonary dysfunction through neuro-immune interactions. These interactions are mediated by ROS, which exacerbate lung inflammation by disrupting the blood–brain barrier, facilitating the systemic spread of inflammatory mediators. For instance, a study demonstrated that TBI can lead to ARDS, where ROS play a significant role in the pathogenesis by promoting inflammation and exacerbating lung damage (Qian et al., 2020).

5.2.2 Immune pathways

The immune response plays a crucial role in bridging brain and lung health, significantly influenced by ROS. ROS are highly reactive chemicals containing oxygen, produced either exogenously or endogenously, and are essential for various biological functions, including cell survival, proliferation, differentiation, and immune response. They are related to a wide variety of human disorders, such as chronic inflammation, age-related diseases, and cancers (Yang et al., 2013).

In the context of neuroinflammation, ROS activate microglia, the resident immune cells of the brain, leading to the production of inflammatory cytokines. This process exacerbates neuroinflammation and can affect pulmonary health by inducing a systemic inflammatory response (Morris et al., 2022). The activation of macrophages by ROS involves metabolic reprogramming and redox factors, leading to the activation of proinflammatory cytokines and chemokines, iNOS, and HIF1α, crucial for maintaining macrophage activation and M1 polarization (Morris et al., 2022). This shift is indispensable for increasing phagocytosis, production of ROS, and proinflammatory cytokines. Conversely, pulmonary infections increase ROS production in lung tissue, affecting the central nervous system by enhancing neuroinflammation through cytokine-mediated mechanisms.

Reactive oxygen species-associated immune response and metabolism are intricately linked to the pathophysiology of various diseases, highlighting the role of metabolic reprogramming in immune responses, particularly in macrophages (Banerjee et al., 2020). The regulation of oxidative stress by ROS is crucial for both initiating and resolving inflammation, underlining the complex role ROS play in immune responses and disease pathogenesis.

5.2.3 Endocrine pathways

Endocrine interactions, particularly those involving oxidative stress and the brain–lung crosstalk, are indeed complex and significantly influenced by the HPA axis. The regulation of the HPA axis and its interaction with oxidative stress mechanisms have profound implications for immune function and susceptibility to infections and inflammation in the lungs (Spiers et al., 2014; Leistner and Menke, 2020; Palma-Gudiel et al., 2021).

A study highlighted that HPA axis dysregulation is associated with altered immune function through epigenetic mechanisms, including DNA methylation changes in genes related to immune and HPA axis function. It found that higher cortisol levels, indicative of blunted HPA axis feedback, were associated with lower DNA methylation at certain gene sites involved in immune response regulation, suggesting a link between chronic stress, HPA axis function, and immune response modulation (Palma-Gudiel et al., 2021). Further research into the HPA axis's role in

TABLE 2 Detailed analysis of the role of ROS in brain–lung crosstalk: bridging neural, immune, and endocrine pathways.

Section	Description	Key mechanisms	References
Neural pathways	Explains how severe TBI induces pulmonary dysfunction through neuro-immune interactions mediated by ROS. This leads to blood–brain barrier disruption, systemic inflammatory mediator spread, and conditions like ARDS.	Neuro-immune interactions Blood–brain barrier disruption	Qian et al., 2020
Immune pathways	Highlights ROS's role in activating brain's immune cells and macrophages, contributing to inflammation and lung health. Discusses ROS's involvement in immune response, metabolic reprogramming, and redox factors.	Activation of microglia and macrophages Metabolic reprogramming and redox factors in immune response	Yang et al., 2013; Banerjee et al., 2020; Morris et al., 2022
Endocrine pathways	Discusses the impact of oxidative stress and the HPA axis on immune function and lung susceptibility to infections and inflammation. Highlights the regulation of oxidative stress by ROS and its implications for health.	HPA axis regulation Oxidative stress mechanisms in immune function	Spiers et al., 2014; Leistner and Menke, 2020; Palma-Gudiel et al., 2021
Molecular and cellular mechanisms	Details how ROS affect key signaling pathways such as NF-κB and MAPK, crucial for inflammation and cellular stress response regulation. Also discusses the role of enzymes like NADPH oxidase in ROS production and cellular defense.	NF-κB and MAPK signaling pathways Enzymatic production of ROS and cellular defense	Morgan and Liu, 2011; Wang et al., 2017; Iqbal et al., 2024

stress responses elucidates how its dysregulation can contribute to various mental and physical health issues (Leistner and Menke, 2020). This research has identified distinct sex differences in the HPA axis's regulation in response to stress, which might explain the variations in susceptibility to stress-related disorders between genders (Leistner and Menke, 2020). Moreover, the activation of the HPA axis and subsequent release of glucocorticoids have been shown to induce oxidative stress within cells, particularly affecting the redox system (Spiers et al., 2014). This system plays a crucial role in managing oxidative phosphorylation and maintaining cellular health. The exposure to glucocorticoids, particularly in the hippocampus, has been linked to increased oxidative stress, highlighting the intricate relationship between HPA axis activity, glucocorticoid release, and cellular oxidative balance (Spiers et al., 2014).

These findings collectively underscore the intricate interplay between the HPA axis, endocrine responses, oxidative stress, and immune function. Understanding these relationships is crucial for developing interventions aimed at mitigating the adverse effects of stress and oxidative stress on health, particularly in the context of lung health and susceptibility to infections and inflammation.

5.2.4 Molecular and cellular mechanisms

At the molecular level, ROS influence several key signaling pathways, including NF-κB and MAPK pathways, which play a significant role in the regulation of inflammation and cellular stress responses in various diseases affecting the brain and lungs. The activation of these pathways by ROS can lead to an increased expression of inflammatory cytokines, chemokines, and adhesion molecules, thereby promoting the recruitment of immune cells to sites of injury or infection.

Reactive oxygen species are produced by a variety of enzymes, including NADPH oxidase, which is crucial for cellular defense mechanisms. However, excessive ROS can lead to oxidative stress, damaging intracellular proteins, lipids, and nucleic acids. In response to ROS, cells may activate pathways such as NF-κB, promoting survival by increasing the expression of antioxidant proteins and preventing excessive inflammation and cellular damage (Morgan and Liu, 2011). Furthermore, the MAPK pathway is another key signaling cascade activated by ROS, leading to the phosphorylation and activation of transcription factors such as AP-1 and NF-κB. These factors regulate the expression of genes involved in cell survival, proliferation, and apoptosis, highlighting the complex balance between ROS production and cellular signaling mechanisms (Iqbal et al., 2024). Specifically, in lung diseases, urban particulate matter has been demonstrated to trigger lung inflammation through the activation of ROS-mediated MAPK and NF-κB signaling pathways, emphasizing the molecular mechanisms by which environmental pollutants can exacerbate inflammatory responses in respiratory diseases (Wang et al., 2017).

These findings collectively underscore the complex interplay between ROS and key cellular signaling pathways in regulating inflammation and stress responses, elucidating potential therapeutic targets for diseases characterized by aberrant inflammation and oxidative stress.

5.3 Oxidative stress and glycation in brain–lung crosstalk

Recent studies have underscored the intricate relationship between oxidative stress and glycation, notably through the generation of advanced glycation end products (AGEs) and their impact on brain–lung interactions. Oxidative stress, characterized by an imbalance between the production of ROS and antioxidant defense mechanisms, plays a pivotal role in initiating and accelerating the glycation process. Glycation, a non-enzymatic reaction where reducing sugars react with proteins, lipids, and nucleic acids, leads to the formation of AGEs. These AGEs accumulate in various tissues, including the brain and lungs,

causing cellular dysfunction and disease progression (Xu et al., 2023).

In the context of brain–lung interactions, the accumulation of AGEs has been demonstrated to exacerbate oxidative stress, thereby creating a vicious cycle that promotes neurodegeneration and the development and progression of pulmonary diseases. For instance, AGEs can compromise the blood–brain barrier, leading to increased neuronal vulnerability and inflammation, hallmark features of several brain disorders (Dobi et al., 2021). Similarly, in the lungs, AGEs contribute to the pathogenesis of COPD and pulmonary fibrosis through the enhancement of oxidative stress and inflammatory responses (Otoupalova et al., 2020). Furthermore, the receptor for AGEs (RAGE) mediates many of the deleterious effects of AGEs in both the brain and lungs. Specifically, AGEs, through their interaction with RAGE, trigger signaling pathways that further promote oxidative stress, inflammation, and cellular damage (Tóbon-Velasco et al., 2014). This interaction underscores the critical role of the oxidative stress-glycation axis in regulating brain–lung interactions and highlights the potential of therapeutic interventions targeting this pathway. Strategies aimed at reducing AGE accumulation, inhibiting RAGE signaling, or enhancing antioxidant defense systems offer promising avenues for mitigating the adverse effects of oxidative stress and glycation in brain–lung interactions. Antioxidant therapies, AGE breakers, and RAGE antagonists represent some of the interventions currently under investigation, holding the potential to disrupt this harmful cycle and improve disease outcomes (Firuzi et al., 2011).

In summary, the interplay between oxidative stress and glycation represents a key mechanism influencing the pathophysiology of brain and lung diseases. Further understanding of this relationship and the development of targeted therapeutic strategies may significantly impact the management and treatment of conditions associated with oxidative stress and the accumulation of AGEs.

6 In-depth exploration of molecular mechanisms

In this chapter, we embark on a detailed exploration of the complex molecular mechanisms involved in oxidative stress, focusing on two key areas: the role of essential molecular pathways (see section "6.1 Role of key molecular pathways") and the potential of biomarkers in biomedical research (see section "6.2 The potential of biomarkers in biomedical research"). In section "6.1 Role of key molecular pathways," we delve into several pivotal molecular pathways such as NRF2-ARE, NF-κB, and MAPK pathways. These pathways play crucial roles in regulating the oxidative stress response. By examining their specific functions in brain and lung diseases, we gain insights into the pathogenesis of these conditions and identify important molecular targets for potential therapeutic strategies.

Following this, section "6.2 The potential of biomarkers in biomedical research" explores the significance of biomarkers in identifying and quantifying levels of oxidative stress. This section emphasizes the role of oxidative stress biomarkers in various diseases, particularly their applications in brain and lung disorders. Identifying these biomarkers allows researchers to more accurately monitor oxidative stress levels, thereby facilitating a more effective assessment of disease states and treatment outcomes.

Together, these two sections form the foundation for an in-depth exploration of the molecular mechanisms of oxidative stress, offering new perspectives for understanding and combating brain and lung diseases at the molecular level. **Table 3** shows comparative overview of key molecular pathways and biomarkers of oxidative stress in various diseases.

6.1 Role of key molecular pathways

Central to the oxidative stress response is the NRF2-ARE pathway. NRF2, a pivotal transcription factor in combating oxidative stress, orchestrates cellular defense against ROS-induced harm by regulating the expression of genes responsible for antioxidation and detoxification. Within the cerebral context, activation of the NRF2-ARE pathway fortifies the antioxidative defense mechanism, attenuating neuronal injury caused by oxidative stress. Studies reveal that activation of the NRF2-ARE pathway post-cerebral injury diminishes mitochondrial oxidative stress triggered by singlet oxygen and superoxide radicals, thereby aiding in the recuperation of cognitive functions (Yan et al., 2008). In pulmonary conditions, NRF2 emerges as a critical defensive element, lessening pulmonary tissue damage from ROS by enhancing the expression of genes for detoxifying enzymes responsive to oxidative stress (Pall and Levine, 2015).

Another integral molecular pathway is the NF-κB pathway. NF-κB, a transcription factor, assumes a pivotal role in the oxidative stress response. In the brain, oxidative stress catalyzes NF-κB activation, leading to escalated production of inflammatory mediators and increased neuronal apoptosis. Investigations have demonstrated a correlation between cerebral oxidative stress and the NF-κB pathway, suggesting that inhibiting this pathway may alleviate brain injuries induced by oxidative stress (Chen et al., 2021). In pulmonary diseases, activation of the NF-κB pathway is thought to play a role in modulating oxidative stress-related inflammatory responses. Studies indicate that suppressing NF-κB pathway activity can reduce oxidative stress and inflammatory reactions in pulmonary fibrosis, thereby promoting repair of lung tissue (Lingappan, 2018).

In addition to the NRF2-ARE and NF-κB pathways, other critical molecular pathways also partake in the regulation of oxidative stress. The MAPK pathway, extensively studied and linked with oxidative stress, is one such example. In the brain, MAPK pathway activation due to oxidative stress can result in increased cell apoptosis and inflammatory responses. Research has shown that inhibiting MAPK pathway activation can mitigate the oxidative stress-induced damage to neural cells, thereby safeguarding the brain from oxidative injury (Fan et al., 2019). In pulmonary diseases, the MAPK pathway also contributes to the modulation of oxidative stress. Findings reveal that activation of the MAPK pathway induced by oxidative stress escalates the production of inflammatory and fibrotic factors, thus aggravating lung damage (Maselli et al., 2002; Rezatabar et al., 2019).

To gain a more comprehensive understanding of the molecular mechanisms underpinning oxidative stress in brain–lung interactions, further investigation into other key molecular

TABLE 3 Comparative overview of key molecular pathways and biomarkers of oxidative stress in various diseases.

Disease	Key molecular pathways	Biomarkers	Level changes	Significance	References
Cerebral injury	NRF2-ARE (regulates genes for antioxidation and detoxification)	Mitochondrial oxidative stress indicators, 8-OHdG	Post-injury increase in oxidative markers and 8-OHdG	Indicates oxidative stress damage and efficacy of antioxidative therapies	Yan et al., 2008
Pulmonary conditions	NRF2 (reduces pulmonary tissue damage from ROS)	AOPPs, Ox-LDL, gene expression of detoxifying enzymes	Elevated AOPPs, Ox-LDL during oxidative stress	Reflects ROS impact and NRF2 activation effectiveness	Pall and Levine, 2015
Neurodegenerative diseases (AD and PD)	NF-κB (linked to oxidative stress-induced brain injuries)	8,12-Iso-PGF2α, oxidized lipids, nitrotyrosine, MDA	Increased lipid peroxidation markers (8,12-iso-PGF2α, MDA) and protein nitration	Markers of inflammation, cellular damage in neurodegeneration	Mythri et al., 2011; Butterfield, 2020
Pulmonary fibrosis	NF-κB (modulates oxidative stress-related inflammatory responses)	Ox-LDL, AOPP levels, 8-OHdG, MDA	Elevated AOPP, Ox-LDL, 8-OHdG, and MDA levels	Indicative of oxidative stress and inflammation in lung tissue	Shen et al., 2013; Gao et al., 2021
General oxidative stress	MAPK pathway, HO-1, SOD	8,12-Iso-PGF2α, 8-OHdG, 8-OHdA, oxidized lipids, nitrotyrosine	Varies with oxidative stress levels	General indicators of oxidative stress and damage	Maselli et al., 2002; Méthy et al., 2004; Ryter and Choi, 2005; Fan et al., 2019; Rezatabar et al., 2019

pathways, such as heme oxygenase-1 (HO-1) (Ryter and Choi, 2005) and SOD (Méthy et al., 2004), which also play substantial roles in oxidative stress responses, is essential. Additionally, given the intricacy of brain–lung interplay, future research endeavors should embrace an integrative methodology, incorporating transcriptomics, proteomics, and metabolomics, to thoroughly unravel the molecular intricacies of oxidative stress within the brain–lung nexus.

6.2 The potential of biomarkers in biomedical research

Biomarkers are instrumental as molecular or indicative targets for the assessment of specific biological processes or states of disease. In exploring the molecular mechanisms of oxidative stress and its brain–lung interactions, identifying suitable biomarkers for measuring the degree and impact of oxidative stress is of paramount importance.

In the context of AD, an increase in the levels of 8,12-iso-prostaglandin F2α (8,12-iso-PGF2α), indicative of enhanced lipid peroxidation within the body, has been noted (Praticò et al., 2000). This lipid peroxidation, a consequence of oxidative stress, is a marker for inflammation and cellular damage (Praticò et al., 2000), suggesting that 8,12-iso-PGF2α could be a potential biomarker for determining the extent of oxidative stress in the brain. In neurodegenerative diseases such as AD and PD, oxidative stress leads to increased lipid peroxidation chain reactions and protein nitration (Mythri et al., 2011; Butterfield, 2020). Therefore, the by-products of lipid peroxidation and protein nitration, like oxidized lipids and nitrotyrosine, are viewed as potential biomarkers for assessing the severity of oxidative stress in these neurodegenerative conditions.

In pulmonary diseases, oxidative protein products such as AOPPs and oxidized low-density lipoprotein (Ox-LDL) are considered potential biomarkers for gauging the level of oxidative stress (Shen et al., 2013; Gao et al., 2021). Studies have shown that AOPP levels are elevated in lung diseases like pneumonia and COPD, while Ox-LDL is linked to pulmonary fibrosis and airway inflammation (Shen et al., 2013).

Additionally, oxidative stress can lead to oxidative modifications in DNA and RNA. Biomarkers such as 8-hydroxyguanosine (8-OHdG) and 8-hydroxyadenine (8-OHdA) are extensively used to indicate oxidative damage in DNA and RNA (Valavanidis et al., 2009; Guo et al., 2020). The levels of these biomarkers, measurable in urine, blood, or tissue samples, serve to assess the degree of oxidative stress. However, their role in the interplay between the brain and lungs remains to be further elucidated.

7 Clinical applications of oxidative stress in brain–lung crosstalk

This section elaborates on the progress and trends of oxidative stress diagnostic tools, treatment methods, and future treatment strategies. Regarding oxidative stress diagnostic tools, emphasis is placed on the role of 8-OHdG and other related biomarkers in monitoring oxidative stress under different health conditions, as well as the development of advanced 8-OHdG measurement methods. In terms of innovative treatments for oxidative stress-related diseases, approaches such as enhancing NRF2 synthesis or inhibiting its degradation to alleviate oxidative stress, and utilizing non-toxic electron-affine substances to bind KEAP1 are mentioned. Additionally, innovative methods for treating cardiovascular diseases, neurodegenerative diseases, and glioblastoma are introduced. Lastly, future strategies for treating oxidative stress-related diseases are pointed out, such as applying machine learning to drug discovery, developing targeted drugs for specific diseases, and regulating the role of ROS in the wound healing process. **Table 4** demonstrates summary of treatment strategies for oxidative stress-related diseases.

TABLE 4 Summary of treatment strategies for oxidative stress-related diseases.

Treatment strategy	Description	Application	Mechanism of action	References
Drug therapy	Traditional pharmacological approaches targeting specific symptoms or pathways of diseases.	Used in various oxidative stress-related diseases like neurodegenerative diseases, cardiovascular diseases, and cancer.	Often involves modulation of specific pathways or inhibition of pathological processes.	Firuzi et al., 2011; Zhang et al., 2011; Sá et al., 2017
Antioxidant therapy	Utilization of antioxidants like vitamin E, vitamin C, and beta-carotene to neutralize free radicals.	Commonly used in conditions with excessive oxidative stress, such as COPD and neurodegenerative diseases.	Directly reacts with free radicals to reduce oxidative stress and protect cells from damage.	Sorriento et al., 2018; Ashok et al., 2022
Mitochondrial targeting strategies	Strategies focusing on protecting or repairing mitochondrial function to reduce oxidative stress.	Emerging approach in diseases like neurodegenerative disorders where mitochondrial dysfunction is prominent.	Involves enhancing mitochondrial resilience to oxidative stress or repairing oxidative damage.	Cobley et al., 2018; Gonçalves and Romeiro, 2019
Machine learning in drug discovery	Integration of machine learning techniques to accelerate the identification and development of new therapeutic agents.	Applied in the discovery of novel drugs for treating oxidative stress-related conditions.	Improves efficiency and accuracy in identifying potential therapeutic compounds.	Vassalle et al., 2020
NRF2 synthesis enhancement	Enhancing the synthesis of NRF2 or inhibiting its degradation.	Investigated in various oxidative stress-related conditions for its antioxidant role.	NRF2 regulates the expression of antioxidant genes, thus protecting cells from oxidative damage.	Forman and Zhang, 2021
Antioxidant lipid peptides (via 3D-QSAR CoMSIA)	Identification of antioxidant lipid peptides through computational models.	A novel approach in antioxidant therapy, potentially applicable in various diseases.	Aims to optimize antioxidant properties of peptides for therapeutic use.	Forman and Zhang, 2021

7.1 Development of diagnostic tools

In recent years, oxidative stress biomarkers, particularly 8-OHdG, have received considerable attention due to their role in indicating oxidative DNA damage. This has been identified as a key biomarker of oxidative stress and has been shown to play an important role in the process of cancer development. Systematic reviews evaluating the assessment of 8-OHdG in various biological samples, including urine, have highlighted its utility in monitoring oxidative stress under different health conditions (Valavanidis et al., 2009; Graille et al., 2020). Further research has demonstrated the versatility of 8-OHdG in reflecting oxidative damage in occupational settings, particularly among workers exposed to nanomaterials (Omari Shekaftik and Nasirzadeh, 2021). Advanced methods for measuring 8-OHdG have been developed, such as the combination of terbium oxide nanoparticles and reduced graphene oxide, demonstrating progress in sensitive detection techniques for this biomarker (Manavalan et al., 2018).

Additionally, a non-invasive method for measuring another oxidative stress biomarker, 8-hydroxyguanine, in saliva, has been reported using high-performance liquid chromatography with electrochemical detection (HPLC-ECD). This method offers a simple and cost-effective option for monitoring oxidative stress (Kawai et al., 2018). In the context of specific diseases, MDA and 8-OHdG have been reported as reliable biomarkers of oxidative stress in ischemic stroke. The presence of these biomarkers in extracellular space, cerebrospinal fluid, and blood further validates their potential in diagnosing and monitoring neurodegenerative diseases (Tugasworo et al., 2023).

This new evidence on oxidative stress diagnostic tools, particularly focusing on 8-OHdG and related biomarkers, can provide important references for your review, offering comprehensive views on the current status and future prospects of oxidative stress diagnostics.

7.2 Innovation in treatment methods

In recent years, there have been numerous innovative treatment approaches in the field of oxidative stress-related diseases, aiming to alleviate oxidative stress through different mechanisms for the treatment or prevention of such diseases.

Nuclear factor erythroid 2-related factor 2, a key transcription factor within cells, protects cells from oxidative damage by regulating the expression of antioxidant genes. Studies have found that enhancing the synthesis of NRF2 or inhibiting its degradation could serve as a potential antioxidant treatment approach. Additionally, using non-toxic electrophiles to alkylate KEAP1 has also emerged as an important therapeutic means (Forman and Zhang, 2021). Furthermore, research has focused on how to prevent and treat diseases by targeting oxidative stress, including the utilization of innovative strategies such as identifying antioxidant lipid peptides through machine learning-integrated 3D-QSAR CoMSIA models (Vassalle et al., 2020).

In cardiovascular diseases, the imbalance of oxidative stress is one of the key factors leading to these diseases. It has been found that antioxidant treatment strategies, such as the use of antioxidants and drugs inhibiting oxidative stress generation, can serve as effective methods for treating these diseases (Pavlidis, 2022). Moreover, for neurodegenerative diseases like AD and PD, oxidative stress is considered a key driving factor in the pathological process. Treatment strategies involve the use of

therapeutic agents like hydrogen sulfide to alleviate oxidative stress-induced neurodegeneration (Ienco et al., 2011). Additionally, in the treatment of glioblastoma, researchers are exploring potential therapeutic targets to modulate the extent of oxidative stress. This includes regulating the expression of key proteins like PKM2 to enhance resistance against oxidative stress (Liu S. et al., 2022).

These innovative treatment approaches demonstrate the rapid progress in the field of oxidative stress research, offering new perspectives and possibilities for the treatment of oxidative stress-related diseases. With further research, more innovative treatment strategies may emerge in the future.

7.3 Future strategies for oxidative stress-related diseases treatment

Researchers are exploring multiple novel strategies for the treatment of oxidative stress-related diseases in the future. These include applying machine learning techniques in drug discovery, specifically in the 3D-QSAR CoMSIA model for identifying antioxidant lipid peptides, which can improve the efficiency of antioxidant identification and design (Vassalle et al., 2020). Additionally, drugs targeting specific diseases such as Ebselen are being developed for inhibiting lung cancer cell growth through cell cycle arrest and cell death, as well as depleting glutathione (Vassalle et al., 2020). New anti-inflammatory and analgesic drugs such as LQFM291 have demonstrated their anti-inflammatory and analgesic effects, as well as good safety and toxicological properties (Vassalle et al., 2020). In intensive care units, the use of antioxidants has shown potential in counteracting oxidative stress (Vassalle et al., 2020). The regulation of ROS during wound healing process has also been shown to be an effective therapeutic pathway for promoting healing (Wang et al., 2023). Mitochondria-targeted therapeutic strategies, such as using light-sensitive NO-releasing molecules, are being studied for regulating mitochondrial oxidative stress (Yamada et al., 2020). Finally, modulating the role of oxidative stress in cancer and inflammation by controlling the production of endogenous ROS during tumor growth is a research focus (Fang et al., 2009). These studies demonstrate the innovative trends and potential strategies in the field of oxidative stress treatment, indicating the emergence of more innovative treatment methods in the future.

8 Conclusion

8.1 Summary of main findings

This comprehensive review has extensively explored the significance of oxidative stress in the brain–lung interaction, revealing its crucial role in various diseases. Biomarkers of oxidative stress, particularly 8-OHdG, have played important roles in the diagnosis and monitoring of this process. The medical community is striving to mitigate the impact of oxidative stress through various innovative therapeutic approaches, including drug therapies, machine learning techniques, and mitochondrial-targeted strategies. These findings offer new perspectives on the role of oxidative stress in brain and lung diseases and lay the foundation for future research and clinical interventions.

8.2 Discussion of future research directions

Future research should focus on further understanding the specific mechanisms of oxidative stress in brain–lung interactions and how to more effectively use this information to prevent and treat related diseases: (i) the impact of individual variations on oxidative stress responses should be considered, along with how to adjust treatment plans accordingly; (ii) the discovery and validation of novel biomarkers and the development of new drug delivery systems are also areas worth exploring; (iii) the application of machine learning and artificial intelligence technologies in drug discovery and disease prediction models is an important direction for future research; (iv) there is an urgent need for further research to dissect the molecular and cellular mechanisms that promote brain–lung interactions, with a special emphasis on the role of oxidative stress in mediating these interactions. This includes identifying key oxidative stress pathways common to brain and lung diseases; (v) the development of innovative therapeutic approaches targeting these oxidative stress pathways is expected to become a new treatment modality.

These strategies may include specially designed antioxidant therapies to alleviate oxidative stress in the brain and lungs, and the application of precision medicine approaches to tailor treatment methods according to the individual circumstances of patients. Exploring these areas will greatly promote our understanding of the complex relationship between brain and lung diseases, leading to more effective interventions.

8.3 Clinical and research implications of the review

This review emphasizes the clinical and research significance of oxidative stress in brain and lung diseases. A deeper understanding of oxidative stress can provide new strategies for early diagnosis and treatment of diseases. Furthermore, the mentioned treatment innovations, particularly advancements in drug development and the application of biomarkers, offer clinicians more treatment options and researchers new avenues to explore. These advancements not only help improve the quality of patients' lives but also pave the way for new trends in scientific research.

Author contributions

JK: Conceptualization, Data curation, Formal analysis, Funding acquisition, Investigation, Methodology, Project administration, Resources, Software, Supervision, Validation, Visualization, Writing – original draft, Writing – review & editing. RF: Conceptualization, Data curation, Formal analysis, Funding acquisition, Investigation, Methodology, Project administration, Resources, Software, Supervision, Validation,

Visualization, Writing – original draft. YZ: Conceptualization, Data curation, Formal analysis, Funding acquisition, Investigation, Methodology, Project administration, Resources, Software, Supervision, Validation, Visualization, Writing – original draft. ZJ: Conceptualization, Data curation, Formal analysis, Funding acquisition, Investigation, Methodology, Project administration, Resources, Software, Supervision, Validation, Visualization, Writing – original draft. JZ: Conceptualization, Data curation, Formal analysis, Funding acquisition, Investigation, Methodology, Project administration, Resources, Software, Supervision, Validation, Visualization, Writing – review & editing. HP: Conceptualization, Data curation, Formal analysis, Funding acquisition, Investigation, Methodology, Project administration, Resources, Software, Supervision, Validation, Visualization, Writing – review & editing. QW: Conceptualization, Data curation, Formal analysis, Funding acquisition, Investigation, Methodology, Project administration, Resources, Software, Supervision, Validation, Visualization, Writing – review & editing.

Funding

The author(s) declare financial support was received for the research, authorship, and/or publication of this article. This work was supported by grants from the Central Government Guides Local Science and Technology Development Funds (YDZX2022091).

Conflict of interest

The authors declare that the research was conducted in the absence of any commercial or financial relationships that could be construed as a potential conflict of interest.

Publisher's note

All claims expressed in this article are solely those of the authors and do not necessarily represent those of their affiliated organizations, or those of the publisher, the editors and the reviewers. Any product that may be evaluated in this article, or claim that may be made by its manufacturer, is not guaranteed or endorsed by the publisher.

References

Aboelella, N., Brandle, C., Kim, T., Ding, Z., and Zhou, G. (2021). Oxidative stress in the tumor microenvironment and its relevance to cancer immunotherapy. *Cancers* 13:986. doi: 10.3390/cancers13050986

Alharbi, K., Afzal, O., Almalki, W., Kazmi, I., Javed Shaikh, M., Thangavelu, L., et al. (2022). Nuclear factor-kappa B (NF-κB) inhibition as a therapeutic target for plant nutraceuticals in mitigating inflammatory lung diseases. *Chem. Biol. Interact.* 354:109842. doi: 10.1016/j.cbi.2022.109842

Allen, C. L., and Bayraktutan, U. (2009). Oxidative stress and its role in the pathogenesis of ischaemic stroke. *Int. J. Stroke* 4, 461–470. doi: 10.1111/j.1747-4949.2009.00387.x

Arredondo, F., Echeverry, C., Abin-Carriquiry, J., Blasina, F., Antúnez, K., Jones, D., et al. (2010). After cellular internalization, quercetin causes Nrf2 nuclear translocation, increases glutathione levels, and prevents neuronal death against an oxidative insult. *Free Radic. Biol. Med.* 49, 738–747. doi: 10.1016/j.freeradbiomed.2010.05.020

Arunachalam, K., Anand, K., Palanisamy, S., and Anathy, V. (2022). Editorial: Oxidative stress related to cellular metabolism in lung health and diseases. *Front. Pharmacol.* 13:1015423. doi: 10.3389/fphar.2022.1015423

Ashok, A., Andrabi, S., Mansoor, S., Kuang, Y., Kwon, B., and Labhasetwar, V. (2022). Antioxidant therapy in oxidative stress-induced neurodegenerative diseases: Role of nanoparticle-based drug delivery systems in clinical translation. *Antioxidants* 11:408. doi: 10.3390/antiox11020408

Banerjee, S., Ghosh, S., Mandal, A., Ghosh, N., and Sil, P. (2020). ROS-associated immune response and metabolism: A mechanistic approach with implication of various diseases. *Arch. Toxicol.* 94, 2293–2317. doi: 10.1007/s00204-020-02801-7

Bedard, K., and Krause, K. H. (2007). The NOX family of ROS-generating NADPH oxidases: Physiology and pathophysiology. *Physiol. Rev.* 87, 245–313. doi: 10.1152/physrev.00044.2005

Begum, R., Thota, S., Abdulkadir, A., Kaur, G., Bagam, P., and Batra, S. (2022). NADPH oxidase family proteins: Signaling dynamics to disease management. *Cell Mol. Immunol.* 19, 660–686. doi: 10.1038/s41423-022-00858-1

Bezerra, F., Lanzetti, M., Nesi, R., Nagato, A., Silva, C., Kennedy-Feitosa, E., et al. (2023). Oxidative stress and inflammation in acute and chronic lung injuries. *Antioxidants* 12:548. doi: 10.3390/antiox12030548

Butterfield, D. (2020). Brain lipid peroxidation and Alzheimer disease: Synergy between the butterfield and mattson laboratories. *Ageing Res. Rev.* 64:101049. doi: 10.1016/j.arr.2020.101049

Caliri, A. W., Tommasi, S., and Besaratinia, A. (2021). Relationships among smoking, oxidative stress, inflammation, macromolecular damage, and cancer. Mutation research. *Rev. Mutat. Res.* 787:108365. doi: 10.1016/j.mrrev.2021.108365

Chaudhary, P., Janmeda, P., Docea, A., Yeskaliyeva, B., Abdull Razis, A., Modu, B., et al. (2023). Oxidative stress, free radicals and antioxidants: Potential crosstalk in the pathophysiology of human diseases. *Front. Chem.* 11:1158198. doi: 10.3389/fchem.2023.1158198

Chen, R., Wang, Z., Zhi, Z., Tian, J., Zhao, Y., and Sun, J. (2021). Targeting the TLR4/NF-κB pathway in β-amyloid-stimulated microglial cells: A possible mechanism that oxysophoridine exerts anti-oxidative and anti-inflammatory effects in an in vitro model of Alzheimer's disease. *Brain Res. Bull.* 175, 150–157. doi: 10.1016/j.brainresbull.2021.07.019

Cho, S. J., and Stout-Delgado, H. W. (2020). Aging and lung disease. *Annu. Rev. Physiol.* 82, 433–459. doi: 10.1146/annurev-physiol-021119-034610

Chtourou, Y., Fetoui, H., Garoui el, M., Boudawara, T., and Zeghal, N. (2012). Improvement of cerebellum redox states and cholinergic functions contribute to the beneficial effects of silymarin against manganese-induced neurotoxicity. *Neurochem. Res.* 37, 469–479. doi: 10.1007/s11064-011-0632-x

Cobley, J., Fiorello, M., and Bailey, D. (2018). 13 reasons why the brain is susceptible to oxidative stress. *Redox Biol.* 15, 490–503. doi: 10.1016/j.redox.2018.01.008

Cong, X., Hubmayr, R., Li, C., and Zhao, X. (2017). Plasma membrane wounding and repair in pulmonary diseases. *Am. J. Physiol. Lung. Cell Mol. Physiol.* 312, L371–L391. doi: 10.1152/ajplung.00486.2016

Costanzi, E., Martino, S., Persichetti, E., Tiribuzi, R., Massini, C., Bernardi, G., et al. (2008). Effects of vitamin C on fibroblasts from sporadic Alzheimer's disease patients. *Neurochem. Res.* 33, 2510–2515. doi: 10.1007/s11064-007-9539-y

Dobi, A., Rosanaly, S., Devin, A., Baret, P., Meilhac, O., Harry, G., et al. (2021). Advanced glycation end-products disrupt brain microvascular endothelial cell barrier: The role of mitochondria and oxidative stress. *Microvasc. Res.* 133:104098. doi: 10.1016/j.mvr.2020.104098

Elsayed, W. M., Abdel-Gawad, E.-H. A., Mesallam, D. I., and El-Serafy, T. S. (2020). The relationship between oxidative stress and acute ischemic stroke severity and functional outcome. *Egypt. J. Neurol. Psychiatry Neurosurg.* 56, 1–6.

Fan, Z., Wang, X., Zhang, M., Zhao, C., Mei, C., and Li, P. (2019). Pathway inhibitors attenuated hydrogen peroxide induced damage in neural cells. *Biomed. Res. Int.* 2019:5962014. doi: 10.1155/2019/5962014

Fang, J., Seki, T., and Maeda, H. (2009). Therapeutic strategies by modulating oxygen stress in cancer and inflammation. *Adv. Drug Deliv. Rev.* 61, 290–302. doi: 10.1016/j.addr.2009.02.005

Feitosa, C., da Silva Oliveira, G., do Nascimento Cavalcante, A., Morais Chaves, S., and Rai, M. (2018). Determination of parameters of oxidative stress in vitro models of neurodegenerative diseases-a review. *Curr. Clin. Pharmacol.* 13, 100–109. doi: 10.2174/1574884713666180301091612

Firuzi, O., Miri, R., Tavakkoli, M., and Saso, L. (2011). Antioxidant therapy: Current status and future prospects. *Curr. Med. Chem.* 18, 3871–3888. doi: 10.2174/092986711803414368

Forman, H. J., and Zhang, H. (2021). Targeting oxidative stress in disease: Promise and limitations of antioxidant therapy. *Nat. Rev. Drug Discov.* 20, 689–709. doi: 10.1038/s41573-021-00233-1

Franco, R., and Vargas, M. R. (2018). Redox biology in neurological function, dysfunction, and aging. *Antioxid. Redox Signal.* 28, 1583–1586. doi: 10.1089/ars.2018.7509

Franzoni, F., Scarfò, G., Guidotti, S., Fusi, J., Asomov, M., and Pruneti, C. (2021). Oxidative stress and cognitive decline: The neuroprotective role of natural antioxidants. *Front. Neurosci.* 15:729757. doi: 10.3389/fnins.2021.729757

Fujioka, S., Niu, J., Schmidt, C., Sclabas, G., Peng, B., Uwagawa, T., et al. (2004). NF-kappaB and AP-1 connection: Mechanism of NF-kappaB-dependent regulation of AP-1 activity. *Mol. Cell Biol.* 24, 7806–7819. doi: 10.1128/MCB.24.17.7806-7819.2004

Galiniak, S., Rohovyk, N., and Rachel, M. (2023). Biomarkers of nitrosative stress in exhaled breath condensate and serum among patients with cystic fibrosis. *Adv. Med. Sci.* 68, 202–207. doi: 10.1016/j.advms.2023.05.002

Gao, S., Duan, Y., Chen, J., and Wang, J. (2021). Evaluation of blood markers at admission for predicting community acquired pneumonia in chronic obstructive pulmonary disease. *Copd* 18, 557–566. doi: 10.1080/15412555.2021.1976739

Gao, W., Yuan, C., Zhang, J., Li, L., Yu, L., Wiegman, C., et al. (2015). Klotho expression is reduced in COPD airway epithelial cells: Effects on inflammation and oxidant injury. *Clin. Sci.* 129, 1011–1023. doi: 10.1042/CS20150273

Gonçalves, P. B., and Romeiro, N. C. (2019). Multi-target natural products as alternatives against oxidative stress in Chronic Obstructive Pulmonary Disease (COPD). *Eur. J. Med. Chem.* 163, 911–931. doi: 10.1016/j.ejmech.2018.12.020

Graille, M., Wild, P., Sauvain, J., Hemmendinger, M., Guseva Canu, I., and Hopf, N. (2020). Urinary 8-OHdG as a biomarker for oxidative stress: A systematic literature review and meta-analysis. *Int. J. Mol. Sci.* 21:3743. doi: 10.3390/ijms21113743

Guo, C., Chen, Q., Chen, J., Yu, J., Hu, Y., Zhang, S., et al. (2020). 8-Hydroxyguanosine as a possible RNA oxidative modification marker in urine from colorectal cancer patients: Evaluation by ultra performance liquid chromatography-tandem mass spectrometry. *J. Chromatogr. B Analyt. Technol. Biomed. Life Sci.* 1136:121931. doi: 10.1016/j.jchromb.2019.121931

Hall, E. D., Vaishnav, R. A., and Mustafa, A. G. (2010). Antioxidant therapies for traumatic brain injury. *Neurotherapeutics* 7, 51–61. doi: 10.1016/j.nurt.2009.10.021

Hall, E. D., Wang, J. A., Miller, D. M., Cebak, J. E., and Hill, R. L. (2019). Newer pharmacological approaches for antioxidant neuroprotection in traumatic brain injury. *Neuropharmacology* 145, 247–258. doi: 10.1016/j.neuropharm.2018.08.005

Hecker, L. (2018). Mechanisms and consequences of oxidative stress in lung disease: Therapeutic implications for an aging populace. *Am. J. Physiol. Lung. Cell Mol. Physiol.* 314, L642–L653. doi: 10.1152/ajplung.00275.2017

Hill, R. L., Singh, I. N., Wang, J. A., and Hall, E. D. (2017). Time courses of post-injury mitochondrial oxidative damage and respiratory dysfunction and neuronal cytoskeletal degradation in a rat model of focal traumatic brain injury. *Neurochem. Int.* 111, 45–56. doi: 10.1016/j.neuint.2017.03.015

Ienco, E., LoGerfo, A., Carlesi, C., Orsucci, D., Ricci, G., Mancuso, M., et al. (2011). Oxidative stress treatment for clinical trials in neurodegenerative diseases. *J. Alzheimers Dis.* 24(Suppl. 2), 111–126. doi: 10.3233/JAD-2011-110164

Iqbal, M., Kabeer, A., Abbas, Z., Siddiqui, H., Calina, D., Sharifi-Rad, J., et al. (2024). Interplay of oxidative stress, cellular communication and signaling pathways in cancer. *Cell Commun. Signal.* 22:7. doi: 10.1186/s12964-023-01398-5

Jakubczyk, K., Dec, K., Kałduńska, J., Kawczuga, D., Kochman, J., and Janda, K. (2020). Reactive oxygen species - sources, functions, oxidative damage. *Pol. Merkur Lekarski* 48, 124–127.

Jelinek, M., Jurajda, M., and Duris, K. (2021). Oxidative stress in the brain: Basic concepts and treatment strategies in stroke. *Antioxidants* 10:1886. doi: 10.3390/antiox10121886

Katsi, V., Marketou, M., Maragkoudakis, S., Didagelos, M., Charalambous, G., Parthenakis, F., et al. (2020). Blood-brain barrier dysfunction: The undervalued frontier of hypertension. *J. Hum. Hypertens.* 34, 682–691. doi: 10.1038/s41371-020-0352-2

Kawai, K., Kasai, H., Li, Y., Kawasaki, Y., Watanabe, S., Ohta, M., et al. (2018). Measurement of 8-hydroxyguanine as an oxidative stress biomarker in saliva by HPLC-ECD. *Genes Environ.* 40:5. doi: 10.1186/s41021-018-0095-2

Kim, G., Kim, J., Rhie, S., and Yoon, S. (2015). The role of oxidative stress in neurodegenerative diseases. *Exp. Neurobiol.* 24, 325–340. doi: 10.5607/en.2015.24.4.325

Kim, G., Weiss, S., and Levine, R. (2014). Methionine oxidation and reduction in proteins. *Biochim. Biophys. Acta* 1840, 901–905. doi: 10.1016/j.bbagen.2013.04.038

Kim, J. W., Lee, J. Y., Oh, M., and Lee, E. W. (2023). An integrated view of lipid metabolism in ferroptosis revisited via lipidomic analysis. *Exp. Mol. Med.* 55, 1620–1631. doi: 10.1038/s12276-023-01077-y

Kontush, K., and Schekatolina, S. (2004). Vitamin E in neurodegenerative disorders: Alzheimer's disease. *Ann. N. Y. Acad. Sci.* 1031, 249–262. doi: 10.1196/annals.1331.025

Kurtz, D. (2004). Microbial detoxification of superoxide: The non-heme iron reductive paradigm for combating oxidative stress. *Acc. Chem. Res.* 37, 902–908. doi: 10.1021/ar0200091

Lee, K. H., Cha, M., and Lee, B. H. (2020). Neuroprotective effect of antioxidants in the brain. *Int. J. Mol. Sci.* 21:7152. doi: 10.3390/ijms21197152

Leichtle, S., Sarma, A., Strein, M., Yajnik, V., Rivet, D., Sima, A., et al. (2020). High-dose intravenous ascorbic acid: Ready for prime time in traumatic brain injury? *Neurocrit. Care* 32, 333–339. doi: 10.1007/s12028-019-00829-x

Leistner, C., and Menke, A. (2020). Hypothalamic-pituitary-adrenal axis and stress. *Handb. Clin. Neurol.* 175, 55–64. doi: 10.1016/b978-0-444-64123-6.00004-7

Lingappan, K. (2018). NF-κB in oxidative stress. *Curr. Opin. Toxicol.* 7, 81–86. doi: 10.1016/j.cotox.2017.11.002

Liu, K., Hua, S., and Song, L. (2022). PM2.5 exposure and asthma development: The key role of oxidative stress. *Oxid. Med. Cell.Longev.* 2022:3618806. doi: 10.1155/2022/3618806

Liu, S., Dong, L., Shi, W., Zheng, Z., Liu, Z., Meng, L., et al. (2022). Potential targets and treatments affect oxidative stress in gliomas: An overview of molecular mechanisms. *Front. Pharmacol.* 13:921070. doi: 10.3389/fphar.2022.921070

Liu, Y., Li, H., Ouyang, Y., Zhang, Y., and Pan, P. (2023). Exploration of the role of oxidative stress-related genes in LPS-induced acute lung injury via bioinformatics and experimental studies. *Sci. Rep.* 13:21804. doi: 10.1038/s41598-023-49165-3

Liu, Z., Zhou, T., Ziegler, A., Dimitrion, P., and Zuo, L. (2017). Oxidative stress in neurodegenerative diseases: From molecular mechanisms to clinical applications. *Oxid. Med. Cell Longev.* 2017:2525967. doi: 10.1155/2017/2525967

Lovell, M. A., and Markesbery, W. R. (2007). Oxidative DNA damage in mild cognitive impairment and late-stage Alzheimer's disease. *Nucleic Acids Res.* 35, 7497–7504. doi: 10.1093/nar/gkm821

Lushchak, V. (2014). Free radicals, reactive oxygen species, oxidative stress and its classification. *Chem. Biol. Interact.* 224, 164–175. doi: 10.1016/j.cbi.2014.10.016

Lushchak, V. I. (2015). Free radicals, reactive oxygen species, oxidative stresses and their classifications. *Ukr. Biochem. J.* 87, 11–18. doi: 10.15407/ubj87.06.011

Manavalan, S., Rajaji, U., Chen, S. M., Govindasamy, M., Chen, T. W., Ali, M. A., et al. (2018). Determination of 8-hydroxy-2′-deoxyguanosine oxidative stress biomarker using dysprosium oxide nanoparticles@ reduced graphene oxide. *Inorg. Chem. Front.* 5, 2885–2892.

Mansour, O. Y., Megahed, M. M., and Elghany, E. H. S. (2015). Acute ischemic stroke prognostication, comparison between Glasgow Coma Score, NIHS scale and full outline of unresponsiveness score in intensive care unit. *Alexandria J. Med.* 51, 247–253. doi: 10.1016/j.ajme.2014.10.002

Manzanero, S., Santro, T., and Arumugam, T. V. (2013). Neuronal oxidative stress in acute ischemic stroke: Sources and contribution to cell injury. *Neurochem. Int.* 62, 712–718. doi: 10.1016/j.neuint.2012.11.009

Maselli, R., Grembiale, R., Pelaia, G., and Cuda, G. (2002). Oxidative stress and lung diseases. *Monaldi Arch. Chest Dis.* 57, 180–181.

Mastruzzo, C., Crimi, N., and Vancheri, C. (2002). Role of oxidative stress in pulmonary fibrosis. *Monaldi Arch. Chest Dis.* 57, 173–176.

Mendioroz, M., Fernández-Cadenas, I., Rosell, A., Delgado, P., Domingues-Montanari, S., Ribó, M., et al. (2011). Osteopontin predicts long-term functional outcome among ischemic stroke patients. *J. Neurol.* 258, 486–493. doi: 10.1007/s00415-010-5785-z

Méthy, D., Bertrand, N., Prigent-Tessier, A., Stanimirovic, D., Beley, A., and Marie, C. (2004). Differential MnSOD and HO-1 expression in cerebral endothelial cells in response to sublethal oxidative stress. *Brain Res.* 1003, 151–158. doi: 10.1016/j.brainres.2003.12.031

Michaeloudes, C., Abubakar-Waziri, H., Lakhdar, R., Raby, K., Dixey, P., Adcock, I., et al. (2022). Molecular mechanisms of oxidative stress in asthma. *Mol. Aspects Med.* 85:101026. doi: 10.1016/j.mam.2021.101026

Morgan, M. J., and Liu, Z. G. (2011). Crosstalk of reactive oxygen species and NF-κB signaling. *Cell Res.* 21, 103–115. doi: 10.1038/cr.2010.178

Morris, G., Gevezova, M., Sarafian, V., and Maes, M. (2022). Redox regulation of the immune response. *Cell Mol. Immunol.* 19, 1079–1101. doi: 10.1038/s41423-022-00902-0

Mumby, S., and Adcock, I. M. (2022). Recent evidence from omic analysis for redox signalling and mitochondrial oxidative stress in COPD. *J. Inflamm.* 19:10. doi: 10.1186/s12950-022-00308-9

Mythri, R., Venkateshappa, C., Harish, G., Mahadevan, A., Muthane, U., Yasha, T., et al. (2011). Evaluation of markers of oxidative stress, antioxidant function and astrocytic proliferation in the striatum and frontal cortex of Parkinson's disease brains. *Neurochem. Res.* 36, 1452–1463. doi: 10.1007/s11064-011-0471-9

Niedzielska, E., Smaga, I., Gawlik, M., Moniczewski, A., Stankowicz, P., Pera, J., et al. (2016). Oxidative stress in neurodegenerative diseases. *Mol. Neurobiol.* 53, 4094–4125. doi: 10.1007/s12035-015-9337-5

Nucera, F., Mumby, S., Paudel, K., Dharwal, V., Di Stefano, A., Casolaro, V., et al. (2022). Role of oxidative stress in the pathogenesis of COPD. *Minerva Med.* 113, 370–404. doi: 10.23736/S0026-4806.22.07972-1

Ohl, K., Tenbrock, K., and Kipp, M. (2016). Oxidative stress in multiple sclerosis: Central and peripheral mode of action. *Exp. Neurol.* 277, 58–67. doi: 10.1016/j.expneurol.2015.11.010

Omari Shekaftik, S., and Nasirzadeh, N. (2021). 8-Hydroxy-2′-deoxyguanosine (8-OHdG) as a biomarker of oxidative DNA damage induced by occupational exposure to nanomaterials: A systematic review. *Nanotoxicology* 15, 850–864. doi: 10.1080/17435390.2021.1936254

Otoupalova, E., Smith, S., Cheng, G., and Thannickal, V. (2020). Oxidative stress in pulmonary fibrosis. *Compr. Physiol.* 10, 509–547. doi: 10.1002/cphy.c190017

Pall, M. L., and Levine, S. (2015). Nrf2, a master regulator of detoxification and also antioxidant, anti-inflammatory and other cytoprotective mechanisms, is raised by health promoting factors. *Sheng Li Xue Bao* 67, 1–18.

Palma-Gudiel, H., Prather, A., Lin, J., Oxendine, J., Guintivano, J., Xia, K., et al. (2021). HPA axis regulation and epigenetic programming of immune-related genes in chronically stressed and non-stressed mid-life women. *Brain Behav. Immun.* 92, 49–56. doi: 10.1016/j.bbi.2020.11.027

Pavlidis, G. (2022). Oxidative stress and antioxidant therapy in cardiovascular diseases-clinical challenge. *J. Clin. Med.* 11:3784. doi: 10.3390/jcm11133784

Pinzaru, A., Mihai, C., Chisnoiu, T., Pantazi, A., Lupu, V., Kassim, M., et al. (2023). Oxidative stress biomarkers in cystic fibrosis and cystic fibrosis-related diabetes in children: A literature review. *Biomedicines* 11:2671. doi: 10.3390/biomedicines11102671

Pisoschi, A. M., and Pop, A. (2015). The role of antioxidants in the chemistry of oxidative stress: A review. *Eur. J. Med. Chem.* 97, 55–74. doi: 10.1016/j.ejmech.2015.04.040

Praticò, D., Clark, C., Lee, V., Trojanowski, J., Rokach, J., and FitzGerald, G. (2000). Increased 8,12-iso-iPF2alpha-VI in Alzheimer's disease: Correlation of a noninvasive index of lipid peroxidation with disease severity. *Ann. Neurol.* 48, 809–812.

Qian, Y., Gao, C., Zhao, X., Song, Y., Luo, H., An, S., et al. (2020). Fingolimod attenuates lung injury and cardiac dysfunction after traumatic brain injury. *J. Neurotrauma.* 37, 2131–2140. doi: 10.1089/neu.2019.6951

Quijano, C., Castro, L., Peluffo, G., Valez, V., and Radi, R. (2007). Enhanced mitochondrial superoxide in hyperglycemic endothelial cells: Direct measurements and formation of hydrogen peroxide and peroxynitrite. *Am. J. Physiol. Heart Circ. Physiol.* 293, H3404–H3414. doi: 10.1152/ajpheart.00761.2007

Radak, Z., Zhao, Z., Goto, S., and Koltai, E. (2011). Age-associated neurodegeneration and oxidative damage to lipids, proteins and DNA. *Mol. Aspects Med.* 32, 305–315. doi: 10.1016/j.mam.2011.10.010

Rahman, I. (2005). The role of oxidative stress in the pathogenesis of COPD: Implications for therapy. *Treat. Respir. Med.* 4, 175–200. doi: 10.2165/00151829-200504030-00003

Rezatabar, S., Karimian, A., Rameshknia, V., Parsian, H., Majidinia, M., Kopi, T., et al. (2019). RAS/MAPK signaling functions in oxidative stress, DNA damage response and cancer progression. *J. Cell Physiol.* 234, 14951–14965. doi: 10.1002/jcp.28334

Ryter, S. W., and Choi, A. M. (2005). Heme oxygenase-1: Redox regulation of a stress protein in lung and cell culture models. *Antioxid. Redox Signal.* 7, 80–91. doi: 10.1089/ars.2005.7.80

Sá, N., Lima, C., Lino, C., Barbeira, P., Baltazar, L., Santos, D., et al. (2017). Heterocycle thiazole compounds exhibit antifungal activity through increase in the production of reactive oxygen species in the *Cryptococcus neoformans-Cryptococcus gattii* species complex. *Antimicrob. Agents Chemother.* 61, e2700–e2716. doi: 10.1128/AAC.02700-16

Sadowska-Bartosz, I., Adamczyk-Sowa, M., Galiniak, S., Mucha, S., Pierzchala, K., and Bartosz, G. (2013). Oxidative modification of serum proteins in multiple sclerosis. *Neurochem. Int.* 63, 507–516. doi: 10.1016/j.neuint.2013.08.009

Schieber, M., and Chandel, N. S. (2014). ROS function in redox signaling and oxidative stress. *Curr. Biol.* 24, R453–R462. doi: 10.1016/j.cub.2014.03.034

Shen, Q., Hiebert, J., Hartwell, J., Thimmesch, A., and Pierce, J. (2016). Systematic review of traumatic brain injury and the impact of antioxidant therapy on clinical outcomes. *Worldviews Evid. Based Nurs.* 13, 380–389. doi: 10.1111/wvn.12167

Shen, Y., Yang, T., Guo, S., Li, X., Chen, L., Wang, T., et al. (2013). Increased serum ox-LDL levels correlated with lung function, inflammation, and oxidative stress in COPD. *Mediat. Inflamm.* 2013:972347. doi: 10.1155/2013/972347

Sies, H., and Jones, D. P. (2020). Reactive oxygen species (ROS) as pleiotropic physiological signalling agents. *Nat. Rev. Mol. Cell Biol.* 21, 363–383. doi: 10.1038/s41580-020-0230-3

Simon, D. K., and Standaert, D. G. (1999). Neuroprotective therapies. *Med. Clin.* 83, 509–523.

Snezhkina, A., Kudryavtseva, A., Kardymon, O., Savvateeva, M., Melnikova, N., Krasnov, G., et al. (2019). ROS generation and antioxidant defense systems in normal and malignant cells. *Oxid. Med. Cell Longev.* 2019:6175804. doi: 10.1155/2019/6175804

Sokolowska, M., Quesniaux, V., Akdis, C., Chung, K., Ryffel, B., and Togbe, D. (2019). Acute respiratory barrier disruption by ozone exposure in mice. *Front. Immunol.* 10:2169. doi: 10.3389/fimmu.2019.02169

Song, K., Li, Y., Zhang, H., An, N., Wei, Y., Wang, L., et al. (2020). Oxidative stress-mediated blood-brain barrier (BBB) disruption in neurological diseases. *Oxid. Med. Cell. Longev.* 2020, 1–27.

Sorriento, D., De Luca, N., Trimarco, B., and Iaccarino, G. (2018). The antioxidant therapy: New insights in the treatment of hypertension. *Front. Physiol.* 9:258. doi: 10.3389/fphys.2018.00258

Spiers, J. G., Chen, H. J., Sernia, C., and Lavidis, N. A. (2014). Activation of the hypothalamic-pituitary-adrenal stress axis induces cellular oxidative stress. *Front. Neurosci.* 8:456. doi: 10.3389/fnins.2014.00456

Teleanu, D., Niculescu, A., Lungu, I., Radu, C., Vladâcenco, O., Roza, E., et al. (2022). An Overview of oxidative stress, neuroinflammation, and neurodegenerative diseases. *Int. J. Mol. Sci.* 23:5938. doi: 10.3390/ijms23115938

Tóbon-Velasco, J. C., Cuevas, E., and Torres-Ramos, M. A. (2014). Receptor for AGEs (RAGE) as mediator of NF-kB pathway activation in neuroinflammation and oxidative stress. *CNS & Neurol. Disord. Drug Targets* 13, 1615–1626. doi: 10.2174/1871527313666140806144831

Tugasworo, D., Prasetyo, A., Kurnianto, A., Retnaningsih, R., Andhitara, Y., Ardhini, R., et al. (2023). Malondialdehyde (MDA) and 8-hydroxy-2′-deoxyguanosine (8-OHdG) in ischemic stroke: A systematic review. *Egypt. J. Neurol. Psychiatry Neurosurg.* 59:87.

Tung, E., Philbrook, N., Macdonald, K., and Winn, L. (2012). DNA double-strand breaks and DNA recombination in benzene metabolite-induced genotoxicity. *Toxicol. Sci.* 126, 569–577. doi: 10.1093/toxsci/kfs001

Valavanidis, A., Vlachogianni, T., and Fiotakis, C. (2009). 8-hydroxy-2′-deoxyguanosine (8-OHdG): A critical biomarker of oxidative stress and carcinogenesis. *J. Environ. Sci. Health C Environ. Carcinog. Ecotoxicol. Rev.* 27, 120–139. doi: 10.1080/10590500902885684

Vassalle, C., Maltinti, M., and Sabatino, L. (2020). Targeting oxidative stress for disease prevention and therapy: Where do we stand, and where do we go from here. *Molecules* 25:2653. doi: 10.3390/molecules25112653

Vermot, A., Petit-Härtlein, I., Smith, S. M. E., and Fieschi, F. (2021). NADPH Oxidases (NOX): An overview from discovery, molecular mechanisms to physiology and pathology. *Antioxidants* 10:980. doi: 10.3390/antiox10060890

Walters, D., Cho, H., and Kleeberger, S. (2008). Oxidative stress and antioxidants in the pathogenesis of pulmonary fibrosis: A potential role for Nrf2. *Antioxid. Redox Signal.* 10, 321–332. doi: 10.1089/ars.2007.1901

Wang, G., Yang, F., Zhou, W., Xiao, N., Luo, M., and Tang, Z. (2023). The initiation of oxidative stress and therapeutic strategies in wound healing. *Biomed. Pharmacother.* 157:114004. doi: 10.1016/j.biopha.2022.114004

Wang, J., Huang, J., Wang, L., Chen, C., Yang, D., Jin, M., et al. (2017). Urban particulate matter triggers lung inflammation via the ROS-MAPK-NF-κB signaling pathway. *J. Thorac. Dis.* 9, 4398–4412. doi: 10.21037/jtd.2017.09.135

Wiegman, C., Li, F., Ryffel, B., Togbe, D., and Chung, K. (2020). Oxidative stress in ozone-induced chronic lung inflammation and emphysema: A facet of chronic obstructive pulmonary disease. *Front. Immunol.* 11:1957. doi: 10.3389/fimmu.2020.01957

Wiegman, C., Michaeloudes, C., Haji, G., Narang, P., Clarke, C., Russell, K., et al. (2015). Oxidative stress-induced mitochondrial dysfunction drives inflammation and airway smooth muscle remodeling in patients with chronic obstructive pulmonary disease. *J. Allergy Clin. Immunol.* 136, 769–780. doi: 10.1016/j.jaci.2015.01.046

Wu, Y., Hu, Q., Cheng, H., Yu, J., Gao, L., and Gao, G. (2023). USP30 impairs mitochondrial quality control and aggravates oxidative damage after traumatic brain injury. *Biochem. Biophys. Res. Commun.* 671, 58–66. doi: 10.1016/j.bbrc.2023.05.069

Xu, K., Zhang, L., Yu, N., Ren, Z., Wang, T., Zhang, Y., et al. (2023). Effects of advanced glycation end products (AGEs) on the differentiation potential of primary

stem cells: A systematic review. *Stem Cell Res. Ther.* 14:74. doi: 10.1186/s13287-023-03324-5

Yamada, Y., Takano, Y., Satrialdi, Abe, J., Hibino, M., and Harashima, H. (2020). Therapeutic strategies for regulating mitochondrial oxidative stress. *Biomolecules* 10:83. doi: 10.3390/biom10010083

Yan, W., Wang, H. D., Hu, Z. G., Wang, Q. F., and Yin, H. X. (2008). Activation of Nrf2-ARE pathway in brain after traumatic brain injury. *Neurosci. Lett.* 431, 150–154. doi: 10.1016/j.neulet.2007.11.060

Yanagi, S., Tsubouchi, H., Miura, A., Matsuo, A., Matsumoto, N., and Nakazato, M. (2017). The impacts of cellular senescence in elderly pneumonia and in age-related lung diseases that increase the risk of respiratory infections. *Int. J. Mol. Sci.* 18:503. doi: 10.3390/ijms18030503

Yang, Y., Bazhin, A. V., Werner, J., and Karakhanova, S. (2013). Reactive oxygen species in the immune system. *Int. Rev. Immunol.* 32, 249–270. doi: 10.3109/08830185.2012.755176

Yaribeygi, H., Panahi, Y., Javadi, B., and Sahebkar, A. (2018). The underlying role of oxidative stress in neurodegeneration: A mechanistic review. *CNS Neurol Disord. Drug Targets* 17, 207–215. doi: 10.2174/1871527317666180425122557

Zarkovic, N. (2020). Roles and functions of ROS and RNS in cellular physiology and pathology. *Cells* 9:767. doi: 10.3390/cells9030767

Zhang, F., Lau, S. S., and Monks, T. J. (2011). The cytoprotective effect of N-acetyl-L-cysteine against ROS-induced cytotoxicity is independent of its ability to enhance glutathione synthesis. *Toxicol. Sci.* 120, 87–97. doi: 10.1093/toxsci/kfq364

Ziaka, M., and Exadaktylos, A. (2021). Brain-lung interactions and mechanical ventilation in patients with isolated brain injury. *Crit. Care* 25:358.

Zinellu, E., Zinellu, A., Fois, A., Pau, M., Scano, V., Piras, B., et al. (2021). Oxidative stress biomarkers in chronic obstructive pulmonary disease exacerbations: A systematic review. *Antioxidants* 10:710. doi: 10.3390/antiox10050710

frontiers | Frontiers in Aging Neuroscience

TYPE Original Research
PUBLISHED 21 May 2024
DOI 10.3389/fnagi.2024.1393351

OPEN ACCESS

EDITED BY
Caroline Haikal,
NewYork-Presbyterian, United States

REVIEWED BY
Kemal Ugur Tufekci,
Izmir Democracy University, Türkiye
Anna Vilalta,
Minoryx Therapeutics SL, Spain

*CORRESPONDENCE
Po-Wah So
✉ po-wah.so@kcl.ac.uk

RECEIVED 28 February 2024
ACCEPTED 26 April 2024
PUBLISHED 21 May 2024

CITATION
Ashraf AA, Aljuhani M, Hubens CJ, Jeandriens J, Parkes HG, Geraki K, Mahmood A, Herlihy AH and So P-W (2024) Inflammation subsequent to mild iron excess differentially alters regional brain iron metabolism, oxidation and neuroinflammation status in mice. *Front. Aging Neurosci.* 16:1393351. doi: 10.3389/fnagi.2024.1393351

Inflammation subsequent to mild iron excess differentially alters regional brain iron metabolism, oxidation and neuroinflammation status in mice

Azhaar Ahmad Ashraf[1], Manal Aljuhani[1], Chantal J. Hubens[1], Jérôme Jeandriens[1,2], Harold G. Parkes[1], Kalotina Geraki[3], Ayesha Mahmood[1], Amy H. Herlihy[4] and Po-Wah So[1]*

[1]Department of Neuroimaging, Institute of Psychiatry, Psychology and Neuroscience, King's College London, London, United Kingdom, [2]Department of Human Biology and Toxicology, Faculty of Medicine, University of Mons, Mons, Belgium, [3]Diamond Light Source, Harwell Science and Innovation Campus, Didcot, United Kingdom, [4]Perspectum Diagnostics Ltd., Oxford, United Kingdom

Iron dyshomeostasis and neuroinflammation, characteristic features of the aged brain, and exacerbated in neurodegenerative disease, may induce oxidative stress-mediated neurodegeneration. In this study, the effects of potential priming with mild systemic iron injections on subsequent lipopolysaccharide (LPS)-induced inflammation in adult C57Bl/6J mice were examined. After cognitive testing, regional brain tissues were dissected for iron (metal) measurements by total reflection X-ray fluorescence and synchrotron radiation X-Ray fluorescence-based elemental mapping; and iron regulatory, ferroptosis-related, and glia-specific protein analysis, and lipid peroxidation by western blotting. Microglial morphology and astrogliosis were assessed by immunohistochemistry. Iron only treatment enhanced cognitive performance on the novel object location task compared with iron priming and subsequent LPS-induced inflammation. LPS-induced inflammation, with or without iron treatment, attenuated hippocampal heme oxygenase-1 and augmented 4-hydroxynonenal levels. Conversely, in the cortex, elevated ferritin light chain and xCT (light chain of System X_c^-) were observed in response to LPS-induced inflammation, without and with iron-priming. Increased microglial branch/process lengths and astrocyte immunoreactivity were also increased by combined iron and LPS in both the hippocampus and cortex. Here, we demonstrate iron priming and subsequent LPS-induced inflammation led to iron dyshomeostasis, compromised antioxidant function, increased lipid peroxidation and altered neuroinflammatory state in a brain region-dependent manner.

KEYWORDS

iron metabolism, inflammation, lipid peroxidation, cortex, hippocampus, aging, System X_c^-, hyper-ramified microglia

Introduction

Iron is essential for crucial reactions in brain cells, including neurotransmitter, adenosine triphosphate (ATP), and myelin syntheses. If unregulated, excess iron enhances reactive oxygen species (ROS) production and oxidative stress, thus cellular iron levels are under strict homeostatic control. Iron import proteins that regulate cellular iron entry include the

transferrin receptor (TfR) and divalent metal transporter 1 (DMT1) (Ashraf et al., 2018). Excess cellular iron is either sequestered by ferritin in a non-toxic yet bioavailable form or exported out of the cell via ferroportin aided by a ferroxidase, ceruloplasmin. In aging and neurodegenerative diseases, the iron homeostatic cascade appears to be disrupted (Ward et al., 2014). Ferroptosis, a recently discovered form of iron-induced cell death (Dixon et al., 2012), is thought to be a significant contributor to neurodegeneration, including in Alzheimer's disease (AD) (Ashraf and So, 2020; Ashraf et al., 2020).

Previously, we established that iron dyshomeostasis and neuroinflammation are two facets of brain aging in C57Bl/6J mice (Walker et al., 2016; Ashraf et al., 2019a). Iron is known to stimulate microglia via NFκB activation and increase production of pro-inflammatory cytokines (Saleppico et al., 1996). Inflammation can induce iron dyshomeostasis through altering ferritin expression and other players implicated in iron homeostasis (Zhang et al., 2015; Ashraf et al., 2018; Ward et al., 2022). We propose the combination of increasing iron dysregulation and chronic neuroinflammation with aging contributes to advanced age being the major risk factor in neurodegenerative disease. However, the effect of peripheral administration of iron and/or lipopolysaccharide (LPS)-induced inflammation on the young adult mouse brain remains to be understood.

In this study, we initially administered (mild) iron injections into 8-week-old mice. From 8-weeks of age, iron has been shown to enter the mouse brain, albeit relatively slowly and accumulate as brain iron export is minimal (Holmes-Hampton et al., 2012). At this age, the mouse brain has not had the opportunity to accrete iron, or exhibit chronic neuroinflammation, as would be observed in older mice (Walker et al., 2016; Ashraf et al., 2019a). Contrary to previous iron dietary supplementation studies (Sobotka et al., 1996; Malecki et al., 2002), we chose to systemically administer relatively lower iron doses to represent the insidious brain accumulation of iron that is more representative of aging, similar to other previous studies (Maaroufi et al., 2009, 2014). Supplementation of iron via the diet has been as high as 20,000 parts of million (ppm) of carbonyl iron (Sobotka et al., 1996) which approximates to ingestion of 0.86–1.43 mmol iron per day as compared to approximately 0.0002 mmol iron per day as in our and other studies (Maaroufi et al., 2009, 2014). Two weeks after iron treatment, mice underwent a mild LPS dosing regime known to modify brain immunological responses (Ifuku et al., 2012). We induced an inflammatory insult sometime after the systemic iron injections to allow/mimic the accretion of brain iron and subsequent chronic neuroinflammation as seen with aging.

We determined whether proteins involved in iron homeostasis and antioxidation, and lipid peroxidation protein adduct levels were modulated by systemic inflammation/neuroinflammation subsequent to previous acute mild iron doses. Furthermore, we assessed whether iron priming prior to inflammation/neuroinflammation modulates subsequent glial morphology and spatial learning ability. We focused on the hippocampus, cortex and basal ganglia regions, but in particular, the hippocampus and cortex as these regions play major roles in cognition, which is impaired in normal aging and neurodegenerative diseases such as AD (Devanand et al., 2012; Fjell et al., 2014). We also investigated possible changes in the basal ganglia as these brain regions accrete iron to a much greater extent than other brain regions with aging (Hallgren and Sourander, 1958; Ward et al., 2014) and are affected in neurodegenerative diseases (Guan et al., 2022). Prior to brain isolation for metal, western blot and immunohistochemical analyses, mice underwent spatial learning behavioral testing. Total reflection X-ray fluorescence (TXRF) and synchrotron radiation X-ray fluorescence (SRXRF) mapping were used for bulk and spatial iron (metals) analyses, respectively. Ferroptosis-related—iron regulatory and antioxidant proteins, glia-specific proteins, and lipid peroxidation protein adducts were assessed by western blotting. Ionized calcium-binding adaptor molecule 1 (Iba1) and glial fibrillary acidic protein (GFAP) immunohistochemistry, was used to assess microglial morphology and astrogliosis, respectively. Microglia and astroglia are key players in neuroinflammation, and microglial and astroglial measurements were used as putative indicators of neuroinflammation. We hypothesized that iron priming and subsequent neuroinflammation in a normal young mouse model would exhibit protein changes reminiscent of ferroptosis (iron accumulation/dyshomeostasis, impaired antioxidation, lipid peroxidation) in the brain to a greater extent than by systemic iron injections or inflammation alone.

Materials and methods

Animals and treatment

Young male C57Bl/6J mice (3-weeks of age, $n = 56$) were obtained from Envigo (Huntingdon, United Kingdom), housed in pairs on arrival, and acclimatized before experimentation. All experimental procedures were approved by the local ethical review panel of King's College London in accordance with the U.K. Home Office Animals Scientific Procedures Act 1986.

After acclimatization, at 8-weeks of age, mice were injected intraperitoneally with saline ($n = 27$) or 3 mg/kg ferrous sulphate heptahydrate (423731000, Fisher Scientific, Leicestershire, United Kingdom; $n = 29$) daily for 5 days (Maaroufi et al., 2009). Saline- or iron-treated ($n = 5$/group) mice were euthanized two days after the final injection and brains isolated (see below) to study the acute effects of mild iron treatment on the brain (Cohort 1). Similarly, another cohort (saline, $n = 7$; iron-treated, $n = 8$) were killed at three weeks post-dose (aged 12 weeks) and brains isolated (see below) to determine the potential longer term/chronic effect of a single iron treatment (Cohort 2). The remaining saline- or iron-treated mice were subdivided and received either saline (10 mg/kg) or 0.25 mg/kg LPS (L2880, Sigma, Dorset, United Kingdom) intraperitoneally daily for a week, yielding four final groups (Cohort 3): saline only (control group, $n = 7$), iron only ($n = 8$), LPS only ($n = 8$) and iron + LPS group ($n = 8$). Two weeks after the final injection, mice (aged 15-weeks) underwent spatial learning behavioral (cognitive) assessment (see behavior testing) and then brains isolated (see below).

Brains were harvested after exsanguination by transcardial perfusion with phosphate-buffered saline (PBS) under terminal isoflurane-oxygen anesthesia. Hippocampus, cortex, striatum, and substantia nigra were dissected from the right-brain hemisphere and snap-frozen in liquid nitrogen and stored at −80°C for western blotting and TXRF (see below). (Note, the substantia nigra was not dissected out for Cohort 1.) The remaining left-brain hemisphere was fixed in 4% paraformaldehyde in PBS for 48 h before storage in PBS-0.025% sodium azide at 4°C for immunohistochemistry and

SRXRF (see below). An overview of the study design and protocol is shown in Figure 1.

Behavioral (cognitive) testing

Novel object location (NOL) testing was used to evaluate learning and memory in mice, as described previously (Lueptow, 2017). Briefly, testing was performed in an opaque arena (40 cm × 40 cm, and 50 cm high walls), and exposed to light intensity of 50 lux and ambient noise, ~65 dB (supplied by a radio). All behavior trials were recorded using EthoVision XT software (Noldus information technology, VA, United States). Equipment between trials were wiped clean and treated with 0.1% acetic acid to eliminate residual odors.

Mice were placed into the arena and allowed to explore two identical objects for 10 min (training trial) and then returned to their home cage. An hour later, they were re-introduced into the arena after one of the objects had been moved to a novel location and allowed to explore again for 10 min (test trial). The total time each animal spends exploring each object, characterized by active sniffing, or rearing against the object with the nose directed towards the object within 2–3 cm of the object, was recorded. The center-point of the mice defined its position for analysis. We calculated the discrimination index for NOL using Eq. 1:

$$\text{Discrimination index (DI)} = \frac{T_{\text{novel}} - T_{\text{familiar}}}{T_{\text{novel}} + T_{\text{familiar}}} \quad (1)$$

where T_{novel} and T_{familiar} are times spent exploring a novel and familiar location, respectively.

Mice with preserved spatial memory and curiosity will spend more time exploring the object placed in a novel location compared with the familiar location (Lueptow, 2017). A higher discriminatory index (DI) score implies a preference for the novel location, suggesting intact spatial memory and recognition of the change of object location.

Western blotting

For western blotting, lysates of hippocampus, cortex, and striatum were prepared as before (Ashraf et al., 2020), and stored at −80°C until further analysis. Brain lysates (40 µg protein) were mixed with Laemmli buffer (S3401; Sigma, Poole, United Kingdom) and heated (95°C, 5 min). Proteins were separated on NovexTM tris-glycine 4–20% gradient gels (XP04205BOX, Thermo Fisher; 150 V, 90 min), and then transferred onto a 0.45 µm nitrocellulose membrane (GE10600002, GE Healthcare, Amersham, United Kingdom) in tris-glycine buffer supplemented with 20% methanol (80 V, 1 h). Following incubation in a blocking solution (1 h, ambient temperature), membranes were incubated with primary antibodies (overnight, 4°C; Supplementary Table S1) for iron-homeostatic proteins: ferritin-light chain (FTL), ferritin-heavy chain (FTH), transferrin-receptor (TfR), DMT1, iron responsive element binding protein 2 (IRP2), ceruloplasmin, ferroportin, heme-oxygenase-1 (HO-1); for immune

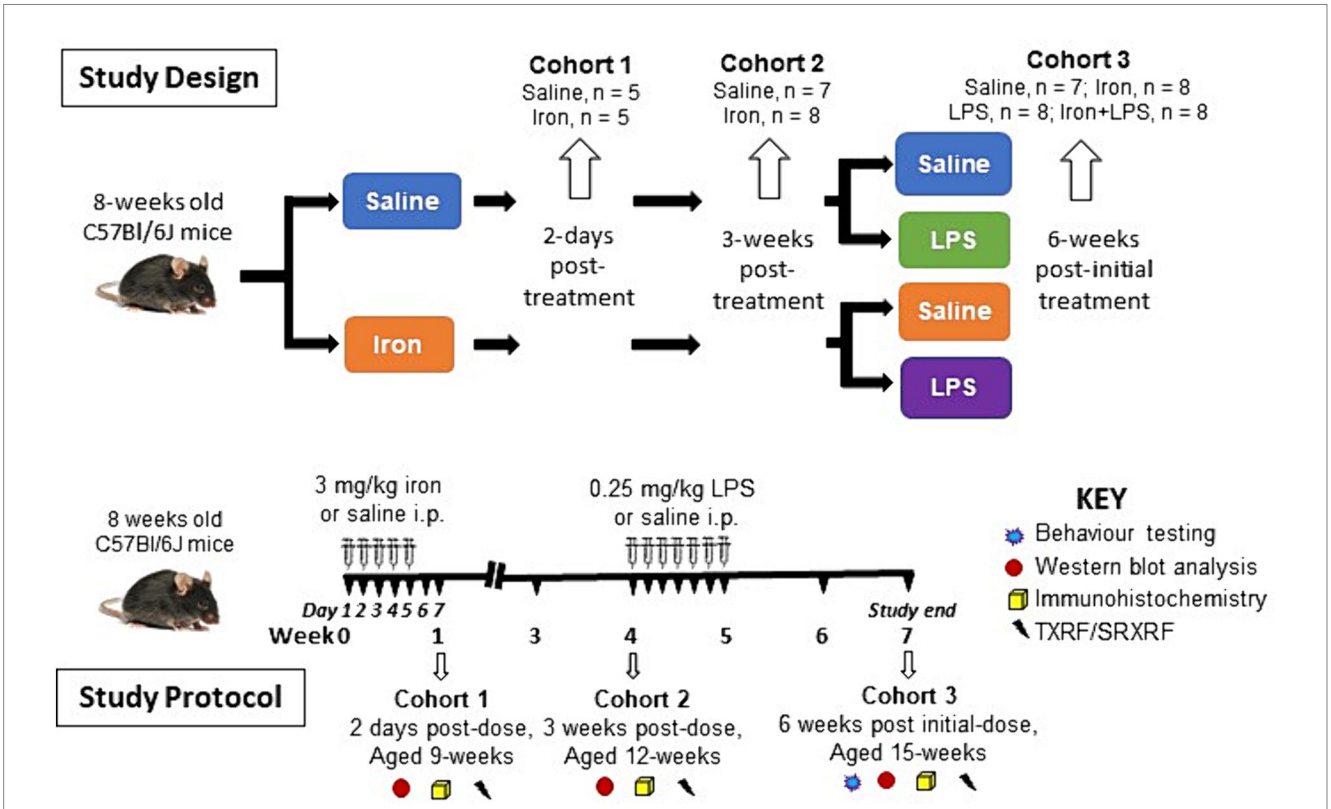

FIGURE 1
Overview of the study design and study protocol. i.p., intraperitoneally; LPS, lipopolysaccharide; SRXRF, synchrotron-radiation X-ray fluorescence; TXRF, total reflection X-ray fluorescence.

cells/inflammation, Iba1, GFAP, NADPH oxidase 2 (NOX2) and triggering receptor expressed on myeloid cells 2 (TREM2); and for ferroptosis, acyl-CoA synthetase long-chain family member 4 (ACSL4), light chain subunit of System X_c^- (xCT), glutathione peroxidase 4 (GPX4) and the lipid-peroxidation marker 4-hydroxynonenal (4-HNE).

After incubation with primary antibodies, protein bands were visualized as described before (Ashraf et al., 2020) with horse-radish peroxidase (HRP)-conjugated secondary antibodies and imaged (BioRad ChemiDoc MP system). For protein quantification, membranes were stripped using Restore Western blot stripping buffer (20159; Thermo Fisher) and re-probed with HRP-conjugated β-actin. Band signal intensities were quantified by densitometry (ImageJ, NIH), and normalized to β-actin.

Total reflection X-ray fluorescence

Brain lysates (hippocampus, cortex and striatum) prepared as detailed above were thawed and diluted 1:5 v/v with Milli-Q distilled water and underwent TXRF as described previously (Ashraf et al., 2020). Briefly, following dilution with polyvinyl alcohol (2 µL, 0.3 g/L water; 843871, Merck, Gillingham, United Kingdom), gallium solution (10 µL, 440 µg/L; TraceCERT® gallium standard for inductive coupled plasma-mass spectrometry; 16639, Merck) was added (final gallium concentration of 200 µg/L). Resultant duplicate samples were placed on acrylic sample carriers for TXRF (PICOFOX, Bruker Nano GmbH, Germany) (Ashraf et al., 2019b). Elemental concentrations of iron, copper and zinc were calculated by reference to the internal gallium standard and normalized to protein concentrations (mg/kg protein) (Ashraf et al., 2020).

Synchrotron radiation X-ray fluorescence

Fixed brain samples were cryoprotected in 30% sucrose in PBS for 48 h and frozen at −20°C before cryosectioning. Cryosections (30 µm thick) were mounted onto 4 µm thick Ultralene film (Spex SamplePrep, NJ, United States) secured to a customized holder and kept at room temperature prior to SRXRF.

Brain cryosections containing the hippocampus, cortex, striatum, and substantia nigra ($n = 4$/group in Cohort 2 and $n = 7$–8/group in Cohort 3) underwent SRXRF at the Diamond Light Source synchrotron radiation facility (microfocus beamline I18; Didcot, United Kingdom), as described previously (Ashraf et al., 2019a). Briefly, cryosections were mounted at a 45° angle with respect to the incoming X-ray beam and the detector, and scanned raster fashion with a beam of 100 µm diameter (resolution) and 11 keV energy. Full energy dispersive spectra were collected for each beam position, deconvolved and areas of the characteristic peaks of iron, zinc, and copper evaluated using PyMca (Solé et al., 2007) to produce elemental metal maps. For quantification, photon flux was estimated by measurement of a reference metal film (AXO, Dresden, GmbH). Regions of interest (ROIs) were placed on the elemental metal maps to obtain metal concentrations (mg/kg) in different brain regions (Supplementary Figure S1).

Immunohistochemistry

Immunohistochemistry was performed in the hippocampus, cortex, striatum and substantia nigra from all mice of all cohorts. Brain cryosections were prepared as detailed for SRXRF, albeit sectioned into wells of 96-well plates containing PBS-0.025% sodium azide (see above) and stored at 4°C prior to analysis. For immunohistochemistry, cryosections were treated with 1% hydrogen peroxide in PBS-0.2% TritonX-100, washed with PBS-0.2% Triton X-100 (2 × 5 min), and blocked in 10% BSA supplemented with PBS-0.2% Triton X-100. Antibodies for Iba1 (microglia, SAB2500042; Sigma) and GFAP (astrocytes; Z0334; DAKO) were incubated overnight (5% BSA in PBS-Triton X-100, 4°C), washed, and then incubated with a secondary biotinylated anti-rabbit antibody (5% BSA in PBS-0.2% Triton X-100, 2 h). Following enhancement with avidin-biotin complex (Vectashield, Vector Laboratories, Burlingame, United States) for 30 min, 3,3′-diaminobenzidine (DAB) was used to develop the staining for 4 min and the reaction was stopped by the addition of distilled water. The sections were then mounted on Superfrost slides (J1800AMNZ; Thermo Fisher Scientific), dehydrated sequentially in 70% ethanol (2 min), 90% ethanol (2 × 2 min), 100% ethanol (2 × 2 min), and xylene before mounting in DPX. Images were acquired with a Leica microscope using a 40× objective connected to a camera using Image-Pro software (National Institutes of Health, Bethesda, Maryland, United States). The stained images were quantified using Fiji/ImageJ software.

Microglial morphology was assessed of Iba1-stained brain tissue section images using the skeletonize plugin for ImageJ (Morrison and Filosa, 2013; Young and Morrison, 2018; Ali et al., 2019). The image of each hemisphere section was skeletonized, and microglial branch endpoints and lengths measured across the image (a cutoff value of 20 for endpoints and lengths was used). The endpoint measure assesses the number of microglial branches or processes, while branch length measures their length. Microglial endpoints and branch lengths were normalized to the microglial soma number to give endpoints/cell and branch length/cell, respectively.

For GFAP-stained brain sections, images were converted to an 8-bit greyscale image, a threshold applied, and then converted to binary format in ImageJ. Signal intensities in an optical field were obtained after applying a thresholding protocol using negative control sections (incubated with secondary antibody only) to identify non-specific background staining. Depending on the brain region analyzed, GFAP-immunoreactivity was analyzed in 2–4 optical fields (Walker et al., 2016).

Statistical analysis

Data normality was assessed using Q-Q, residual, and homoscedasticity plots: values violating these assumptions were identified as outliers and excluded from the analysis.

A two-tailed student's *t*-test was performed on proteins and metals to monitor the acute and chronic effects of saline- and iron-treatment (Cohorts 1 and 2). To correct for multiple *t*-test comparisons, we used an adaptive linear set-up procedure to control the false discovery rate (FDR) at 5%. One-way ANOVA followed by Tukey *post hoc* correction was used to identify the effects of iron only, inflammation only, and

iron-primed inflammation on behavioral performance; levels of iron regulatory, ferroptosis-related, and glial-specific proteins; and metals (Cohort 3). Adjusted p-value ≤0.05 were considered significant.

All statistical analyses were performed using IBM SPSS Statistics 26 and GraphPad Prism 9.

Results

Acute (Cohort 1) and chronic (Cohort 2) effects of iron

Changes in protein, glial cell, and metal measurements at 2 days (Cohort 1) or 3 weeks (Cohort 2) post-iron injection did not surpass FDR-correction in the different brain regions (Supplementary Tables S2–S9).

Effects of iron and/or inflammation treatment (Cohort 3)

The iron only treatment group showed improved NOL performance compared with iron + LPS group ($p = 0.0440$; Figure 2). However, NOL performance was not significantly improved with iron treatment when compared with saline ($p = 0.0924$) or LPS only ($p = 0.1323$) groups.

By western blot analysis, LPS-induced inflammation, with ($p = 0.0061$) or without iron treatment ($p = 0.0149$) was shown to attenuate hippocampal HO-1 compared with saline (Figure 3A and Supplementary Table S10). LPS only group and iron + LPS group demonstrated augmented 4-HNE levels compared with both saline ($p = 0.0462$, $p = 0.0294$, respectively) and iron only groups ($p = 0.0220$, $p = 0.0132$, respectively; Figure 3B and Supplementary Table S10). Hippocampal TREM2 levels were found to be higher in the LPS group compared to both saline ($p = 0.0398$) and iron + LPS ($p = 0.0040$) groups, while the iron + LPS group had lower TREM2 compared to the iron only group ($p = 0.0218$; Figure 3C). The LPS group showed increased levels of Iba1 compared with the saline ($p = 0.0035$) and iron ($p = 0.0247$) groups (Figure 3D). Similarly, LPS group demonstrated augmented levels of GFAP than saline ($p = 0.0174$) and iron ($p = 0.0039$) groups (Figure 3E). None of the other measured proteins were found to be altered by the various treatments (Supplementary Table S10). Similarly, metals—iron, zinc, and copper, as assessed by bulk and spatial analyses, TXRF and SRXRF, were comparable between groups in Cohort 3.

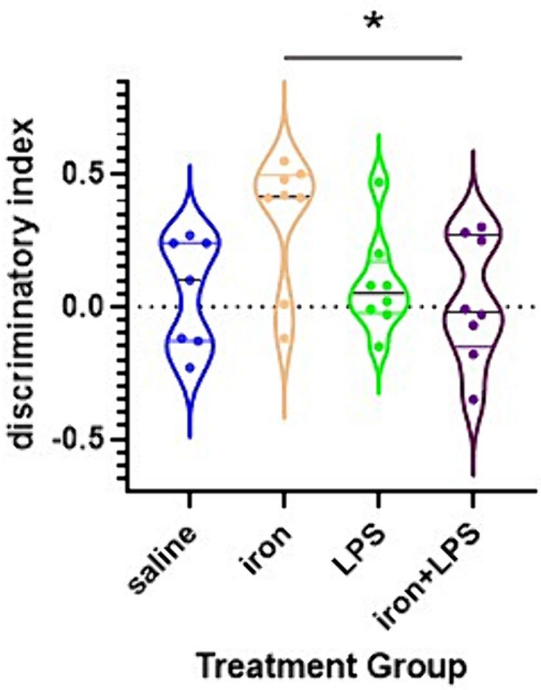

FIGURE 2
Effects of iron-priming and inflammation on the novel object location (NOL) assessment. *$p < 0.05$.

Analysis of Iba-1 stained immunohistochemical stained images revealed longer hippocampal microglial branch length/cell in the iron + LPS group compared with saline ($p = 0.0158$) or iron ($p = 0.0071$) groups (Figures 3F, 4A). Similarly, augmented GFAP-immunoreactivity was observed in the iron + LPS group compared with either saline ($p = 0.0022$) or iron ($p = 0.0251$) groups (Figures 3G, 4B). However, microglial endpoints/cell were similar between groups ($p = 0.25$; Supplementary Table S10).

The cortex exhibited different changes compared with the hippocampus. Cortical FTL was significantly increased in response to LPS-induced inflammation, with $p = 0.0498$ and $p = 0.0343$, when comparing with and without iron priming to the saline group, respectively (Figure 5A). Meanwhile, IRP2 was higher in the iron + LPS group compared to saline ($p = 0.0382$) and iron ($p = 0.0131$; Figure 5B, Supplementary Table S11). Combinatorial iron + LPS treatment increased cortical DMT1 compared to LPS only treatment ($p = 0.0299$, Figure 5C). Increased xCT in the cortex was observed in response to LPS-induced inflammation, without and with iron-priming compared to saline ($p = 0.0464$ and $p = 0.0306$, respectively; Figure 5D). Surprisingly, the lipid peroxidation marker, 4-HNE, was attenuated in the iron + LPS group relative to iron ($p = 0.0274$, Figure 5E). Levels of other proteins or metals measured were similar irrespective of treatments (Supplementary Table S11).

By Iba1-immunohistochemistry, cortical microglial endpoints/cell were found to be comparable between groups ($p = 0.35$, Supplementary Table S11). However, longer microglial branch length/cell was observed in the iron + LPS group compared to saline ($p = 0.0422$) and iron only ($p = 0.0081$) groups (Figure 5F, 6A). Further, cortical GFAP-immunoreactivity was augmented in the iron+LPS group compared to the iron only group ($p = 0.0187$; Figures 5G, 6B).

The response of the striatum to iron and/or LPS treatment was different from that in both the hippocampus and cortex. Striatal ferroportin levels were decreased in response to LPS-induced inflammation without ($p = 0.0315$) and with iron priming ($p = 0.0304$) compared to saline treatment, respectively (Figure 7A). Levels of ACSL4 were increased in the iron + LPS group relative to the iron only group ($p = 0.0474$; Figure 7B and Supplementary Table S12). Striatal microglial endpoints/cell were decreased by iron-treatment compared to the saline group ($p = 0.0315$, Figure 7C). Conversely, microglial branch length/cell were longer in the iron+LPS treated mice compared to those only treated with iron ($p = 0.0038$; Figures 7D, 8A and Supplementary Table S12).

10.3389/fnagi.2024.1393351

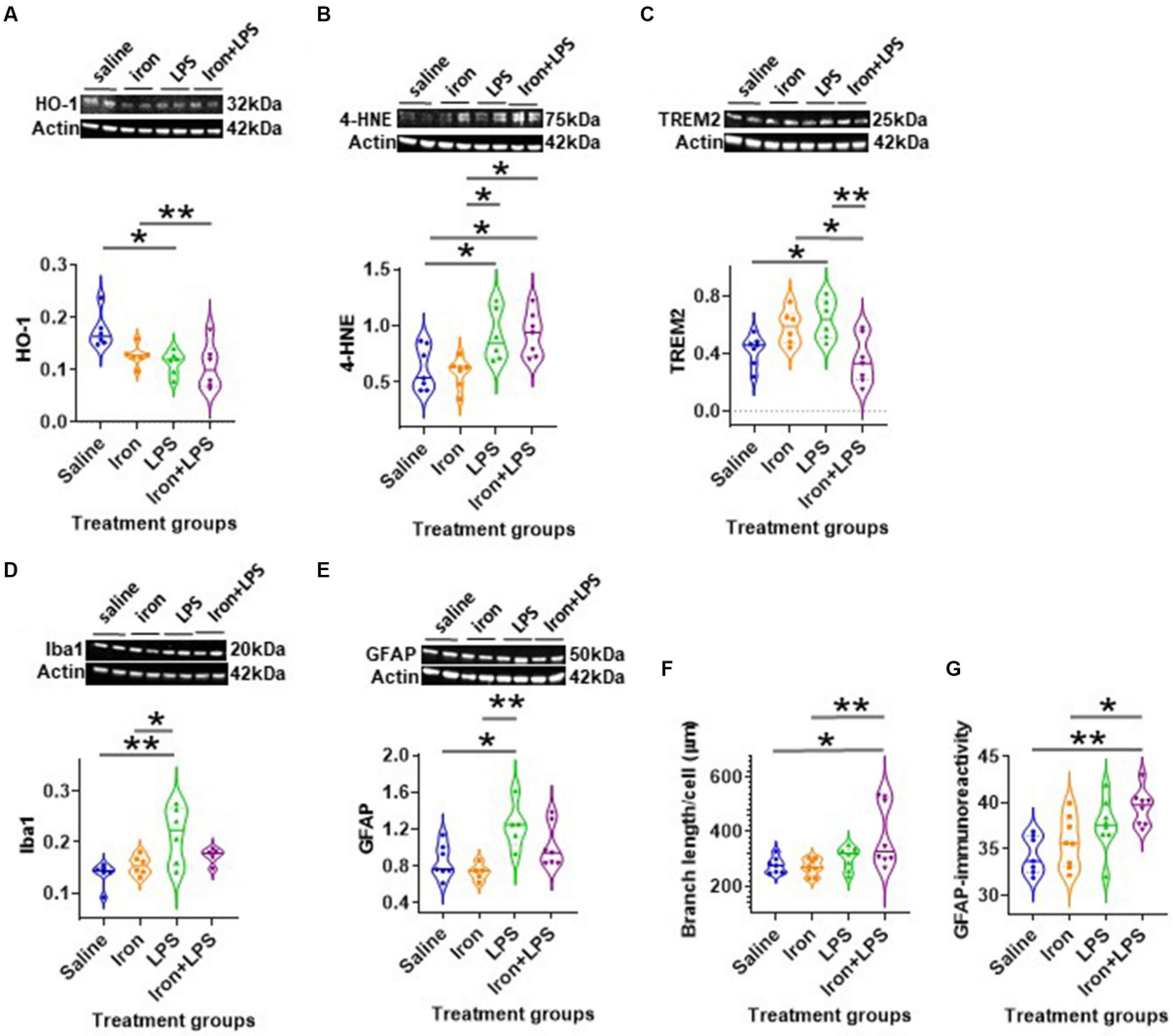

FIGURE 3
Effect of iron-priming and inflammation in the hippocampus (Cohort 3). Western blot analysis of **(A)** Heme oxygenase-1 (HO-1), **(B)** 4-hydroxynonenal (4-HNE), **(C)** triggering receptor expressed on myeloid cells 2 (TREM2), **(D)** ionized calcium-binding adaptor molecule 1 (Iba1) and **(E)** glial fibrillary acidic protein (GFAP). Immunohistochemical analysis of **(F)** microglial branch length/cell (assessed by Iba1 staining) and **(G)** GFAP signal intensity (SI, arbitary units, a.u.). (Proteins used in western blot were normalised against actin). *$p < 0.05$ and **$p < 0.01$. LPS, lipopolysaccharide.

The substantia nigra also exhibited a regional-specific response to iron and/or LPS. Longer nigral microglial branch lengths were observed in the iron + LPS group compared to saline ($p = 0.0004$), iron ($p = 0.0018$), and LPS groups ($p = 0.0403$, Figures 7E, 8B and Supplementary Table S13). However, the microglial endpoints/cell ($p = 0.53$, Supplementary Table S14) and GFAP-immunoreactivity ($p = 0.32$, Supplementary Table S13) were similar between groups. Likewise, metal levels, including iron, were also similar between groups (Supplementary Table S14).

Discussion

We demonstrate iron dyshomeostasis, neuroinflammation, inhibition of System X_c^- (cystine/glutamate antiporter), and modulation of lipid peroxidation in young C57Bl/6J mice exposed to peripheral iron and subsequent LPS-induced inflammation, in a brain region-dependent manner.

We reveal neuroprotective effects from a previous short duration of relatively mild systemic iron treatment in young C57Bl/6J mice (Cohort 3), with improved spatial learning on the NOL task, when compared with mice treated with both iron + LPS. We suggest that mild systemic iron injections in mice led to iron being partitioned beneficially towards fulfilling metabolic demands (e.g., iron-dependent brain maturation processes including synaptogenesis) rather than enhancing the labile iron pool and potentially, inducing iron toxicity via lipid peroxidation and oxidative stress. This is consistent with our molecular findings where iron only treatment demonstrated a significant attenuation of hippocampal lipid peroxidation 7-weeks after iron-treatment compared with iron + LPS and LPS only groups. Lipid peroxidation was assessed by measurement of 4-HNE, a reactive aldehyde that can detrimentally alter signaling pathways in aging (Zhang and Forman, 2017).

The brain is particularly susceptible to lipid peroxidation-mediated oxidative stress due to its high oxygen consumption and lipid-rich content. Mice subjected to LPS-induced inflammation,

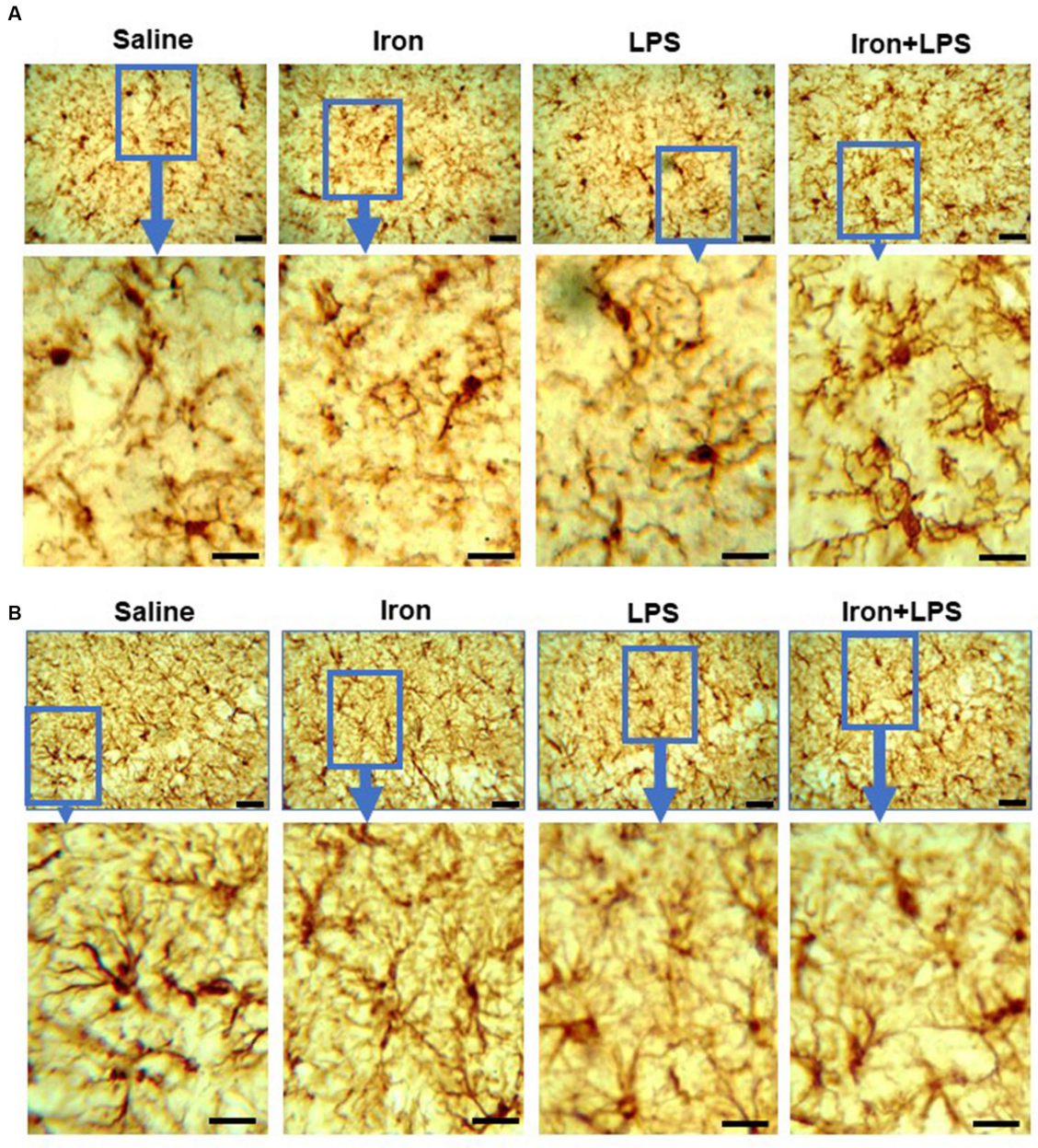

FIGURE 4
Effect of iron-priming and inflammation on micro- and astro-glial morphology in the hippocampus (Cohort 3). **(A)** ionized calcium-binding adaptor molecule 1 and **(B)** glial fibrillary acidic protein immunochemistry. Micrographs were acquired at 40× magnification. Scale bar represents 25 μm (top panels) and 12.5 μm (bottom panels, magnified images). LPS, lipopolysaccharide.

with or without iron-priming, demonstrated augmented lipid peroxidation. This may be attributed to the reduced HO-1 levels observed in LPS-treated mice, irrespective of prior treatment with iron or not. HO-1 is an antioxidant enzyme that catalyzes the detoxification/degradation of heme (from hemoglobin) to ferrous iron (to be sequestered by ferritin), biliverdin/bilirubin (lipid antioxidant), and carbon monoxide (Eskew et al., 1999; Sung et al., 2000; Vanacore et al., 2000; Wu and Hsieh, 2022). HO-1 attenuates the generation of ROS (e.g., superoxide) and lipid peroxidation (Chao et al., 2013), and an integral part of the antioxidant system: HO-1 null mice exhibit increased lipid peroxides (Ishikawa et al., 2012). Diminished HO-1 levels (and enzymatic activity) prevent heme-detoxification and increases heme availability for the generation of ROS, thereby increasing the susceptibility of cells to oxidative stress (Pirota et al., 2016; Righy et al., 2016; Chiabrando et al., 2018).

We showed that LPS only treatment increased hippocampal levels of Iba1 (microglia) and GFAP (astrocytes) compared with saline and iron only treatments. Increased numbers of microglia and astrocytes have been previously demonstrated in response to LPS administration in mice (Ifuku et al., 2012). LPS has been shown to augment pro-inflammatory cytokine secretion from microglia and astrocytes (Godbout et al., 2005; Qin et al., 2007; Henry et al., 2009; Ifuku et al., 2012; Wohleb et al., 2012). LPS likely induces microglia to secrete IL1β

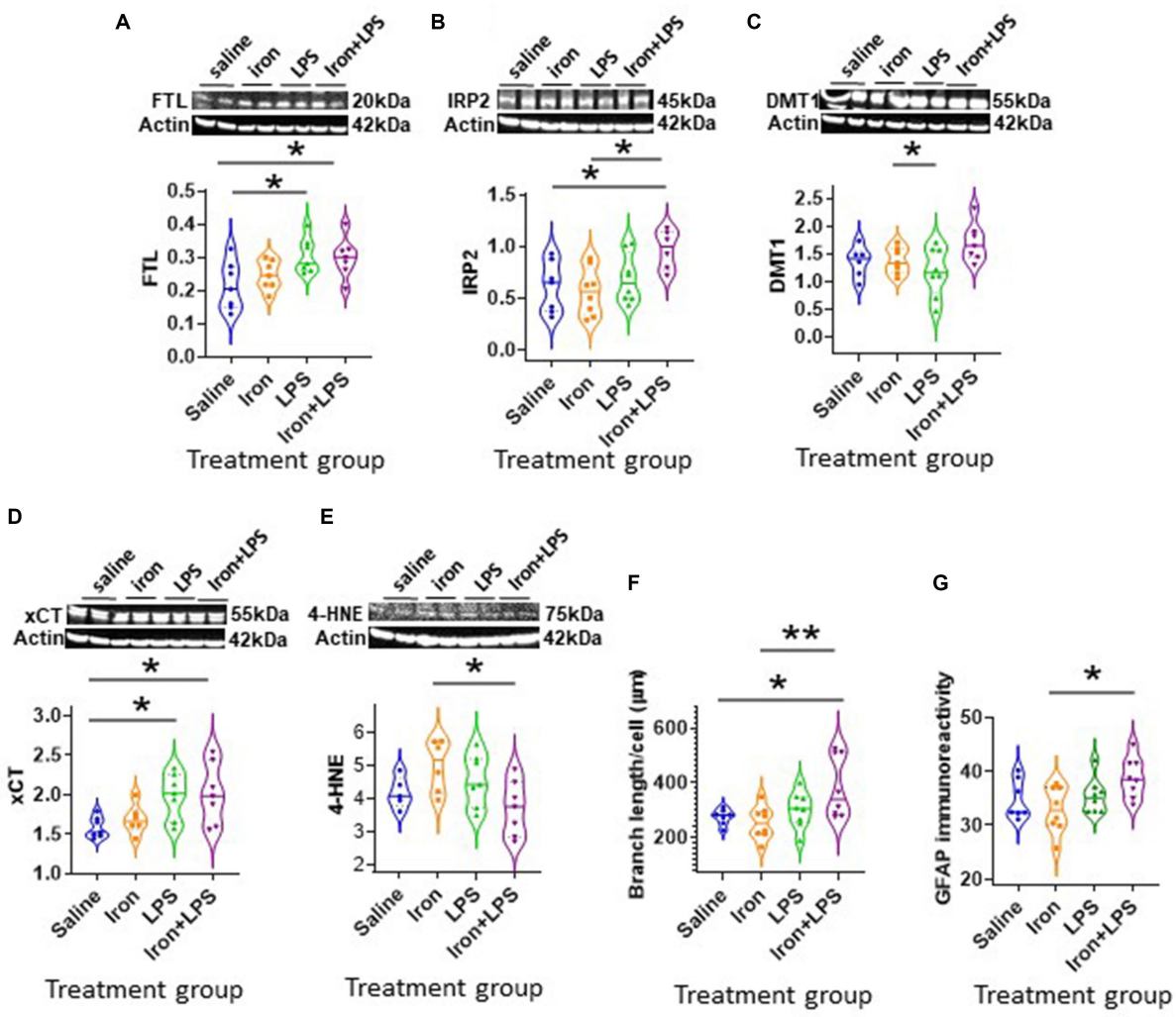

FIGURE 5
Effect of iron-priming and inflammation in the cortex (Cohort 3). Western blot analysis of **(A)** ferritin light-chain (FTL), **(B)** iron regulatory protein 2 (IRP2), **(C)** divalent metal transporter 1 (DMT1), **(D)** light-chain subunit of system X_c^- (xCT), **(E)** 4-hydroxynonenal (4-HNE). Immunohistochemical analysis of **(F)** microglial branch length/cell (assessed from ionized calcium binding adaptor molecule 1-immunohistochemistry) and **(G)** glial fibrillary acidic protein (GFAP) signal intensity (SI, measured in arbitrary units, a.u.). (Proteins measured by western blot analysis were normalized against actin.) Significant results were * and ** for $p < 0.05$ and 0.01, respectively. LPS, lipopolysaccharide.

which in turn stimulates astrocytic levels/activation (Norris et al., 2005; Sama et al., 2008; Perry et al., 2010).

Mice receiving LPS after iron-priming exhibited longer microglial branch length/cell compared to saline and iron only groups. Little is known about the initiation of microglial hyper-ramification (i.e., branching) and how this phenotype relates to microglial functionality (Hinwood et al., 2013). However, exposure of mice to chronic psychological stress, e.g., depression or post-traumatic stress disorder, in the absence of injury or neurodegeneration, has been shown to increase microglial ramification (unaltered microglial numbers) in various brain regions (Hinwood et al., 2013; Walker et al., 2013; Hellwig et al., 2016; Smith et al., 2019). Anti-depressant treatment which ameliorates depression like-behavior was shown to attenuate microglial hyper-ramification and restore microglial morphology. Moreover, microglia exhibited hyper-ramification in a DNA-repair deficient model of accelerated aging (Ercc1 mutant mice) (Raj et al., 2014). Microglia in these mice displayed an exaggerated response to LPS stimulation with augmented expression of pro-inflammatory cytokines (IL1β, IL6, and TNFα) and generation of ROS. We suggest that a LPS challenge following iron-priming leads to hyper-ramified microglia which may represent a primed microglial state. Primed microglia are not acutely activated but may exhibit differential expression patterns, e.g., increased CD68, and mount an exaggerated inflammatory response to a subsequent immune challenge (Witcher et al., 2015). Notably, acute iron loading in mouse macrophages has been found to potentiate the inflammatory response to a consequent LPS challenge (Hoeft et al., 2017). Moreover, pre-treatment of macrophages with an iron-chelator in normal mice attenuated the LPS-induced inflammatory response (Wang et al., 2009). In primary cultured ventral mesencephalic (VM) neurons, augmented release of IL1β and TNFα was observed in LPS-activated microglia exhibiting iron overload (Wang et al., 2013). Iron treatment increases microglial secretion of proinflammatory cytokines which can augment ROS and lipid peroxidation (Yang et al., 2007, 2013; Hoeft et al., 2017; Yauger et al., 2019). Our study

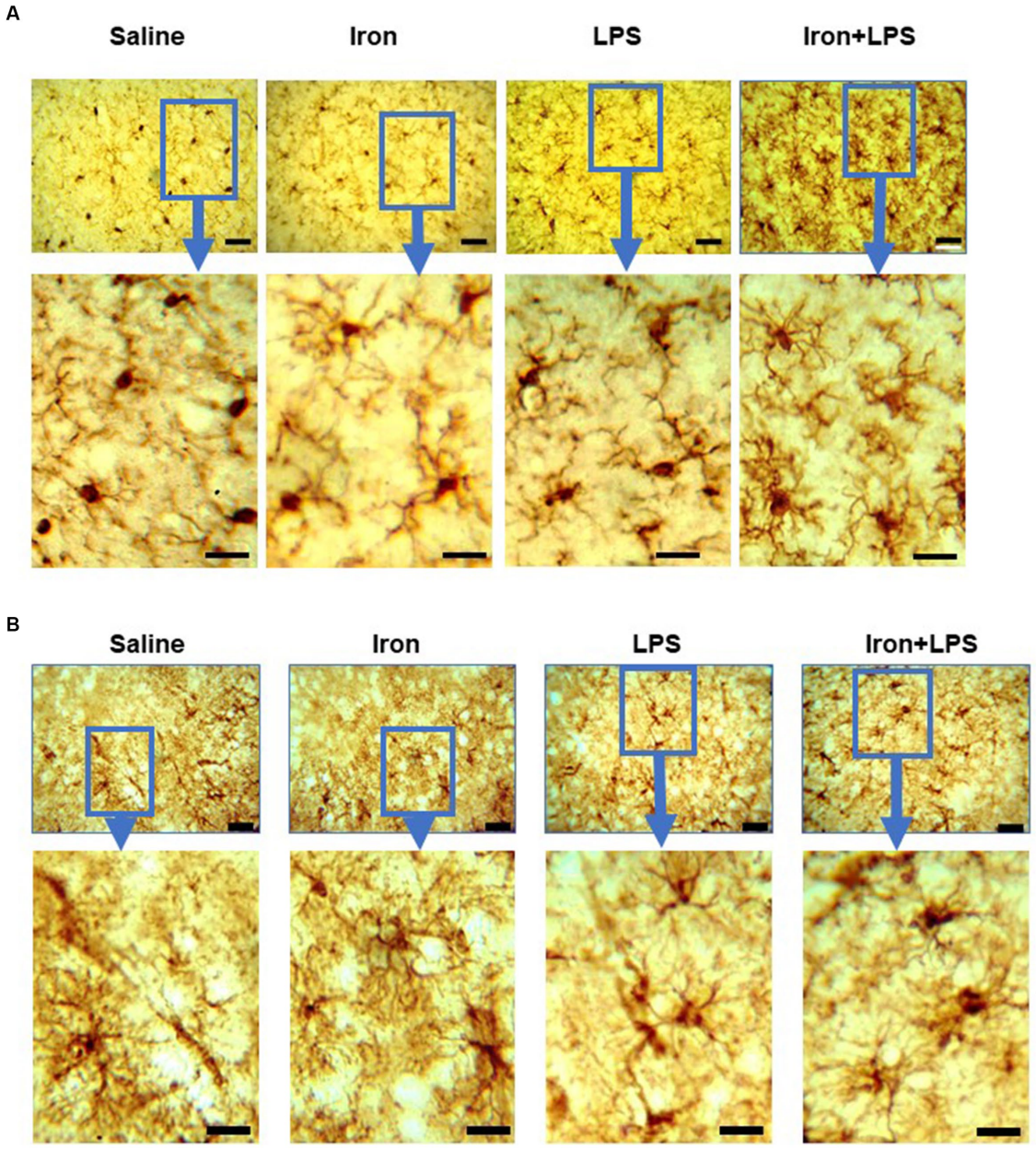

FIGURE 6
Effect of iron-priming and inflammation on micro- and astro-glial morphology in the cortex (Cohort 3). **(A)** ionized calcium-binding adaptor molecule 1 and **(B)** glial fibrillary acidic protein immunochemistry. Micrographs were acquired at 40× magnification. Scale bar represents 25 μm (top panels) and 12.5 μm (bottom panels, magnified images). LPS, lipopolysaccharide.

demonstrates that excess iron and subsequent inflammation alters hippocampal microglial morphology (observed as hyper-ramification of processes) alongside increased lipid peroxidation.

Decreased hippocampal TREM2 was observed following LPS treatment, but only with iron priming, suggesting that iron-primed hippocampal microglia may not be able to respond appropriately to a subsequent inflammation stimulus, e.g., attenuated phagocytosis. TREM2 is exclusively expressed by microglia and is known to promote phagocytic function and regulate inflammation (Takahashi et al., 2005, 2007; Hsieh et al., 2009). TREM2 is pivotal in sustaining trophic functions of microglial in the aging brain (Poliani et al., 2015) and microglial TREM2 expression has been to be reduced in aged mice (Hickman et al., 2013). Further, loss of function mutations of TREM2 is associated with Nasu-Hakola disease, an inflammatory degenerative disease of the brain and bone, leading to premature dementia and death (Bianchin et al., 2010). Rare variants of TREM2 have augmented risk of developing late-onset AD (Jonsson et al., 2013).

Hippocampal GFAP-immunoreactivity was also significantly increased in iron-primed mice subjected to a subsequent LPS challenge, which has also been observed in the aging mouse brain (Kohama et al., 1995). GFAP is not detectable in all astrocytes but a common feature of reactive/activated astrocytes (Zamanian et al., 2012). We suggest astrocytic phagocytosis may be detrimentally increased to compensate for microglial dysfunction we proposed

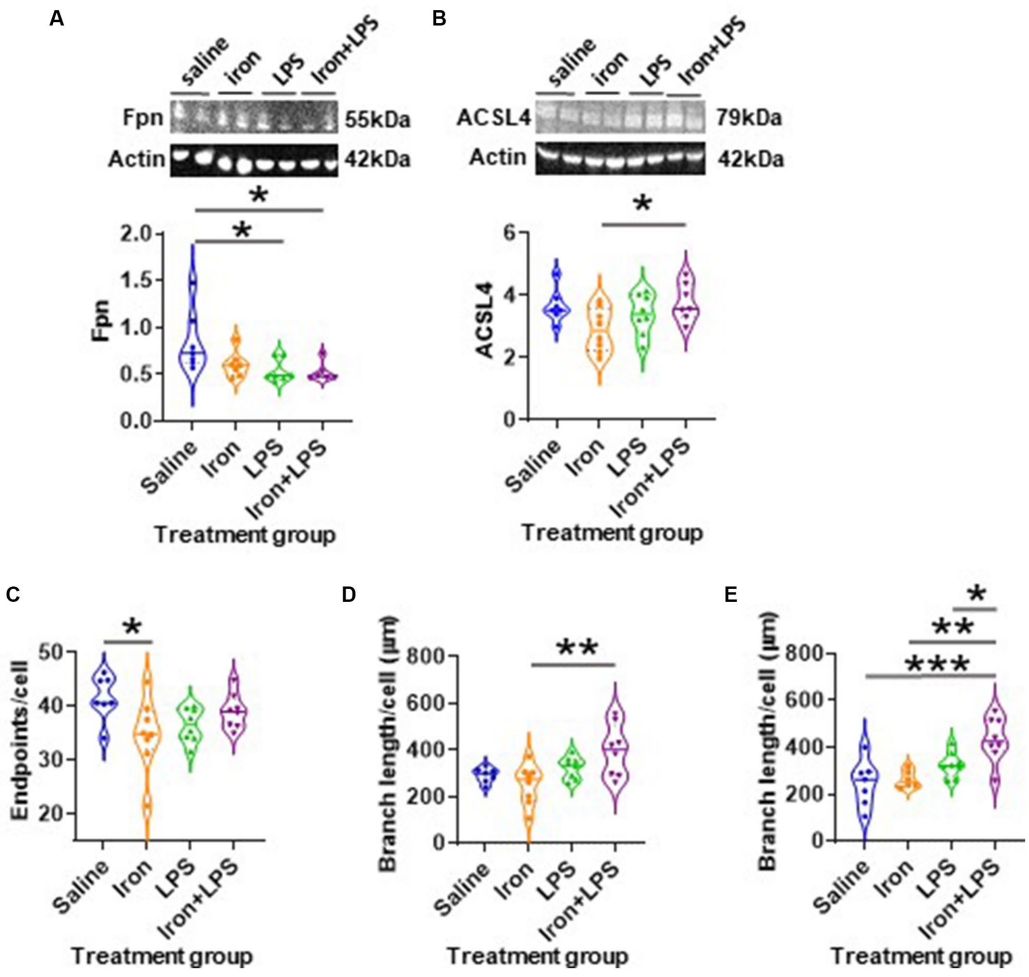

FIGURE 7
The effects of iron-priming and inflammation in the striatum and substantia nigra (Cohort 3). Western blot analysis of **(A)** ferroportin (Fpn) and **(B)** acyl-CoA synthetase long-chain family member 4 (ACSL4). Ionized calcium binding adaptor molecular 1-immunohistochemical analysis of **(C)** microglial endpoints/cell and **(D)** branch length/cell in the striatum and **(E)** microglial branch length/cell in the substantia nigra. (Proteins measured by western blot analysis were normalized against actin.) Significant results were *, ** and *** for $p < 0.05$, 0.01 and 0.001, respectively. LPS, lipopolysaccharide.

above (Konishi et al., 2020). However, we did not measure proteins, e.g., ATP-binding cassette transporter A1, which are better surrogate measures of astroglial phagocytosis (Morizawa et al., 2017), compared to GFAP-immunoreactivity used in this study.

While iron only treatment unexpectedly improved hippocampal function compared with iron-primed inflammation group (see above), iron appeared to have detrimental effects in the cortex as evidenced by increased cortical lipid peroxidation, compared with iron-primed inflammation. We suggest regional differences in the brain arise from variable iron requirements, with the cortex being relatively iron-sufficient compared to the hippocampus, the latter being particularly vulnerable to iron deficiency (Rao et al., 2013). Moreover, higher cortical oxygen consumption renders the cortex particularly vulnerable to lipid peroxidation (Nair et al., 1987). We propose greater cortical oxygen consumption alongside iron over-sufficiency in the cortex explains greater lipid peroxidation in the cortex compared with the hippocampus following iron treatment.

Increased FTL expression was observed in the brain cortex of mice exposed to LPS, with or without iron-priming. Ferritin consists of two subunits, FTH and FTL, which have distinct functions. Predominantly found in oligodendrocytes and neurons, FTH is a ferroxidase that oxidizes ferrous iron to ferric iron for storage. Microglia and astrocytes are equipped with FTL, which better sequestrates iron (Meadowcroft et al., 2015; Ashraf et al., 2018). Augmented microglial hyper-ramification and GFAP-immunoreactivity were observed only in the cortex of iron-primed mice subjected to LPS-induced inflammation, comparable to that in the hippocampus. Iron priming prior to subsequent mild inflammation in the cortex appears to induce a (functional) cellular iron overload prompting glial cells to increase FTL expression. Further evidence for apparently increased cellular iron is indicated by elevated IRP2 levels with iron-primed inflammation, but not with inflammation only. IRP2 expression has been shown to be increased in a 6-hydroxydopamine (6-OHDA)-model of Parkinson's disease (PD), concomitant with increased iron accumulation (Jiang et al., 2010). In conditions of increased iron, a lack of IRP2 binding (signified by increased IRP2 levels) to the iron-responsive element (IRE) of ferritin mRNA leads to increased translation and expression of FTL (Rouault, 2006; Leipuviene and Theil, 2007). The apparent elevated cellular iron in iron + LPS mice compared to those treated with LPS

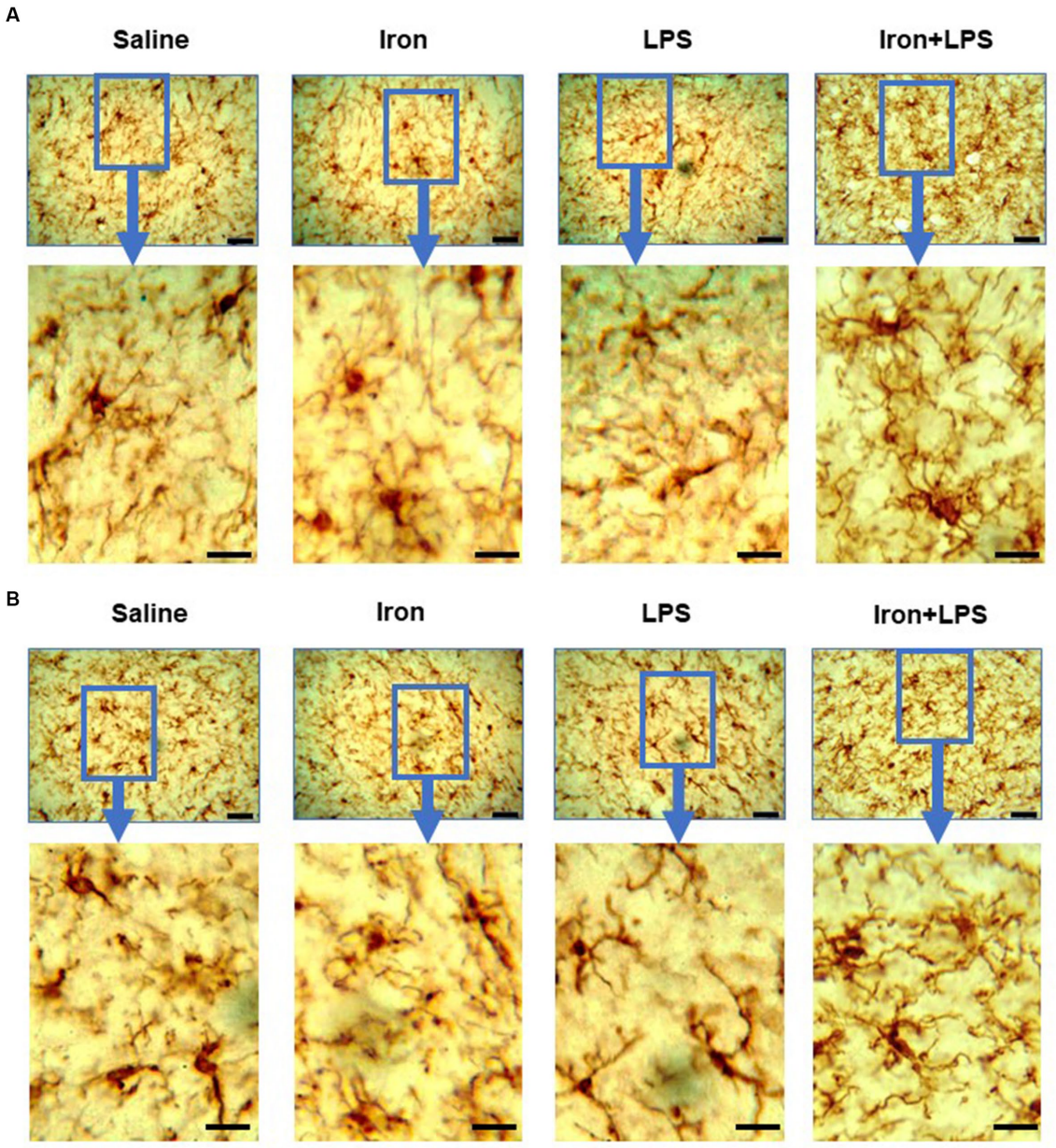

FIGURE 8
Effect of iron-priming and inflammation in the striatum (Cohort 3) on **(A)** ionized calcium-binding adaptor molecule 1 and **(B)** glial fibrillary acidic protein immunochemistry. Micrographs were acquired at 40× magnification. Scale bar represents 25 μm (top panels) and 12.5 μm (bottom panels, magnified images). LPS, lipopolysaccharide.

only may arise from increased cellular iron import since we demonstrated elevated DMT1 in the former mice. DMT1 mediates both cellular iron uptake and endosomal iron export to increase cellular iron (Moos et al., 2007).

Notably, we show inflammation, with and without iron-priming, increased expression levels of cortical xCT, which has been demonstrated when System X_c^- is inhibited (Yu et al., 2017). System X_c^- comprises the widely expressed 4F2 heavy chain subunit, common to several amino acid transporters, and a specific xCT light chain subunit (Sato et al., 1999). Predominantly in glia, System X_c^- is responsible for importing cystine in exchange for glutamate at the plasma membrane and is also called a cystine/glutamate antiporter (Sato et al., 1999; Gasol et al., 2004). Cystine is reduced to cysteine, the rate-limiting substrate for glutathione synthesis and crucial for GPX4 function. Inflammation-mediated inhibition of System X_c^- may compromise cellular uptake of cystine, attenuate GPX4 activity, and increase susceptibility to oxidative stress. However, deletion of the xCT gene attenuated production of pro-inflammatory cytokines including nitric oxide, TNFα, and IL-6, while the expression of anti-inflammatory cytokines, e.g., Tm1/Chil3 were augmented, suggesting xCT also regulates microglial functions (Mesci et al., 2015).

Responses to iron and/or LPS-induced inflammation, not only differed in the hippocampus and cortex, but also in the basal ganglia regions, the striatum and substantia nigra. Mice exposed to

LPS-induced inflammation, with or without iron-priming, showed decreased striatal ferroportin levels. Decreased ferroportin may be caused by increased hepcidin, a peptide hormone that enhances cellular degradation of ferroportin. Previously, systemic injection of hepcidin has been shown to decrease striatal ferroportin (Wang et al., 2010). Further, elevated striatal hepcidin has been observed under inflammatory conditions including ischemia and systemic bacterial inflammation (Ding et al., 2011; Lieblein-Boff et al., 2013). Increased degradation of ferroportin, the only known cellular iron exporter, attenuates iron egress and may lead to (functional) cellular iron overload in the striatum. LPS used in the present study originates from bacteria and can explain the concordance between our results and previous studies (Ding et al., 2011; Lieblein-Boff et al., 2013).

Elevated ACSL4 was also observed in iron + LPS mice in the striatum. ACSL4 catalyzes the insertion of arachidonic acid into phospholipids, specifically phosphatidylethanolamines. Phosphatidylethanolamines appear to be particularly susceptible to lipid peroxidation and the major lipid source for lipid peroxidation in ferroptosis and shown to be significant contributors to elevated 4-HNE adducts/lipid peroxidation products (Doll et al., 2017). Interestingly, mice with ACSL4-ablation, with limited ability to insert arachidonic acid into phosphatidylethanolamines, exhibited attenuated lipid peroxidation (Killion et al., 2018). The increased ACSL4 in response to iron-primed inflammation suggests increased susceptibility of the striatum to ferroptosis.

The alterations in ferroportin and ACSL4 in the striatum were not observed in the hippocampus and cortex. The striatum is known to have higher iron and microglial content than the cortex and hippocampus (Ramos et al., 2014; Ward et al., 2014; Grabert et al., 2016; Keller et al., 2018; Saba et al., 2020), which may explain the differential regional response. Further, GFAP-immunoreactivity was unaltered in the striatum but was increased in both the hippocampus and the cortex. This is unsurprising as astrocytes from the mouse striatum and hippocampus display diversity as confirmed by transcriptomic, proteomic, morphological, and functional evidence (Chai et al., 2017). Further, cortical astrocytes have been shown to release greater amounts of TNFα in response to LPS stimulation than striatal astrocytes (Saba et al., 2020), consistent with our findings of increased astroglial immunoreactivity in the cortex but not in the striatum.

Regional molecular comparisons were not possible with the substantia nigra as only metal and histological analyses were performed. However, we observed hyper-ramified microglia in the iron + LPS group compared with saline, iron, and LPS treatment groups. We suggest that iron activates microglia in the substantia nigra but revert to their usual surveillance mode unless exposed to a subsequent inflammatory episode. The substantia nigral neurons contain neuromelanin, which is known to sequester excess iron and inhibit free radical production (Zecca et al., 2008a). However, iron-loaded neuromelanin itself can be a source of redox-active iron to induce microgliosis and impair dopamine neuronal functioning (Faucheux et al., 2003; Zecca et al., 2008b; Zhang et al., 2011; Ward et al., 2014). A caveat of the study was that a comprehensive protein analysis of the substantia nigra to investigate iron dyshomeostasis and ferroptosis-like changes was not performed to allow comparison with other brain regions. Moreover, a functional readout of this anatomical region would have been useful to associate with molecular changes.

The total iron levels in the current study were unchanged despite iron treatment. A limitation of our study is that both spatial and bulk iron analysis by SRXRF and TXRF, respectively, measure all forms of iron and were used as proxy measures for the labile iron pool. The labile iron pool is relatively small compared to the total iron content and such iron measurements may not be sensitive/accurate to subtle fluctuations in the labile iron pool (Ashraf et al., 2019a, 2020). Ideally, future studies should directly measure changes in the labile iron pool.

We did not evaluate the mechanism of microglial and astrocytic activation in inflammation, but LPS has been shown to induce inflammation via crosstalk between microglia and astrocytes (Norris et al., 2005; Sama et al., 2008). Moreover, it is challenging to translate glial morphological plasticity to functionality. A limitation of the study is the lack of measurement of relevant pro- and anti-inflammatory cytokines in the brain and plasma that can be correlated with microglial priming. Additional functional readouts from *in vitro* experiments evaluating changes in microglial phenotype by flow cytometry may offer deeper mechanistic insights. To ascertain the propositions in this exploratory study, future studies are warranted to measure pro- and anti-inflammatory cytokines to determine their association with different microglial morphological states.

Conclusion

We demonstrate inflammation following priming with systemic injections of mild iron doses in normal C57Bl/6J mice alters brain molecular profile suggestive of iron dyshomeostasis, lipid peroxidation, and neuroinflammation, in a region-dependent manner.

Data availability statement

The original contributions presented in the study are included in the article/Supplementary material, further inquiries can be directed to the corresponding author.

Ethics statement

The animal study was approved by local ethical review panel of King's College London in accordance with the UK Home Office Animals Scientific Procedures Act 1986. The study was conducted in accordance with the local legislation and institutional requirements.

Author contributions

AA: Conceptualization, Data curation, Formal analysis, Investigation, Methodology, Project administration, Visualization, Writing – original draft, Writing – review & editing. MA: Investigation, Writing – review & editing. CH: Investigation, Project administration, Writing – review & editing. JJ: Formal analysis, Investigation, Writing – review & editing. HP: Formal analysis, Investigation, Methodology, Writing – review & editing. KG: Formal analysis, Investigation,

Methodology, Software, Writing – review & editing. AM: Formal analysis, Investigation, Writing – review & editing. AH: Funding acquisition, Resources, Writing – review & editing. P-WS: Conceptualization, Formal analysis, Funding acquisition, Investigation, Methodology, Project administration, Resources, Software, Supervision, Validation, Writing – original draft, Writing – review & editing.

Funding

The author(s) declare that financial support was received for the research, authorship, and/or publication of this article. This study was sponsored by the Biotechnology and Biological Sciences Research Council (BBSRC), King's College London, and Perspectum Diagnostics Ltd. by funding AA's industrial PhD studentship. Perspectum Diagnostics Ltd. was not involved in the study design, collection, analysis, interpretation of data, the writing of this article, or the decision to submit it for publication. Also, we would like to thank the Wellcome Trust for funding the London Metallomics Facility (Grant reference 202902/Z/16/Z) where the TXRF was performed.

Acknowledgments

The authors thank the Diamond Light Source for access to the I18 beamline for synchrotron-radiation X-ray fluorescence elemental mapping, beamline proposals: SP19447 and SP22661.

Conflict of interest

KG was employed by Diamond Light Source. AH was employed by Perspectum Diagnostics Ltd.

The remaining authors declare that the research was conducted in the absence of any commercial or financial relationships that could be construed as a potential conflict of interest.

The author(s) declared that they were an editorial board member of Frontiers, at the time of submission. This had no impact on the peer review process and the final decision.

Publisher's note

Supplementary material

The Supplementary material for this article can be found online at: https://www.frontiersin.org/articles/10.3389/fnagi.2024.1393351/full#supplementary-material

References

Ali, S., Liu, X., Queen, N. J., Patel, R. S., Wilkins, R. K., Mo, X., et al. (2019). Long-term environmental enrichment affects microglial morphology in middle age mice. *Aging* 11, 2388–2402. doi: 10.18632/aging.101923

Ashraf, A., Clark, M., and So, P. W. (2018). The aging of iron man. *Front. Aging Neurosci.* 10:65. doi: 10.3389/fnagi.2018.00065

Ashraf, A., Jeandriens, J., Parkes, H. G., and So, P. W. (2020). Iron dyshomeostasis, lipid peroxidation and perturbed expression of cystine/glutamate antiporter in Alzheimer's disease: evidence of ferroptosis. *Redox Biol.* 32:101494. doi: 10.1016/j.redox.2020.101494

Ashraf, A., Michaelides, C., Walker, T. A., Ekonomou, A., Suessmilch, M., Sriskanthanathan, A., et al. (2019a). Regional distributions of iron, copper and zinc and their relationships with glia in a normal aging mouse model. *Front. Aging Neurosci.* 11:351. doi: 10.3389/fnagi.2019.00351

Ashraf, A., and So, P. W. (2020). Spotlight on ferroptosis: iron-dependent cell death in Alzheimer's disease. *Front. Aging Neurosci.* 12:196. doi: 10.3389/fnagi.2020.00196

Ashraf, A., Stosnach, H., Parkes, H. G., Hye, A., Powell, J., So, P. W., et al. (2019b). Pattern of altered plasma elemental phosphorus, calcium, zinc, and iron in Alzheimer's disease. *Sci. Rep.* 9:3147. doi: 10.1038/s41598-018-37431-8

Bianchin, M. M., Martin, K. C., De Souza, A. C., De Oliveira, M. A., and Rieder, C. R. (2010). Nasu–Hakola disease and primary microglial dysfunction. *Nat. Rev. Neurol.* 6:523. doi: 10.1038/nrneurol.2010.17-c1

Chai, H., Diaz-Castro, B., Shigetomi, E., Monte, E., Octeau, J. C., Yu, X., et al. (2017). Neural circuit-specialized astrocytes: transcriptomic, proteomic, morphological, and functional evidence. *Neuron* 95, 531–549.e9. doi: 10.1016/j.neuron.2017.06.029

Chao, X. D., Ma, Y. H., Luo, P., Cao, L., Lau, W. B., Zhao, B. C., et al. (2013). Up-regulation of heme oxygenase-1 attenuates brain damage after cerebral ischemia via simultaneous inhibition of superoxide production and preservation of NO bioavailability. *Exp. Neurol.* 239, 163–169. doi: 10.1016/j.expneurol.2012.09.020

Chiabrando, D., Fiorito, V., Petrillo, S., and Tolosano, E. (2018). Unraveling the role of heme in neurodegeneration. *Front. Neurosci.* 12:712. doi: 10.3389/fnins.2018.00712

Devanand, D. P., Bansal, R., Liu, J., Hao, X., Pradhaban, G., and Peterson, B. S. (2012). MRI hippocampal and entorhinal cortex mapping in predicting conversion to Alzheimer's disease. *NeuroImage* 60, 1622–1629. doi: 10.1016/j.neuroimage.2012.01.075

Ding, H., Yan, C. Z., Shi, H., Zhao, Y. S., Chang, S. Y., Yu, P., et al. (2011). Hepcidin is involved in iron regulation in the ischemic brain. *PLoS One* 6:e25324. doi: 10.1371/journal.pone.0025324

Dixon, S. J., Lemberg, K. M., Lamprecht, M. R., Skouta, R., Zaitsev, E. M., Gleason, C. E., et al. (2012). Ferroptosis: an iron-dependent form of nonapoptotic cell death. *Cell* 149, 1060–1072. doi: 10.1016/j.cell.2012.03.042

Doll, S., Proneth, B., Tyurina, Y. Y., Panzilius, E., Kobayashi, S., Ingold, I., et al. (2017). ACSL4 dictates ferroptosis sensitivity by shaping cellular lipid composition. *Nat. Chem. Biol.* 13, 91–98. doi: 10.1038/nchembio.2239

Eskew, J. D., Vanacore, R. M., Sung, L., Morales, P. J., and Smith, A. (1999). Cellular protection mechanisms against extracellular heme. Heme-hemopexin, but not free heme, activates the N-terminal c-jun kinase. *J. Biol. Chem.* 274, 638–648. doi: 10.1074/jbc.274.2.638

Faucheux, B. A., Martin, M. E., Beaumont, C., Hauw, J. J., Agid, Y., and Hirsch, E. C. (2003). Neuromelanin associated redox-active iron is increased in the substantia nigra of patients with Parkinson's disease. *J. Neurochem.* 86, 1142–1148. doi: 10.1046/j.1471-4159.2003.01923.x

Fjell, A. M., Mcevoy, L., Holland, D., Dale, A. M., and Walhovd, K. B.Alzheimer's Disease Neuroimaging Initiative (2014). What is normal in normal aging? Effects of aging, amyloid and Alzheimer's disease on the cerebral cortex and the hippocampus. *Prog. Neurobiol.* 117, 20–40. doi: 10.1016/j.pneurobio.2014.02.004

Gasol, E., Jimenez-Vidal, M., Chillaron, J., Zorzano, A., and Palacin, M. (2004). Membrane topology of system X_c^- light subunit reveals a re-entrant loop with substrate-restricted accessibility. *J. Biol. Chem.* 279, 31228–31236. doi: 10.1074/jbc.M402428200

Godbout, J. P., Chen, J., Abraham, J., Richwine, A. F., Berg, B. M., Kelley, K. W., et al. (2005). Exaggerated neuroinflammation and sickness behavior in aged mice following activation of the peripheral innate immune system. *FASEB J.* 19, 1329–1331. doi: 10.1096/fj.05-3776fje

Grabert, K., Michoel, T., Karavolos, M. H., Clohisey, S., Baillie, J. K., Stevens, M. P., et al. (2016). Microglial brain region-dependent diversity and selective regional sensitivities to aging. *Nat. Neurosci.* 19, 504–516. doi: 10.1038/nn.4222

Guan, X., Guo, T., Zhou, C., Wu, J., Zeng, Q., Li, K., et al. (2022). Altered brain iron depositions from aging to Parkinson's disease and Alzheimer's disease: a quantitative susceptibility mapping study. *NeuroImage* 264:119683. doi: 10.1016/j.neuroimage.2022.119683

Hallgren, B., and Sourander, P. (1958). The effect of age on the non-haemin iron in the human brain. *J. Neurochem.* 3, 41–51. doi: 10.1111/j.1471-4159.1958.tb12607.x

Hellwig, S., Brioschi, S., Dieni, S., Frings, L., Masuch, A., Blank, T., et al. (2016). Altered microglia morphology and higher resilience to stress-induced depression-like

behavior in CX3CR1-deficient mice. *Brain Behav. Immun.* 55, 126–137. doi: 10.1016/j.bbi.2015.11.008

Henry, C. J., Huang, Y., Wynne, A. M., and Godbout, J. P. (2009). Peripheral lipopolysaccharide (LPS) challenge promotes microglial hyperactivity in aged mice that is associated with exaggerated induction of both pro-inflammatory IL-1beta and anti-inflammatory IL-10 cytokines. *Brain Behav. Immun.* 23, 309–317. doi: 10.1016/j.bbi.2008.09.002

Hickman, S. E., Kingery, N. D., Ohsumi, T. K., Borowsky, M. L., Wang, L. C., Means, T. K., et al. (2013). The microglial sensome revealed by direct RNA sequencing. *Nat. Neurosci.* 16, 1896–1905. doi: 10.1038/nn.3554

Hinwood, M., Tynan, R. J., Charnley, J. L., Beynon, S. B., Day, T. A., and Walker, F. R. (2013). Chronic stress induced remodeling of the prefrontal cortex: structural re-organization of microglia and the inhibitory effect of minocycline. *Cereb. Cortex* 23, 1784–1797. doi: 10.1093/cercor/bhs151

Hoeft, K., Bloch, D. B., Graw, J. A., Malhotra, R., Ichinose, F., and Bagchi, A. (2017). Iron loading exaggerates the inflammatory response to the toll-like receptor 4 ligand lipopolysaccharide by altering mitochondrial homeostasis. *Anesthesiology* 127, 121–135. doi: 10.1097/ALN.0000000000001653

Holmes-Hampton, G. P., Chakrabarti, M., Cockrell, A. L., Mccormick, S. P., Abbott, L. C., Lindahl, L. S., et al. (2012). Changing iron content of the mouse brain during development. *Metallomics* 4, 761–770. doi: 10.1039/c2mt20086d

Hsieh, C. L., Koike, M., Spusta, S. C., Niemi, E. C., Yenari, M., Nakamura, M. C., et al. (2009). A role for TREM2 ligands in the phagocytosis of apoptotic neuronal cells by microglia. *J. Neurochem.* 109, 1144–1156. doi: 10.1111/j.1471-4159.2009.06042.x

Ifuku, M., Katafuchi, T., Mawatari, S., Noda, M., Miake, K., Sugiyama, M., et al. (2012). Anti-inflammatory/anti-amyloidogenic effects of plasmalogens in lipopolysaccharide-induced neuroinflammation in adult mice. *J. Neuroinflammation* 9:197. doi: 10.1186/1742-2094-9-197

Ishikawa, K., Navab, M., and Lusis, A. J. (2012). Vasculitis, atherosclerosis, and altered HDL composition in heme-oxygenase-1-knockout mice. *Int. J. Hypertens.* 2012:948203. doi: 10.1155/2012/948203

Jiang, H., Song, N., Xu, H., Zhang, S., Wang, J., and Xie, J. (2010). Up-regulation of divalent metal transporter 1 in 6-hydroxydopamine intoxication is IRE/IRP dependent. *Cell Res.* 20, 345–356. doi: 10.1038/cr.2010.20

Jonsson, T., Stefansson, H., Steinberg, S., Jonsdottir, I., Jonsson, P. V., Snaedal, J., et al. (2013). Variant of TREM2 associated with the risk of Alzheimer's disease. *N. Engl. J. Med.* 368, 107–116. doi: 10.1056/NEJMoa1211103

Keller, D., Ero, C., and Markram, H. (2018). Cell densities in the mouse brain: a systematic review. *Front. Neuroanat.* 12:83. doi: 10.3389/fnana.2018.00083

Killion, E. A., Reeves, A. R., El Azzouny, M. A., Yan, Q. W., Surujon, D., Griffin, J. D., et al. (2018). A role for long-chain acyl-CoA synthetase-4 (ACSL4) in diet-induced phospholipid remodeling and obesity-associated adipocyte dysfunction. *Mol. Metab.* 9, 43–56. doi: 10.1016/j.molmet.2018.01.012

Kohama, S. G., Goss, J. R., Finch, C. E., and Mcneill, T. H. (1995). Increases of glial fibrillary acidic protein in the aging female mouse brain. *Neurobiol. Aging* 16, 59–67. doi: 10.1016/0197-4580(95)80008-F

Konishi, H., Okamoto, T., Hara, Y., Komine, O., Tamada, H., Maeda, M., et al. (2020). Astrocytic phagocytosis is a compensatory mechanism for microglial dysfunction. *EMBO J.* 39:e104464. doi: 10.15252/embj.2020104464

Leipuviene, R., and Theil, E. C. (2007). The family of iron responsive RNA structures regulated by changes in cellular iron and oxygen. *Cell. Mol. Life Sci.* 64, 2945–2955. doi: 10.1007/s00018-007-7198-4

Lieblein-Boff, J. C., Mckim, D. B., Shea, D. T., Wei, P., Deng, Z., Sawicki, C., et al. (2013). Neonatal *E. coli* infection causes neuro-behavioral deficits associated with hypomyelination and neuronal sequestration of iron. *J. Neurosci.* 33, 16334–16345. doi: 10.1523/JNEUROSCI.0708-13.2013

Lueptow, L. M. (2017). Novel object recognition test for the investigation of learning and memory in mice. *J. Vis. Exp.* 2017:55718. doi: 10.3791/55718

Maaroufi, K., Had-Aissouni, L., Melon, C., Sakly, M., Abdelmelek, H., Poucet, B., et al. (2009). Effects of prolonged iron overload and low frequency electromagnetic exposure on spatial learning and memory in the young rat. *Neurobiol. Learn. Mem.* 92, 345–355. doi: 10.1016/j.nlm.2009.04.002

Maaroufi, K., Had-Aissouni, L., Melon, C., Sakly, M., Abdelmelek, H., Poucet, B., et al. (2014). Spatial learning, monoamines and oxidative stress in rats exposed to 900 MHz electromagnetic field in combination with iron overload. *Behav. Brain Res.* 258, 80–89. doi: 10.1016/j.bbr.2013.10.016

Malecki, E. A., Cable, E. E., Isom, H. C., and Connor, J. R. (2002). The lipophilic iron compound TMH-ferrocene [(3,5,5-trimethylhexanoyl)ferrocene] increases iron concentrations, neuronal L-ferritin, and heme oxygenase in brains of BALB/c mice. *Biol. Trace Elem. Res.* 86, 73–84. doi: 10.1385/BTER:86:1:73

Meadowcroft, M. D., Connor, J. R., and Yang, Q. X. (2015). Cortical iron regulation and inflammatory response in Alzheimer's disease and APPSWE/PS1DeltaE9 mice: a histological perspective. *Front. Neurosci.* 9:255. doi: 10.3389/fnins.2015.00255

Mesci, P., Zaidi, S., Lobsiger, C. S., Millecamps, S., Escartin, C., Seilhean, D., et al. (2015). System xC- is a mediator of microglial function and its deletion slows symptoms in amyotrophic lateral sclerosis mice. *Brain* 138, 53–68. doi: 10.1093/brain/awu312

Moos, T., Rosengren Nielsen, T., Skjorringe, T., and Morgan, E. H. (2007). Iron trafficking inside the brain. *J. Neurochem.* 103, 1730–1740. doi: 10.1111/j.1471-4159.2007.04976.x

Morizawa, Y. M., Hirayama, Y., Ohno, N., Shibata, S., Shigetomi, E., Sui, Y., et al. (2017). Reactive astrocytes function as phagocytes after brain ischemia via ABCA1-mediated pathway. *Nat. Commun.* 8:28. doi: 10.1038/s41467-017-00037-1

Morrison, H. W., and Filosa, J. A. (2013). A quantitative spatiotemporal analysis of microglia morphology during ischemic stroke and reperfusion. *J. Neuroinflammation* 10:4. doi: 10.1186/1742-2094-10-4

Nair, P. K., Buerk, D. G., and Halsey, J. H. Jr. (1987). Comparisons of oxygen metabolism and tissue PO_2 in cortex and hippocampus of gerbil brain. *Stroke* 18, 616–622. doi: 10.1161/01.STR.18.3.616

Norris, C. M., Kadish, I., Blalock, E. M., Chen, K. C., Thibault, V., Porter, N. M., et al. (2005). Calcineurin triggers reactive/inflammatory processes in astrocytes and is upregulated in aging and Alzheimer's models. *J. Neurosci.* 25, 4649–4658. doi: 10.1523/JNEUROSCI.0365-05.2005

Perry, V. H., Nicoll, J. A., and Holmes, C. (2010). Microglia in neurodegenerative disease. *Nat. Rev. Neurol.* 6, 193–201. doi: 10.1038/nrneurol.2010.17

Pirota, V., Monzani, E., Dell'acqua, S., and Casella, L. (2016). Interactions between heme and tau-derived R1 peptides: binding and oxidative reactivity. *Dalton Trans.* 45, 14343–14351. doi: 10.1039/C6DT02183B

Poliani, P. L., Wang, Y., Fontana, E., Robinette, M. L., Yamanishi, Y., Gilfillan, S., et al. (2015). TREM2 sustains microglial expansion during aging and response to demyelination. *J. Clin. Invest.* 125, 2161–2170. doi: 10.1172/JCI77983

Qin, L., Wu, X., Block, M. L., Liu, Y., Breese, G. R., Hong, J. S., et al. (2007). Systemic LPS causes chronic neuroinflammation and progressive neurodegeneration. *Glia* 55, 453–462. doi: 10.1002/glia.20467

Raj, D. D., Jaarsma, D., Holtman, I. R., Olah, M., Ferreira, F. M., Schaafsma, W., et al. (2014). Priming of microglia in a DNA-repair deficient model of accelerated aging. *Neurobiol. Aging* 35, 2147–2160. doi: 10.1016/j.neurobiolaging.2014.03.025

Ramos, P., Santos, A., Pinto, N. R., Mendes, R., Magalhaes, T., and Almeida, A. (2014). Iron levels in the human brain: a post-mortem study of anatomical region differences and age-related changes. *J. Trace Elem. Med. Biol.* 28, 13–17. doi: 10.1016/j.jtemb.2013.08.001

Rao, R., Tkac, I., Unger, E. L., Ennis, K., Hurst, A., Schallert, T., et al. (2013). Iron supplementation dose for perinatal iron deficiency differentially alters the neurochemistry of the frontal cortex and hippocampus in adult rats. *Pediatr. Res.* 73, 31–37. doi: 10.1038/pr.2012.143

Righy, C., Bozza, M. T., Oliveira, M. F., and Bozza, F. A. (2016). Molecular, cellular and clinical aspects of intracerebral hemorrhage: are the enemies within? *Curr. Neuropharmacol.* 14, 392–402. doi: 10.2174/1570159X14666151230110058

Rouault, T. A. (2006). The role of iron regulatory proteins in mammalian iron homeostasis and disease. *Nat. Chem. Biol.* 2, 406–414. doi: 10.1038/nchembio807

Saba, J., Lopez Couselo, F., Turati, J., Carniglia, L., Durand, D., De Laurentiis, A., et al. (2020). Astrocytes from cortex and striatum show differential responses to mitochondrial toxin and BDNF: implications for protection of striatal neurons expressing mutant huntingtin. *J. Neuroinflammation* 17:290. doi: 10.1186/s12974-020-01965-4

Saleppico, S., Mazzolla, R., Boelaert, J. R., Puliti, M., Barluzzi, R., Bistoni, F., et al. (1996). Iron regulates microglial cell-mediated secretory and effector functions. *Cell. Immunol.* 170, 251–259. doi: 10.1006/cimm.1996.0159

Sama, M. A., Mathis, D. M., Furman, J. L., Abdul, H. M., Artiushin, I. A., Kraner, S. D., et al. (2008). Interleukin-1beta-dependent signaling between astrocytes and neurons depends critically on astrocytic calcineurin/NFAT activity. *J. Biol. Chem.* 283, 21953–21964. doi: 10.1074/jbc.M800148200

Sato, H., Tamba, M., Ishii, T., and Bannai, S. (1999). Cloning and expression of a plasma membrane cystine/glutamate exchange transporter composed of two distinct proteins. *J. Biol. Chem.* 274, 11455–11458. doi: 10.1074/jbc.274.17.11455

Smith, K. L., Kassem, M. S., Clarke, D. J., Kuligowski, M. P., Bedoya-Perez, M. A., Todd, S. M., et al. (2019). Microglial cell hyper-ramification and neuronal dendritic spine loss in the hippocampus and medial prefrontal cortex in a mouse model of PTSD. *Brain Behav. Immun.* 80, 889–899. doi: 10.1016/j.bbi.2019.05.042

Sobotka, T. J., Whittaker, P., Sobotka, J. M., Brodie, R. E., Quander, D. Y., Robl, M., et al. (1996). Neurobehavioral dysfunctions associated with dietary iron overload. *Physiol. Behav.* 59, 213–219. doi: 10.1016/0031-9384(95)02030-6

Solé, V. A., Papillon, E., Cotte, M., Walter, P., and Susini, J. (2007). A multiplatform code for the analysis of energy-dispersive X-ray fluorescence spectra. *Spectrochim. Acta B* 62, 63–68. doi: 10.1016/j.sab.2006.12.002

Sung, L., Shibata, M., Eskew, J. D., Shipulina, N., Morales, P. J., and Smith, A. (2000). Cell-surface events for metallothionein-1 and heme oxygenase-1 regulation by the hemopexin-heme transport system. *Antioxid. Redox Signal.* 2, 753–765. doi: 10.1089/ars.2000.2.4-753

Takahashi, K., Prinz, M., Stagi, M., Chechneva, O., and Neumann, H. (2007). TREM2-transduced myeloid precursors mediate nervous tissue debris clearance and facilitate recovery in an animal model of multiple sclerosis. *PLoS Med.* 4:e124. doi: 10.1371/journal.pmed.0040124

Takahashi, K., Rochford, C. D., and Neumann, H. (2005). Clearance of apoptotic neurons without inflammation by microglial triggering receptor expressed on myeloid cells-2. *J. Exp. Med.* 201, 647–657. doi: 10.1084/jem.20041611

Vanacore, R. M., Eskew, J. D., Morales, P. J., Sung, L., and Smith, A. (2000). Role for copper in transient oxidation and nuclear translocation of MTF-1, but not of NF-kappa B, by the heme-hemopexin transport system. *Antioxid. Redox Signal.* 2, 739–752. doi: 10.1089/ars.2000.2.4-739

Walker, T., Michaelides, C., Ekonomou, A., Geraki, K., Parkes, H. G., Suessmilch, M., et al. (2016). Dissociation between iron accumulation and ferritin upregulation in the aged substantia nigra: attenuation by dietary restriction. *Aging* 8, 2488–2508. doi: 10.18632/aging.101069

Walker, F. R., Nilsson, M., and Jones, K. (2013). Acute and chronic stress-induced disturbances of microglial plasticity, phenotype and function. *Curr. Drug Targets* 14, 1262–1276. doi: 10.2174/13894501113149990208

Wang, S. M., Fu, L. J., Duan, X. L., Crooks, D. R., Yu, P., Qian, Z. M., et al. (2010). Role of hepcidin in murine brain iron metabolism. *Cell. Mol. Life Sci.* 67, 123–133. doi: 10.1007/s00018-009-0167-3

Wang, L., Harrington, L., Trebicka, E., Shi, H. N., Kagan, J. C., Hong, C. C., et al. (2009). Selective modulation of TLR4-activated inflammatory responses by altered iron homeostasis in mice. *J. Clin. Invest.* 119, 3322–3328. doi: 10.1172/JCI39939

Wang, J., Song, N., Jiang, H., Wang, J., and Xie, J. (2013). Pro-inflammatory cytokines modulate iron regulatory protein 1 expression and iron transportation through reactive oxygen/nitrogen species production in ventral mesencephalic neurons. *Biochim. Biophys. Acta* 1832, 618–625. doi: 10.1016/j.bbadis.2013.01.021

Ward, R. J., Dexter, D. T., and Crichton, R. R. (2022). Iron, neuroinflammation and neurodegeneration. *Int. J. Mol. Sci.* 23:7267. doi: 10.3390/ijms23137267

Ward, R. J., Zucca, F. A., Duyn, J. H., Crichton, R. R., and Zecca, L. (2014). The role of iron in brain ageing and neurodegenerative disorders. *Lancet Neurol.* 13, 1045–1060. doi: 10.1016/S1474-4422(14)70117-6

Witcher, K. G., Eiferman, D. S., and Godbout, J. P. (2015). Priming the inflammatory pump of the CNS after traumatic brain injury. *Trends Neurosci.* 38, 609–620. doi: 10.1016/j.tins.2015.08.002

Wohleb, E. S., Fenn, A. M., Pacenta, A. M., Powell, N. D., Sheridan, J. F., and Godbout, J. P. (2012). Peripheral innate immune challenge exaggerated microglia activation, increased the number of inflammatory CNS macrophages, and prolonged social withdrawal in socially defeated mice. *Psychoneuroendocrinology* 37, 1491–1505. doi: 10.1016/j.psyneuen.2012.02.003

Wu, Y. H., and Hsieh, H. L. (2022). Roles of heme oxygenase-1 in neuroinflammation and brain disorders. *Antioxidants* 11:923. doi: 10.3390/antiox11050923

Yang, D., Elner, S. G., Bian, Z. M., Till, G. O., Petty, H. R., and Elner, V. M. (2007). Pro-inflammatory cytokines increase reactive oxygen species through mitochondria and NADPH oxidase in cultured RPE cells. *Exp. Eye Res.* 85, 462–472. doi: 10.1016/j.exer.2007.06.013

Yang, C. M., Hsieh, H. L., Lin, C. C., Shih, R. H., Chi, P. L., Cheng, S. E., et al. (2013). Multiple factors from bradykinin-challenged astrocytes contribute to the neuronal apoptosis: involvement of astroglial ROS, MMP-9, and HO-1/CO system. *Mol. Neurobiol.* 47, 1020–1033. doi: 10.1007/s12035-013-8402-1

Yauger, Y. J., Bermudez, S., Moritz, K. E., Glaser, E., Stoica, B., and Byrnes, K. R. (2019). Iron accentuated reactive oxygen species release by NADPH oxidase in activated microglia contributes to oxidative stress *in vitro*. *J. Neuroinflammation* 16:41. doi: 10.1186/s12974-019-1430-7

Young, K., and Morrison, H. (2018). Quantifying microglia morphology from photomicrographs of immunohistochemistry prepared tissue using ImageJ. *J. Vis. Exp.* 2018:57648. doi: 10.3791/57648-v

Yu, H., Guo, P., Xie, X., Wang, Y., and Chen, G. (2017). Ferroptosis, a new form of cell death, and its relationships with tumourous diseases. *J. Cell. Mol. Med.* 21, 648–657. doi: 10.1111/jcmm.13008

Zamanian, J. L., Xu, L., Foo, L. C., Nouri, N., Zhou, L., Giffard, R. G., et al. (2012). Genomic analysis of reactive astrogliosis. *J. Neurosci.* 32, 6391–6410. doi: 10.1523/JNEUROSCI.6221-11.2012

Zecca, L., Casella, L., Albertini, A., Bellei, C., Zucca, F. A., Engelen, M., et al. (2008a). Neuromelanin can protect against iron-mediated oxidative damage in system modeling iron overload of brain aging and Parkinson's disease. *J. Neurochem.* 106, 1866–1875. doi: 10.1111/j.1471-4159.2008.05541.x

Zecca, L., Wilms, H., Geick, S., Claasen, J. H., Brandenburg, L. O., Holzknecht, C., et al. (2008b). Human neuromelanin induces neuroinflammation and neurodegeneration in the rat substantia nigra: implications for Parkinson's disease. *Acta Neuropathol.* 116, 47–55. doi: 10.1007/s00401-008-0361-7

Zhang, X. Y., Cao, J. B., Zhang, L. M., Li, Y. F., and Mi, W. D. (2015). Deferoxamine attenuates lipopolysaccharide-induced neuroinflammation and memory impairment in mice. *J. Neuroinflammation* 12:20. doi: 10.1186/s12974-015-0238-3

Zhang, H., and Forman, H. J. (2017). 4-hydroxynonenal-mediated signaling and aging. *Free Radic. Biol. Med.* 111, 219–225. doi: 10.1016/j.freeradbiomed.2016.11.032

Zhang, W., Phillips, K., Wielgus, A. R., Liu, J., Albertini, A., Zucca, F. A., et al. (2011). Neuromelanin activates microglia and induces degeneration of dopaminergic neurons: implications for progression of Parkinson's disease. *Neurotox. Res.* 19, 63–72. doi: 10.1007/s12640-009-9140-z

frontiers | Frontiers in Aging Neuroscience

TYPE Review
PUBLISHED 17 June 2024
DOI 10.3389/fnagi.2024.1417989

OPEN ACCESS

EDITED BY
Robert Weissert,
University of Regensburg, Germany

REVIEWED BY
Hongquan Wang,
Peking University Aerospace School of Clinical Medicine, China
Yukari Shigemoto-mogami,
National Institute of Health Sciences (NIHS), Japan

*CORRESPONDENCE
Jin-yong Tian
tjy8877@yeah.net

RECEIVED 15 April 2024
ACCEPTED 06 June 2024
PUBLISHED 17 June 2024

CITATION
Liu Y, Feng D, Shui L, Wang Y-j, Yu L, Liu Y-q and Tian J-y (2024) The research landscape of ferroptosis in neurodegenerative disease: a bibliometric analysis.
Front. Aging Neurosci. 16:1417989.
doi: 10.3389/fnagi.2024.1417989

The research landscape of ferroptosis in neurodegenerative disease: a bibliometric analysis

Yun Liu[1], Dan Feng[1], Ling Shui[2], Yu-jie Wang[1], Li Yu[1], Yu-qi Liu[1] and Jin-yong Tian[2]*

[1]First Clinical Medical College, Guizhou University of Traditional Chinese Medicine, Guiyang, China, [2]Department of General Practice, Guizhou Provincial People's Hospital, Guiyang, China

Background: Ferroptosis, a newly proposed concept of programmed cell death, has garnered significant attention in research across different diseases in the last decade. Despite thorough citation analyses in neuroscience, there is a scarcity of information on ferroptosis research specifically related to neurodegenerative diseases.

Method: The Web of Science Core Collection database retrieved relevant articles and reviews. Data on publications, countries, institutions, authors, journals, citations, and keywords in the included studies were systematically analyzed using Microsoft Excel 2019 and CiteSpace 6.2.R7 software.

Result: A comprehensive analysis and visualization of 563 research papers on ferroptosis in neurodegenerative diseases from 2014 to 2023 revealed emerging research hotspots and trends. The number of annual publications in this field of study has displayed a pattern of stabilization in the early years of the decade, followed by a notable increase in the later years and peaking in 2023 with 196 publications. Regarding publication volume and total citations, notable research contributions were observed from countries, institutions, and authors in North America, Western Europe, and China. Current research endeavors primarily focus on understanding the intervention mechanisms of neurodegenerative diseases through the ferroptosis pathway and exploring and identifying potential therapeutic targets.

Conclusion: The study highlights key areas of interest and emerging trends in ferroptosis research on neurodegenerative diseases, offering valuable insights for further exploration and potential directions for diagnosing and treating such conditions.

KEYWORDS

ferroptosis, neurodegenerative diseases, bibliometric analysis, hotspots, CiteSpace, knowledge graph

1 Introduction

The progressive loss of neuronal structure and function or neuronal death in the brain and spinal cord characterizes neurodegenerative diseases (ND). Common examples include Alzheimer's disease (AD), Parkinson's disease (PD), Huntington's disease (HD), amyotrophic lateral sclerosis, and multiple sclerosis (Dugger and Dickson, 2017; Agnello and Ciaccio, 2022; Temple, 2023). Iron tends to accumulate in specific brain regions with advancing age,

triggering oxidative stress in cells and contributing to the onset of ND (Chen, 2019). Epidemiological studies have identified ferroptosis markers such as reduced GSH levels, iron deposition, and glutathione peroxidase 4 (GPX4) downregulation in cell and animal models of AD and PD (Cozzi et al., 2019). A study finds that ALOX5-mediated ferroptosis acts as a distinct cell death pathway upon oxidative stress in HD, it provides potential new targets for the treatment of HD (Song et al., 2023). Other researchers also explored the susceptibility to ferroptosis in fused in sarcoma-amyotrophic lateral sclerosis cell models, uncovering mitochondrial disturbances and heightened vulnerability to ferroptosis in cells containing amyotrophic lateral sclerosis-causing fused in sarcoma mutations. This result indicates that ferroptosis could play a substantial role in amyotrophic lateral sclerosis (Ismail et al., 2024). Additionally, One study highlights the benefits of dabrafenib in the treatment of multiple sclerosis by showing its ability to inhibit ferroptosis in microglia through the up-regulation of the Axl receptor. This mechanism ultimately helps to slow down the progression of multiple sclerosis (Liu et al., 2024a). Numerous research results indicate that inhibition of ferroptosis may be a potential strategy for treating ND.

Ferroptosis is a newly identified type of iron-dependent cell death, distinguished by an accumulation of intracellular iron ions that disturb the equilibrium of the intracellular lipid peroxidation system, leading to lipid peroxidation and eventual cell demise (Nikseresht et al., 2019; Costa et al., 2023). In contrast to apoptosis, ferroptosis is an irregular and disordered way of cell death usually induced by external factors such as oxidative stress and drug impacts. Ferroptosis plays a significant role in a variety of diseases (Wang et al., 2023a), including nervous system diseases (Lei et al., 2020; Yao et al., 2021; Ou et al., 2022), cancers (Chen et al., 2021), lung diseases (Xu W. et al., 2021; Yu S. et al., 2021), cardiovascular diseases (Li N. et al., 2021; Yu Y. et al., 2021; Fang et al., 2023), liver diseases (Guo G. et al., 2023; Wang X. et al., 2023), and kidney diseases (Guo R. et al., 2023). The core mechanisms of ferroptosis (Figure 1) involve triggering cell death through the catalysis of lipid peroxidation of unsaturated fatty acids found in high levels on the cell membrane in the presence of divalent ferroptosis or ester oxygenase (Wu et al., 2021). The key enzyme responsible for this process is GPX4, which facilitates the conversion of phospholipid hydroperoxides into less harmful lipid alcohols, thereby safeguarding the cell from damage caused by lipid peroxidation. Inhibition or reduction of GPX4 activity enhances cellular susceptibility to ferroptosis (Bersuker et al., 2019; Xie et al., 2023). Additional regulatory factors of ferroptosis include disruptions in iron metabolism, accumulation of lipid peroxides, and imbalances in the antioxidant system. For instance, excessive iron intake or depleted iron reserves, along with heightened reactive oxygen species (ROS) generation through the Fenton reaction, can precipitate ferroptosis (Park and Chung, 2019). The mechanism of ferroptosis is intricate, involving the interplay of various factors and molecules. By modulating these factors, the sensitivity and response of cells to ferroptosis can be influenced. Pharmacological inhibition of ferroptosis by bioactive small-molecule compounds (ferroptosis inhibitors) could be effective for treatments of ND (Wang et al., 2023b). Aging is an unavoidable process of gradual deterioration of physiological functions caused by a combination of factors (Stockwell, 2022). As cellular senescence proceeds, the physiological functions of tissues and organs of the organism become progressively disturbed and decline, thereby increasing the risk of disease and death, such as ND, cancer and cardiovascular diseases (Goldsteins et al., 2022; Xu et al., 2024). At present, scholars have gradually discovered the intricate connection between ferroptosis and aging, and specific types of cellular senescence and aging-associated diseases are sometimes accompanied by features of cellular ferroptosis (Zheng et al., 2021).

Bibliometric analysis plays a vital role in assessing research performance and identifying influential papers within a specific field (Wang S. Q. et al., 2020). While citation analyses have been conducted in various areas of neuroscience, there is limited information on ferroptosis research related to ND, with only a few studies published. Citation counts significantly measure a study's impact on a research field (Yi et al., 2022). Previous reviews have primarily relied on individual literature summaries and study extractions, which may not fully capture the spatial and temporal distribution of researchers, institutions, and journals. Additionally, visualizing the knowledge base's internal structure and research focus has been challenging, with few systematic, comprehensive, and visual studies available. Current bibliometric analyses on ferroptosis primarily concentrate on specific diseases within the ND series, such as PD and AD. Researchers have identified pathogenesis and treatment (Chen et al., 2024) as key areas of interest in PD research, with 'ferroptosis,' 'immunohistochemistry,' 'diagnosis,' and 'microenvironment' being highlighted as frequent keywords (Lu et al., 2023). Similarly, in AD research, the focus lies on molecular mechanisms (Liu et al., 2024b), with 'Ferroptosis in AD,' 'Pyrptosis in AD,' and 'Neoptosis in AD' emerging as cutting-edge terms that indicate the present and future research directions in this field (Yeerlan et al., 2024). These studies have significantly contributed to the field of bibliometric analysis on ferroptosis and offer valuable research insights for further exploration in ND. Therefore, this study aims to perform a bibliometric analysis of papers published on ferroptosis in ND from 2014 to 2023, comprehensively analyzing the current research status, hot spots, and trends in this area. The goal is to identify journal publications, collaborators, keywords, and research trends that could enhance understanding of these diseases' causes, mechanisms, and treatments. These findings offer valuable insights for future researchers conducting further research.

2 Materials and methods

2.1 Data source

This study utilized the Web of Science Core Collection (WoSCC) database, enriched by the Science Citation Index, as the primary data source. The WoSCC database is well-known for its comprehensive coverage, systematic methodology, and authoritative nature, spanning over 12,000 influential and high-quality journals globally. It is a commonly used resource in scientometric analyses and visualization of scientific literature across various research domains (Hassan et al., 2021; Ge et al., 2022). An advanced search was conducted in the WoSCC database using the search formula TS = (ferroptosis) AND TS = (Neurodegenerative Disease OR Neurologic Degenerative Disease OR Degenerative Neurologic Disease OR Nervous System Degenerative Diseases OR Neurodegenerative Disorder OR Neurologic Degenerative Condition OR Neurologic Degenerative

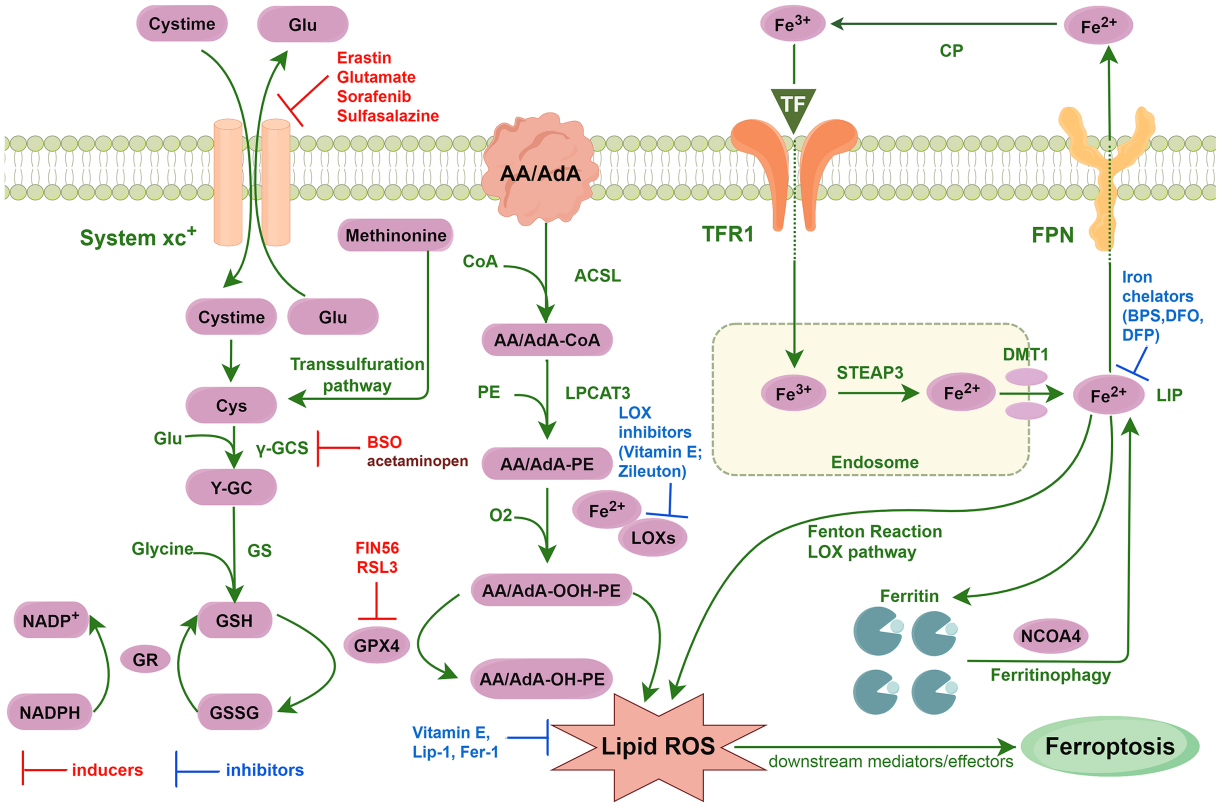

FIGURE 1
Core mechanisms of ferroptosis.

Diseases OR Degenerative OR Neurologic Disorders OR Degenerative Neurologic Disorder) for a comprehensive investigation, focusing on articles and reviews in the English language published until December 2023. This search resulted in a total of 563 relevant documents.

2.2 Data import and merging

All data records from the WoSCC were extracted, including details such as annual research, countries/regions, funding agencies, source journals, institutions, authors, keywords, citations, impact factors, and Journal Citation Reports. Download the bibliographic record from the WoSCC database in Plain Text File format, selecting Record Content as Full Records and Cited References. Import the bibliographic record into NoteExpress and merge the entries in the fields manually after screening and verifying. We identified three situations where data needed to be merged and proposed solutions accordingly. These cases included: (1) full names or abbreviations of the same country name, such as different writing conventions for United States of America and USA; (2) different abbreviations of the same author's name or variations in the order of the last name and the first name, which we solved by using ORCID information and author affiliation; and (3) different terms or expressions that refer to the same concept, for example, ND and neurodegenerative diseases will be merged into neurodegenerative diseases.

2.3 Data analysis and visualization

After data merging, the plain text was imported into Microsoft Excel 2019 and CiteSpace 6.2.R7 (Chen, 2004; Chen and Song, 2019) for analysis. Microsoft Excel was utilized to generate visualizations of the yearly publication volume, whereas CiteSpace was used to visualize collaborations among countries/regions, institutions, and authors. The analysis of cited literature primarily includes network maps, high-frequency co-cited literature, and keywords analysis comprising keywords co-occurrence analysis, keywords clustering analysis, and keywords citation burst analysis.

3 Results

3.1 Publication outputs and time trend

A total of 563 documents on ferroptosis in ND research were published between 2014 and 2023. The publication trend exhibited stability in the initial years, followed by a notable surge in later years, as illustrated in Figure 2. From 2014 to 2017, the number of publications remained relatively low and consistent, with an annual range of 2–6 articles. Subsequently, there was a significant rise in publications from 2018 to 2020, with an average annual growth of 30 articles. Although there was a slight decline in 2021, the numbers remained comparable to 2020, indicating a sustained high activity level. A rapid growth trend is observed in 2022–2023, with an average

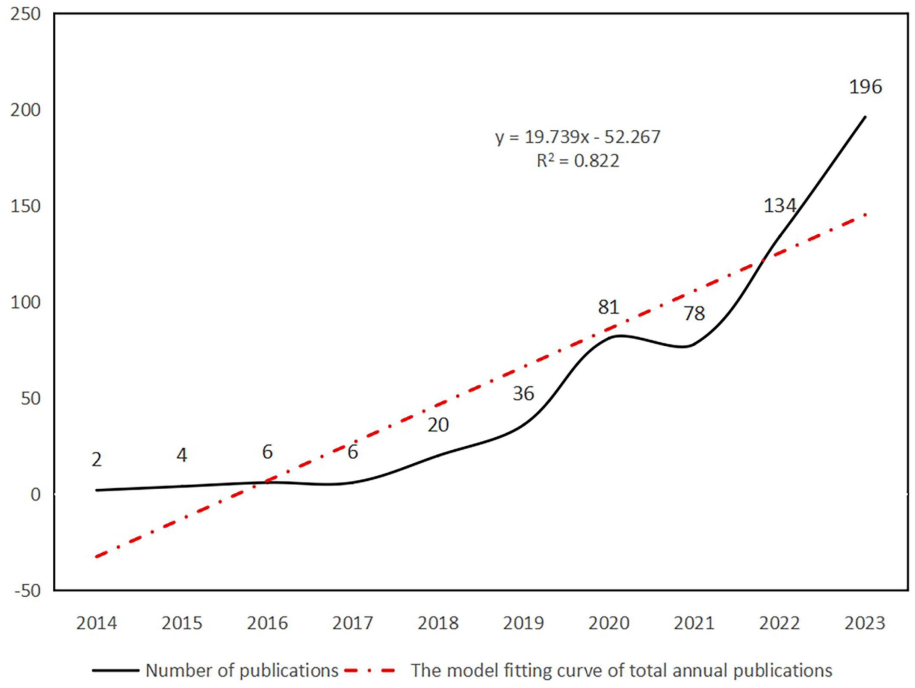

FIGURE 2
Number of publications and the model fitting curve of total annual publications.

increase of 79 articles per year, matching the total publications in 2021. Furthermore, linear regression analysis reveals a positive correlation between the annual total of published articles and the years ($y = 19.739x - 52.267$, $R^2 = 0.822$). These results indicate a promising outlook for ongoing growth and advancement in this research field.

3.2 Distribution of journals

The dataset consists of 563 journal articles from 280 different journals. The journal 'FREE RADICAL BIOLOGY AND MEDICINE' has the highest number of publications with 24 articles, followed by 'INTERNATIONAL JOURNAL OF MOLECULAR SCIENCES' with 20 articles. 90 journals have published more than 2 articles, making up 32.14% of the total number of journals and accounting for 69.8% of the total articles. The top 15 journals contribute to 32.33% of the total articles. These figures indicate a concentrated distribution of articles among journals, with those having high-impact factors publishing a significant number of articles. The top 15 journals by publication volume can be seen in Figure 3.

3.3 Analysis of countries/regions and institutions

A total of 52 countries participated in the studies analyzed, with 11 countries publishing more than 10 studies each. China emerged as the leading contributor with 43.6% of the studies, followed by the United States at 15.82% and Germany at 5.09%. The top 10 contributing countries are detailed in Table 1. CiteSpace analysis was utilized to create a visualization of country collaborations; as depicted in Figure 4, the network consists of 52 nodes and 141 links, illustrating the interconnected academic collaborations among high-producing countries. The top five countries identified are China, the United States, Germany, Australia, and Japan. Among these, the United States, England, and China emerge as the top three countries in terms of centrality, with values of 0.53, 0.37, and 0.18. Analysis based on publication numbers and centrality metrics highlights the United States, China, England, and Germany as the significant research powerhouses in this study.

A total of 486 institutions participated in publishing research papers, with 59 institutions (12.14%) contributing more than 5 papers. The top 10 institutions, detailed in Table 1, each produced at least 13 papers. The University of Melbourne and the Helmholtz Association led with 21 papers each. Collaborative institution mapping results, illustrated in Figure 5, showcased 486 nodes and 1,365 links, indicating cooperative solid relationships. The University of Melbourne, Helmholtz Association, Helmholtz-Center Munich-German Research Center for Environmental Health, Florey Institute of Neuroscience & Mental Health, and the University of Texas System emerged as the top five institutions in collaboration. Noteworthy is the joint top position in centrality rankings held by the University of Melbourne, Florey Institute of Neuroscience & Mental Health, University of Texas System, and Institut National de la Sante et de la Recherche Medicale.

3.4 Analysis of authors and co-cited representative literature

There are 803 authors involved in Ferroptosis in ND. The top 10 most active authors and their related information are shown in Table 2. The top 10 authors collectively published 78 articles. Conrad Marcus published 14 papers and ranked first among all authors,

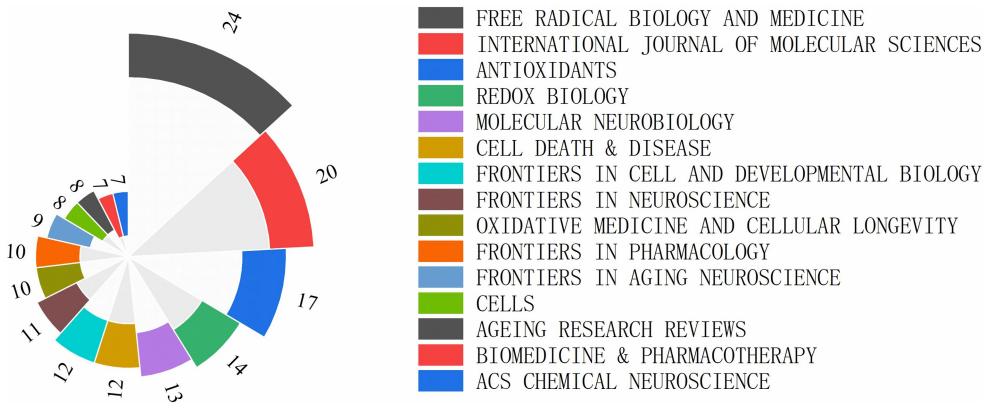

FIGURE 3
Top 15 journals of ferroptosis in ND research ranked by publication number.

TABLE 1 Top 10 countries and institutions in the field of ferroptosis in ND among 563 included studies (2014–2023).

Rank	Country	Count	Centrality	Institute (Country)	Count	Centrality
1	CHINA	317	0.18	University of Melbourne (Australia)	21	0.12
2	USA	115	0.53	Helmholtz Association (Germany)	21	0.04
3	GERMANY	37	0.08	Helmholtz-Center Munich - German Research Center for Environmental Health (Germany)	18	0.03
4	AUSTRALIA	25	0.15	Florey Institute of Neuroscience & Mental Health (Australia)	17	0.12
5	JAPAN	24	0	University of Texas System (USA)	17	0.12
6	ITALY	22	0.02	Institut National de la Sante et de la Recherche Medicale (France)	16	0.12
7	FRANCE	21	0.15	Harvard University (USA)	14	0.07
8	ENGLAND	20	0.37	China Medical University (China)	14	0.01
9	INDIA	17	0.08	Shanghai Jiao Tong University (China)	13	0.07
10	RUSSIA	14	0	Huazhong University of Science & Technology (China)	13	0.01

followed by Maher Pamela ($n = 10$) and Hirata Yoko ($n = 9$). These top 10 authors were affiliated with 8 different research institutions. Table 3 displays the top 10 most cited original articles on ferroptosis in ND research. Nature Chemical Biology and Cell have had a significant scientific impact on researchers and scholars in this field, with nearly half of the top 10 highly cited original articles being published in these journals. All of the top 10 publications have collectively received over 1,030 citations. The study by Doll S et al., published in Nature Chemical Biology, is the most cited article with 182 citations (Doll et al., 2017). Figure 6 presents the results of the CiteSpace analysis of literature co-citations, which includes 646 nodes and 3,293 links. Both nodes and links show the richness of co-citations.

3.5 Keyword analysis

3.5.1 Keywords co-occurrence analysis

Keywords related to ferroptosis in ND research papers were identified and analyzed using CiteSpace software. The keywords were analyzed over The publication period of 2014–2023. The Top five keywords were oxidative stress ($n = 229$), cell death ($n = 206$), lipid peroxidation ($n = 150$), AD ($n = 115$), and PD ($n = 103$). Larger values of centrality represent more cooperation of The node with other nodes. Centrality analysis revealed that cancer cells ($n = 0.16$), activation ($n = 0.12$), ferroptosis ($n = 0.11$), cell death ($n = 0.09$), and mechanisms ($n = 0.09$) exhibited high centrality and emerged as the most influential keywords.

3.5.2 Keywords clusters analysis

The keyword clustering graph reflects the structural features between clusters, highlighting their key nodes and essential connections (Qin et al., 2020). Based on the results of the co-occurrence analysis, a keyword clustering network map was generated with LLR. The network map has a rich clustering structure, and the structure is persuasive, as indicated by the Modularity Q= 0.4174 > 0.3 and Mean Silhouette= 0.7295 > 0.5 of the keyword clustering map, signifying that the clustering structure is clear and reasonable, with high credibility. As is shown in Figure 7, the top 9 clustered tag groups (#0-8), examined and filtered using clustered keywords, represent a general research framework for ferroptosis in ND research. Among the nine keyword clusters, the research topics can be categorized into three groups: (#0), (#1), and (#7) form the first group, mainly related to the study of diseases caused by

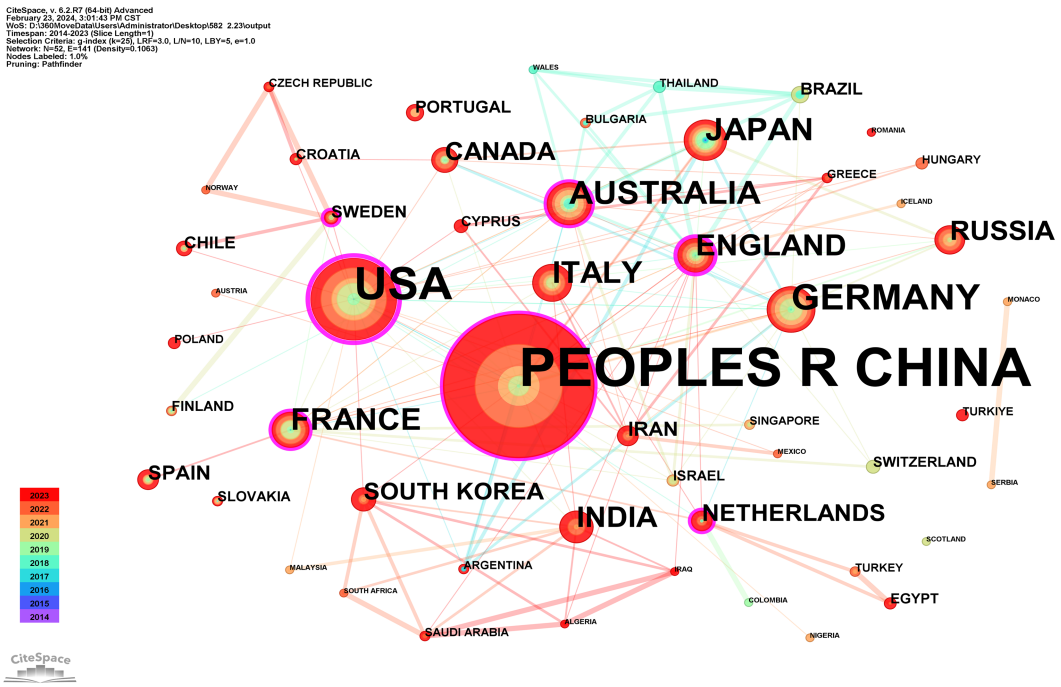

FIGURE 4
CiteSpace network visualization map of country/regions involved in ferroptosis of ND research.

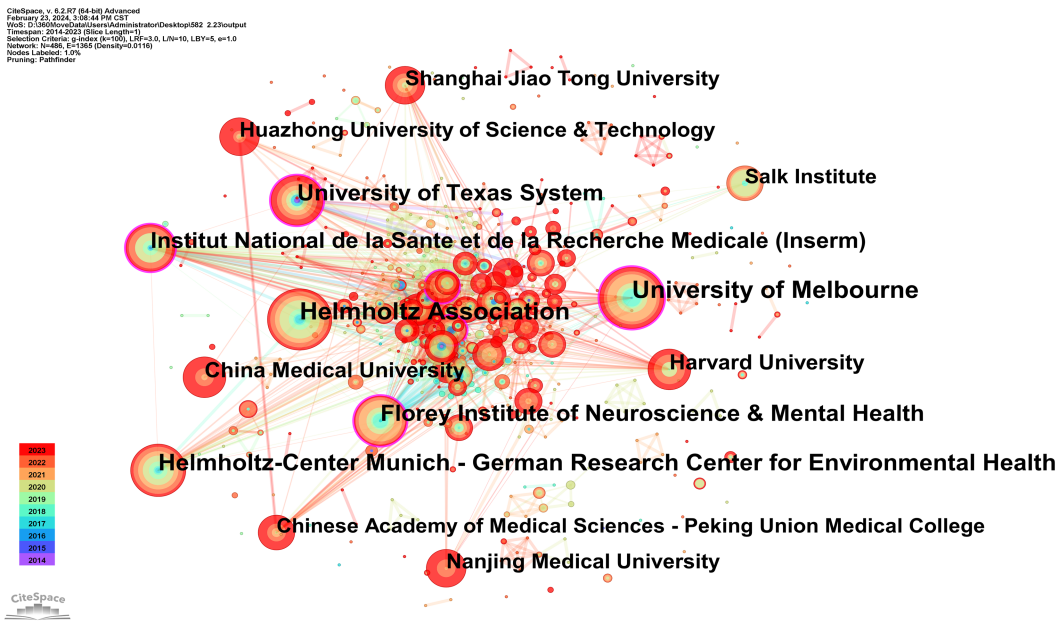

FIGURE 5
CiteSpace network visualization map of institutions involved in ferroptosis of ND research.

ferroptosis; (#2), (#5), and (#6) form the second group, mainly related to the study of the effects of ferroptosis on body tissues and cells; (#3), (#4), and (#8) form the third group, mainly involved in the study of the primary mechanism of ferroptosis in ND. The number of labels in the keyword clusters is inversely proportional to the size of the clusters, with the most prominent clustered label being (#0) AD (n=76), indicating that AD is the primary disease in ferroptosis in ND research.

3.5.3 Keywords citation burst analysis

The analysis of keyword citation bursts can reveal the research trends within a specific timeframe (Wang Z. et al., 2020). Based on

TABLE 2 Top 10 authors who published literature on ferroptosis in ND among 563 included studies (2014–2023).

Rank	Author	Institute	Count	Centrality
1	Conrad, Marcus	Helmholtz Zentrum Munchen	14	0.00
2	Maher, Pamela	Salk Institute for Biological Studies	10	0.00
3	Hirata, Yoko	Gifu University	9	0.00
4	Devos, David	Lille University	7	0.01
5	Furuta, Kyoji	Gifu University	7	0.00
6	Currais, Antonio	Salk Institute for Biological Studies	7	0.00
7	Bush, Ashley I	University of Melbourne	6	0.02
8	Ayton, Scott	University of Melbourne	6	0.01
9	Tang, Daolin	Guangzhou Medical University	6	0.00
10	Stockwell, Brent R.	Columbia University	6	0.00

keyword co-occurrence analysis, Keyword citation burst analysis was utilized to determine the top 25 cited keywords, see Figure 8. In the Keywords citation burst analysis, "Begin" and "End" indicate the time of the burst. "Strength" means the strength of the burst, representing credibility over time. By focusing on keywords with a high burst rate, researchers can uncover the current hot topics in the field.

The Keywords citation burst analysis reveals three phases of results. The first phase, from 2014 to 2017, highlights keywords like 'cancer cells, death, injury, 12/15 lipoxygenase, glutamate, gpx4, biomolecules, AD', focusing on physiological changes and disease effects. For instance, the proliferation of cancer cells was linked to ferroptosis, which was also identified as a pathogenic mechanism in AD. The second phase, spanning 2017 to 2020, explores keywords such as 'amyloid precursor protein, HD, neurofibrillary tangles, antioxidant, peroxidation, inactivation, cell death mechanisms, metabolism, toxicity, heme oxygenase 1, Friedreich's ataxia,' emphasizing the impact of ferroptosis on ND. Lastly, the third phase, from 2020 to 2023, concentrates on 'homeostasis, cellular, binding, NLRP3 inflammasome, cancer therapy, ablation,' indicating a sustained focus on mechanism and pathway studies. This phase also underscores the increasing significance of inhibition of ferroptosis for disease treatment. The keywords from the third phase remain relevant today and represent emerging trends and future research directions.

4 Discussion

4.1 General information

In the past decade, there has been a notable increase in scholarly interest and research on ferroptosis in ND, leading to a growing number of related studies annually. This bibliometric analysis employs CiteSpace to examine and illustrate 563 papers on the subject to identify critical research hotspots and trends. The evolution of research activity and output in publications related to this topic can be observed in three distinct phases. Before 2018, a relatively consistent and limited number of papers were published. In 2012, the discovery of a small molecule compound called erastin revolutionized the field by affecting a wide range of cells, including neurons and tumor cells. Erastin enhances the process of peroxide accumulation during $Fe2^{+}$ synthesis, leading to intracellular mitochondrial atrophy and increased membrane density. This unique mechanism results in a distinctive form of cell death known as ferroptosis, setting it apart from other forms of cell death (Li et al., 2020). Initially, research on ferroptosis was limited. However, from 2018 to 2021, there was a substantial increase in the number of papers, indicating a broadening scope and depth of research. Post-2021, there has been a rapid growth trend, with an average annual increase of approximately 79 articles. This trend underscores the immense research potential of ferroptosis in ND, drawing increasing attention from scholars (Reichert et al., 2020; Xu et al., 2023). Consequently, it is foreseeable that this research area will continue to gain traction in the future.

Among the top 10 countries publishing papers in this research field, 9 are developed, while China is the sole developing country. Despite China having the highest number of publications, its low centrality score of 0.18 suggests limited connections with developed countries in the field, indicating a lack of international cooperation. The United States, Germany, the United Kingdom, and Australia dominate this area. Analysis of the institutional cooperation network reveals that national institutions in Australia, the United States, and Germany, such as the University of Melbourne, Helmholtz Association, Helmholtz-Center Munich - German Research Center for Environmental Health, Florey Institute of Neuroscience & Mental Health, and the University of Texas System, are leading in research on ferroptosis in ND. The most active and prominent institutions are predominantly renowned universities from developed countries with abundant academic resources, with China following closely behind. There is an imbalance in the exchange of academic resources between developing and developed countries. This disparity may be attributed to financial constraints and insufficient attention in developing countries, resulting in delayed research initiation and a lack of high-quality research outcomes.

The distribution of author clusters exhibits similarities to the distribution of country and institutional clusters. The top 10 authors listed in Table 2 are predominantly associated with research institutions in developed countries. Among these top 10 authors, Conrad Marcus, Maher Pamela, and Hirata Yoko emerge as the leading researchers in this particular field. Conrad Marcus has proposed that ferroptosis plays a significant role in the development of organ injuries and degenerative pathologies. He has also suggested that the manipulation of ferroptosis, through both its induction and inhibition, holds promise in treating drug-resistant cancers, ischaemic organ injuries, and other degenerative diseases characterized by high levels of lipid peroxidation (Jiang et al., 2021). Maher Pamela and her

TABLE 3 Top 10 co-citation representative literature of ferroptosis in ND among the 563 articles included (2014–2023).

Rank	Cited number	Title	Type	Year	Centrality	Journal	JCR (2022)	IF (2022)	Reference
1	182	ACSL4 dictates ferroptosis sensitivity by shaping cellular lipid composition	Article	2017	0.04	Nature Chemical Biology	Q1	14.8	Doll et al. (2017)
2	161	Ferroptosis: A Regulated Cell Death Nexus Linking Metabolism, Redox Biology, and Disease	Review	2017	0.00	Cell	Q1	64.5	Stockwell et al. (2017)
3	120	The CoQ oxidoreductase FSP1 acts parallel to GPX4 to inhibit ferroptosis	Article	2019	0.02	Nature	Q1	64.8	Bersuker et al. (2019)
4	94	Oxidized arachidonic and adrenic PEs navigate cells to ferroptosis	Article	2017	0.02	Nature Chemical Biology	Q1	14.8	Kagan et al. (2017)
5	88	Ablation of ferroptosis regulator glutathione peroxidase 4 in forebrain neurons promotes cognitive impairment and neurodegeneration	Article	2017	0.01	Redox biology	Q1	11.4	Hambright et al. (2017)
6	82	Ferroptosis: mechanisms, biology and role in disease	Review	2021	0.00	Nature reviews Molecular cell biology	Q1	112.7	Jiang et al. (2021)
7	79	Ferroptosis: past, present and future	Review	2020	0.01	Cell Death & Disease	Q1	9.0	Li et al. (2020)
8	78	Molecular mechanisms of cell death: recommendations of the Nomenclature Committee on Cell Death 2018	Review	2018	0.09	Cell Death and Differentiation	Q1	12.4	Galluzzi et al. (2018)
9	76	Selenium Utilization by GPX4 Is Required to Prevent Hydroperoxide-Induced Ferroptosis	Article	2018	0.04	Cell	Q1	64.5	Ingold et al. (2018)
10	70	Ferroptosis: process and function	Review	2016	0.00	Cell Death and Differentiation	Q1	12.4	Xie et al. (2016)

*IF, impact factor; *JCR, Category Quartile of Journal Citation Report.

colleagues have emphasized the involvement of the oxytosis/ferroptosis is regulated with cell death pathway in aging and ND and the AMPK/ACC1 pathway in cell death induced by an oxytosis/ferroptosis inducer (Currais et al., 2022). Additionally, Hirata Yoko and his team discovered that N,N-dimethylaniline derivatives had been identified as potent inhibitors of ferroptosis. Despite not forming a chelating structure with $Fe2^{+}$, N,N-dimethylaniline derivatives are capable of creating stable monodentate complexes with hydrated ferrous ions, with the assistance of aliphatic tertiary amine molecules to stabilize the complexes. Those discoveries could potentially aid in developing more effective lysosomal ferroptosis inhibitors for treating ND (Hirata et al., 2023).

Analysis of publication output and citations reveals that approximately one-third of the papers are published in the top 15 journals. Notably, 'Nature Chemical Biology' and 'Cell' have had a significant scientific impact on researchers and scholars in the field. For instance, 'Nature Chemical Biology', a journal under the NATURE PORTFOLIO, boasts an IF of 14.8 in 2022. The journal covers diverse research on the role of ferroptosis in ND, including lipid metabolism, autophagy, and mitochondria, which significantly advances people's understanding of this field. An article in the journal investigated the relationship between the structure, activity, and distribution of compounds that modulate ferroptosis using fluorescence and stimulated Raman scattering imaging. The study found that lipid peroxidation triggering ferroptosis occurs across different subcellular membranes, with the endoplasmic reticulum membrane being identified as the primary site. The research revealed a sequential pattern of membrane peroxidation during iron metabolism, starting with accumulation on the endoplasmic reticulum membrane before spreading to the plasma membrane. By targeting inhibitors and inducers specifically at the endoplasmic reticulum, it may be possible to precisely regulate lipid peroxidation dynamics in cells undergoing ferroptosis. This targeted approach shows promise as a potential

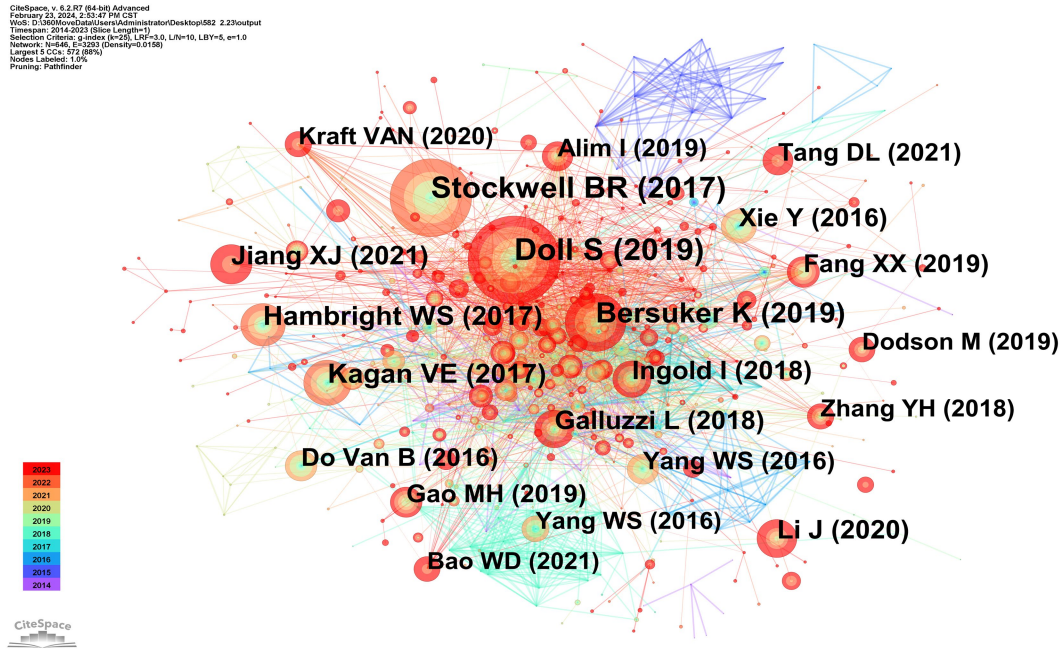

FIGURE 6
CiteSpace network visualization map of co-cited references involved in ferroptosis of ND research.

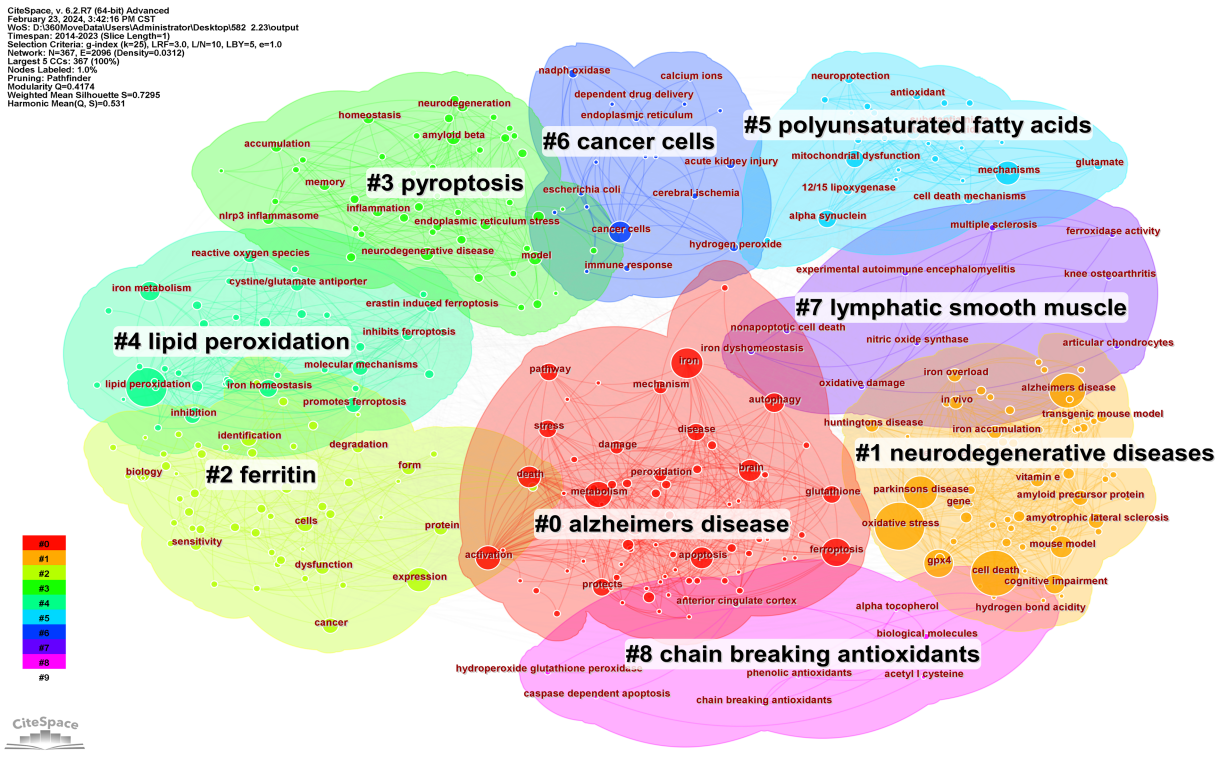

FIGURE 7
CiteSpace network visualization map of keywords clusters analysis involved in ferroptosis of ND research.

therapeutic strategy for drug-resistant cancers and could have implications for the pathogenesis of certain degenerative diseases (Von Krusenstiern et al., 2023). Furthermore, other prestigious journals like 'Nature', 'Nature Reviews Molecular Cell Biology', and 'Cell Death and Differentiation' have also made valuable contributions to the field of ferroptosis to ND research.

10.3389/fnagi.2024.1417989

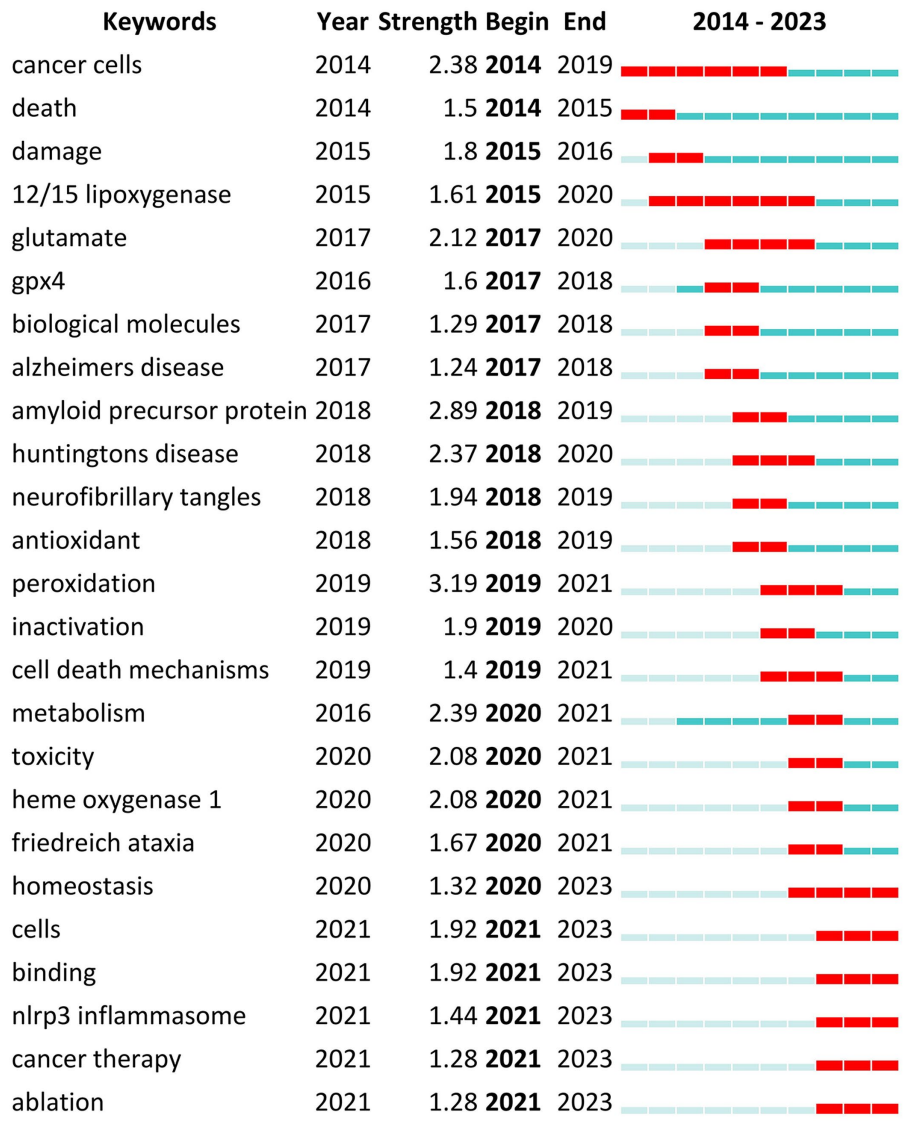

FIGURE 8
Keywords citation bursts analysis of related literature. The red line shows the time frame during which the keyword bursts were discovered, while the blue line shows the time interval.

4.2 Important research findings

Based on a literature citation analysis, the paper 'ACSL4 dictates ferroptosis sensitivity by shaping cellular lipid composition' by Doll S et al. published in 'Nature Chemical Biology' in 2017 (Doll et al., 2017) has received the highest number of citations. The study highlights the crucial role of CoA synthetase long-chain family member 4 (ACSL4) in driving ferroptosis. GPX4-ACSL4 double-knockout cells displayed significant resistance to ferroptosis. Targeting ACSL4 with thiazolidinediones, a type of antidiabetic compound, reduced tissue damage in a mouse model of ferroptosis, suggesting that inhibiting ACSL4 could be a promising therapeutic approach for ferroptosis-related diseases. The second most cited work is a review by Stockwell BR et al. published in Cell in 2017 (Stockwell et al., 2017), which underscores that recent research indicates ferroptosis is triggered by integrating polyunsaturated fatty acids into cellular membranes. Sensitivity to ferroptosis is intricately linked to various biological processes, including amino acid, iron, and polyunsaturated fatty acid metabolism and the synthesis of glutathione, phospholipids, and coenzyme Q10. Ferroptosis has been implicated in pathological cell death in conditions such as ND, cancer progression, stroke, intracerebral hemorrhage, and traumatic brain injury.

In addition, in an article published in Nature Chemical Biology, Kagan et al. (2017) demonstrated that ferroptosis is characterized by a highly organized oxygenation center. They discovered that inhibiting ACSL4 can prevent the esterification of arachidonic acid or adrenic acid into phosphatidylethanolamine, serving as a specific pathway to rescue cells from ferroptotic cell death. Lipoxygenase was identified as

the enzyme responsible for generating doubly and triply-oxygenated-diacylated phosphatidylethanolamine species, which signal cell death. Additionally, tocopherols and tocotrienols were found to suppress lipoxygenase activity and protect cells from ferroptosis, indicating a potential physiological role for vitamin E in maintaining cellular homeostasis. The authors propose that targeting this oxidative phosphatidylethanolamine death pathway could be a promising approach for drug development (Kagan et al., 2017).

4.3 Research hotspots and frontiers

Keywords play a crucial role in identifying emerging trends and guiding future research directions (Synnestvedt et al., 2005). In this instance, keywords citation burst analysis was conducted using CiteSpace. Five research frontier keywords burst from 2021. We summarize the existing research results and provide insights into the future research direction hotspots of ferroptosis on ND.

4.3.1 Cells

Ferroptosis is a unique type of regulated cell death characterized by the lethal buildup of lipid peroxides in plasma membranes (Martinez et al., 2020). This process is intricately linked to various biological pathways and has been implicated in the pathogenesis of cancer and ND. These discoveries have paved the way for developing innovative cytoprotective approaches aimed at safeguarding cells in conditions such as neurodegenerative, hematologic, and cardiovascular disorders through inhibiting ferroptosis (Qiu et al., 2020). The study of microglia has been increasingly emphasized by scholars, and research on microglia ferroptosis in ND has been carried out. A study found that human-induced pluripotent stem cell-derived microglia when cultivated in a tri-culture system, demonstrate heightened reactivity to iron and are prone to ferroptosis. Excessive iron levels cause a notable shift in the transcriptional profile of microglia, resembling a gene expression pattern seen in postmortem brain microglia of PD patients. This microglial reaction contributes to neurodegeneration, as evidenced by the delayed onset of iron-induced neurotoxicity upon microglia removal from the tri-culture setup. These results underscore the critical role of microglial iron overload and ferroptosis in the neurodegenerative process (Ryan et al., 2023).

Aberrations in programmed cell death signaling pathways, such as apoptosis, necroptosis, pyroptosis, ferroptosis, autophagy-associated cell death, and unprogrammed necrosis, are observed in the development of various neurological disorders. These mechanisms of cell death can be initiated by cellular stress and inflammatory reactions. The dysregulated activation of programmed cell death pathways is a common feature in neurodegenerative conditions, resulting in the unwanted loss of neuronal cells and their functionality (Moujalled et al., 2021). Mitochondria are pivotal in the process of apoptotic cell death, with mitochondrial outer membrane permeabilization (MOMP) typically leading to cell death (Vringer and Tait, 2023). MOMP triggers a range of pro-inflammatory signaling pathways, and recent research indicating cell survival after MOMP suggests that mitochondria-derived signaling from pro-apoptotic triggers may have non-lethal functions. Targeting MOMP to modulate cell death shows great promise for therapeutic interventions in ND (Bock and Tait, 2020). Research has been conducted on the cellular level of ferroptosis in the context of drug treatment for ND. Experimental animal studies have demonstrated that salidroside exhibits neuroprotective effects by inhibiting neuronal ferroptosis in Amyloid beta peptide (Aβ)1-42-induced AD mice and Glu-injured HT22 cells. This neuroprotective mechanism is associated with the activation of the Nrf2/HO1 signaling pathway. This area of research shows promise for future exploration (Yang et al., 2022).

4.3.2 Binding

GPX4 is identified as a crucial regulator of ferroptosis. Autoantibodies and interferon-α found in the serum have been shown to trigger neutrophil ferroptosis by increasing the binding of the transcriptional repressor CREMα to the GPX4 promoter. This results in reduced expression of GPX4 and an increase in lipid-ROS (Li P. et al., 2021). High mobility group box 1 (HMGB1) is a nonhistone nuclear protein known for its role as a DNA chaperone, maintaining chromosome structure and function. Additionally, HMGB1 can induce autophagy by interacting with the BECN1 protein. The secretion and release of HMGB1 are regulated by various factors, such as posttranslational modifications like phosphorylation and methylation, as well as cell death mechanisms like apoptosis, necroptosis, and ferroptosis (Chen et al., 2022).

The RNA-binding protein ZFP36 ring finger protein is essential in regulating ferroptosis in hepatic stellate cells (HSCs). Treatment with erastin and sorafenib in mice helped alleviate murine liver fibrosis by promoting HSC ferroptosis. Overexpression of ZFP36, specifically in HSCs, hindered the induction of HSC ferroptosis by erastin or sorafenib. In human HSCs, sorafenib treatment alone resulted in ZFP36 downregulation, activation of ferritinophagy, and induction of ferroptosis. These findings shed light on new molecular mechanisms and signaling pathways involved in ferroptosis (Zhang et al., 2020). Another study (Zhang et al., 2021) suggests that ferroptosis is a tightly regulated process suppressing tumors. The RNA-binding protein RBMS1 plays a role in lung cancer development by facilitating the evasion of ferroptosis, making it a crucial regulator of this process. Inhibiting RBMS1 led to decreased translation of SLC7A11, resulting in reduced cystine uptake mediated by SLC7A11 and ultimately promoting ferroptosis. Exploring the role of RNA-binding proteins in disease development through mediating ferroptosis evasion could be a promising area for further research.

4.3.3 NLRP3 inflammasome

Deferoxamine, an iron chelator, has demonstrated the ability to inhibit neuron degeneration by reducing the accumulation of iron, lipid peroxides, and ROS and modulating the expression of ferroptosis-related indicators. Furthermore, Deferoxamine has shown potential in reducing NLRP3 activation through the ROS/NF-κB pathway, influencing microglial polarization, decreasing neutrophil and macrophage infiltration, and inhibiting the release of inflammatory factors following traumatic brain injury. Moreover, Deferoxamine may also attenuate the activation of neurotoxic responsive astrocytes (Jia et al., 2023). It has been proposed that therapeutic interventions for neuropsychiatric disorders may benefit from targeting not only oxidative stress and inflammatory processes in general but also specific factors such as TNF-α, PARP-1, NLRP3 inflammasome, and RIP3. Activation of these factors can lead to peripheral inflammation and neuroinflammation, even in the absence

of cell death, highlighting their potential as treatment targets (Morris et al., 2018).

Aβ has been identified as a key contributor to AD. In a study involving APP/PS1 mice, treatment with non-toxic tetrahydroxy stilbene glycoside (TSG) demonstrated a dose-dependent protection against Aβ-induced neuronal cell death by modulating ferroptosis-related proteins and enzymes. TSG was found to enhance the activation of GSH/GPX4/ROS and Keap1/Nrf2/ARE signaling pathways. Additionally, TSG administration led to a decrease in markers associated with ferroptosis, such as lipid peroxidation and neuroinflammation markers like NLRP3 and ACSL4 (Gao et al., 2021). Elevated expression of Heme oxygenase-1 in ND has been linked to the accumulation of neurotoxic ferric iron deposits. In mouse models, inflammation-induced stimulation leads to changes in various iron-related metabolic proteins, ultimately causing an upsurge in ferroptosis, iron deposition, and oxidative stress. Additionally, microglia demonstrate a primed phenotype with heightened levels of inflammatory markers, including iNOS, TNF-α, IL-1β, and NLRP3 (Fernández-Mendívil et al., 2021). Exploring the NLRP3 inflammasome pathway and its molecular interactions may reveal additional potential avenues for the development of inflammasome-targeting drugs.

4.3.4 Cancer therapy

Ferroptosis induction has recently gained attention as a promising approach to cancer treatment. Elevated iron levels within cells lead to increased production of ROS. Molecules that induce ferroptosis enhance ROS production and suppress the antioxidant defense system, thereby promoting ferroptosis in cancer cells (Maru et al., 2022). Cancer cells accumulate elevated levels of iron and ROS to enhance their metabolic activity and proliferation. Notably, the metabolic reprogramming of cancer cells is frequently linked with increased vulnerability to ferroptosis. This indicates that ferroptosis could serve as an adaptive reaction to metabolic dysregulation and potentially offer a novel approach to eliminating cancerous cells (Battaglia et al., 2020).

RSL3 and other small-molecule GPX4 inhibitors have been shown to induce ferroptosis in both cultured cancer cells and tumor xenografts in mice. Likewise, erastin and other system Xc- inhibitors can reduce intracellular glutathione levels necessary for GPX4 activity, resulting in lipid peroxidation and ferroptosis. Given that therapy-resistant cancer cells are particularly vulnerable to GPX4-targeted treatments, the potential of ferroptosis-inducing agents to enhance existing cancer therapies is promising (Wang L. et al., 2022). Glioblastoma is recognized as the predominant malignant tumor affecting the brain. The complexity of this cancer poses challenges in treatment, attributed to its significant heterogeneity and the presence of an immunosuppressive microenvironment. Recent research indicates that directing interventions toward ferroptosis could serve as a promising approach to addressing resistance to conventional tumor therapies and immune evasion strategies (Zhuo et al., 2022). The integration of ferroptosis-targeted therapies with existing treatments holds the potential to enhance the management of cancer.

4.3.5 Ablation

In various neurodegenerative disorders, the intracellular accumulation of TAU aggregates is a defining feature. When TAU was conditionally removed from excitatory neurons, it led to a decrease in epilepsy and the overactivation of the PI3K/AKT pathway (Shao et al., 2022). Using CRISPR to introduce point mutations and express human tau in AD model mice, it was demonstrated that the interaction between specific sites regulates both normal physiological phosphorylation and the development of amyloid-associated cognitive impairments. Furthermore, a combined approach targeting key phosphorylation sites and p38α synergistically ablated hyperphosphorylation (Stefanoska et al., 2022). Additionally, Shank3, a protein primarily found in the heart, plays a role in regulating age-related ND. Removal of Shank3 was found to increase the process of mitophagy, decrease the production of harmful superoxide from mitochondria, reduce cell death, and protect against heart dysfunction in older individuals. When aging heart cells treated with D-galactose were studied, it was observed that mitophagy decreased while Shank3 expression significantly increased. Knocking down Shank3 resulted in the restoration of mitophagy, leading to improved health of mitochondria, reduced oxidative stress within mitochondria, and decreased cell death. Conversely, overexpression of Shank3 mimicked the inhibitory effects of D-galactose on mitophagy and caused dysfunction in mitochondria (Wang Y. et al., 2022). Another study reported that aconitate decarboxylase 1 ablation abates Tumor-infiltrating neutrophils infiltration, constrains metastasis, and bolsters antitumor T cell immunity (Zhao et al., 2023). Previously, we mentioned GPX4's research on cancer; in a new study, it was found that the loss of GPX4 leads to an excessive buildup of lipid peroxides and ferroptosis in Treg cells when T cell receptor/CD28 co-stimulation occurs. Additionally, Treg-specific ablation of GPX4 inhibits tumor growth and enhances the body's ability to fight against tumors (Xu C. et al., 2021).

A recent study delved into the concept of 'ablation' within the realm of treatment technology (Pfannenstiel et al., 2022). Microwave ablation (MWA) is gaining attention as an alternative method for treating unresectable tumors. Studies suggest that MWA may impact the process of ferroptosis within tumors, potentially regulating cancer cell ferroptosis. This mechanism could play a role in the tumor-killing effects of MWA (Bozaykut et al., 2016). Research indicates that inducing ferroptosis is a promising therapy for cancer treatment, suggesting that combining MWA with ferroptosis inducers could be a novel approach in tumor therapy (Gai et al., 2020; Yu et al., 2023). In conclusion, the specific ablation of TAU, Shank3, and GPX4, along with utilizing MWA technology, presents new opportunities for studying ND and cancer induced by ferroptosis.

4.4 Limitations

This study utilized CiteSpace 6.2.R7 software to visualize and analyze the literature on ferroptosis in ND within the WoSCC database. However, several limitations were identified. Firstly, disparities in economic strength and population size among countries may influence research progress in this field, potentially leading to bias. Secondly, only English literature from the WoSCC database was included in the visualization analysis, suggesting that future studies should consider incorporating additional databases such as CNKI and Scopus. Lastly, since citations are expected to peak gradually

3–10 years after publication, the current analysis may not highlight recently published articles.

5 Conclusion

Research on ferroptosis for ND is still in its early stages of development. Based on the current global trend, there is expected to be a significant increase in publications on this topic and the number of researchers actively involved. Noteworthy advancements have been achieved in ferroptosis research related to ND, particularly in China, Europe, and the United States, with Europe and the United States emerging as leaders in this field. Existing literature can be broadly classified into two main categories: 'mechanism studies' and 'treatment and effects'. Future research is likely to focus more on areas such as cells, binding, nlrp3 inflammasome, cancer therapy, and ablation, indicating potential new directions for investigation.

Author contributions

YL: Data curation, Funding acquisition, Investigation, Project administration, Resources, Software, Supervision, Validation, Visualization, Writing – original draft, Writing – review & editing. DF: Methodology, Software, Validation, Visualization, Writing – review & editing. LS: Data curation, Investigation, Project administration, Visualization, Writing – review & editing. Y-jW: Formal analysis, Visualization, Writing – review & editing. LY: Validation, Writing – review & editing. Y-qL: Investigation, Validation, Writing – review & editing. J-yT: Funding acquisition, Supervision, Writing – review & editing.

Funding

The author(s) declare that financial support was received for the research, authorship, and/or publication of this article. This work was supported by the Guizhou Province Science and Technology Planning Project (No. [2020]1Z059).

Conflict of interest

The authors declare that the research was conducted in the absence of any commercial or financial relationships that could be construed as a potential conflict of interest.

Publisher's note

References

Agnello, L., and Ciaccio, M. (2022). Neurodegenerative diseases: from molecular basis to therapy. *Int. J. Mol. Sci.* 23:12854. doi: 10.3390/ijms232112854

Battaglia, A. M., Chirillo, R., Aversa, I., Sacco, A., Costanzo, F., and Biamonte, F. (2020). Ferroptosis and cancer: mitochondria meet the "iron maiden" cell death. *Cells* 9:1505. doi: 10.3390/cells9061505

Bersuker, K., Hendricks, J. M., Li, Z., Magtanong, L., Ford, B., Tang, P. H., et al. (2019). The coq oxidoreductase fsp1 acts parallel to gpx4 to inhibit ferroptosis. *Nature* 575, 688–692. doi: 10.1038/s41586-019-1705-2

Bock, F. J., and Tait, S. (2020). Mitochondria as multifaceted regulators of cell death. *Nat. Rev. Mol. Cell Biol.* 21, 85–100. doi: 10.1038/s41580-019-0173-8

Bozaykut, P., Ozer, N. K., and Karademir, B. (2016). Nrf2 silencing to inhibit proteolytic defense induced by hyperthermia in ht22 cells. *Redox Biol.* 8, 323–332. doi: 10.1016/j.redox.2016.03.001

Chen, C. (2004). Searching for intellectual turning points: progressive knowledge domain visualization. *Proc. Natl. Acad. Sci. USA* 101, 5303–5310. doi: 10.1073/pnas.0307513100

Chen, J. J. (2019). Functional mri of brain physiology in aging and neurodegenerative diseases. *NeuroImage* 187, 209–225. doi: 10.1016/j.neuroimage.2018.05.050

Chen, X., Kang, R., Kroemer, G., and Tang, D. (2021). Organelle-specific regulation of ferroptosis. *Cell Death Differ.* 28, 2843–2856. doi: 10.1038/s41418-021-00859-z

Chen, R., Kang, R., and Tang, D. (2022). The mechanism of hmgb1 secretion and release. *Exp. Mol. Med.* 54, 91–102. doi: 10.1038/s12276-022-00736-w

Chen, C., and Song, M. (2019). Visualizing a field of research: a methodology of systematic scientometric reviews. *PLoS One* 14:e223994. doi: 10.1371/journal.pone.0223994

Chen, Y., Wu, Z., Li, S., Chen, Q., Wang, L., Qi, X., et al. (2024). Mapping the research of ferroptosis in parkinson's disease from 2013 to 2023: a scientometric review. *Drug Des. Devel. Ther.* 18, 1053–1081. doi: 10.2147/DDDT.S458026

Costa, I., Barbosa, D. J., Benfeito, S., Silva, V., Chavarria, D., Borges, F., et al. (2023). Molecular mechanisms of ferroptosis and their involvement in brain diseases. *Pharmacol. Ther.* 244:108373. doi: 10.1016/j.pharmthera.2023.108373

Cozzi, A., Orellana, D. I., Santambrogio, P., Rubio, A., Cancellieri, C., Giannelli, S., et al. (2019). Stem cell modeling of neuroferritinopathy reveals iron as a determinant of senescence and ferroptosis during neuronal aging. *Stem Cell Rep.* 13, 832–846. doi: 10.1016/j.stemcr.2019.09.002

Currais, A., Kepchia, D., Liang, Z., and Maher, P. (2022). The role of amp-activated protein kinase in oxytosis/ferroptosis: protector or potentiator? *Antioxid. Redox Signal.* 4:13. doi: 10.1089/ars.2022.0013

Doll, S., Proneth, B., Tyurina, Y. Y., Panzilius, E., Kobayashi, S., Ingold, I., et al. (2017). Acsl4 dictates ferroptosis sensitivity by shaping cellular lipid composition. *Nat. Chem. Biol.* 13, 91–98. doi: 10.1038/nchembio.2239

Dugger, B. N., and Dickson, D. W. (2017). Pathology of neurodegenerative diseases. *Cold Spring Harb. Perspect. Biol.* 9:a028035. doi: 10.1101/cshperspect.a028035

Fang, X., Ardehali, H., Min, J., and Wang, F. (2023). The molecular and metabolic landscape of iron and ferroptosis in cardiovascular disease. *Nat. Rev. Cardiol.* 20, 7–23. doi: 10.1038/s41569-022-00735-4

Fernández-Mendívil, C., Luengo, E., Trigo-Alonso, P., García-Magro, N., Negredo, P., and López, M. G. (2021). Protective role of microglial ho-1 blockade in aging: implication of iron metabolism. *Redox Biol.* 38:101789. doi: 10.1016/j.redox.2020.101789

Gai, C., Yu, M., Li, Z., Wang, Y., Ding, D., Zheng, J., et al. (2020). Acetaminophen sensitizing erastin-induced ferroptosis via modulation of nrf2/heme oxygenase-1 signaling pathway in non-small-cell lung cancer. *J. Cell. Physiol.* 235, 3329–3339. doi: 10.1002/jcp.29221

Galluzzi, L., Vitale, I., Aaronson, S. A., Abrams, J. M., Adam, D., Agostinis, P., et al. (2018). Molecular mechanisms of cell death: recommendations of the nomenclature committee on cell death 2018. *Cell Death Differ.* 25, 486–541. doi: 10.1038/s41418-017-0012-4

Gao, Y., Li, J., Wu, Q., Wang, S., Yang, S., Li, X., et al. (2021). Tetrahydroxy stilbene glycoside ameliorates alzheimer's disease in app/ps1 mice via glutathione peroxidase related ferroptosis. *Int. Immunopharmacol.* 99:108002. doi: 10.1016/j.intimp.2021.108002

Ge, Y., Chao, T., Sun, J., Liu, W., Chen, Y., and Wang, C. (2022). Frontiers and hotspots evolution in psycho-cardiology: a bibliometric analysis from 2004 to 2022. *Curr. Probl. Cardiol.* 47:101361. doi: 10.1016/j.cpcardiol.2022.101361

Goldsteins, G., Hakosalo, V., Jaronen, M., Keuters, M. H., Lehtonen, Š., and Koistinaho, J. (2022). Cns redox homeostasis and dysfunction in neurodegenerative diseases. *Antioxidants* 11:405. doi: 10.3390/antiox11020405

Guo, R., Duan, J., Pan, S., Cheng, F., Qiao, Y., Feng, Q., et al. (2023). The road from Aki to ckd: molecular mechanisms and therapeutic targets of ferroptosis. *Cell Death Dis.* 14:426. doi: 10.1038/s41419-023-05969-9

Guo, G., Yang, W., Sun, C., and Wang, X. (2023). Dissecting the potential role of ferroptosis in liver diseases: an updated review. *Free Radic. Res.* 57, 282–293. doi: 10.1080/10715762.2023.2232941

Hambright, W. S., Fonseca, R. S., Chen, L., Na, R., and Ran, Q. (2017). Ablation of ferroptosis regulator glutathione peroxidase 4 in forebrain neurons promotes cognitive impairment and neurodegeneration. *Redox Biol.* 12, 8–17. doi: 10.1016/j.redox.2017.01.021

Hassan, W., Zafar, M., Duarte, A. E., Kamdem, J. P., and Teixeira, D. R. J. (2021). Pharmacological research: a bibliometric analysis from 1989 to 2019. *Pharmacol. Res.* 169:105645. doi: 10.1016/j.phrs.2021.105645

Hirata, Y., Hashimoto, T., Ando, K., Kamatari, Y. O., Takemori, H., and Furuta, K. (2023). Structural features localizing the ferroptosis inhibitor gif-2197-r to lysosomes. *RSC Adv.* 13, 32276–32281. doi: 10.1039/d3ra06611h

Ingold, I., Berndt, C., Schmitt, S., Doll, S., Poschmann, G., Buday, K., et al. (2018). Selenium utilization by gpx4 is required to prevent hydroperoxide-induced ferroptosis. *Cell* 172, 409–422.e21. doi: 10.1016/j.cell.2017.11.048

Ismail, M., Großmann, D., and Hermann, A. (2024). Increased vulnerability to ferroptosis in fus-als. *Biology* 13:215. doi: 10.3390/biology13040215

Jia, H., Liu, X., Cao, Y., Niu, H., Lan, Z., Li, R., et al. (2023). Deferoxamine ameliorates neurological dysfunction by inhibiting ferroptosis and neuroinflammation after traumatic brain injury. *Brain Res.* 1812:148383. doi: 10.1016/j.brainres.2023.148383

Jiang, X., Stockwell, B. R., and Conrad, M. (2021). Ferroptosis: mechanisms, biology and role in disease. *Nat. Rev. Mol. Cell Biol.* 22, 266–282. doi: 10.1038/s41580-020-00324-8

Kagan, V. E., Mao, G., Qu, F., Angeli, J. P., Doll, S., Croix, C. S., et al. (2017). Oxidized arachidonic and adrenic pes navigate cells to ferroptosis. *Nat. Chem. Biol.* 13, 81–90. doi: 10.1038/nchembio.2238

Lei, J., Chen, Z., Song, S., Sheng, C., Song, S., and Zhu, J. (2020). Insight into the role of ferroptosis in non-neoplastic neurological diseases. *Front. Cell. Neurosci.* 14:231. doi: 10.3389/fncel.2020.00231

Li, J., Cao, F., Yin, H. L., Huang, Z. J., Lin, Z. T., Mao, N., et al. (2020). Ferroptosis: past, present and future. *Cell Death Dis.* 11:88. doi: 10.1038/s41419-020-2298-2

Li, P., Jiang, M., Li, K., Li, H., Zhou, Y., Xiao, X., et al. (2021). Glutathione peroxidase 4-regulated neutrophil ferroptosis induces systemic autoimmunity. *Nat. Immunol.* 22, 1107–1117. doi: 10.1038/s41590-021-00993-3

Li, N., Jiang, W., Wang, W., Xiong, R., Wu, X., and Geng, Q. (2021). Ferroptosis and its emerging roles in cardiovascular diseases. *Pharmacol. Res.* 166:105466. doi: 10.1016/j.phrs.2021.105466

Liu, N., Yu, W., Sun, M., Li, X., Zhang, W., and Wang, M. (2024a). Dabrafenib mitigates the neuroinflammation caused by ferroptosis in experimental autoimmune encephalomyelitis by up regulating axl receptor. *Eur. J. Pharmacol.* 973:176600. doi: 10.1016/j.ejphar.2024.176600

Liu, N., Yu, W., Sun, M., Zhou, D., Sun, J., Jiang, T., et al. (2024b). Research trends and hotspots of ferroptosis in neurodegenerative diseases from 2013 to 2023: a bibliometrics study. *Heliyon* 10:e29418. doi: 10.1016/j.heliyon.2024.e29418

Lu, Y., Chen, Y., Jiang, Z., Ge, Y., Yao, R., Geng, S., et al. (2023). Research progress of ferroptosis in parkinson's disease: a bibliometric and visual analysis. *Front. Aging Neurosci.* 15:1278323. doi: 10.3389/fnagi.2023.1278323

Martinez, A. M., Kim, A., and Yang, W. S. (2020). Detection of ferroptosis by bodipy™ 581/591 c11. *Methods Mol. Biol.* 2108, 125–130. doi: 10.1007/978-1-0716-0247-8_11

Maru, D., Hothi, A., Bagariya, C., and Kumar, A. (2022). Targeting ferroptosis pathways: a novel strategy for cancer therapy. *Curr. Cancer Drug Targets* 22, 234–244. doi: 10.2174/1568009622666220211122745

Morris, G., Walker, A. J., Berk, M., Maes, M., and Puri, B. K. (2018). Cell death pathways: a novel therapeutic approach for neuroscientists. *Mol. Neurobiol.* 55, 5767–5786. doi: 10.1007/s12035-017-0793-y

Moujalled, D., Strasser, A., and Liddell, J. R. (2021). Molecular mechanisms of cell death in neurological diseases. *Cell Death Differ.* 28, 2029–2044. doi: 10.1038/s41418-021-00814-y

Nikseresht, S., Bush, A. I., and Ayton, S. (2019). Treating alzheimer's disease by targeting iron. *Br. J. Pharmacol.* 176, 3622–3635. doi: 10.1111/bph.14567

Ou, M., Jiang, Y., Ji, Y., Zhou, Q., Du, Z., Zhu, H., et al. (2022). Role and mechanism of ferroptosis in neurological diseases. *Mol. Metab.* 61:101502. doi: 10.1016/j.molmet.2022.101502

Park, E., and Chung, S. W. (2019). Ros-mediated autophagy increases intracellular iron levels and ferroptosis by ferritin and transferrin receptor regulation. *Cell Death Dis.* 10:822. doi: 10.1038/s41419-019-2064-5

Pfannenstiel, A., Iannuccilli, J., Cornelis, F. H., Dupuy, D. E., Beard, W. L., and Prakash, P. (2022). Shaping the future of microwave tumor ablation: a new direction in precision and control of device performance. *Int. J. Hyperth.* 39, 664–674. doi: 10.1080/02656736.2021.1991012

Qin, Y., Zhang, Q., and Liu, Y. (2020). Analysis of knowledge bases and research focuses of cerebral ischemia-reperfusion from the perspective of mapping knowledge domain. *Brain Res. Bull.* 156, 15–24. doi: 10.1016/j.brainresbull.2019.12.004

Qiu, Y., Cao, Y., Cao, W., Jia, Y., and Lu, N. (2020). The application of ferroptosis in diseases. *Pharmacol. Res.* 159:104919. doi: 10.1016/j.phrs.2020.104919

Reichert, C. O., de Freitas, F. A., Sampaio-Silva, J., Rokita-Rosa, L., Barros, P. L., Levy, D., et al. (2020). Ferroptosis mechanisms involved in neurodegenerative diseases. *Int. J. Mol. Sci.* 21:8765. doi: 10.3390/ijms21228765

Ryan, S. K., Zelic, M., Han, Y., Teeple, E., Chen, L., Sadeghi, M., et al. (2023). Microglia ferroptosis is regulated by sec24b and contributes to neurodegeneration. *Nat. Neurosci.* 26, 12–26. doi: 10.1038/s41593-022-01221-3

Shao, E., Chang, C. W., Li, Z., Yu, X., Ho, K., Zhang, M., et al. (2022). Tau ablation in excitatory neurons and postnatal tau knockdown reduce epilepsy, sudep, and autism behaviors in a dravet syndrome model. *Sci. Transl. Med.* 14:eabm5527. doi: 10.1126/scitranslmed.abm5527

Song, S., Su, Z., Kon, N., Chu, B., Li, H., Jiang, X., et al. (2023). Alox5-mediated ferroptosis acts as a distinct cell death pathway upon oxidative stress in huntington's disease. *Genes Dev.* 37, 204–217. doi: 10.1101/gad.350211.122

Stefanoska, K., Gajwani, M., Tan, A., Ahel, H. I., Asih, P. R., Volkerling, A., et al. (2022). Alzheimer's disease: ablating single master site abolishes tau hyperphosphorylation. *Sci. Adv.* 8:eabl8809. doi: 10.1126/sciadv.abl8809

Stockwell, B. R. (2022). Ferroptosis turns 10: emerging mechanisms, physiological functions, and therapeutic applications. *Cell* 185, 2401–2421. doi: 10.1016/j.cell.2022.06.003

Stockwell, B. R., Friedmann, A. J., Bayir, H., Bush, A. I., Conrad, M., Dixon, S. J., et al. (2017). Ferroptosis: a regulated cell death nexus linking metabolism, redox biology, and disease. *Cell* 171, 273–285. doi: 10.1016/j.cell.2017.09.021

Synnestvedt, M. B., Chen, C., and Holmes, J. H. (2005). CiteSpace ii: visualization and knowledge discovery in bibliographic databases. *AMIA Annu. Symp. Proc.* 2005, 724–728

Temple, S. (2023). Advancing cell therapy for neurodegenerative diseases. *Cell Stem Cell* 30, 512–529. doi: 10.1016/j.stem.2023.03.017

Von Krusenstiern, A. N., Robson, R. N., Qian, N., Qiu, B., Hu, F., Reznik, E., et al. (2023). Identification of essential sites of lipid peroxidation in ferroptosis. *Nat. Chem. Biol.* 19, 719–730. doi: 10.1038/s41589-022-01249-3

Vringer, E., and Tait, S. (2023). Mitochondria and cell death-associated inflammation. *Cell Death Differ.* 30, 304–312. doi: 10.1038/s41418-022-01094-w

Wang, L., Chen, X., and Yan, C. (2022). Ferroptosis: an emerging therapeutic opportunity for cancer. *Genes Dis.* 9, 334–346. doi: 10.1016/j.gendis.2020.09.005

Wang, Y., Hu, J., Wu, S., Fleishman, J. S., Li, Y., Xu, Y., et al. (2023a). Targeting epigenetic and posttranslational modifications regulating ferroptosis for the treatment of diseases. *Signal Transduct. Target. Ther.* 8:449. doi: 10.1038/s41392-023-01720-0

Wang, Z., Huang, C., and Li, X. (2020). Research trends and hotspot analysis of conjunctival bacteria based on citeSpace software. *Biomed. Res. Int.* 2020:2580795. doi: 10.1155/2020/2580795

Wang, S. Q., Wang, J. X., Zhang, C., Sun, F. H., Xie, Y. J., Jiang, W., et al. (2020). What you should know about osteoarthritis rehabilitation: a bibliometric analysis of the 50 most-cited articles. *Geriatr. Orthop Surg. Rehabil.* 11:1466742900. doi: 10.1177/2151459320973196

Wang, Y., Wu, S., Li, Q., Sun, H., and Wang, H. (2023b). Pharmacological inhibition of ferroptosis as a therapeutic target for neurodegenerative diseases and strokes. *Adv. Sci.* 10:e2300325. doi: 10.1002/advs.202300325

Wang, Y., Xu, Y., Guo, W., Fang, Y., Hu, L., Wang, R., et al. (2022). Ablation of shank3 alleviates cardiac dysfunction in aging mice by promoting camkii activation and parkin-mediated mitophagy. *Redox Biol.* 58:102537. doi: 10.1016/j.redox.2022.102537

Wang, X., Zhou, Y., Min, J., and Wang, F. (2023). Zooming in and out of ferroptosis in human disease. *Front. Med.* 17, 173–206. doi: 10.1007/s11684-023-0992-z

Wu, X., Li, Y., Zhang, S., and Zhou, X. (2021). Ferroptosis as a novel therapeutic target for cardiovascular disease. *Theranostics* 11, 3052–3059. doi: 10.7150/thno.54113

Xie, Y., Hou, W., Song, X., Yu, Y., Huang, J., Sun, X., et al. (2016). Ferroptosis: process and function. *Cell Death Differ.* 23, 369–379. doi: 10.1038/cdd.2015.158

Xie, Y., Kang, R., Klionsky, D. J., and Tang, D. (2023). Gpx4 in cell death, autophagy, and disease. *Autophagy* 19, 2621–2638. doi: 10.1080/15548627.2023.2218764

Xu, W., Deng, H., Hu, S., Zhang, Y., Zheng, L., Liu, M., et al. (2021). Role of ferroptosis in lung diseases. *J. Inflamm. Res.* 14, 2079–2090. doi: 10.2147/JIR.S307081

Xu, C., Sun, S., Johnson, T., Qi, R., Zhang, S., Zhang, J., et al. (2021). The glutathione peroxidase gpx4 prevents lipid peroxidation and ferroptosis to sustain treg cell activation and suppression of antitumor immunity. *Cell Rep.* 35:109235. doi: 10.1016/j.celrep.2021.109235

Xu, Y., Xu, M., Zhou, C., Sun, L., Cai, W., and Li, X. (2024). Ferroptosis and its implications in treating cognitive impairment caused by aging: a study on the mechanism of repetitive transcranial magnetic stimulation. *Exp. Gerontol.* 192:112443. doi: 10.1016/j.exger.2024.112443

Xu, Y., Zhao, J., Zhao, Y., Zhou, L., Qiao, H., Xu, Q., et al. (2023). The role of ferroptosis in neurodegenerative diseases. *Mol. Biol. Rep.* 50, 1655–1661. doi: 10.1007/s11033-022-08048-y

Yang, S., Xie, Z., Pei, T., Zeng, Y., Xiong, Q., Wei, H., et al. (2022). Salidroside attenuates neuronal ferroptosis by activating the nrf2/ho1 signaling pathway in aβ(1-42)-induced alzheimer's disease mice and glutamate-injured ht22 cells. *Chin. Med.* 17:82. doi: 10.1186/s13020-022-00634-3

Yao, M. Y., Liu, T., Zhang, L., Wang, M. J., Yang, Y., and Gao, J. (2021). Role of ferroptosis in neurological diseases. *Neurosci. Lett.* 747:135614. doi: 10.1016/j.neulet.2020.135614

Yeerlan, J., He, B., Hu, X., and Zhang, L. (2024). Global research trends and hotspots for ferroptosis, necroptosis, and pyroptosis in alzheimer's disease from the past to 2023: a combined bibliometric review. *J Alzheimers Dis. Rep.* 8, 129–142. doi: 10.3233/ADR-230092

Yi, K., Xu, J. G., Yang, K. L., Zhang, X., Ma, L., You, T., et al. (2022). The top-100 most cited articles of biomarkers in congenital heart disease: a bibliometric analysis. *Ann. Palliat Med.* 11, 1700–1713. doi: 10.21037/apm-21-2422

Yu, L., Cheng, M., Liu, J., Ye, X., Wei, Z., Xu, J., et al. (2023). Crosstalk between microwave ablation and ferroptosis: the next hot topic? *Front. Oncol.* 13:1099731. doi: 10.3389/fonc.2023.1099731

Yu, S., Jia, J., Zheng, J., Zhou, Y., Jia, D., and Wang, J. (2021). Recent progress of ferroptosis in lung diseases. *Front. Cell Dev. Biol.* 9:789517. doi: 10.3389/fcell.2021.789517

Yu, Y., Yan, Y., Niu, F., Wang, Y., Chen, X., Su, G., et al. (2021). Ferroptosis: a cell death connecting oxidative stress, inflammation and cardiovascular diseases. *Cell Death Discov.* 7:193. doi: 10.1038/s41420-021-00579-w

Zhang, Z., Guo, M., Li, Y., Shen, M., Kong, D., Shao, J., et al. (2020). Rna-binding protein zfp36/ttp protects against ferroptosis by regulating autophagy signaling pathway in hepatic stellate cells. *Autophagy* 16, 1482–1505. doi: 10.1080/15548627.2019.1687985

Zhang, W., Sun, Y., Bai, L., Zhi, L., Yang, Y., Zhao, Q., et al. (2021). Rbms1 regulates lung cancer ferroptosis through translational control of slc7a11. *J. Clin. Invest.* 131:e152067. doi: 10.1172/JCI152067

Zhao, Y., Liu, Z., Liu, G., Zhang, Y., Liu, S., Gan, D., et al. (2023). Neutrophils resist ferroptosis and promote breast cancer metastasis through aconitate decarboxylase 1. *Cell Metab.* 35, 1688–1703.e10. doi: 10.1016/j.cmet.2023.09.004

Zheng, H., Jiang, L., Tsuduki, T., Conrad, M., and Toyokuni, S. (2021). Embryonal erythropoiesis and aging exploit ferroptosis. *Redox Biol.* 48:102175. doi: 10.1016/j.redox.2021.102175

Zhuo, S., He, G., Chen, T., Li, X., Liang, Y., Wu, W., et al. (2022). Emerging role of ferroptosis in glioblastoma: therapeutic opportunities and challenges. *Front. Mol. Biosci.* 9:974156. doi: 10.3389/fmolb.2022.974156

frontiers | Frontiers in Immunology

TYPE Brief Research Report
PUBLISHED 08 August 2024
DOI 10.3389/fimmu.2024.1458713

OPEN ACCESS

EDITED BY
Robert Weissert,
University of Regensburg, Germany

REVIEWED BY
Chunbo Dong,
Dalian Medical University, China
Jinming Han,
Capital Medical University, China

*CORRESPONDENCE
Piotr Alster
piotr.alster@gmail.com

RECEIVED 02 July 2024
ACCEPTED 29 July 2024
PUBLISHED 08 August 2024

CITATION
Alster P, Otto-Ślusarczyk D, Kutyłowski M, Migda B, Wiercińska-Drapało A, Jabłońska J, Struga M and Madetko-Alster N (2024) The associations between common neuroimaging parameters of Progressive Supranuclear Palsy in magnetic resonance imaging and non-specific inflammatory factors – pilot study. *Front. Immunol.* 15:1458713. doi: 10.3389/fimmu.2024.1458713

The associations between common neuroimaging parameters of Progressive Supranuclear Palsy in magnetic resonance imaging and non-specific inflammatory factors – pilot study

Piotr Alster[1]*, Dagmara Otto-Ślusarczyk[2], Michał Kutyłowski[3], Bartosz Migda[4], Alicja Wiercińska-Drapało[5], Joanna Jabłońska[5], Marta Struga[2] and Natalia Madetko-Alster[1]

[1]Department of Neurology, Medical University of Warsaw, Warsaw, Masovian, Poland, [2]Department of Biochemistry, Medical University of Warsaw, Warsaw, Masovian, Poland, [3]Department of Diagnostic Imaging, Mazowiecki Hospital Brodnowski, Warsaw, Poland, [4]Diagnostic Ultrasound Lab, Department of Pediatric Radiology, Medical University of Warsaw, Warsaw, Masovian, Poland, [5]Department of Infectious and Tropical Diseases and Hepatology, Medical University of Warsaw, Warsaw, Masovian, Poland

Progressive Supranuclear Palsy is an atypical parkinsonism based on tauopathic pathology. Growing interest is associated with the pathomechanism of this disease. Among theories analyzing this issue can be mentioned the one highlighting the significance of inflammation. In this study authors examined 14 patients with PSP-Richardson syndrome (PSP-RS) and 13 healthy volunteers using laboratory testing based on the analysis of interleukins 1 and 6 (IL-1 and IL-6), tau in the cerebrospinal fluid (CSF) and non-specific parameters of peripheral inflammation in the serum (IL-1, IL-6, neutrophils, lymphocytes, monocytes, platelets and the ratios based on the factors). All of the patients underwent neuroimaging using magnetic resonance imaging using 3 Tesla. The serum levels of IL-1 were positively correlated with the area of the mesencephalon, suggesting that higher levels of IL-1 are not linked with atrophic changes in this region, whereas serum levels IL-6 was positively correlated with frontal horn width and negatively correlated with superior cerebellar area. Additionally IL-6 in the serum was found to be correlated with neutrophil-to-high density lipoprotein ratio. The observations were not confirmed in the analysis of the levels of interleukins in the CSF. To the best of our knowledge this work is one of the first analyzing this issue. The outcome of the work shows that the role of interleukins associated with microglial activation may possibly differ in the context of neurodegenerative changes, moreover the role of peripheral inflammation in PSP requires further analysis.

KEYWORDS

neuroinflammation, neurodegeneration, PSP, atypical parkinsonisms, tauopathy

Introduction

Progressive Supranuclear Palsy (PSP) is a four repeats tauopathy in the group of atypical parkinsonism (1). Clinically it is defined as a syndrome associated with postural deficiencies, oculomotor dysfunction, akinesia and cognitive/language disorders (1). The disease was discovered in the seventh decade of the twentieth century, primarily it was defined as a single entity, since the release of the most contemporary criteria of diagnosis in 2017, it is presented as a group of clinical subtypes differing in the context of correlation of primary features (1, 2). The two major subtypes of PSP – Richardson's syndrome (PSP-RS) and Parkinsonism Predominant (PSP-P) comprise up to 90% of cases (3). The main subtypes significantly differ in the context of progression, clinical manifestation and response to levodopa treatment (4). Though the descriptions of PSP subtypes seem more and more detailed, the pathophysiology of PSP is not fully explored. It is not verified whether certain mechanisms, commonly associated with PSP, as inflammation, oxidative stress, vascular abnormalities are a cause or consequence of these processes (5, 6). It is also not specified whether these pathways affect certain regions of interest in the central nervous system more severely (7). The inflammatory hypothesis regarding the pathogenesis of PSP described in contemporary literature does not clearly indicate whether the mechanism should be directly associated with clinical deterioration or whether its certain aspect provide a protective role in the course of neurodegeneration. The example of chronic traumatic encephalopathy due to its certain overlaps in context of tauopathic pathology may suggest that repeated stimulation causing inflammatory activation could be a factor in the pathogenesis of neurodegenerative diseases (8). The McGeer theory rccognized the chronic impact of microglial activation as an aspect of neurodegeneration (9). Nevertheless though neurodegenerative processes may present certain similarities, the studies performed on patients with parkinsonisms, revealed that generally the inflammatory activation is more pronounced in atypical parkinsonisms, when compared to Parkinson's disease (PD) (10, 11). The data concerning this issue is not sufficiently explored due to the small number of researches evaluating inflammatory processes in atypical parkinsonisms and the lack of such works evaluating correlations between the inflammatory factors and atrophic changes in neuroimaging as in this study.

Based on previous examinations of this research group concerning the role of interleukins and neurotrophic factors in the analysis of PSP, it was revealed that the agents may have a significant in the differential diagnosis of two major subtypes of PSP – PSP Richardson's syndrome (PSP-RS) and PSP-Parkinsonism Predominant (PSP-P) (12, 13). The goal of this work was to verify whether the processes associated with inflammation can be linked with the neurodegenerative changes in the disease manifested by atrophy in neuroimaging.

Material and methodology

In this study 14 patients with PSP and 13 healthy volunteers aged 50-80 years old were recruited. All of the patients with PSP included in the study had possible or probable diagnosis of PSP according to the most contemporary Movement Disorders Society criteria of diagnosis released in 2017 (1). The deficits among patients were evaluated using the third part of Unified Parkinson's Disease Rating Scale (UPDRS-III). The results of UPDRS-III of patients with PSP varied between 20 and 30. None of the patients received levodopa treatment or any drug associated with the impact on dopaminergic system. The duration of the disease among PSP patients varied from 3 to 6 years. Among exclusion criteria could be mentioned neoplasms, autoimmune disease, infectious diseases, dyslipidemia, other neurodegenerative disease, vascular changes in the central nervous system. Authors excluded from the study patients and healthy controls using drugs possibly impacting the inflammatory parameters, as well as using medications affecting the level of cholesterol (due to Neutrophil-to-High Density Lipoprotein Cholesterol evaluation) according to characteristics of medicinal product or literature were excluded from the study. The comorbidities were excluded due to their possible impact on the evaluated parameters in laboratory and neuroimaging examination. All of the participants included in the study were examined in the Department of Neurology and Department of Hepatology and Infectious and Tropical Diseases of the Medical University of Warsaw. The patients were examined by neurologists experienced in movement disorders. Each patient underwent blood collection, lumbar puncture and Magnetic Resonance Imaging (MRI). The MRIs were evaluated by a radiologist experienced in neuroimaging of parkinsonisms (14, 15).

Blood and cerebrospinal fluid (CSF) collection

The blood samples were obtained from 14 patients with PSP, all of whom were hospitalized in the Department of Neurology at the Medical University of Warsaw. Blood samples and CSF (5 mL) were drawn into test tubes without anticoagulant and then centrifuged. The resulting serum and CSF samples were subsequently frozen at −80°C until analysis. The analysis involved determining the levels of IL-6 and IL-1β using commercial enzyme-linked immunosorbent assays (ELISAs), employing human (h) IL-6 HS and IL-1β ELISA kits from Diaclon SAS and Tau protein ELISA kit from Cloud-Clone Corp). Absorbance readings were measured at 450 nm using a plate reader, and marker concentrations were calculated based on standard curves.

All patients underwent comprehensive laboratory examinations, including blood morphology analysis, assessment of C-reactive protein (CRP) levels, and biochemical analysis, which included lipids profile and ferritin levels. None of the patients exhibited elevated infection markers, such as CRP or leukocytosis. Several ratios, including the neutrophil-to-lymphocyte ratio (NLR), lymphocyte-to-monocyte ratio (LMR), neutrophil-to-high density lipoprotein cholesterol (HDL-C) ratio (NHR), platelet-to-lymphocyte ratio (PLR), and neutrophil-to-monocyte ratio (NMR) were calculated. These ratios were determined by dividing the number of neutrophils by the number of lymphocytes, the number of lymphocytes by the number of monocytes, the number of neutrophils by the number of HDL-C, the number of platelets by

the number of lymphocytes, and the number of neutrophils by the number of monocytes from the same blood sample, respectively. The initial assessment of neutrophil and lymphocyte counts was conducted utilizing the Sysmex XT 4000i automated hematology analyzer within the Department of Laboratory Diagnostics at the Mazovian Bródno Hospital in Warsaw.

Magnetic resonance imaging

In the conducted study, all participants underwent magnetic resonance imaging (MRI) utilizing the Siemens 3.0T equipment, with subsequent assessment performed by a radiologist possessing over 5 years of expertise in neuroimaging, utilizing dedicated software (Syngovia Siemens) specialized software. Quantitative measurements were acquired from T2-weighted sequences, encompassing the evaluation of the pons (P) and midbrain (M) areas using freehand region of interest in the midsagittal plane, the average widths of the middle cerebellar peduncles (MCP) in the sagittal plane, the average widths of the superior cerebellar peduncles (SCP) in the coronal plane, the third ventricle based on three measurements (V3) in the axial plane at the level of anterior and posterior commissures, and the maximal width of the frontal horns of the lateral ventricles (FH). The Magnetic Resonance Parkinsonism Index (MRPI) was derived from the formula MRPI = (P/M) × (MCP/SCP), while the Magnetic Resonance Parkinsonism Index 2.0 (MRPI 2.0) was calculated as MRPI 2.0 = MRPI × (V3/FH), serving as quantitative measures for assessing parkinsonism based on structural ratios obtained from the MRI data.

Statistical analysis

Data analysis were performed by using GraphPad Prism 8 (GraphPad Software, San Diego, CA, USA). The arithmetic means (X) along with their standard deviations (SDs) were calculated. A significance level of $p<0.05$ was deemed statistically significant, and appropriate statistical tests were employed for comparisons between means. All the data were tested normally distribution (normality estimation) of analyzed variables was assessed using the Shapiro–Wilk W test. Pearson's correlation coefficients were employed to evaluate the significance of correlations between the various laboratory and neuroimaging markers. Due to the limited number of patients, lack of neuropathological verification and the singular evaluation, authors considered a sharpened threshold regarding correlations (r above 0.5 or below -0.5).

Results

Clinical characteristics of PSP patients and HCs

The clinical characteristics of the patients are comprehensively described in Table 1. This study included patients with PSP 14 (9 males and 5 females) and 13 HCs (5 males and 8 females). The average age of the patients with PSP was 70 ± 3.6 years, and that of the HCs was 50 ± 8.8 years. There were significant differences between patients with PSP and HCs in age ($p < 0.0001$).

TABLE 1 Characteristics of PSP patients and HCs.

	Healthy controls (n= 13)	PSP patients (n=14)	p
Sex (male:female)	5/8	9/5	
Age (years)	50 ± 8.8	70 ± 3.6	0.0001
Duration (years)		3-6	
WBC ($x10^9$/L)	6.29 ± 3.9		
Neutrophils ($x10^9$/L)	4.03 ± 3.06	4.36 ± 1.48	
Monocytes ($x10^9$/L)		0.48 ± 0.17	
Lymohocytes ($x10^9$/L)	1.25 ± 0.58	2.21 ± 1.30	0.0001
Plateles ($x10^{12}$/L)	149 ± 90.1	208.7 ± 49.8	0.0001
RBC ($x10^{12}$/L)	3.44 ± 0.68		
NLR	2.82 ± 1.89	1.85 ± 0.62	0.01
LMR		4.53± 1.14	
NHR	0.15 ± 0.19	0.10 ± 0.05	
PLR	92.5 ± 60	107.3 ± 37	0.05
NMR		9.28 ± 2.11	

WBC, white blood cells; RBC, red blood cells, NLR, neutrophil to lymphocyte ratio, LMR, lymphocye to monocyte ratio, NHR, neutrophil to high density lipoprotein ratio, PLR, platelet to lymphocyte ratio, NMR, neutrophile to monocyte ratio; the data shown are the means ± SD; a comparison of variables between PSP patients and HCs was performed by student's t-test; $p < 0.05$ was considered to indicate statistical significance.

Also, there were substantial differences between the PSP patients and HCs in terms of the lymphocyte, platelets count, NLR and PLR ($p < 0.05$). Patients with PSP had substantially similar plasma neutrophiles counts but lower NLR than HCs ($p < 0.01$). In addition, the plasma platelets count, and PLR were significantly elevated in patients with PSP than in HCs ($p < 0.0001$, $p<0,05$ respectively).

Pearson's correlation analysis of the all variables in PSP patients

This study showed that the levels of IL-1 in the serum are positively correlated with the area of mesencephalon. The Pearson's correlation coefficient between serum IL-1 levels and the area of the mesencephalon was found to be r=0.535208, p< 0.02. This positive correlation indicates that as IL-1 levels increase, there is no corresponding decrease in the mesencephalon area, implying a lack of detrimental impact on this region (Table 2). The concentration of IL-6 in is correlated positively with the frontal horn width (r=0.516973, p<0.02) and negatively and the area of superior

10.3389/fimmu.2024.1458713

cerebellar peduncle (r=-0.563613,p<0.01), which may suggest partial association with enhancement of neurodegenerative changes (Table 2). In the context of interleukins no other correlations were detected in the serum and CSF (Tables 2, 3). Ferritin was found to be positively correlated with the levels of interleukin-1 (r=0,539486, p<0,02) and interleukin-6 (r=0,547016, p<0,02). IL-6 was found to be positively correlated with NHR (r=0,5229, p<0,02). The observations were not confirmed among healthy volunteers. Additionally, tau evaluation in the CSF, which was performed due to the lack of neuropathological verification, revealed significantly increased levels in the CSF when compared to control group. No significant correlation was detected in the context of tau concentration in the CSF and atrophic changes in MRI (Table 4).

Discussion

The outcome of the study may suggest that inflammatory interleukins possibly play different roles depending on the regions of interest of the central nervous system. The unfavorable abnormalities within the SCP and FH, which were positively correlated with the level of IL-6, did not show any association with the levels of IL-1. On the other hand IL-1 was found to be positively correlated with the area of mesencephalon, which may suggest its role possibly counteracting neurodegeneration. Previous evaluations regarding the expression of IL-1 beta transcripts, revealed its increased levels in the substantia nigra (11). IL-1 beta and IL-6 as well as other cytokines secreted as a consequence of microglial activation were linked with neurodegeneration in atypical parkinsonisms (16). The increase of microglial derived cytokines was interpreted as a factor differentiating atypical parkinsonisms with PD (17).

The results obtained in this study may seem interesting in the context of staging of PSP based on MRI charts, which were indicated in a work by Planche et al. in 2024 (18). This work indicated major stages of progress in atrophic abnormalities. Among them could be mentioned: ventral diencephalon, pallidum, brainstem, striatum, amygdala, thalamus, frontal and occipital lobe (18). The outcome of this work and the discrepancies in the context of the impact of IL-1 and IL-6 on certain regions of interest may highlight the vulnerability to different factors depending on the stage. On the other hand previous studies performed by this research group on the possible role of IL-1 and IL-6 in the differential diagnosis of PSP subtypes – PSP-RS and PSP-P, showed that in the serum and cerebrospinal fluid the level of both interleukins was higher in the clinically more favorable subtype (PSP-P), than in PSP-RS which is affected by more rapid deterioration (13). A study by Nubling et al. indicated that though Cathepsin S is associated with the impact on tau oligomer formation through limited cleavage, the IL-6 serum levels correlated positively with disease severity in PSP (19). The outcome of the work by Nubling et al, combined with the results of this study, may suggest that IL-6 may have a role in the neurodegeneration of PSP. Additionally the fact that the level of IL-6 in the serum is positively correlated with NHR, may suggest that there is a possible link between peripheral inflammation and

TABLE 2 Correlation analysis of all variables in patients with PSP.

Variable	NLR		LMR		NHR		PLR		Neutrophiles		Monocyte		Lymphocytes		IL-6		IL-1b	
	r	*P*	r	*p*	r	*p*	r	*p*	r	*P*	r	*p*	r	*P*	r	*p*	r	*p*
III vent	0.072	0.40	0.326	0.12	0.07	0.39	0.267	0.17	0.072	0.40	-0.195	0.25	0.077	0.39	0.436	0.05	0.264	0.18
V3	0.137	0.32	0.370	0.19	0.146	0.30	0.416	0.05	0.137	0.32	-0.076	0.39	0.186	0.26	0.405	0.07	0.247	0.19
FH	0.02	0.47	0.08	0.78	0.021	0.47	-0.208	0.23	0.020	0.47	-0.310	0.14	-0.101	0.36	**0.516**	**0.02**	0.331	0.12
P	0.02	0.93	0.107	0.35	0.096	0.37	-0.285	0.16	0.022	0.46	-0.177	0.27	-0.09	0.37	-0.342	0.11	0.391	0.08
M	0.028	0.46	0.326	0.12	0.038	0.44	-0.235	0.20	0.028	0.46	-0.09	0.37	0.024	0.46	-0.082	0.39	**0.535**	**0.02**
MCP	0.497	0.03	0.272	0.17	0.169	0.28	0.295	0.15	0.497	0.03	0.263	0.18	0.273	0.17	-0.344	0.11	0.225	0.21
SCP	0.112	0.35	0.162	0.28	0.074	0.40	0.067	0.40	0.112	0.35	0.402	0.07	0.287	0.15	**-0.563**	**0.01**	-0.129	0.33
M/P	0.02	0.46	0.113	0.35	0.013	0.48	-0.150	0.30	0.022	0.46	-0.031	0.45	0.078	0.39	0.056	0.42	0.461	0.04
MRPI	0.08	0.38	-0.182	0.26	-0.043	0.44	0.197	0.24	0.087	0.38	-0.090	0.37	-0.108	0.35	-0.127	0.33	-0.311	0.13
MRPI 2.0	0.162	0.28	0.047	0.43	0.082	0.77	0.488	0.03	0.162	0.28	-0.014	0.48	0.05	0.42	-0.035	0.45	-0.184	0.26

These data were assessed based on the Pearson correlation test.
Pearson correlation was performed to evaluate the relationship between two continuous variables; p < 0.05 was considered to indicate statistical significance.
NLR, neutrophil to lymphocyte ratio; LMR, lymphocyte to monocyte ratio; NHR, neutrophil to high density lipoprotein ratio; PLR, platelet to lymphocyte ratio; V3; III vent, the third ventricle; FH, the lateral ventricles; P, pons; M, midbrain areas; MCP, the middle cerebellar peduncles; SCP, the superior cerebellar peduncles; MRPI, magnetic resonance parkinsonism index; MRPI 2.0, the magnetic resonance parkinsonism index 2.0.
Bolded - p values below 0.05 and r values below -0.5 or above 0.5.

TABLE 3 Correlation analysis between plasma IL-6, IL-1 beta.

	IL-6		IL-1 beta	
	r	p	r	P
Neutrophils (x10^9/L)	0.379	0.08	0.435	0.05
Monocytes (x10^9/L)	0.100	0.36	0.012	0.48
Lymohocytes (x10^9/L)	0.398	0.07	0.398	0.14
Plateles (x10^{12}/L)				
PLR	0.387	0.08	0.242	0.20
NLR	0.177	0.27	0.435	0.05
LMR	-0.238	0.20	0.347	0.11
NHR	**0.522**	**0.02**	0.387	0.08
NMR	0.027	0.46	0.295	0.15

Pearson correlation was performed to evaluate the relationship between two continuous variables; $p < 0.05$ was considered to indicate statistical significance.
PLR, platelet to lymphocyte ratio; NLR, neutrophil to lymphocyte ratio; LMR, lymphocyte to monocyte ratio; NHR, neutrophil to high density lipoprotein ratio NMR- neutrophil to monocyte ratio.
Bolded - p values below 0.05 and r values below -0.5 or above 0.5.

HDL (20). This seems possibly crucial in the context of previous studies regarding the permeability of brain-blood barrier in dyslipidemia and HDL abnormalities (21, 22). Both of the interleukins were found to be positively correlated with the concentration of ferritin. This fact combined by diversed links between the levels of interleukins in the serum and atrophic changes in MRI, highlights the limited feasibility of ferritin evaluation in the serum in the context of possible associations with commonly observed abnormalities in the neuroimaging of PSP.

TABLE 4 Correlation analysis of CSF IL-6, IL1- beta and Tau with all variables in patients with PSP.

Variable	IL-6		IL-1 beta		Tau	
	r	*p*	r	*p*	r	*P*
III vent	0.020	0.47	0.319	0.13	0.07	0.39
V3	0.08	0.38	0.308	0.14	0.146	0.30
FH	- 0.02	0.46	0.04	0.44	0.021	0.47
P	- 0.278	0.46	0.266	0.17	0.096	0.37
M	0.113	0.34	0.309	0.14	0.038	0.44
MCP	-0.152	0.30	-0.438	0.06	0.169	0.28
SCP	0.087	0.38	-0.260	0.18	0.074	0.40
M/P	0.145	0.30	0.289	0.15	0.013	0.48
MRPI	-0.313	0.13	-0.341	0.11	-0.043	0.44
MRPI 2.0	-0.187	0.26	0.098	0.36	0.082	0.77

These data were assessed based on the Pearson correlation test. Pearson correlation was performed to evaluate the relationship between two continuous variables; $p < 0.05$ was considered to indicate statistical significance.
V3, III vent, the third ventricle; FH, the lateral ventricles; P, pons; M, midbrain areas; MCP, the middle cerebellar peduncles; SCP, the superior cerebellar peduncles; MRPI, magnetic resonance parkinsonism index; MRPI 2.0, magnetic resonance parkinsonism index 2.0.

The fact that no correlations were detected between the levels of interleukins in the CSF and atrophic changes evaluated in this study could be explained by the fact that the most significant impact of the inflammatory factors could be more pronounced in the initial year of the disease. In favor of this argument could be mentioned the results of the study regarding the assessment of interleukins in subtypes of PSP. In this the levels of both interleukins were higher in the serum and CSF among patients with PSP-P, the subtype linked with gradual deterioration and less pronounced atrophic changes of the brainstem. In this study the majority of patients were diagnosed with PSP-RS, in which the abnormalities in the context of levels of interleukins were found to be less deviated than in PSP-P in the previous study of this research group (13). Inflammatory factors may also play a role prior to initial symptoms of PSP, however these hypotheses cannot be verified using this study. Undoubtedly the role of certain interleukins associated with microglial activation may differ, this could be partly justified by the diversity of clinical manifestations in the initial years of PSP, which could likely be an effect of different profiles of cytokines affecting their pathomechanisms. Additionally possible evaluations of atrophic changes in other regions of interest associated with the pathogenesis of PSP e.g. pallidum, putamen, caudate, amygdala, supplementary motor cortex, thalamus, frontal pole, precentral gyrus, occipital fusiform gyrus could provide a broader perspective on the issue (17, 18, 23).

Due to the fact that the issue concerning inflammation in PSP is not widely explored, the work could not be sufficiently discussed in the context of consistencies and discrepancies in other studies. Apart from the study performed by this research group, which indicated interleukin-1 and interleukin-6 as factors possibly differentiating PSP-P and PSP-RS, there were several works evaluating inflammatory factors in PSP examination. The majority of these work were based on the examination of small numbers of patients. One of the studies showed the increase of expression of IL-1beta transcript in substantia nigra among patients with PSP (24). Other works revealed increased levels of interferon γ, IL-10, IL-18, IL-1β, IL-4, IL-6, transforming growth factor β1, and Tumor Necrosis Factor-α in PSP and Multiple System Atrophy when compared to PD (10). Evaluations concerning the possible significance of NLR on one hand showed significantly higher levels of PSP, when compared to PD, on the other no pronounced differences with Corticobasal Syndrome (CBS) were detected (11, 25). The possible modulation of microglial-derived factors may be interpreted as a target point in future therapies in neurodegenerative, however contemporarily the data on its significance in PSP is insufficient (26).

Authors are aware of the limitations of the study among which could be mentioned the limited number of patients, single evaluation and lack of neuropathological verification. The small number of patients is related to the rarity of the disease. Additionally the recruitment of patients with PSP is affected by pronounced cognitive and motor deterioration. Taking into account the fact that the median life expectancy of PSP-RS patients after diagnosis was estimated at the level of 5.6 years, the examination of patients with 3-6 years duration is on one hand initially affected by significant obstacles in recruitment, on the other the study though limited by its pilot character may provide information on the

inflammatory profile of advanced stage patients (27). In this context obtaining a larger sample of advanced stage patients in a single center study is difficult. The generalizability of the results of this pilot study is undoubtfully affected by the limitations mentioned above, however due to its novelty, it can be interpreted as a point in further discussions, especially in exploring the pathogenesis and possible therapeutic binding factors. As the patients included in the study are alive, no neuropathological verification was performed, a verification of the increased level of tau among patients with PSP in the CSF due to the lack of neuropathological verification was performed. The work does not indicate subtypes of PSP. The assessment is based on the evaluation of non-specific inflammatory parameters. Moreover the imaging is based on selected regions of interest, which are most commonly evaluated in PSP. Due to the fact that authors intended to obtain a control group without significant comorbidities, based on the fact that the recruitment was partly performed during COVID-19 pandemic, authors were forced to obtain a control group significantly younger than the examined group, as the age-matched controls were excluded due to comorbidities possibly jeopardizing the results. Additionally some of the patients which could be age-matched with PSP patients were unwilling to perform examination during COVID-19 pandemic. Apart from the indicated limitations, this pilot study stresses an issue which is unexplored in contemporary literature.

Conclusion

The work, though presenting the outcome of a pilot study, may suggest that the role of inflammatory factors in neurodegenerative diseases is not unequivocal. The possible significance of certain peripheral agents may depend on the type of inflammatory factor and the vulnerability of regions of interest affected by PSP. The evaluation of peripheral inflammatory factors should be interpreted as an initiatory point in further discussions concerning the course of neurodegeneration in tauopathic atypical parkinsonisms. Additional evaluation of the issue based on larger groups of patients is required.

Data availability statement

The original contributions presented in the study are included in the article/supplementary material. Further inquiries can be directed to the corresponding author.

Ethics statement

The studies involving humans were approved by the Bioethical Committee of Medical University of Warsaw—approval numbers: KB/139/2020 and KB/1243/2016. The studies were conducted in accordance with the local legislation and institutional requirements. The participants provided their written informed consent to participate in this study.

Author contributions

PA: Conceptualization, Formal analysis, Funding acquisition, Investigation, Methodology, Project administration, Validation, Writing – original draft, Writing – review & editing. DO: Formal analysis, Investigation, Methodology, Software, Writing – original draft, Writing – review & editing. MK: Formal analysis, Investigation, Methodology, Software, Writing – original draft, Writing – review & editing. BM: Formal analysis, Investigation, Methodology, Software, Writing – original draft, Writing – review & editing. AW: Formal analysis, Investigation, Methodology, Software, Writing – original draft, Writing – review & editing. JJ: Formal analysis, Investigation, Methodology, Software, Writing – original draft, Writing – review & editing. MS: Data curation, Formal analysis, Investigation, Methodology, Resources, Software, Writing – original draft, Writing – review & editing. NM: Data curation, Formal analysis, Investigation, Methodology, Resources, Software, Writing – original draft, Writing – review & editing.

Funding

The author(s) declare financial support was received for the research, authorship, and/or publication of this article. The project was funded by an internal grant nr MB/M/09 (16).

Conflict of interest

The authors declare that the research was conducted in the absence of any commercial or financial relationships that could be construed as a potential conflict of interest.

Publisher's note

All claims expressed in this article are solely those of the authors and do not necessarily represent those of their affiliated organizations, or those of the publisher, the editors and the reviewers. Any product that may be evaluated in this article, or claim that may be made by its manufacturer, is not guaranteed or endorsed by the publisher.

References

1. Höglinger GU, Respondek G, Stamelou M, Kurz C, Josephs KA, Lang AE, et al. Clinical diagnosis of progressive supranuclear palsy: The movement disorder society criteria. *Mov Disord*. (2017) 32:853–64. doi: 10.1002/mds.26987

2. Pearce JM. Progressive supranuclear palsy (Steele-Richardson-Olszewski syndrome): a short historical review. *Neurologist*. (2007) 13:302–4. doi: 10.1097/01.nrl.0000254743.69160.b3

3. Alster P, Madetko N, Koziorowski D, Friedman A. Progressive supranuclear palsy-parkinsonism predominant (PSP-P)-A clinical challenge at the boundaries of PSP and parkinson's disease (PD). *Front Neurol*. (2020) 11:180. doi: 10.3389/fneur.2020.00180

4. Necpál J, Borsek M, Jeleňová B. Parkinson's disease" on the way to progressive supranuclear palsy: a review on PSP-parkinsonism. *Neurol Sci*. (2021) 42:4927–36. doi: 10.1007/s10072-021-05601-8

5. Koziorowski D, Figura M, Milanowski ŁM, Szlufik S, Alster P, Madetko N, et al. Mechanisms of neurodegeneration in various forms of parkinsonism-similarities and differences. *Cells*. (2021) 10:656. doi: 10.3390/cells10030656

6. Krzosek P, Madetko N, Migda A, Migda B, Jaguś D, Alster P. Differential diagnosis of rare subtypes of progressive supranuclear palsy and PSP-like syndromes-infrequent manifestations of the most common form of atypical parkinsonism. *Front Aging Neurosci*. (2022) 14:804385. doi: 10.3389/fnagi.2022.804385

7. Spinelli EG, Ghirelli A, Bottale I, Basaia S, Canu E, Castelnovo V, et al. Stepwise functional brain architecture correlates with atrophy in progressive supranuclear palsy. *Mov Disord*. doi: 10.1002/mds.29887. Epub ahead of print.

8. Chancellor KB, Chancellor SE, Duke-Cohan JE, Huber BR, Stein TD, Alvarez VE, et al. Altered oligodendroglia and astroglia in chronic traumatic encephalopathy. *Acta Neuropathol*. (2021) 142:295–321. doi: 10.1007/s00401-021-02322-2

9. McGeer PL, Itagaki S, Boyes BE, McGeer EG. Reactive micro-glia are positive for HLA-DR in the substantia nigra of Parkinson's and Alzheimer's disease brains. *Neurology*. (1988) 38:1285–91. doi: 10.1212/WNL.38.8.1285

10. Amrami A, Singh NA, Ali F, Pham NTT, Stephens YC, Josephs KA, et al. Clinical utility of tectal plate measurements on magnetic resonance imaging in progressive supranuclear palsy. *Mov Disord*. (2024). doi: 10.1002/mds.29806. Epub ahead of print.

11. Fernández-Botrán R, Ahmed Z, Crespo FA, Gatenbee C, Gonzalez J, Dickson DW, et al. Cytokine expression and microglial activation in progressive supranuclear palsy. *Parkinsonism Relat Disord*. (2011) 17:683–8. doi: 10.1016/j.parkreldis.2011.06.007

12. Alster P, Otto-Ślusarczyk D, Szlufik S, Duszyńska-Wąs K, Drzewińska A, Wiercińska-Drapało A, et al. The significance of glial cell line-derived neurotrophic factor analysis in Progressive Supranuclear Palsy. *Sci Rep*. (2024) 14:2805. doi: 10.1038/s41598-024-53355-y

13. Madetko-Alster N, Otto-Ślusarczyk D, Wiercińska-Drapało A, Koziorowski D, Szlufik S, Samborska-Ćwik J, et al. Clinical phenotypes of progressive supranuclear palsy-the differences in interleukin patterns. *Int J Mol Sci*. (2023) 24:15135. doi: 10.3390/ijms242015135

14. Quattrone A, Nicoletti G, Messina D, Fera F, Condino F, Pugliese P, et al. MR imaging index for differentiation of Progressive Supranuclear Palsy from Parkinson disease and the Parkinson variant of multiple system atrophy. *Radiology*. (2008) 246:214–21. doi: 10.1148/radiol.2453061703

15. Quattrone A, Morelli M, Nigro S, Quattrone A, Vescio B, Arabia G, et al. A new MR imaging index for differentiation of Progressive Supranuclear Palsy-parkinsonism from Parkinson's disease. *Parkinsonism Relat Disord*. (2018) 54:3–8. doi: 10.1016/j.parkreldis.2018.07.016

16. van Olst L, Verhaege D, Franssen M, Kamermans A, Roucourt B, Carmans S, et al. Microglial activation arises after aggregation of phosphorylated-tau in a neuron-specific P301S tauopathy mouse model. *Neurobiol Aging*. (2020) 89:89–98. doi: 10.1016/j.neurobiolaging.2020.01.003

17. Hall S, Janelidze S, Surova Y, Widner H, Zetterberg H, Hansson O. Cerebrospinal fluid concentrations of inflammatory markers in Parkinson's disease and atypical parkinsonian disorders. *Sci Rep*. (2018) 8:13276. doi: 10.1038/s41598-018-31517-z

18. Planche V, Mansencal B, Manjon JV, Meissner WG, Tourdias T, Coupé P. Staging of progressive supranuclear palsy-Richardson syndrome using MRI brain charts for the human lifespan. *Brain Commun*. (2024) 6:fcae055. doi: 10.1093/braincomms/fcae055

19. Nübling G, Schuberth M, Feldmer K, Giese A, Holdt LM, Teupser D, et al. Cathepsin S increases tau oligomer formation through limited cleavage, but only IL-6, not cathespin S serum levels correlate with disease severity in the neurodegenerative tauopathy progressive supranuclear palsy. *Exp Brain Res*. (2017) 235:2407–12. doi: 10.1007/s00221-017-4978-4

20. Guerra-Vázquez CM, Martínez-Ávila M, Guajardo-Flores D, Antunes-Ricardo M. Punicic acid and its role in the prevention of neurological disorders: A review. *Foods*. (2022) 11:252. doi: 10.3390/foods11030252

21. Bowman GL, Kaye JA, Quinn JF. Dyslipidemia and blood-brain barrier integrity in Alzheimer's disease. *Curr Gerontol Geriatr Res*. (2012). doi: 10.1155/2012/184042

22. Knox EG, Aburto MR, Clarke G, Cryan JF, O'Driscoll CM. The blood-brain barrier in aging and neurodegeneration. *Mol Psychiatry*. (2022) 27:2659–73. doi: 10.1038/s41380-022-01511-z

23. Quattrone A, Franzmeier N, Huppertz HJ, Klietz M, Roemer SN, Boxer AL, et al. Magnetic resonance imaging measures to track atrophy progression in progressive supranuclear palsy in clinical trials. *Mov Disord*. (2024). doi: 10.1002/mds.29866. ahead of print.

24. Inci I, Kusbeci OY, Eskut N. The neutrophil-to-lymphocyte ratio as a marker of peripheral inflammation in progressive supranuclear palsy: a retrospective study. *Neurol Sci*. (2020) 41:1233–7. doi: 10.1007/s10072-019-04208-4

25. Alster P, Madetko N, Friedman A. Neutrophil-to-lymphocyte ratio (NLR) at boundaries of Progressive Supranuclear Palsy Syndrome (PSPS) and Corticobasal Syndrome (CBS). *Neurol Neurochir Pol*. (2021) 55:97–101. doi: 10.5603/PJNNS.a2020.0097

26. Przewodowska D, Marzec W, Madetko N. Novel therapies for parkinsonian syndromes-recent progress and future perspectives. *Front Mol Neurosci*. (2021) 14:720220. doi: 10.3389/fnmol.2021.720220

27. Litvan I, Mangone CA, McKee A, Verny M, Parsa A, Jellinger K, et al. Natural history of progressive supranuclear palsy (Steele-Richardson-Olszewski syndrome) and clinical predictors of survival: a clinicopathological study. *J Neurol Neurosurg Psychiatry*. (1996) 60:615–20. doi: 10.1136/jnnp.60.6.615

frontiers | Frontiers in Immunology

TYPE Original Research
PUBLISHED 12 August 2024
DOI 10.3389/fimmu.2024.1443464

OPEN ACCESS

EDITED BY
Robert Weissert,
University of Regensburg, Germany

REVIEWED BY
Yejun Tan,
University of Minnesota Health Twin Cities, United States
Marijana Lisak,
Sisters of Charity Hospital, Croatia
Lorna Galleguillos,
Clínica Alemana, Chile
Meral Seferoğlu,
Bursa Yuksek Ihtisas Training and Research Hospital, Türkiye

*CORRESPONDENCE
Yihua An
riveran@ccmu.edu.cn
Shouwei Li
lishouwei@ccmu.edu.cn

†These authors have contributed equally to this work and share first authorship

RECEIVED 04 June 2024
ACCEPTED 25 July 2024
PUBLISHED 12 August 2024

CITATION
An W, Zhou J, Qiu Z, Wang P, Han X, Cheng Y, He Z, An Y and Li S (2024) Identification of crosstalk genes and immune characteristics between Alzheimer's disease and atherosclerosis. *Front. Immunol.* 15:1443464. doi: 10.3389/fimmu.2024.1443464

Identification of crosstalk genes and immune characteristics between Alzheimer's disease and atherosclerosis

Wenhao An[1†], Jiajun Zhou[1†], Zhiqiang Qiu[1], Peishen Wang[2], Xinye Han[2], Yanwen Cheng[2], Zi He[2], Yihua An[1*] and Shouwei Li[1*]

[1]Department of Neurosurgery, Sanbo Brain Hospital, Capital Medical University, Beijing, China, [2]Department of Research and Development, Beijing Yihua Biotechnology Co., Ltd, Beijing, China

Background: Advancements in modern medicine have extended human lifespan, but they have also led to an increase in age-related diseases such as Alzheimer's disease (AD) and atherosclerosis (AS). Growing research evidence indicates a close connection between these two conditions.

Methods: We downloaded four gene expression datasets related to AD and AS from the Gene Expression Omnibus (GEO) database (GSE33000, GSE100927, GSE44770, and GSE43292) and performed differential gene expression (DEGs) analysis using the R package "limma". Through Weighted gene correlation network analysis (WGCNA), we selected the gene modules most relevant to the diseases and intersected them with the DEGs to identify crosstalk genes (CGs) between AD and AS. Subsequently, we conducted functional enrichment analysis of the CGs using DAVID. To screen for potential diagnostic genes, we applied the least absolute shrinkage and selection operator (LASSO) regression and constructed a logistic regression model for disease prediction. We established a protein-protein interaction (PPI) network using STRING (https://cn.string-db.org/) and Cytoscape and analyzed immune cell infiltration using the CIBERSORT algorithm. Additionally, NetworkAnalyst (http://www.networkanalyst.ca) was utilized for gene regulation and interaction analysis, and consensus clustering was employed to determine disease subtypes. All statistical analyses and visualizations were performed using various R packages, with a significance level set at $p<0.05$.

Results: Through intersection analysis of disease-associated gene modules identified by DEGs and WGCNA, we identified a total of 31 CGs co-existing between AD and AS, with their biological functions primarily associated with immune pathways. LASSO analysis helped us identify three genes (C1QA, MT1M, and RAMP1) as optimal diagnostic CGs for AD and AS. Based on this, we constructed predictive models for both diseases, whose accuracy was validated by external databases. By establishing a PPI network and employing four topological algorithms, we identified four hub genes (C1QB, CSF1R, TYROBP, and FCER1G) within the CGs, closely related to immune cell infiltration. NetworkAnalyst further revealed the regulatory networks of these hub genes. Finally, defining C1 and C2 subtypes for AD and AS respectively based on the expression profiles of CGs, we found the C2 subtype exhibited immune overactivation.

Conclusion: This study utilized gene expression matrices and various algorithms to explore the potential links between AD and AS. The identification of CGs revealed interactions between these two diseases, with immune and inflammatory imbalances playing crucial roles in their onset and progression. We hope these findings will provide valuable insights for future research on AD and AS.

KEYWORDS

Alzheimer's disease, atherosclerosis, crosstalk genes, bioinformatics analysis, immunology

1 Introduction

With the continuous progress of modern society and medical technology, human life expectancy is steadily increasing, which is a delightful development (1–3). However, this brings along a series of challenges, one of which is the rise in age-related diseases (4). Among these ailments, Alzheimer's disease and atherosclerosis stand out as two significant focal points. Alzheimer's disease leads to cognitive decline, while atherosclerosis triggers cardiovascular diseases, causing immense suffering not only to the patients themselves but also imposing a heavy burden on their families and society at large (5, 6).

Alzheimer's disease (AD) is a progressive neurodegenerative disorder, typically characterized by memory loss, cognitive decline, and behavioral abnormalities (7). Currently, it affects a significant number of individuals globally, with a growing trend. Data shows that in the United States alone, there are approximately 6.7 million AD patients aged 65 and older, and this number is projected to exceed 13.8 million by 2060 (8). The exact cause of AD remains unclear, but research suggests that genetic factors, abnormal protein metabolism, and neuroinflammation may be involved in its pathogenesis, with neuronal death and abnormal protein accumulation likely playing significant roles (9, 10). Initial symptoms of AD typically include mild memory issues, such as forgetting important dates or events, progressing to severe memory loss and the inability to navigate familiar surroundings (11). As the disease progresses, patients may also experience language impairments, mood swings, social withdrawal, and other symptoms (12). Currently, there is no cure for Alzheimer's disease, but some medications and non-pharmacological therapies can help slow disease progression and alleviate symptoms (13). Therefore, early diagnosis and intervention are crucial for managing this condition.

Atherosclerosis (AS) is a chronic, progressive arterial disease characterized by the deposition of lipid plaques within the blood vessel walls and thickening of the vessel walls (14). Rough estimates suggest that currently there are billions of individuals globally afflicted by this condition (15). The primary causes of AS include dyslipidemia, chronic inflammatory responses, and endothelial dysfunction within the blood vessels, among other factors (16). This disease has a wide-ranging impact, affecting various arteries throughout the body, including those of the heart, carotid, cerebral, and peripheral arteries, leading to cardiovascular diseases such as myocardial infarction, and cerebrovascular diseases such as stroke, making it a leading cause of death worldwide (17–19). When confronting AS, prevention, early diagnosis, and aggressive treatment are often paramount in controlling and managing the disease (20).

Advancements in molecular biology and genomics have significantly propelled scientists' understanding of the genetic basis of complex diseases (21, 22). Gene expression represents the activity level of specific genes at particular times and under specific conditions, determining cellular characteristics and functions, and largely influencing the health and disease states of an organism (23). By studying gene expression, we can discern which genes are activated or suppressed under certain conditions, thus unveiling the biochemical reactions and signal transduction processes within cells (24). Transcriptomic analysis, by comprehensively examining all mRNA expression in a cell or tissue, provides a systematic understanding of gene expression regulatory networks (25). This research approach not only allows for the quantitative analysis of the expression levels of tens of thousands of genes but also captures the interactions and regulatory relationships between different genes. It holds significant importance in revealing gene expression differences under various physiological states and disease conditions, aiding scientists in identifying potential pathogenic genes and biomarkers (26, 27).

Currently, there is increasing evidence suggesting a close association between Alzheimer's disease (AD) and atherosclerosis (AS) (28–30). They both belong to age-related diseases and are largely regulated by the immune system. Recent advancements in AD research have confirmed the significant role of peripheral immune dysfunction in its pathogenesis (31–33). Meanwhile, vascular aging and endothelial dysfunction also appear to be common triggers between the two diseases (34). However, there is relatively limited research on the correlation between these two diseases based on gene expression levels. To address this gap, we conducted in-depth analysis utilizing public online databases, involving 888 patients with either AD or AS, along with their corresponding healthy population. Our study aimed to explore the association between these two diseases, striving to identify shared crosstalk genes (CGs) and analyze the

primary biological effects of these genes. Through the application of machine learning algorithms, we successfully identified the optimal diagnostic genes and hub genes shared by AD and AS. This finding was supported by consistent expression patterns across four databases, validating the accuracy of our results. Furthermore, we delved into understanding these two diseases through immune infiltration analysis and confirmed the associated networks of key genes. Finally, we successfully identified subtypes of these two diseases using CGs. In conclusion, through this study, we aim to provide new insights for future researchers in predicting these two diseases and exploring the mechanisms underlying their association.

2 Materials and methods

2.1 Data download and processing

We retrieved four gene expression datasets (GSE33000, GSE100927, GSE44770, and GSE43292) from the GEO database (https://www.ncbi.nlm.nih.gov/geo/). Among these, GSE33000 and GSE100927 were analyzed as disease experimental groups. The former includes 310 samples of Alzheimer's disease patients and 157 samples of normal brain tissue, while the latter comprises 69 samples of atherosclerosis patients and 35 samples of normal arterial tissue. On the other hand, GSE44770 and GSE43292 were analyzed as disease validation groups. The former consists of 80 samples of Alzheimer's symptomatic patients and 173 samples of normal brain tissue, whereas the latter includes 32 samples of atherosclerosis patients and 32 samples of normal arterial tissue. All gene expression datasets underwent standardization using the "normalizeBetweenArrays" package in R software.

2.2 Differential gene expression analysis

We utilized the "limma" package in R software to perform differential gene expression analysis on the standardized GSE33000 and GSE100927 datasets. For the GSE33000 dataset, the criteria for screening differential expression genes (DEGs) were set as $|\log FC| \geq 0.5$ and p-value<0.05, while for the GSE100927 dataset, the criteria were $|\log FC| \geq 1$ and p-value<0.05. Using volcano plots, we displayed the DEGs that met these criteria, highlighting genes with $|\log FC| \geq 1$ in AD and $|\log FC| \geq 2$ in AS. Additionally, gene expression heatmaps were generated to illustrate the top 30 upregulated or downregulated DEGs.

2.3 Weighted gene correlation network analysis identifies disease-related gene modules

Weighted gene correlation network analysis (WGCNA) is employed to discover highly correlated gene clusters (modules), and these modules are associated with external sample features and other modules through a module feature gene network approach (35). We utilized the "WGCNA" package in R software to construct the gene co-expression network. Firstly, the quality of samples and genes was inspected to ensure data quality met the requirements. Secondly, hierarchical clustering was performed on samples to detect outlier samples, and outliers were removed based on corresponding high values. Thirdly, the pickSoftThreshold function was used to compute an appropriate soft threshold, and a biologically meaningful scale-free network was established. Fourthly, the dynamic tree-cutting algorithm was employed to construct a topological overlap matrix, establish the gene co-expression network, and identify gene modules. Fifthly, by computing gene significance and module membership, gene modules were linked to clinical features, and the structure and associations of feature gene networks were visualized. Finally, genes from the respective modules were selected for subsequent analysis.

2.4 Identification and enrichment analysis of crosstalk genes

DEGs identified from GSE33000 and GSE100927, as well as gene modules obtained from WGCNA analysis from both datasets, were analyzed by taking their intersection. Overlapping genes were considered as crosstalk genes (CGs) related to both diseases. The CGs were uploaded to https://david.ncifcrf.gov/ for Gene Ontology (GO) analysis and Kyoto Encyclopedia of Genes and Genomes (KEGG) analysis. Bubble plot tools were utilized to visually represent the results. Relevant immune processes were selected from the c5.all.v7.5.1 gene set, and Gene Set Variation Analysis (GSVA) from the R package "GSVA" was used to calculate enrichment scores for each patient. Heatmaps were generated using the "pheatmap" package for visualization.

2.5 Filtering potential diagnostic genes in CGs

The Least Absolute Shrinkage and Selection Operator (LASSO) is a regularization method for linear regression. It adds an L1 regularization term to the loss function of the regression model to limit the sum of the absolute values of the model parameters. This allows many model parameters to become zero, achieving the goal of feature selection and model sparsity (36). We used 5-fold cross-validation to determine the optimal regularization parameter for AD (GSE33000) and AS (GSE100927) respectively, and analyzed the two databases using the "glmnet" package. Ultimately, we selected their intersection as the best diagnostic genes in the CGs of the two diseases. The expression patterns of these genes in the two diseases were displayed through box plots, and their diagnostic effectiveness was observed by the area under the receiver operating characteristic (ROC) curve (37). We also included datasets GSE44770 and GSE43292 for validation.

2.6 Building disease prediction model based on diagnostic genes

We utilized the "Irm" package in R software to incorporate the three identified optimal diagnostic genes and constructed a logistic regression model for predicting the occurrence of the related disease,

generating a nomogram (38). "Scores" represent the scoring situation of each identified gene, while "Total Score" indicates the sum of scores for each gene. The accuracy of the model in disease prediction was evaluated through ROC curves, while calibration curves and decision curves were employed to assess the consistency between prediction and actual observation, incorporating the corresponding validation group for comprehensive model evaluation.

2.7 Construction of PPI network and screening of hub CGs

The construction and analysis of PPI networks help uncover the interactions between important proteins underlying diseases, thereby inferring key functions and pathways in disease progression (39). We utilized the online analysis tool STRING (https://string-db.org/) to compute PPI networks of CGs and visualized the results using Cytoscape software. In the process of screening hub CGs, the cytoHubba plugin was employed, along with four topological analysis methods, including Maximal Clique Centrality (MCC), Degree, Maximum Neighborhood Component (MNC), and Edge Percolated Component (EPC), to jointly identify hub expression genes. The expression profiles of hub expression genes across four databases were demonstrated using violin plots.

2.8 Analysis of immune cell infiltration

Immune cells exhibit specific patterns of infiltration and residence during the onset and progression of diseases. These patterns provide crucial clues and guidance for understanding their roles in disease mechanisms and offer key information for the development of novel therapeutic approaches (40). Utilizing tissue-based gene expression matrices, we employed the CIBERSORT algorithm to compute the infiltration levels of 24 immune cell types. Through box plots, stacked bar charts, and correlation heatmaps, we presented the infiltration results of immune cells along with their associated features.

2.9 Gene regulation and network analysis of interactions with diseases, drugs, and chemical substances

NetworkAnalyst (http://www.networkanalyst.ca) is an online platform used for complex meta-analysis of gene expression (41). In this study, we utilized the NetworkAnalyst platform for multifaceted analyses. Construction of the Gene-miRNA interaction network was based on the TarBase v8.0 database, while the TF-Gene interaction network relied on the ChEA database, and the study of TF-miRNA crosstalk was based on the RegNetwork database. Additionally, we employed the DisGeNET database, DrugBank database, and Comparative Toxicogenomics Database (CTD) to analyze associations between genes and diseases, interactions between proteins and drugs, and interactions between proteins and chemical substances.

2.10 Consensus clustering analysis identifies disease subtypes associated with CGs

The consensus clustering method is an unsupervised algorithm that effectively distinguishes different subtypes or subgroups within a dataset by identifying and clustering individual samples. Using CGs, we employed the Pam algorithm from the "ConsensusClusterPlus" package to determine subtypes for both AD and AS (42). Subsequently, through immune infiltration analysis and the GSVA algorithm, we analyzed the relevant features of the subtypes for these two diseases separately and presented these results using box plots and heatmaps.

2.11 Statistical analysis and visualization processing

This study employed R software (version 4.2.3, Windows platform), in conjunction with various software packages, for statistical analysis and plotting. To assess significant differences between two groups of data, we utilized two-sided Wilcoxon tests for analysis; while for evaluating correlations between two groups of data, Pearson correlation analysis was employed. In statistical terms, we defined a p-value less than 0.05 as having significance.

3 Result

3.1 Identification of DEGs in AD and AS

After standardizing the required datasets, we identified 550 DEGs (Supplementary Table 1) in the AD dataset GSE33000, comprising 252 upregulated genes and 298 downregulated genes. In the AS dataset GSE100927, we identified 463 DEGs (Supplementary Table 2), including 326 upregulated genes and 137 downregulated genes. The volcano plots illustrate all DEGs in AD and AS (Figures 1A, B), while the heatmap displays the top 30 upregulated or downregulated DEGs with the highest differences between the two diseases (Figures 1C, D).

3.2 Weighted gene correlation network analysis and key module selection

In the AD dataset GSE33000 and AS dataset GSE100927, we employed WGCNA to construct an unsigned co-expression network to identify the gene sets most associated with AD and AS, respectively. For the soft thresholding, we chose a value of 14 for both datasets (Figures 2A, D). Under the conditions of a minimum module size of 50 and a merge cut height of 0.25, we generated cluster dendrograms for AD and AS (Figures 2B, E). Through clinical correlation analysis, we obtained 9 gene module sets for both diseases (Figures 2C, F). Without considering the grey module, we selected the modules MEgreen and Meturquoise (Supplementary Table 3), which had the highest positive correlation with AD and

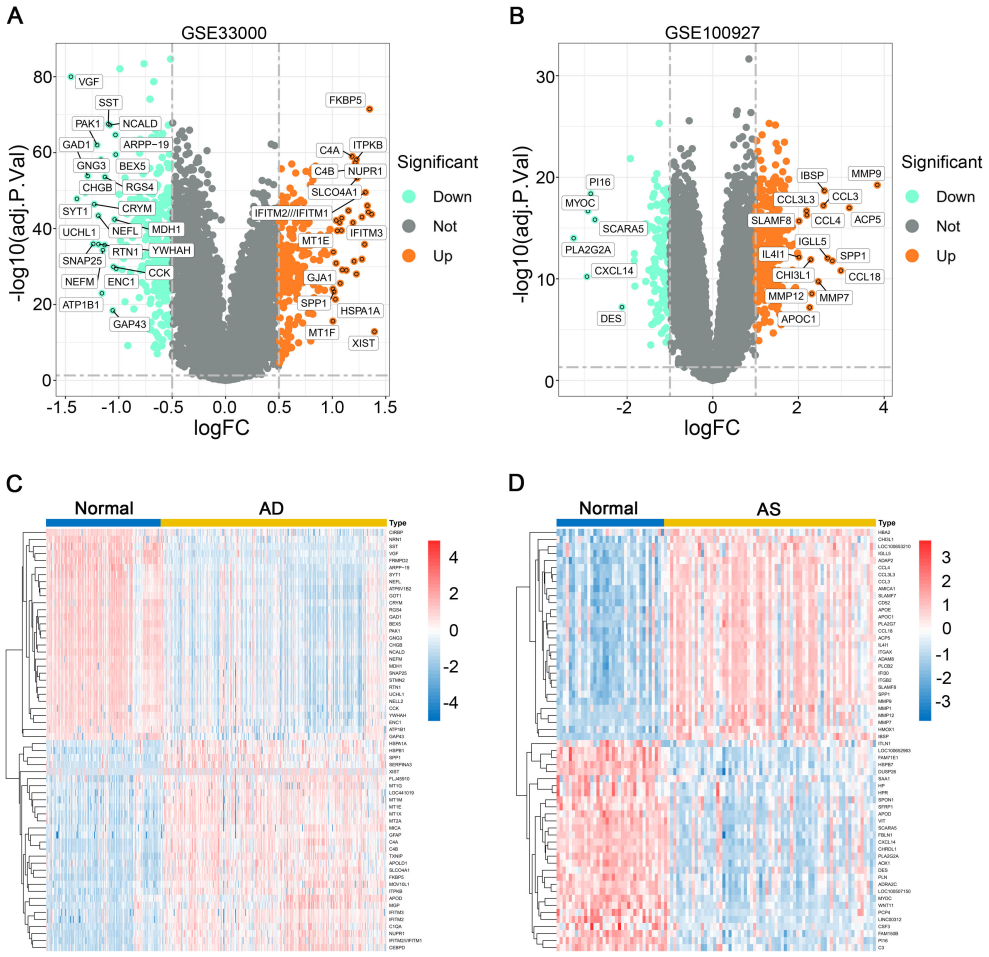

FIGURE 1
Differential gene expression analysis. **(A, B)** Volcano plots depict the differential expression genes (DEGs) in GSE33000 and GSE100927. **(C, D)** Heatmaps illustrate the expression patterns of corresponding DEGs in GSE33000 and GSE100927.

AS, respectively, as well as the modules MEturquoise and MEblue (Supplementary Table 4), which had the highest negative correlation, for further analysis.

3.3 Identification and functional analysis of CGs in AD and AS

To identify the most closely associated crosstalk gene sets with AD and AS, we performed an intersection analysis between the differentially expressed genes in AD and AS and the relevant gene module sets determined through WGCNA, resulting in 31 CGs for both diseases (Figure 3A). Subsequently, we conducted GO functional enrichment analysis for CGs, displaying the results of various aspects sorted by ascending p-values (Figure 3B). Biological process analysis demonstrated enriched contents closely related to immune function, such as antigen processing and presentation of exogenous peptide antigen via MHC class II, innate immune response, neutrophil activation involved in immune response, and complement activation classical pathway. In addition, cellular component and molecular function analyses also revealed immune-related contents, including complement components C1 complex and MHC class II receptor activity. Most results from KEGG analysis were also related to the immune system, such as complement and coagulation cascades, antigen processing and presentation, and efferocytosis (Figure 3C). Therefore, we inferred a certain correlation between the pathogenesis of AD and AS in the immune system, further validated by GSVA. We selected immune-related biological processes of interest and calculated scores for each patient in the AD dataset GSE33000 and AS dataset GSE100927. The results (Figures 3D, E) clearly demonstrated varying degrees of activation of various immune responses in both diseases compared to the normal group.

3.4 Identification of the optimal diagnostic genes in CGs through LASSO analysis

The CGs identified in the previous step were subjected to LASSO regression analysis using the AD dataset GSE33000 and the AS dataset GSE100927 (Figures 4A, B). The λ values were selected as lambda.min for both datasets, followed by intersection

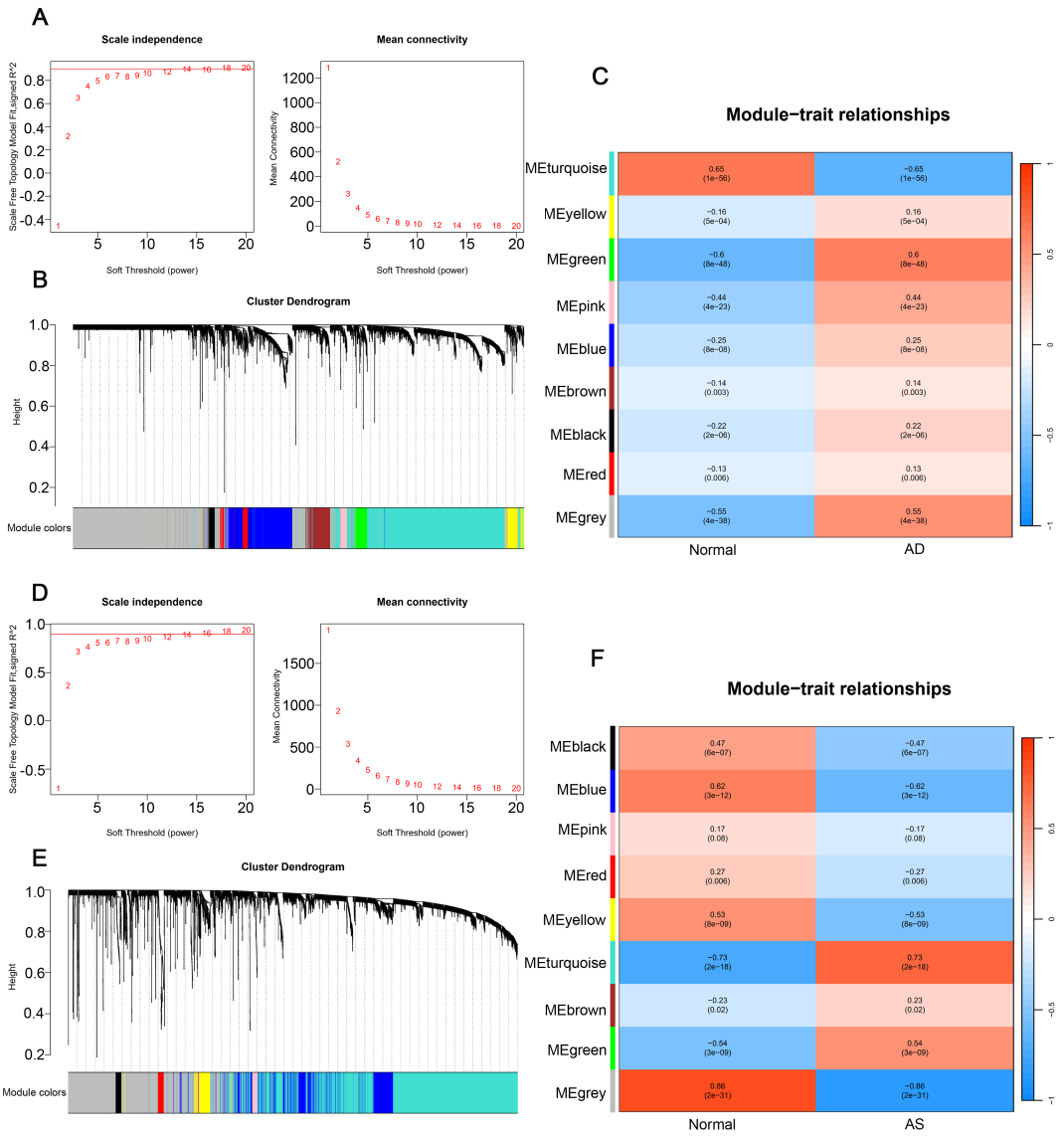

FIGURE 2
Weighted gene co-expression network analysis. **(A, D)** Determination of soft threshold powers in GSE33000 and GSE100927, R^2 = 0.90. **(B, E)** Gene cluster trees in GSE33000 and GSE100927. **(C, F)** Relationships between gene modules and traits in disease and normal groups, with numbers in the modules representing correlation coefficients and p-values.

analysis. Eventually, we determined three optimal diagnostic genes: C1QA, MT1M, and RAMP1 (Figure 4C). To observe the expression patterns of these three genes in the diseases, we analyzed a total of four databases including GSE33000 and GSE100927 as experimental groups for AD and AS, respectively, and GSE44770 and GSE43292 as validation groups for AD and AS, respectively. In the AD dataset, all three genes were found to be highly expressed in the disease (Figures 4D, F). In the AS dataset, MT1M showed low expression in the disease, while the remaining genes exhibited high expression (Figures 4E, G). Furthermore, to evaluate the predictive accuracy of the three genes for the diseases, we plotted receiver operating characteristic (ROC) curves using the four databases. The area under the curve (AUC) values of the ROC curves were used as indicators of predictive accuracy. The results (Figures 4H–K) indicated that in all four databases, the AUC values of the three genes were mostly distributed above 80%, suggesting that the diagnostic genes we identified possess excellent disease prediction capabilities.

3.5 Construction and evaluation of AD and AS diagnostic models

To further ascertain the predictive capabilities of the identified diagnostic genes, we intentionally incorporated the three diagnostic genes into the GSE33000 and GSE100927 databases to respectively construct AD and AS disease prediction models. Utilizing ROC curves, we assessed the disease prediction accuracy of the two models across four databases, and the results (Figures 5A–D) indicated that in both the corresponding experimental and

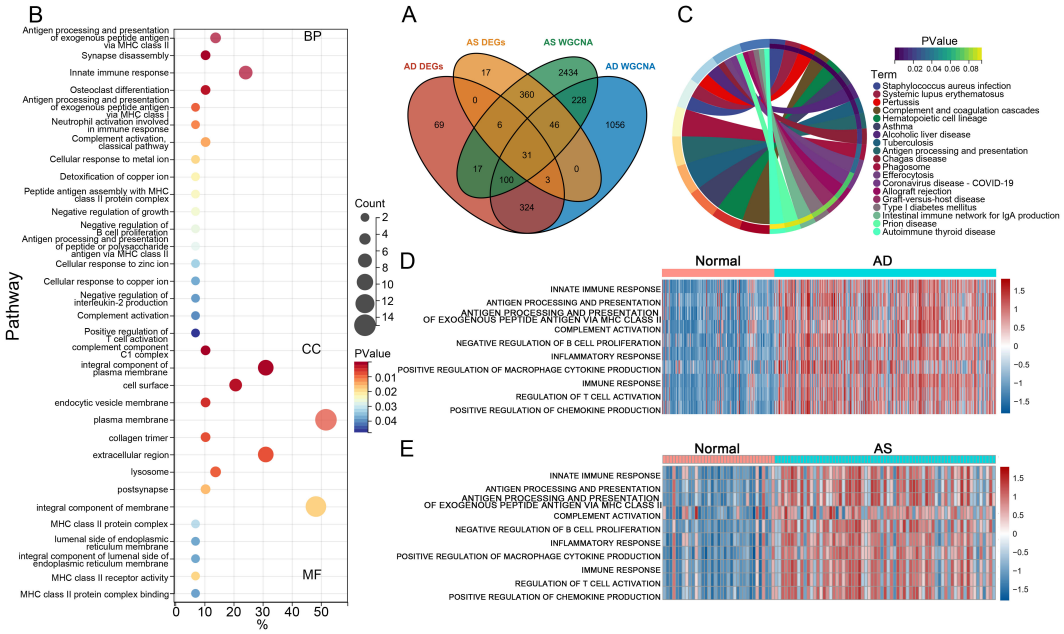

FIGURE 3
Functional and pathway enrichment analysis. **(A)** Venn diagram illustrates the intersection analysis of DEGs in AD and AS, as well as the gene sets associated with respective traits, determining the crosstalk genes (CGs) for AD and AS. **(B, C)** GO and KEGG enrichment analysis of CGs. **(D, E)** Gene set variation analysis (GSVA) in GSE33000 and GSE100927.

validation groups for the two diseases, the AUC values exceeded 0.85. Moreover, in the calibration curves (Figures 5E–H), the deviation correction curves for the AD and AS cohorts closely approximated the ideal curve, indicating good model consistency. Additionally, clinical decision curve analysis (DCA) brought deeper clinical significance (Figures 5I–L). Across various databases, the net benefits of clinical intervention based on the predicted probabilities from the constructed models were higher within the majority of threshold probability ranges compared to intervening for all or none. Finally, we detailed the characteristics of the AD and AS disease prediction models constructed based on the three diagnostic genes through nomograms (Figures 5M, N). In summary, through the aforementioned study, we confirmed the excellent predictive abilities of C1QA, MT1M, and RAMP1 expression as well as the corresponding models in AD and AS.

3.6 Selection of hub genes in CGs

To identify potential interactions within CGs, we constructed a protein-protein interaction (PPI) network using the STRING database in Cytoscape software, resulting in a network comprising 31 nodes and 79 edges (Figure 6A). Simultaneously, we employed four topological analysis methods, including MCC, Degree, MNC, and EPC, to collectively explore hub genes within CGs. According to the results, all four topological analysis methods converged on four common genes: C1QB, CSF1R, TYROBP, and FCER1G (Figure 6B). Further analysis of disease expression patterns revealed that these four hub genes exhibited significantly high expression in both the experimental and validation groups for AD and AS (Figures 6C–F).

3.7 Immune cell infiltration analysis

In order to thoroughly investigate the mechanisms underlying disease pathogenesis, we explored the patterns of immune cell infiltration in AD and AS cohorts. Utilizing the CIBERSORT algorithm, we obtained infiltration scores of various immune cells in the relevant disease tissues. In the GSE33000 dataset, the distribution of immune cells revealed (Figures 7A, B) that compared to the normal group, the AD group exhibited a significantly elevated infiltration pattern of M2 macrophages, while B cell memory, B cell plasma, and Mast cell resting showed pronounced decreases in infiltration. In the GSE100927 dataset (Figures 7D, E), the AS group displayed an exaggerated increase in infiltration of M0 macrophages compared to the normal group, while B cell plasma, T cell CD4+ memory resting, and Monocyte showed noticeable decreases in infiltration. Correlation analysis (Figures 7C, F) demonstrated a high consistency between the identified hub genes in CGs and the relationship with immune cells observed in both diseases' immune infiltration characteristics. This confirms the inseparable relationship between the expression of the hub genes identified earlier and the development of both diseases.

3.8 Construction of hub gene interaction networks

To confirm the upstream and downstream interactions of hub genes and their associated content, we separately constructed regulatory networks of hub genes and associated networks of

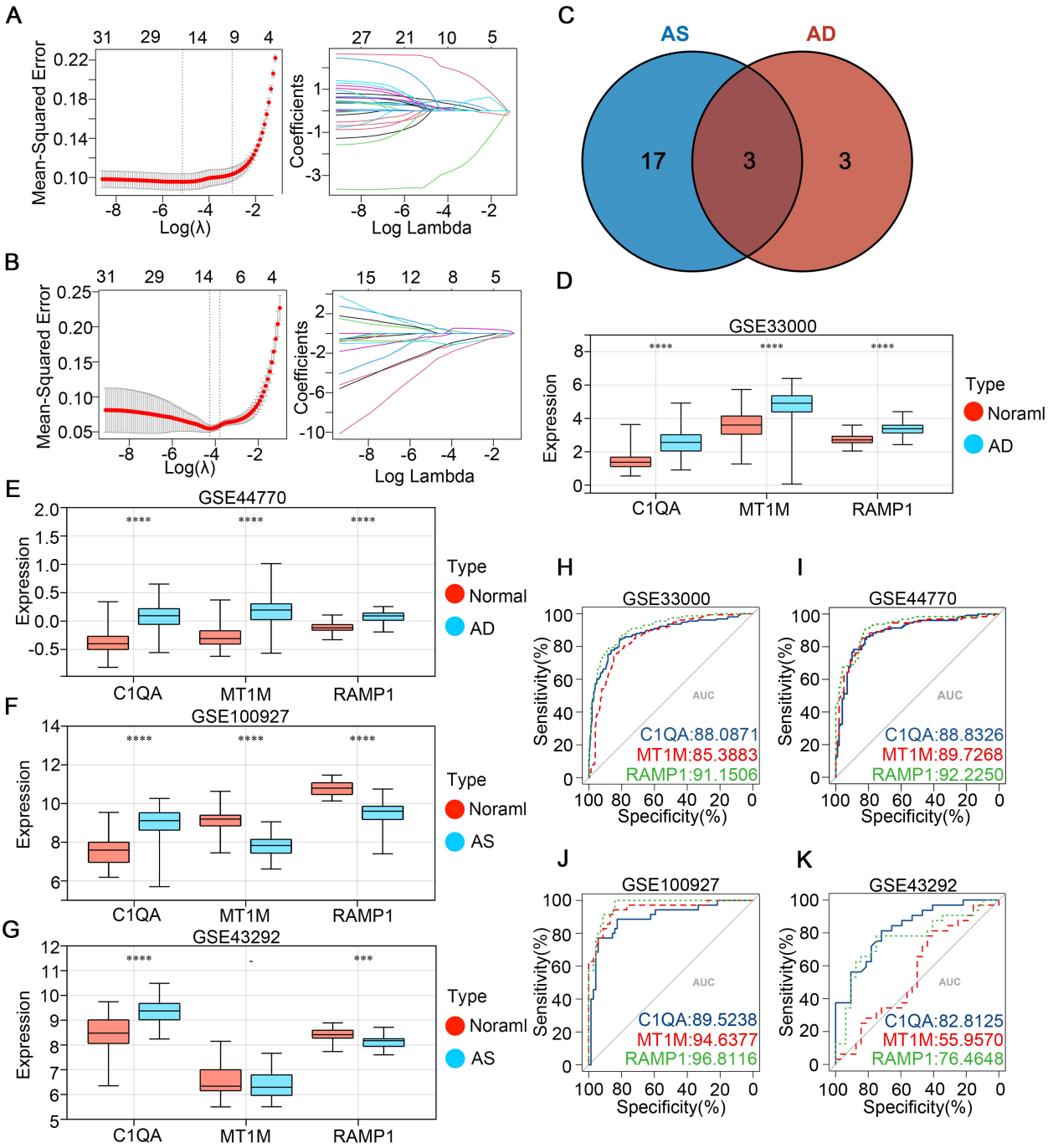

FIGURE 4
Identifying potential shared disease diagnostic CGs. **(A, B)** LASSO algorithm screening for potential diagnostic CGs in GSE33000 and GSE100927, respectively. **(C)** Venn diagram shows the intersection of potential diagnostic CGs for AD and AS. **(D-G)** Expression patterns of potential shared diagnostic CGs in GSE33000, GSE44770, GSE100927, and GSE43292 for AD and AS. **(H-K)** ROC curve analysis demonstrates the disease prediction ability of shared diagnostic CGs in GSE33000, GSE44770, GSE100927, and GSE43292. ***p < 0.001; ****p < 0.0001.

diseases, drugs, and chemicals. The gene regulatory network includes gene-miRNA interaction network, TF-gene interaction network, and TF-miRNA co-regulation network (Figure 8A). It can be observed that C1QB occupies a central position in hub gene interactions, with regulatory factors TCF4, MYC, STAT3, and SCLY playing a co-regulatory role in hub genes. has-mir-146a-5p, has-mir-124-3p, has-mir-129-2-3p, and has-mir-99b-5p are important miRNAs in the hub gene network. In the protein-chemical, protein-drug, and gene-disease associated networks (Figure 8B), associated diseases and drugs mainly focus on the action of C1QB, while chemicals such as Nickel, Tretinoin, Calcitriol, Methotrexate, and Antirheumatic Agents are significant relevant substances. These findings demonstrate closely associated networks of actions with hub genes in both diseases.

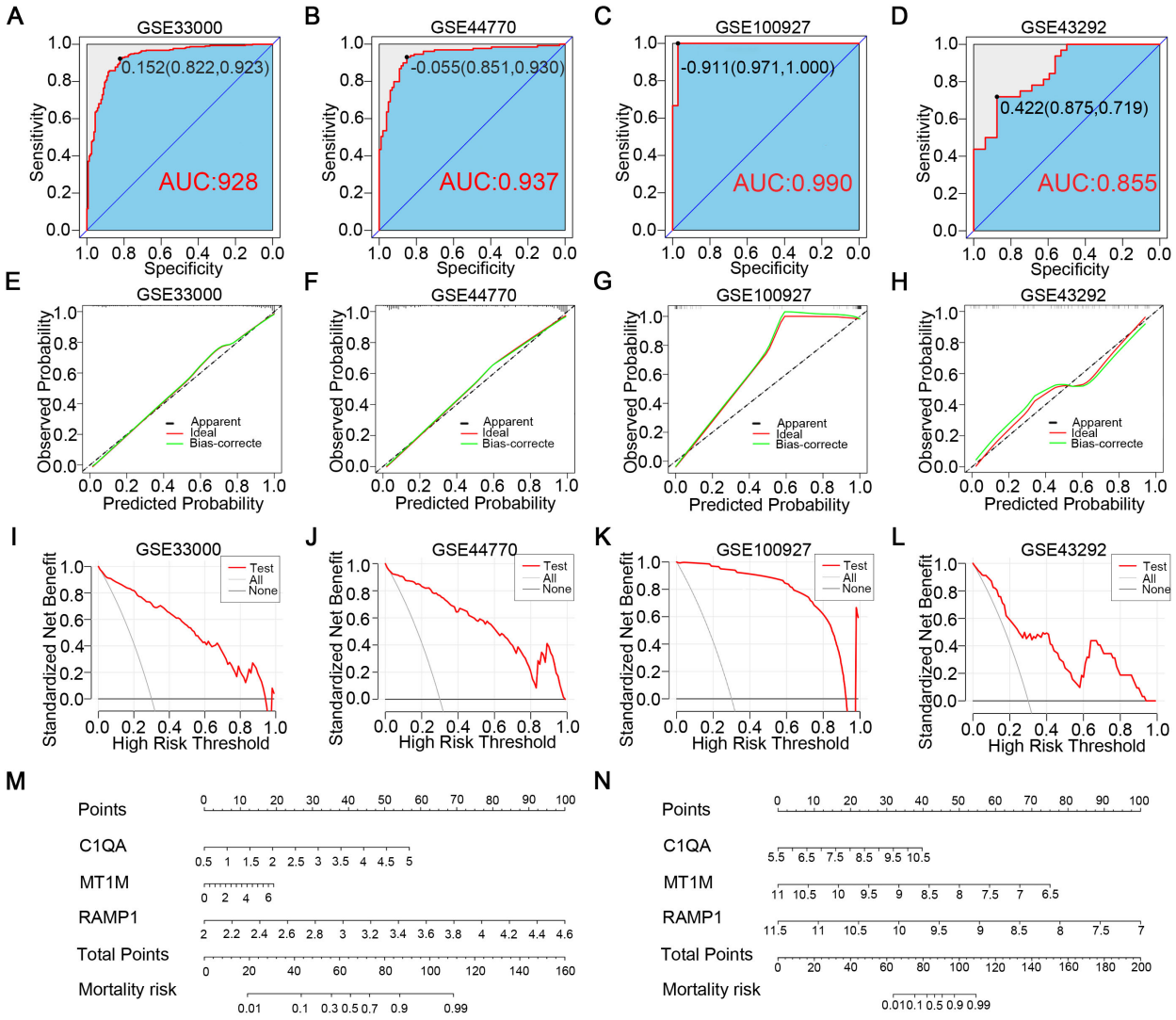

FIGURE 5
Construction of disease prediction models related to diagnostic CGs. **(A, B)** ROC curves demonstrate the predictive ability of the AD diagnostic model in GSE33000 and GSE44770. **(C, D)** ROC curves demonstrate the predictive ability of the AS diagnostic model in GSE100927 and GSE43292. **(E, F)** Calibration curves of the AD diagnostic model in GSE33000 and GSE44770. **(G, H)** Calibration curves of the AS diagnostic model in GSE100927 and GSE43292. **(I, J)** Clinical decision curves of the AD diagnostic model in GSE33000 and GSE44770. **(K, L)** Clinical decision curves of the AS diagnostic model in GSE100927 and GSE43292. **(M, N)** Disease prediction scoring models established based on diagnostic CGs for AD and AS.

3.9 Identification and characteristic analysis of subtypes in two disease types based on CGs

Finally, to comprehensively understand the impact of CGs expression on AD and AS, we identified subtypes of CGs through consensus clustering analysis for each disease. Consensus clustering analysis of CGs expression profiles in AD identified two subtypes, C1 and C2, among AD patients in GSE33000 (Figures 9A–C). Similarly, consensus clustering analysis of CGs expression profiles in AS also identified two subtypes, C1 and C2, among AS patients in GSE100927 (Figures 9E–G). Heatmaps were generated to illustrate the expression patterns of CGs in the two subtypes of AD and AS (Figures 9D, H). Subsequently, we performed immune infiltration analysis and enrichment score calculation of disease-related pathways using the CIBERSORT algorithm and GSVA algorithm for the subtypes of both diseases. Results indicated that, compared to the C1 subtype, the C2 subtype in both AD and AS largely exhibited expression patterns of immune cell infiltration consistent with the inherent immune infiltration characteristics of the diseases, particularly in macrophage infiltration features (Figures 10A, B). Calculation of enrichment scores (Figures 10C, D) revealed a significant immune activation state in the C2 subgroups of both diseases, including activation of various immune cells and regulation of inflammatory cells. Furthermore, in their respective disease mechanisms, pathways such as amyloid precursor protein biosynthesis and positive regulation of neuroinflammatory responses in AD, as well as positive regulation of macrophage-

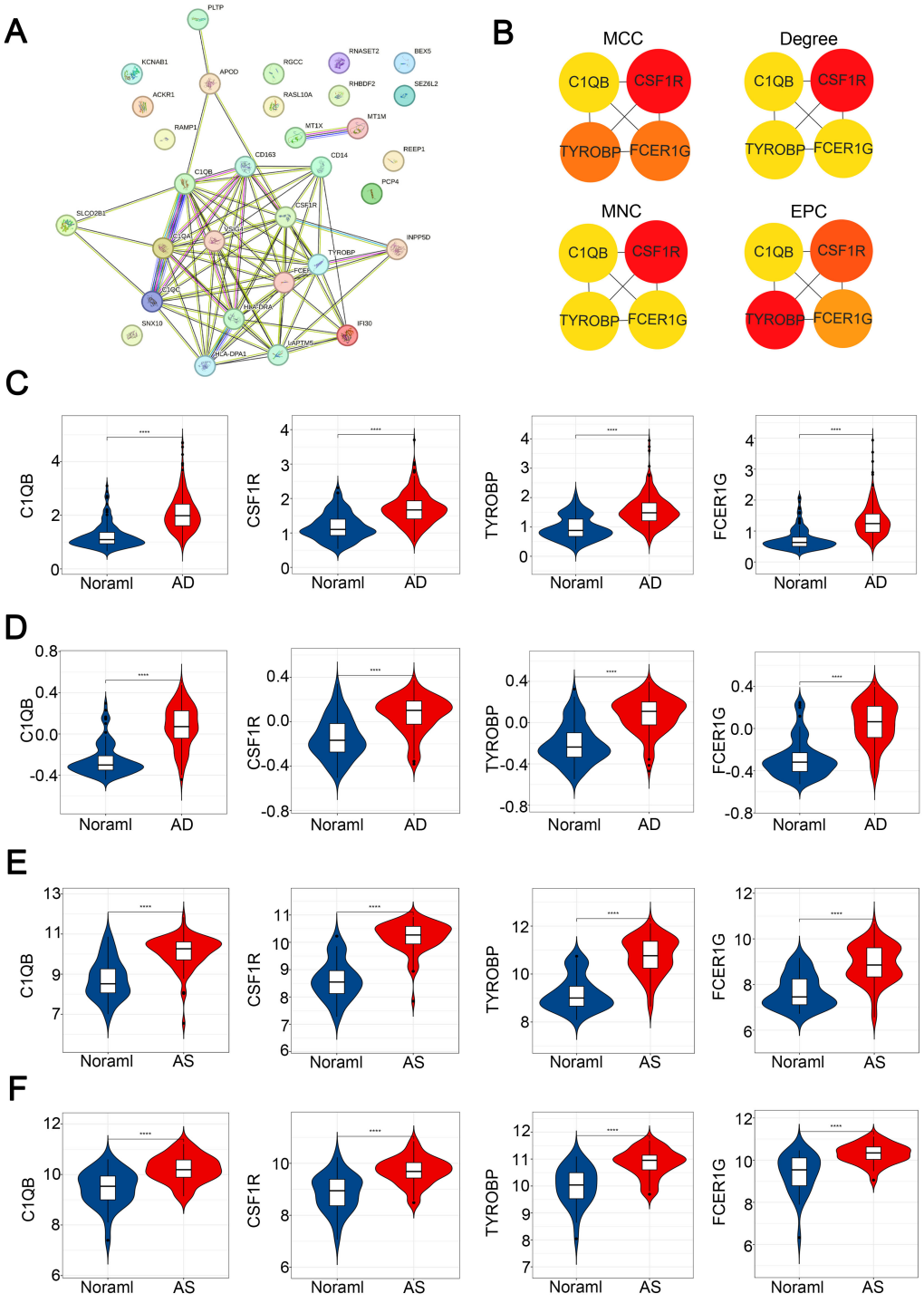

FIGURE 6
Construction of PPI network and identification of hub CGs. **(A)** PPI network of CGs. **(B)** Hub CGs determined by MCC, Degree, MNC, and EPC algorithms. **(C–F)** Expression patterns of hub CGs in GSE33000, GSE44770, GSE100927, and GSE43292, respectively. ****p < 0.0001.

derived foam cell differentiation in AS, showed significant activation in the C2 compared to the C1 subtype. Overall, these consistent pieces of evidence suggest a key role of CGs in the pathogenesis of AD and AS, indicating important connections between AD and AS at their core disease level.

4 Discussion

Alzheimer's disease (AD) and atherosclerosis (AS), as two major diseases in the world today, pose significant challenges to human society due to their progressive courses and increasing

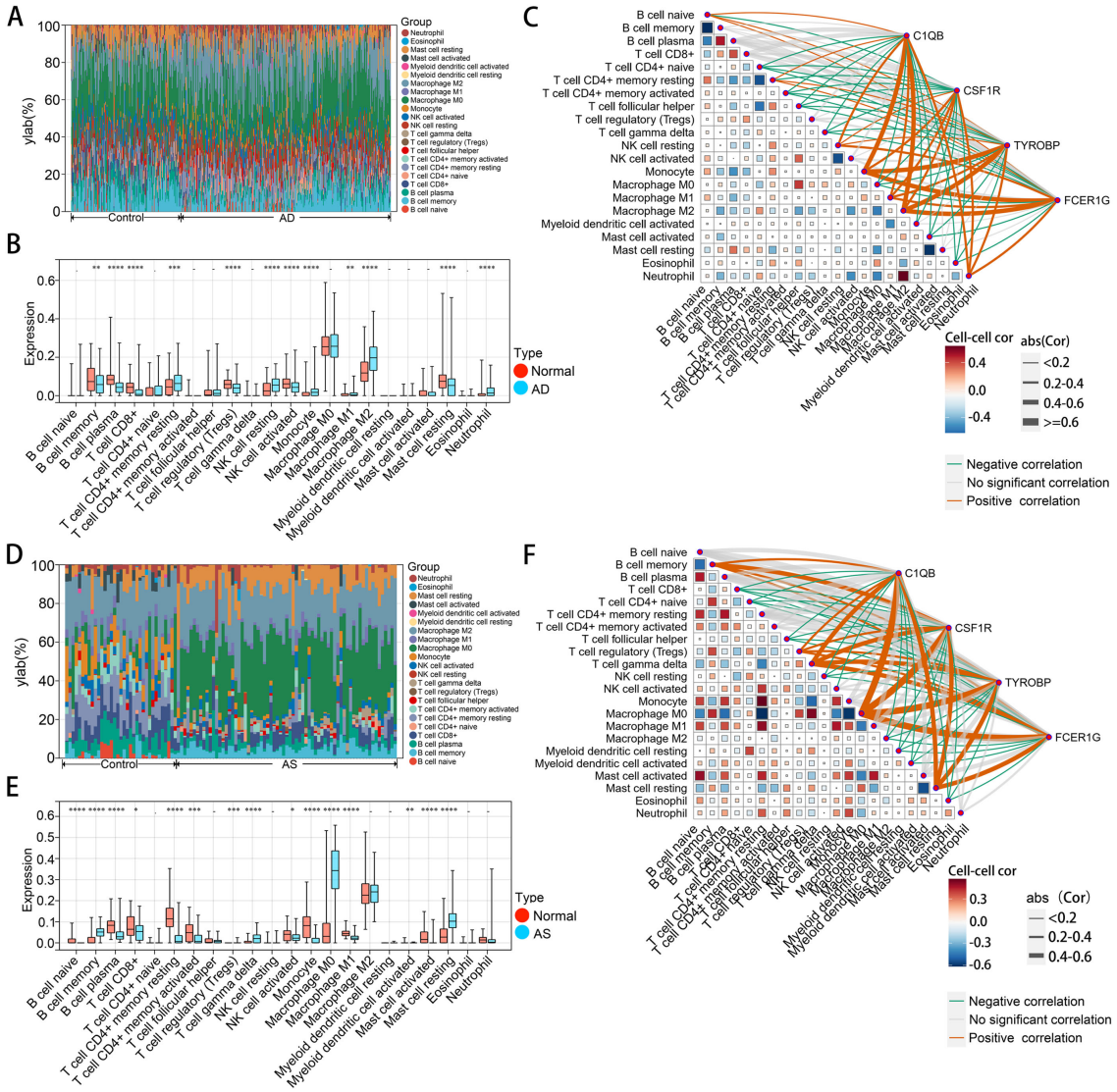

FIGURE 7
Immune cell infiltration analysis of AD and AS. **(A, D)** Analysis of the proportions of various immune cell infiltrates in GSE33000 and GSE100927 using the CIBERSORT algorithm. **(B, E)** Comparison of levels of various immune cell infiltrates between disease and normal groups in GSE33000 and GSE100927. **(C, F)** Analysis of the correlation between hub CGs and various infiltrating immune cells, as well as among infiltrating immune cells. The upper panel represents AD, and the lower panel represents AS. *p < 0.05; **p < 0.01; ***p < 0.001; ****p < 0.0001.

prevalence (43, 44). Although they are different diseases, there are important associations and interactions between them. AD patients often have a higher risk of cardiovascular diseases, such as hypertension, high cholesterol, and diabetes, which may be related to the development of AS (45). AS may accelerate the progression of AD by damaging the vascular endothelium, allowing harmful substances to enter the brain (46). Additionally, some pathophysiological changes in AD, such as amyloid plaques and abnormal tau protein deposition within neurons, may be associated with blood supply insufficiency and disrupted neuronal energy metabolism caused by AS (47). It is important to note that both diseases are related to chronic low-grade inflammation caused by aging, and shared inflammatory responses and immune dysregulation mechanisms may be key links between them (34). Given the intricate interaction mechanisms between them, a thorough understanding of their potential comorbid mechanisms is crucial for the prevention of both diseases.

This study identified 31 CGs between AD and AS, and functional analysis results showed significantly enhanced immune and inflammatory responses in both diseases compared to healthy patients. Previous research on neurodegenerative diseases has shown that inflammation is not only a result of these diseases but also a key participant in the process (48). In the case of AS, chronic inflammation of the arterial wall has long been considered a key cause of its pathogenesis (33). Nowadays, there has been significant progress in understanding the inflammatory and immune responses in AD and AS, and targeted treatments for long-term immune and inflammatory responses have gained increasing consensus (49, 50). In our subsequent research, three biomarkers (C1QA, MT1M, and RAMP1) were finally identified and demonstrated good diagnostic

10.3389/fimmu.2024.1443464

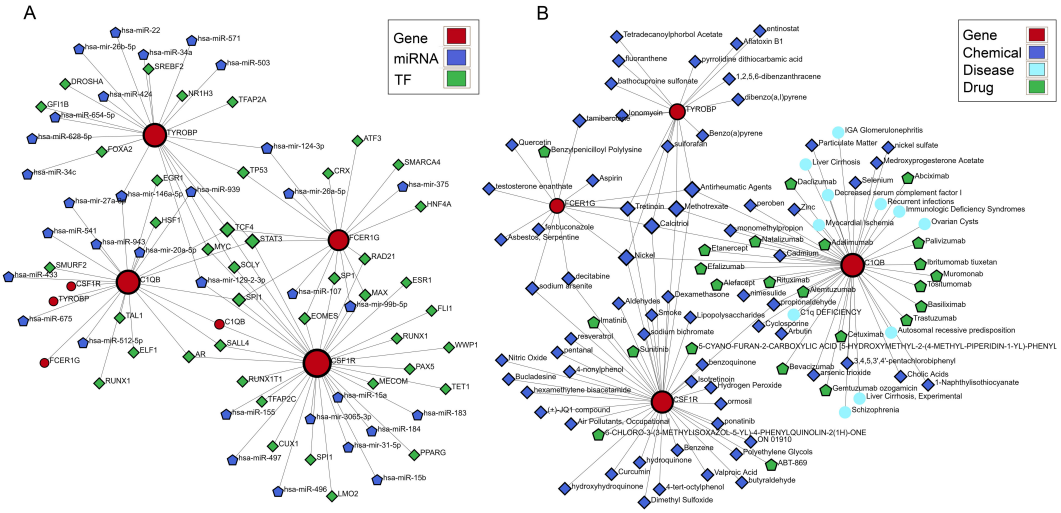

FIGURE 8
Building the interacting network of hub CGs. **(A)** Gene-miRNA interaction network, TF-gene interaction network, and TF-miRNA co-regulatory network. **(B)** Protein-chemical association, protein-drug association, and gene-disease association networks.

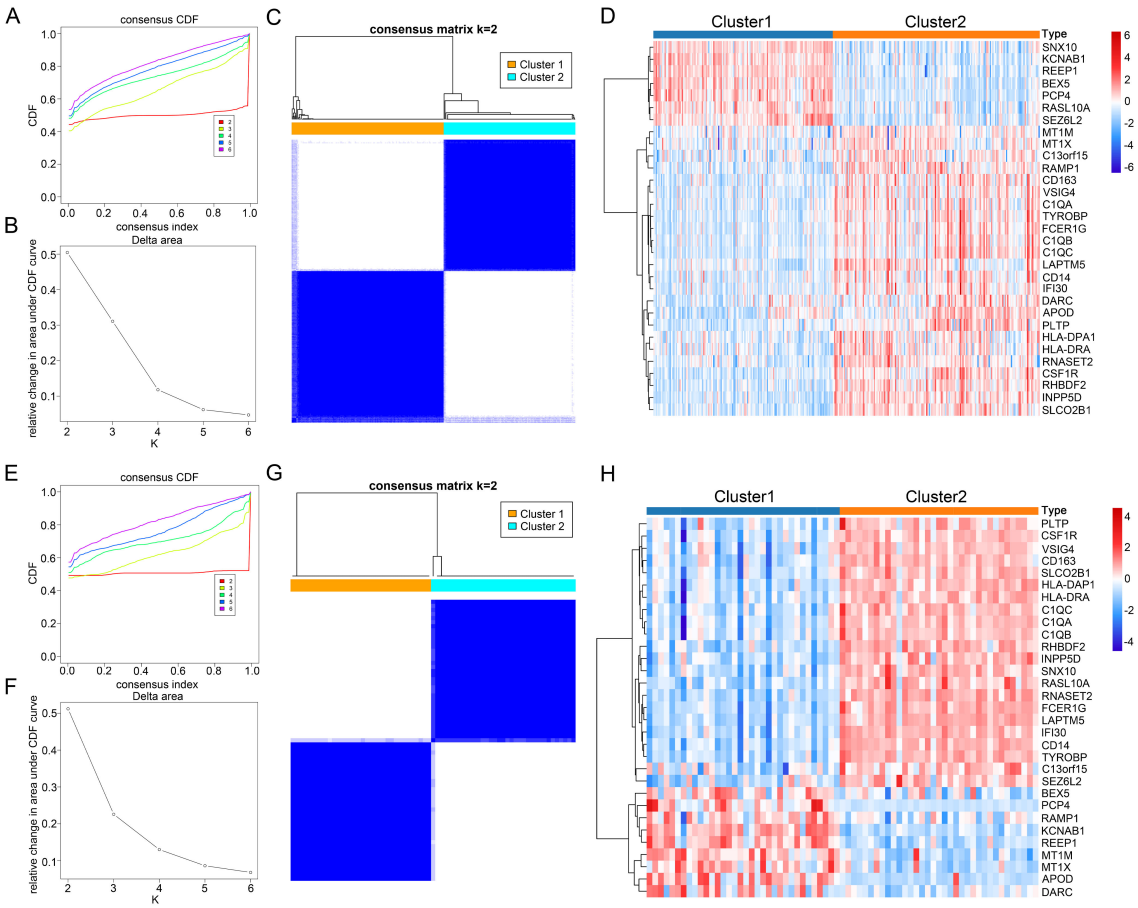

FIGURE 9
Identification of AD and AS disease subtypes related to consensus clustering of CGs. **(A, B)** Changes in the values of CDF and the corresponding area under the CDF curve in GSE33000 for k = 2-6. **(E, F)** Changes in the values of CDF and the corresponding area under the CDF curve in GSE100927 for k = 2-6. **(C)** Consensus matrix heatmap of AD subtype at k = 2. **(G)** Consensus matrix heatmap of AS subtype at k = 2. **(D)** Expression heatmap of different subtype CGs in AD cohort. **(H)** Expression heatmap of different subtype CGs in AS cohort.

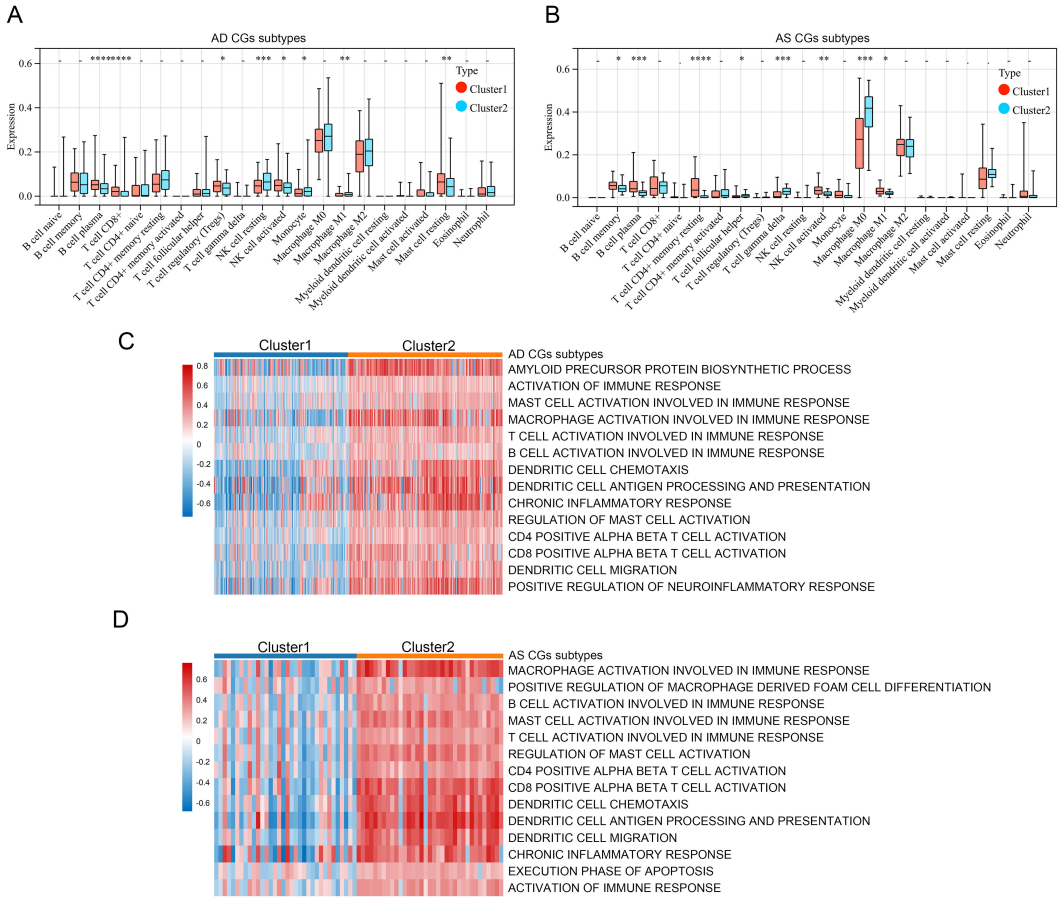

FIGURE 10
Relevant features of AD and AS disease subtypes. **(A, B)** Analysis of immune cell infiltration levels of C1 and C2 subtypes in AD and AS using the CIBERSORT algorithm. **(C, D)** GSVA demonstrates the enrichment status of different functional pathways in C1 and C2 subtypes. *p < 0.05; **p < 0.01; ***p < 0.001; ****p < 0.0001.

capabilities for both diseases. C1q is an important component of the complement system, playing a crucial role in maintaining immune homeostasis (51). The A-chain peptide of serum subcomponent C1q is encoded by the C1QA gene, and research has shown that C1QA may promote synaptic loss and be associated with progressive neurodegeneration (52, 53). Furthermore, clinical research results confirm the involvement of C1q in the development of atherosclerosis, plaque instability, and obstructive coronary artery disease (54, 55). Metallothionein 1M (MT1M) is a zinc-binding protein belonging to the metallothionein family, rich in cysteine, and plays an important role in regulating oxidative stress (56, 57). It is widely expressed in various tissues and protects cells from oxidative stress damage by scavenging free radicals and releasing zinc into the cytoplasm (58, 59). Interestingly, previous studies have also shown the involvement of MT1M in the inflammatory process, as pro-inflammatory factors can increase MT1M expression (60). RAMP1 belongs to the receptor activity-modifying protein (RAMP) family, best known for its role in modulating the activity of the calcitonin receptor (CLR), which has significant implications in the treatment of migraines (61, 62). Recently, there have also been reports of a close association between RAMP1 and tumors (63). Although research on RAMP1 is limited, increasing evidence suggests that RAMP1 plays important roles in the nervous, immune, endocrine, and circulatory systems, making it a potential new hotspot for disease development (64–67). Subsequently, the disease risk prediction model based on C1QA, MT1M, and RAMP1 was thoroughly validated using a verification database, suggesting that these three biomarkers are worthy of further in-depth study.

In studying the CGs that play a central role, we incorporated four topological analysis methods to jointly identify four hub CGs (C1QB, CSF1R, TYROBP, and FCER1G). C1QB is a polypeptide chain of the serum complement subcomponent C1q, and the effects of C1q on the nervous system and atherosclerosis have already been described earlier. CSF1R is a transmembrane receptor that initiates signal transduction pathways within cells by binding with ligands CSF-1 and IL-34 (68–70). Studies have indicated that CSF1R signaling is involved in regulating the activity of immune cells, promoting cell survival, proliferation, and differentiation, especially in macrophages, microglia, osteoclasts, and bone marrow dendritic cells (71). Moreover, excessive CSF1R signaling can sustain microglial activation, leading to the occurrence of chronic neuroinflammation and subsequent neurodegenerative changes (72, 73). TYROBP, also known as DAP12, is a transmembrane

adaptor protein widely expressed on immune cells, serving as a downstream adapter and presumed signaling partner for various receptors associated with AD, notorious for its role (74). Additionally, research suggests that TYROBP can promote lipid deposition and plaque inflammation during the AS process (75). FCER1G has been identified as a marker for human aging and neurodegenerative diseases in microglial cells (76). Recent studies have also confirmed the significant role of FCER1G in promoting immune cell infiltration into atherosclerotic plaques and intraplaque hemorrhage (77). Overall, these four hub CGs are intricately linked to both AD and AS.

The results of immune cell infiltration analysis show a significant enrichment of M2 macrophages in the AD environment. It is believed that the recruitment of peripheral macrophages to the central nervous system is likely a potential therapeutic target for AD (78). Currently, activated macrophages are mainly divided into two subtypes: M1 and M2. M1 macrophages primarily promote inflammatory responses, while M2 macrophages mainly inhibit inflammatory responses (79). An interesting study found that in AD model rats, transplantation of M2 macrophages could reduce intracranial inflammatory responses, decrease neuronal loss, and improve cognitive dysfunction, suggesting that M2 macrophages have a protective role in AD (80). The enrichment of M2 macrophages in the brains of AD patients is hypothesized to be a form of self-protection by the body. How to utilize this phenomenon may be worth further in-depth research by future scholars. In the AS environment, M0 macrophages exhibit more significant infiltration. This aligns with the pathogenesis of AS, where macrophages engulf modified low-density lipoprotein particles and form foam cells (a hallmark of atherosclerosis), leading to the formation of early atherosclerotic lesions (81, 82). Nowadays, since lipid-lowering therapy cannot completely halt the progression of AS and macrophage polarization is involved in various stages of atherosclerosis, an increasing number of AS treatment strategies are focusing on targeting macrophages (83–85).

The construction of gene interaction networks provides a more detailed illustration of the regulatory mechanisms of hub CGs and their associated diseases, drugs, and chemicals, enhancing our understanding of disease onset and aiding in the development of treatment strategies. The regulatory factors TCF4, MYC, STAT3, and SCLY play the most extensive co-regulatory roles in CGs. TCF4, a member of the helix-loop-helix (HLH) protein family, is expressed in various cell types and tissues throughout the body (86). Research has shown that TCF4 is a key regulator of neural function and is closely associated with neurodevelopmental disorders such as intellectual disability and schizophrenia (87, 88). Recent studies have also indicated that TCF4 influences IL-17RA/IL-17RE signaling, which is involved in inflammatory feedback loops (89). Current research on MYC primarily focuses on its role in cancer (90). MYC is a super-transcription factor encoded by the MYC gene located on chromosome 8q24.21, playing a crucial role in cell growth, proliferation, and apoptosis (91, 92). STAT3's mechanisms have been confirmed in Alzheimer's disease (AD) model mice, where inhibiting STAT3 expression improves pathological and behavioral abnormalities (93). Additionally, STAT3 has been shown to promote the progression of ankylosing spondylitis (AS) through mechanisms such as interference with the Akt/mTOR signaling cascade and pyroptosis (94–96). Studies on SCLY indicate its involvement in selenium methionine metabolism and its potential role in oxidative stress and cellular protection (97). Chemical compounds such as Nickel, Tretinoin, Calcitriol, Methotrexate, and Antirheumatic Agents have been closely linked to pivotal CGs in analyses. These compounds may play significant roles in future research.

Consensus clustering analysis based on CGs revealed two distinct subtypes of immune and inflammatory activation intensities within AD and AS. This finding highlights the crucial role of CGs in the pathogenesis of AD and AS and underscores the importance of immune and inflammatory dysregulation in the occurrence and progression of these diseases.

Despite the aforementioned analyses, this study still has certain limitations. Utilizing online databases, we analyzed and identified CGs for both AD and AS; however, the database itself may not be comprehensive, and we lack experimental validation in aspects such as gene function and immune infiltration. Additionally, disease prediction models and disease subtypes built based on CGs may require further clinical validation before entering formal applications. Therefore, in the future, we hope to see more researchers joining this study.

5 Conclusion

In recent years, age-related diseases have garnered increasing attention. We are dedicated to filling the gap in understanding the interaction mechanisms between Alzheimer's disease (AD) and atherosclerosis (AS) and have identified crosstalk genes between AD and AS. C1QA, MT1M, and RAMP1 have been identified as potential diagnostic biomarkers, and predictive models for both diseases have been constructed based on these genes. Additionally, C1QB, CSF1R, TYROBP, and FCER1G have been recognized as key genes in the crosstalk between AD and AS, showing close associations with immune cells in immune infiltration analysis. By establishing a gene interaction network, we have more clearly demonstrated the regulatory mechanisms and related functions of these key genes. Overall, we have identified seven important crosstalk genes, which have been confirmed in extensive studies to play significant roles in the immune process. However, the specific roles of these genes in AD and AS still require further research. In the future, these findings are expected to provide new clues for exploring targeted therapeutic approaches for both diseases.

Data availability statement

The datasets analyzed for this study can be found in the GEO database; GSE33000, GSE100927, GSE44770, and GSE43292.

Author contributions

WA: Writing – original draft. JZ: Writing – original draft. ZQ: Writing – original draft. PW: Writing – original draft. XH: Writing

– original draft. YC: Writing – original draft. ZH: Writing – original draft. YA: Writing – review & editing. SL: Writing – review & editing.

Funding

The author(s) declare that no financial support was received for the research, authorship, and/or publication of this article.

Acknowledgments

Sincere thanks for the open access to the GEO database, as well as the contributions from researchers, volunteers, and patients providing data.

Conflict of interest

Authors PW, XH, YC, and ZH are employed by Beijing Yihua Biotechnology Co., Ltd.

The remaining authors declare that the research was conducted in the absence of any commercial or financial relationships that could be construed as a potential conflict of interest.

Publisher's note

Supplementary material

The Supplementary Material for this article can be found online at: https://www.frontiersin.org/articles/10.3389/fimmu.2024.1443464/full#supplementary-material

SUPPLEMENTARY TABLE 1
DEGs in the expression matrix of GSE33000.

SUPPLEMENTARY TABLE 2
DEGs in the expression matrix of GSE100927.

SUPPLEMENTARY TABLE 3
Identification of the MEgreen module most positively correlated with AD and the MEturquoise module most positively correlated with AS by WGCNA.

SUPPLEMENTARY TABLE 4
Identification of the MEturquoise module most negatively correlated with AD and the MEblue module most negatively correlated with AS by WGCNA

References

1. Smulders L, Deelen J. Genetics of human longevity: From variants to genes to pathways. *J Intern Med*. (2024) 295:416–35. doi: 10.1111/joim.13740

2. Dugan B, Conway J, Duggal NA. Inflammaging as a target for healthy ageing. *Age Ageing*. (2023) 52:afac328. doi: 10.1093/ageing/afac328

3. Crimmins EM. Lifespan and healthspan: past, present, and promise. *GERONT*. (2015) 55:901–11. doi: 10.1093/geront/gnv130

4. Kemoun P, Ader I, Planat-Benard V, Dray C, Fazilleau N, Monsarrat P, et al. A gerophysiology perspective on healthy ageing. *Ageing Res Rev*. (2022) 73:101537. doi: 10.1016/j.arr.2021.101537

5. Zhang XX, Tian Y, Wang ZT, Ma YH, Tan L, Yu JT. The epidemiology of alzheimer's disease modifiable risk factors and prevention. *J Prev Alzheimers Dis*. (2021) 8:313–21. doi: 10.14283/jpad.2021.15

6. Biondi-Zoccai G, Garmendia CM, Abbate A, Giordano A, Frati G, Sciarretta S, et al. Atherothrombosis prevention and treatment with anti-interleukin-1 agents. *Curr Atheroscler Rep*. (2020) 22:4. doi: 10.1007/s11883-020-0819-1

7. Jalbert JJ, Daiello LA, Lapane KL. Dementia of the alzheimer type. *Epidemiol Rev*. (2008) 30:15–34. doi: 10.1093/epirev/mxn008

8. 2023 Alzheimer's disease facts and figures. *Alzheimer's Dementia*. (2023) 19:1598–695. doi: 10.1002/alz.13016

9. Scheltens P, De Strooper B, Kivipelto M, Holstege H, Chételat G, Teunissen CE, et al. Alzheimer's disease. *Lancet*. (2021) 397:1577–90. doi: 10.1016/S0140-6736(20)32205-4

10. Bloom GS. Amyloid-β and tau: the trigger and bullet in alzheimer disease pathogenesis. *JAMA Neurol*. (2014) 71:505. doi: 10.1001/jamaneurol.2013.5847

11. Porsteinsson AP, Isaacson RS, Knox S, Sabbagh MN, Rubino I. Diagnosis of early alzheimer's disease: clinical practice in 2021. *J Prev Alz Dis*. (2021) 8(3):371–386. doi: 10.14283/jpad.2021.23

12. van der Wee N, Bilderbeck AC, Cabello M, Ayuso-Mateos JL, Saris IMJ, Giltay EJ, et al. Working definitions, subjective and objective assessments and experimental paradigms in a study exploring social withdrawal in schizophrenia and Alzheimer's disease. *Neurosci Biobehav Rev*. (2019) 97:38–46. doi: 10.1016/j.neubiorev.2018.06.020

13. Passeri E, Elkhoury K, Morsink M, Broersen K, Linder M, Tamayol A, et al. Alzheimer's disease: treatment strategies and their limitations. *Int J Mol Sci*. (2022) 23:13954. doi: 10.3390/ijms232213954

14. Libby P, Buring JE, Badimon L, Hansson GK, Deanfield J, Bittencourt MS, et al. Atherosclerosis. *Nat Rev Dis Primers*. (2019) 5:56. doi: 10.1038/s41572-019-0106-z

15. Aday AW, Matsushita K. Epidemiology of peripheral artery disease and polyvascular disease. *Circ Res*. (2021) 128:1818–32. doi: 10.1161/CIRCRESAHA.121.318535

16. Frostegård J. Immunity, atherosclerosis and cardiovascular disease. *BMC Med*. (2013) 11:117. doi: 10.1186/1741-7015-11-117

17. Herrington W, Lacey B, Sherliker P, Armitage J, Lewington S. Epidemiology of atherosclerosis and the potential to reduce the global burden of atherothrombotic disease. *Circ Res*. (2016) 118:535–46. doi: 10.1161/CIRCRESAHA.115.307611

18. Malekmohammad K, Sewell RDE, Rafieian-Kopaei M. Antioxidants and atherosclerosis: mechanistic aspects. *Biomolecules*. (2019) 9:301. doi: 10.3390/biom9080301

19. Fan J, Watanabe T. Atherosclerosis: known and unknown. *Pathol Int*. (2022) 72:151–60. doi: 10.1111/pin.13202

20. Raitakari O, Pahkala K, Magnussen CG. Prevention of atherosclerosis from childhood. *Nat Rev Cardiol*. (2022) 19:543–54. doi: 10.1038/s41569-021-00647-9

21. McGuire AL, Gabriel S, Tishkoff SA, Wonkam A, Chakravarti A, Furlong EEM, et al. The road ahead in genetics and genomics. *Nat Rev Genet*. (2020) 21:581–96. doi: 10.1038/s41576-020-0272-6

22. Gonzaga-Jauregui C, Lupski JR, Gibbs RA. Human genome sequencing in health and disease. *Annu Rev Med*. (2012) 63:35–61. doi: 10.1146/annurev-med-051010-162644

23. Naumova O, Lee M, Rychkov S, Vlasova NV, Grigorenko EL. Gene expression in the human brain: the current state of the study of specificity and spatio-temporal dynamics. *Child Dev*. (2013) 84:76–88. doi: 10.1111/cdev.12014

24. Gibney ER, Nolan CM. Epigenetics and gene expression. *Heredity (Edinb)*. (2010) 105:4–13. doi: 10.1038/hdy.2010.54

25. Segundo-Val IS, Sanz-Lozano CS. Introduction to the gene expression analysis. *Methods Mol Biol*. (2016) 1434:29–43. doi: 10.1007/978-1-4939-3652-6_3

26. Dorado G, Gálvez S, Rosales TE, Vásquez VF, Hernández P. Analyzing modern biomolecules: the revolution of nucleic-acid sequencing – review. *Biomolecules*. (2021) 11:1111. doi: 10.3390/biom11081111

27. Brazma A, Vilo J. Gene expression data analysis. *FEBS Lett*. (2000) 480:17–24. doi: 10.1016/s0014-5793(00)01772-5

28. Lathe R, Sapronova A, Kotelevtsev Y. Atherosclerosis and Alzheimer–diseases with a common cause? Inflammation, oxysterols, vasculature. *BMC Geriatr*. (2014) 14:36. doi: 10.1186/1471-2318-14-36

29. Gustavsson AM, van Westen D, Stomrud E, Engström G, Nägga K, Hansson O. Midlife atherosclerosis and development of alzheimer or vascular dementia. *Ann Neurol*. (2020) 87:52–62. doi: 10.1002/ana.25645

30. Stakos DA, Stamatelopoulos K, Bampatsias D, Sachse M, Zormpas E, Vlachogiannis NI, et al. The alzheimer's disease amyloid-beta hypothesis in cardiovascular aging and disease: JACC focus seminar. *J Am Coll Cardiol*. (2020) 75:952–67. doi: 10.1016/j.jacc.2019.12.033

31. Heneka MT, Carson MJ, El Khoury J, Landreth GE, Brosseron F, Feinstein DL, et al. Neuroinflammation in alzheimer's disease. *Lancet Neurol*. (2015) 14:388–405. doi: 10.1016/S1474-4422(15)70016-5

32. Heppner FL, Ransohoff RM, Becher B. Immune attack: the role of inflammation in Alzheimer disease. *Nat Rev Neurosci*. (2015) 16:358–72. doi: 10.1038/nrn3880

33. Roy P, Orecchioni M, Ley K. How the immune system shapes atherosclerosis: roles of innate and adaptive immunity. *Nat Rev Immunol*. (2022) 22:251–65. doi: 10.1038/s41577-021-00584-1

34. Stahr N, Galkina EV. Immune response at the crossroads of atherosclerosis and alzheimer's disease. *Front Cardiovasc Med*. (2022) 9:870144. doi: 10.3389/fcvm.2022.870144

35. Langfelder P, Horvath S. WGCNA: an R package for weighted correlation network analysis. *BMC Bioinf*. (2008) 9:559. doi: 10.1186/1471-2105-9-559

36. Friedman J, Hastie T, Tibshirani R. Regularization paths for generalized linear models via coordinate descent. *J Stat Software*. (2010) 33:1–22. doi: 10.18637/jss.v033.i01

37. Obuchowski NA, Bullen JA. Receiver operating characteristic (ROC) curves: review of methods with applications in diagnostic medicine. *Phys Med Biol*. (2018) 63:07TR01. doi: 10.1088/1361-6560/aab4b1

38. Shariat SF, Capitanio U, Jeldres C, Karakiewicz PI. Can nomograms be superior to other prediction tools? *BJU Int*. (2009) 103:492–495; discussion 495-497. doi: 10.1111/j.1464-410X.2008.08073.x

39. Chen H, Cai Y, Ji C, Selvaraj G, Wei D, Wu H. AdaPPI: identification of novel protein functional modules via adaptive graph convolution networks in a protein-protein interaction network. *Brief Bioinform*. (2023) 24:bbac523. doi: 10.1093/bib/bbac523

40. Makowski L, Chaib M, Rathmell JC. Immunometabolism: From basic mechanisms to translation. *Immunol Rev*. (2020) 295:5–14. doi: 10.1111/imr.12858

41. Xia J, Gill EE, Hancock REW. NetworkAnalyst for statistical, visual and network-based meta-analysis of gene expression data. *Nat Protoc*. (2015) 10:823–44. doi: 10.1038/nprot.2015.052

42. Wilkerson MD, Hayes DN. ConsensusClusterPlus: a class discovery tool with confidence assessments and item tracking. *Bioinformatics*. (2010) 26:1572–3. doi: 10.1093/bioinformatics/btq170

43. Monteiro AR, Barbosa DJ, Remião F, Silva R. Alzheimer's disease: Insights and new prospects in disease pathophysiology, biomarkers and disease-modifying drugs. *Biochem Pharmacol*. (2023) 211:115522. doi: 10.1016/j.bcp.2023.115522

44. Wojtasińska A, Frąk W, Lisińska W, Sapeda N, Młynarska E, Rysz J, et al. Novel insights into the molecular mechanisms of atherosclerosis. *Int J Mol Sci*. (2023) 24:13434. doi: 10.3390/ijms241713434

45. Leszek J, Mikhaylenko EV, Belousov DM, Koutsouraki E, Szczechowiak K, Kobusiak-Prokopowicz M, et al. The links between cardiovascular diseases and alzheimer's disease. *Curr Neuropharmacol*. (2021) 19:152–69. doi: 10.2174/1570159X18666200729093724

46. Sweeney MD, Sagare AP, Zlokovic BV. Blood–brain barrier breakdown in Alzheimer's disease and other neurodegenerative disorders. *Nat Rev Neurol*. (2018) 14:133–50. doi: 10.1038/nrneurol.2017.188

47. Cermakova P, Eriksdotter M, Lund LH, Winblad B, Religa P, Religa D. Heart failure and Alzheimer′s disease. *J Intern Med*. (2015) 277:406–25. doi: 10.1111/joim.12287

48. Zhang W, Xiao D, Mao Q, Xia H. Role of neuroinflammation in neurodegeneration development. *Signal Transduct Target Ther*. (2023) 8:267. doi: 10.1038/s41392-023-01486-5

49. Thakur S, Dhapola R, Sarma P, Medhi B, Reddy DH. Neuroinflammation in alzheimer's disease: current progress in molecular signaling and therapeutics. *Inflammation*. (2023) 46:1–17. doi: 10.1007/s10753-022-01721-1

50. Kong P, Cui ZY, Huang XF, Zhang DD, Guo RJ, Han M. Inflammation and atherosclerosis: signaling pathways and therapeutic intervention. *Signal Transduct Target Ther*. (2022) 7:131. doi: 10.1038/s41392-022-00955-7

51. Zhang W, Chen Y, Pei H. C1q and central nervous system disorders. *Front Immunol*. (2023) 14:1145649. doi: 10.3389/fimmu.2023.1145649

52. Zhang C, Qi H, Jia D, Zhao J, Xu C, Liu J, et al. Cognitive impairment in Alzheimer's disease FAD4T mouse model: Synaptic loss facilitated by activated microglia via C1qA. *Life Sci*. (2024) 340:122457. doi: 10.1016/j.lfs.2024.122457

53. Li S, Zhu Y, Wei C, Li C, Chen W, Jiang S, et al. Identification of molecular correlations between DHRS4 and progressive neurodegeneration in amyotrophic lateral sclerosis by gene co-expression network analysis. *Front Immunol*. (2022) 13:874978. doi: 10.3389/fimmu.2022.874978

54. Sasaki S, Nishihira K, Yamashita A, Fujii T, Onoue K, Saito Y, et al. Involvement of enhanced expression of classical complement C1q in atherosclerosis progression and plaque instability: C1q as an indicator of clinical outcome. *PloS One*. (2022) 17:e0262413. doi: 10.1371/journal.pone.0262413

55. Guo S, Mao X, Li X, Ouyang H, Gao Y, Ming L. Serum complement C1q activity is associated with obstructive coronary artery disease. *Front Cardiovasc Med*. (2021) 8:618173. doi: 10.3389/fcvm.2021.618173

56. Formigari A, Irato P, Santon A. Zinc, antioxidant systems and metallothionein in metal mediated-apoptosis: biochemical and cytochemical aspects. *Comp Biochem Physiol C Toxicol Pharmacol*. (2007) 146:443–59. doi: 10.1016/j.cbpc.2007.07.010

57. Shelton RC, Claiborne J, Sidoryk-Wegrzynowicz M, Reddy R, Aschner M, Lewis DA, et al. Altered expression of genes involved in inflammation and apoptosis in frontal cortex in major depression. *Mol Psychiatry*. (2011) 16:751–62. doi: 10.1038/mp.2010.52

58. Mao J, Yu H, Wang C, Sun L, Jiang W, Zhang P, et al. Metallothionein MT1M is a tumor suppressor of human hepatocellular carcinomas. *Carcinogenesis*. (2012) 33:2568–77. doi: 10.1093/carcin/bgs287

59. Yu T, Huang Z, Pu Z. Identification of potential diagnostic biomarkers and biological pathways in hypertrophic cardiomyopathy based on bioinformatics analysis. *Genes (Basel)*. (2022) 13:530. doi: 10.3390/genes13030530

60. Lappas M. Expression and regulation of metallothioneins in myometrium and fetal membranes. *Am J Reprod Immunol*. (2018) 80:e13040. doi: 10.1111/aji.13040

61. McLatchie LM, Fraser NJ, Main MJ, Wise A, Brown J, Thompson N, et al. RAMPs regulate the transport and ligand specificity of the calcitonin-receptor-like receptor. *Nature*. (1998) 393:333–9. doi: 10.1038/30666

62. Mullard A. FDA approves second GPCR-targeted antibody. *Nat Rev Drug Discovery*. (2018) 17:613. doi: 10.1038/nrd.2018.153

63. Xie L, Xiao W, Fang H, Liu G. RAMP1 as a novel prognostic biomarker in pan-cancer and osteosarcoma. *PloS One*. (2023) 18:e0292452. doi: 10.1371/journal.pone.0292452

64. Mizuta H, Takakusaki A, Suzuki T, Otake K, Dohmae N, Simizu S. C-mannosylation regulates stabilization of RAMP1 protein and RAMP1-mediated cell migration. *FEBS J*. (2023) 290:196–208. doi: 10.1111/febs.16592

65. Yang D, Jacobson A, Meerschaert KA, Sifakis JJ, Wu M, Chen X, et al. Nociceptor neurons direct goblet cells via a CGRP-RAMP1 axis to drive mucus production and gut barrier protection. *Cell*. (2022) 185:4190–4205.e25. doi: 10.1016/j.cell.2022.09.024

66. Tsuru S, Ito Y, Matsuda H, Hosono K, Inoue T, Nakamoto S, et al. RAMP1 signaling in immune cells regulates inflammation-associated lymphangiogenesis. *Lab Invest*. (2020) 100:738–50. doi: 10.1038/s41374-019-0364-0

67. Pinho-Ribeiro FA, Deng L, Neel DV, Erdogan O, Basu H, Yang D, et al. Bacteria hijack a meningeal neuroimmune axis to facilitate brain invasion. *Nature*. (2023) 615:472–81. doi: 10.1038/s41586-023-05753-x

68. Rojo R, Raper A, Ozdemir DD, Lefevre L, Grabert K, Wollscheid-Lengeling E, et al. Deletion of a Csf1r enhancer selectively impacts CSF1R expression and development of tissue macrophage populations. *Nat Commun*. (2019) 10:3215. doi: 10.1038/s41467-019-11053-8

69. Hume DA, Caruso M, Ferrari-Cestari M, Summers KM, Pridans C, Irvine KM. Phenotypic impacts of CSF1R deficiencies in humans and model organisms. *J Leukoc Biol*. (2020) 107:205–19. doi: 10.1002/JLB.MR0519-143R

70. Sehgal A, Donaldson DS, Pridans C, Sauter KA, Hume DA, Mabbott NA. The role of CSF1R-dependent macrophages in control of the intestinal stem-cell niche. *Nat Commun*. (2018) 9:1272. doi: 10.1038/s41467-018-03638-6

71. Emoto T, Lu J, Sivasubramaniyam T, Maan H, Khan AB, Abow AA, et al. Colony stimulating factor-1 producing endothelial cells and mesenchymal stromal cells maintain monocytes within a perivascular bone marrow niche. *Immunity*. (2022) 55:862–878.e8. doi: 10.1016/j.immuni.2022.04.005

72. Wang Y, Wernersbach I, Strehle J, Li S, Appel D, Klein M, et al. Early posttraumatic CSF1R inhibition via PLX3397 leads to time- and sex-dependent effects on inflammation and neuronal maintenance after traumatic brain injury in mice. *Brain Behav Immun*. (2022) 106:49–66. doi: 10.1016/j.bbi.2022.07.164

73. Henry RJ, Ritzel RM, Barrett JP, Doran SJ, Jiao Y, Leach JB, et al. Microglial depletion with CSF1R inhibitor during chronic phase of experimental traumatic brain injury reduces neurodegeneration and neurological deficits. *J Neurosci*. (2020) 40:2960–74. doi: 10.1523/JNEUROSCI.2402-19.2020

74. Haure-Mirande JV, Audrain M, Ehrlich ME, Gandy S. Microglial TYROBP/DAP12 in Alzheimer's disease: Transduction of physiological and pathological signals across TREM2. *Mol Neurodegener*. (2022) 17:55. doi: 10.1186/s13024-022-00552-w

75. Wang HM, Gao JH, Lu JL. Pravastatin improves atherosclerosis in mice with hyperlipidemia by inhibiting TREM-1/DAP12. *Eur Rev Med Pharmacol Sci*. (2018) 22(15):4995–5003. doi: 10.26355/eurrev_201808_15640

76. Mukherjee S, Klaus C, Pricop-Jeckstadt M, Miller JA, Struebing FL. A microglial signature directing human aging and neurodegeneration-related gene networks. *Front Neurosci*. (2019) 13:2. doi: 10.3389/fnins.2019.00002

77. Li S, Zhang Q, Huang Z, Tao W, Zeng C, Yan L, et al. Comprehensive analysis of immunocyte infiltration and the key genes associated with intraplaque hemorrhage in carotid atherosclerotic plaques. *Int Immunopharmacol*. (2022) 106:108633. doi: 10.1016/j.intimp.2022.108633

78. Lin C, Xu C, Zhou Y, Chen A, Jin B. Identification of biomarkers related to M2 macrophage infiltration in alzheimer's disease. *Cells*. (2022) 11:2365. doi: 10.3390/cells11152365

79. Yunna C, Mengru H, Lei W, Weidong C. Macrophage M1/M2 polarization. *Eur J Pharmacol*. (2020) 877:173090. doi: 10.1016/j.ejphar.2020.173090

80. Zhu D, Yang N, Liu YY, Zheng J, Ji C, Zuo PP. M2 macrophage transplantation ameliorates cognitive dysfunction in amyloid-β-treated rats through regulation of microglial polarization. *J Alzheimers Dis*. (2016) 52:483–95. doi: 10.3233/JAD-151090

81. Bazzi S, Frangie C, Azar E, Daher J. The effect of myeloperoxidase-oxidized LDL on THP-1 macrophage polarization and repolarization. *Innate Immun*. (2022) 28:91–103. doi: 10.1177/17534259221090679

82. Khatana C, Saini NK, Chakrabarti S, Saini V, Sharma A, Saini RV, et al. Mechanistic insights into the oxidized low-density lipoprotein-induced atherosclerosis. *Oxid Med Cell Longev*. (2020) 2020:5245308. doi: 10.1155/2020/5245308

83. Wu J, He S, Song Z, Chen S, Lin X, Sun H, et al. Macrophage polarization states in atherosclerosis. *Front Immunol*. (2023) 14:1185587. doi: 10.3389/fimmu.2023.1185587

84. Chen W, Schilperoort M, Cao Y, Shi J, Tabas I, Tao W. Macrophage-targeted nanomedicine for the diagnosis and treatment of atherosclerosis. *Nat Rev Cardiol*. (2022) 19:228–49. doi: 10.1038/s41569-021-00629-x

85. Gao C, Huang Q, Liu C, Kwong CHT, Yue L, Wan JB, et al. Treatment of atherosclerosis by macrophage-biomimetic nanoparticles via targeted pharmacotherapy and sequestration of proinflammatory cytokines. *Nat Commun*. (2020) 11:2622. doi: 10.1038/s41467-020-16439-7

86. Jung M, Häberle BM, Tschaikowsky T, Wittmann MT, Balta EA, Stadler VC, et al. Analysis of the expression pattern of the schizophrenia-risk and intellectual disability gene TCF4 in the developing and adult brain suggests a role in development and plasticity of cortical and hippocampal neurons. *Mol Autism*. (2018) 9:20. doi: 10.1186/s13229-018-0200-1

87. Teixeira JR, Szeto RA, Carvalho VMA, Muotri AR, Papes F. Transcription factor 4 and its association with psychiatric disorders. *Transl Psychiatry*. (2021) 11:19. doi: 10.1038/s41398-020-01138-0

88. Quednow BB, Brzózka MM, Rossner MJ. Transcription factor 4 (TCF4) and schizophrenia: integrating the animal and the human perspective. *Cell Mol Life Sci*. (2014) 71:2815–35. doi: 10.1007/s00018-013-1553-4

89. Jiang Y, Gruszka D, Zeng C, Swindell WR, Gaskill C, Sorensen C, et al. Suppression of TCF4 promotes a ZC3H12A-mediated self-sustaining inflammatory feedback cycle involving IL-17RA/IL-17RE epidermal signaling. *JCI Insight*. (2024) 9:e172764. doi: 10.1172/jci.insight.172764

90. Venkatraman S, Balasubramanian B, Thuwajit C, Meller J, Tohtong R, Chutipongtanate S. Targeting MYC at the intersection between cancer metabolism and oncoimmunology. *Front Immunol*. (2024) 15:1324045. doi: 10.3389/fimmu.2024.1324045

91. Chen H, Liu H, Qing G. Targeting oncogenic Myc as a strategy for cancer treatment. *Signal Transduct Target Ther*. (2018) 3:5. doi: 10.1038/s41392-018-0008-7

92. Meyer N, Penn LZ. Reflecting on 25 years with MYC. *Nat Rev Cancer*. (2008) 8:976–90. doi: 10.1038/nrc2231

93. Reichenbach N, Delekate A, Plescher M, Schmitt F, Krauss S, Blank N, et al. Inhibition of Stat3-mediated astrogliosis ameliorates pathology in an Alzheimer's disease model. *EMBO Mol Med*. (2019) 11:e9665. doi: 10.15252/emmm.201809665

94. Xu S, Ni H, Chen H, Dai Q. The interaction between STAT3 and nAChRα1 interferes with nicotine-induced atherosclerosis via Akt/mTOR signaling cascade. *Aging (Albany NY)*. (2019) 11:8120–38. doi: 10.18632/aging.102296

95. Wei Y, Lan B, Zheng T, Yang L, Zhang X, Cheng L, et al. GSDME-mediated pyroptosis promotes the progression and associated inflammation of atherosclerosis. *Nat Commun*. (2023) 14:929. doi: 10.1038/s41467-023-36614-w

96. Dong G, Yu J, Shan G, Su L, Yu N, Yang S. N6-Methyladenosine Methyltransferase METTL3 Promotes Angiogenesis and Atherosclerosis by Upregulating the JAK2/STAT3 Pathway via m6A Reader IGF2BP1. *Front Cell Dev Biol*. (2021) 9:731810. doi: 10.3389/fcell.2021.731810

97. Seale LA, Ha HY, Hashimoto AC, Berry MJ. Relationship between selenoprotein P and selenocysteine lyase: Insights into selenium metabolism. *Free Radic Biol Med*. (2018) 127:182–9. doi: 10.1016/j.freeradbiomed.2018.03.037

frontiers | Frontiers in Aging Neuroscience

TYPE Original Research
PUBLISHED 11 September 2024
DOI 10.3389/fnagi.2024.1424056

OPEN ACCESS

EDITED BY
Robert Weissert,
University of Regensburg, Germany

REVIEWED BY
Vanessa A. Johanssen,
La Trobe University, Australia
Khairiah Razali,
International Islamic University Malaysia, Malaysia

*CORRESPONDENCE
Jiajun Chen
✉ cjj@jlu.edu.cn

RECEIVED 27 April 2024
ACCEPTED 20 August 2024
PUBLISHED 11 September 2024

CITATION
Qin Y, Wang L, Song J, Quan W, Xu J And Chen J (2024) Plasma lipidome, circulating inflammatory proteins, and Parkinson's disease: a Mendelian randomization study. *Front. Aging Neurosci.* 16:1424056. doi: 10.3389/fnagi.2024.1424056

Plasma lipidome, circulating inflammatory proteins, and Parkinson's disease: a Mendelian randomization study

Yidan Qin, Lin Wang, Jia Song, Wei Quan, Jing Xu and Jiajun Chen*

Department of Neurology, China-Japan Union Hospital of Jilin University, Changchun, Jilin, China

Background: Observational studies have suggested that plasma lipidome play a pivotal role in the occurrence of Parkinson's disease (PD). However, it remains unknown which lipids among plasma lipidome affect PD and how they exert their influence. Clarity is lacking regarding the causal relationship between plasma lipidome and PD, as well as whether circulating inflammatory proteins serve as mediators.

Methods: Single nucleotide polymorphisms (SNPs) significantly associated with 179 plasma lipidome were selected as instrumental variables to assess their causal impact on PD. PD data, serving as the outcome, were sourced from the International Parkinson's Disease Genomics Consortium, which boasts the largest sample size to date. The inverse variance weighted (IVW), Weighted median method, MR-Egger method, Simple mode method, Weighted mode method and MR-PRESSO were employed to evaluate the influence of the 179 plasma lipidome on PD. Heterogeneity, pleiotropy tests, and reverse causality analyses were conducted accordingly. Additionally, we analyzed the causal relationship between 91 circulating inflammatory proteins and PD, exploring whether these proteins serve as mediators in the pathway from plasma lipidome to PD.

Results: Among the 179 plasma lipidome, three were found to be associated with a reduced risk of PD: Phosphatidylcholine (14:0_18:2) (IVW, OR = 0.877; 95%CI, 0.787–0.978; p = 0.018), Phosphatidylcholine (16:0_16:1) levels (IVW, OR = 0.835; 95%CI, 0.717–0.973; p = 0.021), and Phosphatidylcholine (O-17:0_17:1) levels (IVW, OR = 0.854; 95%CI, 0.779–0.936; p = 0.001). Meanwhile, Sphingomyelin (d38:1) was linked to an increased risk of PD (IVW, OR = 1.095; 95%CI, 1.027–1.166; p = 0.005). Among the 91 circulating inflammatory proteins, three were associated with a lower PD risk: Fibroblast growth factor 21 levels (IVW, OR = 0.817; 95%CI, 0.674–0.990; p = 0.039), Transforming growth factor-alpha levels (IVW, OR = 0.825; 95%CI, 0.683–0.998; p = 0.048), and Tumor necrosis factor receptor superfamily member 9 levels (IVW, OR = 0.846; 95%CI, 0.744–0.963; p = 0.011). Two were associated with a higher risk of PD: Interleukin-17A levels (IVW, OR = 1.285; 95%CI, 1.051–1.571; p = 0.014) and TNF-beta levels (IVW, OR = 1.088; 95%CI, 1.010–1.171; p = 0.026). Additionally, a positive correlation was observed between Phosphatidylcholine (14:0_18:2) levels and Fibroblast growth factor 21 levels (IVW, OR = 1.125; 95%CI, 1.006–1.257; p = 0.038), suggesting that Fibroblast growth factor 21 levels may serve as a mediating factor in the pathway between Phosphatidylcholine (14.0_18.2) levels and PD. The mediation effect was estimated to be −0.024, accounting for approximately 18% of the total effect.

Conclusion: Both plasma lipidome and circulating inflammatory proteins demonstrate a causal relationship with PD. Additionally, circulating inflammatory proteins may serve as mediators in the pathway from plasma lipidome to PD. These findings may contribute to the prediction and diagnosis of PD and potentially pave the way for targeted therapies in the future.

KEYWORDS

Parkinson's disease, plasma lipidome, circulating inflammatory proteins, Mendelian randomization, causal relationship

1 Introduction

Parkinson's disease (PD) is a progressive neurodegenerative disorder characterized by the loss of dopaminergic neurons in the substantia nigra and the deposition of α-synuclein. Its typical manifestations include resting tremor, bradykinesia, postural instability, and rigidity of the limbs (Tansey et al., 2022). With the aging population, the prevalence of PD is expected to gradually increase (Beitz, 2014), potentially doubling over the next 30 years (Tolosa et al., 2021), posing a significant burden on patients' daily activities and society's healthcare system. However, the pathogenesis of PD remains unclear, early diagnosis is challenging, and current treatments are not curative. Therefore, it is crucial to explore predictive factors for PD to improve early diagnosis rates and develop better targeted therapies.

Lipids, an essential component of cell membranes, are primarily classified in mammals as glycerides, sphingolipids, and sterols. Initially regarded as structural components, lipids have been found to regulate various cellular physiological functions and play a crucial role in cell signaling and the production of bioactive metabolites (Cockcroft, 2021). Studies have shown that lipid metabolism is not only associated with immune diseases, cardiovascular diseases, and diabetes (Luo et al., 2008; Duan et al., 2022; Zhang et al., 2022), but also intimately linked to PD. Decreased catabolism of lipid substrates in lysosomes can affect lysosomal function, thereby impeding the clearance of α-synuclein (Galper et al., 2022). Additionally, lipids can mediate the onset of PD by regulating immune responses, oxidative stress, endolysosomal function, and endoplasmic reticulum stress (Xicoy et al., 2019). Notably, lipids are part of a complex network regulating numerous cellular and molecular processes, particularly inflammation, playing a significant role in modulating inflammatory factors (Gonçalves et al., 2012; Leuti et al., 2020).

Neuroinflammation is a key pathogenic mechanism in PD (Minchev et al., 2022; Morris et al., 2024). Numerous studies have demonstrated that inflammatory factors can modulate the occurrence of neuroinflammation, thus participating in the pathogenesis of PD (Wang et al., 2019; Gautam et al., 2023). Both neurohistological and neuroimaging studies support the persistent presence of neuroinflammatory processes throughout the development and terminal stages of PD. Inflammatory markers in peripheral blood and cerebrospinal fluid may also trigger or exacerbate neuroinflammation, leading to neurodegeneration (Tansey et al., 2022). Furthermore, Belarbi et al. (2020) suggested that metabolic dysregulation of glycosphingolipids may be associated with the occurrence of neuroinflammation in PD.

Research indicates altered plasma lipidome profiles in PD patients (Guo et al., 2015), suggesting a possible association between PD and plasma lipidome metabolism disorders (Hu et al., 2020). Although several meta-analyses have shown that serum triglyceride, low-density lipoprotein cholesterol, and total cholesterol levels have a protective effect on PD (Fu et al., 2020; Jiang et al., 2020; Lu et al., 2021; Hong et al., 2022), these are based solely on observational studies, and the causal relationship between these lipids and PD remains unclear. It is also unknown which other lipids are associated with PD and the underlying mechanisms involved. Additionally, meta-analyses have demonstrated significantly elevated IL-17 levels in PD patients (Gautam et al., 2023), leading us to speculate that circulating inflammatory proteins may mediate the pathway from plasma lipidome to PD. The identification of plasma lipidome may aid in the prediction and diagnosis of PD and potentially serve as therapeutic targets for PD in the future. Therefore, we conducted a Mendelian randomization study to address these questions.

Mendelian randomization (MR) is a genetic analytical approach that relies on the random allocation of parental alleles to offspring. It aims to estimate the causal relationship between a specific exposure and outcome by using genetic variations in exposure as instrumental variables. Serving as a natural randomized controlled trial (RCT), MR can reduce the confounding effects of environmental factors and reverse causality inherent in observational studies (Skrivankova et al., 2021). In this study, we conducted a comprehensive MR analysis using the latest and largest genome-wide association studies (GWAS) for 179 plasma lipidome, 91 circulating inflammatory proteins, and PD. This analysis aimed to reveal the causal relationship between these plasma lipidome and PD risk and explore whether the circulating inflammatory proteins serve as mediators in the pathway from plasma lipidome to PD.

2 Materials and methods

This study is a re-analysis of previously collected and published data and does not require additional ethical approval.

2.1 Study design

This study mainly comprises two parts. Firstly, we analyzed the causal effects of 179 plasma lipidome groups and 91 circulating inflammatory proteins on PD, respectively, and conducted sensitivity analysis and reverse analysis. Secondly, we employed a two-step and

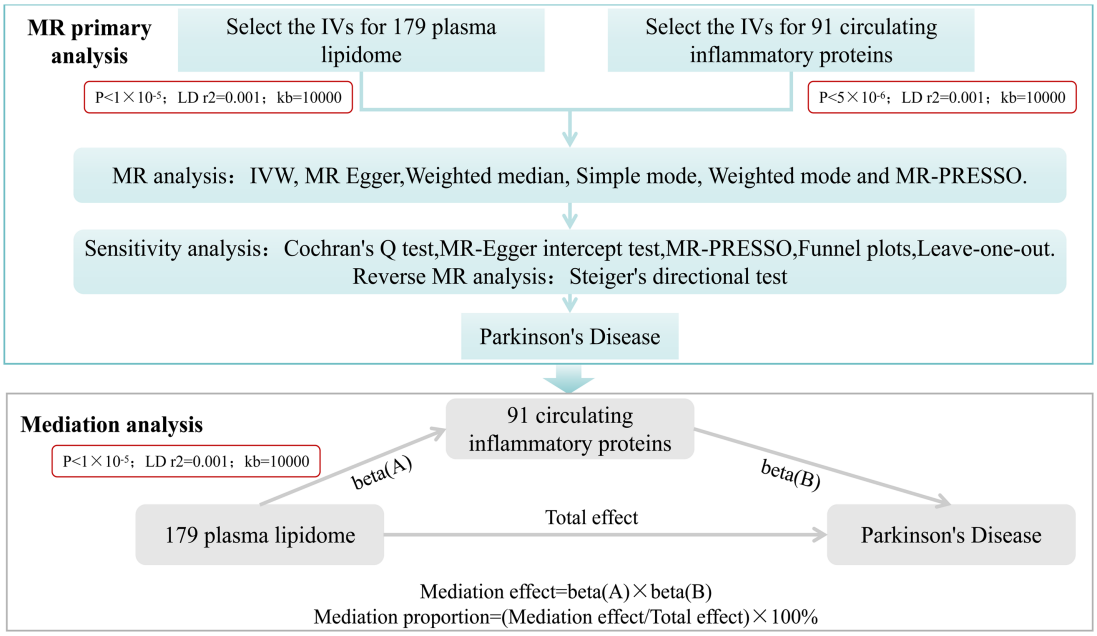

FIGURE 1
Study desige. Overview of the research design. It is mainly divided into two parts: MR primary analysis and mediation analysis.

multivariate MR (MVMR) analysis to investigate the mediating role of circulating inflammatory proteins in the relationship between plasma lipidome and PD (Figure 1).

2.2 Data source

The genetic data for plasma lipidome were derived from a 2023 GWAS summary dataset encompassing 7,174 Finnish individuals. This comprehensive dataset includes 179 lipid species belonging to 13 lipid classes covering 4 major lipid categories: glycerolipids, glycerophospholipids, sphingolipids, and sterols (Ottensmann et al., 2023). On the other hand, the genetic data for circulating inflammatory proteins were sourced from a 2023 GWAS study involving 14,824 European individuals across 11 cohorts. This dataset encompasses 91 inflammation-related plasma proteins (Zhao et al., 2023).

The GWAS summary data for PD were obtained from the International Parkinson's Disease Genomics Consortium, which has been archived by the ieu open gwas project (GWAS ID: ieu-b-7). Representing the largest sample size available thus far, this dataset comprises 33,674 PD patients and 449,056 control cases, encompassing 14 cohorts (Nalls et al., 2019).

2.3 Instrumental variables selection

In MR analysis, the instrumental variables (IVs) selected must satisfy three assumptions: first, the genetic variant must be strongly associated with the exposure; second, it must be independent of confounding factors; and third, its effect on the outcome can only be mediated through the exposure (Skrivankova et al., 2021).

Using the R package TwoSampleMR (version 0.5.7), SNPs significantly associated with plasma lipidome were chosen with a threshold of $p < 1 \times 10^{-5}$, while SNPs significantly associated with circulating inflammatory proteins were selected using a threshold of $p < 5 \times 10^{-6}$. Subsequently, SNPs in linkage disequilibrium were excluded based on the criteria of r2 < 0.001 and a distance of >10,000 kb. After matching, palindromic SNPs were further removed. The resulting selected IVs were then utilized for MR estimation of the causal relationships between plasma lipidome or circulating inflammatory proteins and PD.

Additionally, we calculated the F-statistic for each IV and discarded weak IVs with an F-statistic <10 (Burgess et al., 2017).

2.4 MR primary analysis

To evaluate the causal impacts of plasma lipidome and circulating inflammatory proteins on PD, we conducted two-sample Mendelian randomization (MR) analyses using R version 4.3.1 and the TwoSampleMR package (version 0.5.7) for plasma lipidome and circulating inflammatory proteins, respectively. Inverse-variance weighted (IVW) analysis was employed as the primary analytical approach. Additionally, we complemented our findings using MR Egger, weighted median, simple mode, weighted mode and MR-PRESSO. Heterogeneity among the selected IVs was tested using the Cochran's Q test. Multicollinearity was examined using the MR-Egger test, with a significant intercept term indicating horizontal pleiotropy (Burgess and Thompson, 2017). Furthermore, we employed the Mendelian randomization pleiotropy residual sum and outlier (MR-PRESSO) approach to assess pleiotropy and exclude outliers that could potentially bias our estimates (Verbanck et al., 2018). Finally, scatter plots, funnel plots, and leave-one-out sensitivity tests were generated to further validate our results. Statistical significance was considered when the p-value from IVW was less than 0.05 and the directions of IVW and MR Egger were concordant. These rigorous

analytical approaches ensure the robustness and reliability of our findings.

2.5 Bi-directional causality analysis

To assess the impact of reverse causality on our findings, we performed MR analysis with PD as the exposure and plasma lipidome or circulating inflammatory proteins associated with PD as the outcomes. SNPs significantly associated with PD were selected using a threshold of $p < 1 \times 10^{-5}$, with the remaining steps identical to the forward analysis. Furthermore, the Steiger's directional test was also conducted to further verify the correctness of the causal relationship direction.

2.6 Mediation analysis

After completing MR primary analysis, we incorporated those plasma lipidome and circulating inflammatory proteins that exhibited significant causal effects on PD without any reverse causality into step 2. we employed a two-step MR approach and further examined the causal relationships between PD-associated plasma lipidome and PD-related circulating inflammatory proteins. The threshold for selecting SNPs significantly associated with plasma lipidome was set at $p < 1 \times 10^{-5}$. Similarly, results were considered statistically significant when the p-value from IVW analysis was less than 0.05 and the directions of IVW and MR Egger were concordant. Under these conditions, the mediation effect was calculated as Beta(A) * Beta(B), and the proportion of mediation effect was expressed as a percentage of the total effect (Figure 1). Finally, a multivariate Mendelian randomization analysis was performed.

Additionally, we conducted a reverse causality analysis by treating the circulating inflammatory proteins as the exposure and plasma lipidome as the outcome, using the same MR analytical approach as in the forward analysis.

3 Results

3.1 The causal effects of 179 plasma lipidome on PD

The present study comprehensively analyzed the association between 179 plasma lipidome and PD, with 3,981 SNPs being selected as instrumental variables (IVs) for the 179 plasma lipidome (Supplementary Table S1). The results (Figure 2; Supplementary Table S2) revealed that three plasma lipidome were significantly associated with a reduced risk of PD. Notably, these three plasma lipidome belonged to different subtypes within the same category. Specifically, (1) higher levels of Phosphatidylcholine (14:0_18:2) exhibited a negative correlation with PD risk (IVW, OR = 0.877; 95%CI, 0.787–0.978; $p = 0.018$). (2) Similarly, increased Phosphatidylcholine (16:0_16:1) levels were inversely associated with PD risk (IVW, OR = 0.835; 95%CI, 0.717–0.973; $p = 0.021$). (3) Furthermore, Phosphatidylcholine (O-17:0_17:1) levels also demonstrated a negative association with PD risk (IVW, OR = 0.854; 95%CI, 0.779–0.936; $p = 0.001$).

Contrarily, one plasma lipidome was identified to be positively associated with an increased risk of PD (Figure 2). Specifically, higher levels of Sphingomyelin (d38:1) were positively correlated with PD risk (IVW, OR = 1.095; 95%CI, 1.027–1.166; $p = 0.005$). Finally, the results were further verified using MR-PRESSO, and all results showed $p < 0.05$ (Supplementary Table S3).

3.2 The causal effects of 91 circulating inflammatory proteins on PD

The present study comprehensively examined the association between 91 circulating inflammatory proteins and PD, with 1,435 SNPs selected as instrumental variables (IVs) for the 91 circulating inflammatory proteins (Supplementary Table S4). The results (Figure 3; Supplementary Table S5) revealed that three circulating inflammatory proteins were significantly associated with a reduced risk of PD. Specifically, (1) higher levels of Fibroblast growth factor 21 levels exhibited a negative correlation with PD risk (IVW, OR = 0.817; 95%CI, 0.674–0.990; $p = 0.039$). (2) Similarly, increased levels of Transforming growth factor-alpha levels were inversely associated with PD risk (IVW, OR = 0.825; 95%CI, 0.683–0.998; $p = 0.048$). (3) Furthermore, Tumor necrosis factor receptor superfamily member 9 levels also demonstrated a negative association with PD risk (IVW, OR = 0.846; 95%CI, 0.744–0.963; $p = 0.011$).

Contrarily, two circulating inflammatory proteins were identified to be positively associated with an increased risk of PD (Figure 3). Specifically, (1) higher levels of Interleukin-17A levels were positively correlated with PD risk (IVW, OR = 1.285; 95%CI, 1.051–1.571; $p = 0.014$). (2) Additionally, TNF-beta levels also exhibited a positive association with PD risk (IVW, OR = 1.088; 95%CI, 1.010–1.171; $p = 0.026$). Finally, the results were further verified using MR-PRESSO (Supplementary Table S3).

3.3 Sensitivity analyses and reverse causal effects of PD on plasma lipidome and circulating inflammatory proteins

In the Cochran's Q test, both MR-Egger and IVW yielded p-values greater than 0.05, indicating no heterogeneity. Furthermore, the MR-Egger intercept test showed a p-value above 0.05, and MR-PRESSO reported a global p-value also exceeding 0.05, collectively suggesting the absence of pleiotropy (Supplementary Table S6). No significant abnormalities were observed in the leave-one-out analysis, forest plots, Scatter plots, and funnel plots (Supplementary Figures S1–S8).

Additionally, a reverse causality analysis was conducted with PD as the exposure and four lipid profiles and five circulating inflammatory proteins as the outcomes. The results demonstrated no causal relationship between PD and these analytes (Supplementary Table S7).

Finally, the Steiger's directional test was conducted to further validate the correctness of the causal relationship directions between plasma lipidome, circulating inflammatory proteins and PD, respectively. The results showed that snp_r2.exposure was greater than snp_r2.outcome, indicating a stronger association between SNPs and exposure variables. All correct_causal_direction values were TRUE,

Trait	Method	nSNP	*P* Value	OR (95% CI)
Phosphatidylcholine (14:0_18:2) levels	MR Egger	24	0.562	0.909 (0.663 – 1.247)
Phosphatidylcholine (14:0_18:2) levels	Weighted median	24	0.131	0.896 (0.776 – 1.033)
Phosphatidylcholine (14:0_18:2) levels	IVW	24	0.018	0.877 (0.787 – 0.978)
Phosphatidylcholine (14:0_18:2) levels	Simple mode	24	0.137	0.831 (0.656 – 1.052)
Phosphatidylcholine (14:0_18:2) levels	Weighted mode	24	0.868	1.014 (0.862 – 1.193)
Phosphatidylcholine (16:0_16:1) levels	MR Egger	16	0.760	0.929 (0.586 – 1.474)
Phosphatidylcholine (16:0_16:1) levels	Weighted median	16	0.674	0.955 (0.771 – 1.183)
Phosphatidylcholine (16:0_16:1) levels	IVW	16	0.021	0.835 (0.717 – 0.973)
Phosphatidylcholine (16:0_16:1) levels	Simple mode	16	0.874	0.972 (0.694 – 1.364)
Phosphatidylcholine (16:0_16:1) levels	Weighted mode	16	0.885	0.976 (0.706 – 1.349)
Phosphatidylcholine (O−17:0_17:1) levels	MR Egger	33	0.150	0.839 (0.664 – 1.059)
Phosphatidylcholine (O−17:0_17:1) levels	Weighted median	33	0.137	0.908 (0.799 – 1.031)
Phosphatidylcholine (O−17:0_17:1) levels	IVW	33	0.001	0.854 (0.779 – 0.936)
Phosphatidylcholine (O−17:0_17:1) levels	Simple mode	33	0.874	0.979 (0.757 – 1.267)
Phosphatidylcholine (O−17:0_17:1) levels	Weighted mode	33	0.656	0.951 (0.764 – 1.184)
Sphingomyelin (d38:1) levels	MR Egger	35	0.165	1.094 (0.967 – 1.237)
Sphingomyelin (d38:1) levels	Weighted median	35	0.095	1.090 (0.985 – 1.207)
Sphingomyelin (d38:1) levels	IVW	35	0.005	1.095 (1.027 – 1.166)
Sphingomyelin (d38:1) levels	Simple mode	35	0.374	1.077 (0.916 – 1.267)
Sphingomyelin (d38:1) levels	Weighted mode	35	0.086	1.092 (0.991 – 1.203)

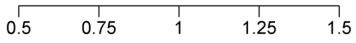

FIGURE 2
Forest plot of 179 plasma lipidome and PD. Forest plots showed the causal associations between plasma lipidome and PD by using different methods. IVW, inverse variance weighting; CI, confidence interval; OR, odds ratio.

Trait	Method	nSNP	*P* Value	OR (95% CI)
Fibroblast growth factor 21 levels	MR Egger	13	0.391	0.802 (0.494 – 1.302)
Fibroblast growth factor 21 levels	Weighted median	13	0.303	0.880 (0.691 – 1.122)
Fibroblast growth factor 21 levels	IVW	13	0.039	0.817 (0.674 – 0.990)
Fibroblast growth factor 21 levels	Simple mode	13	0.535	1.168 (0.725 – 1.881)
Fibroblast growth factor 21 levels	Weighted mode	13	0.013	0.616 (0.444 – 0.854)
Interleukin−17A levels	MR Egger	12	0.390	1.245 (0.772 – 2.009)
Interleukin−17A levels	Weighted median	12	0.126	1.231 (0.943 – 1.608)
Interleukin−17A levels	IVW	12	0.014	1.285 (1.051 – 1.571)
Interleukin−17A levels	Simple mode	12	0.363	1.229 (0.803 – 1.880)
Interleukin−17A levels	Weighted mode	12	0.332	1.239 (0.819 – 1.877)
Transforming growth factor−alpha levels	MR Egger	12	0.824	0.945 (0.579 – 1.540)
Transforming growth factor−alpha levels	Weighted median	12	0.492	0.911 (0.699 – 1.188)
Transforming growth factor−alpha levels	IVW	12	0.048	0.825 (0.683 – 0.998)
Transforming growth factor−alpha levels	Simple mode	12	0.493	0.845 (0.529 – 1.347)
Transforming growth factor−alpha levels	Weighted mode	12	0.816	0.957 (0.670 – 1.369)
TNF−beta levels	MR Egger	19	0.145	1.094 (0.975 – 1.227)
TNF−beta levels	Weighted median	19	0.051	1.092 (1.000 – 1.192)
TNF−beta levels	IVW	19	0.026	1.088 (1.010 – 1.171)
TNF−beta levels	Simple mode	19	0.243	1.136 (0.924 – 1.398)
TNF−beta levels	Weighted mode	19	0.047	1.095 (1.007 – 1.191)
Tumor necrosis factor receptor superfamily member 9 levels	MR Egger	23	0.191	0.806 (0.589 – 1.102)
Tumor necrosis factor receptor superfamily member 9 levels	Weighted median	23	0.079	0.840 (0.692 – 1.020)
Tumor necrosis factor receptor superfamily member 9 levels	IVW	23	0.011	0.846 (0.744 – 0.963)
Tumor necrosis factor receptor superfamily member 9 levels	Simple mode	23	0.236	0.816 (0.588 – 1.132)
Tumor necrosis factor receptor superfamily member 9 levels	Weighted mode	23	0.228	0.855 (0.667 – 1.096)

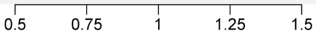

FIGURE 3
Forest plot of 91 circulating inflammatory proteins and PD. Forest plots showed the causal associations between circulating inflammatory proteins and PD by using different methods. IVW, inverse variance weighting; CI, confidence interval; OR, odds ratio.

and $p < 0.05$, indicating that the inferred causal directions were correct (Supplementary Table S8).

3.4 Mediation analysis

A two-step MR analysis was conducted to explore the mediating effects of plasma lipidome on PD via circulating inflammatory proteins. The results (Supplementary Table S9), revealed a positive correlation between Phosphatidylcholine (14:0_18:2) levels and Fibroblast growth factor 21 levels (IVW, OR = 1.125; 95%CI, 1.006–1.257; $p = 0.038$). Notably, both Phosphatidylcholine (14:0_18:2) levels and Fibroblast growth factor 21 levels exhibited a negative association with the risk of PD. Based on these findings, this suggests that Fibroblast growth factor 21 levels may serve as a mediator in the pathway linking Phosphatidylcholine (14:0_18:2) levels and PD, with a mediation effect of −0.024 and total effect of −0.131, the mediation effect accounts for approximately 18% of the total effect.

Additionally, when the circulating inflammatory proteins were considered as the exposure and the plasma lipidome as the outcome, MR analysis did not reveal any reverse causal influence (IVW, $p = 0.116$). Moreover, the results of the Steiger's directional test showed that snp_r2.exposure was 0.103, snp_r2.outcome was 0.009, correct_causal_direction was TRUE, and p value was 3.96E-57, indicating that the inferred causal direction was correct.

Finally, a multivariate MR analysis was performed with Phosphatidylcholine (14:0_18:2) levels and Fibroblast growth factor 21 levels as exposures and PD as the outcome. Unfortunately, both exposure results were negative ($p = 0.889$ and $p = 0.395$).

4 Discussion

The brain ranks second only to adipose tissue in terms of lipid concentration and diversity. Within the central nervous system, metabolic disturbances of lipids have been linked to the occurrence, progression, and severity of PD (Castellanos et al., 2021). Furthermore, research has identified a shared genetic risk between lipids, lipoproteins, and PD, where genetic variations associated with PD regulate the blood levels of specific lipid species that play crucial roles in the pathogenesis of PD (Klemann et al., 2017; Xicoy et al., 2021).

Investigations have shown that abnormal metabolism of lipids such as triglycerides, glycerophosphoethanolamine, diglycerides, polyunsaturated fatty acids, sphingolipids, gangliosides, glycerophospholipids, and cholesterol can lead to aberrant formation of α-synuclein, triggering neuroinflammation in PD through various innate and adaptive immune responses (Hatton and Pandey, 2022). Notably, glycerophosphoethanolamine has been found to facilitate the binding of acidic phospholipids with α-synuclein, thereby promoting its abnormal aggregation (Jo et al., 2000). Sphingolipids, a specialized class of lipids primarily confined to the nervous system, play a pivotal role in inflammatory diseases, including PD (Quinville et al., 2021). Ceramide, a central molecule in sphingolipid metabolism, serves as a crucial regulator of cellular functions and can be degraded into sphingosine (Ventura et al., 2019). Research has demonstrated that the synthesis of ceramide, sphingosine, and sphingosine-1-phosphate is associated with α-synuclein aggregation in PD patients (Gaspar et al., 2018). Low levels of ceramide have also been associated with α-synuclein aggregation in PD (Abbott et al., 2014), suggesting that the conversion of ceramide to sphingosine may be a crucial step in α-synuclein aggregation in PD (Hatton and Pandey, 2022).

Scholars such as Avisar et al. (2021) have employed machine learning algorithms to analyze 517 lipids across 37 categories and discovered that dihydrosphingomyelin (dhSM-20:0), plasmalogen phosphatidylethanolamine (PEp-38:6; 42:7), glucosylceramide (GlcCer-16:0; 24:1), dihydroglycosphingosine-based ceramide (dhGB3-22:0;16:0), and to a lesser extent, dihydroganglioside GM3 (dhGM3-16:0), can aid in predicting the severity of PD. Additionally, Avisar et al. (2021) have demonstrated that various lipids, such as those derived from vegetable oils, animal fats, or fatty acids, can suppress cytotoxicity induced by pathological processes including mitochondrial dysfunction, oxidative stress, apoptosis, and inflammation. Targeted use of these oils or fatty acids may thus contribute to the prevention of neurodegenerative diseases. Furthermore, Alarcon-Gil et al. (2022) have shown that linoleic acid exhibits neuroprotective and anti-inflammatory effects in PD models. Exploring the relationship between lipids and PD not only facilitates the identification of predictive factors for early diagnosis and treatment but also aids in discovering therapeutic targets for PD. However, the intricate interplay between PD and lipid metabolism precludes a straightforward analysis of the plasma lipidome that influence PD through observational studies. As a result, the exact causal relationships and underlying mechanisms remain elusive. To address this, we employed a two-sample MR analysis to investigate the causal relationship between 179 plasma lipidome and PD, identifying four plasma lipidome with significant causal associations. Reverse causation analysis was also conducted. Nevertheless, the precise mechanisms underlying how these plasma lipidome contribute to PD remain unknown. We hypothesize that circulating inflammatory proteins may mediate the relationship between these plasma lipidome and PD. Consequently, we further analyzed the causal relationships between 91 circulating inflammatory proteins and PD, discovering five circulating inflammatory proteins with significant causal associations, which were also subjected to reverse causation analysis. Moreover, our MR analysis revealed a causal link between PD-associated plasma lipidome and PD-related circulating inflammatory proteins, suggesting that these circulating inflammatory proteins may serve as mediators in the pathway between plasma lipidome and PD. However, further multivariate MR analysis showed no correlation between the phosphatidylcholine (14:0_18:2), Fibroblast growth factor 21 and PD, and in the future, we still need more data to verify this result.

The MR results indicated that elevated serum levels of phosphatidylcholine (14:0_18:2), phosphatidylcholine (16:0_16:1), and phosphatidylcholine (O-17:0_17:1) were associated with a reduced risk of PD. Phosphatidylcholine, a zwitterionic phospholipid composed of a hydrophilic head and hydrophobic tail, is a crucial component of eukaryotic cell membranes. Its anti-inflammatory properties have been implicated in the treatment of ulcerative colitis (Treede et al., 2007). Additionally, phosphatidylcholine plays a pivotal role in intracellular cholesterol transport and maintaining membrane lipid homeostasis (Lagace, 2015). Genetic studies have shown a shared etiology and significant negative correlation between PD and blood levels of phosphatidylcholine aa 32:3 (Xicoy et al., 2021). Farmer et al. (2015) observed downregulation of phosphatidylcholine and lysophosphatidylcholine lipid classes in the

substantia nigra of a PD animal model. Consistently, Chang et al. (2022) reported a downregulation of phosphatidylcholine (35:6) in the plasma of PD patients. However, López de Frutos et al. (2022) found increased levels of phosphatidylcholine and decreased levels of lysophosphatidylcholine in the plasma of PD patients from the Iberian Peninsula, which may be attributed to the species diversity of phosphatidylcholine and its varying roles in different metabolic pathways.

Furthermore, through a more profound analysis, it has been revealed that Fibroblast growth factor 21 levels may serve as a mediating factor in the pathway between phosphatidylcholine (14:0_18:2) and PD. Elevated levels of phosphatidylcholine (14:0_18:2) promote the increase of Fibroblast growth factor 21 levels, thereby exerting a protective effect on PD. The mediating effect is estimated to be −0.024, accounting for approximately 18% of the total effect. Research has shown that the phospholipase/lysophospholipase PNPLA8-PNPLA7 axis can break down phosphatidylcholine, enabling the endogenous choline stored in hepatic phosphatidylcholine to be utilized for methyl metabolism and providing methyl groups for the methionine cycle. In PNPLA7-deficient mice, due to reduced phosphatidylcholine breakdown, methionine deficiency and disrupted methionine cycling trigger the expression of Fibroblast growth factor 21 levels, mediating metabolic alterations (Hirabayashi et al., 2023). Fibroblast growth factor 21 levels have been proven to ameliorate brain metabolic disorders and behavioral deficits in PD mouse models by promoting a favorable colonic microbiota composition and influencing the microbiota-gut-brain metabolic axis (Yang et al., 2023). Additionally, it regulates microglial polarization through the sirtuin 1 (SIRT1)/nuclear factor-κ B (NF-κB) pathway, thus alleviating neurodegeneration in PD mice models and PD cellular models (Yang et al., 2021). Therefore, We hypothesize that an increase in phosphatidylcholine (14:0_18:2) levels may lead to a reduction in the availability of methyl groups for the methionine cycle, impeding the regeneration of methionine and the methyl donor S-adenosylmethionine. This disruption in the methionine cycle, in turn, promotes an increase in Fibroblast growth factor 21 levels, exerting a protective effect against PD. Therefore, a decrease in phosphatidylcholine (14:0_18:2) levels may serve as a predictor for PD.

Our MR analysis revealed that the risk of PD increases with elevated serum levels of sphingomyelin (d38:1). Sphingomyelin, a sphingolipid composed of ceramide linked to phosphocholine (or phosphoethanolamine) at the C-1 hydroxyl group, is synthesized from palmitic acid and serine through the intermediate sphingosine, followed by conjugation with acyl-CoA and phosphocholine. Prior studies have demonstrated a shared genetic etiology and positive correlation between PD and blood levels of Sphingomyelin26:0 (Xicoy et al., 2021). Consistent with our findings, Gusev et al. (2020) observed increased concentrations of seven out of 12 sphingomyelins in the blood of preclinical subjects with PD risk. Xicoy et al. (2020a) also reported increased levels of three sphingomyelin species in a PD cell model. However, contrasting results have emerged from lipid and transcriptome analyses of putamen samples from PD patients, revealing decreased levels of most sphingomyelins, particularly saturated sphingomyelins (Xicoy et al., 2020b). Similarly, Chang et al. (2022) analyzed lipid changes in the plasma of PD patients and found downregulation of sphingomyelins (d30:1), (d32:1), and (d39:1). The differences in these results may be related to the species diversity of sphingomyelins.

Sphingomyelins play diverse roles in PD, yet their specific functions remain elusive due to the complexity of their metabolic pathways. Decreased levels of acid sphingomyelinase in PD may lead to sphingomyelin accumulation, causing cellular toxicity. In addition, reduced neutral sphingomyelinase activity may be associated with decreased exocytosis of α-synuclein-containing exosomes, leading to intracellular accumulation of α-synuclein (Signorelli et al., 2021). Mutations in the sphingomyelin phosphodiesterase (SMPD1) gene, which cleaves the phosphocholine head group of sphingomyelin to produce ceramide (Schuchman et al., 1992), have been identified as a risk factor for PD (Foo et al., 2013; Mao et al., 2017). Low ceramide levels are also associated with α-synuclein aggregation in PD (Abbott et al., 2014). These suggesting that SMPD1 mutations may disrupt the conversion of sphingomyelin to ceramide, leading to sphingomyelin accumulation, ceramide depletion, and subsequent α-synuclein aggregation, which may trigger neuroinflammation and the occurrence of PD.

We further explored the mediating role of circulating inflammatory proteins between sphingomyelin (d38:1) and PD, but unfortunately, no positive conclusions were obtained. The relationship between sphingomyelin (d38:1) and PD may involve an exceptionally complex metabolic network, necessitating further investigation.

To the best of our knowledge, this study is the first to utilize MR analysis to investigate the causal relationship between 179 plasma lipidome and PD, and it was discovered that circulating inflammatory proteins may serve as intermediates. Our findings are reliable, grounded in MR analysis of published large-scale GWAS results, which circumvents issues of reverse causality and confounding factors. We identified four plasma lipidome with a causal link to PD and demonstrated that phosphatidylcholine (14:0_18:2) levels may reduce PD risk by promoting fibroblast growth factor 21 levels. This discovery may lead to the development of predictive biomarkers for PD, enhancing early diagnosis rates and facilitating the development of targeted therapeutics. However, several limitations should be acknowledged. Firstly, as the GWAS data used in this study were derived from European populations, our findings may not be generalizable to other ethnic groups. Secondly, the 179 plasma lipidome and 91 circulating inflammatory proteins analyzed were measured in blood, not cerebrospinal fluid. Future studies should expand sample sizes, include cerebrospinal fluid analysis, and investigate diverse populations to further elucidate the mechanisms and pathways underlying the role of plasma lipidome in PD. Finally, our mediation analysis revealed that further multivariate MR analysis showed no correlation between phosphatidylcholine (14:0_18:2), fibroblast growth factor 21, and PD. More data are still needed in the future to validate this result.

5 Conclusion

Utilizing a comprehensive MR analysis, we delved into the causal relationships among plasma lipidome, circulating inflammatory proteins, and PD. Our findings revealed three negative and one positive causal effects between genetic predisposition to plasma lipidome and PD. Similarly, there were three negative and two positive causal effects between circulating inflammatory proteins and PD. Furthermore, we discovered that fibroblast growth factor 21 levels appear to mediate the pathway from phosphatidylcholine

(14:0_18:2) levels to PD. Our research offers valuable insights into the intricate relationship between plasma lipidome and PD risk, which can not only guide future exploration of PD pathogenesis but also aid in the prediction, diagnosis, and even potential targeted therapy of PD.

Data availability statement

Publicly available datasets were analyzed in this study. This data can be found at: All data used in the study were obtained from published articles or publicly available GWAS platform (https://gwas.mrcieu.ac.uk/), and all data can be obtained for free.

Ethics statement

Ethical approval was not required for the study involving humans in accordance with the local legislation and institutional requirements. Written informed consent to participate in this study was not required from the participants or the participants' legal guardians/next of kin in accordance with the national legislation and the institutional requirements.

Author contributions

YQ: Writing – review & editing, Writing – original draft, Software, Methodology, Data curation, Conceptualization. LW: Writing – review & editing, Supervision, Project administration, Methodology, Conceptualization. JS: Writing – review & editing, Validation, Supervision, Software. WQ: Writing – review & editing, Project administration, Methodology, Data curation, Conceptualization. JX: Writing – review & editing, Validation, Resources, Conceptualization. JC: Writing – review & editing, Supervision, Project administration, Investigation, Funding acquisition, Conceptualization.

Funding

The author(s) declare that financial support was received for the research, authorship, and/or publication of this article. This study was supported by the Jilin Science and Technology Department Project (20240305084YY and YDZJ202402026CXJD).

Acknowledgments

The authors would like to express their gratitude to the investigators involved in this study for sharing the GWAS summary statistics.

Conflict of interest

The authors declare that the research was conducted in the absence of any commercial or financial relationships that could be construed as a potential conflict of interest.

Publisher's note

Supplementary material

The Supplementary material for this article can be found online at: https://www.frontiersin.org/articles/10.3389/fnagi.2024.1424056/full#supplementary-material

References

Abbott, S. K., Li, H., Muñoz, S. S., Knoch, B., Batterham, M., Murphy, K. E., et al. (2014). Altered ceramide acyl chain length and ceramide synthase gene expression in Parkinson's disease. *Mov. Disord.* 29, 518–526. doi: 10.1002/mds.25729

Alarcon-Gil, J., Sierra-Magro, A., Morales-Garcia, J. A., Sanz-SanCristobal, M., Alonso-Gil, S., Cortes-Canteli, M., et al. (2022). Neuroprotective and anti-inflammatory effects of linoleic acid in models of Parkinson's disease: the implication of lipid droplets and Lipophagy. *Cells* 11:2297. doi: 10.3390/cells11152297

Avisar, H., Guardia-Laguarta, C., Area-Gomez, E., Surface, M., Chan, A. K., Alcalay, R. N., et al. (2021). Lipidomics prediction of Parkinson's disease severity: a machine-learning analysis. *J. Parkinsons Dis.* 11, 1141–1155. doi: 10.3233/jpd-202476

Beitz, J. M. (2014). Parkinson's disease: a review. *Front. Biosci.* 6, 65–74. doi: 10.2741/s415

Belarbi, K., Cuvelier, E., Bonte, M. A., Desplanque, M., Gressier, B., Devos, D., et al. (2020). Glycosphingolipids and neuroinflammation in Parkinson's disease. *Mol. Neurodegener.* 15:59. doi: 10.1186/s13024-020-00408-1

Burgess, S., Small, D. S., and Thompson, S. G. (2017). A review of instrumental variable estimators for Mendelian randomization. *Stat. Methods Med. Res.* 26, 2333–2355. doi: 10.1177/0962280215597579

Burgess, S., and Thompson, S. G. (2017). Interpreting findings from Mendelian randomization using the MR-Egger method. *Eur. J. Epidemiol.* 32, 377–389. doi: 10.1007/s10654-017-0255-x

Castellanos, D. B., Martín-Jiménez, C. A., Rojas-Rodríguez, F., Barreto, G. E., and González, J. (2021). Brain lipidomics as a rising field in neurodegenerative contexts: perspectives with machine learning approaches. *Front. Neuroendocrinol.* 61:100899. doi: 10.1016/j.yfrne.2021.100899

Chang, K. H., Cheng, M. L., Tang, H. Y., Huang, C. Y., Wu, H. C., and Chen, C. M. (2022). Alterations of sphingolipid and phospholipid pathways and ornithine level in the plasma as biomarkers of Parkinson's disease. *Cells* 11:395. doi: 10.3390/cells11030395

Cockcroft, S. (2021). Mammalian lipids: structure, synthesis and function. *Essays Biochem.* 65, 813–845. doi: 10.1042/ebc20200067

Duan, Y., Gong, K., Xu, S., Zhang, F., Meng, X., and Han, J. (2022). Regulation of cholesterol homeostasis in health and diseases: from mechanisms to targeted therapeutics. *Signal Transduct. Target. Ther.* 7:265. doi: 10.1038/s41392-022-01125-5

Farmer, K., Smith, C. A., Hayley, S., and Smith, J. (2015). Major alterations of phosphatidylcholine and Lysophosphotidylcholine lipids in the substantia Nigra using an early stage model of Parkinson's disease. *Int. J. Mol. Sci.* 16, 18865–18877. doi: 10.3390/ijms160818865

Foo, J. N., Liany, H., Bei, J. X., Yu, X. Q., Liu, J., Au, W. L., et al. (2013). Rare lysosomal enzyme gene SMPD1 variant (p.R591C) associates with Parkinson's disease. *Neurobiol. Aging* 34:2890.e13-5. doi: 10.1016/j.neurobiolaging.2013.06.010

Fu, X., Wang, Y., He, X., Li, H., Liu, H., and Zhang, X. (2020). A systematic review and meta-analysis of serum cholesterol and triglyceride levels in patients with Parkinson's disease. *Lipids Health Dis.* 19:97. doi: 10.1186/s12944-020-01284-w

Galper, J., Dean, N. J., Pickford, R., Lewis, S. J. G., Halliday, G. M., Kim, W. S., et al. (2022). Lipid pathway dysfunction is prevalent in patients with Parkinson's disease. *Brain* 145, 3472–3487. doi: 10.1093/brain/awac176

Gaspar, R., Pallbo, J., Weininger, U., Linse, S., and Sparr, E. (2018). Ganglioside lipids accelerate α-synuclein amyloid formation. *Biochim. Biophys. Acta Proteins Proteom.* 1866, 1062–1072. doi: 10.1016/j.bbapap.2018.07.004

Gautam, A. S., Pulivarthi, C. B., and Singh, R. K. (2023). Proinflammatory IL-17 levels in serum/cerebrospinal fluid of patients with neurodegenerative diseases: a meta-analysis study. *Naunyn Schmiedeberg's Arch. Pharmacol.* 396, 577–588. doi: 10.1007/s00210-022-02357-6

Gonçalves, I., Edsfeldt, A., Ko, N. Y., Grufman, H., Berg, K., Björkbacka, H., et al. (2012). Evidence supporting a key role of Lp-PLA2-generated lysophosphatidylcholine in human atherosclerotic plaque inflammation. *Arterioscler. Thromb. Vasc. Biol.* 32, 1505–1512. doi: 10.1161/atvbaha.112.249854

Guo, X., Song, W., Chen, K., Chen, X., Zheng, Z., Cao, B., et al. (2015). The serum lipid profile of Parkinson's disease patients: a study from China. *Int. J. Neurosci.* 125, 838–844. doi: 10.3109/00207454.2014.979288

Gusev, E. I., Katunina, E. A., Martinov, M. Y., Blokhin, V. E., Kalinkin, A. L., Alesenko, A. V., et al. (2020). Development of early diagnosis of Parkinson's disease based on the search for biomarkers such as premotor symptoms and changes in blood. *Zh. Nevrol. Psikhiatr. Im. S S Korsakova* 120, 7–17. doi: 10.17116/jnevro20201201217

Hatton, S. L., and Pandey, M. K. (2022). Fat and protein combat triggers immunological weapons of innate and adaptive immune systems to launch neuroinflammation in Parkinson's disease. *Int. J. Mol. Sci.* 23:1089. doi: 10.3390/ijms23031089

Hirabayashi, T., Kawaguchi, M., Harada, S., Mouri, M., Takamiya, R., Miki, Y., et al. (2023). Hepatic phosphatidylcholine catabolism driven by PNPLA7 and PNPLA8 supplies endogenous choline to replenish the methionine cycle with methyl groups. *Cell Rep.* 42:111940. doi: 10.1016/j.celrep.2022.111940

Hong, X., Guo, W., and Li, S. (2022). Lower blood lipid level is associated with the occurrence of Parkinson's disease: a meta-analysis and systematic review. *Int. J. Clin. Pract.* 2022:9773038. doi: 10.1155/2022/9773038

Hu, L., Dong, M. X., Huang, Y. L., Lu, C. Q., Qian, Q., Zhang, C. C., et al. (2020). Integrated metabolomics and proteomics analysis reveals plasma lipid metabolic disturbance in patients with Parkinson's disease. *Front. Mol. Neurosci.* 13:80. doi: 10.3389/fnmol.2020.00080

Jiang, Z., Xu, X., Gu, X., Ou, R., Luo, X., Shang, H., et al. (2020). Effects of higher serum lipid levels on the risk of Parkinson's disease: a systematic review and Meta-analysis. *Front. Neurol.* 11:597. doi: 10.3389/fneur.2020.00597

Jo, E., McLaurin, J., Yip, C. M., St George-Hyslop, P., and Fraser, P. E. (2000). Alpha-Synuclein membrane interactions and lipid specificity. *J. Biol. Chem.* 275, 34328–34334. doi: 10.1074/jbc.M004345200

Klemann, C., Martens, G. J. M., Sharma, M., Martens, M. B., Isacson, O., Gasser, T., et al. (2017). Integrated molecular landscape of Parkinson's disease. *NPJ Parkinsons Dis* 3:14. doi: 10.1038/s41531-017-0015-3

Lagace, T. A. (2015). Phosphatidylcholine: greasing the cholesterol transport machinery. *Lipid Insights* 8, 65–73. doi: 10.4137/lpi.S31746

Leuti, A., Fazio, D., Fava, M., Piccoli, A., Oddi, S., and Maccarrone, M. (2020). Bioactive lipids, inflammation and chronic diseases. *Adv. Drug Deliv. Rev.* 159, 133–169. doi: 10.1016/j.addr.2020.06.028

López de Frutos, L., Almeida, F., Murillo-Saich, J., Conceição, V. A., Guma, M., Queheberger, O., et al. (2022). Serum phospholipid profile changes in Gaucher disease and Parkinson's disease. *Int. J. Mol. Sci.* 23:10387. doi: 10.3390/ijms231810387

Lu, Y., Jin, X., and Zhao, P. (2021). Serum lipids and the pathogenesis of Parkinson's disease: a systematic review and meta-analysis. *Int. J. Clin. Pract.* 75:e13865. doi: 10.1111/ijcp.13865

Luo, C., Wang, K., Liu, D. Q., Li, Y., and Zhao, Q. S. (2008). The functional roles of lipid rafts in T cell activation, immune diseases and HIV infection and prevention. *Cell. Mol. Immunol.* 5, 1–7. doi: 10.1038/cmi.2008.1

Mao, C. Y., Yang, J., Wang, H., Zhang, S. Y., Yang, Z. H., Luo, H. Y., et al. (2017). SMPD1 variants in Chinese Han patients with sporadic Parkinson's disease. *Parkinsonism Relat. Disord.* 34, 59–61. doi: 10.1016/j.parkreldis.2016.10.014

Minchev, D., Kazakova, M., and Sarafian, V. (2022). Neuroinflammation and autophagy in Parkinson's disease-novel perspectives. *Int. J. Mol. Sci.* 23:14997. doi: 10.3390/ijms232314997

Morris, H. R., Spillantini, M. G., Sue, C. M., and Williams-Gray, C. H. (2024). The pathogenesis of Parkinson's disease. *Lancet* 403, 293–304. doi: 10.1016/s0140-6736(23)01478-2

Nalls, M. A., Blauwendraat, C., Vallerga, C. L., Heilbron, K., Bandres-Ciga, S., Chang, D., et al. (2019). Identification of novel risk loci, causal insights, and heritable risk for Parkinson's disease: a meta-analysis of genome-wide association studies. *Lancet Neurol.* 18, 1091–1102. doi: 10.1016/s1474-4422(19)30320-5

Ottensmann, L., Tabassum, R., Ruotsalainen, S. E., Gerl, M. J., Klose, C., Widén, E., et al. (2023). Genome-wide association analysis of plasma lipidome identifies 495 genetic associations. *Nat. Commun.* 14:6934. doi: 10.1038/s41467-023-42532-8

Quinville, B. M., Deschenes, N. M., Ryckman, A. E., and Walia, J. S. (2021). A comprehensive review: sphingolipid metabolism and implications of disruption in sphingolipid homeostasis. *Int. J. Mol. Sci.* 22:5793. doi: 10.3390/ijms22115793

Schuchman, E. H., Levran, O., Pereira, L. V., and Desnick, R. J. (1992). Structural organization and complete nucleotide sequence of the gene encoding human acid sphingomyelinase (SMPD1). *Genomics* 12, 197–205. doi: 10.1016/0888-7543(92)90366-z

Signorelli, P., Conte, C., and Albi, E. (2021). The multiple roles of sphingomyelin in Parkinson's disease. *Biomol. Ther.* 11:1311. doi: 10.3390/biom11091311

Skrivankova, V. W., Richmond, R. C., Woolf, B. A. R., Yarmolinsky, J., Davies, N. M., Swanson, S. A., et al. (2021). Strengthening the reporting of observational studies in epidemiology using Mendelian randomization: the STROBE-MR statement. *JAMA* 326, 1614–1621. doi: 10.1001/jama.2021.18236

Tansey, M. G., Wallings, R. L., Houser, M. C., Herrick, M. K., Keating, C. E., and Joers, V. (2022). Inflammation and immune dysfunction in Parkinson disease. *Nat. Rev. Immunol.* 22, 657–673. doi: 10.1038/s41577-022-00684-6

Tolosa, E., Garrido, A., Scholz, S. W., and Poewe, W. (2021). Challenges in the diagnosis of Parkinson's disease. *Lancet Neurol.* 20, 385–397. doi: 10.1016/s1474-4422(21)00030-2

Treede, I., Braun, A., Sparla, R., Kühnel, M., Giese, T., Turner, J. R., et al. (2007). Anti-inflammatory effects of phosphatidylcholine. *J. Biol. Chem.* 282, 27155–27164. doi: 10.1074/jbc.M704408200

Ventura, A. E., Mestre, B., and Silva, L. C. (2019). Ceramide domains in health and disease: a biophysical perspective. *Adv. Exp. Med. Biol.* 1159, 79–108. doi: 10.1007/978-3-030-21162-2_6

Verbanck, M., Chen, C. Y., Neale, B., and Do, R. (2018). Detection of widespread horizontal pleiotropy in causal relationships inferred from Mendelian randomization between complex traits and diseases. *Nat. Genet.* 50, 693–698. doi: 10.1038/s41588-018-0099-7

Wang, S., Yuan, Y. H., Chen, N. H., and Wang, H. B. (2019). The mechanisms of NLRP3 inflammasome/pyroptosis activation and their role in Parkinson's disease. *Int. Immunopharmacol.* 67, 458–464. doi: 10.1016/j.intimp.2018.12.019

Xicoy, H., Brouwers, J. F., Kalnytska, O., Wieringa, B., and Martens, G. J. M. (2020a). Lipid analysis of the 6-Hydroxydopamine-treated SH-SY5Y cell model for Parkinson's disease. *Mol. Neurobiol.* 57, 848–859. doi: 10.1007/s12035-019-01733-3

Xicoy, H., Brouwers, J. F., Wieringa, B., and Martens, G. J. M. (2020b). Explorative combined lipid and transcriptomic profiling of substantia Nigra and putamen in Parkinson's disease. *Cells* 9:1966. doi: 10.3390/cells9091966

Xicoy, H., Klemann, C. J., De Witte, W., Martens, M. B., Martens, G. J., and Poelmans, G. (2021). Shared genetic etiology between Parkinson's disease and blood levels of specific lipids. *NPJ Parkinsons Dis* 7:23. doi: 10.1038/s41531-021-00168-9

Xicoy, H., Wieringa, B., and Martens, G. J. M. (2019). The role of lipids in Parkinson's disease. *Cells* 8:27. doi: 10.3390/cells8010027

Yang, C., Wang, W., Deng, P., Li, C., Zhao, L., and Gao, H. (2021). Fibroblast growth factor 21 modulates microglial polarization that attenuates neurodegeneration in mice and cellular models of Parkinson's disease. *Front. Aging Neurosci.* 13:778527. doi: 10.3389/fnagi.2021.778527

Yang, C., Wang, W., Deng, P., Wang, X., Zhu, L., Zhao, L., et al. (2023). Fibroblast growth factor 21 ameliorates behavior deficits in Parkinson's disease mouse model via modulating gut microbiota and metabolic homeostasis. *CNS Neurosci. Ther.* 29, 3815–3828. doi: 10.1111/cns.14302

Zhang, J., Xiao, Y., Hu, J., Liu, S., Zhou, Z., and Xie, L. (2022). Lipid metabolism in type 1 diabetes mellitus: Pathogenetic and therapeutic implications. *Front. Immunol.* 13:999108. doi: 10.3389/fimmu.2022.999108

Zhao, J. H., Stacey, D., Eriksson, N., Macdonald-Dunlop, E., Hedman, Å. K., Kalnapenkis, A., et al. (2023). Genetics of circulating inflammatory proteins identifies drivers of immune-mediated disease risk and therapeutic targets. *Nat. Immunol.* 24, 1540–1551. doi: 10.1038/s41590-023-01588-w

Frontiers in
Aging Neuroscience

Explores the mechanisms of central nervous system aging and age-related neural disease

The third most-cited journal in the field of geriatrics and gerontology, with a focus on understanding the mechanistic processes associated with central nervous system aging.

Discover the latest Research Topics

See more →

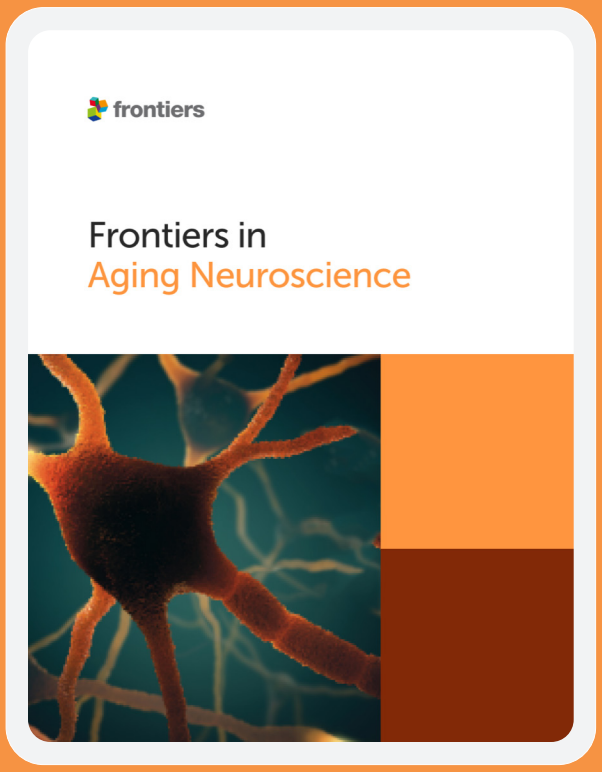

Frontiers

Avenue du Tribunal-Fédéral 34
1005 Lausanne, Switzerland
frontiersin.org

Contact us

+41 (0)21 510 17 00
frontiersin.org/about/contact